# BABBAGE RIVER DELTA AND LAGOON: HYDROLOGY AND SEDIMENTOLOGY OF AN ARCTIC ESTUARINE SYSTEM

by

DONALD LAWRENCE FORBES
M.A., University of Toronto, 1973

A THESIS SUBMITTED IN PARTIAL FULFILMENT OF
THE REQUIREMENTS FOR THE DEGREE OF
DOCTOR OF PHILOSOPHY

in

THE FACULTY OF GRADUATE STUDIES
(Department of Geography)

We accept this thesis as conforming
to the required standard

THE UNIVERSITY OF BRITISH COLUMBIA
April 1981

© Donald Lawrence Forbes, 1981

In presenting this thesis in partial fulfilment of the requirements for an advanced degree at the University of British Columbia, I agree that the Library shall make it freely available for reference and study. I further agree that permission for extensive copying of this thesis for scholarly purposes may be granted by the Head of my Department or by his representatives. It is understood that copying or publication of this thesis for financial gain shall not be allowed without my written permission.

Department of Geography

The University of British Columbia
2075 Wesbrook Place
Vancouver, Canada
V6T 1W5

Date 10 September 1981

BP 75-511E

ABSTRACT

Inputs, transfer processes, and storage characteristics of water and sediment have been investigated in a 40-km² estuarine system on the central Yukon coast. The setting is transgressive, microtidal, and high-latitude (69°N). The Babbage Estuary system can be subdivided into fluvial, tidal-distributary, delta-plain, intertidal, lagoon, marginal-supratidal, and barrier subsystems, each associated with one or more distinctive depositional environments and characteristic lithofacies assemblages. The structure of the system has been examined in terms of links between subsystems and overall system response to input perturbations. Although the propagation of tide and surge within the estuary may be treated as a quasi-linear stochastic process, transfers of fluvial water and sediment through the system are highly non-linear. Furthermore, the parameters of the system change dramatically on an annual cycle.

Inputs and associated system responses are dominated in the short run by seasonal- and synoptic-scale variance, the former reflecting major seasonal adjustments in the phase distribution, circulation process, and input regime of the estuary. The annual salinity cycle, with a range of at least 60 ppt, exhibits a short reaction and long relaxation response to major snowmelt runoff inputs in May or June, when salt water

is flushed completely out of the estuary. Wind-generated waves are effectively absent from the system during 8-9 months of the year, but play a major role during the open-water season. Although direct transport of sediment by ice is relatively unimportant, ice effects are pervasive; they include, in addition to restriction of winter runoff and surface wave generation, creation of hypersaline conditions, control of the sedimentologically important flood events on deltaic supratidal flats, enhanced rates of coastal recession due to thermal degradation of ground ice, and production of distinctive thermokarst morphology on supratidal surfaces. Water level, storage volume, salinity, and suspended sediment series during the open-water season in the lagoon are dominated by synoptic-scale wind effects. In the delta, the major synoptic-scale anomalies of sediment concentration are related to storm runoff. Fluvial clastic sediment inputs to the estuary exceed $10^8$ kg $a^{-1}$, almost an order of magnitude greater than the estimated littoral transport input. More than 97% of the fluvial input may occur in June; of this, approximately half may be exported directly from the system.

At long time scales, the estuarine system has been dominated by rising sea level and coastal recession; Holocene climatic fluctuations may also have been important. A transgressive sequence has developed, including various distinctive features, notably the absence or limited development of aeolian, backbarrier-margin, tidal-delta, and intertidal marsh facies, a largely afaunal intertidal

component, and deltaic deposits with poorly developed levees and abundant lake basins. The basal fluvial component includes a sinuous gravel channel assemblage of a hitherto poorly documented type. The Babbage Estuary barrier sequence is primarily transgressive, but incorporates localized elements of progradational and inlet-migration models. Examples of major transgressive, progradational, and inlet-fill barrier sequences occur in close proximity on the central Yukon coast.

TABLE OF CONTENTS

ABSTRACT ii

LIST OF TABLES viii

LIST OF FIGURES xii

ACKNOWLEDGEMENTS xxxiii

INTRODUCTION 1

1.1 Preamble 1

1.1.1 Definition of study 1

1.2 Conceptual approach 4

1.2.1 Geophysical systems 4

1.2.2 Environments and facies 9

1.2.3 Estuarine systems 11

1.3 The present study 17

1.3.1 Babbage estuarine system 17

REGIONAL CONTEXT: NORTHERN YUKON AND BEAUFORT SEA 26

2.1 Geography and palaeogeography 26

2.1.1 Contemporary geography 26

2.1.2 Late-Quaternary palaeogeography 38

2.2 Atmospheric environment 45

2.2.1 Contemporary climate 45

2.2.2 Low-frequency variability of climate 56

2.3 Oceanographic environment 62

2.3.1 Water and circulation in Mackenzie Bay 62

2.3.2 Ice in the southern Beaufort Sea 69

2.3.3 Tides and storm surges 76

2.3.4 Wave climate 84

HYDROLOGICAL SUBSYSTEM 94
3.1 Freshwater inputs to the estuary 94
3.1.1 Runoff and precipitation inputs 94
3.2 Marine inputs to the estuary 118
3.2.1 Water levels at the marine boundary 118
3.3 System response 144
3.3.1 Tidal propagation within the estuary 144
3.3.2 Supratidal flooding 155
3.3.3 Ice in the estuary 170
3.3.4 Properties of water in the estuary 185
3.3.5 The non-tidal circulation 207
3.3.6 Water budget and structure of the system 230
SEDIMENTOLOGICAL SUBSYSTEM 243
4.1 Fluvial sediment inputs to the estuary 243
4.1.1 Sediment sources and materials 243
4.1.2 Fluvial transport processes 252
4.1.3 Total fluvial sediment input 289
4.2 Marine sediment inputs to the estuary 296
4.2.1 Sediment sources and materials 296
4.2.2 Littoral transport processes 303
4.2.3 Total marine sediment input 314
4.3 System response 317
4.3.1 Sediment transfers within the estuary 317
4.3.2 Sedimentation and erosion 347
4.3.3 Sediment budget and structure of the system 367
4.4 Sediment storage component 376
4.4.1 General characteristics 376
4.4.2 Fluvial facies 392

4.4.3 Delta plain facies 398

4.4.4 Distributary and intertidal facies 414

4.4.5 Lagoon, barrier, and marginal facies 422

4.4.6 The transgressive sequence 435

CONCLUSIONS 447

REFERENCES 457

APPENDICES 495

LIST OF TABLES


1 Scales of variance in Arctic estuarine systems 15

2 Morphometry of lagoons and barriers of the Yukon coast 34

3 Monthly precipitation data, Kay Point 49

4 Selected observations of surface salinity in embayments of the central Yukon coast and in adjacent waters of Mackenzie Bay 68

5 Potential fetch with ≤3/10 ice, Kay Point, 1975 74

6 Potential fetch with ≤3/10 ice, Kay Point, 1976 75

7 Principal tidal constituents at Tuktoyaktuk and Kay Point 77

8 Mean sea level and summer anomaly, Tuktoyaktuk, 1962-1975 82

9 Summary statistics for catchments draining to Babbage Estuary 95

10 Estimates of annual peak discharge, Babbage River at B1 and Deep Creek at D1, 1974-1977 100

11 Major tidal constituents at Kay Point by month 121

12 Summary of dissolved constituents in water samples from the Babbage Estuary system and Phillips Bay 189

13 Stratification and circulation parameters for the Babbage Estuary at station 12 during successive ten-day intervals in the summer of 1976. 210

14 Product-moment correlation coefficients for mean density, transverse stratification, and vertical stratification in Babbage Estuary entrance (stations 5-7) 223

15 Comparison of water transfer estimates for Babbage Estuary entrance section (M1) as obtained from current meter data and by equation 3.3.6-1 233

16 Water budget for Babbage Estuary, January 1976 and June-August 1976 240

17 Summary of dissolved constituents in water samples from the Babbage River and Deep Creek drainage basins 248

18 Petrographic analyses of sand and gravel from Babbage River channel between Tulugaq (Crow) River confluence and section B1 250

19 Sediment transport summary, Babbage River below Crow River 290

20 Sediment transport summary, Deep Creek above Babbage distributary 291

21 Distribution of sediment transport by type, Babbage River and Deep Creek 294

22 Summary of net wave-generated longshore sediment transport for proximal and distal Kay Point spit and Niakolik foreshore, 1975-1976 315

23 Statistics of Secchi extinction depth for stations in the Babbage Estuary, 1976 341

24 Flushing times for the Babbage Estuary 343

25 Thickness of freshly deposited sediment at sites on vegetated supratidal flats, Babbage Delta, 8 June 1976 349

26 Erosion and sedimentation on intertidal surfaces of the Babbage Delta, summer 1976 355

27 Sediment accumulation rates in traps deployed in Babbage Lagoon and in lakes of the Babbage Delta, 1976 358

28 Analysis of variance to determine significance of differences in sediment trap data between sites, Babbage Estuary, 1976 359

29 Approximate sediment budget for Babbage Estuary system, January,June, July, and August, 1976 369

30 Lithofacies types of lower Babbage River and Babbage Estuary 379

31 Benthic invertebrates in Ekman dredge samples from the Babbage Estuary near station 7a, 24 July 1975 425

32 A: Delaware surficial transgressive sequence (adapted from Kraft, 1971); B: Babbage Lagoon surficial transgressive sequence 437

33 Babbage Delta surficial transgressive sequence 444

LIST OF FIGURES

1 Map of the Yukon coast, showing location of Babbage Estuary system and other topographic features, including major lagoons and estuaries 2

2 Map of the Babbage Estuary system, showing major sampling stations, locations of tide and stage recorders, hydrometric sections, and location of meteorological station at Kay Point 18

3 Bathymetry of Babbage Estuary in 1975; view across main entrance section toward Kay Point spit, with Babbage Lagoon to right, Kay Point in distance, and Niakolik Point in foreground 19

4 A: view of the Babbage Delta, showing intertidal and supratidal surfaces; B: lower Babbage River, looking downstream toward section B1 21

5 Babbage Delta and southern lagoon, showing coordinate system, intertidal transects, sites where the thickness of fresh sediment was measured on the delta plain and on ice, and locations of sediment traps, excluding sites in the northern lagoon 22

6 Babbage Estuary system, showing grid network, borehole locations and locations of short cores or exposures 24

7 Western part of Yukon Coastal Plain with British Mountains in background; A: Backhouse Lagoon; B: Firth River fan with Nunaluk Lagoon in foreground 27

8 A: headwaters of Babbage River with Tertiary pediment and icing, 29 August 1976; B: upper Trail River basin in British Mountains near Mount Sedgewick 28

9 Massive ground ice in ice-thrust sediments exposed between Kay Point and King Point, Mackenzie Bay coast 30

10 Barriers and lagoons at Stokes Point (A) and at King Point (B), central Yukon coast 33

11 Hypsometric curves for Babbage River and Deep Creek drainage basins 36

12 Tentative late-Wisconsinan and 1826 palaeogeography between Kay Point and Herschel Island 39

13 Profile along axis of Babbage Valley and Herschel Basin, showing hypothesized late-Wisconsinan water level in Lake Herschel and present valley-axis slopes of Babbage River and tributaries 42

14 Data base and tentative history of late Wisconsinan and Holocene sea levels in Mackenzie Delta and on the Yukon coast (after Forbes, 1980) 44

15 Monthly temperature and precipitation data for Komakuk Beach and Shingle Point on the Yukon coast and for Old Crow (south of the mountains) 46

16 Cumulative precipitation at stations in the northern Yukon Territory, summer 1974 51

17 Variance density spectrum of hourly atmospheric pressure at Kay Point, summer 1976 52

18 Relative frequencies of hourly wind speed (m/s) by direction, 1975 and 1976 summer records, Kay Point. 53

19 Variance density spectra for northeasterly and northwesterly components of hourly wind stress, Kay Point, 1976 55

20 Representative temperature and salinity profiles in Mackenzie Bay 64

21 Landsat image 1-1422-20185-5, 18 September 1973, showing Mackenzie River plume spreading north and east, with an abrupt western boundary in Mackenzie Bay 66

22 Portion of Landsat image 1-1460-20292-6, 26 October 1973, showing open water in Mackenzie Bay and thin ice in Herschel Basin, in Phillips Bay, west of Herschel Island, and in all lagoons 71

23 Portion of Landsat image 1-1317-20374-6, 5 June 1973, showing narrow band of landfast ice west of Herschel Island, extensive landfast ice in Mackenzie Bay, and lead in the shear-zone between landfast ice and seasonal pack 71

24 Frequency distribution of extreme monthly water levels at Tuktoyaktuk 81

25 Plots of estimated versus observed wave period and height, Kay Point spit 88

26 Refraction of waves at T=4.2s approaching from the NNW and of waves at T=4.9s approaching from the east; sites for which hindcast computations and longshore sediment transport estimates were obtained are also plotted 90

27 Frequency distributions of tangential and normal components of wave power at the distal end of Kay Point spit, based on hindcast wave analysis 93

28 Daily runoff (Babbage River at B1) and daily precipitation at Kay Point and Shingle Point, 1974-1976 97

29 Cumulative precipitation at Shingle Point and cumulative runoff in Babbage River (B1) and Deep Creek (D1), 1975 and 1976 101

30 Time of diurnal peak flow during summer recession in Babbage River at B1, 1975 and 1976 106

31 Babbage River discharge, section B1, 21 June to 2 July 1976 108

32 Storm hydrographs, Babbage River, August 1976, showing non-exponential character of recessions 110

33 Frequency distributions of daily runoff for snowmelt and summer seasons 1974-1976, Babbage River at B1 113

34 Variance density spectra of hourly discharge: Babbage River at B1, summer 1975; Deep Creek at D1, summer 1976 115

35 Hourly water level at marine boundary of Babbage Estuary: summer 1974, summer 1975, and breakup+summer 1976 119

36 Variance density spectrum of hourly water level at Kay Point spit (gauge A, CHS station 6515), 12 July to 12 September 1975 120

37 Cumulative normalized variance spectra for hourly water level at marine boundary, Babbage Estuary 124

38 Variance density spectrum of hourly water temperature at station 5, Babbage Estuary, during 20 days of record in August 1975 128

39 Wind, atmospheric pressure, and water level at Kay Point during 1975, illustrating phase correspondence between low-pass water level and northwesterly wind speed but variable amplitude of surge response 131

40 Wind, atmospheric pressure, and water level at Kay Point during 1976, illustrating phase correspondence between low-pass water level and northwesterly wind speed 132

41 Partial coherence between water level and northwesterly wind stress 135

42 Frequency distributions of daily-maximum hourly water level for the late June to early September season in three different years, Kay Point spit data 138

43 High-frequency and transient response of water level to wind associated with cold-front passage, 30 July 1976 140

44 Minor surge with abrupt shock front and high-frequency low-amplitude variance superimposed on Niakolik Point (gauge-B) tidal record for 6 August 1976 141

45 Water levels at gauges A and E, 19-25 August 1975 146

46 Water level sequence at gauge C, distal Babbage Delta, late July 1976 146

47 Partial coherence: (A) between gauge-A and gauge-E water levels; (B) between B1 and gauge-E water levels 148

48 Comparison between variance density spectra of $\zeta_E(t)$ and of $\zeta_E(t)$, showing close agreement at $f<10^{-1}$ c $h^{-1}$ 151

49 Gain function for Babbage Estuary cooscillating tidal system 152

50 Lag function for Babbage Estuary cooscillating tidal system 154

51 Complete duration sequences for hourly water level, Babbage Estuary marine boundary, summer 1975 and spring-summer 1976 156

52 Driftwood deposits marking the present transgressive limit near Kay Point and near gauge E in the valley 158

53 Distribution of major driftwood deposits in the Babbage Estuary system, 22 August 1944 and 20 August 1970 159

54 Record of storm-surge event, 27 August 1975: water levels at gauges A and E 162

55 Water level at Niakolik Point (gauge B) as a function of Babbage River discharge, spring and summer 1976 164

56 Babbage River discharge, gauge-B water level, and bottomfast ice thickness at a site in the Babbage Estuary near gauge B, 1-30 June 1976 166

57 Supratidal flooding of Babbage Delta with bottomfast ice in the lagoon, 9th and 10th of June 1974 167

58 Schematic plot of monthly ice thickness (after Schell, 1974) and proportions of estuarine storage volume in solid and liquid phases 171

59 Ice in the northern Babbage Lagoon and in the proximal Babbage Delta, late May 1974 172

60 Chronology of breakup in the Babbage Estuary, 1974-1976 177

61 A: Spring River, showing snowmelt runoff contained and deflected by the Spring River barrier; overflow of Babbage River water onto ice outside Babbage Estuary is visible in the background, 30 May 1974; B: ice floating in main distributary channel of Babbage Estuary between distal delta and Niakolik Point, 9 June 1974 178

62 Drainage holes through ice outside main entrance section and general view of central lagoon, showing limited extent of flooding over-ice and open water in entrance channel 30 May 1974 182

63 Schematic plot of monthly water temperature and salinity in the Babbage Estuary, based on 1976 observations for the summer months and 1974 data (after Steigenberger et al., 1975) for April, with other values interpolated 191

64 Daily sequence of water temperature, $\Theta$, salinity, s, density, $\rho$, and viscosity, $\eta$, in Babbage Estuary entrance, June-September 1976 194

65 Daily sequence of water temperature, $\Theta$, salinity, s, density, $\rho$, and viscosity, $\eta$, at station 12, Babbage Delta, June-September 1976 195

66 Daily temperature, salinity, density, and viscosity in Babbage Estuary, 24 July to 5 August 1977 197

67 Estimates of the variance of water density for sets of data at various sampling intervals, $\Delta t$ 199

68 Time sequence including the storm surge event of 27 August 1975: 12h maximum, minimum, and instantaneous air temperature; half-hourly water temperature; wind speed and direction at Kay Point; water level at gauge A; and Babbage River discharge at B1

202

69 Surface salinity in the Babbage Estuary following the storm of 27 August 1975

204

70 Examples of salinity stratification in main distributary channel and entrance section of Babbage Estuary, 1 September 1976 and 31 July 1975

213

71 Change in pattern of salinity stratification in main distributary and entrance section of Babbage Estuary over a 3-4h period of ebb flow, 30 July 1975

214

72 Changes in the pattern of salinity stratification over nine-hour interval, 31 July to 1 August 1975

215

73 Surface velocity distribution in M1 section, Babbage Estuary, during ebb 1423-1603h 10 August 1976

218

74 Surface and near-bottom velocities in M1 section, Babbage Estuary entrance, during flood 1200-1330h 3 August 1976, showing continued ebb flow at all depths over the central shoal, with water entering at depth via channels near stations 5 and 7

220

75 Time sequence of surface and bottom salinity at stations 2, 5, and 7 in Babbage Estuary, of gauge-A water level, and of wind speed and direction at Kay Point, showing response of vertical salinity distributions to wind-induced mixing; wave heights are superimposed on the salinity sequence

221

76 Longitudinal and transverse components of velocity at station 5, low-pass and high-pass filtered components, and water level at gauge A, Babbage Estuary, 12-31 August 1975 225

77 Capacity of the Babbage Estuary as a function of water level 231

78 Net exchange flow through M1 section, gauge-B water level, and Babbage River discharge through B1 section, June 1976 234

79 Hourly storage volume in the Babbage Estuary during summer 1975 235

80 Variance density spectrum of hourly storage volume in the Babbage Estuary during summer 1975 237

81 Partial coherence between Babbage River discharge, $Q_f(t)$, and M1 net output sequence, $Q_{\tilde{Q}}(t)$, showing extreme non-linearity of runoff transfers through the estuary, particularly in the synoptic frequency band in which most of the variance of runoff resides 238

82 Simplified canonical structure of the hydrological subsystem during late-winter, snowmelt, and summer seasons, showing dramatic changes in the number and character of internal and external links 242

83 Incised middle course of Babbage River: (A) major exposure of Cretaceous or earlier sediments adjacent to the channel; (B) Tertiary gravel over older sediments in a spur above the river 244

84 A: steep braided channels draining unvegetated ridges in Barn Mountains, eastern part of Babbage River basin, August 1976; B: block slumping due to thermo-erosional niche development, lower Babbage River, late July 1976 245

85 Representative particle-size distributions for source materials and for sediments stored in the channel system, Babbage River basin 250

86 A: incombustible suspended sediment and total dissolved solids concentrations (mg/L) in Babbage River at B1, 1975; B: incombustible suspended sediment and total dissolved solids transport (kg/s) 254

87 A: total suspended sediment and total dissolved solids concentrations (mg/L) in Babbage River at B1, 1976; B: total suspended and total dissolved solids transport (kg/s) 255

88 A: total suspended sediment and total dissolved solids concentrations (mg/L) in Deep Creek at D1, 1976; B: total suspended and total dissolved solids transport (kg/s) 256

89 Dissolved, suspended, and bedload ratings, Babbage River at B1, 1976 258

90 Dissolved, suspended, and bedload ratings, Deep Creek at D1, 1976 259

91 Total dissolved solids concentration as a function of discharge, Babbage River at B1, 1976 262

92 Total dissolved solids concentration as a function of dischargeDeep Creek at D1, 1976 263

93 Water discharge and total dissolved solids concentration (estimated from specific conductivity corrected for $\Theta_w$ ), showing two transients of high TDS concentration during breakup and snowmelt flood of June 1975, Babbage River 266

94 Phase relations between incombustible suspended sediment concentration (mg/L) and discharge ($m^3s^{-1}$), Babbage River at B1, 1975 and 1976 269

95 Phase relations between incombustible suspended sediment concentration (mg/L) and discharge ($m^3s^{-1}$), Deep Creek at D1, 1975 and 1976, showing hysteresis during annual snowmelt floods 270

96 Hysteresis in suspended-sediment/discharge relation during Babbage River flood of 8 June 1974, showing peaks in TSS concentration both before and after peak stage and counter-clockwise hysteresis loop for the flood as a whole 272

97 Sample data and theoretical ratings for bedload transport, Babbage River at B1, 1976 277

98 Particle-size distributions for various samples of sediment in channel deposits or moving as bedload, Babbage River at B1 281

99 Three sets of empirical results for the hiding factor$\xi$ as a function of $D/D_{50}$ in rough turbulent flow 282

100 Channel bed profiles at section B1 (Babbage River) between 28 May and 8 June 1975, showing degradation of bottomfast ice 286

101 Channel bed profiles at section B1 (Babbage River); A, 1975: scour during rising limb of annual snowmelt hydrograph, showing development of scour-hole against bank in thalweg; B, 1976: profiles shortly after peak flow on 6 June and 26 June, net fill 10-15 June, and net scour 15-19 June 288

102 Cumulative percent of total sediment transport in Babbage River at B1 in 1975 and 1976 293

103 A: coastal segment 1 near Kay Point, showing undercutting and failure of polygonal blocks formed by ice-wedge thaw or fracture, July 1976; B: coastal segment 2, showing major impact of retrogressive-thaw and associated mudflow transport of fine sediment across the beach, August 1977 298

104 Turbid Mackenzie River water off central Yukon coast; A: part of Landsat image 1-1089-20020-5, 17 July 1975, showing advection of suspended sediment past Kay Point; B: leading edge of Mackenzie River plume off Kay Point, 28 July 1976 301

105 Vertical photograph of Kay Point and Babbage Estuary, showing longshore transport of suspended sediment westward past Kay Point and wide shore-normal dispersion in Phillips Bay; part of NAPL photograph A22975-56, 4 August 1972 304

106 Daily longshore sediment transport at distal end of Kay Point spit, positive toward the main entrance section (M1), computed from hindcast wave data using equation 4.2.2-6 310

107 Proximal end of Kay Point spit, showing temporary (M3) inlet; part of NAPL photograph A21830-2, 18 August 1970 312

108 Viscosity, Stokes settling velocity for D=1 μm, and total suspended solids concentration at station 7, Babbage Estuary, 1976 319

109 Scanning electron micrographs of sediment from the Babbage Estuary (site 021125), showing silt- and clay-size mineral particles and various composite particles of silt size 322

110 Scanning electron micrographs of sediment from the Babbage Estuary (site 010140), showing both pelletized and angular forms of agglomeration 323

111 Particle-size distributions for bottom sediment and for suspended sediment collected in traps at site 010140, Babbage Lagoon, showing effects of various treatments 325

112 Longitudinal thalweg profiles in the main distributary channel of the Babbage Delta, showing (A) predominance of ebb-directed transport and (B) rare occurrence of flood-directed bedforms downstream from station 10 329

113 Horizontal reflectors in cross-sections of lower Deep Creek channel, suggesting presence of fluid-mud 331

114 Time sequence of total suspended solids concentration at station 12, Babbage Delta, with wind speed and direction at Kay Point and Babbage River discharge, spring and summer 1976 333

115 Distribution of $C_T(0)$ in the Babbage Estuary during the storm-surge of 27 August 1975 (A) and on 14 August 1976 (B), when a plume of turbid water filled Phillips Bay as far northeast as Kay Point 337

116 Water level and longitudinal velocity (station 5; h-z=0.9 m), second half of August 1975; uppermost record is time sequence current speed, showing distribution of values exceeding an approximate entrainment threshold of 0.15 m/s 338

117 Estimated concentration of total suspended sediment, based on hourly Secchi extinction data at stations 5, 6, and 7 in the entrance section and station 12 in the delta during a 48-h period in July 1976 340

118 Ice rafting of sediment onto supratidal delta plain, June 1976 346

119 Ice in Babbage Delta lakes after spring flooding, showing basins with and without sediment on ice; (A) 15 June 1974; (B) 18 June 1976 351

120 Sediment on ice, formerly bottomfast; (A) in lagoon near the distal end of the spit (015080), apparently rafted from a location closer to the delta; and (B) in Phillips Bay near section M1 (site 000050) 353

121 Sediment trap locations and distribution of accumulation rates (kg $m^{-2}day^{-1}$) for the interval 24 June to 16 July in 1976 357

122 Rates of sediment accumulation (kg $m^{-2}day^{-1}$) in traps deployed at lagoon- and lake-bottom sites in the Babbage Estuary system, June-September 1976 360

123 Distribution of sediment accumulation (kg $m^{-2}day^{-1}$) in traps in the Babbage Estuary, 8/9-14/15 August 1976 362

124 Area of supratidal flat lost to bank erosion along western and main distributary channels of the Babbage Delta, August 1944 to August 1970, determined from air photographs; extent of erosion indicated by shading 365

125 Degradation of vegetated supratidal flats, distal Babbage Delta, August 1975 366

126 Total suspended sediment concentration at section B1, Babbage River, and estimated total suspended sediment concentration, based on Secchi extinction depth, at stations 5, 6, 7, and 7a in the estuary during June 1976 371

127 Part of NAPL photograph A13383-151, 1952, showing configuration of distributary channels seaward of the distal delta margin very different from the 1972 morphology (cf. Figure 105) 373

128 Canonical structure of the sedimentary component of the Babbage Estuary system, showing seasonal changes in the linkage network 374

129 Map of Babbage Estuary system showing distribution of major depositional environments and representative lithofacies types 378

130 Sediment sampling locations in the Babbage Estuary, classified according to depositional environment 381

131 Ternary diagrams showing proportions of sand plus gravel, silt, and clay, for various components of the Babbage Estuary system 382

132 Ternary diagram showing proportions of gravel, sand, and mud in sediments of the Babbage River and Estuary 386

133 Relation between graphic standard deviation $\tilde{s}$ and graphic mean $\tilde{D}$ for surface sediments of the Babbage Delta and Estuary 388

134 Borehole data, Babbage Estuary and Delta 390

135 Distribution of Holocene channel deposits in the lower valley, as interpreted from surface morphology and limited exposures, showing major impact of Tulugaq river fan on sedimentation in this part of the valley 393

136 Lower Babbage River between Trail River and furthest-seaward gravel riffle, in 1954 (left) and 1976 (right); parts of NAPL photographs A14406-48 and A24502-170 394

137 Distribution of lithofacies types at the surface, Babbage River and distributary channel immediately downstream from section B1; part of NAPL photograph A21826-87, August 1970 395

138 Air and ground views of Babbage Delta, showing distributary, lacustrine, and supratidal components of the sediment system 399

139 Topographic profile of central Babbage Delta along grid line yyy=040 (see Figure 5); proximal delta at left, distal margin with anomalous elevated surface at right 400

140 Frequency distributions of surface area for various subsets of the pond and lake population on the Babbage Delta; also plotted are distributions for an area of lagoon-margin supratidal flats, for anomalous surface with rugged microrelief on distal delta, and for a representative area in the lower valley 402

141 Long profile of tidal channel and cross-profiles of three lakes in the central Babbage Delta 403

142 Levees in the Babbage Delta; A: prominent levee beside minor distributary channel, northern distal margin of delta plain; B: bank with negligible levee development, more typical of the distal delta, right bank of main distributary channel between stations 10 and 12 405

143 Proximal delta plain; (A) looking upvalley, showing vegetated supratidal surface with lakes at left and flood-splay unit at bottom right; note abandonned Babbage River channel in middle distance; (B) sparsely vegetated supratidal flood-splay surface 406

144 Flood-splay sedimentation surface adjacent to main distributary channel, central Babbage Delta; part of NAPL photograph A21826-81, August 1970 407

145 A: spruce logs (driftwood) in supratidal sediments of the Babbage Delta; B: stratified organic silts of the supratidal delta plain, part of section 405 in the central delta

409

146 Anomalous raised surface of rugged microrelief at distal margin of central delta plain, June 1976

411

147 Marginal supratidal flats of Babbage Delta, showing thermokarst morphology arising in part, at least, from degradation of ice-wedge polygon nets

412

148 A: 7-kHz record from main distributary channel, proximal delta; B: interpretation of 7-kHz record from main distribuary, distal delta near station 10

415

149 A: flood-directed dune- and ripple-scale bedforms on distributary-margin surface near transect 4, proximal Babbage Delta; B: ice-rafted gravel on distributary-margin intertidal surface, central delta

416

150 Channel-margin and lagoon-margin intertidal surfaces in the Babbage Delta, August 1974

418

151 A: intertidal flats near transect 8, distal Babbage Delta, showing tidal channel network, with patches of colonizing Puccinellia on levees, and erosion of supratidal surface, September 1976; B: dessication cracks, associated small-scale scour, and drainage vents on low intertidal surface.

419

152 Core sections from high intertidal surface in shallow basin, distal delta plain (site 406, Figure 6)

420

153 Profile of M1 (main entrance) section, Babbage Estuary marine boundary 423

154 Gravel forming low intertidal shoal in Babbage Lagoon (site 032080), showing linear grooves attributed to ice scour 425

155 A: Kay Point barrier, with Phillips Bay at right and Babbage Lagoon at left, showing wide backshore surface largely snow-free, May 1976; B: Shingle Point spit, showing extensive and complex backbarrier deposits 427

156 A: Distal Kay Point spit, 27 August 1975, following a severe storm and moderate surge, showing limited extent of washover deposits, aeolian sand accumulation near large logs on berm, and ice incorporated in foreshore sediments; (B) distal end of spit, 2 August 1974, showing subtidal backbarrier platform and post-1972 extension of the spit 428

157 Schematic section through Kay Point spit, showing distribution of upper barrier lithofacies 429

158 A: lagoon-margin supratidal flats at north end of Babbage Lagoon, showing numerous lakes and ponds, local rugged microrelief, and marginal beach and washover facies; B: Carex-Puccinellia and Elymus communities and the landward limit of marginal washover sand 432

159 Parts of core taken in ephemeral pond near edge of supratidal flats, showing (at left) near-surface interlaminated algal mud, peat, and sand, and (at right) pebbly sand washover unit at a depth of 400 mm 433

160 Section through Babbage Lagoon, Kay Point spit, and Phillips Bay, showing the distribution of sand and gravelly-sand lithofacies and the transgressive character of the barrier sequence 438

161 Changes in the King Point barrier, 1954-1972, showing development of an inlet-fill sequence by distal extension of the spit; parts of NAPL photographs A14363-54 (1954) and A22879-105 (1972) 440

162 A: low-level oblique photograph of surface morphology on the King Point barrier backshore, August 1975; B: Running River delta near Shingle Point, showing beach and washover facies at the seaward margin of deltaic supratidal flats 441

163 Spring River barrier in 1952 (part of NAPL photograph A13383-155) and changes occurring between 1952 and 1970 442

164 Schematic diagram showing hypothetical distribution of lithofacies forming transgressive sequence beneath the Babbage Delta 445

ACKNOWLEDGEMENTS

It is a pleasure to acknowledge the help of many individuals and organizations during the course of this study. The project was supported by the Geological Survey of Canada, Terrain Sciences Division. Major contributions were also received from the National Research Council of Canada (now NSERC) through grants to Dr M. Church and from the University of British Columbia. Personal support was provided by the Geological Survey, by a National Research Council Postgraduate Scholarship, and by a MacMillan Family Fellowship. Logistical support was provided by Technical Field Support Services, by the Polar Continental Shelf Project, and by the Inuvik Research Laboratory (now ISRC).

I wish to express particular appreciation to two individuals for their wide-ranging support and general encouragement over the years. I am grateful to M. Church, who acted as research supervisor, for his concern, helpful criticism, and persistent confidence; and to C.P. Lewis, for his part in initiating the study, for invaluable administrative and technical support, and for help and collaboration in the field.

I thank F. Stephenson, Institute of Ocean Sciences, Patricia Bay, for provision of water level recorders and current meters and for assistance in the field; Dr J.W. Murray,

University of British Columbia, for lending coring equipment; L. Veto, University of British Columbia, for SEM imagery; H. Wood, Water Survey of Canada, Inuvik, for lending hydrometric equipment; and Dr W. Blake, Jr, Geological Survey of Canada, for radiocarbon analyses.

For major assistance in the field, under conditions that were at times very difficult and at times idyllic, I am especially grateful to Bill Barrie, Linda Forbes, Ian Gale, Stuart Hotzel, Annie Krasker, Michael Krastman, and John O'Loughlin. Important contributions were also made by Dr R. Gilbert, Roland Wahlgren, and many other individuals involved in the coastal studies project at Kay Point. I am especially indebted to Helen Kerfoot for much friendly assistance with logistical problems, both in and out of the field, and for substantial contributions to the field data.

Richard Leslie provided valuable technical advice and assistance. Audrey Vycinas carried out much of the laboratory work in Vancouver. Peter Richards helped with the tidal analysis. Naomi Bergh, Linda Forbes, Julia Purcell, and Margaret Ritchie helped with production of the report.

I am grateful to Dr B.C. McDonald for early support of the project and to Dr C.F.M. Lewis for his interest and encouragement. Finally, I am happy to acknowledge the guidance and support of Dr J.R. Mackay, Dr W.H. Mathews, and Dr O. Slaymaker, members of my research supervisory committee at the University of British Columbia.

# 1 INTRODUCTION

## 1.1 PREAMBLE

### 1.1.1 DEFINITION OF STUDY

This is a study of water and sediment transfers in a small delta-estuary of the southern Beaufort Sea coast (Figure 1). It is an investigation of sediments and geomorphology on a transgressive microtidal coast under Arctic conditions. It is also an analysis of structure and variability in an estuarine system, wherein energy and mass inputs imposed by the regional and local environments produce associated outputs and storage components.

The physical configuration of an estuary reflects patterns of mass storage in dynamically interacting hydrological and sedimentological subsystems. The storage component of the hydrological subsystem is related to water level and affects, among other factors, the net non-tidal circulation, through the effect of density stratification on circulation in the estuary. The storage component of the sedimentological subsystem determines, in large part, the surface morphology of the estuary and, to the extent that a net gain in storage occurs over time, may yield a partial historical record and a model for interpretation of similar ancient deposits.

The Babbage Estuary system exhibits distinctive water and

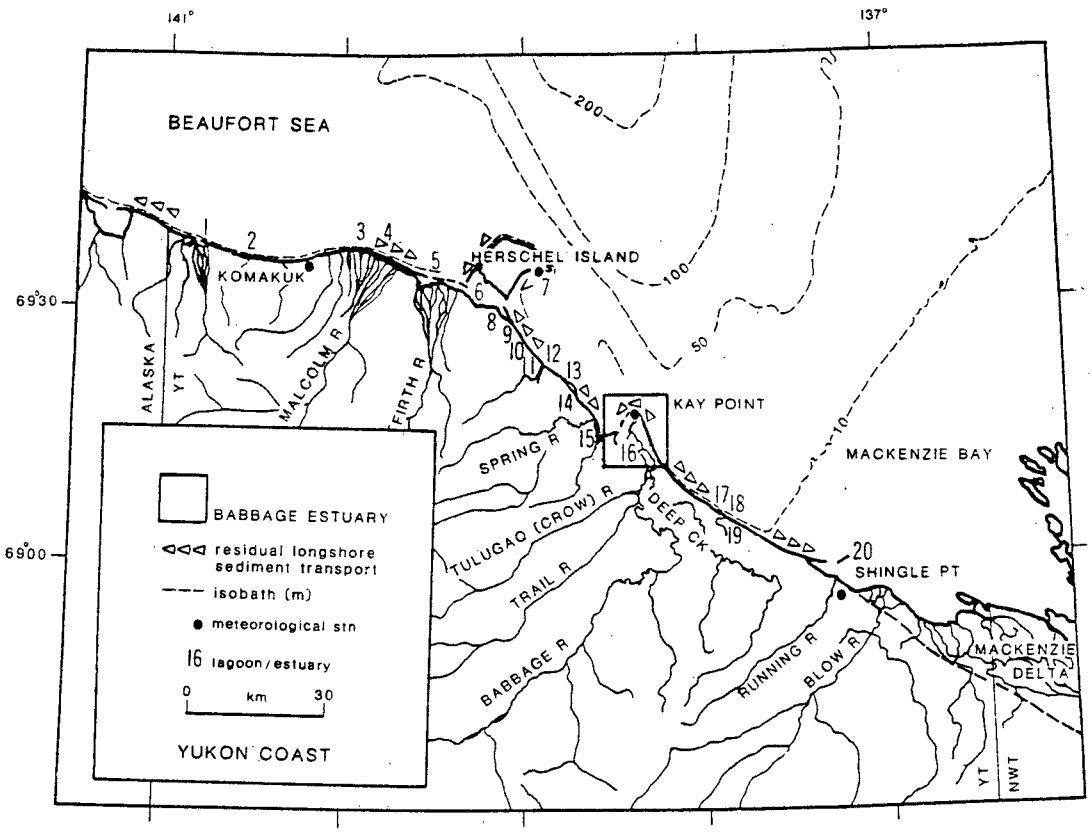


FIGURE 1

Map of the Yukon coast, showing location of Babbage Estuary system and other topographic features, including major lagoons and estuaries (code numbers defined in Table 2).

sediment storage patterns and distinctive system response characteristics reflecting various aspects of the geographical setting. These provide, in some cases, new insights into the effects of ice, runoff regime, coastal setting, and historical context in the development of an estuarine system. Furthermore, they indicate the relative importance of various scales of input and parameter variance for different components of the estuarine system. The Babbage system exhibits significant variability at time scales ranging from $10^3$ to $10^{12}$s, the range corresponding to scales of observed or inferred fluctuations of mass inputs and system parameters. The nature of these fluctuations, the patterns of system response (including system structure, reaction-relaxation effects, and storage distribution), and distinctive features of the system related to its transgressive, microtidal, or high-latitude setting, are major themes of the present study.

## 1.2 CONCEPTUAL APPROACH

### 1.2.1 GEOPHYSICAL SYSTEMS

Relationships among various geophysical phenomena may be examined in the context of geophysical systems, structured sets "of components or variables ... that exhibit discernible relationships with one another and operate together as a complex whole, according to some observed pattern" (Chorley and Kennedy, 1971, pp.1-2). Geophysical systems may be variously defined, with variables having different or like dimensions. A simple system may involve an independent or input variable, $x(t)$; an intermediate operation or transformation, f, conditioned by the structure, parameters, and state of the system; and a dependent, or response, or output variable, $y(t)=f[x(t)]$.

Geophysical systems may involve energy or mass transfers within and between geographically definable physical entities; they may involve structured geometrical, statistical, or other relationships among physical properties; or they may involve both. Chorley and Kennedy (1971) have distinguished three types of geophysical system: the cascade system, the morphological system, and the process-response system. A cascade system, representing energy or mass transfer processes, generally incorporates a chain of subsystems, with mass or energy passing from subsystem to subsystem, in each of which one or more storage compartments may occur. A morphological system incorporates a structured set of physical properties, which may or may not have morphological expression, and which

take on particular instantaneous values as a result of interaction with energy or mass cascades; this type of system may be termed, with more generality, a parameter system. Interacting parameter and cascade systems may be considered to form together a process-response system, in which the parameters and storage product of the cascade system are represented by individual components and structures of the parameter system [cf. Chorley and Kennedy (1971, figure 1.3); this formulation and terminology are in debt to earlier 'process-response model' concepts enunciated by, among others, Krumbein and Sloss (1963, chapter 7), Krumbein (1963), and Whitten (1964)]. Components of the parameter system may be morphological (e.g. channel geometry or sediment texture) or non-morphological (e.g. density or albedo); most parameter systems include both.

Cascade systems may have multiple inputs and outputs. The intervening transfers or transformations involve storage locations and distribution control terms or regulators (Chorley and Kennedy, 1971, pp.5-7). The transformation from input to output may involve various routes, rates, and interruptions (storage), yielding variable reaction and relaxation effects in the output (cf. Allen, 1974). In the case of sediment cascades, the transfer processes are characteristically size-dependent; as a result, sedimentary deposits commonly exhibit size sorting effects, which contribute to lithofacies differentiation, while size-dependent lag times may also be anticipated. The identification of lags is in some cases

diagnostic and may constitute a valuable finding in itself [cf. Stenborg (1970) for an example in glacial hydrology and Allen (1973) for examples involving sedimentary bedforms].

System response behaviour reflects a number of factors, including the state of internal storage and regulation terms, the magnitude, variance, and frequency distribution of system inputs, the existence of thresholds, the complexity of the system, and the integration of various output component lags. In particular, thresholds and feedback mechanisms in the system may produce transient unstable or metastable responses, involving abrupt shifts of the mean, while variable internal trajectories may give lag or relaxation effects that are frequency-dependent (cf. Bendat and Piersol, 1971, p.31).

If the input process of a simple single-input, single-output, physical cascading system is stationary and ergodic, if the system is free of thresholds or unstable positive feedback within some range of inputs, and if the system response is linear within this range, then theoretical results for linear systems may be applied. The output of a physically-realizable linear system is given by the convolution

$$y(t) = \int_0^\infty h(\tau)x(t-\tau)d\tau, \qquad (1.2.1\text{-}1)$$

where $h(\tau)$ is a weighting function and $\tau$ is a lag term in the time domain. In the frequency domain, the Fourier transforms, $X(f)$ and $Y(f)$ of $x(t)$ and $y(t)$, are related through a frequency response function, $H(f)$:

$$Y(f) = H(f)\ X(f), \qquad (1.2.1\text{-}2)$$

where $H(f)$ is the Fourier transform of $h(\tau)$. The modulus,

$|H(f)|$, is the gain factor of the system and the argument, $\Phi(f)$, is the phase factor. For a hypothetical sinusoidal input at frequency f, $|H(f)|$ is the ratio of the output amplitude to the input amplitude and $\Phi(f)$ defines the phase shift of the system (Bendat and Piersol, 1971, p.41).

Frequency-dependent system response characteristics can be investigated by this strategy if the system satisfies the rather stringent assumptions listed above. Linear system theory can be extended to cover multiple-input and -output systems and the approach can be applied, with greater complexity, to some non-linear systems as well (cf., for example, Amorocho and Brandstetter, 1971). In any case, the results are limited to fixed-parameter system response with stationary inputs.

Most geophysical systems are non-linear beyond some limited range of input conditions and many are non-linear throughout. In an energy cascade between coupled water and sediment cascade systems, water and sediment transfers may be considered to represent parameters of the process-response system that forms the coupling. In general, this system is non-linear, viz.:

$$J = aQ^{b}+c+e, \quad b\neq 1,$$

where J is the sediment transport rate, Q is the water discharge, a, b, and c are empirical coefficients and e is an error or variance term. For bedload transport, in particular, the exponent is typically very high ($b>>1$) and dependent on discharge ($db/dQ\neq 0$; see section 4.1.2). In the case of

suspended sediment transport, because $J = C_s Q$ where $C_s$ is the sediment concentration, the exponent $b=1$ if and only if $dC_s/dQ=0$ (i.e. if the concentration is constant). In many natural systems, it is found that the concentration of suspended sediment varies as a positive logarithmic function of discharge,

$$\ln(C_s) = a \ln(Q) + c + e,$$

and the $J=f(Q)$ system may be treated as linear after logarithmic transformation (cf. Sharma and Dickinson, 1979).

## 1.2.2 ENVIRONMENTS AND FACIES

An environment may be viewed as the totality of external phenomena affecting the nature and time-space distribution of inputs to a system and constraints on its response. In a sense, this definition involves two parameter systems, one external and one internal to a given process-response system. The external parameters are part of larger process-response systems in which the given system is imbedded; the internal parameters constitute the parametric component of the given system.

A sedimentary environment has been defined as a "complex of physical, chemical, and biological conditions under which a sediment accumulates" (Krumbein and Sloss, 1963, p.324; cf. Scruton, 1960, pp.92-93). In this sense, a sedimentary environment and associated sediments are equivalent to a sedimentary process-response system as defined above. Moreover, a close functional relationship exists between the geomorphology of a particular sedimentary environment and the storage components of the sedimentary system.

It has long been recognized that landscapes and deposits may be classified into distinctive groups, not only by evolutionary or stratigraphic position, but also in terms of environmental context or associated process sets. Gressly (1838) introduced the term 'facies' to distinguish stratigraphically equivalent units that differ laterally in lithology or palaeontology. The facies concept has since been

broadened to include sedimentary sets sharing common environmental attributes but not necessarily related in a stratigraphic context. Facies may be viewed as the morphological or depositional products of individual cascade subsystems, and in particular as storage components of these subsystems within the sediment transport cascade.

Distinctive depositional environments usually generate deposits having distinctive sets of textural and structural characteristics (see, for example, Blatt et al., 1972, chapter 6; Reineck and Singh, 1973; and Walker, 1979). These lithological attributes may be described by use of various ratio-scale measures and statistics derived from them. They may also usefully be summarized in terms of distinctive assemblages of standard lithofacies types, each defined by a limited range of particle size, specified compositional properties, structural characteristics, or other criteria. A lithofacies classification of this kind, developed by Miall (1977, 1978) for application to braided river deposits, has been adopted for the present study in an amended and expanded form (see section 4.4.1).

### 1.2.3 ESTUARINE SYSTEMS

An estuary or estuarine system may be defined as a set of phenomena caused by or pertaining to the inflow of freshwater runoff to an ocean or marginal sea [this formulation is simpler than the widely cited definition proposed by Cameron and Pritchard (1963)]. As coastal filters through which runoff enters the sea, estuaries form part of a relatively minor link in the global hydrological system, passing only about seven per cent of total precipitation (More, 1967). However, due to the occurrence of cooscillating tides, due to the difference in density between freshwater runoff and seawater, and due to the extraordinary variety of circulation processes which occur as a result of these and other effects, estuaries form remarkably complex hydrological systems. These systems frequently form sediment traps (cf. Meade, 1969) and are of considerable ecological and socioeconomic importance (cf. Officer et al., 1977).

Periodic tidal storage of water is a characteristic feature of estuarine systems. The volume of water stored during a given tide is a function of the tidal range and of certain morphological parameters of the estuary, which determine the potential storage volume and control tidal-current hydraulics. Non-periodic water storage fluctuations occur due to various other effects, including steric adjustments (cf. Pattullo et al., 1955; Beal, 1968), meteorological forcing processes (see, for example, Doodson, 1924; Proudman, 1955; Smith, 1979; Wang, 1979), and changes in

the backwater curve due to fluctuations of river discharge (Volker, 1966). Individual systems differ in the relative importance of the various storage components; indeed, significant seasonal and other fluctuations in the distribution of variance may occur within a given system. Furthermore, the freshwater fraction or volume of runoff water stored in the estuary may be highly variable, depending on the circulation regime and other system parameters. This has important implications with respect to flushing rates and the partition between short- and long-term storage of suspended sediment and other pollutants.

Estuarine systems commonly store large volumes of sediment in a variety of distinctive deposits, including marine-deltaic, intertidal, barrier, lagoon, and marsh facies (cf. Postma, 1967; Hayes, 1975; Frey and Basan, 1978) and in fine-sediment suspensions, which can achieve very high concentrations (Inglis and Allen, 1957; Allersma et al., 1966; Kirby and Parker, 1977) and represent a form of short- or medium-term storage. The depositional product in many deltas is significantly influenced by estuarine effects, including density stratification and tidal motions (cf. Bates, 1953; Scruton, 1960; Coleman et al., 1970; Nelson, 1970; Wright, 1970; Galloway, 1976).

Sediment transport in the estuarine system is powered primarily by water motions and associated energy dissipation (cf. Bagnold, 1966). It is therefore appropriate to treat water and sediment transport and storage as energetically-coupled cascading subsystems. Although sediments

are predominantly conservative, sediment suspensions are not; as a result, sedimentological and hydrological subsystems may respond differently to a given input event. Nevertheless, certain structural similarities can be anticipated. Furthermore, sediment storage phenomena determine in part the morphological parameters of the hydrological subsystem, while sedimentary facies or facies assemblages may be identified with geographically defined subsystems of the hydrological cascade.

The present study is concerned with an Arctic estuarine system, characterized by great seasonal variance of net radiation, extreme temperatures and abundant ice. It is a thesis of the present work that distinctive dynamic and morphological characteristics may be associated with estuaries occurring in such an environment. Relatively few comprehensive studies of Arctic estuaries have preceded this investigation; contributions that deal with various physical aspects of the Arctic estuarine environment include reports by Alexander et al. (1974), Barber (1968), Barnes and Reimnitz (1972), Dygas and Burrell (1976), Ford and Hattersley-Smith (1965), Hume (1971), Ince (1962), Kinney et al. (1972), Knight (1971), Knight and Church (1970), Lake and Walker (1973), Lewellen (1973), Lewis (1977), Mackay (1963a), Matthews (1979, in press), Morison and Taylor (1978), Reimnitz and Bruder (1972), Short (1979), Tucker and Burrell (1977), Walker (1969, 1971, 1972, 1973, 1974), and Wiseman (1979).

An approach to Arctic estuarine systems as a potentially distinctive set involves certain assumptions about the

relevance of global-scale variability to the mechanics of small hydrodynamic systems. Global-scale variables include inertial or Coriolis effects and large-scale energy sources, notably solar radiation and gravitational potential energy. The tidal potential exhibits some latitude-dependence and tides in the Arctic Ocean are generally small in amplitude and predominantly semidiurnal. Coriolis effects are particulary strong at higher latitudes and the inertial period in the southern Beaufort Sea is approximately semidiurnal (Sverdrup, 1926). Finally, the high-latitude radiation regime exhibits a pronounced annual cycle that, directly or indirectly, affects a great variety of processes operating in the estuarine environment. Most distinctive features of high-latitude estuarine systems can be ascribed ultimately to the radiation and temperature regime.

The recognition of a quasi-homogeneous depositional product or lithofacies assemblage implies an assumption of equilibrium in the estuarine sedimentary environment, broadly analogous to concepts of equilibrium in erosional systems (see, e.g., Strahler, 1950; Langbein and Leopold, 1964). Both may be interpreted in terms of the consistent behaviour of a constant-parameter process-response system under a statistically stationary input regime. Changes in the system output and in the pattern of internal storage may occur due to changes of system parameters, which may be due to a threshold effect or may result from non-stationarity of one or more input variables.

Non-stationarity of inputs arises due to changes in other

TABLE 1

Scales of variance in Arctic estuarine systems.

| class | scale | characteristic process | period |
|---|---|---|---|
| micro- | subdiurnal | turbulence gravity waves | $T<10^3$ s |
| micro- | diurnal | tidal and diurnal variance | $10^3<T<10^5$ s<br>$0.01<T<2$ d |
| meso- | synoptic | cyclonic systems | $2<T<100$ d |
| meso- | seasonal | earth orbit | $100<T<366$ d |
| macro- | annual | year-to-year variance of hemispheric circulation | $1<T<10$ a |
| macro- | decadal | short-term climatic variance | $10<T<100$ a |
| mega- | millenial | long-term climatic changes | $T>100$ a |

s seconds
d days
a years

cascade systems that interface with the system under consideration. For example, adjustments of this sort may occur as a result of climatic fluctuations, changes in land-use, tectonic activity, or erosional thresholds. Apart from such discrete changes, it appears that the definition of stationarity for any given input series depends on the time scale considered (Båth, 1974, p.108; cf. Schumm and Lichty, 1965; Mandelbrot and Wallis, 1969). The inputs to an estuarine system may be stationary over intervals of a few minutes, weeks, or years, but highly non-stationary over intervals corresponding to tidal, synoptic, seasonal, or longer-term variance. For the purposes of this work, the time scale of a process is taken to connote the characteristic, dominant, or modal period (inverse frequency) and the terminology presented in Table 1 is employed.

## 1.3 THE PRESENT STUDY

### 1.3.1 BABBAGE ESTUARINE SYSTEM

The estuarine system at the confluence of the Babbage River and Deep Creek, on the central Yukon coast near Kay Point (69°18'N, 138°24'W; see Figure 1), was chosen as the focus of the present investigation. The project was inititiated in 1974 under the auspices of the Geological Survey of Canada, together with a companion study designed to examine aspects of coastal erosion, nearshore sediment transport, and beach dynamics in the vicinity of Kay Point (Lewis, 1975). Early results of the combined investigation were reported by Lewis and Forbes (1974, 1975).

The major features of the Babbage Estuary system are illustrated in Figure 2. The setting can be summarized as low-Arctic, transgressive, and microtidal, with seasonally restricted fetch and a highly variable nival runoff regime. A barrier-spit some 4.4 km in length extends southwestward from Kay Point, partially enclosing an extensive shallow lagoon (Figure 3). Depths in the lagoon average about 1 m relative to mean water level. A long narrow shoal parallel to the barrier transects the main lagoon basin. A small, quasi-permanent tidal inlet occurs toward the distal end of the barrier (M2, Figure 2) and short-lived inlets (denoted M3) develop from time to time near the proximal end. A major inlet, 2 km wide, referred to as the estuary entrance or main entrance section (M1), lies between the distal end of Kay Point spit and Niakolik Point. This inlet is characterized by a broad central

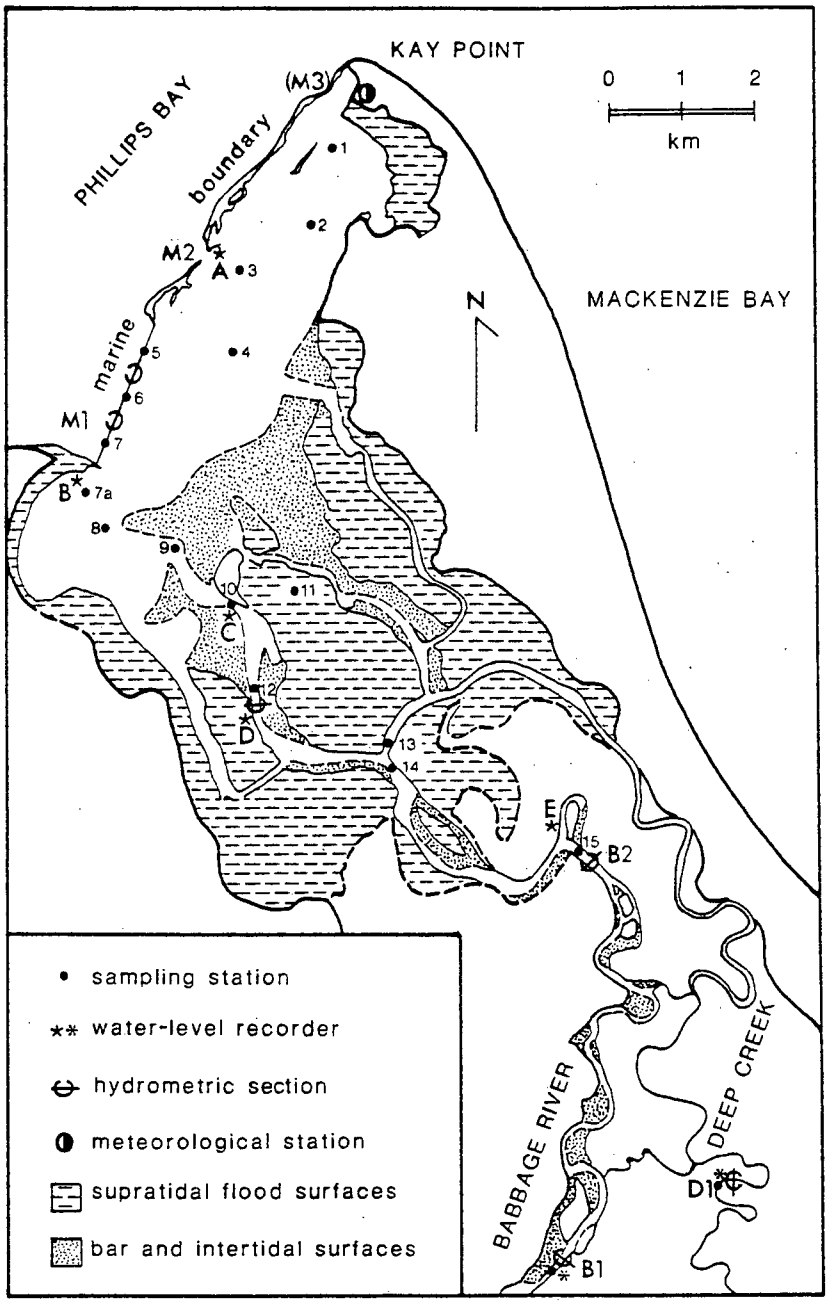


FIGURE 2

Map of the Babbage Estuary system, showing major sampling stations, locations of tide and stage recorders, hydrometric sections, and the location of the meteorological station at Kay Point (see Figure 1 for regional setting).

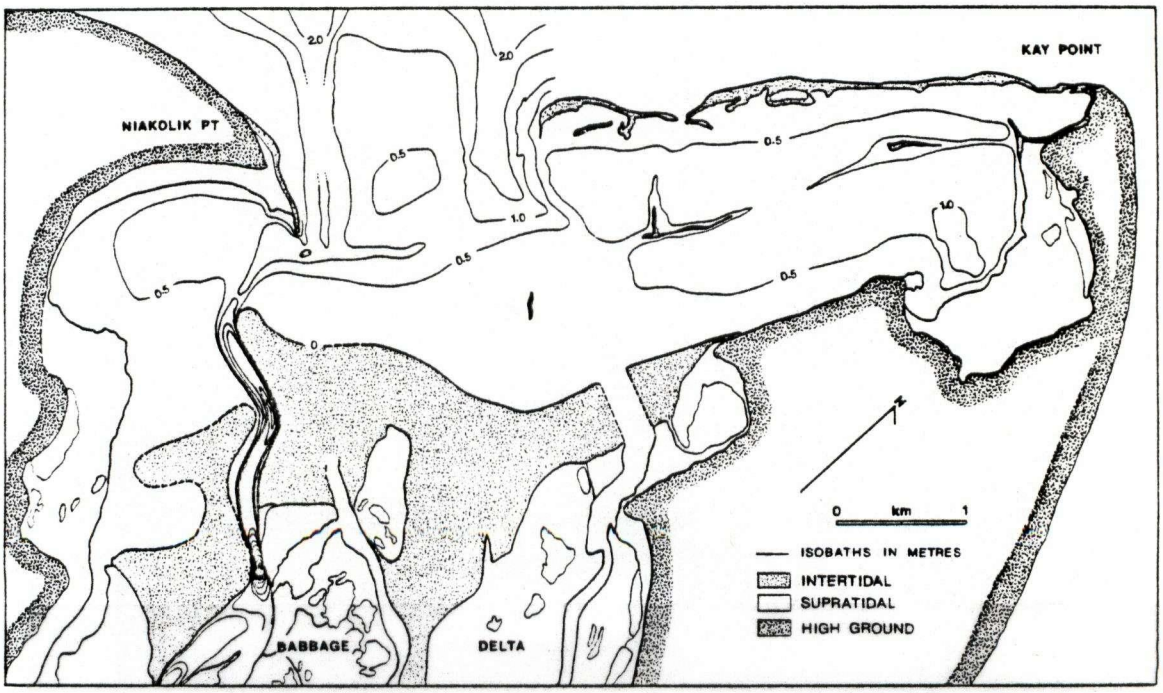


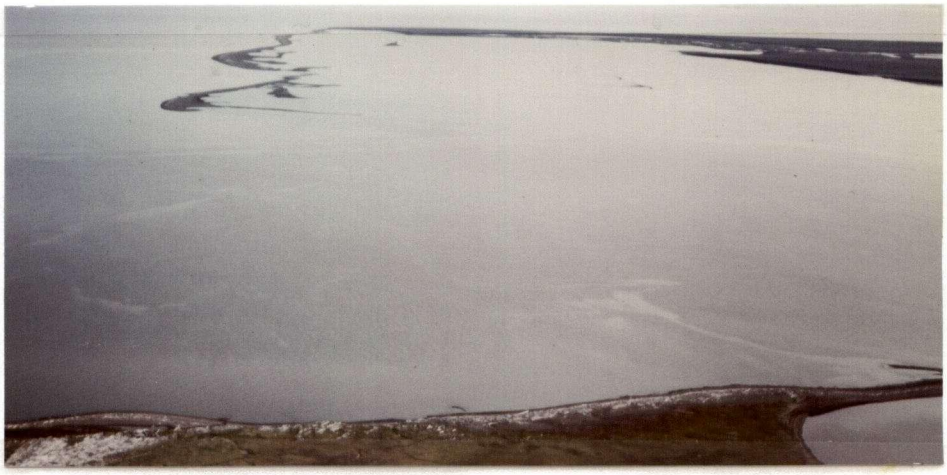

FIGURE 3

Bathymetry of Babbage Estuary in 1975 and view across main entrance section toward Kay Point spit with Babbage Lagoon to right, Kay Point in distance, and Niakolik Point in foreground.

platform and two marginal channels, with maximum depths of about 2 m at mean tide.

Supratidal (storm-flood) surfaces are found at the northeast and southwest ends of the lagoon; supratidal flats of the Babbage Delta extend across the valley opposite the entrance section. Four major distributary channels carry fluvial discharge across the delta to the lagoon. The largest of these, referred to as the main distributary channel, can be identified in Figure 2 by the line of sampling stations. Extensive intertidal surfaces occur on the lagoon margin of the delta plain and locally within the delta (Figure 4A). A large part of the delta plain is occupied by lakes and ponds, some of which are connected by narrow tidal channels to the main distributary channel network (Figure 5). The total subaqueous and subaerial area of the delta and lagoon complex below the limit of recent storm-surge flooding is a little over 40 $km^2$.

Deep Creek, the Babbage River, and two non-tidal distributaries flowing to Deep Creek from the Babbage, form an anastomosing channel system in the lower valley above the delta. The limit of storm-surge backwater extends upstream to the lower of these distributaries (Figure 2). The lower Babbage River is a sinuous gravel-bed stream with a low-Arctic nival discharge regime. The channel is locally divided and is dominated by alternating lateral or point bars, by diagonal bars in some reaches, and by a prominent pool-riffle sequence (Figure 4B).

FIGURE 4

A: intertidal and supratidal surfaces of the Babbage Delta, with main distributary channel in distance, September 1976; lagoon is out of the picture to the right;
B: lower Babbage River, looking downstream toward hydrometric section B1, 2 August 1974.

FIGURE 5

Babbage Delta and southern lagoon, showing coordinate system, intertidal transects (——), sites where sediment accumulation was measured on the delta plain (●) and on ice (◇), and locations of sediment traps (⊘), excluding traps in the northern lagoon; part of NAPL photograph A22975-55, 4 August 1972.

The estuarine system as defined for the present study is laterally bounded by the pre-Holocene upland surface and delimited at the marine end by Kay Point spit and the main entrance section (the 'marine boundary'). At the headward end, the limits of the system are determined by the locations of hydrometric sections (Figure 2) that were established on Deep Creek at D1 and on the Babbage River at B1 (Figure 4B), above the uppermost distributary. Section B1 was located 5 km downstream from the confluence with two major tributaries, the Trail and the Tulugaq (also known as the Crow).[1]

Positions within the estuarine system have been referred to a grid network (Figures 5 and 6), with lines at 500-m intervals. Six-digit coordinates (xxxyyy) identify positions to the nearest 50 m. Standard stations established in the lagoon and delta for regular sampling and in situ observations of water properties and suspended sediment concentrations are shown in Figure 2, which also includes locations of the meteorological station, of hydrometric sections, and of water level recorders. Drillhole sites and other locations for which shallow stratigraphic information is available are indicated in Figure 6. A brief summary of the observation program and procedures is given in Appendix A.2; further details are presented where appropriate within the text and in other appendices (A.3, A.4, A.8, and A.12).

---

[1] 'Tulugaq River' is the official name, but 'Crow River' appears on many maps.

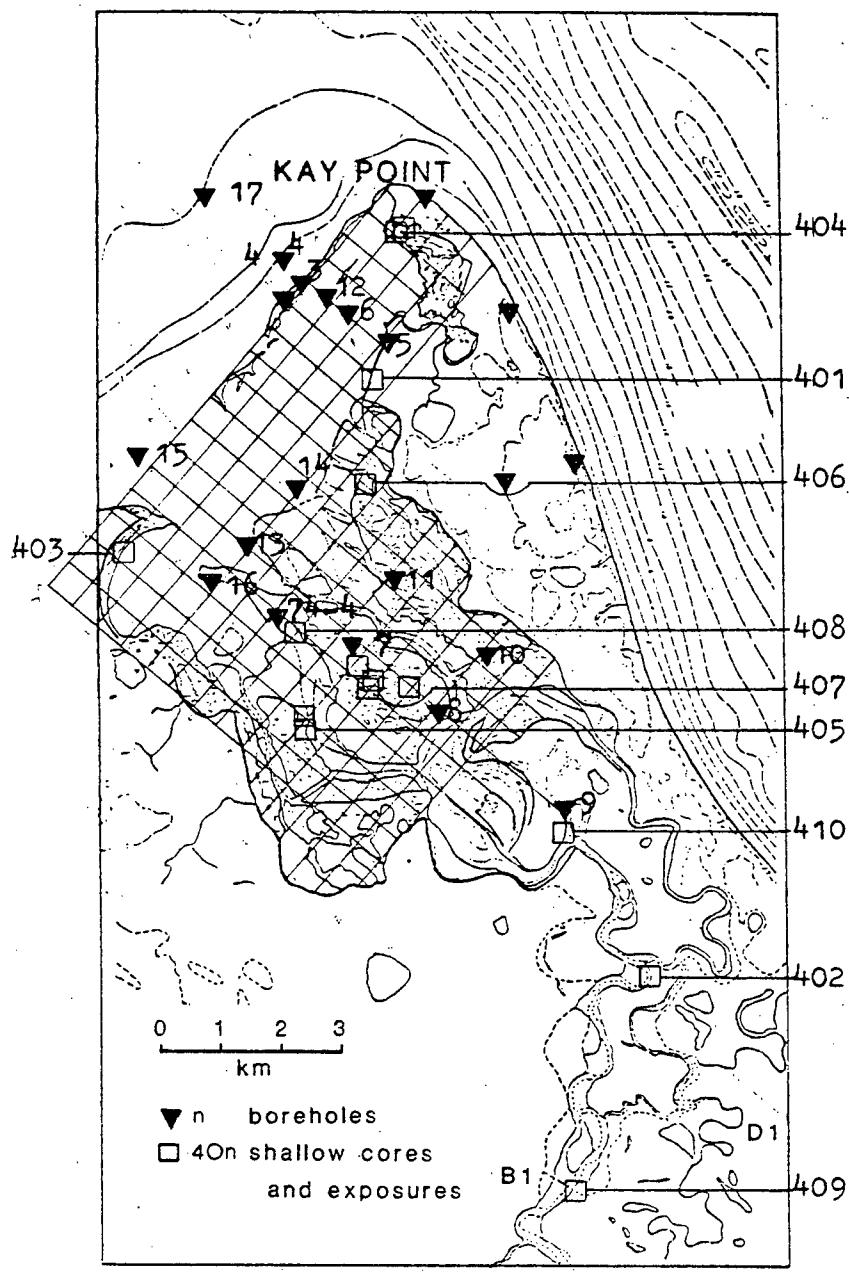


FIGURE 6

Babbage Estuary system, showing grid network and locations of boreholes, short cores, and exposures.

The cascade system of the Babbage Estuary may be subdivided into fluvial, tidal-distributary, delta-plain, intertidal, lagoon, marginal supratidal, and barrier subsystems. The structure of the system may be examined in terms of the varying nature of links between these subsystems. Each subsystem may be viewed as a single depositional environment or, depending upon the scale, may be seen to encompass a number of subenvironments. Thus, the fluvial subsystem includes channel and overbank environments; the tidal channel subsystem includes channel and channel-margin environments and may be extended to include lakes without closure; the delta plain incorporates vegetated high and low supratidal flats, ephemeral ponds, and lakes with closure; the intertidal subsystem can be divided into high and low intertidal surfaces on the basis of exposure frequency or other criteria; the marginal supratidal includes vegetated supratidal flats, lakes with and without closure, ephemeral ponds, and marginal beach and washover environments; the lagoon subsystem can be subdivided into exposed lagoon ('open-estuary'), protected basin ('lagoon'), and lagoon shoal environments; and, finally, the barrier encompasses foreshore, backshore, and back-barrier platform components.

# 2 REGIONAL CONTEXT: NORTHERN YUKON AND BEAUFORT SEA

## 2.1 GEOGRAPHY AND PALAEOGEOGRAPHY

### 2.1.1 CONTEMPORARY GEOGRAPHY

The present configuration of the Yukon coast is illustrated in Figure 1. Previous general investigations include surveys by Franklin (1828), O'Neill (1924), Bostock (1948), Mackay (1960), Hughes (1972), McDonald and Lewis (1973), Lewis and Forbes (1974), and Rampton (1974a, in press). The coast is conterminous with the north Alaska coast in the west, where the subaerial coastal plain is less than 10 km wide near the Backhouse River (Figure 7A); further east, the plain expands to approach 40 km in width near the Babbage River. The coastal plain is flanked on the south by the British, Barn, and Richardson Mountains, parts of the Romanzoff Uplift and Aklavik Arch (Norris, 1973), with elevations up to 1600 m in the northern Yukon (Figures 7 and 8).

The Yukon Coastal Plain is underlain by Jurassic and Cretaceous flysch, molasse, and epicontinental clastic sediments. Palaeozoic clastics and carbonates occur in the Richardson, Barn, and British mountains, including parts of the upper Babbage River basin (Norris et al., 1963). Precambrian metaclastics of the Neruokpuk Formation are exposed in the British Mountains, including parts of the western Babbage (Tulugaq and Trail) basins; crystalline intrusives of Devonian

FIGURE 7

Western part of Yukon Coastal Plain with British Mountains in background; A: Backhouse Lagoon; B: Firth River fan with Nunaluk Lagoon in foreground.

FIGURE 8

A: headwaters of Babbage River with Tertiary pediment and icing, 29 August 1976; B: upper Trail River basin in British Mountains near Mount Sedgewick.

age are found at Mount Sedgewick in the upper Trail River basin (Norris et al., 1963; Pelletier, 1980).

An extensive post-Palaeocene pediment (Hughes, 1972; Rampton, in press) rises from the coastal plain toward and into the mountains (Figure 8A); this surface and underlying beds have a mean slope toward the northwest of about $7.5 \times 10^{-4}$ (Rampton, in press), such that the coastal bluff west of the Malcolm River is generally less than 10 m high (Figure 7A), while in the east near the Blow River it exceeds 30 m in height. The major rivers west of Herschel Island (Malcolm and Firth) are predominantly aggradational on the coastal plain, forming large fans that extend north to the coast (Figure 7B), similar to the extensive fans along the eastern north Alaska coast. Further east, the major rivers (notably Spring, Babbage, Running, and Blow) are incised below the general level of the coastal plain, the depth of incision increasing eastward.

Permafrost is continuous beneath most subaerial surfaces, excepting large lakes, and extends to depths of 600 m or more (J.R. Mackay, personal communication, 1981; cf. Gold and Lachenbruch, 1973, p.10). It occurs also under parts of the Beaufort Sea shelf (Mackay, 1972; Hunter et al., 1978). Widespread massive ground ice, some of which is older than 40000 years (Mackay et al., 1972, p.1322), outcrops in coastal and other exposures, where thaw processes exert a major erosional impact (Figure 9).

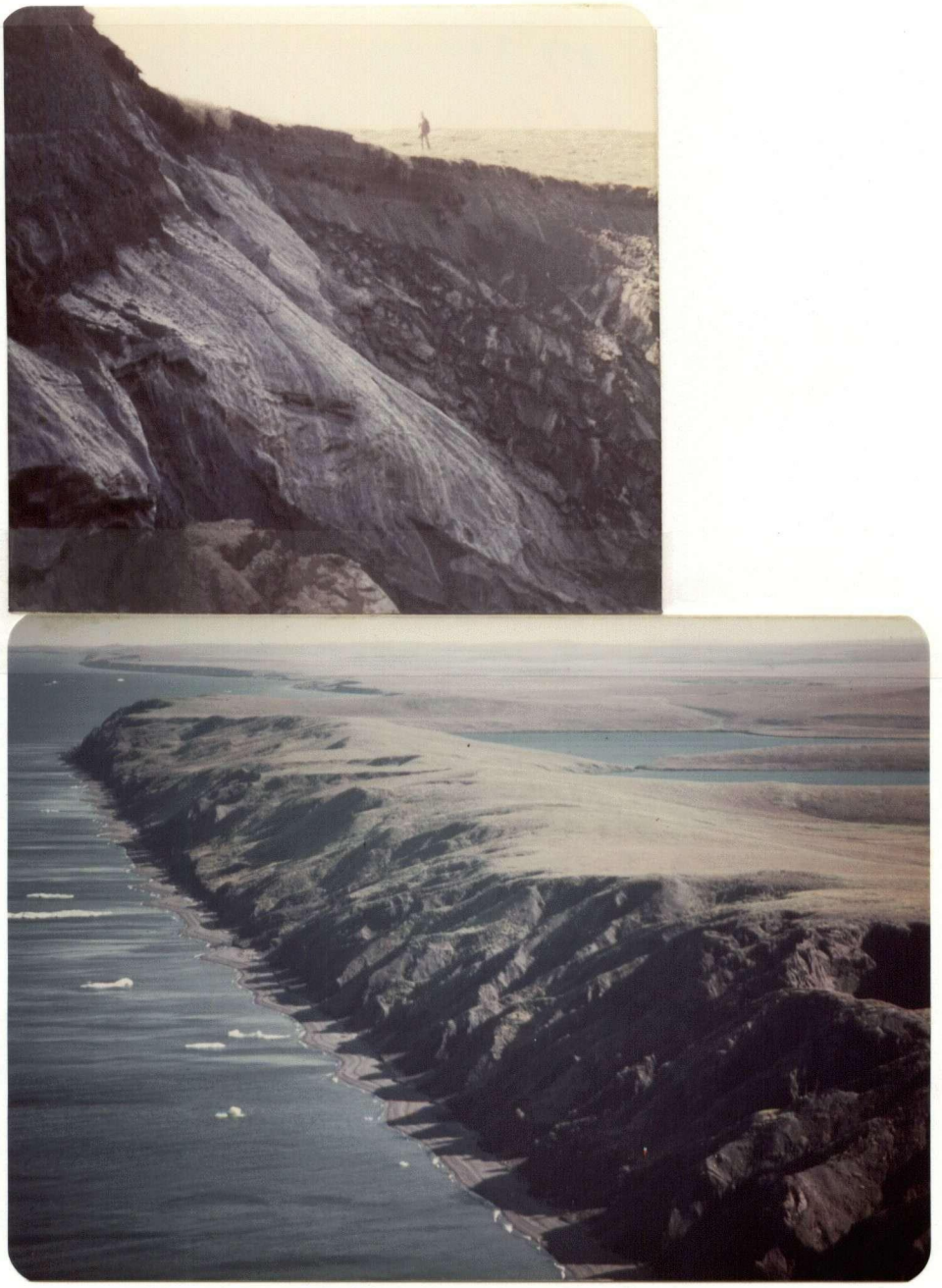

FIGURE 9

Massive ground ice in ice-thrust sediments exposed between Kay Point and King Point, Mackenzie Bay coast; A: August 1977; B: August 1975.

The Yukon Coastal Plain is an area of tundra vegetation, characterized by wet sedge meadows in flat areas and sedge tussock tundra on sites with better drainage (Welsh and Rigby, 1971). Low shrub willow (Salix sp.) and birch (Betula nana and B. glandulosa) are locally abundant, while tall shrub willow (especially Salix alexensis) is a major element of riparian vegetation, particularly on the eastern coastal plain. Spruce (Picea glauca) occurs locally in the lower Firth Valley to within 30 km of the coast (Wein et al., 1974) and in the upper Babbage River basin at Spruce Creek.

The Yukon coast is bounded on the east by the Mackenzie Delta, which occupies a glacially scoured structural depression, developed by late-Cretaceous block faulting (Yorath, 1973). This depression extends seaward to Mackenzie Canyon as a partially infilled box-like trough (Shearer, 1972) trending northwest across the shelf to intersect the continental slope at a depth of about 400 m. East of the canyon, the shelf has a width of about 100 km to the shelf break at a depth of about 70 m; west of the canyon, the shelf is approximately 50 km wide. Depths near the coast are highly variable, being less than 10 m in the east over the subaqueous Mackenzie Delta, increasing to 50 m within 10 km of Kay Point and to 100 m the same distance off Herschel Island. A submarine ridge, with a maximum depth of about 14 m, extends from Kay Point northwest to Herschel Island, separating a deep depression known informally as Herschel Basin from Mackenzie Bay. Herschel Basin shoals toward the southeast and the waters

of Phillips Bay, off the Babbage Estuary, are generally shallow with depths in the range 5-7 m some 3 km offshore.

The total length of the Yukon coast is approximately 250 km. Of this, some 58 per cent takes the form of a coastal cliff developed in frozen unconsolidated Quaternary sediments, fronted by a narrow beach (Figures 7A and 9). The remainder consists of deltaic, barrier-lagoon, and tidal inlet features. The combined length of barrier shoreline is approximately 67 km. Extensive shallow lagoons are present behind the coastal barriers (Figure 10). Morphometric data for Yukon coast barriers and lagoons are given in Table 2.

Twenty lagoons have been catalogued, ranging in area from $6.8 \times 10^4$ to $4.5 \times 10^7$ m$^2$; the Babbage Estuary is among the largest. Individual barrier systems range in length from $\sim$100 m to more than 20 km (including inlets), with inlet/barrier length ratios ranging from zero to more than one. The barriers are typically narrow and low (mean width less than 200 m, mean berm height less than 2 m).

Many of the lagoon systems are strongly influenced by freshwater runoff, particularly during and following the snowmelt season. Values of the ratio $A_L/A_D$, where $A_L$ is lagoon area and $A_D$ the area draining to the lagoon system, provide a rough measure of potential snowmelt runoff impact on the estuarine system, although the hypsometry of the drainage basin may be important and deeper submerged-valley estuaries can be expected to respond in a manner different to that of shallow

FIGURE 10

Barriers and lagoons at Stokes Point (A) and at King Point (B), central Yukon coast; A: August 1976; B: August 1975.

TABLE 2

Morphometry of lagoons and barriers of the Yukon coast.

| map code[a] | name[b] | $A_L$ ($m^2$)[c] | $A_D$ ($m^2$)[d] | $A_L/A_D$ | $L_I$ (m)[e] | $L_B$ (m)[f] | $b^*_L$ (m)[g] | $b_B$ (m)[h] | $H_B$ (m)[i] | tan$\beta_f$[j] | tan$\beta_n$[k] |
|---|---|---|---|---|---|---|---|---|---|---|---|
| 1 | Clarence | $3.2\times10^6$ | $2.9\times10^8$ | 0.01 | 30 | 2750 | 1200 | | | | |
| 2 | Backhouse | $1.9\times10^5$ | $8.6\times10^7$ | 0.00 | ≈20 | ≈200 | 860 | | | | |
| 3 | Malcolm-1 | $2.8\times10^6$ | $1.8\times10^7$ | 0.02 | 0 | 1500 | 190 | | | | |
| 4 | Malcolm-2 | $1.4\times10^7$ | $3.3\times10^9$ | 0.04 | 0 | 5250 | 270 | | | | |
| 5 | Nunaluk | $1.5\times10^7$ | $7.3\times10^7$ | 0.00 | [1370] | 18750 | 750 | 163 | 1.49 | 0.041 | 0.017 |
| 6 | Workboat | $4.5\times10^5$ | $4.4\times10^7$ | 1.0 | [2125] | 6050 | 5500 | | | | |
| 7 | Pauline | $2.6\times10^6$ | $2.7\times10^6$ | 0.10 | 750 | 525 | 200 | | | | |
| 8 | Ptarmigan | $4.1\times10^6$ | $5.2\times10^7$ | 0.08 | [ 0] | 5000 | 820 | | | | |
| 9 | un-named | $9.0\times10^4$ | $1.1\times10^6$ | 0.08 | 0 | 675 | 130 | | | | |
| 10 | Whale | $2.3\times10^6$ | $1.9\times10^7$ | 0.12 | <40 | 1550 | 1500 | | | | |
| 11 | ria-1 | $1.3\times10^5$ | $5.1\times10^6$ | 0.03 | 0 | ≈100 | 1300 | | | | |
| 12 | Roland | $1.8\times10^6$ | $2.7\times10^8$ | 0.01 | <70 | 570 | 2800 | | | | |
| 13 | Stokes-1 | $1.9\times10^6$ | $3.7\times10^6$ | 0.51 | [<300][m] | <3000 | 630 | | | | |
| 14 | Stokes-2 | $6.1\times10^5$ | $1.1\times10^8$ | 0.56 | [ 0] | ≈2000 | 310 | | | | |
| 15 | Spring-Phillips | $1.6\times10^7$ | $8.0\times10^9$ | 0.00 | <400 | 5250 | 280 | | | | |
| 16 | Babbage | $2.8\times10^5$ | $5.0\times10^6$ | 0.01 | 2020 | 4380 | 4400 | 61 | 0.90 | 0.066 | 0.010 |
| 17 | King | $6.3\times10^7$ | $1.6\times10^5$ | 0.39 | 0[n] | 1500 | 420 | | | | |
| 18 | ria-2 | $6.8\times10^4$ | $3.6\times10^5$ | 0.19 | <10 | 120 | 566 | | | | |
| 19 | ria-3 | $6.3\times10^7$ | $4.7\times10^7$ | 0.01 | <20 | 350 | 1800 | | | | |
| 20 | Shingle | $4.0\times10^7$ | $4.7\times10^8$ | 0.09 | 10500 | 7250 | 2300 | 141 | 1.53 | 0.085 | 0.006 |

a: see Figure 1
b: some names informal
c: area of lagoon
d: drainage area (in part after McDonald and Lewis, 1973, table II)
e: total inlet width
f: lagoon width measure $b^*_L = A_L/(L_I+L_B)$
[]: excludes passages between lagoons
h: mean subaerial barrier width
i: mean berm height
j: mean foreshore slope
k: mean nearshore slope
} after Lewis and Forbes, 1974
m: opened between 1970 and 1972
n: closed before 1972; in 1954, geometry was: $L_I$≈300m, $L_B$≈1200m

estuaries such as the Babbage. The ratio $A_L/A_D$ ranges from less than 0.01 to a maximum of 1.02; for the Babbage Estuary, $A_L/A_D=0.01$.

The ratio of lagoon area to barrier-plus-inlet length, $A_L/(L_B+L_I)$, has the dimension of length and may be considered a measure of mean coast-normal lagoon width. By this measure, the Babbage Estuary, Workboat Passage (between Herschel Island and the mainland shore), Roland Bay, the embayment behind Shingle Point spit, and the large submerged valley east of King Point ('ria 3') stand apart from the other systems. Roland Bay, ria-3, and the Babbage Estuary are all valley systems submerged during the late-Holocene transgression, as are the Backhouse Lagoon, the southern portion of the Spring-Phillips system, and the other unnamed lagoons identified as rias in Table 2. The Spring River valley was undoubtedly flooded also, but has since been filled with sediment. Other lagoons, such as those at King Point and Whale Bay, appear to have developed in former lake basins breached by coastal erosion.

McDonald and Lewis (1973) have presented morphometric data for thirteen drainage basins that empty into the Beaufort Sea along the Yukon coast. These include the Firth, with a drainage area of 6200 km², the Babbage with 5000 km², the Blow with 3700 km², and the Malcolm with 1100 km². Hypsometric curves for the Babbage and for Deep Creek, the two rivers of primary interest in the present context, are given in Figure 11. There is a marked contrast between the two basins, Deep Creek being largely confined to the coastal plain, while

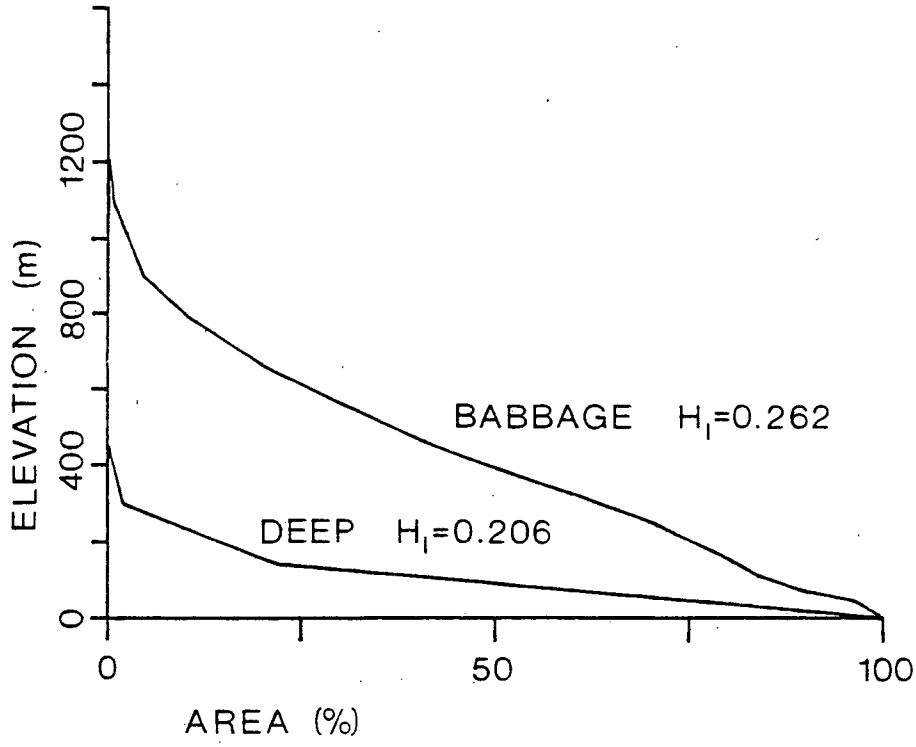


FIGURE 11

Hypsometric curves for Babbage River and Deep Creek drainage basins (modified after McDonald and Lewis, 1973, figure 6).

the Babbage and tributaries drain parts of the Barn and British Mountains. As a result, runoff response from the two basins, particularly snowmelt runoff, may be expected to differ significantly (McDonald and Lewis, 1973, p.22; cf. section 3.1.1 below).

Accumulations of deltaic sediment at the coast vary considerably in size and morphology. The fan deltas of the Malcolm and Firth and in eastern Clarence Lagoon are dominated by braided channel networks; at other locations, the deltas are characterized by low supratidal floodplains with numerous lakes and tidal distributary channels. The largest deltas of the latter type are the Blow and the Babbage (McCloy, 1970, 1971; McDonald and Lewis, 1973; Lewis and Forbes, 1974).

Major changes in the physical environment of the Yukon coast region have occurred during late Quaternary time; indeed, rapid coastal erosion has produced substantial changes in the coastal configuration during the past century and a half, since the reconnaissance by Franklin (1828). The existing geomorphology, long-term trends in the behaviour of the estuarine systems, and the nature of sediment storage, can only be understood in the context of these changes, which are the subject of the following section.

## 2.1.2 LATE-QUATERNARY PALAEOGEOGRAPHY

Rapid erosional transgression is occurring along much of the Yukon coast at present. Photogrammetric work carried out by G. Mizerovsky (McDonald and Lewis, 1973) has revealed that as much as 88 m of coastal recession occurred at Kay Point during the interval 1952-1970. Mackay (1963b) discussed historical and geomorphological evidence for long-term coastal recession, including the virtual disappearance of a major promontory at Sabine Point since 1905, substantial changes during the same interval at King Point (Figure 10B) amounting to several metres of recession per year at the western end of the lagoon, and remarkably rapid coastal retreat at Kay Point since Franklin's survey in 1826. Kay Point is the most rapidly retreating part of the coast at the present time (McDonald and Lewis, 1973). An interpretation of Franklin's map, taking into account the present bathymetry and his observation of latitude (69°18'45"N) in the vicinity of the 1826 spit (Franklin, 1828, appendix V), suggests the tentative 1826 shoreline plotted in Figure 12. This interpretation yields an extraordinary mean recession rate for the Kay Point promontory in excess of 40 m $a^{-1}$. It indicates that the planform and dynamic environment of the Babbage Estuary may have been radically different as recently as 150 years ago.

Continental ice of early- or pre-Wisconsin age flowed west along the Yukon coast as far as the present Firth River outlet, west of Herschel Island (Hughes, 1972). This advance has been termed the Buckland Glaciation by Rampton (in press). It

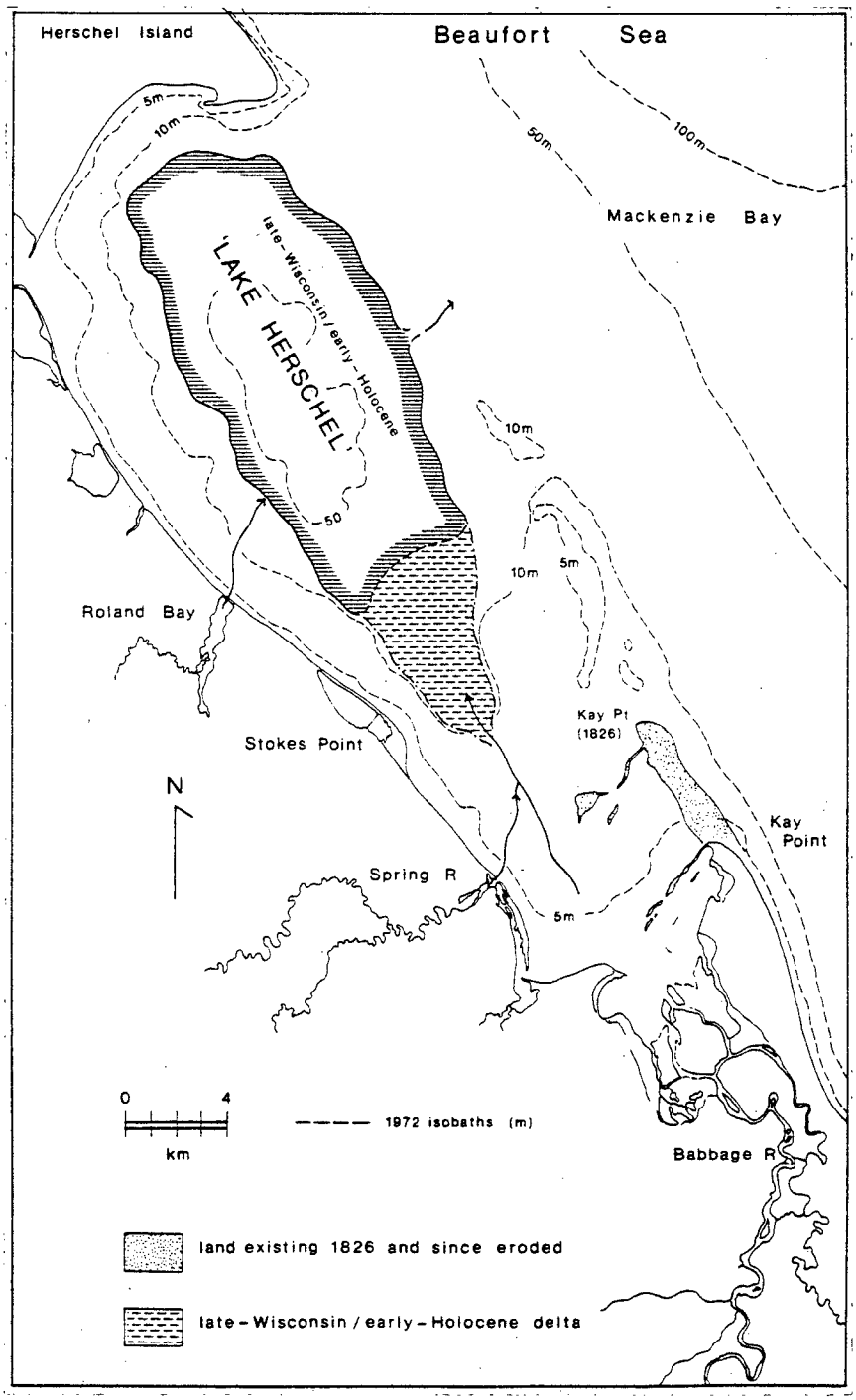


FIGURE 12

Tentative late-Wisconsinan and 1826 palaeogeography between Kay Point and Herschel Island (in part after Franklin, 1826).

caused widespread deformation of pre-existing frozen sediments and associated ground ice (Mackay, 1959; Mackay et al., 1972) and may have created Herschel Basin, emplacing much of the material now forming Herschel Island (Mackay, 1959). A prominent moraine ridge parallel to the Yukon coast, previously considered a possible late-Wisconsinan ice limit (cf. Hughes, 1972; Mackay et al., 1972), is now considered to represent the southern margin of a major stillstand or readvance, termed the Sabine phase, of the Buckland Glaciation (Rampton, in press). The major valley now occupied by Deep Creek and the Babbage Delta, parallel to the Yukon coast and aligned with the major axis of Herschel Basin, may be attributable in part to glacial scour and in part to late-Buckland proglacial runoff (cf. Mackay, 1959).

Ice of the late-Wisconsinan glaciation advanced seaward through the Mackenzie Delta to a limit in the vicinity of the distal delta (J.R. Mackay, personal communication, 1979; Rampton, in press). This limit is based on the intersection of the upper ice surface with present sea level (Rampton, in press, figure 18). Late-Wisconsinan ice is believed to have attained its maximum extent in the region between 13500 and 14000 radiocarbon years B.P. (Prest, 1969). The Yukon coast was not directly affected by glaciation at that time.

Evidence for post-Buckland marine transgression to levels higher than present sea level in the northern Yukon and Mackenzie Delta region is fragmentary and inconclusive (see Forbes, 1980, pp.76-77). During the late-Wisconsinan

glaciation, on the other hand, sea level appears to have dropped to a minimum some 60-80 m below the present level (Forbes, 1980), leading to creation of a lake (here designated Lake Herschel) at about -15±1 m elevation in Herschel Basin (Figure 12). The Babbage River may have drained to Lake Herschel for 15000 years or more. An extensive terrace at the southeast end of the Lake Herschel basin (Figures 12 and 13) is interpreted as a delta formed by sediments from the Babbage River and tributaries, including Spring River.

Available data and associated ambiguities relating to postglacial sea levels in the southern Beaufort Sea have been discussed in detail by Forbes (1980). Information relevant to the Holocene transgression is extremely fragmentary. It appears that limited isostatic depression beneath late-Wisconsinan ice may have occurred in the Mackenzie Delta area and to the southeast, while a marginal forebulge may have existed to the north and west. There is some evidence, also, of recent and perhaps continuing regional submergence. Despite ambiguities at individual sites, data available from the Yukon coast (Appendix A.13), from the outer Mackenzie Delta (Mackay, 1963a, pp.88-94; Mackay and Stager, 1966), and from the Alaska coast (Faas, 1966; E. Reimnitz, personal communication, 1978), provide strong collective support for rising sea level throughout the mid- to late Holocene, in excess of the trend attributable to global variation in glacial volume during the past few thousand years (cf. Walcott, 1975). The data therefore point to a hypothesis of broad regional submergence

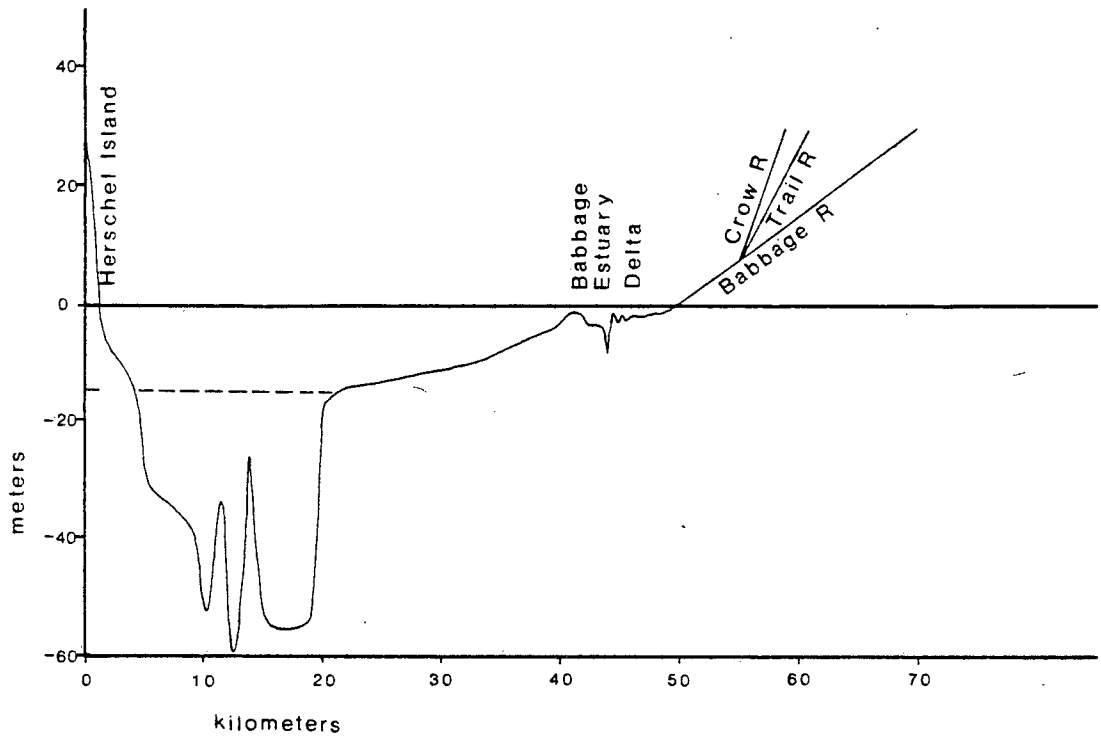


FIGURE 13

Profile along axis of Babbage Valley and Herschel Basin, showing hypothesized late-Wisconsinan water level in Lake Herschel (broken line) and present valley-axis slopes of Babbage River and tributaries.

on the Yukon coast during the Holocene.

The tentative sea level history illustrated in Figure 14 should be regarded for the time being as an educated guess at best. It conforms in general outline to a plausible sequence involving some isostatic rebound in the Mackenzie Delta following deglaciation, followed by subsidence as a marginal forebulge moved through the area, accompanied by rapid sedimentation (Forbes, 1980). On this basis, the beginning of the Holocene marine transgression in Herschel Basin and the Babbage River valley may be assigned a tentative date of about 6000 years B.P. Dates from the Babbage Delta and Herschel Island (Appendix A.13) suggest that sea level in this area may have been as much as 1 m below present datum as recently as 1000 years ago; the data are somewhat ambiguous, due to the possibility of thaw subsidence at the sites.

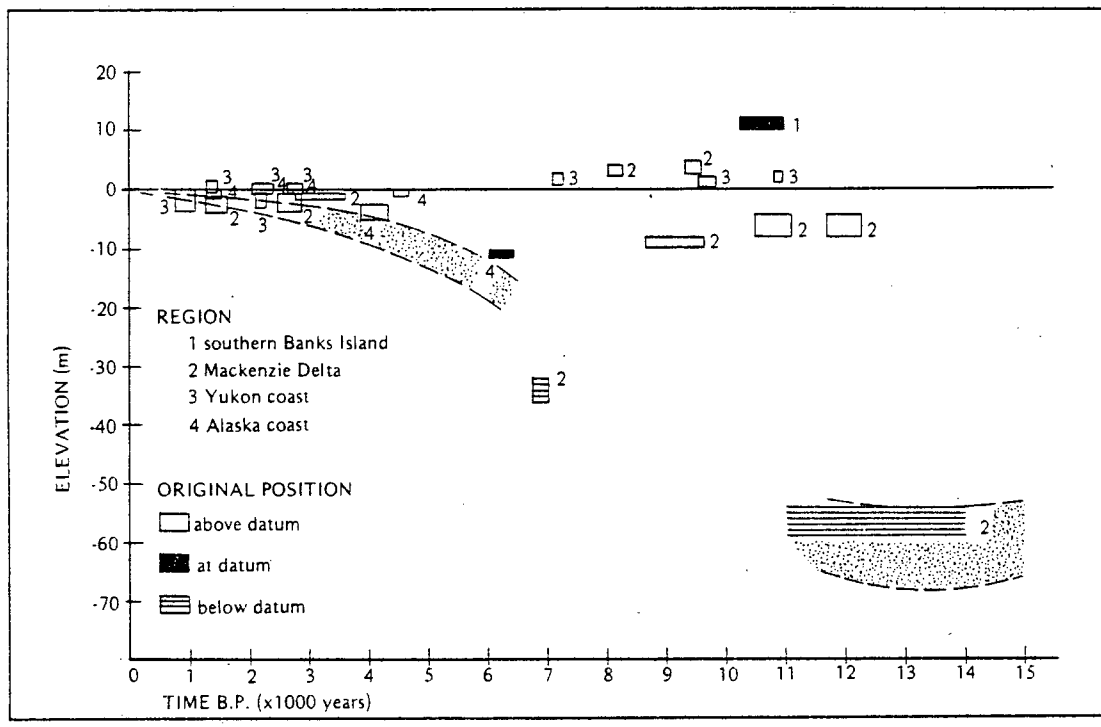


FIGURE 14

Data base and tentative history of late Wisconsinan and Holocene sea levels in Mackenzie Delta and on the Yukon coast (after Forbes, 1980).

## 2.2 ATMOSPHERIC ENVIRONMENT

### 2.2.1 CONTEMPORARY CLIMATE

The present regional climate of the northern Yukon and southern Beaufort Sea is strongly seasonal, with severe winters and cool summers, marked by a pronounced mesoscale temperature gradient normal to the coast. The monthly mean air temperature at Shingle Point (68°57'N, 137°13'W) ranges from a maximum of 10.7°C in July to a minimum of -27.7°C in February (Figure 15). The temperature regime at Komakuk Beach, some 75 km to the west of Kay Point, is similar, with somewhat cooler temperatures in July, due in part to the persistence of sea ice close to the coast west of Herschel Island. The mean annual screen temperature is -10.4°C at Shingle Point (1959-1973) and -11.6°C at Komakuk Beach (R.E. Wahl, A.E.S. Yukon Weather Office, personal communication, 1978); this compares with a contemporary mean annual near-surface ground temperature on the Yukon Coastal Plain of approximately -8.5±1.5°C (Mackay, 1975b, pp.173-174). Equilibrium ground temperature varies locally with varying snow conditions (Judge, 1973; Mackay and MacKay, 1974), with proximity to major water bodies, and of course with depth. Mean annual precipitation totals are low throughout the region, amounting to 188 mm (of which 76 mm falls as snow) at Shingle Point, 127 mm (51 mm as snow) at Komakuk Beach, and 206 mm (97 mm as snow) at Old Crow, south of the mountains.

In winter, the region is dominated by a dome of relatively cold and stable continental Arctic (cA) air, which diverts most frontal lows around its periphery (Burns, 1973, pp.18-19).

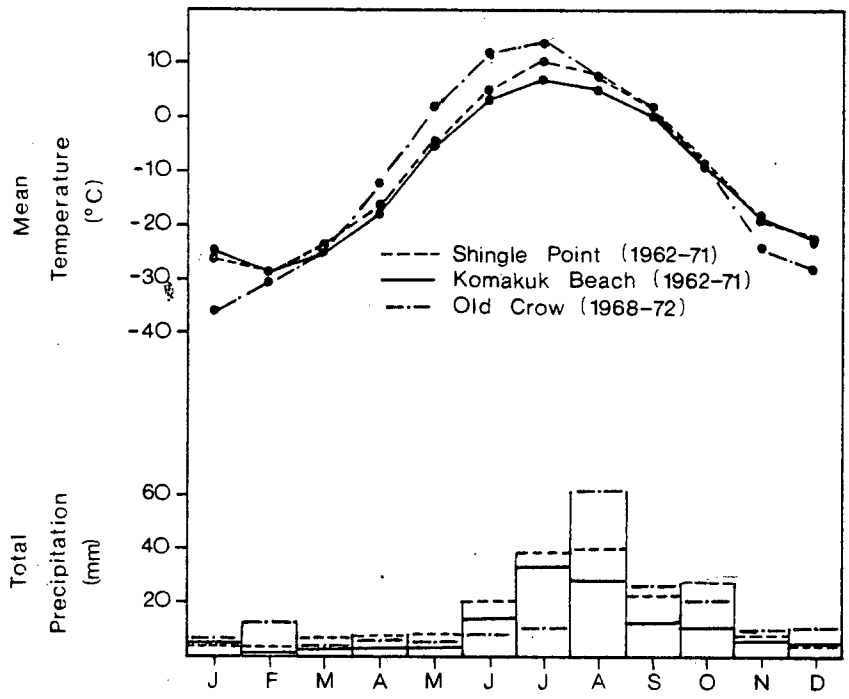


FIGURE 15

Monthly temperature and precipitation data for Komakuk Beach and Shingle Point, on the Yukon coast, and for Old Crow, south of the mountains (data courtesy Atmospheric Environment Service).

Anomalous warming trends associated with occasional penetration of low-pressure centres into the region may produce temperature excursions as great as +30K (Wiseman and Short, 1976, p.236); in some cases, these events culminate in positive air temperatures along the Yukon coast and may generate winter storm surges.

The transition from winter to summer, of particular importance because of the major role of snowmelt runoff in the sediment transport process, is marked by rapidly increasing radiation inputs, changes in albedo due to snow ablation, northward retreat of cA air, and more frequent cyclonic activity (Burns, 1973, p.16). In summer, the Yukon coast is dominated by cool and moist maritime Arctic (mA) air, while relatively warm and dry Pacific air penetrates to the coast, on average, about 20 per cent of the time in July (Bryson, 1966). The modal July position of the Arctic/Pacific frontal zone lies across the northern Yukon (Reed and Kunkel, 1960; Bryson, 1966). Low pressure systems passing eastward through the region along the Arctic front generate much of the summer precipitation (Hare, 1969, p.188; Burns, 1973, p.19). Cyclonic activity is at a maximum in July and August, which are the wettest months of the year (Burns, 1973, p.18; Figure 15). Precipitation also arises from instability of mA air moving across the warmer coastal plain and adjacent mountains, where it is heated from below. Extensive low cloudiness and fog are common during the summer months, when coastal waters are largely ice-free.

Precipitation was measured at Kay Point during parts of the 1974-1976 summer seasons, in support of the hydrological investigations described below. Summary statistics are presented in Table 3. Note the striking differences between years, particularly the high July precipitation in 1974 and the large number of trace events in 1975. The greater part of July 1975 precipitation occurred near the end of the month; the total for the 30-day interval 16 June to 15 July amounted to only 2.03 mm plus nine trace events (this resulted in extremely low runoff rates in the Babbage River in late July: $Q<0.2$ mm/day; see section 3.1.1).

Given the size and hypsometry of the Babbage River basin (Figure 11), it is improbable that precipitation at the coast is representative of the mean basin precipitation. There are no stations in the mountains of the northern Yukon Territory, but data for a single summer season (1974) are available from a camp at Sam Lake (68°25'N, 138°37'W; Pearson and Nagy, 1976). These data (furnished by R.E. Wahl, personal communication, 1978) provide some indication of the spatial variability of near-surface conditions during an unusually cool and wet season. Precipitation data were also collected at Herschel Island in 1974 (Canada, Atmospheric Environment Service, Monthly Record) and an unusually complete picture of geographic variability is therefore available for that season. Cumulative precipitation series, beginning with the first date of observations at Kay Point, have been computed for Komakuk Beach, Herschel Island, Kay Point, and Shingle Point, to yield

TABLE 3

Monthly precipitation data, Kay Point.

| month/year | proportion of record missing | observed precipitation | number of trace events | estimated total precipitation | total snow water |
|---|---|---|---|---|---|
| | % | mm | | mm | mm |
| July 1974 | 32 | (17.74) | 3 | >18.1 | 0 |
| Aug 1974 | 32 | (22.34) | 3 | >22.7 | 0 |
| June 1975 | 40 | ( 2.03) | 4 | > 2.5 | >0 |
| July 1975 | 0 | 7.07 | 14 | 8.8 | 0 |
| Aug 1975 | 0 | 25.47 | 17 | 27.6 | ≈1 |
| June 1976 | 0 | 29.76 | 6 | 30.5 | T |
| July 1976 | 0 | 8.74 | 1 | 8.9 | 4 |
| Aug 1976 | 0 | 24.10 | 3 | 24.5 | 0 |
| Sept 1976 | 67 | ( 3.00) | 1 | > 3.1 | >0 |

an east-west transect along the coast, and for Sam Lake and Old Crow, to yield a north-south transect across the mountains; the series are plotted in Figure 16. In 1974, the precipitation totals were very much higher on the south flank of the mountains than along the coast. Apart from the Herschel Island data, precipitation totals appear to have been relatively consistent along the coast, being somewhat higher in the east at Shingle Point; this pattern held for 1975 and 1976 also. It appears that Shingle Point data may provide the best available estimates of precipitation in the Deep Creek basin but are a relatively unreliable guide to conditions in the upper Babbage River.

Much of the important synoptic-scale variance in estuarine systems of the Yukon coast is associated with cyclonic activity in July and August. The variance density spectrum of hourly pressure at Kay Point during summer 1976 is presented in Figure 17. The spectrum is essentially monotonic, with variance density varying as $f^{-5}$, approximately, in the range $0.5<T<2.5$ days. The poorly defined structure at T=1 day may reflect the development of a weak land-sea breeze pattern in summer. The greatest part of the variance clearly resides at lower frequencies.

Hourly mean wind velocities were recorded at Kay Point during the 1974-1976 field seasons. The measurements were obtained approximately 16 m above sea level, 10 m above the tundra surface. Frequency distributions for the summer seasons (mid-July to early September) of 1975 and 1976 are shown in

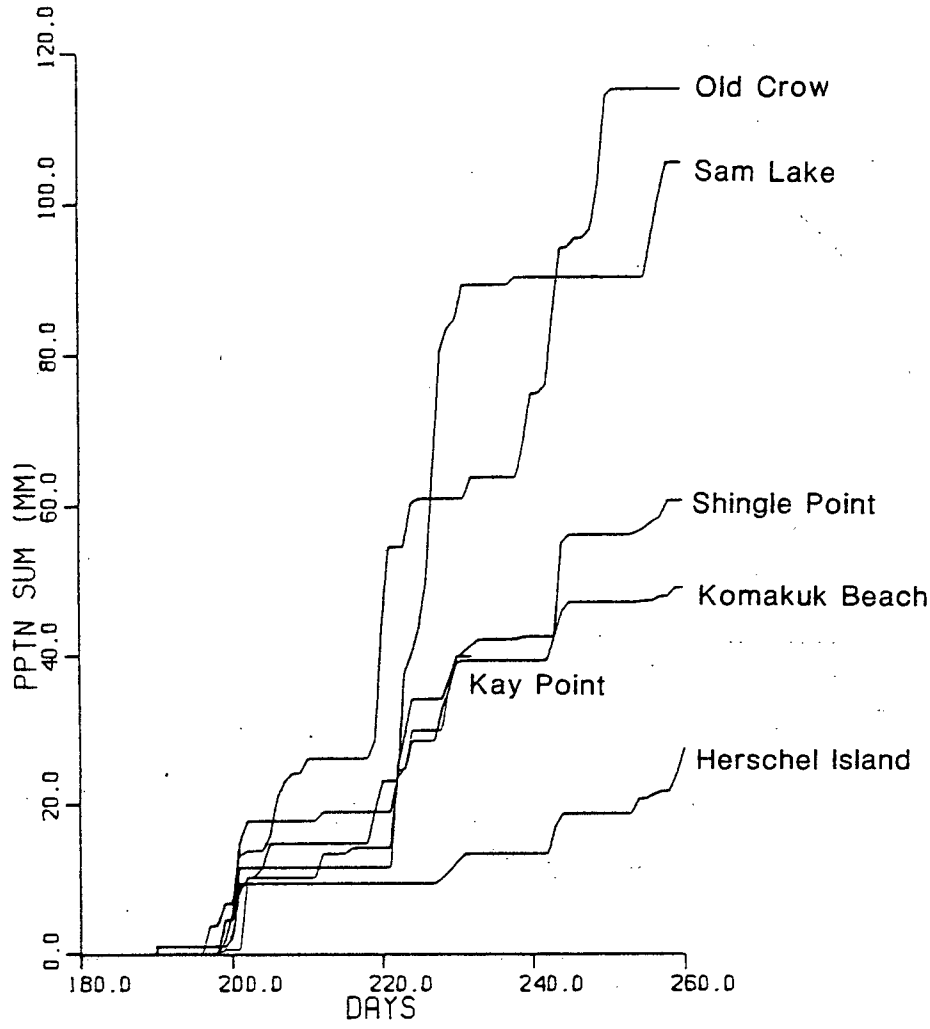


FIGURE 16

Cumulative precipitation at stations in the northern Yukon Territory, summer 1974.

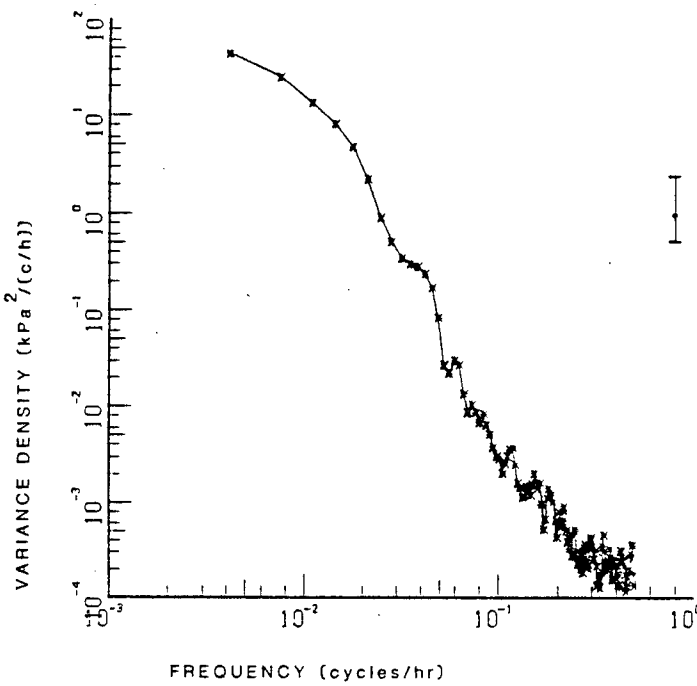


FIGURE 17

Variance density spectrum of hourly atmospheric pressure at Kay Point, summer 1976; the 90% confidence interval, assuming a chi-square distribution with 10 degrees of freedom, is given at upper right.

1975

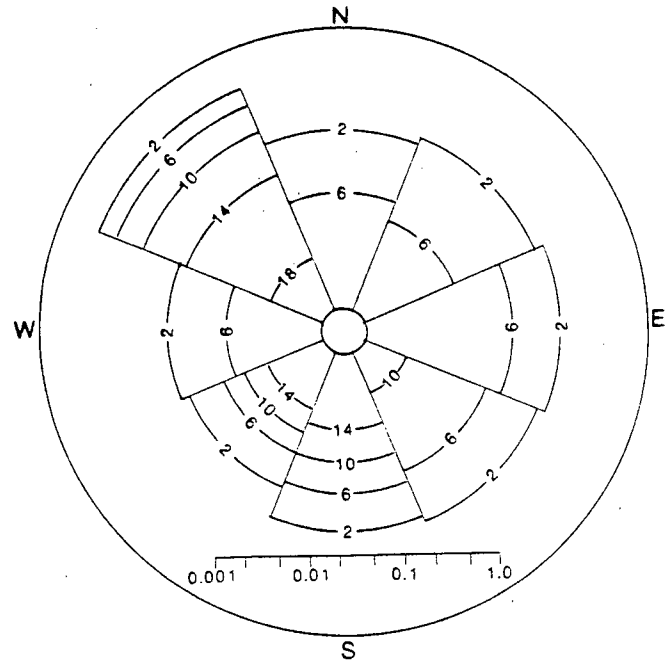


1976

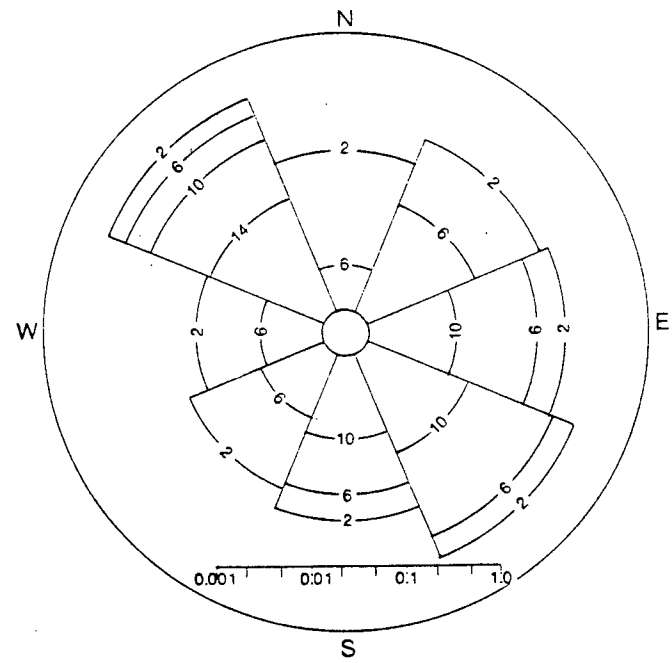


FIGURE 18

Relative frequencies of hourly wind speed (m/s) by direction, 1975 and 1976 summer records, Kay Point.

Figure 18. The Kay Point data indicate prevailing and dominant winds from the northwest in these two seasons, with a strong secondary maximum out of the southeast in 1976. Winds at the coast may differ significantly from winds offshore; Burns (1973, p.176) has pointed out that winds over the water may be two to four times greater than at nearby coastal stations, particularly in the presence of a surface cold front or of a trough of warm air aloft.

Variance density spectra of northeasterly and northwesterly components of wind stress at Kay Point (Figure 19) show maxima at approximately T=5 days, while the northeasterly component exhibits a peak at T=1 day, ascribed to a land-sea breeze effect. However, the particular frequencies or periods corresponding to variance density peaks in the synoptic range are of less concern here than the relative distribution of variance among macroscale, mesoscale, and microscale processes. In an analysis of the estuarine system, the partition between mesoscale (synoptic- and seasonal-scale) events and events associated with diurnal or shorter periods (especially tidal effects) is of major interest. Synoptic-scale processes, in particular, may assume considerable importance in microtidal settings such as the southern Beaufort Sea.

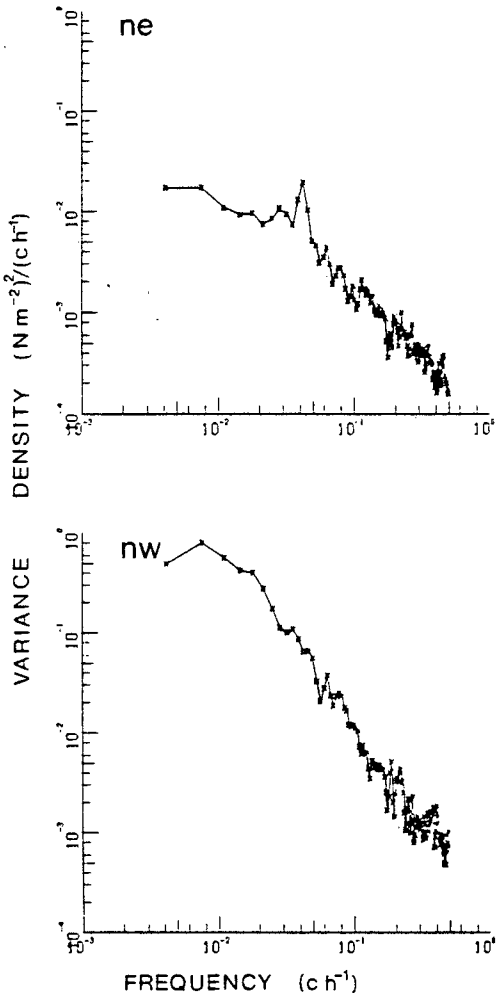


FIGURE 19

Variance density spectra for northeasterly and northwesterly components of hourly wind stress, Kay Point, 1976.

### 2.2.2 LOW-FREQUENCY VARIABILITY OF CLIMATE

When a natural hydrological or sedimentological system is observed over a period of a few years only, hypotheses and conclusions may be seriously biased by the presence of undetected trends in input variables (see below) or even in the parameters of the system, as exemplified by the trends of sea level and coastal retreat described above (section 2.1.2). Furthermore, while significant differences may be detected between years, the nature and magnitude of the low-frequency variance may not be readily determined. For these reasons, the year-to-year and longer-term variability of the ocean-atmosphere system, as they affect conditions on the central Yukon coast, are of great relevance to the present study.

Walsh and Johnson (1979) have identified year-to-year variations of Arctic ice extent exceeding five degrees of latitude at most longitudes and a significant positive trend of total ice cover over the past few years. Markham (1975, pp.35-45) presented a classification of summer ice conditions in the southern Beaufort Sea and related these to a simple model of ice circulation driven by the early winter surface pressure over the Arctic Ocean (cf. Ackley and Hibler, 1977). Other models have been investigated, including correlations with mean summer temperatures at coastal stations and with long-term periodicities in temperature (Rogers, 1978). Classifications such as that of Markham (1975) have led to the interpretation that a four- or five-year periodicity is

characteristic of ice conditions off the Beaufort Sea coast (e.g. McLeod and Hodder, 1978).

Analysis of summer temperatures at Point Barrow (Rogers, 1978) shows statistically non-significant variance peaks in the band $4<T<5$ years. Furthermore, Roger's results suggest the possibility of a marked non-stationarity of variance in the temperature process over the interval 1921-1974.

Changes in mean temperature have been observed in many parts of the Northern Hemisphere during the present century (cf. Mitchell, 1961; Bryson, 1974). Evidence for a rising trend of temperature prior to 1950 in the western Arctic comes from analyses of ground temperature profiles (e.g. Lachenbruch and Brewer, 1961; Garland and Lennox, 1962; Judge, 1973), from ring-width series in white spruce in the southern Brooks Range of Alaska (Garfinkel and Brubaker, 1980), from timberline advance in the Brooks Range (Griggs, 1937, p.253), from the development of thaw lakes in the Yukon and western Northwest Territories (Mackay, 1975b, p.174; M.W. Smith, personal communication, 1980), and from instrumental records.

Burns (1973, pp.80-81, 139-140) has summarized observed trends of temperature and precipitation in the Mackenzie Valley during the present century. At Fort McPherson (67°26'N, 134°57'W), the most northerly station for which records extending back into the 1890s are available, July temperatures have shown no significant trends; January temperatures, on the other hand, have undergone a distinct pattern of fluctuation.

Estimates of associated changes in mean annual ground temperature suggest an increase of 3-4K on the North Slope and in the lower Mackenzie Valley (Lachenbruch and Brewer, 1961; Lachenbruch and Marshall, 1969; Mackay, 1975b, p.173), followed by a decrease of order 1K since c.1950 (Mackay, 1975b, p.175).

Mackay (1976) has documented the widespread occurrence along the southern Beaufort Sea coast of secondary or tertiary ice wedges attesting to recent upward aggradation of permafrost. In alluvial environments, where permafrost is aggrading due to net sedimentation, climatic trends such as the post-1950 cooling process can increase the rate of aggradational ice segregation.

The relevance of the heat and water budgets of the Arctic Ocean to any discussion of climatic trends in the western Canadian Arctic deserves particular mention. Treshnikov et al. (1968) have argued that, because the net annual advective transport of heat by Atlantic water into the Arctic Ocean exceeds the radiation balance, fluctuations of Atlantic water transport must affect atmospheric conditions throughout the Arctic. The annual inflow of Atlantic water is reported to vary between $6.5 \times 10^{13}$ and $1.5 \times 10^{14}$ $m^3$ or more (Treshnikov, 1977; Aagaard and Coachman, 1977); appears to fluctuate with periods between two and seven years or longer (Treshnikov and Baranov, 1977); and declined during the late 1960s and early 1970s (Treshnikov, 1977, p.27; cf. Walsh and Johnson, 1979).

Data currently available are insufficient for an

examination of temperature trends or low-frequency variability in the Beaufort Sea. Shpaikher et al. (1968) presented an analysis of temperature data for the Chukchi Sea for the years 1941-1966, indicating a maximum in the early 1960s, following a pronounced minimum in 1957. Substantial fluctuations may occur, not only in the annual heat input with Atlantic water transport, but in the net advection of heat through Bering Strait and in the upward loss to the atmosphere. Shpaikher et al. (1968, p.21) have indicated a range of net transfers through Bering Strait between $-6.7 \times 10^{19}$ J $a^{-1}$ and $+1.5 \times 10^{20}$ J $a^{-1}$. Ackley and Hibler (1977, p.237) have suggested that large fluctuations of heat loss to the atmosphere may occur on a year-to-year basis in the central Beaufort Sea, due to large ice divergence events associated with the occurrence of atmospheric high pressure systems in the region.

While the 1920-1950 period may have been the warmest interval of the past 1000 years in many parts of the Northern Hemisphere (Bryson, 1974), the northward expansion of Boreal Forest on the Tuktoyaktuk Peninsula in the interval 8500-4000 years B.P. (Ritchie and Hare, 1971; Ritchie, 1972) and related changes in faunal distributions, including northward migration of beaver, have been taken to indicate summer temperatures warmer than present during the Hypsithermal Interval. The evidence for a warm interval includes also a widespread thaw unconformity, dated c.10000-5500 years B.P., occurring 1 to 5 m below the present ground surface at the top of Pleistocene

permafrost (Mackay, 1975a, 1978). However, the effect of coastal transgression in association with a marked coast-normal temperature gradient should also be considered in the interpretation of the palaeobotanical results (J.R. Mackay, personal communication, 1981). It is apparent, from evidence of relict ice-thrust permafrost beyond the limits of the late-Wisconsinan glaciation, that the mean annual ground temperature cannot have exceeded 0°C for more than a few years at most during the past 40000 radiocarbon years (Mackay et al., 1972; Mackay, 1978). Nevertheless, some amelioration of the climate did apparently occur on the Yukon Coastal Plain, beginning c.10000 radiocarbon years B.P. Rampton (in press) has discussed the evidence for such a warming trend, including extensive activation of retrogressive-thaw processes.

Without data on changes in precipitation that may have accompanied the Hypsithermal anomaly in the northern Yukon, it is difficult to assess the probable nature of the fluvial response. Increased rates of sediment production due to more active thaw processes would not necessarily generate higher sediment inputs to the estuary if precipitation were reduced. On the other hand, if precipitation remained constant or increased, the total sediment yield from the basin may have been greater.

In the coastal zone, the major inferred impacts of a Holocene warm interval are an increase in the length of the open-water season, a concomitant increase in the rate of coastal erosion and littoral sediment transport, and

accelerated thermal erosion of the coast. These developments are believed have had little impact in the Babbage Estuary system until roughly 6000 years B.P. (cf. section 2.1.2) and possibly not until 4000 years B.P., by which time the Hypsithermal anomaly was at an end (Ritchie, 1972, p.46).

## 2.3 OCEANOGRAPHIC ENVIRONMENT

### 2.3.1 WATER AND CIRCULATION IN MACKENZIE BAY

The nearshore environment off the Babbage Estuary is strongly influenced by conditions in Mackenzie Bay and adjacent waters of the Beaufort Sea. Mackenzie Bay is dominated by two large features, the Mackenzie Delta and Mackenzie Canyon, which contribute to the development of a distinctive oceanographic environment in this part of the Beaufort Sea. The eastern part of Mackenzie Bay forms part of the Mackenzie River estuarine system; coastal waters as far west as Herschel Island may be influenced by interactions between Beaufort Sea water and Mackenzie River runoff. In addition, the deep trough of Mackenzie Canyon provides a route for intrusion of subsurface Arctic Ocean water onto the shelf off the Yukon coast.

Three principal water masses have been recognized in the Arctic Ocean (Coachman, 1963): Arctic bottom water at depths greater than 900 m; Atlantic water at intermediate depths; and Arctic surface water above 200-250 m. The water over the continental shelf in the southern Beaufort Sea is primarily Arctic surface water, with the addition of freshwater discharge from the Mackenzie and other rivers. The Arctic surface layer has been subdivided into three units (Coachman and Barnes, 1962; Coachman, 1963): a lower mixed layer roughly 100 m thick; a middle layer of similar thickness, largely isothermal ($-1.5<\theta<-0.9°C$) but with a strong vertical salinity gradient; and a surface layer which is cold and nearly isohaline, but in which both temperature and salinity show wide temporal and

geographic variation.

Data representative of stations in Mackenzie Bay are plotted in Figure 20 (after Herlinveaux and de Lange Boom, 1975). At depths greater than about 20 m, salinities are typically between 33 and 35 ppt, relatively constant with depth, and temperatures are generally in the range $-1.8<\Theta<-1.3°C$. There is little seasonal variation, but winter cooling is observed above h=50 m. In the top 20 m, a marked seasonal variation is observed, due to summer discharge from the Mackenzie River forming a thin layer of warm low-salinity water at the surface. The mean monthly flow in the Mackenzie River drops to about 3000 $m^3s^{-1}$ in March, rises rapidly in May, and peaks at approximately 22 000 $m^3s^{-1}$ in June. In summer, the depth of the halocline varies between 2 and 10 m (Herlinveaux and de Lange Boom 1975), depending in part on the distribution of sea-ice.

Circulation patterns in the southern Beaufort Sea are not well documented. Over the adjacent Canada Basin, a persistent clockwise circulation produces a westward motion off the western Arctic coast, with a mean speed of order $10^{-1}$ m $s^{-1}$ (Herlinveaux and de Lange Boom, 1975). A net eastward motion immediately adjacent to the coast, predicted from surface wind patterns by Wilson (1974), has been partially documented with limited current-meter data obtained along the Alaska coast (Paquette and Bourke, 1974; Hufford, 1975) and near bottom on the Mackenzie shelf (Huggett et al., 1975), where a mean flow setting northeast with a magnitude of about 0.05 m $s^{-1}$ is

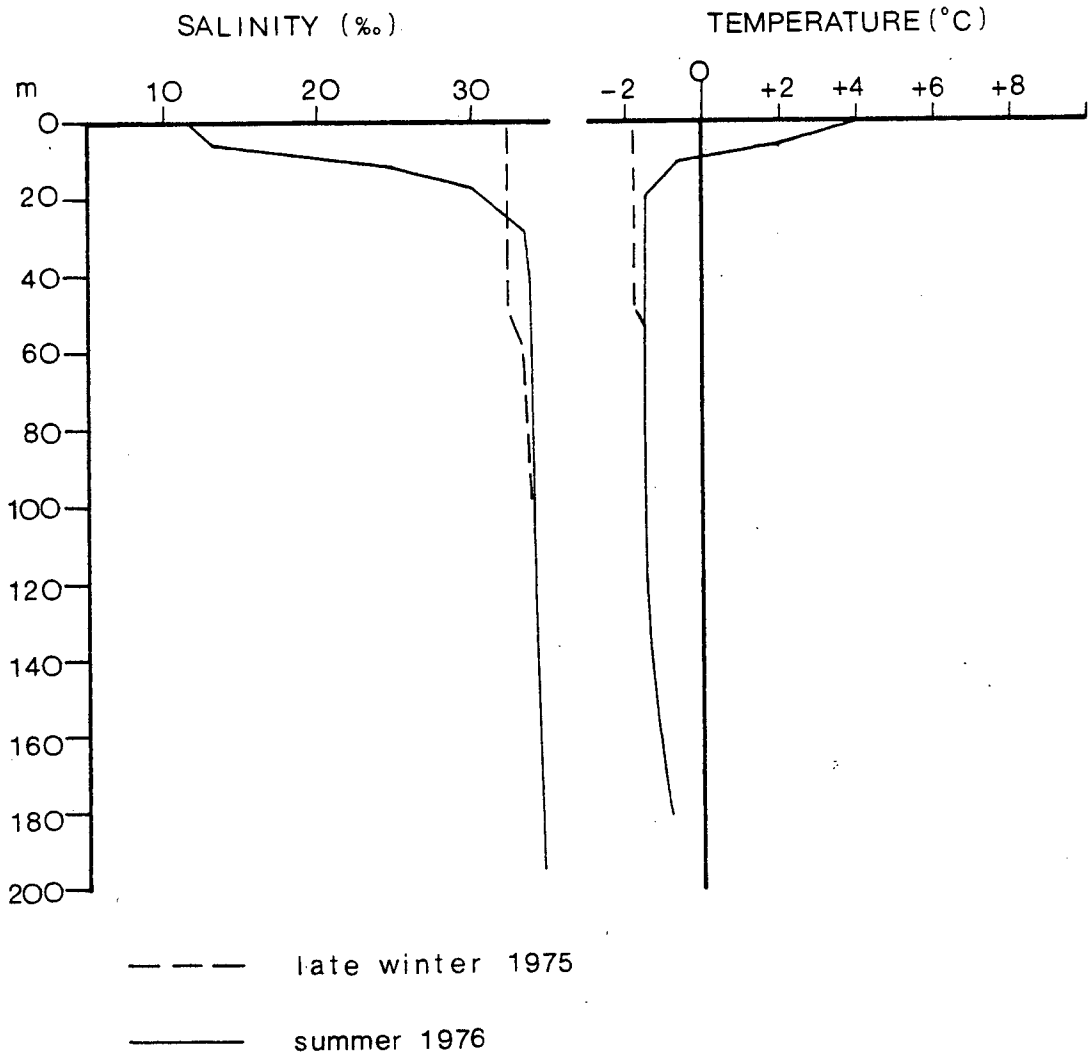


FIGURE 20

Representative temperature and salinity profiles in Mackenzie Bay (after Herlinveaux and de Lange Boom, 1975).

observed. Tidal currents in the region are generally weak, of order $10^{-2}$ m $s^{-1}$, and mainly semi-diurnal. They represent a minor source of variance compared to inertial effects (also semi-diurnal at this latitude and mainly wind-driven) and to fluctuations directly attributable to wind stress or pressure gradient (Huggett et al., 1975). Huggett et al. report near-bottom velocities of order $10^{-1}$ m $s^{-1}$ northeast[1] at various locations on the shelf after prolonged wind. Shearer and Blasco (1975), from observations of resuspended sediment within 5 m above the bottom in depths $h \leq 30$ m, hypothesized that current speeds may be locally increased beneath ice in shallow water; however, the open-water currents reported above would be competent to maintain silt and clay in suspension (see Bornhold, 1975, p.6, for further discussion).

Surface currents in the Mackenzie Delta region are highly variable and strongly affected by surface winds (Cameron, 1953; Healey, 1971; MacNeill and Garrett, 1975). Satellite images illustrate the characteristic responses under different wind conditions: with calm conditions or westerly winds (Figure 21) the plume of Mackenzie River water moves out to a sharp northern boundary and spreads toward the east; with winds from the east, however, Mackenzie water moves offshore and westward (see section 4.2.1), causing upwelling of cold subsurface water of higher salinity (Cameron, 1953). In the latter case,

---

[1]Note that currents are referred to the direction in which they set; this is contrary to the convention for atmospheric flows.

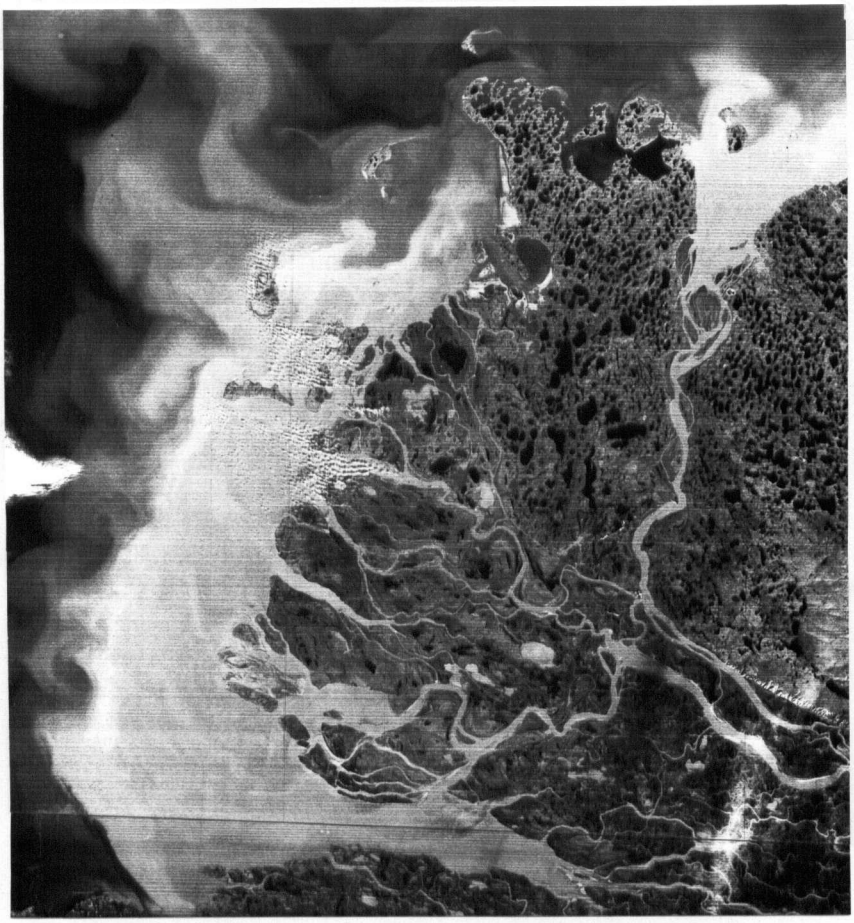

FIGURE 21

Landsat image 1-1422-20185-5, 18 September 1973, showing Mackenzie River plume spreading north and east, with an abrupt western boundary in Mackenzie Bay.

sediment from the Mackenzie River may be advected along the Yukon coast. Indeed a strong current, $u \geq 0.4$ m $s^{-1}$, flowing northwest out of Mackenzie Bay past Herschel Island, was identified as a relatively persistent feature by MacNeill and Garrett (1975). Except under strong easterly winds, however, this current may be relatively free of sediment, being part of a major clockwise gyre in Mackenzie Bay.

Cameron (1953) reported high surface salinities (s>15ppt) against the Yukon coast with both easterly and westerly winds. This situation apparently did not hold in the summer of 1974, when onshore winds and persistent ice cover close to the coast significantly altered the surface circulation and salinity distribution (Table 4).

TABLE 4

Selected observations of surface salinity in embayments of the central Yukon coast and in adjacent waters of Mackenzie Bay.

| station[a] | | source[b] | date | s (ppt) |
|---|---|---|---|---|
| 1974 | | | | |
| Babbage Estuary | 7 | 1 | 12/7/74 | 0.3 |
| Babbage Estuary | nr7 | 2 | 17/7/74 | 0.3 |
| King Pt Lagoon | 114 | 2 | 30/7/74 | 4.0 |
| Stokes Lagoon | 26c | 2 | ? | 2.7 |
| Roland Bay | 30 | 2 | 31/7/74 | 2.0 |
| Mackenzie Bay | 10 (69.67°N,137.15°W) | 3 | 15/8/74 | 2.54 |
| Mackenzie Bay | 11 (69.60°N,137.69°W) | 3 | 16/8/74 | 2.54 |
| near Kay Point | 41 | 2 | 16/8/74 | 2.2 |
| Mackenzie Bay | 16 (69.55°N,138.39°W) | 3 | 18/8/74 | 3.43 |
| Mackenzie Bay | 17 (69.44°N,138.17°W) | 3 | 18/8/74 | 5.16 |
| Mackenzie Bay | 18 (69.40°N,138.13°W) | 3 | 18/8/74 | 5.16 |
| Mackenzie Bay | 19 (69.31°N,138.10°W) | 3 | 18/8/74 | 5.16 |
| Herschel Basin | 20 (69.45°N,138.82°W) | 3 | 21/8/74 | 9.00 |
| Herschel Basin | 23 (69.47°N,138.63°W) | 3 | 22/8/74 | 7.80 |
| Mackenzie Bay | 24 (69.41°N,138.35°W) | 3 | 22/8/74 | 2.91 |
| Babbage Bight | 39 (69.31°N,138.24°W) | 3 | 24/8/74 | 5.16 |
| Mackenzie Bay | 40 (69.37°N,138.33°W) | 3 | 24/8/74 | 5.42 |
| Pauline Cove | 31 | 2 | 24/8/74 | 6.3 |
| 1975 | | | | |
| Babbage Estuary | 7 | 1 | 13/7/75 | 0.7 |
| Babbage Estuary | 7 | 1 | 14/7/75 | 10.5 |
| Babbage Estuary | 7 | 1 | 15/7/75 | 9.0 |
| King Pt Lagoon | 114 | 2 | 29/7/75 | 12.6 |
| Stokes Lagoon | 26c | 2 | 4/8/75 | 13.7 |
| Pauline Cove | 31b | 2 | 5/8/75 | 16.4 |
| Pauline Cove | 7 (69.57°N,138.92°W) | 3 | 10/8/75 | 16.97 |
| Mackenzie Bay | 8 (69.37°N,137.50°W) | 3 | 11/8/75 | 15.01 |
| Mackenzie Bay | 45 (69.75°N,138.12°W) | 3 | 21/8/75 | 14.55 |
| Mackenzie Bay | 46 (69.25°N,138.07°W) | 3 | 21/8/75 | 14.47 |
| Mackenzie Bay | 47 (69.23°N,137.92°W) | 3 | 21/8/75 | 14.63 |

[a] Station numbers are those of the data source, except in the Babbage Estuary, where the observations pertain to station 7 of this study.

[b] Sources: (1) this study; (2) Kendel et al., 1975; (3) Herlinveaux et al., 1976.

## 2.3.2 ICE IN THE SOUTHERN BEAUFORT SEA

Sea ice affects littoral and estuarine systems of the central Yukon coast chiefly by restriction of surface wave generation. Further west, on the Alaska coast, grounding of pressure ridges in the nearshore zone produces frequent direct modification of coastal morphology; ice thrust processes appear to be relatively unimportant on the Yukon coast [see, however, Kovacs and Mellor (1971), McDonald and Lewis (1973), and Lewis and Forbes (1975) for the few reported exceptions to this observation].

The winter distribution of sea-ice off the north Alaska coast has been comprehensively reviewed by Kovacs and Mellor (1974), who distinguished three zones: the landfast ice, extending typically to water 10-20 m deep, largely undeformed and attaining a thickness of about 2 m; the seasonal pack, typically 100-200 km wide, also about 2 m thick in late-winter when undeformed, separated from the landfast ice by a narrow shear zone; and the polar pack, with a large proportion of multi-year ice greater than 2 m thick. The landfast ice is bottomfast in water less than 2 m deep and may exhibit tidal cracks near the 2-m isobath. The landfast ice is stabilized by incorporation of grounded pressure ridges, ridge fragments, and occasional tabular icebergs (the so-called 'ice islands'). It extends seaward to a line, usually defined by the most seaward grounded pressure ridge, and typically near the 20-m isobath (Stringer, 1974).

Landfast ice is a common feature between Herschel Island and Kay Point (early winter development illustrated in Figure 22) and forms a stable cover over most of Mackenzie Bay in some years, although open water may occur close to shore even in February (Cooper, 1974). In Mackenzie Bay, the seaward limit of the landfast ice is also marked by a shear-zone, in which a broad and extensive lead often develops, particularly in response to easterly winds in spring (Figure 23; Marko, 1975).

The areal extent of open water in the southern Beaufort Sea varies considerably from year to year (cf. Markham, 1975; Marko, 1975). Factors affecting the summer ice distribution are not well understood. There is evidence that the evolution of extensive rectilinear lead systems in the polar pack may influence the break-up process (Marko, 1975). However summer winds unquestionably play a major role; in particular, the relative frequency of easterlies seems to be critical. In 1974, east and southeast winds were rare prior to late summer and the ice front remained in the latitude of 70°N, as in 1964, another heavy-ice year. In other years, easterly and southeasterly winds are more frequent and the southern limit of the pack may lie north of 72°N. The area of open water in September 1975 was anomalously small due to storms on August 27 and September 6 that drove pack ice against the coast.

Markham (1975) gives frequencies for various percentages of ice cover in Mackenzie Bay as a function of date. However, because of variability in the pattern of breakup and freezeup

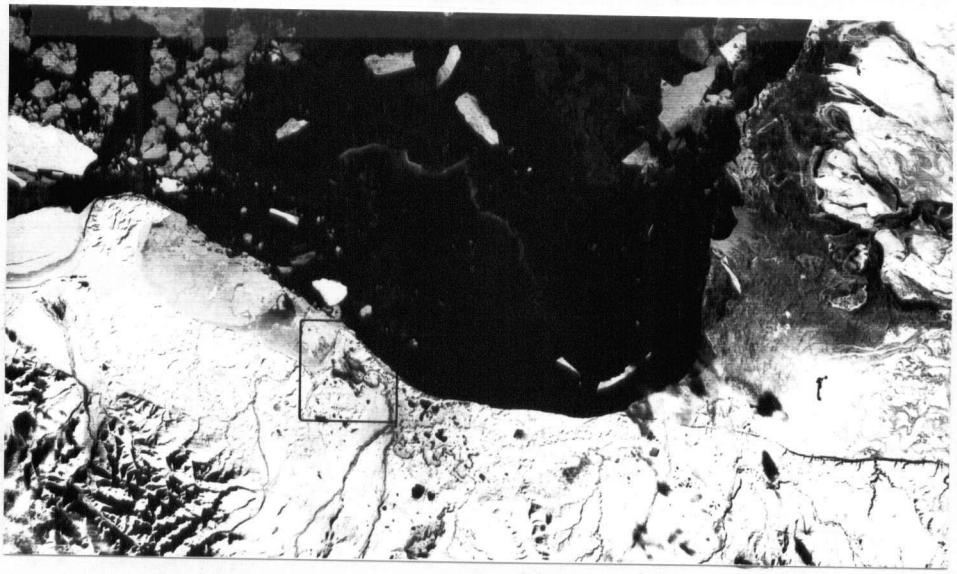

FIGURE 22

Portion of Landsat image 1-1460-20292-6, 26 October 1973, showing open water in Mackenzie Bay and thin ice in Herschel Basin, in Phillips Bay, west of Herschel Island, and in all lagoons.

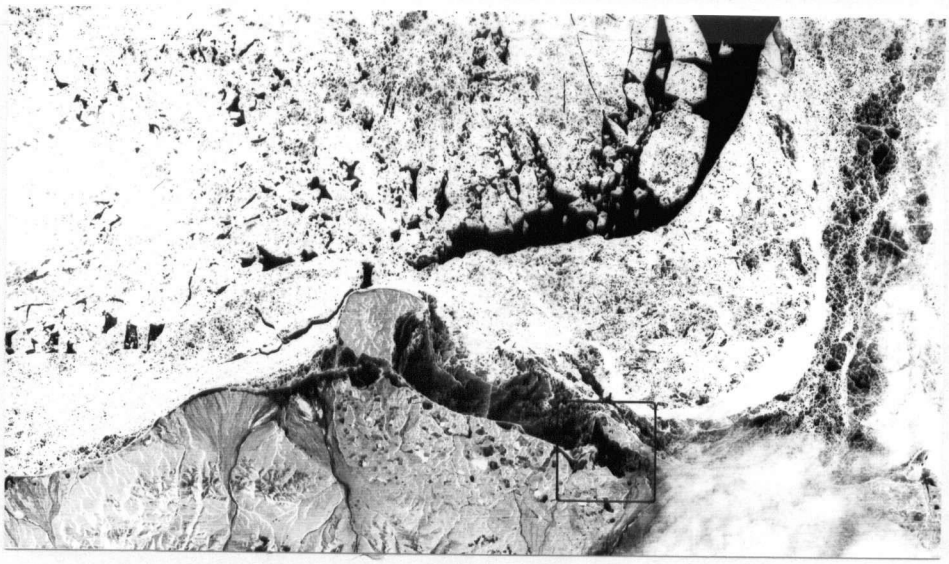

FIGURE 23

Portion of Landsat image 1-1317-20374-6, 5 June 1973, showing narrow band of landfast ice west of Herschel Island, extensive landfast ice in Mackenzie Bay, and lead in the shear-zone between landfast ice and seasonal pack.

along the Yukon coast, these results are somewhat ambiguous as indicators of ice climatology at Kay Point. Breakup usually occurs earlier in the southeast end of Mackenzie Bay due to the effect of Mackenzie River discharge (cf. Dey, 1980). Later expansion of open water from a nucleus in Phillips Bay and from the shear zone in outer Mackenzie Bay (Figure 23) may leave a band of ice along the coast in the vicinity of Kay Point as late as mid-July in some years, despite extensive open water offshore; in other years, Kay Point may be exposed to large fetches early in July. Extensive open water is common in July, August, and September, although pack ice may be moved against the coast during storms.

Weekly charts for 18 years of observation beginning in 1958 indicate that ice concentration never exceeded 2/10 in Mackenzie Bay south of 69°40'N before 24 September (Markham, 1975, figure 2), although the storm of 14 September 1970 is known to have filled the bay almost completely with pack ice as far southeast as Sabine Point, while waters further east and in the lee of Herschel Island were covered with shorefast ice (Canada, Department of Public Works, 1971b, figure 2). Taking a concentration of 8/10 or more as a freezeup criterion, the weekly chart data yield freezeup dates for southern Mackenzie Bay ranging from the end of September to early November.

Freezeup at the coast and in lagoons and estuaries may begin some weeks earlier; slush ice formed in lagoons may be moved out into adjacent coastal waters, where it promotes development of an ice cover adjacent to the coast earlier than

might otherwise occur (Wiseman et al., 1973, p.146). In Mackenzie Bay, and possibly also in Phillips Bay, freezeup may be facilitated when pack ice is concentrated, under appropriate wind and current conditions, in waters adjacent to the coast. This seems to have been the case in 1905, when an anomalously early freezeup occurred ca. 9 September (Amundsen, 1908, vol.2, pp.145-146).

The length of potential fetch containing less than 3/10 ice at weekly intervals in 1975 and 1976 is given, for Kay Point, in Tables 5 and 6. These data demonstrate the pronounced year-to-year variability characteristic of summer ice conditions in the southern Beaufort Sea. In 1975, Kay Point was exposed to open water in Mackenzie Bay during the first week of July and the fetch expanded rapidly toward the northeast, reaching a maximum by 18 July. Expansion toward the northwest was more limited, reaching a maximum around 8 August, after which the storm of 9-10 August drove pack ice toward the coast, effecting sharp reductions in fetch throughout the NE-NW sector. Another abrupt fetch reduction followed the storm of 27 August and the fetch at Kay Point was further diminished to zero by 12 September. In contrast, data for 1976 (Table 6) show that the fetch opened more slowly toward the northeast, more rapidly toward the northwest; there were no major intrusions of the pack during the summer; and extensive open water remained throughout September.

TABLE 5

Potential fetch with ≤3/10 ice, Kay Point, 1975.

(kilometres)

| date | SE | ESE | E | ENE | NE | NNE | N | NNW | NW (1) | WNW (2) |
|---|---|---|---|---|---|---|---|---|---|---|
| 4 Jul | 0 | 0 | 0 | 0 | 0 | 0 | 0 | 0 | 20 | 13* |
| 11 Jul | 50* | 110* | 110* | 140 | 140 | 85 | 75 | 75 | 35* | 13* |
| 18 Jul | 50* | 110* | 110* | 150* | 585 | 360 | 130 | 115 | 35* | 13* |
| 25 Jul | 50* | 110* | 110* | 150* | 385 | 320 | 75 | 85 | 35* | 13* |
| 1 Aug | 50* | 110* | 110* | 150* | 360 | 255 | 265 | 150 | 35* | 13* |
| 8 Aug | 50* | 110* | 110* | 150* | 375 | 255 | 225 | 130 | 35* | 13* |
| 15 Aug | 50* | 110* | 110* | 150* | 20 | 45 | 20 | 10 | 35? | 13? |
| 22 Aug | 50* | 110* | 110* | 150* | 450 | 245 | 130 | 85 | 35* | 13* |
| 29 Aug | 10 | 10 | 6 | 4 | 2 | 2 | 2 | 2 | 35* | 13* |
| 5 Sep | 0 | 0 | 0 | 0 | 0 | 0 | 0 | 0 | <10 | <10 |
| 12 Sep | 0 | 0 | 0 | 0 | 0 | 0 | 0 | 0 | 0 | 0 |

1 Fetch toward northwest is essentially coast-limited by Herschel Island, at a distance of approximately 35 km; under some conditions, refracted deep-water waves generated beyond Herschel Island may affect Kay Point Spit; in most cases, however, most of the refracted wave energy is believed to be dissipated on shoals along the submarine ridge between Kay Point and Collinson Head (Herschel Island); in any case, $K << 1$ for these waves at the Babbage Estuary entrance.

2 Fetch toward west-northwest is restricted by coast between Stokes Point and Spring River, at distances of approximately 13 km from Kay Point and 6 km from distal end of spit.

*Denotes coast-limited maximum fetch.

Sources: Atmospheric Environment Service weekly charts, Landsat imagery, observations from Kay Point, and occasional reconnaissance flights.

TABLE 6

Potential fetch with ≤3/10 ice, Kay Point, 1976.

(kilometres)

| date | SE | ESE | E | ENE | NE | NNE | N | NNW | NW[1] | WNW[2] |
|---|---|---|---|---|---|---|---|---|---|---|
| 2 Jul | 0 | 0 | 0 | 0 | 0 | 0 | 0 | 0 | 10 | 10 |
| 9 Jul | 0 | 0 | 0 | 0 | 0 | 0 | 0 | 0 | 10 | 10 |
| 16 Jul | 50* | 110* | 110* | 150* | 20 | 20 | 20 | 10 | 15 | 13* |
| 23 Jul | 50* | 110* | 110* | 150* | 110 | 95 | 95 | 40 | 35* | 13* |
| 30 Jul | 50* | 110* | 110* | 150* | 190 | 85 | 130 | 200 | 35* | 13* |
| 6 Aug | 50* | 110* | 110* | 150* | 20 | 20 | 30 | 30 | 35* | 13* |
| 13 Aug | 50* | 110* | 110* | 150* | 290 | 150 | 85 | 190 | 35* | 13* |
| 20 Aug | 50* | 110* | 110* | 150* | 215 | 160 | 150 | 200 | 35* | 13* |
| 27 Aug | 50* | 110* | 110* | 150* | 310 | 180 | 160 | 180 | 35* | 13* |
| 3 Sep | 50* | 110* | 110* | 150* | 235 | 215 | 190 | 170 | 35* | 13* |
| 10 Sep | 50* | 110* | 110* | 150* | 300 | 275 | 255 | 190 | 35* | 13* |
| 17 Sep | 50* | 110* | 110* | 150* | 700* | 352 | 385 | 350 | 35* | 13* |
| 24 Sep | 50* | 110* | 110* | 150* | 700* | 373 | 385 | 360 | 35* | 13* |
| 1 Oct | 50* | 110* | 110* | 150* | 700* | 460 | 340 | 425 | 35* | 13* |
| 8 Oct | 0 | 0 | 0 | 0 | 0 | 0 | 0 | 0 | 0 | 0 |
| 15 Oct | 0 | 0 | 0 | 0 | 0 | 0 | 0 | 0 | 0 | 0 |

[1] See Table 2.3.2-1.

[2] See Table 2.3.2-1.

*Denotes coast-limited maximum fetch.

Sources: Atmospheric Environment Service weekly charts, Landsat and NAPL imagery, observations from Kay Point, and occasional reconnaissance flights.

## 2.3.3 TIDES AND STORM SURGES

Astronomical tides in the southern Beaufort Sea are predominantly semidiurnal and the tidal range is small. Representative values of amplitude (in mm) and Greenwich phase lag (in degrees) for the principal tidal constituents at Tuktoyaktuk and Kay Point are presented in Table 7. The semidiurnal M2 constituent is clearly dominant, with an amplitude of 73 mm at Kay Point, as computed from summer 1975 data. The mean spring tide range, $R_S=[(M2)+(S2)]$ (following Defant, 1953), where M2 and S2 refer here to the corresponding amplitudes, is approximately 0.2 m at Kay Point.

The tides are believed to enter from the Atlantic and are significantly influenced by Coriolis effects (Sverdrup, 1926) because the inertial period (12.7 h at 70°N) is close to the periods of the semidiurnal tidal constituents. The dominant M2 tide in the southeastern Beaufort Sea propagates eastward along the shelf with relatively constant amplitude (Huggett et al., 1975). The phase lag at Tuktoyaktuk exceeds the lag at Kay Point for most constituents in Table 7. There is evidence to suggest that the speed of tidal propagation is reduced in the presence of ice cover: the phase of the M2 tide at Tuktoyaktuk exhibits an annual periodicity with the lag in winter being approximately 60° greater than during the open-water season (Henry and Foreman, 1977, p.4 and table 10). The amplitude of the tide is also greater at Tuktoyaktuk during the summer months.

TABLE 7

Principal tidal constituents at Tuktoyaktuk and Kay Point.

| constituent | $f^{-1}$ (h) | Tuktoyaktuk 1/1-31/12/67 a (mm) | Tuktoyaktuk 1/1-31/12/67 g (deg) | Tuktoyaktuk 6/7-9/9/75 a (mm) | Tuktoyaktuk 6/7-9/9/75 g (deg) | Kay Point 6/7-9/9/75 a (mm) | Kay Point 6/7-9/9/75 g (deg) | Kay Point 6/7-9/9/76 a (mm) | Kay Point 6/7-9/9/76 g (deg) |
|---|---|---|---|---|---|---|---|---|---|
| Sa | 8766. | 90. | 188.6 | | | | | | |
| Ssa | 4383. | 84. | 196.6 | | | | | | |
| MSm | 763.5 | 21. | 52.4 | | | | | | |
| Mm | 661.3 | 8. | 301.0 | 65. | 267.2 | 21. | 291.2 | 21. | 224.9 |
| MSf | 354.4 | 14. | 97.3 | 48. | 140.9 | 22. | 114.7 | 62. | 256.0 |
| Mf | 327.9 | 45. | 235.1 | | | | | | |
| Q1 | 26.87 | 6. | 187.6 | 5. | 159.5 | 6. | 119.7 | 4. | 188.9 |
| O1 | 25.82 | 25. | 187.7 | 23. | 171.8 | 30. | 166.8 | 30. | 161.8 |
| P1 | 24.07 | 7. | 149.3 | | | | | | |
| K1 | 23.93 | 32. | 157.9 | 43. | 170.0 | 34. | 143.1 | 34. | 149.8 |
| N2 | 12.66 | 15. | 285.3 | 26. | 243.6 | 13. | 273.2 | 12. | 254.4 |
| OP2 | 12.46 | 14. | 101.9 | | | | | | |
| H1 | 12.44 | 48. | 172.5 | | | | | | |
| M2 | 12.42 | 112. | 309.9 | 149. | 280.6 | 73. | 275.1 | 77. | 267.6 |
| H2 | 12.40 | 39. | 109.8 | | | | | | |
| MKS2 | 12.39 | 18. | 149.0 | | | | | | |
| L2 | 12.19 | 4. | 13.4 | 6. | 241.9 | 5. | 323.5 | 6. | 320.2 |
| T2 | 12.02 | 20. | 44.9 | | | | | | |
| S2 | 12.00 | 48. | 3.3 | 67. | 336.7 | 33. | 326.5 | 35. | 317.1 |
| R2 | 11.98 | 17. | 13.0 | | | | | | |
| K2 | 11.97 | 9. | 340.7 | | | | | | |

$f^{-1}$ period (hours)
a amplitude (mm)
g Greenwich phase lag (degrees)

All computations in GMT.

Results for Tuktoyaktuk 1967 after Henry and Foreman (1977).
Results for Tuktoyaktuk 1975 derived from data in Foreman (1977).

The characteristics of the low-frequency constituents are extremely variable (Table 7). In summer 1976, the amplitude at Kay Point of the MSf tide (T=354.4 h) was 62 mm, second only to the M2 amplitude (77 mm). For the same period in 1975, however, the MSf amplitude was only 22 mm. The great variability of the low-frequency tides in the southern Beaufort Sea reflects the importance of meteorological effects, particularly but not exclusively during the open-water season (see section 3.2.1).

Historical extremes due to positive and negative storm surges are approximately +3 m and -1 m at Tuktoyaktuk (Henry, 1975). The range is therefore about 4 m, an order of magnitude greater than that of the astronomical tide. While the high-frequency waves that accompany many positive storm surges constitute the major source of energy for sediment transport and morphological change during such events (Hume and Schalk, 1967; Wiseman et al., 1973), the low-frequency surge of water level alters the physical boundaries of a coastal system and may change the locus of erosion and sedimentation. This effect is particularly marked along the southern Beaufort Sea coast, characterized as it is by widespread deltaic and other supratidal flats, especially in the outer Mackenzie Delta.

Two outstanding surges, in 1944 and 1970, have been observed and described in some detail (Canada, Public Works, 1971b; Reimnitz and Maurer, 1979). Although no gauges were in operation during either event, it has been suggested that a rise of about 3 m (sum of tide and surge) occurred at

Tuktoyaktuk during the storm of August 1944, while the estimates for September 1970 range from +1.3 m at Herschel Island to more than +2 m at Shingle Point and Tuktoyaktuk (Canada, Public Works, 1971b). It is not clear that wave effects have been eliminated entirely in these estimates.

Positive storm surges in the southern Beaufort Sea are generally associated with west and northwest winds, while negative surges occur in association with an easterly surface air flow (Henry, 1975). A numerical storm-surge simulation incorporating a backwater effect due to Mackenzie River discharge (Henry and Heaps, 1976, figure 12) produced a positive anomaly in Shallow Bay substantially greater than that obtained without backwater. Interaction between storm surges and river discharge is explored further in the present study with data from a smaller coastal system, leading to the conclusion that the two processes are largely decoupled in the Babbage Estuary (see sections 3.3.1 and 3.3.2).

Recurrence frequencies of major surges are not well established, there being only about 20 years of partially complete tidal record at Tuktoyaktuk, and very much less at other sites on the Yukon and Mackenzie coasts. Various estimates of the return period for a storm such as the major 1970 event have been proposed. Recurrence periods for extreme winds, ice conditions, and surge response will not be the same. Burns (1973) estimated a period between 7 and 9 years, based on atmospheric synoptic analysis, which may not account for the variable effectiveness of similar storms moving along slightly

different tracks with respect to open water and under varying conditions of sea ice distribution. Other estimates between 25 and 50 years have been proposed (Canada, Public Works, 1971a, b); the criteria used for these estimates are not well described. Further evidence from the Babbage Delta is presented in section 3.3.2, suggesting that the return period of surges comparable to those of 1944 and 1970 may be greater than 100 years.

Two winter surges have been recorded, in November 1973 and in January 1974. The amplitude was less than 1 m at Herschel Island (Huggett et al., 1975), not significantly different from the amplitude at a site offshore, in contrast to the situation during open-water surges, and considerably less than would be expected in response to similar wind magnitude and duration over open water. Nevertheless, a small winter surge can result in considerable ice movement onshore, may lead to explosive rupture of ice under pressure in rare cases (Reimnitz and Maurer, 1978), and can flood bottomfast ice and coastal flats, as observed in the Babbage Delta in January 1974 (R. MacKenzie, personal communication, 1974) and in the Noatak Delta, western Alaska, in November 1972 (Ugolini, 1975).

Ice cover and fetch limitation by ice are apparently important in reducing the frequency of winter surges and of summer surges in heavy-ice years (Henry, 1975, figure 3). The frequency distribution of extreme monthly water levels at Tuktoyaktuk is plotted in Figure 24. Positive surges are clearly concentrated in the months July-November.

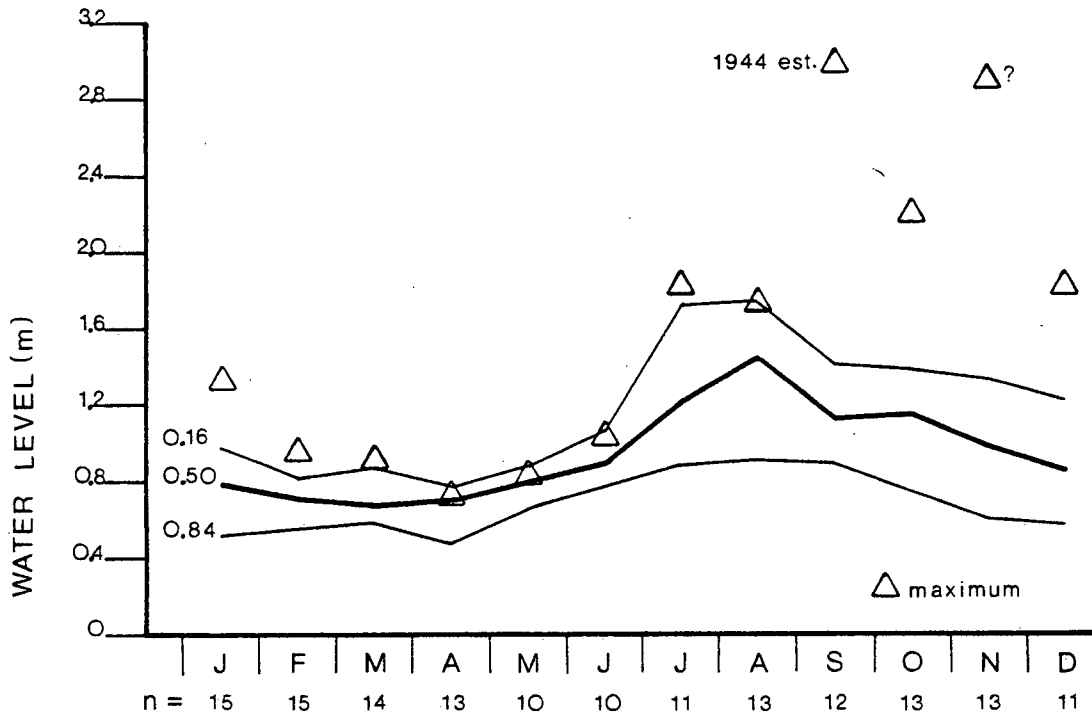


FIGURE 24

Frequency distribution of extreme monthly water levels at Tuktoyaktuk (data courtesy Canadian Hydrographic Service).

TABLE 8

Mean sea level and summer anomaly, Tuktoyaktuk, 1962-1975 (data courtesy Canadian Hydrographic Service).

| year | mean level (m) June-July | mean level (m) January-December |
|---|---|---|
| 1962 | 0.50 | 0.27 |
| 1963 | 0.49 | 0.34 |
| 1964 | 0.61 | 0.39 |
| 1965 | 0.46 | 0.38 |
| 1966 | 0.55 | 0.27 |
| 1967 | 0.57 | 0.43 |
| 1968 | ---- | (0.26) |
| 1969 | ---- | (0.34) |
| 1970 | ---- | (0.25) |
| 1971 | (0.45) | (0.40) |
| 1972 | ---- | (0.33) |
| 1973 | 0.49 | 0.39 |
| 1974 | 0.61 | 0.37 |
| 1975 | (0.33) | (0.42) |

( ) missing data

Tests of hypotheses:

1. Mean sea-level in June-July is significantly greater ($\alpha = 0.001$) than annual mean level (Mann-Whitney $U = 8$, $n_1 = 10$, $n_2 = 10$);

2. Mean sea-level for June-July of 'heavy-ice' years 1964 and 1974 is significantly greater than mean June-July level in other years ($\alpha = 0.05$, Mann-Whitney $U = 0$, $n_1 = 2$, $n_2 = 8$).

Mean sea level also exhibits an annual periodicity. The monthly mean tide during June and July shows a statistically significant positive anomaly at Tuktoyaktuk (Table 8). The early summer anomaly cannot be fully accounted for by the steric effect of the freshwater Mackenzie River plume; although temperature may play a role, dynamic interaction between sea ice and high summer discharge from the Mackenzie River is believed to augment the steric increase in sea level, particularly in heavy-ice years (Henry, 1975). In such years, the summer anomaly is significantly greater ($\alpha$=0.05; see Table 8). Superficially analogous effects occur locally in early June near river outlets along the Yukon coast. There, however, bottomfast ice is a major factor (see section 3.3.2).

## 2.3.4 WAVE CLIMATE

Wind-generated surface gravity waves in the southern Beaufort Sea remain poorly documented. Herlinveaux and de Lange Boom (1975, pp.61-64) have reported wave-buoy data collected in 1975 in Mackenzie Bay, at a site northwest of Pelly Island where the depth was 18 m. The highest waves observed at the site approached 4 m and the peak spectral density occurred at T=5.9 s. Median wave heights for the period of record (8 August to 6 September) were approximately 0.43 m (significant[1]) and 0.70 m (maximum) (Herlinveaux and de Lange Boom, 1975, figure 43). The highest significant wave height was 2.4 m. Wave heights developed during the late August storm in 1975 were lower than those associated with a storm earlier in the month, when the winds were less severe. This reflected the fetch reduction caused by pack ice intrusion following the early August storm (see Table 5).

Average summer wave conditions on the Alaskan Beaufort Sea coast appear to be governed by the local wind field and swell from distant storms is rare (Wiseman et al., 1973, pp.37-39, 110-111). Conditions on the Yukon coast are similar, although the mean ice-free fetch may be greater. An easterly swell was observed at Pingok Island in September 1972 and was apparently fetch-limited by the wind system rather than by ice (Wiseman et al., 1973, p.38).

---

[1]The significant wave height, $H_s$, can be defined as the mean height of waves higher than $H_{67}$.

Wave conditions were to be recorded at Kay Point during the present study using an accelerometer buoy. Unfortunately, the instrument was not delivered and, in the absence of all but limited visual data, recourse has been made to wave hindcast estimates for the computation of incident wave power. Significant wave height and period were computed from Kay Point wind data using the SMB method (U.S.A. Coastal Engineering Research Center, 1973). The wave field was assumed to be determined by local winds only.

The SMB approach, although it fails to describe the full wave spectrum, yields significant wave estimates from which other statistics may be estimated (following Longuet-Higgins, 1952). In the present case, the SMB method was considered to represent an appropriate level of hindcast sophistication, given various uncertainties in the input conditions. As emphasized above (section 2.2.1), wind conditions at the coast may differ significantly from those offshore; however, the major events at the Babbage Estuary entrance were associated with local waves generated by northwesterly winds over Herschel Basin and, for these events, the Kay Point wind data may be fairly representative. A major source of uncertainty is the unknown nature and degree of wave attenuation in a fetch containing scattered ice floes. The maximum fetch adopted for the present computations was defined by the limit ≤3/10 ice concentration, as summarized in Tables 5 and 6. Although coastal waters were essentially ice-free for much of the

open-water season, varying low concentrations of scattered ice may have affected the generation and propagation of surface gravity waves during some events. A third additional source of uncertainty relates to possible systematic variations in air-sea momentum transfer due to synoptic- and seasonal-scale changes in the relative temperature of air and water.

Hindcast values of significant wave height and period were computed for all wind events in the sector 290°T clockwise to 135°T having windspeeds $u > 5.5$ m $s^{-1}$ for more than one hour. The computations were carried out using mean hourly windspeed at Kay Point over the duration of the event, events being partitioned when windspeed was highly variable. Comparison with hourly hindcast estimates for selected storms suggests that the simplified procedure adopted may overestimate the mean significant wave height and period. On the other hand, coastal wind data might be expected to yield unrealistically low values (see discussion in section 2.2.1 above).

The treatment of northwesterly wind events posed some difficulty, inasmuch as Kay Point spit is exposed through a narrow fetch window to deepwater waves with periods $T > 4$ s generated northwest of Herschel Island. The fetch window has a width of about 1.3 km for $T = 5.4$ s. Refracted wave orthogonals converge on the bathymetrically complex shoal area north-northwest of Kay Point. This is the area in which extraordinarily high rates of erosion appear to have occurred in the recent past (see section 2.1.2). The bathymetry is sufficiently complex that operator error in the refraction

analysis is probably quite significant.

Seven sites have been identified with chart depths $0.2 \leq h \leq 1.6$ m relative to 'lowest normal tide' at distances up to 11.6 km north-northwest of Kay Point (Canadian Hydrographic Service, 1971, 1972). These depths may correspond roughly to 1.4 m and 0.0 m, respectively, below the datum adopted in the present study. Although the shallowest site is exposed during periods of unusually low water, northwesterly winds are commonly associated with positive storm surges. Nevertheless, breaker depth computations, following the procedure outlined below and assuming a moderate surge height of 1 m, suggest that extensive breaking may be expected over the shoal area; in any case, considerable energy dissipation must occur in this area and conditions further inshore are not readily predictable. It was therefore decided that the hindcast analysis for northwesterly events would be restricted to waves generated within Herschel Basin. The shallow-water procedures of Bretschneider (U.S.A. Coastal Engineering Research Center, 1973) were employed for these events.

The quality of the hindcast estimates may be judged by comparison with visual observations (Figure 25). Estimates of T are reasonably close to observed values, except at $T > 4.5$ s, for which the hindcast procedure appears to yield unrealistically low estimates. Estimates of breaker height show greater scatter, perhaps reflecting additional errors in the computation of the breaker height index (see below), as well as errors in the visual data due to subjective assessment

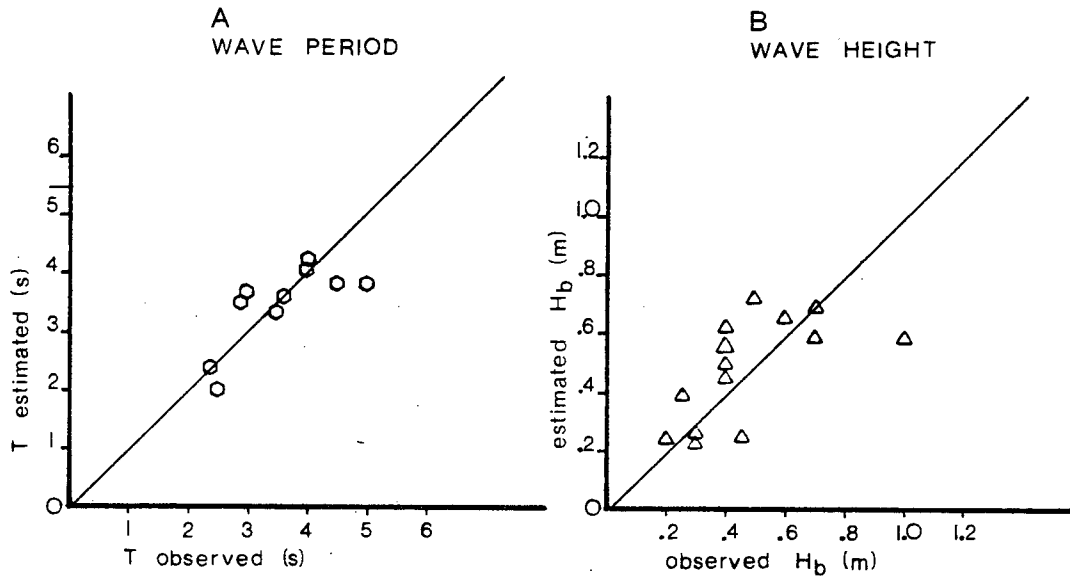


FIGURE 25

Plots of estimated versus observed wave period and height, Kay Point spit.

of predominant wave height.

The breaker height index, $H_b/H_0'$, is a function of $H_0'/\lambda$ and of tan B (Iversen, 1953). $H_b$ is the significant breaker height; $H_0'=K_r H_0$; $K_r$ is a refraction coefficient; $\lambda = gT^2/2\pi$ and $H_0$ are the deepwater wavelength and waveheight, respectively; $H_0'/\lambda$ is a measure of the incident wave stability; and tan B is the shoreface slope. The breaker height index was computed from empirical results of Goda (summarized in U.S.A. Coastal Engineering Research Center, 1973, figure 2-65), and refraction coefficients, $K_r$, were obtained by graphical refraction analysis for all directions of incident wave approach and representative values of incident wave period, following standard procedures (cf. U.S.A. Coastal Engineering Research Center, 1973). Examples of the refraction patterns for waves approaching from the north-northwest and from the east are given in Figure 26. For linear Airy waves, the total wave energy per unit area is given by $E=\rho gH^2/8$ and the energy flux or wave power can be shown to be $P=ECn$, where $C=[gT \tanh(2\pi h/\lambda)]/2\pi$ is the phase speed, Cn is the group speed, and $n=[1+2kh/\sinh(2kh)]/2$, $k=2\pi/\lambda$ (see, for example, Komar, 1976b, p.46). Because sediment transport is apparently governed by the rate of energy dissipation per unit bed area (Bagnold, 1963), and because the longshore transport rate is proportional to the longshore or tangential component of the wave power in the breaker zone (Komar and Inman, 1970), the components ($P_t$,$P_n$) tangential and normal to shore at the depth of breaking are among the most important measures of coastal

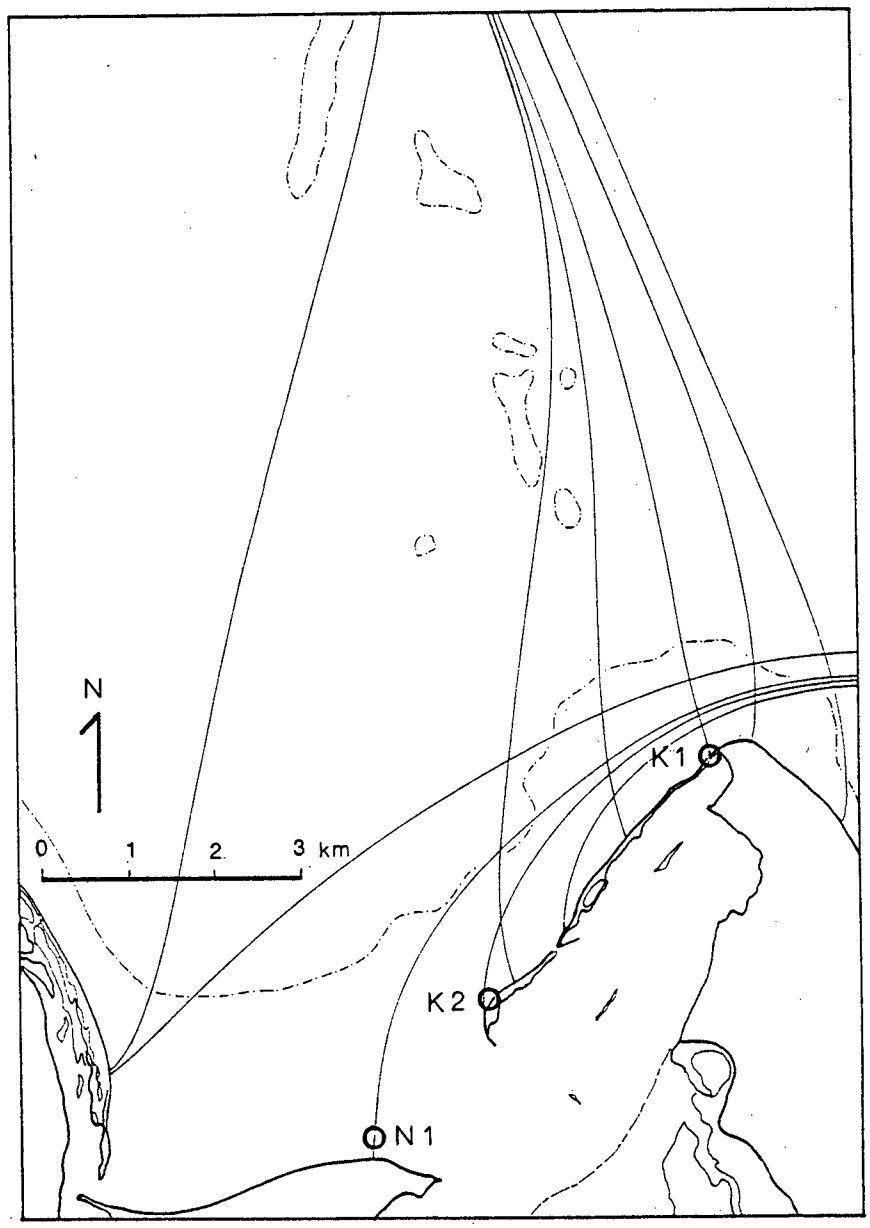


FIGURE 26

Refraction of waves at T=4.2s approaching from the NNW and of waves at T=4.9s approaching from the east; sites for which hindcast computations and longshore sediment transport estimates were obtained are also plotted.

wave climate.

The components of wave power at the breaker depth are given by

$$P_t = (E_b C_b n_b)\sin\alpha_b \qquad (2.3.4\text{-}1)$$

$$P_n = (E_b C_b n_b)\cos\alpha_b \qquad (2.3.4\text{-}2)$$

where $\alpha_b$ is the angle between the breaking wave crests and the shore; $E_b=\rho g H_b^2/16$ because $H_s \tilde{-} 1.42H_{rms}$ (Longuet-Higgins, 1952) and the energy computed from the significant wave height is therefore too high by a factor of two (Komar, 1976b, p.206); $C_b$ and $n_b$ are evaluated using the depth at breaking, $h_b$, and the corresponding wavelength, $\lambda$, obtained using empirical results for $h_b$ as a function of $H_b/gT^2$ and tan B (U.S.A. Coastal Engineering Research Center, 1973, figure 2-66) and numerical solutions for $\lambda(h)$ [tabulated by Weigel (1954) and included in U.S.A. Coastal Engineering Research Center (1973, Appendix C)].

Hindcast estimates of breaking wave conditions were generated from summer 1975 data for a site at the distal end of Kay Point spit, taking the normal component of wave power, $P_n$, positive toward shore and the tangential component, $P_t$, positive in the down-spit direction toward the estuary entrance ($\theta$ =220°T). Estimates were generated from 1976 data for the same site as well as for sites at the proximal end of the spit and along the shore of Phillips Bay west of Niakolik Point (Figure 26). A summary of the synthesized results is given in Appendix A.6.

Figure 27 is a cumulative frequency plot for components of hindcast wave power at the distal spit site in 1975 and 1976, adjusted to the common interval 19 July to 4 September (representing approximately 83 per cent of the open-water season in 1975 and about 70 per cent in 1976). The distributions are highly skewed. The skewness of the tangential components reflects the predominance of low positive values of alongshore wave power. In fact, negative values of $P_t$ had a relative frequency of 0.002 in the 1976 hindcast record and did not occur at all in the 1975 series. This result illustrates the function of coastal promontories such as Kay Point, which may operate as unidirectional gates in the littoral transport system.

The distributions of $P_n$ in Figure 27 exhibit a distinctive break between a low-power segment, $P_n \leq 200$ W m$^{-1}$, with a cumulative frequency greater than 74 per cent in both years, and a high-power segment, $200 < P_n \leq 8100$ W m$^{-1}$. The distribution for $P_n < 200$ W m$^{-1}$ cannot be resolved due to the criteria used to define events. The distributions of alongshore wave power, $P_t$, may also be divided into segments of low power ($-50 < P_t \leq 200$ W m$^{-1}$) and high power ($200 < P_t \leq 1730$ W m$^{-1}$), the former encompassing more than 92 per cent of the hindcast record in both years. If the wave climate is considered on an annual basis, the incident wave power may be negligible, $P=0$ W m$^{-1}$, for as much as 85 per cent of the year, due to the presence of sea ice.

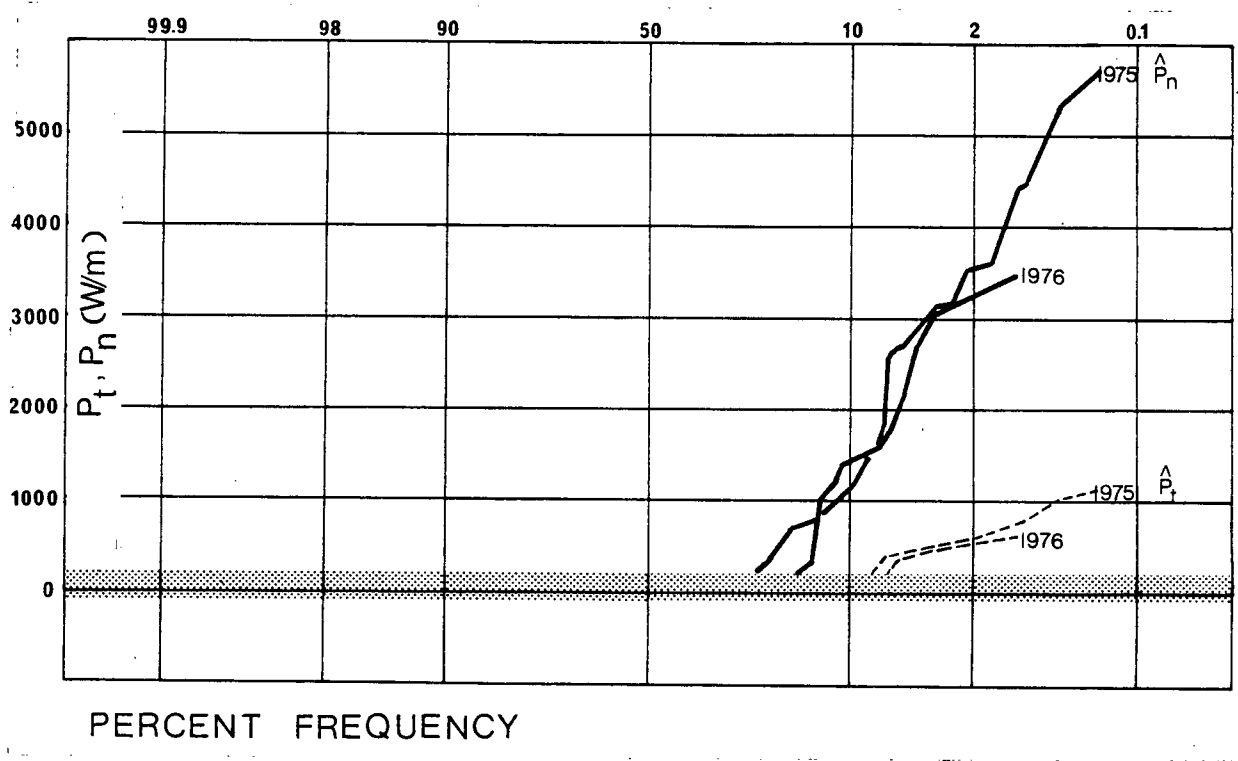


FIGURE 27

Frequency distributions of tangential and normal components of wave power at the distal end of Kay Point spit, based on hindcast wave analysis; shaded area represents portion of the distribution which cannot be resolved.

# 3 HYDROLOGICAL SUBSYSTEM

## 3.1 FRESHWATER INPUTS TO THE ESTUARY

### 3.1.1 RUNOFF AND PRECIPITATION INPUTS

Freshwater runoff can exert a profound influence on the hydrology of an estuary to which it drains (Simmons, 1955), affecting water chemistry, flood levels, circulation dynamics, and dispersion of salt, sediment, and pollutants. The importance of the runoff input to the estuary depends, in large part, on the rate of discharge relative to the tidal prism (volume of water added from ocean reservoir to estuary storage during a flood tide) and to the total storage volume of the estuary.

The surface area draining to the Babbage Estuary is approximately 5000 $km^2$, of which about 4200 $km^2$ drains via the Babbage River through section B1, 700 $km^2$ drains via Deep Creek through section D1 (see Figure 2 for section locations), and the area draining directly to the estuary (contributing runoff unaccounted for by discharge through the B1 and D1 gauging sections) is taken as 100 $km^2$. The character of the two basins contributing gauged runoff is summarized in Table 9.

During three years of record (1974-1976), the observed daily total runoff volume from the Babbage River and Deep Creek ranged between 0.0 and $5.3 \times 10^7$ $m^3$ (Figure 28). This compares

TABLE 9

Summary statistics for catchments draining to Babbage Estuary

| | Deep Creek above delta[1] | Babbage River above delta |
|---|---|---|
| Total area, A | 700 $km^2$ | 4225 $km^2$ |
| Area of lakes[2], $A_L$ | 28 $km^2$ | 16 $km^2$ |
| $100(A_L/A)$ | 4 % | 0.4 % |
| Area of icings[3], $A_I$ | 0 $km^2$ | 12 $km^2$ |
| $100(A_I/A)$ | 0 % | 0.3 % |
| Basin relief | 530 m | 1300 m |
| Hypsometric integral[4], $r_H$ | 0.21 | 0.29 |
| Circularity ratio[5], $r_C$ | 0.26 | 0.43 |

Sources: McDonald and Lewis (1973, p. 23); NTS maps 117A, 117B and 117D, scale 1:250,000; field observations.

[1] Statistics for gauged catchments not significantly different.

[2] Lakes larger than 0.2 $km^2$ in area.

[3] Estimated maximum extent of icings in late winter.

[4] Ratio of area under hypsometric curve to total area bounded by axes (Strahler, 1952).

[5] Ratio of total basin area to area of circle with circumference equal to basin perimeter.

with daily 'tidal' prism totals between 0.0 and $1.9 \times 10^7$ $m^3$ ('tidal' qualified because the maximum and minimum volumes occurred when storm-surge and fluvial effects predominated). The total storage volume of the estuary ranged between $8 \times 10^6$ and $5 \times 10^7$ $m^3$ during the same period (section 3.3.6). These data emphasize the importance of fluvial discharge, and its variability, in the regime of the Babbage Estuary; the impact of variable freshwater runoff on salinity and circulation is examined in detail in sections 3.3.4 and 3.3.5 below.

Both catchments draining to the estuary exhibit pronounced low-Arctic nival runoff regimes, in which the major variance and a large proportion of total annual runoff are concentrated in the month of June. The relatively early date of peak flow distinguishes these low-Arctic basins from higher-latitude analogues in which the major nival flood occurs in July (MacKay, 1966; Pissart, 1967; Church, 1974; Cogley and McCann, 1975). The annual hydrograph is dominated by a long period of negligible flow in winter. Four distinctive runoff seasons may be identified: (1) late-winter zero-flow; (2) snowmelt runoff; (3) summer recession; (4) early-winter recession. These periods correspond to the late-winter, spring, summer plus fall, and early-winter divisions of the hydrological year, recognized by Arnborg et al. (1966, p.202) in their study of the Colville River.

Exceptions to the late-winter zero-flow condition occur at five or more sites of groundwater discharge in the Babbage River basin. Winter groundwater discharge and associated icing

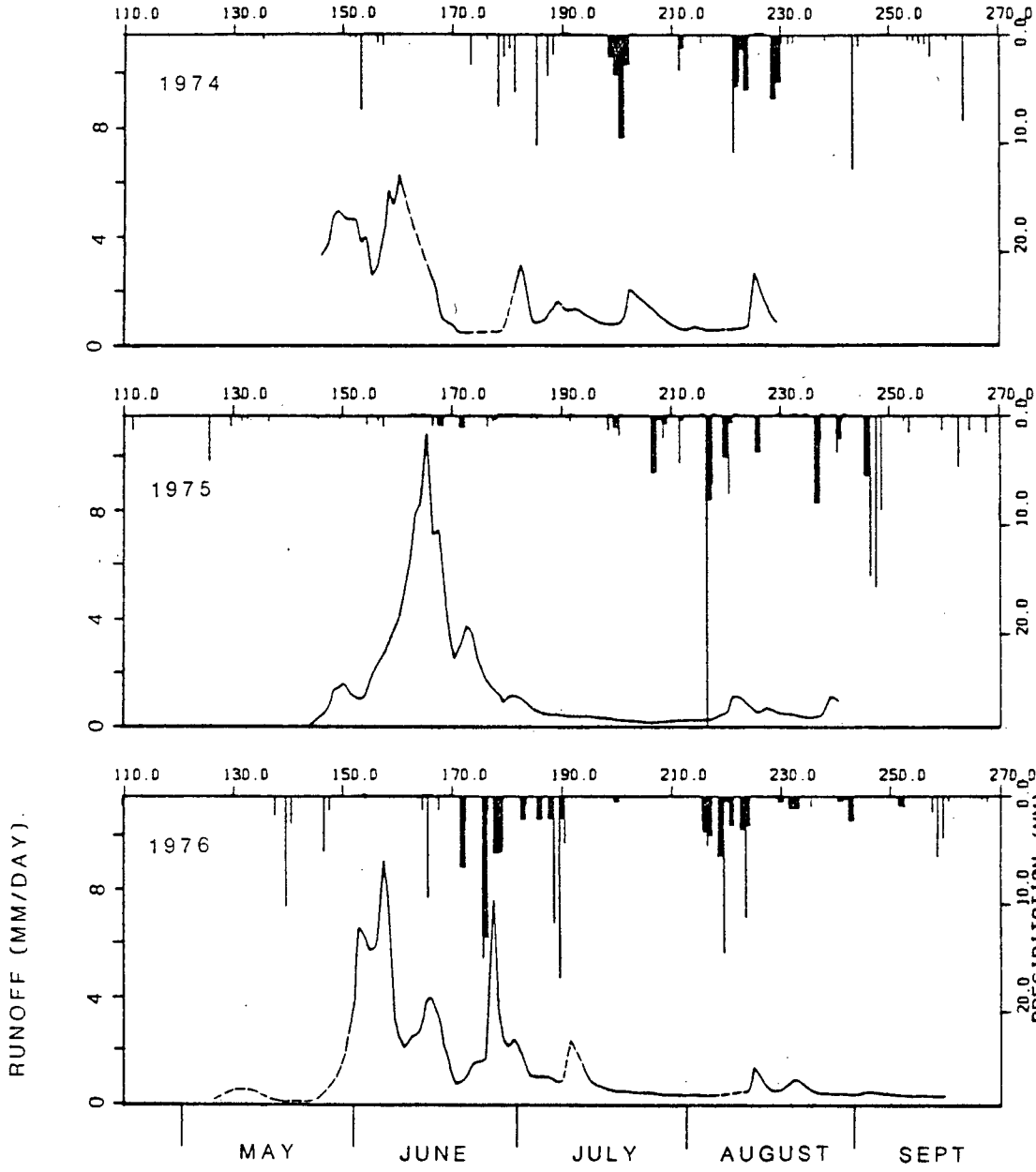


FIGURE 28

Daily runoff (Babbage River at B1) and daily precipitation at Kay Point (■) and Shingle Point (|), 1974-1976.

formation have been reported from most major catchments on the Yukon-Alaska North Slope (van Everdingen, 1974; Childers et al., 1977; Harden et al., 1977). In a few cases, most notably on the Firth and Kongakut Rivers, winter flow occurs at or near the coast. Most of the rivers, however, are believed to have zero discharge at the coast in mid- to late winter, although exceptions during rare winter rain events may occur (see below).

The snowmelt runoff season usually begins in early May with accumulation of meltwater in the ripening snowpack on and adjacent to stream channels (although in many reaches channel ice is blown largely clear of snow). The areal variability of the snowpack and surface retention capacity of the basin have been identified as major variables controlling peak snowmelt runoff on the Alaska coastal plain (Carlson et al., 1972). Runoff production may be positively correlated with air temperature and precipitation during May and June, but is primarily controlled by net radiation (Weller and Holmgren, 1974, pp.859-862; cf. Pissart, 1967, p.219). According to results of Weller and Holmgren, eddy sensible heat flux and evaporation make relatively small contributions to the total snow ablation process at Point Barrow (Alaska). On the other hand, Benson (1969, pp.33-39) reported that evaporation may be quite important, especially where the snow cover is broken by exposed tussocks or other vegetation, a common condition in the Babbage and Deep Creek basins. Furthermore, where vegetation protrudes through the snow, the albedo is greatly reduced and

absorbed radiation correspondingly increased. Under these conditions, rapid ablation may occur at air temperatures below 0°C (cf. extensive early ablation observed in northern Alaska by Holmgren et al., 1975, pp.363-364). In this case, a large proportion of the water equivalent stored in the snowpack may be evaporated (Benson, 1969, p.39) and will not be available for runoff, although some infiltration and refreezing may also occur (Pissart, 1967, p.219).

The highest observed flows in the Babbage River and in Deep Creek (Table 10) were all associated with periods of warm sunny weather and presumed high positive net radiation. The 1974 runoff in the Babbage River was somewhat exceptional in that a considerable volume of snowmelt had already been discharged at moderate flows during the 10 days prior to peak flow (Figure 28) and because the winter precipitation total was anomalously low.

In Deep Creek, the first flow occurred on June 3 in both 1975 and 1976, much later than in the Babbage River; similarly, peak discharge lagged peak flow in the Babbage by two days in 1975 and by five the following year. The 1975 hydrograph in both rivers was characterized by a single large flood, with smaller events superimposed on the Babbage River record (Figure 28). In 1976, two major floods occurred during June, but the second was primarily due to storm runoff.

If Shingle Point precipitation is taken as an index of snow storage in the basin (see section 2.2.1), snowmelt runoff

TABLE 10

Estimates of annual peak discharge, Babbage River at B1 and Deep Creek at D1, 1974-1977.

BABBAGE RIVER

| | | |
|---|---|---|
| 1974 | 380 $m^3s^{-1}$ | 9 June[ab] |
| 1975 | 554 $m^3s^{-1}$ | 15 June[c] |
| 1976 | 529 $m^3s^{-1}$ | 6 June[c] |
| 1977 | 580 $m^3s^{-1}$ | not observed[ace] |

DEEP CREEK

| | | |
|---|---|---|
| 1975 | >97.6 $m^3s^{-1}$ | 17 June[d] |
| 1976 | >63.0 $m^3s^{-1}$ | 11 June[d] |

a: peak stage estimated from debris-line elevation; discharge computed from stage-discharge relation
b: river was not observed during 11-14 June; however stage was falling on the 10th and there was no evidence on the 15th of higher levels during the preceding 5 days
c: peak discharge estimated by extrapolation of stage-discharge relation
d: maximum measured discharge; probably underestimates instantaneous flow
e: river was not observed during the snowmelt runoff; peak discharge may have been overestimated if bottomfast ice or ice-jam backwater occurred at time of peak flow

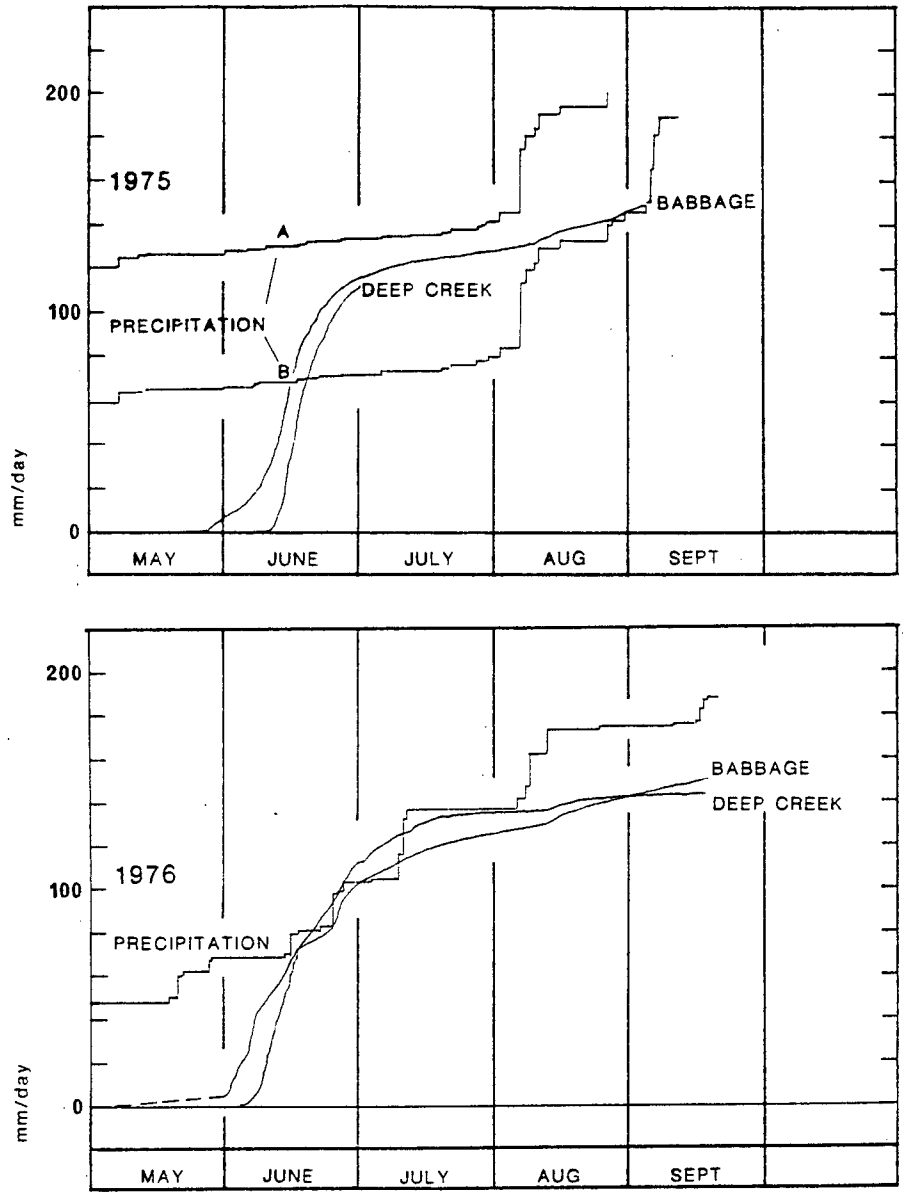


FIGURE 29

Cumulative precipitation at Shingle Point and cumulative runoff in Babbage River (B1) and Deep Creek (D1), 1975 and 1976; see text for explanation of precipitation sequences A and B, 1975.

would appear to have been largely completed by 15 June in 1976 (Figure 29). As the foregoing discussion implies, however, the available data cannot provide reliable estimates of snow storage at the start of runoff. The Shingle Point precipitation total, cumulated from 1 October 1974 (Figure 29A, sequence-A), is thought to overestimate the water equivalent of surface snow storage at the start of May 1975. If a reported reduction in snow depth of approximately 380 mm during January 1975 (Canada, Atmospheric Environment Service, Monthly Record) is assumed to have been lost through evaporation (rather than merely redistributed by blowing or by melt and subsequent refreezing), one may, as an alternative, estimate the water equivalent in storage in the basins from reported late-winter snow depths (Figure 29A, sequence-B). The reported depth of snow on the ground at Shingle Point at the end of May 1975 was 152 mm, yielding a water equivalent of 59 mm if the mean density is taken as 390 kg $m^{-3}$ (cf. Benson, 1969, figure 14). This result probably represents an underestimate of the actual volume of water stored in the basins, because snow depth and snow density are highly variable. The high frequency of blowing snow (Benson, 1969; Wendler, 1978) leads to concentration of a large proportion of total snow in drifts.

Assuming, then, that precipitation sequences A and B in Figure 29A provide upper and lower bounds on the volume of water available for runoff and that all precipitation in May occurred as snow, one may conclude that snowmelt runoff in 1975 was completed sometime between June 15 and late July: a date in

late June is considered realistic. On the 8th of June, well before peak flow in the Babbage River, the lower basin was largely snow-free. However, because the remaining snow was concentrated in drifts, the actual proportion ablated is as difficult to assess as was the original total storage volume. Furthermore, extensive standing water attested to considerable surface retention of meltwater. While surface storage may be expected to have introduced a significant lag into the snowmelt runoff process (the Babbage River peaked on 15 June, Deep Creek on the 17th), it also implies that evaporation of snow-derived water from surface storage may be an important process tending to reduce the overall runoff volume (cf. high evaporation rates in the post-melt period, reported by Weller and Holmgren, 1974, figure 7).

A marked diurnal cycle is apparent in the Babbage River runoff hydrograph during much of the snowmelt season. The time of peak flow is highly variable, depending in part on the area of the basin contributing runoff. Daily recession curves conform approximately to an exponential model

$$Q(t) = Q(t+\tau).\exp(-\tau/t^*) \qquad (3.1.1\text{-}1)$$

where $Q(t)$ is the discharge at time t, $Q(t+\tau)$ the discharge at some time lag $\tau$, and $t^*$ the recession constant. Daily recession constants for the snowmelt runoff period were in the range $33 \leq t^* \leq 86$ h. Because the effective contributing area is unknown, an appropriate normalization of $t^*$ for comparison with other basins is difficult to achieve.

The transition from snowmelt to summer recession in 1975

is believed to correspond to a pronounced change in the slope of the cumulative runoff series (Figure 29A). During the dry early summer of 1975, discharge from the Babbage River declined to $Q < 10$ $m^3s^{-1}$ (specific runoff $Q_s < 0.21$ mm/day). This is an order of magnitude less than the probable mean rate of evapotranspiration (Mather and Thornthwaite, 1956; Brown et al., 1968; Carlson and Kane, 1975). It is believed that a large proportion of the flow at this time was derived from groundwater sources, both directly from spring discharge and indirectly from groundwater stored in icings.

Icings persist until late in the summer (Figure 8A) and survive, in some cases, until accumulation begins again the following winter. A rough estimate of the maximum areal extent of icing development in the Babbage River basin under present conditions in late winter is $A_I$ =12 $km^2$ (Table 9). Assuming a mean thickness of about 1 m, the total volume of groundwater in storage at the beginning of the runoff season would be about $1x10^7$ $m^3$. If one assumes, further, that icing development occupies some 220 days, a mean groundwater discharge rate of 0.5 $m^3s^{-1}$ is obtained. Measured total discharge rates for springs at three sites in the basin range from 0.2 to 2.3 $m^3s^{-1}$ (measurements in November 1972 and April 1973 by Aquatic Environments Ltd, Calgary; cited by van Everdingen, 1974, p.88). The storage estimate appears, therefore, to be of the correct order of magnitude. Assuming that $10^7$ $m^3$ of water is released at a constant rate over 100 days during the runoff season, a constant discharge of 1.2 $m^3s^{-1}$ is obtained,

suggesting a total groundwater baseflow of $\simeq 1.7$ $m^3s^{-1}$. The volume of additional contributions from seasonal thaw in the active layer and from such sources as ice-wedge melt in cut-banks or melting of massive ground-ice in retrogressive-flow headwalls, is difficult to evaluate: neither the total volume of ice nor the effective contributing area are known. Nor are the effects of lake control, although these are believed to be negligible; lakes occupy only 0.4 per cent of the total basin area (Table 9). The runoff data suggest, however, that the sum of contributions from these sources and from groundwater is of the order of 10 $m^3s^{-1}$ in the Babbage River basin in mid-summer.

In Deep Creek, the average discharge declined to $Q<1.0$ $m^3s^{-1}$ ($Q_s$ <0.12 mm/day) during 32 days in August and September of 1976, the minimum being $Q=0.35$ $m^3s^{-1}$ on August 7. Although minor springs occur in the Deep Creek basin (Steigenberger et al., 1975, pp.217-224), no icing formation has been observed there and the baseflow in Deep Creek may be supplied primarily by active-layer storage and by thaw of wedge-ice, massive ground-ice, and segregated ice in the active layer. Lakes occupy some four per cent of the area of this basin and may play a significant role.

The summer recession in the Babbage River is characterized by a distinct diurnal fluctuation, a feature largely absent from the Deep Creek record, suggesting that the diurnal variance may be associated primarily with meltwater production from icings, in particular from the nearby Tulugaq (Crow) River

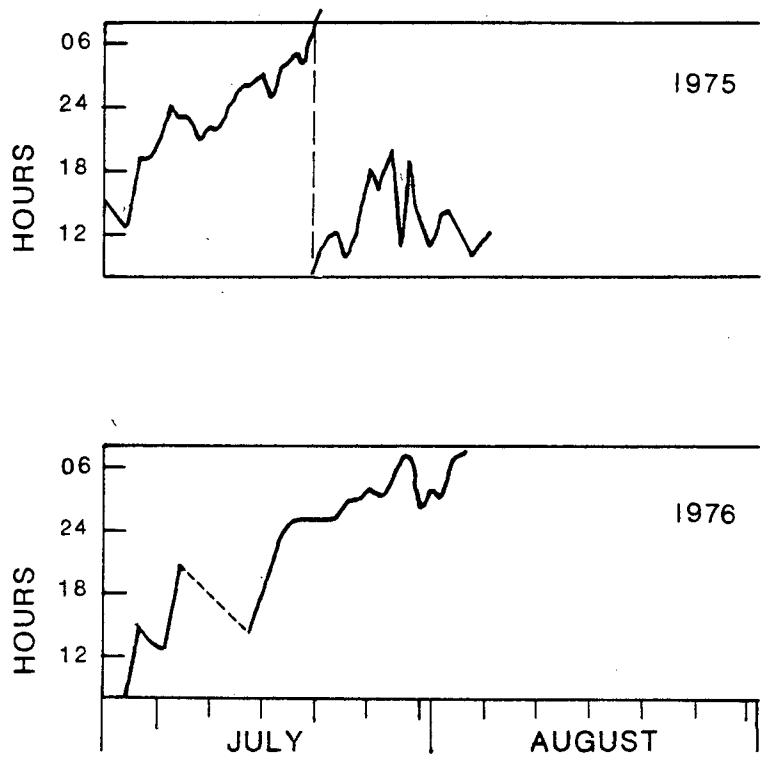


FIGURE 30

Time of diurnal peak flow during summer recession in Babbage River at B1, 1975 and 1976.

icing. As the seasonal recession progresses, peak flow tends to occur later in the day (Figure 30), reflecting greater travel times at lower flow. The diurnal recession curves in summer again conform approximately to an exponential model (equation 3.1.1-1). Although it appears to increase with time, the recession constant for the daily recession in summer is highly variable ($35 \leq t^* \leq 273$ h), in part possibly because of variable contributions to the diurnal runoff from non-icing sources at variable distances from the gauging section. However, total discharge under non-storm conditions during the summer recession is so low that the diurnal variance at this time has little impact on estuarine processes.

A more important feature of the summer flow regime is the storm runoff associated with convectional or cyclonic precipitation (cf. section 2.2.1). While the former may be highly localized and is more common over the southern part of the basin remote from the coast, the latter may deposit varying amounts of water over the entire basin. Frequently, precipitation from cyclonic systems falls as snow at higher levels and the variable lag of runoff associated with subsequent progressive rise of the melting level may be responsible for part of the attenuation and variability of $t^*$ observed in late-summer storm hydrographs.

The highest storm flow recorded in the Babbage River at B1 was $Q=477$ $m^3 s^{-1}$, during the late-spring flood of 26 June 1976 (Figures 28 and 31). The total storm runoff amounted to almost 70 per cent of the 13-mm precipitation recorded near the mouth

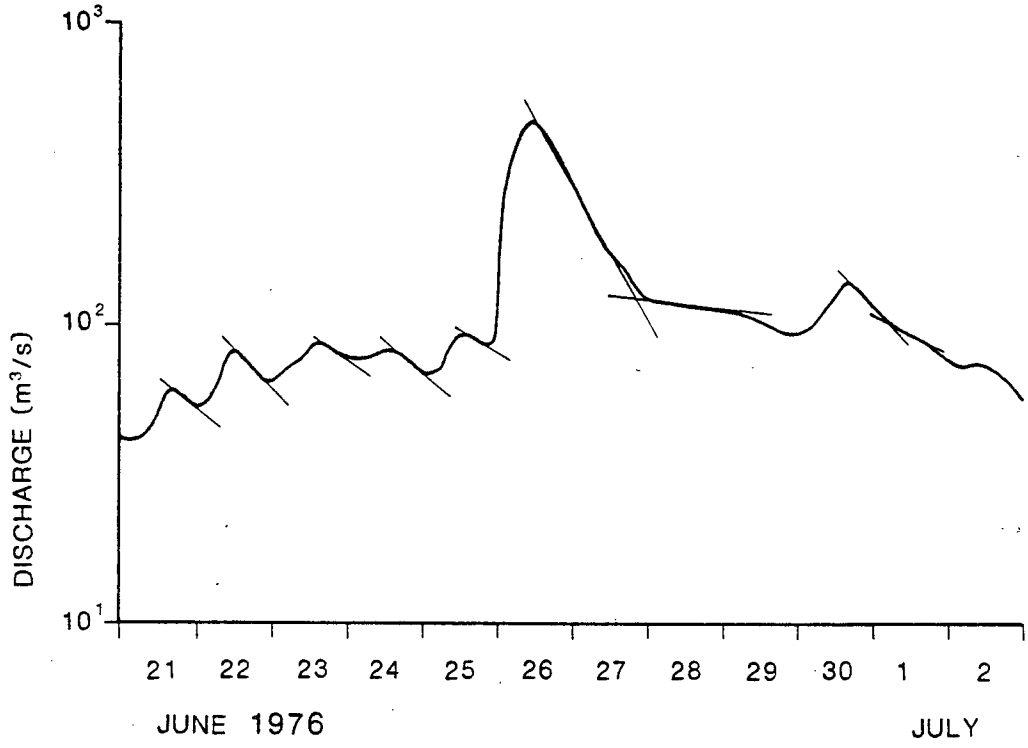


FIGURE 31

Babbage River discharge, section B1, 21 June to 2 July 1976; note exponential recessions, both diurnal- and synoptic-scale.

and 60 per cent of the corresponding precipitation at Shingle Point. Although precipitation may have been greater toward the south, these are remarkably high proportions nonetheless. Brown et al. (1968, p.10) reported runoff/rainfall ratios between 0.01 and 0.69 for a small basin, 1.6 $km^2$ in area, near Point Barrow (Alaska). A mean value of about 0.05 was obtained for summer runoff in 1966, when summer precipitation was above average. Higher proportions (with a mean value of 0.41) prevailed in 1963, an exceptionally wet year when most of the basin may have been contributing runoff. At the time of the Babbage River flood in late June 1976, little seasonal thaw had occurred in the active layer and surface storage in low-relief parts of the basin may have been partially full. It may be that the characteristic Babbage River storm response early in the runoff season is analogous to that observed under very wet antecedent conditions in the small basin near Point Barrow. It is also conceivable that some snow ablation occurred during the event of 26 June 1976 and contributed to an apparent high runoff ratio.

Smaller storm floods characteristic of late summer (Figure 28) are sometimes associated with cyclonic systems that generate positive storm surges at the coast. Although a peak flow of 226 $m^3s^{-1}$ arising from cyclonic precipitation was observed in August 1974, maximum discharge during such events is more commonly less than 100 $m^3s^{-1}$ (Figure 32). Furthermore, the storm recessions are not exponential in late summer but exhibit a progressive increase of the effective decay

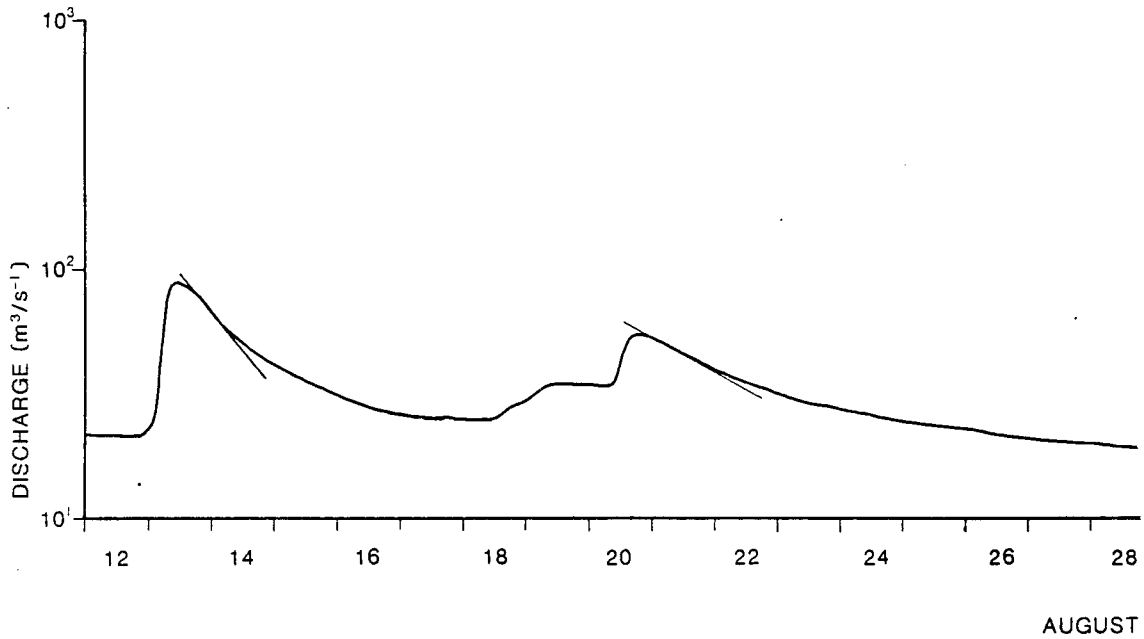


FIGURE 32

Storm hydrographs, Babbage River, August 1976, showing non-exponential character of recessions.

parameter. The final slope of the recession is nearly horizontal, as expected from small-basin studies in similar environments (eg. Brown et al., 1968; Likes, 1966). These indicate extremely large values of t*, due, it is hypothesized, to the large surface storage capacity and highly retentive sodmat characteristic of the coastal plain tundra.

In 1977, the Water Survey of Canada established a gauging station on the Babbage River below Caribou Creek. The drainage area above the station is 1510 $km^2$. Records are complete for August and September 1977 and from January 1978 on. The data suggest a highly variable snowmelt runoff response (maximum daily runoff totals of 30.8mm in 1978 and 4.25mm in 1979), in contrast to more consistent values recorded or estimated for B1 and D1 during the years 1974-1977 (Table 10). In addition, the Water Survey records indicate a major late-summer storm flood, which peaked at 388 $m^3s^{-1}$, with a daily total of 17.5mm on 28 August 1979. This was the largest flow of the year, far surpassing the snowmelt runoff peak.

The early-winter recession, the fourth division of the runoff year recognized above, is taken to begin when temperatures drop sufficiently that some storm precipitation is retained in the basin indefinitely as snow. Precipitation may fall as snow at any season; however, the probability of prolonged snow storage and associated runoff lags generally increases with time after mid-summer. Snow fell over much of the Babbage River basin during 7-9 July 1976, but daily maximum temperatures at the coast remained positive and the associated

lag in the runoff process was not great. In 1975, 43.7 mm water-equivalent, most or entirely snow, fell at Shingle Point during the period 4-7 September (Figure 29A). Although discharge records were terminated on 4 September, casual observation suggested that most of this snow remained in place for about one week before runoff occurred.

The only late-season data available for the Babbage River are the Water Survey records in the upper basin; the last dates for which increases in the daily mean discharge occurred were 26 September in 1978 and 22 September in 1979; the river ceased flowing during the first week of November in both years. Very exceptional circumstances may produce runoff much later in the winter, as in early January 1974, when 0.51 mm of rain fell at Komakuk Beach on 5 January and maximum temperatures of +5.5°C and +4.4°C were recorded on the 4th and 5th respectively. At this time, a positive storm-surge occurred (Huggett et al., 1975), the Babbage Delta area became snow-free, and the delta was partially flooded (R. MacKenzie, personal communication, 1974). A rare mid-winter runoff event may have occurred, terminating on 6 January, when temperatures at Komakuk Beach dropped to -8°C and -22°C maximum and minimum.

The frequency distribution of daily discharge for the snowmelt-runoff and summer-recession seasons (Figure 33) is highly skewed. The skewness would be substantially increased if complete runoff data for the entire year were incorporated in the analysis, because discharge during the two-thirds of the year not included is consistently low or zero. The

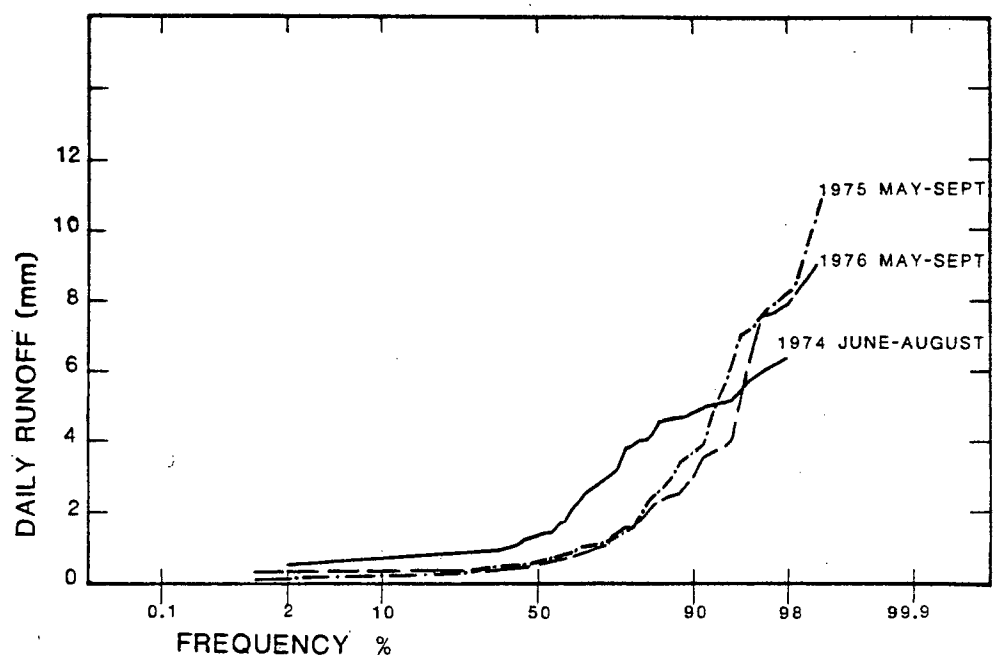


FIGURE 33

Frequency distributions of daily runoff for snowmelt and summer seasons 1974-1976, Babbage River at B1.

distributions plotted in Figure 33 may be considered to incorporate at least three separate populations: baseflow, stormflow, and snowmelt runoff. Indeed significant non-stationarity may exist in the low-flow series, as melt-derived contributions to the baseflow decline throughout the summer, while irregularities in the storm and snowmelt runoff distributions may exist due to inhomogeneities (such as varying contributing area) of runoff production (cf. Likes, 1966; Church, 1972, p.38).

Although both basins yield approximately equivalent volumes of specific runoff, the total discharge from the Babbage River is an order of magnitude greater than that from Deep Creek. Therefore it is the frequency structure of Babbage River runoff that dominates the process of freshwater supply to the estuary. It is noteworthy that considerable differences in the frequency structure of the major runoff inputs to the Babbage Estuary occur between years.

Variance density spectra for Deep Creek and Babbage River discharge are illustrated in Figure 34. Because of the high degree of non-stationarity in the snowmelt runoff portion of the discharge series, the spectral analyses did not include this part of the record and the spectra cannot be used to illustrate the year-to-year variability described above. Rather, they demonstrate the character of summer recession flow and storm runoff during July and August. Spectra for both streams exhibit an essentially monotonic increase of variance density with increasing period. The variance density varies

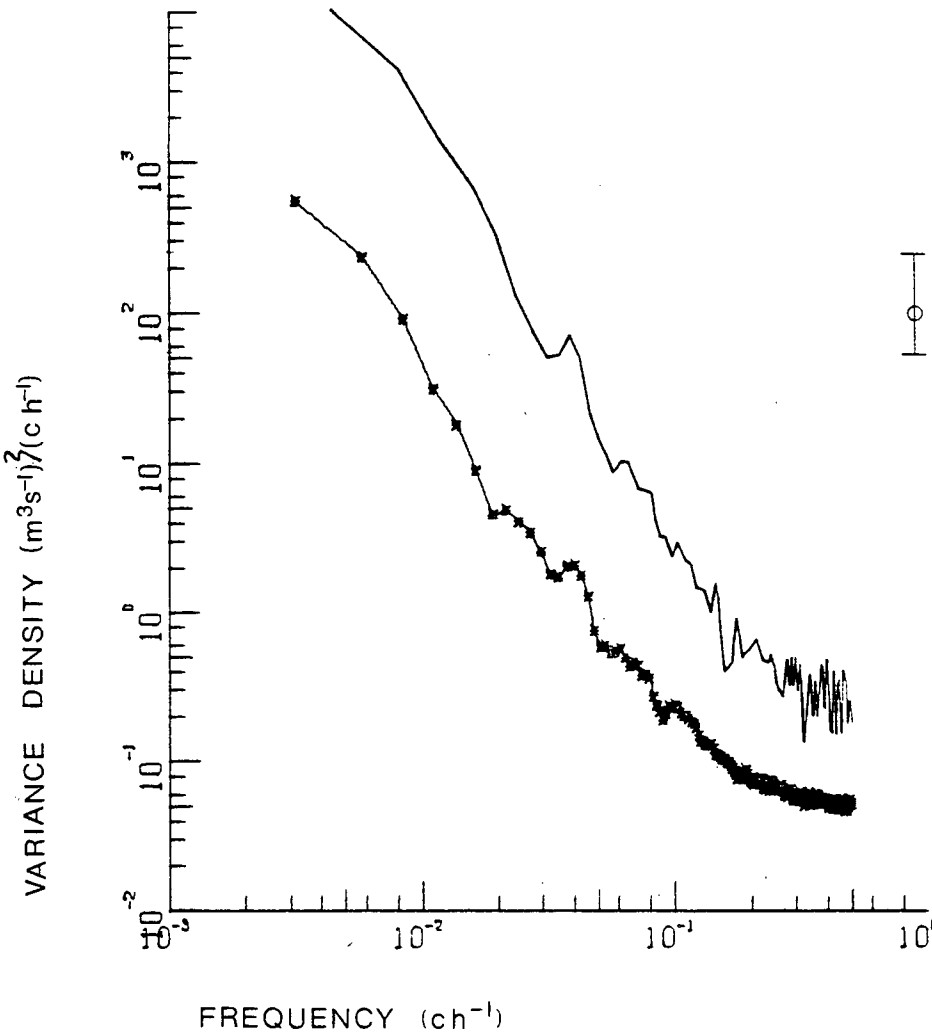


FIGURE 34

Variance density spectra of hourly discharge: Babbage River at B1, summer 1975 (——); Deep Creek at D1, summer 1976 (*—*—).

approximately as $f^{k}$, with k=-3.1 for Babbage River discharge and k=-2.3 for Deep Creek (approximate values prevailing in the frequency range $10^{-2} < f < 10^{-1}$ c $h^{-1}$). A minor peak variance density at T=24 h is prominent in the Babbage River spectrum; an equivalent feature may be present in the spectrum for Deep Creek, revealing a minor diurnal runoff cycle in that basin too. In neither case is the diurnal feature statistically significant; however, the physical reality of a diurnal fluctuation in the Babbage River is well established and a weak diurnal signal in Deep Creek is theoretically plausible, though extreme attenuation may be expected.

In concluding this discussion of the character and sources of runoff inputs to the Babbage Estuary, it may be worthwhile to re-emphasize the predominance of variance at a period of one year. The seasonal trend of runoff, dominated as it is by a very long period of negligible flow in the winter months, after which runoff increases rapidly to peak values of the order of 10 mm/day ($5 \times 10^{7}$ $m^{3}$/day), constitutes one of the overriding external controls on the circulation regime of the estuary.

The mean storage volume of the Babbage Estuary is approximately $2.4 \times 10^{7}$ $m^{3}$. This corresponds to 5.7 mm distributed over the 4200-$km^{2}$ Babbage River catchment and to 34.3 mm over the 700-$km^{2}$ area drained by Deep Creek. Total runoff from the Babbage during June in both 1975 and 1976 was between 100 and 110 mm (Figure 29) or roughly 17-20 times the mean storage volume of the estuary. Total runoff from Deep Creek in June of each year, also approximately 110 mm, amounted

to roughly three times the estuary storage volume.

Contributions of runoff from the nominal 100 km² area draining directly to the estuary and of direct precipitation on the estuary surface (mean area approximately 28 km²) may be estimated by consideration of mean precipitation for Komakuk Beach and Shingle Point (cf. section 2.2.1). Adopting a hydrological year beginning 1 October, the mean annual total precipitation amounted to 170 ±15 mm for the period October 1973 to September 1976 (Canada, Atmospheric Environment Service, Monthly Record). Assuming that 50 per cent of the total annual precipitation runs off (Brown et al., 1968, p.17), we may estimate an annual contribution from the 100-km² direct drainage area of $8.5 \times 10^6$ m³ or 0.35 times the mean storage volume of the estuary. In practice, the proportion of the total precipitation that runs off may be much less than 50 per cent, because of evaporation from the snow and from snowmelt water in surface storage (see discussion above). Total annual direct precipitation on the estuary may amount to an additional $4.8 \times 10^6$ m³. There are insufficient data to estimate the corresponding evaporative loss, which may be of the same order of magnitude. However, direct precipitation, direct drainage and evaporation from the estuary surface are all negligible relative to other terms in the water balance of the estuary (see section 3.3.6).

## 3.2 MARINE INPUTS

### 3.2.1 WATER LEVELS AT THE MARINE BOUNDARY

Hourly water levels recorded at gauge A, located on the lagoon shore of Kay Point spit near a small tidal pass (Figure 2), are illustrated in the summary time series plots of Figure 35. During the breakup period in 1976, water levels were recorded at gauge-B near Niakolik Point, due to ice conditions at gauge-A. The data indicate that high water at gauge-A lagged high water at gauge-B by some 8 minutes (mean lag for period 12-18 July 1976), while the mean range at gauge-B was greater by approximately 14mm. Tidal propagation within the estuary is considered further in section 3.3.1.

Astronomical tides are a major component of meso-frequency variance in most estuaries. The variance spectrum of water surface elevation at the Kay Point spit gauge during the summer of 1975 is illustrated in Figure 36. Significant peaks at diurnal and semidiurnal periods reflect the mixed character of the tide. Results of a conventional harmonic analysis (obtained with a modified version of the program described by Foreman, 1977, following procedures outlined by Godin, 1972) were presented in Table 7.

The semidiurnal M2 constituent is dominant in all cases, with amplitude in the range $51 \leq a \leq 84$mm. One may estimate the mean spring-tide range (Defant, 1953) as

$$R_S = 2(M2+S2) \quad (3.2.1\text{-}1)$$

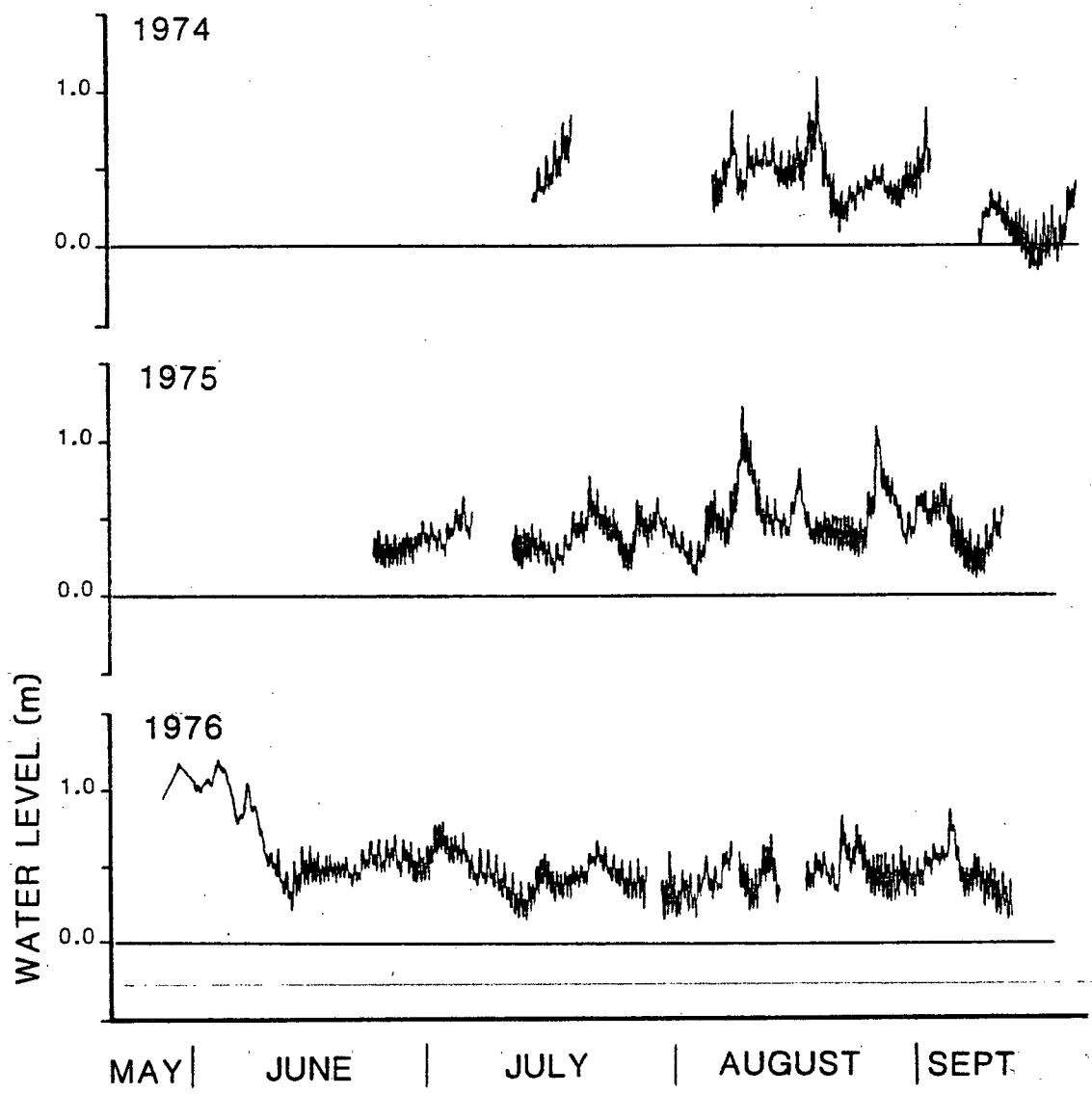


FIGURE 35

Hourly water level at marine boundary of Babbage Estuary, summer 1974, summer 1975, and breakup+summer 1976.

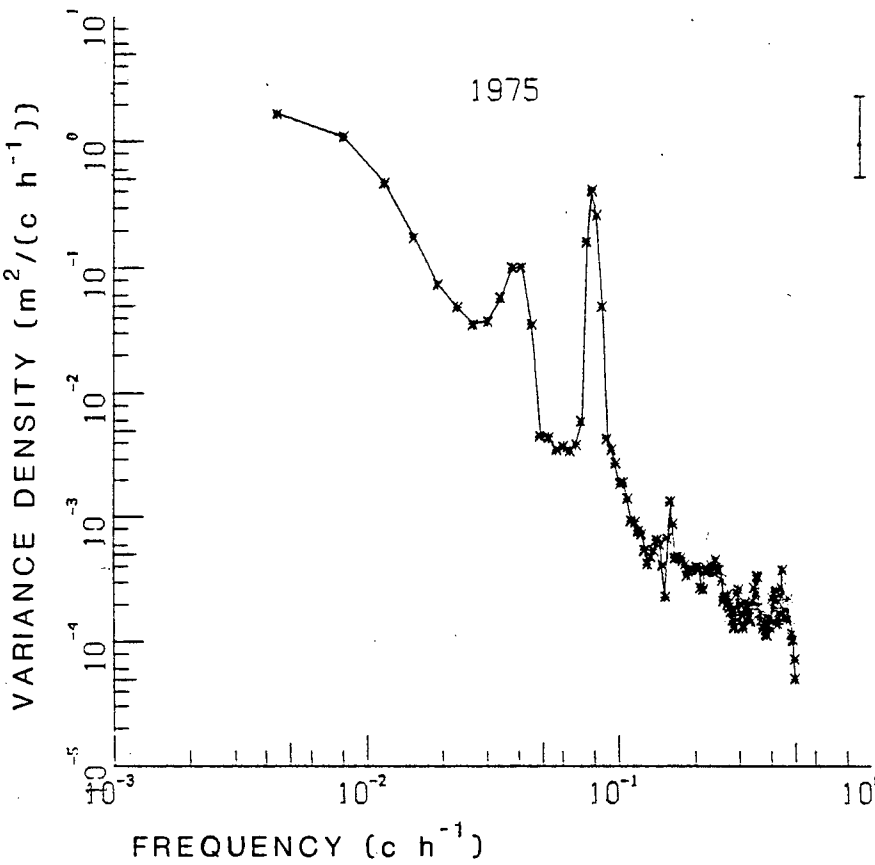


FIGURE 36

Variance density spectrum of hourly water level at Kay Point spit (gauge A, CHS station 6515), 12 July to 12 September 1975; the 90% confidence interval, assuming a chi-squared distribution with 10 degrees of freedom, is given at upper right.

TABLE 11

Major tidal constituents at Kay Point by month.

| | | O1 | | K1 | | M2 | | S2 | |
|---|---|---|---|---|---|---|---|---|---|
| | | a | g | a | g | a | g | a | g |
| August | 1974 | 35. | 167.8 | 31. | 114.2 | 79. | 239.5 | 38. | 293.8 |
| September | 1974 | 34. | 151.0 | 33. | 120.0 | 84. | 242.6 | 45. | 283.2 |
| July | 1975 | 31. | 177.1 | 32. | 153.6 | 72. | 278.5 | 34. | 329.9 |
| August | 1975 | 32. | 173.6 | 33. | 141.0 | 74. | 274.5 | 34. | 328.0 |
| June | 1976 | 28. | 170.5 | 40. | 158.4 | 51. | 289.9 | 27. | 327.8 |
| July | 1976 | 28. | 172.2 | 41. | 140.2 | 77. | 274.7 | 29. | 326.1 |
| August | 1976 | 37. | 144.8 | 25. | 139.3 | 76. | 263.0 | 37. | 312.0 |

a amplitude (mm)

g Greenwich phase lag (degrees)

all computations in GMT

where the constituent symbols denote respective amplitudes. The Kay Point records give $0.15 \leq R_S \leq 0.23$m. Clearly this site represents an extreme microtidal environment, inasmuch as locations with $R_S \leq 2$m are commonly considered microtidal (Davies, 1964; Hayes, 1979, has proposed a new limit $R_S \leq 1$ m). It is of some interest, therefore, to investigate the magnitude of tidal variance relative to variance at other frequencies and to examine the role of tide-generated processes in the Babbage Estuary system.

Seasonal variation of principal tidal constituents is suggested by the monthly analyses in Table 11. The data for June 1976 may be taken to represent a situation with extensive ice cover outside the estuary and partial ice cover within. During the other months of record, representative of the 'open-water' season (see section 2.3.2), varying quantities of ice are present in the southern Beaufort Sea. The M2 amplitude computed for June 1976 is less, and the associated phase lag greater, than in any of the open-water months, although this difference is not significant at $\alpha = 0.05$ ($U=0$, $n_1 = 1$, $n_2 = 6$; Mann and Whitney, 1947). A similar pattern has been identified by Henry and Foreman (1977) in the Tuktoyaktuk and Herschel Island data, which include winter records. Summer anomalies in the phase of M2 are about -10° at Herschel Island and -60° at Tuktoyaktuk, suggesting a relative delay of the M2 tide in winter due to the effects of sea ice. The difference between Herschel Island and Tuktoyaktuk in summer apparently reflects the smaller extent of open water west of Herschel Island (Henry

and Foreman, 1977).

Inspection of the time sequence plots (Figure 35) reveals prominent components of water level variation at lower frequencies (T>1.5 days). Indeed, these low-frequency processes dominate the spectrum of water levels, accounting for as much of 67% of the total variance in the summer of 1976 and 82% in 1975 (Figure 37). The contrast between years is striking, as is that between seasons within a given year. The differences are predominantly in the non-tidal portions of the spectrum.

A portion of the low-frequency variance in the Kay Point records is due to astronomical forcing. However, Henry (1975) noted, with reference to Tuktoyaktuk data, the great variability of computed tidal constituents at periods greater than one day and suggested the probability that meteorological effects are dominant in this frequency range. At Kay Point, the computed amplitude of the fortnightly constituent MSf was 0.06m in 1976 (Table 7), comparable to the amplitude of M2, whereas in 1975 the MSf amplitude was only 0.02m. The overall range of water level in 1975 exceeded 1.1m. Spring tides accounted only for a small portion of the total range; for example, in July 1975, the mean spring tide range was $R_S$=0.212m (equation 3.2.1-1) while the overall range for the month was R=0.625m, almost three times greater.

It is clear that non-tidal low-frequency processes account for most of the variance of water level in the Babbage Estuary.

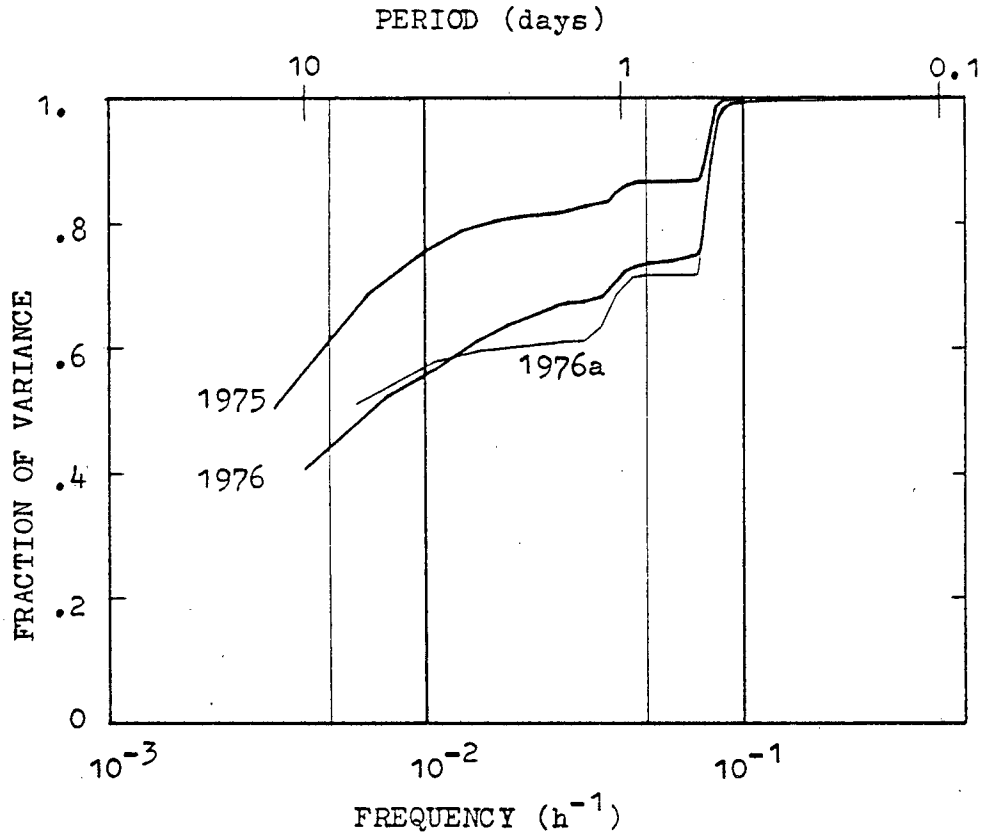


FIGURE 37

Cumulative normalized variance spectra for hourly water levels at marine boundary, Babbage Estuary; gauge-A data for 12/07/75-12/09/75 (1975) and 15/07/76-12/09/76 (1976), gauge-B data for 09/06/76-27/07/76 (1976a).

Several factors influence the low-frequency behaviour of the system. These include: bathymetry, fluvial discharge, surface slope and ice distribution in the estuary, specific volume of the water column, atmospheric pressure, wind stress, and the character of circulation in coastal waters of the Beaufort Sea. The first four factors are essentially parameters of the estuarine response to water levels imposed at the ocean boundary (see sections 3.3.1, 3.3.2, and 3.3.3). Effects of the remaining factors on the imposed water levels are discussed below.

The amplitude of the annual cycle of water level is considerably less than that of synoptic-scale variability. Nevertheless, at a period of one year, specific volume (or steric) fluctuations and hydrostatic pressure effects are known to occur in the Beaufort Sea. The annual range of monthly mean sea level at Tuktoyaktuk is approximately 0.44 ±0.03m (based on six years of relatively complete record in the interval 1961-1975). A maximum seasonal-scale range of 0.43 m was reported at Point Barrow by Beal (1968), who accounted for most of the variation in terms of a 0.23-m steric difference and a 0.10-m hydrostatic pressure effect (due to an observed difference of 1 kPa in the mean atmospheric pressure between summer and winter). In the same paper, Beal (1968, figure 10) reported data from Mackenzie Bay indicating a summer steric anomaly of +0.21 m, equivalent to the value obtained by assuming an 8-m annual range in the depth of the halocline and a density difference $\Delta\rho$ = 25 kg $m^{-3}$ between surface and

underlying water (Henry, 1975). The annual fluctuations of specific volume and hydrostatic equilibrium are generally in-phase, both atmospheric pressure and surface water density being lower in summer.

The Babbage Estuary and most shallow lagoons along this coast are largely frozen to the bottom in mid- to late winter, when the annual minimum sea level commonly occurs. Therefore, annual fluctuations in the frequency of inundation of various intertidal surfaces may be less important for nutrient and sediment budgets in this environment, and in the Arctic generally, than has been postulated for mid-latitude estuaries (e.g. by Kjerfve et al., 1978). A different annual cycle dominated by spring flooding is important in some Beaufort Sea estuaries that receive major runoff inputs during the breakup season. The Babbage Estuary is such a case (see early 1976 data in Figure 35; also section 3.3.2 below).

The tidal records at Kay Point are too short to permit identification of dominant frequencies in the synoptic-scale portion of the spectrum, if indeed the system exhibits any preferred frequencies. It is clear from Figure 37 that most of the variance resides in the range $f < 0.01$ c $h^{-1}$ (corresponding to periods $T > 4$ days). A portion of this variance may relate to non-stationarity of the summer tidal record (including the annual cycle described above), but examination of Figure 35 suggests that much of it relates to synoptic events at periods $2 < T < 20$ days approximately. Atmospheric forcing, particularly in the generation of positive storm surges, is a

widely recognized process and has been well documented in the Beaufort Sea (Matthews, 1970; Henry, 1975). However, storm surges have been treated largely as transient effects and the preponderance of low-frequency variance due to atmospheric forcing throughout the records has received little attention.

Steric effects are believed to play a relatively minor role in the synoptic-frequency range. At the mouth of the Babbage Estuary, density changes as great as $\Delta\rho$ = 13 kg $m^{-3}$ have been observed over one day, associated with the abrupt rising limb of the annual salinity cycle in late July (see section 3.3.4). Fluctuations of the same magnitude can occur over intervals as short as two days in response to river floods later in the summer.

Spectral data for hourly water temperature have been obtained from 20 days of record in the estuary entrance during August 1975 (Figure 38). While the density changes relate primarily to salinity at the estuary entrance, temperature effects also play a minor role and substantial coherence between temperature and salinity spectra can be argued on physical grounds. Although the spectral density for the 1975 water temperature record is greatest at synoptic-scale frequencies, there is relatively high variance at diurnal and semi-diurnal periods also. The diurnal variance may reflect both daytime heating and tidal transport (only the latter will appear in the salinity spectrum); the narrow peak at T = 12.5 h is assumed to reflect advective transport on the semidiurnal tide.

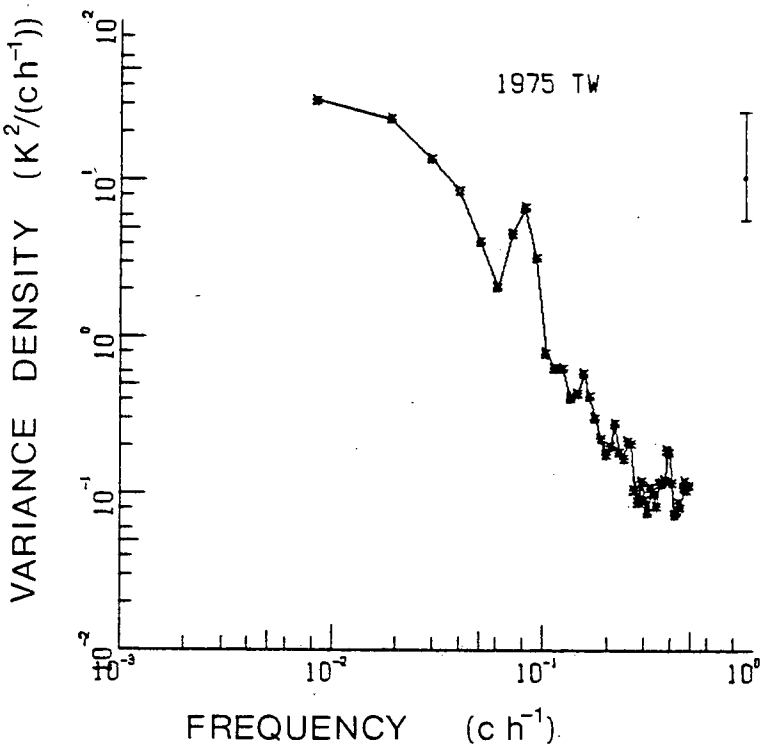


FIGURE 38

Variance density spectrum of hourly water temperature at station 5, Babbage Estuary, during 20 days of record in August 1975; the 90% confidence interval, assuming a chi-squared distribution with 10 degrees of freedom, is given at upper right.

Synoptic-scale temperature and salinity fluctuations are relatively local and are largely confined to a shallow surface layer. If we assume a uniform change $\Delta\rho$ =13.0 kg $m^{-3}$ over the Babbage Estuary and adjacent parts of Phillips Bay with a mean depth of 2 m, the steric effect can be computed for a thin single-layer case such as this without reference to pressure or dynamic units (cf. Defant, 1961, chapter 9). Taking a realistic initial density $\rho_0$ =1002 kg $m^{-3}$ and $h_0$=2 m, the mass of water per unit area is 2004 kg $m^{-2}$. If the density then increases to $\rho_1$ =1015 kg $m^{-3}$, the specific volume is reduced and $h_1$ =2004/1015=1.974 m. The maximum steric change in sea level to be expected at synoptic-scale frequencies is therefore $\Delta$ h=0.026 m, an order of magnitude less than the annual steric effect and roughly two orders less than the observed range of water levels.

The range of atmospheric pressure is approximately 4 kPa in the synoptic-frequency band. Therefore, the maximum response of water level to atmospheric pressure fluctuations is of the order of $10^{-1}$ m, assuming a hydrostatic depression of 0.1 m per 1-kPa rise in pressure. Complete hydrostatic response may not be realized at synoptic frequencies (Doodson, 1924). However, Kjerfve et al. (1978) report an amplified non-hydrostatic response in a small South Carolina estuary.

The variance spectrum of hourly pressure at Kay Point in 1976 was illustrated in Figure 17. The coherence with water level, within the synoptic-frequency range, reaches a maximum

of $\hat{\gamma}^2 = 0.64$. However, assuming a model in which water level responds to three inputs (pressure and two components of wind stress), the maximum partial coherence between water level and pressure is $\hat{\gamma}^2 = 0.35$ at $T = 3.7$ days.[1] The gain at this frequency is $|H(f)| = 0.06$, consistent with an attenuated hydrostatic response.

Smoothed versions of the 1975 and 1976 water level records, obtained using a 25-h moving average as a simple low-pass filter, are plotted in Figures 39 and 40, before and after correction for a hydrostatic pressure effect. The magnitude of the pressure correction is, in most cases, small. In 1975, the variance of observed hourly water levels, $\hat{\sigma}^2 = 0.029$ m$^2$, was reduced by approximately 14% after adjustment for pressure. In 1976, the pressure correction effected an increase in the variance from 0.014 to 0.016 m$^2$. The contrasting response is believed to reflect differences in the character, scale, or track of cyclonic systems producing northwesterly winds at Kay Point.

A strong phase correlation between the water level record and the northwesterly component of wind velocity is apparent in Figures 39 and 40. The general observation that major positive storm surges along this coast are associated with winds from

---

[1]Evidently the relatively high single-input coherence may arise because the surface wind field is coherent with air pressure. This illustrates the point that the choice of parameters is a critical issue in empirical research of this kind (cf. Båth, 1974, p.443).

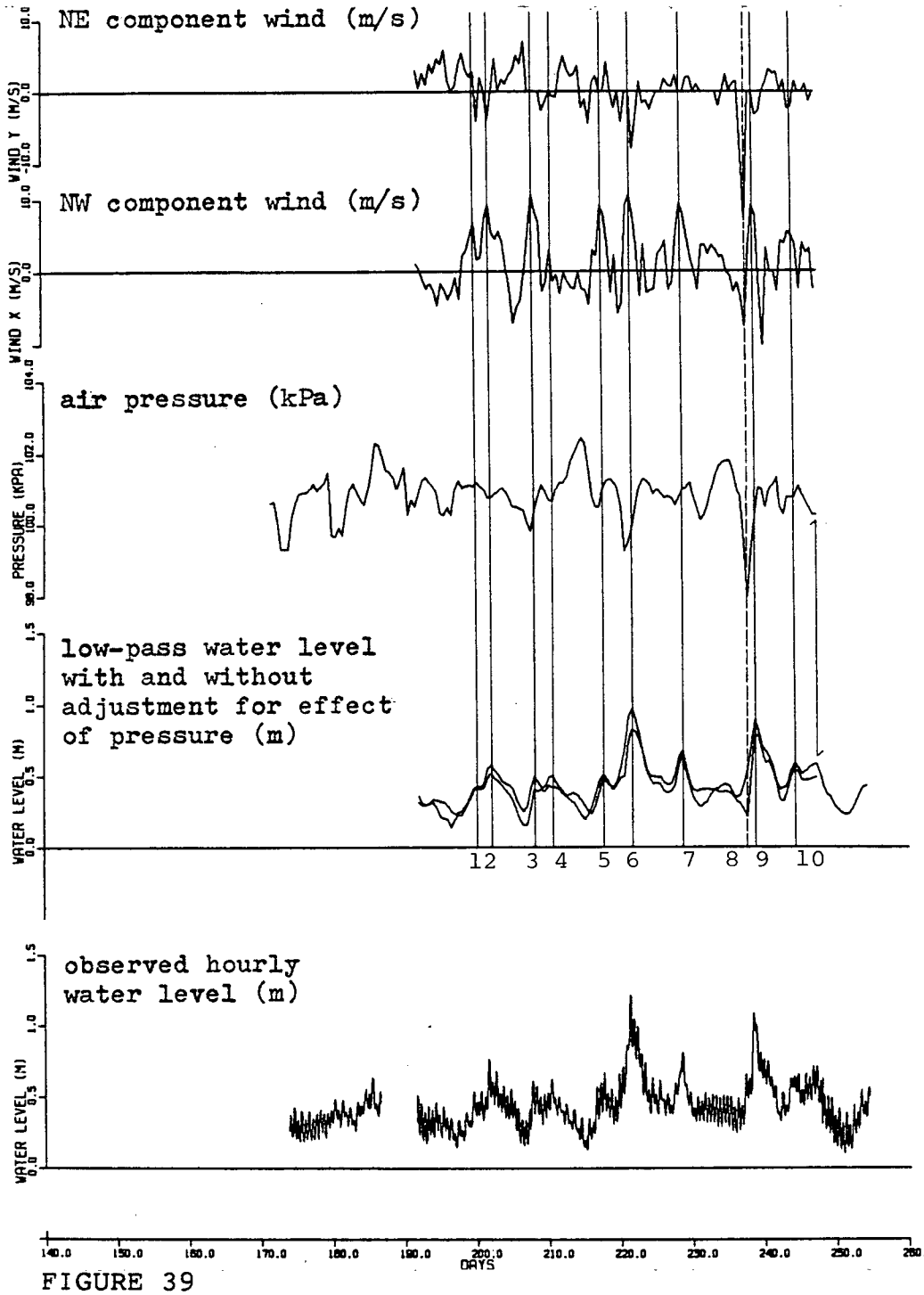


FIGURE 39

Wind, atmospheric pressure, and water level at Kay Point during 1975, illustrating phase correspondence between low-pass water level and northwesterly wind speed but variable amplitude of surge response.

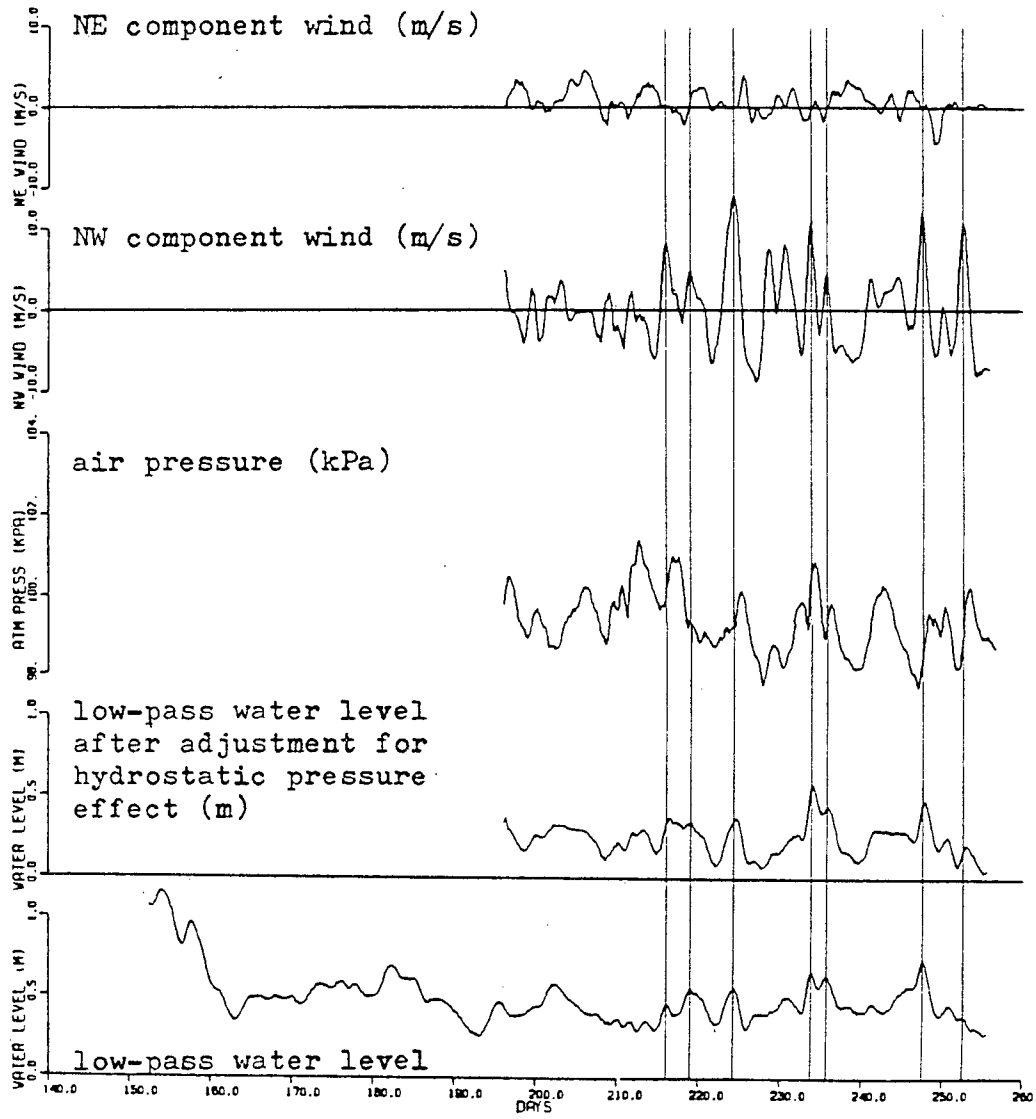


FIGURE 40

Wind, atmospheric pressure, and water level at Kay Point during 1976, illustrating phase correspondence between low-pass water level and northwesterly wind speed.

the northwest and that negative surges are associated with easterly winds, which generate an offshore Ekman transport, was mentioned previously (section 2.3.3). Data in Figures 39 and 40 appear to confirm this pattern for low-frequency fluctuations of small amplitude also.

It is the horizontal shear stress generated by surface winds that appears most directly in the coupling between atmospheric motion and water surface elevation (Groen and Groves, 1962). In the present study, northwesterly and northeasterly components of stress were computed from velocities measured at z = 10 m above the tundra surface at Kay Point. The wind stress was computed as

$$\tau_a = \rho_a C_D u|u| \qquad (3.2.1\text{-}2)$$

assuming air density $\rho_a = 1.25$ kg $m^{-3}$ and adopting a constant drag coefficient $C_D = 1.6 \times 10^{-3}$, based on results from the north Alaska coast (Wiseman et al., 1973). The variability of $\rho_a$ and the conjectural nature of the $C_D$ value, together with its dependence on wind speed and other factors, are recognized but neglected for the purpose of this discussion.

Variance density spectra for the two components of wind stress are plotted in Figure 19 (section 2.2.1). The spectrum for the northeasterly component of wind stress (normal to the coast) levels off at $T \geq 4$ days and exhibits a maximum at T = 1 day, revealing a weak land-sea breeze pattern. The variance density at synoptic frequencies is approximately two orders of magnitude lower than that of the northwesterly component. The latter has a broad maximum in the range

$2.3 < T < 10$ days, with a peak variance density at $T = 5.4$ days.

Partial coherence functions have been estimated, assuming the model outlined above, in which pressure and the two components of wind stress are considered as inputs to a linear system with output (t), the water level at Kay Point spit (gauge A). The northeasterly component of wind stress is essentially incoherent with water level at $T > 1$ day. However, the partial coherence between water level and northwesterly wind stress, (Figure 41), is maximized at $T = 3.7$ days with $^2 = 0.67$; the coherence falls off rapidly at higher and lower frequencies. It may be tempting to conclude that the system is approximately linear at $T = 3.7$ days, inasmuch as pressure exhibited a partial coherence maximum at the same frequency. In neither case, however, is the coherence estimate significant at $= 0.10$ (following Groves and Hannan, 1968, p.153), although for it is nearly so. For other frequency bands, in which the variance of water level remains high, the model is incomplete or the system highly non-linear or both. Major factors contributing to this result include: (1) the inadequacy of local point wind data to describe the wind field influencing a large-scale surge phenomenon; (2) poor correlation between winds at the coast and offshore winds; (3) additional components and nonlinearity in the system; (4) effects of variable sea-ice cover on the atmosphere-ocean coupling.

With reference to factor 3, additional components (in

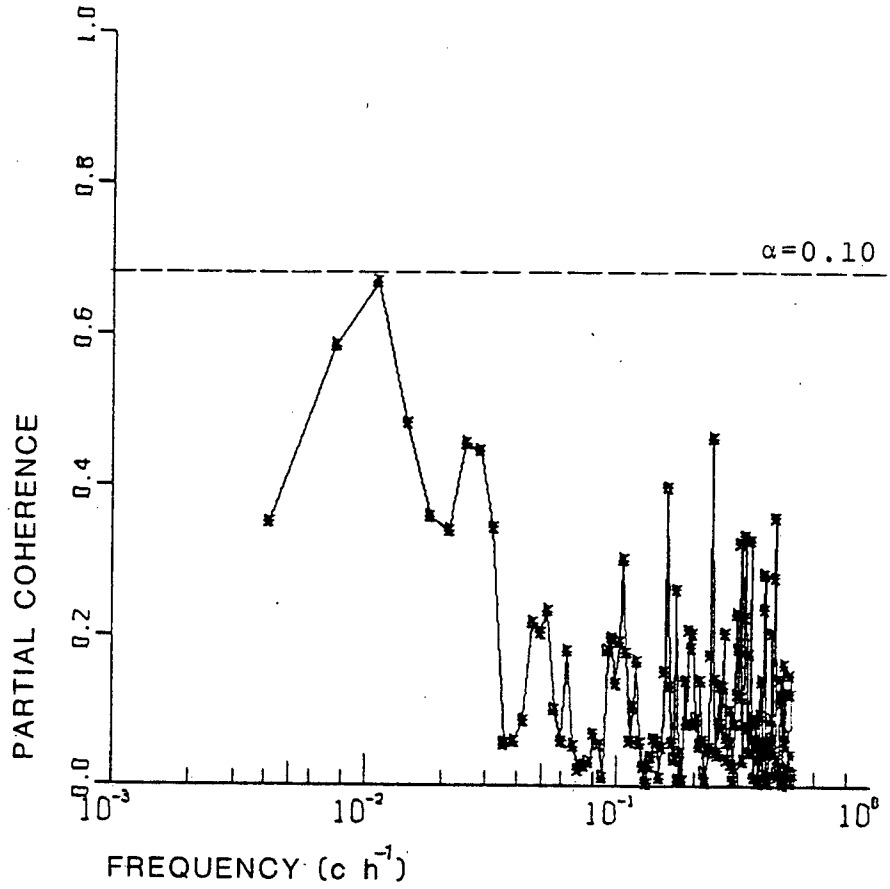


FIGURE 41

Partial coherence between water level and northwesterly wind stress, after removing effects of air pressure and northeasterly wind stress; the 10% level of significance was computed following Groves and Hannan (1968), with 8 degrees of freedom.

effect coupling terms) in the system include a volume transport (or unit-width current) q and a sea-bottom shear stress $\tau_b$. In the equilibrium case, and assuming $q = 0$ and $\tau_b = -m$ $(m<<1)$ (Bowden, 1953), the surface tilt developed in an enclosed or semi-enclosed basin of uniform depth h may be expressed as a linear function of wind stress (van Dorn, 1953):

$$\Delta\zeta/\Delta x = (\tau_a - \tau_b)/\rho_w gh. \qquad (3.2.1\text{-}3)$$

To test the hypothesis that low-frequency fluctuations of water level at Kay Point are due to local equilibrium forcing by northwesterly wind acting along the axis of Herschel Basin, assume $m=0$, $h = 20$ m, $\Delta x = 30$ km, and $\tau_a \leq 0.5$ N m$^{-2}$ ($u \leq 16$ m s$^{-1}$). The maximum rise of water level indicated by this model is no greater than 0.08 m. Clearly, equation 3.2.1-3 cannot account for many of the events illustrated in Figures 39 and 40. Most of the low-frequency variance of water level is believed to result from non-local forcing involving a volume transport $q\neq0$. Even maintaining the assumption of equilibrium response, the coupling then incorporates axial and coaxial components of q, Coriolis acceleration, and an additional non-linear function of q in $\tau_b$ (Groen and Groves, 1962).

Sea-ice is another major factor causing variable response of water level to observed weather inputs. The presence of sea-ice reduces momentum transfer from air to water and limits open-water fetch. Relatively little is known about momentum transfer through ice, particularly in the case of partial ice cover. Wind over an ice-covered sea can generate tangential

stress sufficient to produce significant storm surges, although the role of open-water leads and associated slack in the ice cover may be important (Henry and Heaps, 1976). Winter storm surges recorded in the Beaufort Sea are considerably lower than would be expected under equivalent wind stress over open water. Similar effects have been noted in the Gulf of Bothnia (Lisitzin, 1957).

It would seem that the distribution of sea ice is a major parameter of the physical system linking low-frequency variance of atmospheric and water level processes. It is a parameter that changes throughout any given year and, in the mean, between years (cf. section 2.3.2). In other words, any observable realization of the process incorporates a varying system parameter, so that the response behaviour cannot readily be evaluated.

Frequency distributions of Babbage Estuary water level were examined for a general indication of the shape of the probability function or functions that characterize the imposed water level. Distributions of daily maximum water level for the interval late-June to early-September 1974-1976 are presented in Figure 42. Whereas 1976 summer data are normally distributed, 1975 water levels are positively skewed and apparently incorporate two component distributions. The difference can be seen in Figure 39, where the first four numbered events contrast with events 6 and 9, two moderate surges in August. These latter events may have involved both larger weather systems and more extensive open water than those

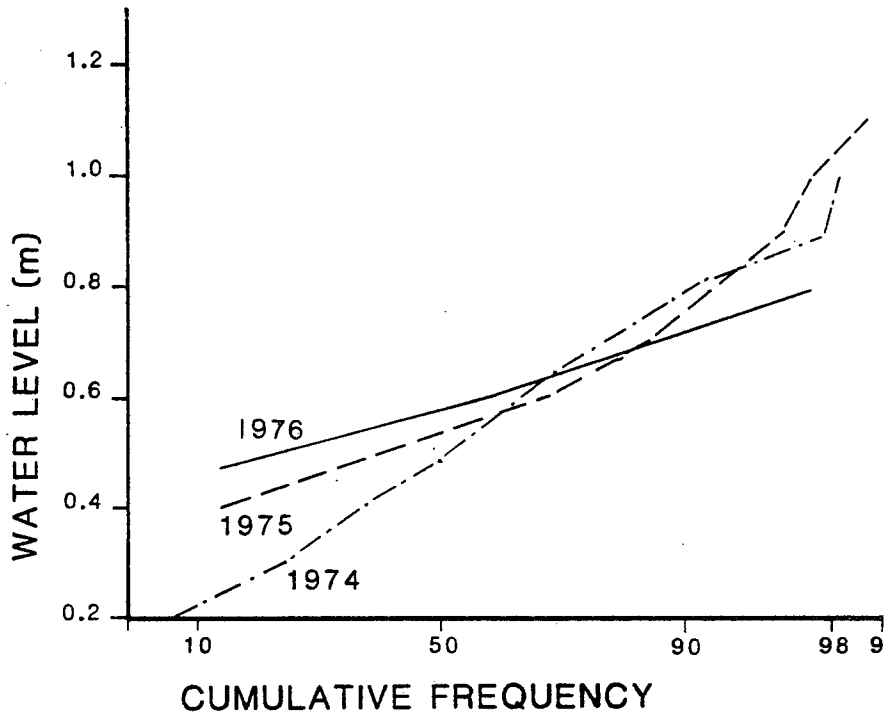


FIGURE 42

Frequency distributions of daily-maximum hourly water level for the late June to early September season in three different years, Kay Point spit data.

earlier in the season. In the case of event 3, which followed a period of easterly winds during which water levels were depressed, the northwesterly wind stress was equivalent to that during events 6 and 9, but the low-pass adjusted high water was some 0.3 m lower than during event 6. In 1974, the distribution of daily maxima at Kay Point (Figure 42) was different again, reflecting the occurrence of a minor positive surge in late-August and of persistent low water levels (a wind-induced negative surge) in early-September.

Serial correlation is present in the daily maximum series, such that the relative frequencies plotted cannot be taken as unbiased probabilities. Nevertheless, it is likely that there exist real differences in the probability distributions for different years, related to differences in the global-scale atmospheric circulation and to year-to-year variations in ice cover. Very low-frequency persistence and intermittency may be anticipated, such that the long-term variability may not be open to unbiased resolution (Mandelbrot and Wallis, 1969).

At the other extreme of the spectrum, transient high-frequency variance ($f>0.5$ c $h^{-1}$) is superimposed on tidal records from the Babbage Estuary. An example from the Niakolik Point record for 30 July 1976 is presented in Figure 43. The most prominent feature of this record is an abrupt transient of height $H = 0.11$ m, associated with a sudden wind shift and increase in $\tau_{nw}$, peak water level lagging the local wind shift by less than one hour. A similar phenomenon was observed on 6 August 1976 (Figure 44), although the lag was greater and the

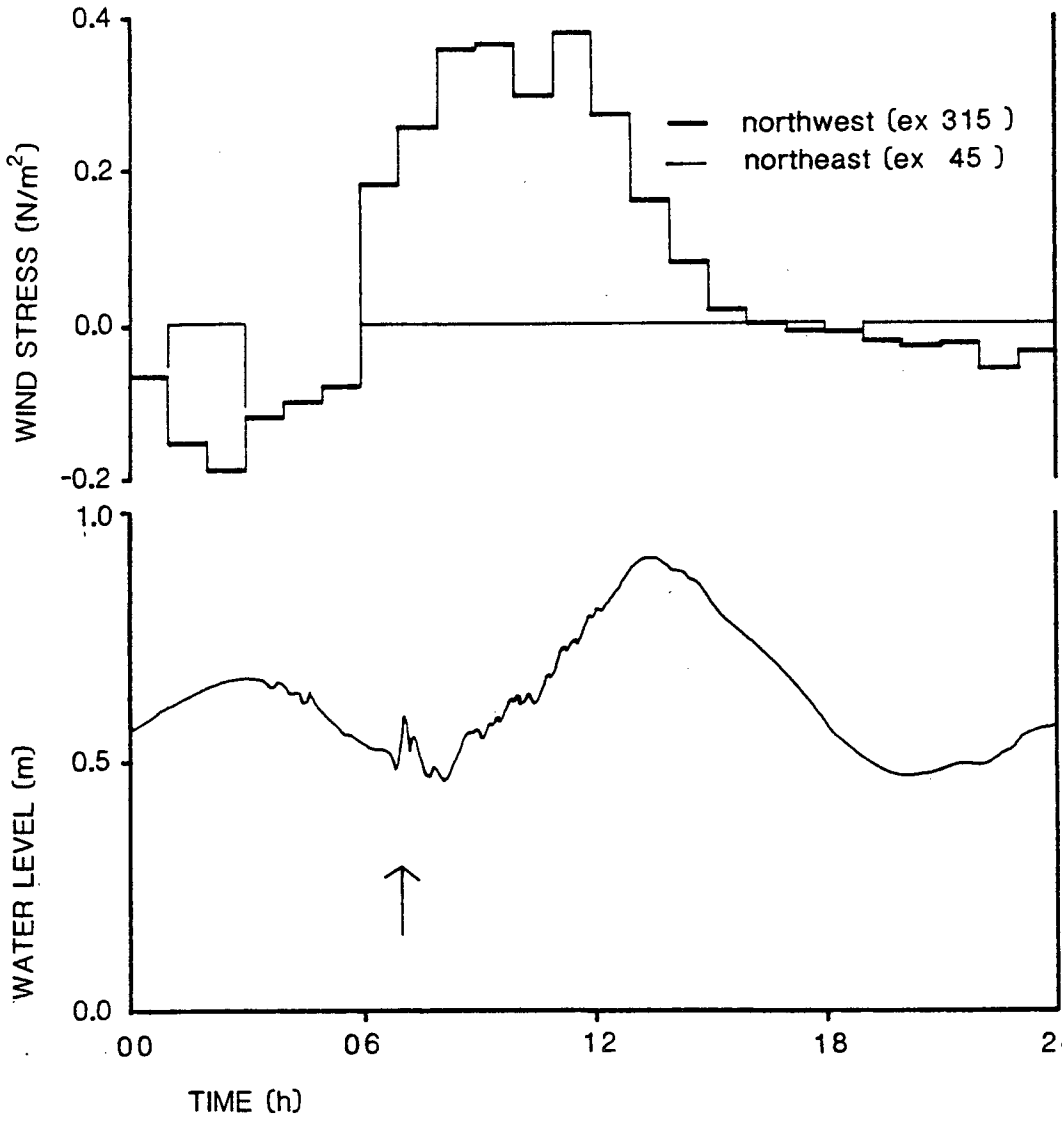


FIGURE 43

High-frequency and transient response of water level to wind associated with cold-front passage, 30 July 1976.

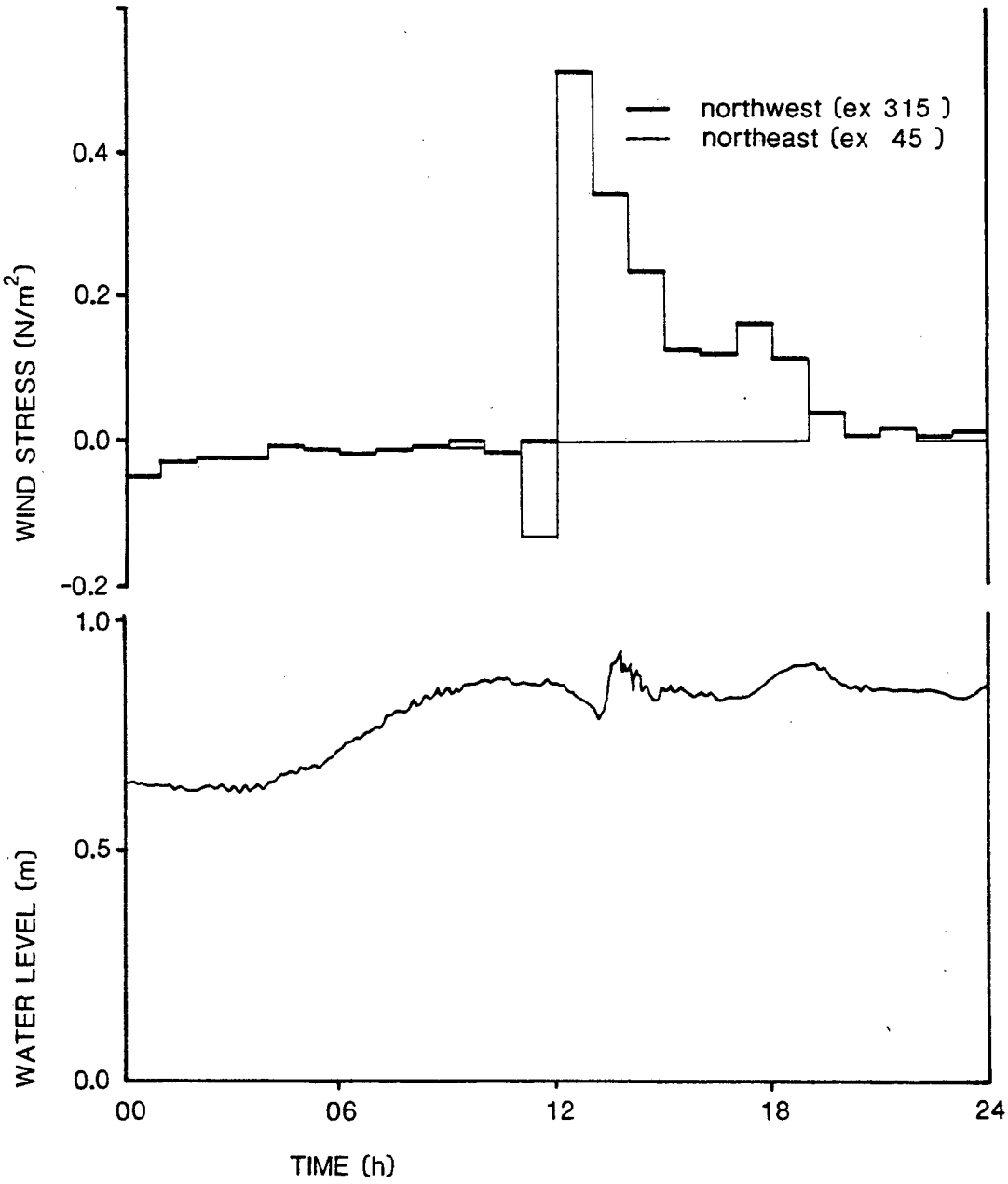


FIGURE 44

Minor surge with abrupt shock front and high-frequency low-amplitude variance superimposed on Niakolik Point (gauge-B) tidal record for 6 August 1976.

relaxation more prolonged.

The records in Figures 43 and 44 also show very low-amplitude variance with periods in the range $0.2 < T < 1$ h approximately. As is evident from the data for 6 August, these long waves are not correlated with local winds. The amplitude and frequency are consistent with a hypothesis of shelf resonance (cf. Munk, 1962). Although no particular exciting mechanism can be identified, internal waves over the shelf (or in Mackenzie Canyon) and far-field meteorological effects are plausible candidates. It is possible that this oscillation is also amplified by resonance within the Babbage Estuary (for example, within the elliptical basin south of Niakolik Point, for which a fundamental period T=0.5 h has been estimated). It is not known whether this 'surging' phenomenon has any appreciable effect on circulation in the Babbage Estuary.

In summary, variability of water level at the ocean boundary, relevant to the estuarine circulation and water budget, occupies a very broad spectral band in the range $T > 10^3$ s, the upper bound being perhaps of order $10^{10}$ s, comparable to the age of the estuary (see section 2.1.2). Annual and synoptic-scale variance related to weather effects dominate the system in the short term. If we consider tidal and higher-frequency variance as noise superimposed on a synoptic-scale signal, we obtain a signal-to-noise ratio of order $10^1$ [cf. $10^0$ for the Texas Gulf coast near Corpus Christi (Smith, 1977), $10^{-2}$ for Bermuda (Wunsch, 1972)]. Sea-ice is identified as a major factor affecting the generation of

synoptic-scale fluctuations in this region. The forcing mechanisms are identified as predominantly far-field, in the sense that they are initiated at a distance or operate over a broad region of the shelf, but local effects at high frequency may occur.

Water levels at the ocean boundary are of fundamental importance to the estuarine and deltaic systems. They represent the base level for river discharge and influence the surface slope within the estuary, such that tidal and other gravity waves can propagate into the lagoon and delta. In particular, over a range of frequencies with periods from 0.2 h to one year and longer, variations in the ocean surface elevation control the storage volume of the estuary, influence the extent of flooding in intertidal and supratidal zones, and drive a fluctuating net exchange between the estuary and Phillips Bay.

## 3.3 SYSTEM RESPONSE

### 3.3.1 TIDAL PROPAGATION WITHIN THE ESTUARY

Water level fluctuations at the ocean boundary propagate into the estuary as gravity waves, generating a cooscillating tide. In general, frequency remains constant but amplitude and phase vary in response to several effects, notably reflection, refraction, and friction, according to the detailed morphology of the estuary.

The cooscillating tide is of interest here because, under most river discharge conditions, it determines the pressure gradient and associated water transfers within the estuary; because it determines the distribution of tidal amplitudes and therefore the vertical extent of the intertidal zone; because, through its dependence on the geomorphology, it reveals a feedback process linking the hydrological and sedimentological subsystems of the estuary; and finally because the dynamics of tidal propagation provide a measure of the tidal energy available for mixing, a major factor in the nontidal circulation.

The tide undergoes relatively minor modification within the Babbage Estuary. The amplitude is reduced headward from Niakolik Point through the delta and also up the lagoon toward Kay Point. High water at gauge E (11 km upstream from the entrance section; see Figure 2 for gauge locations) lags high water at the marine boundary by roughly 50 minutes. Representative gauge-E and gauge-A (marine boundary, section

M2) records are superimposed in Figure 45 to show the minor differences in mean, amplitude, and phase. The mean water level appears to be slightly higher at gauge E than at gauge A [$(\bar{\zeta}_E - \bar{\zeta}_A)$ = 26 mm], as is appropriate for maintenance of river discharge seaward through the estuary. A more pronounced surface slope may exist during high snowmelt discharge and, of course, in the event of ice-jam backwater at gauge E.

The tidal range at gauge E is significantly less than at the marine boundary [$\alpha$ =0.025, (n-2)=134, Student's t=1.22], although the difference is not great ($R_E/R_A$=0.912). In addition, some asymmetry of the gauge-E tide is evident in Figure 45. This is a common feature of shallow-water tidal waves, due to the depth-dependence of the phase velocity $C_0=(gh)^{1/2}$. It is seen too in the delta, for example at gauge C (Figure 46), although the detailed form of the tidal curve varies considerably. Pronounced asymmetry can be seen in part of the record, notably 26-27 July, and the prolonged low tides of the 28th and 29th may represent the same phenomenon. Distortion and high-frequency fluctuations associated with weather or other effects are also present in the gauge-C data (e.g. 20-21 July, Figure 46). Note also the transient event of 30 July discussed earlier (section 3.2.1).

The cooscillating tide may be treated as a mechanical system that is excited at the marine boundary and at entry-points of tributary streams. The system has (n+m) input functions, where n is the number of tributaries and m the number of tidal inlets. The major parameters of the system

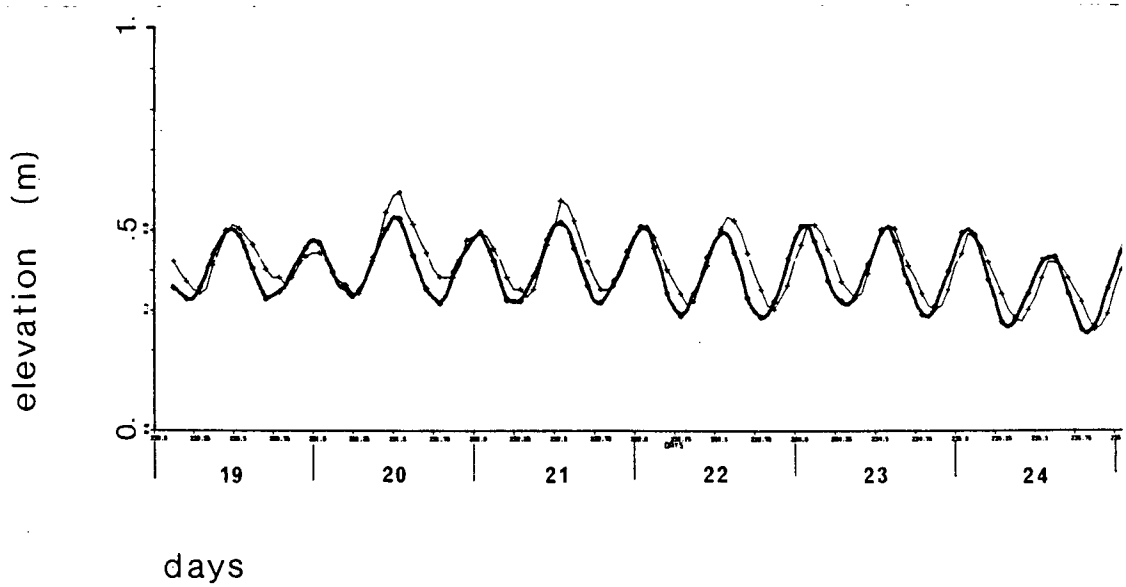


FIGURE 45

Water levels at gauge A (——) and at gauge E (——), 19-25 August 1975.

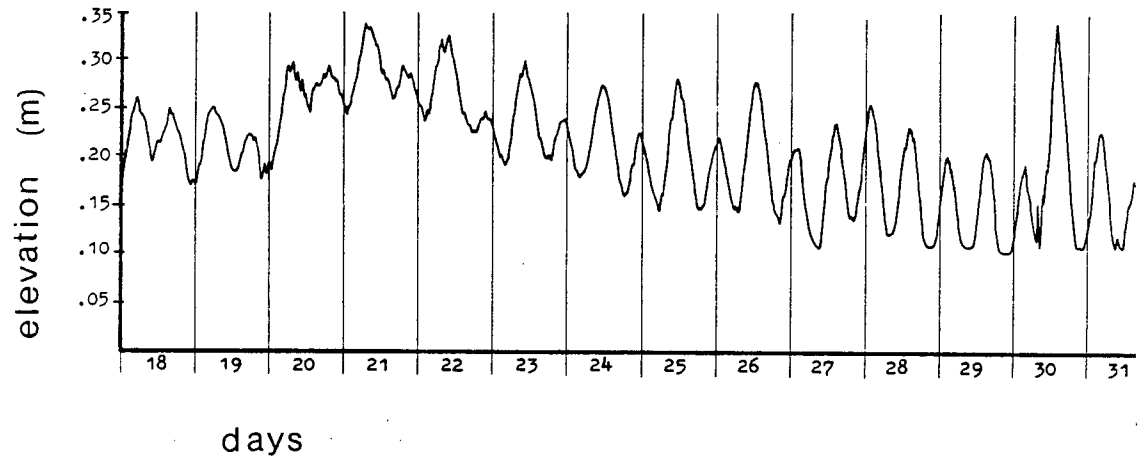


FIGURE 46

Water level sequence at gauge C, distal Babbage Delta, late July 1976.

depend on the morphology at various scales. Refraction and reflection of the tidal wave are determined by the gross morphology of the estuary, while the boundary shear and turbulent energy dissipation reflect in large part the frictional effects of small-scale channel roughness.

The cooscillating system in the Babbage Estuary can be represented by a two-input model, assuming discharge from Deep Creek and exchange flow through inlet section M2 to be negligible. The water level at gauge E may be adopted arbitrarily as the system output function, while stage at B1 on the Babbage River and water level at gauge A are taken as the input functions. Although the physical system is undoubtedly nonlinear (cf. Fjeldstad, 1929), the partial coherence, $\hat{\gamma}_p^2(f)=0.98$, between the gauge-A and the gauge-E records at T=12.5 h, computed for a sample of length N=512 h in August 1975, demonstrates that the semidiurnal tide can be represented by a linear approximation. The partial coherence function is plotted in Figure 47A, which shows also that more than 80 per cent of the residual variance is coherent at periods T>24 h, with a peak of $\hat{\gamma}_p^2(f)=0.92$ at T=2.2 days; in other words, the system behaves in a quasi-linear fashion at synoptic frequencies as well. These results accord with the reported success of linearized versions of the classical theory (e.g. Ippen and Harleman, 1961).

The partial coherence between stage at B1 (which is a surrogate, dimensionally more appropriate in this case, for Babbage River discharge) and water level at gauge E is plotted

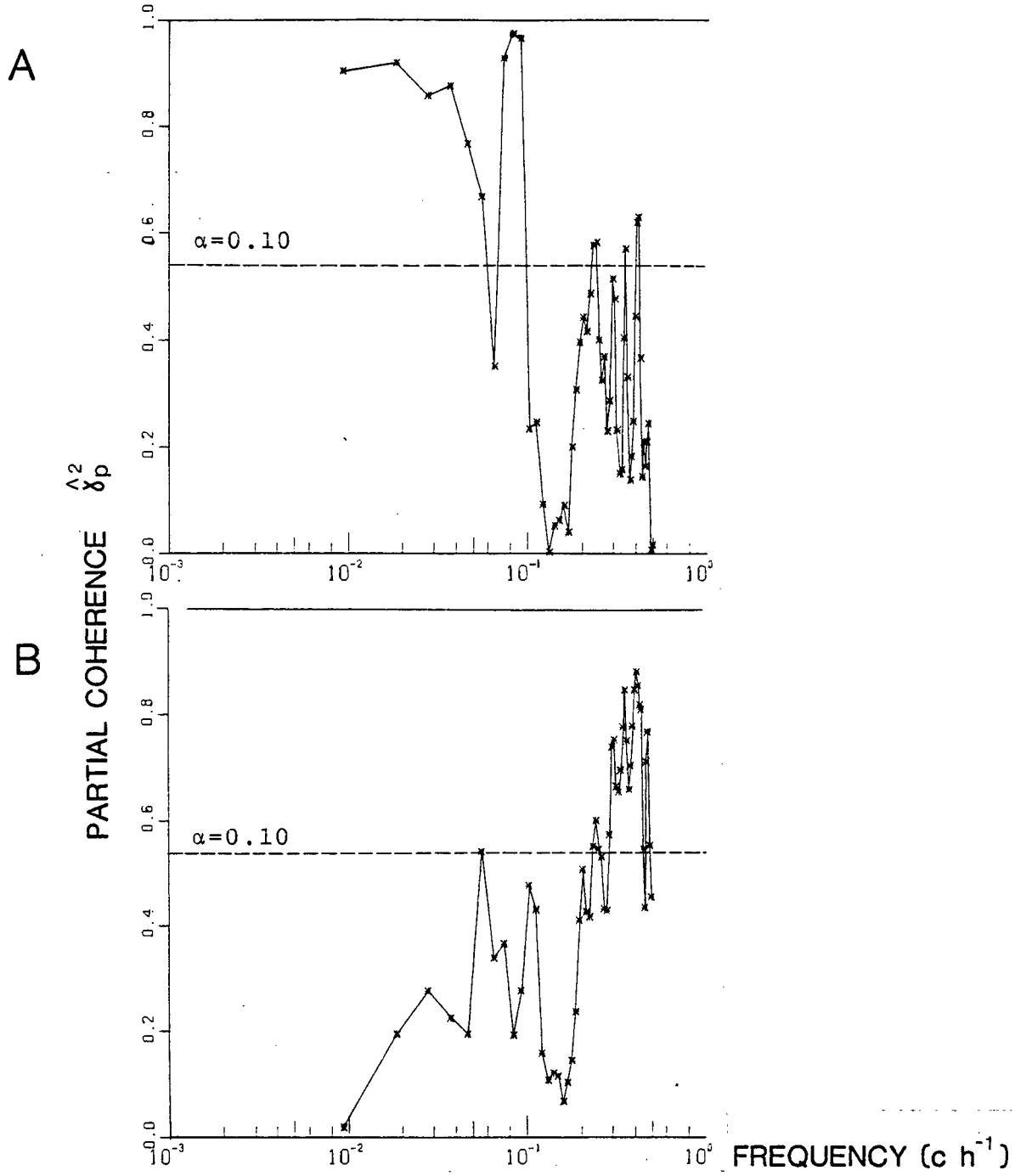


FIGURE 47

Partial coherence: (A) between gauge-A and gauge-E water levels; (B) between B1 and gauge-E water levels.

in Figure 47B. Apart from the high coherence at T<3 h, for which the output variance density is negligible, the results are not significant at $\alpha$ =0.10, and it is concluded that runoff at discharges Q<75 $m^3 s^{-1}$, the highest value in the late summer record examined here, has little effect on the storage volume of the estuary or that any such effect is highly nonlinear. This does not mean, however, that fluctuations of discharge have no influence on the estuarine circulation, density structure, or sediment transport process. The data do suggest that the cooscillating tide at gauge E may be represented by a simple single-input model with the marine boundary tide as the input.

Consider a single-input, time-invariant, linear stochastic model of the form

$$\zeta_E(t) = \int_{-\infty}^{\infty} h(\tau)\zeta_A(t-\tau)d\tau + e(t) \qquad (3.3.1\text{-}1)$$

$$= \hat{\zeta}_E(t) + e(t)$$

where $\zeta_E(t)$ and $\zeta_A(t)$ are observed water levels adjusted to zero mean ( $\bar{\zeta}_E = \bar{\zeta}_A = 0$), e(t) is a noise function, and $h(\tau)$ is the system weighting (impulse response) function. In the frequency domain, the Fourier transform of $\hat{\zeta}_E(t)$ is

$$\hat{Z}_E(f) = N^{-1}\int_{-N/2}^{N/2} \hat{\zeta}_E(t)\, e^{-2\pi fit}\, dt \qquad (3.3.1\text{-}2)$$

where N is the total length of record, $i=(-1)^{1/2}$, and f is frequency. Then

$$\hat{Z}_E(f) = H(f)\ \hat{Z}_A(f) \qquad (3.3.1\text{-}3)$$

where $Z_A(f)$ is the Fourier transform of $\zeta_A(t)$ and $H(f)$ is the system frequency response function, the Fourier transform of the weighting function $h(\tau)$ (Bendat and Piersol, 1971, p.40). The frequency response function represents the system filter behaviour, in this case the effects of estuarine morphology and channel roughness on the amplitude and phase of the cooscillating tide. The amplitude is governed by the gain function, $|H(f)|$, while the phase is determined by the argument of $H$, $\Phi(f)$.

The variance density spectrum of the estimated gauge-E water level, $\hat{\zeta}_E(t)$, computed from gauge-A data, $\zeta_A(t)$, is compared in Figure 48 with the spectrum of observed water level at gauge E, $\zeta_E(t)$. The model is relatively unsuccessful at high frequencies, $f>0.1$ c $h^{-1}$, reflecting in part the nonlinearity of the system in the range $0.1<f<0.2$ c $h^{-1}$ and in part, perhaps, the relatively high coherence with river stage at frequencies $f>0.3$ c $h^{-1}$. Within the range of frequencies containing most of the variance, however, the model is a useful representation and we may examine the response function, $H(f)$, for evidence of frequency dependence in the tidal propagation system.

The computed gain function, $|\hat{H}(f)|$, is plotted in Figure 49. The partial gain function, in which the linear effects of river stage on the gauge-E water level are eliminated, is shown not to differ significantly from the single-input simplification adopted in the model. Furthermore,

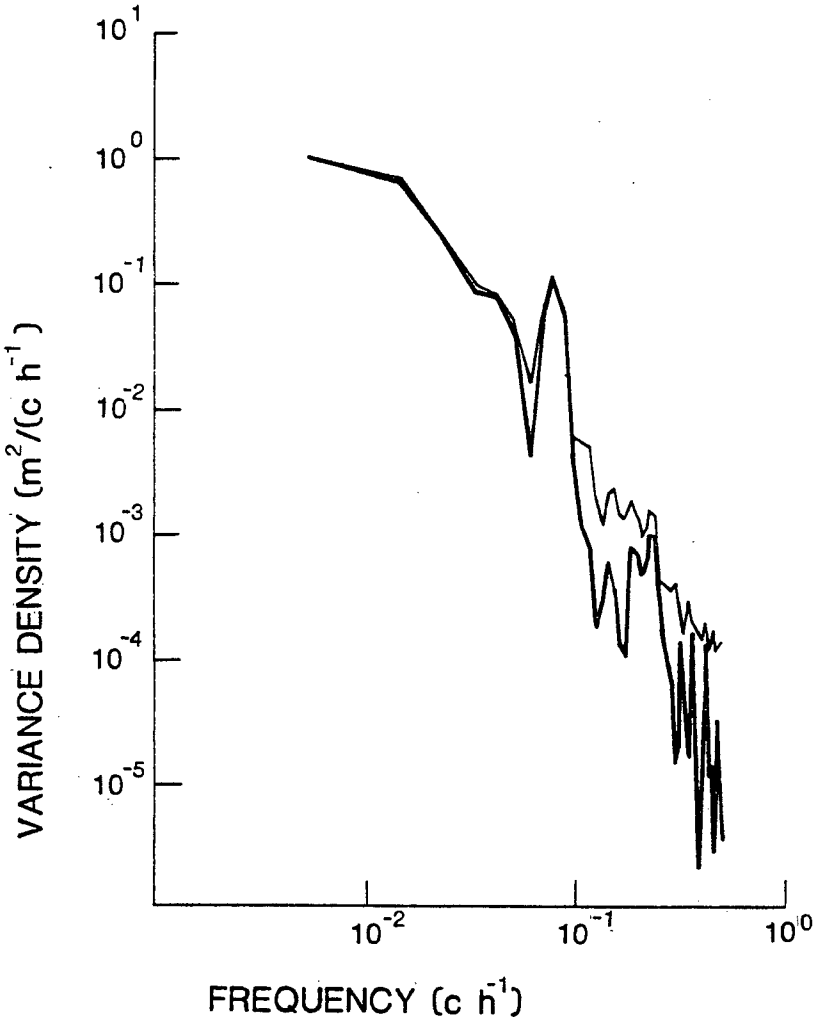


FIGURE 48

Comparison between variance density spectra of $\hat{\zeta}_E(t)$ (——) and of $\zeta_E(t)$ (——), showing close agreement at $f<10^{-1}$ c $h^{-1}$.

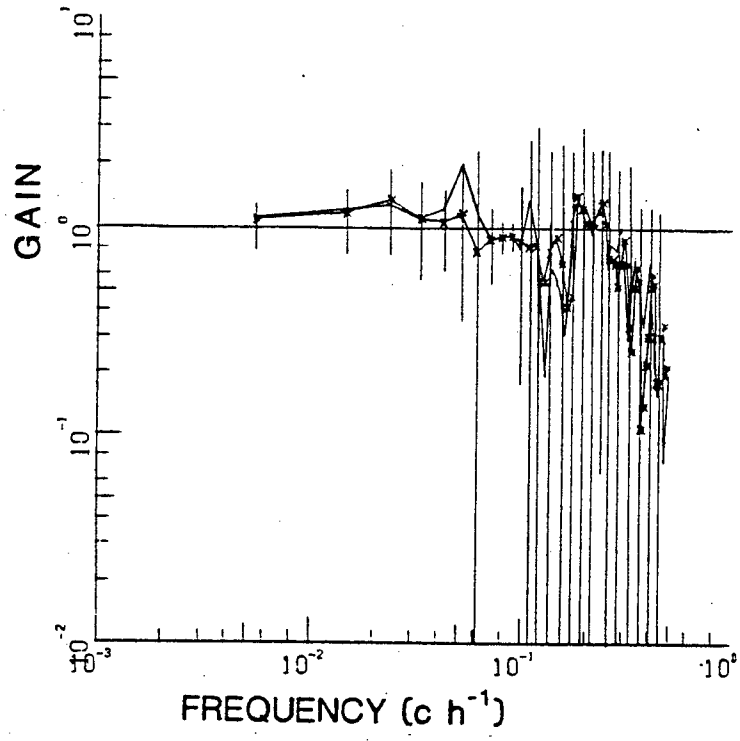


FIGURE 49

Gain function (—*—) for Babbage Estuary cooscillating tidal system; partial gain function, with effects of stage fluctuations at B1 eliminated, is also plotted (——); vertical bars represent 95% confidence limits on $|H(f)|$.

at $\alpha=0.05$, we cannot reject the hypothesis that $|H(f)|=1$ for all observed f. Nevertheless, the sample values exhibit an interesting frequency dependence. For the semidiurnal tide, $f=0.08$ c $h^{-1}$, $|\hat{H}(f)|<1$ as the earlier discussion of tidal range would suggest, given the predominance of the semidiurnal constituent M2. For $f\leq 0.05$ c $h^{-1}$ ($T\geq 20$ h), however, $|\hat{H}(f)|>1$, indicating an amplification of the tide. Indeed, some amplification is discernible at T=24 h in Figure 45 and storm surge data presented in section 3.3.2 below indicate strong amplification of synoptic-scale inputs.

The phase function, $\Phi(f)$, provides an indication of the time lag between high water at the entrance and high water at the response location as a function of frequency f. The phase lag is given by the negative of $\Phi(f)$ (Kanasewich, 1975, p.34) and we may compute the lag as

$$\hat{\tau}(f) = [-\hat{\Phi}(f)/2\pi f] \qquad (3.3.1\text{-}4)$$

(Bendat and Piersol, 1971, p.34). This function is plotted in Figure 50. Within the range of frequencies for which the linear model holds (roughly $f<0.1$ c $h^{-1}$), the mean lag is $\bar{\tau}=1.3$ h. The lag is less for the semidiurnal tide and again in the range T=1.7 days; greater for the diurnal tide and in the range T>2 days. Finally, while the phase lag, $-\hat{\Phi}(f)$, decreases with increasing period in the synoptic range of the spectrum, the time lag $\hat{\tau}(f)$ becomes greater.

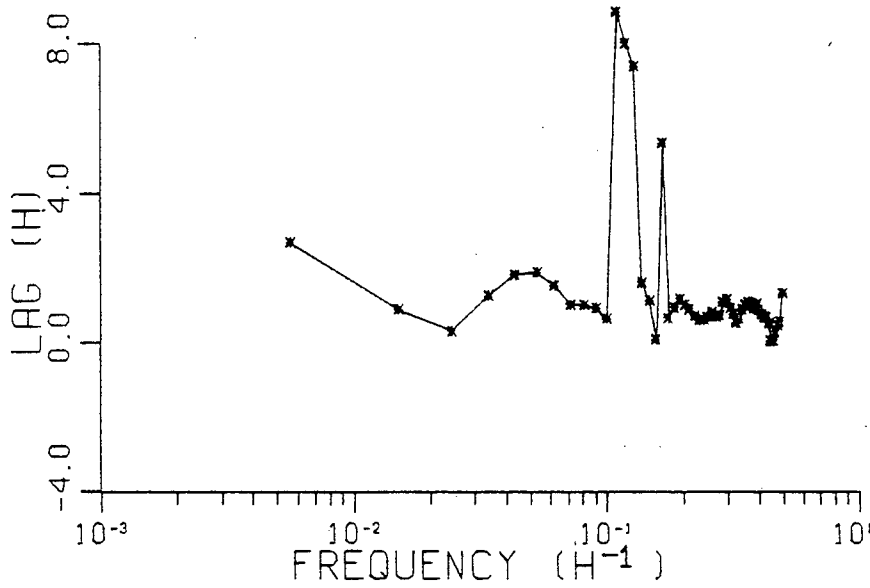


FIGURE 50

Lag function for Babbage Estuary cooscillating tidal system.

### 3.3.2 SUPRATIDAL FLOODING

The lower limit of the supratidal zone in the Babbage Estuary has been taken at $\zeta = 0.70$ m, which corresponds to the approximate lower boundary of continuous vegetation on the delta plain. Although vegetation limits may reflect a variety of physical and biotic factors integrated over time (cf. Dahlskog, 1966, p.86; Gill, 1972) and may not be related simply to parameters of the water level distribution (some colonizing vegetation appears on lower surfaces), the 0.70 m limit is equivalent to $\zeta_{97}$ for summer 1976 water levels (when meteorological effects were few and minor) and to $\zeta_{93}$ for summer 1975 (when three storm surges were recorded). It should be emphasized that the delta plain does not become extensively flooded below a level of roughly $\zeta = 0.75$ m ($\zeta_{98.8}$ for summer 1976; see Figure 51).

Supratidal flood events are generated independently by storm surges and by river flood discharge. Ice effects are important in both cases, although the circumstances differ. The generation of storm surges and the moderating influence of sea ice on surge height were discussed in section 3.2.1. While surges have been recorded in the winter months, the frequency and mean height are greatest in late summer and early fall, when ice cover in the Beaufort Sea is typically least extensive. The parameters of the flood-level distribution associated with storm surge events in the Babbage Estuary may vary with a period of one year in a pattern qualitatively similar to that of Figure 24. The frequency distribution of

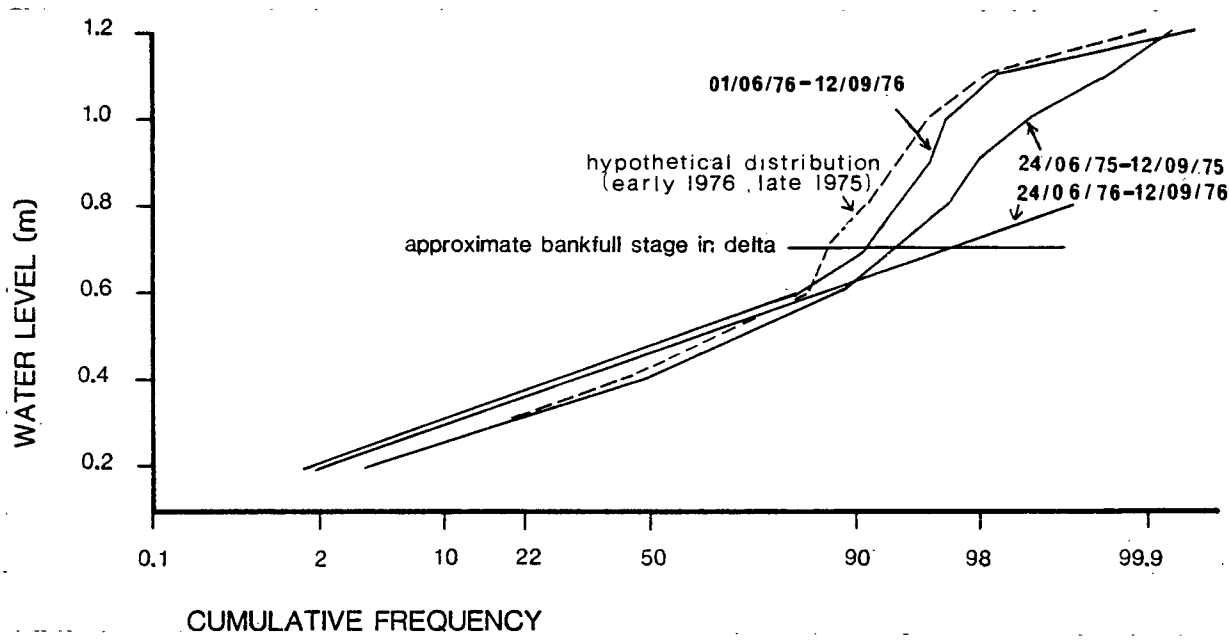


Figure 51

Complete duration sequences for hourly water level, Babbage Estuary marine boundary, summer 1975 and spring-summer 1976.

flood levels associated with high river discharge also varies on an annual cycle (major floods being largely confined to the snowmelt-breakup season) and is strongly influenced by the occurrence of ice in the lagoon, the ice in this case tending to increase the height of flooding (see below).

The approximate upper limit of recent storm surge flooding is delineated by a discontinuous driftwood deposit (Figure 52). Lower surfaces seaward of this limit include Kay Point spit, islands and shoals in the lagoon, supratidal surfaces at the north and south ends of the lagoon, and most of the Babbage Delta (Figure 53). That these surfaces are subject to intermittent flooding is apparent not only from the distribution of driftwood and other debris, but also from morphological and botanical evidence, notably the nature of thermokarst development on supratidal surfaces and the occurrence of salt-tolerant flora (see sections 4.4.2 and 4.4.4).

At the scale of Figure 53, the maximum horizontal extent of supratidal flooding is well defined. The distribution of driftwood 18 days before the major storm of 1944 is plotted in Figure 53A. Figure 53B shows the distribution approximately 28 days before the major storm of September 1970. Photographs taken in 1972 show no significant changes attributable to the 1970 storm, which was reported to have been the worst in the memory of the oldest residents of Tuktoyaktuk, although the criteria are not specified and the 1944 storm was considered almost as severe (Father LeMeur and Codex Historicus de la

FIGURE 52

Driftwood deposits marking the present transgressive limit near Kay Point (A and B) and near gauge E in the valley (C); see Figure 53B for locations.

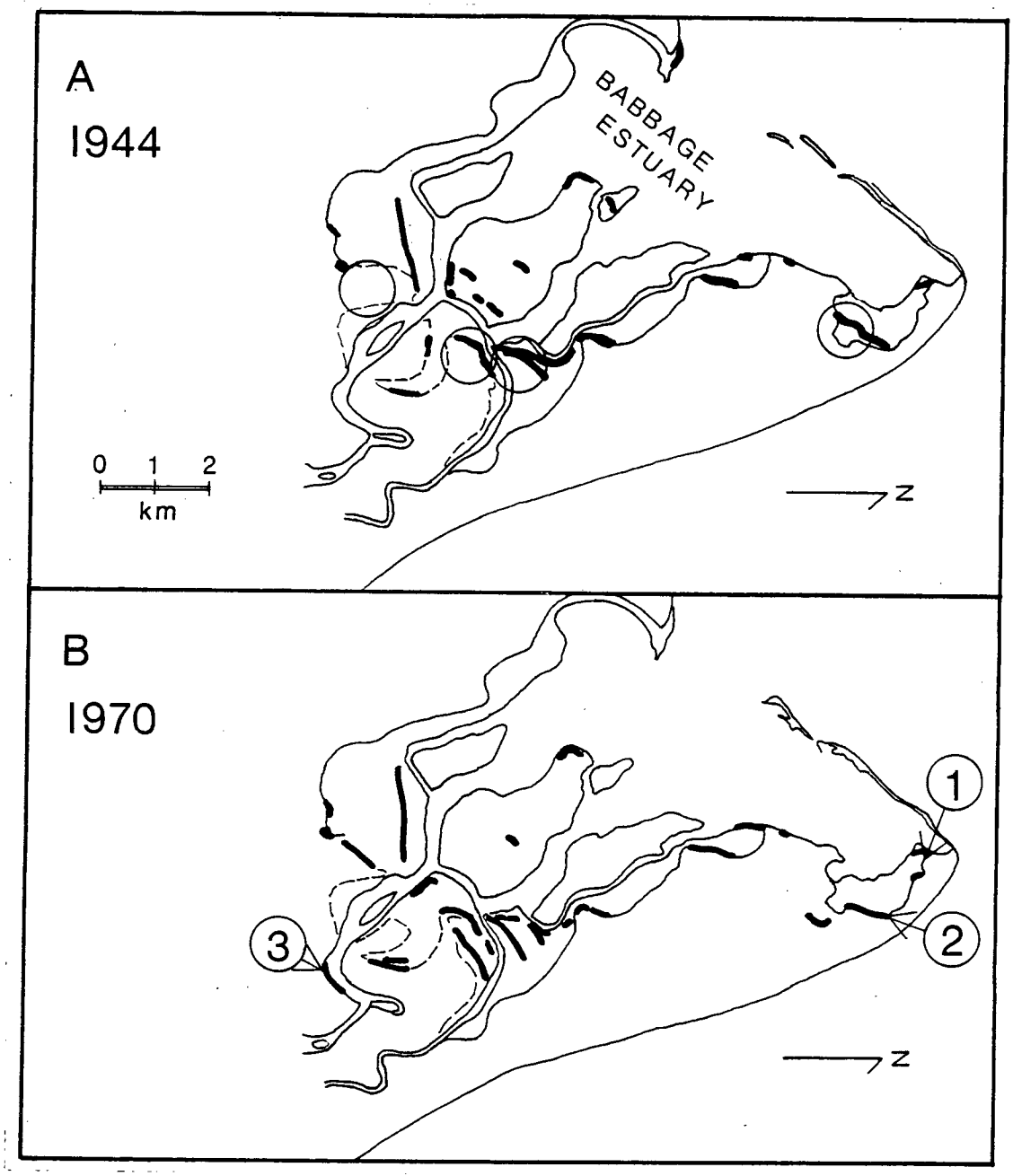


FIGURE 53

Distribution of major driftwood deposits in the Babbage Estuary system, 22 August 1944 and 20 August 1970; circles in A identify areas where major changes occurred between 1952 and 1970; circled numbers in B identify locations and orientation of photographs in Figure 52: (1) 52A; (2) 52B; (3) 52C.

Mission de Tuktoyaktuk, cited in Canada, Public Works, 1971b, pp.17 and 22). Evidence from the north Alaska coast suggests that the 1970 surge was the highest since 1889 or earlier, although a very old driftwood deposit 1-2 m above the 1970 limit has been reported in the vicinity of Harrison Bay (Reimnitz and Maurer, 1979, pp.337-338). Two major surges occurred in the Mackenzie Delta area in 1905 and 1929 (R.F. Henry, cited by Reimnitz and Maurer, 1978, p.14). However, considering the excellent state of preservation and exposure of 1944 driftwood visible in 1970 photography, one may assume that the 1905 and 1929 surges did not extend beyond the limits indicated on Figure 53A.

The extraordinary feature of the driftwood record in the Babbage Estuary is that 1952 photography shows no change from the distribution prior to the 1944 event. In short, the two major documented storms of recent decades (1944 and 1970) caused no detectable redistribution of driftwood; yet, sometime between 1952 and 1970, a substantial transgression of major driftwood deposits occurred near Kay Point and in the valley (see sites circled in Figure 53). It is considered improbable that such a change could occur as a result of snowmelt/breakup flooding (see below). The alternative hypothesis, however, is that a storm surge higher than the 1944 and 1970 events occurred on the central Yukon coast between 1952 and 1970. Anecdotal and incomplete water level data include no evidence of an exceptional surge during this interval in the vicinities of Prudhoe Bay and Tuktoyaktuk, suggesting that the extreme

flood event may be quite localized. This result raises interesting questions concerning spatial variability of flood frequency on the Beaufort Sea coast.

Although the horizontal extent of flooding in the study area is readily mapped from the distribution of driftwood on air photographs, the vertical limits are more difficult to establish. Surge propagation within an estuarine system may be treated as a cooscillation analogous to that of the astronomical tides (cf. section 3.3.1 above). In contrast to the semidiurnal tide, however, storm surges are amplified within the Babbage Estuary. This behaviour yields the positive gain observed at low frequencies in Figure 49. Data are available for three relatively small surges in August 1975 (see Figure 35). The records for the August 27 event (Figure 54) are typical: on this occasion the surge peaked at the head of the estuary (gauge E) approximately three hours later and 240 mm higher than at the spit (gauge A). The ratio of the amplitude at the head of the system to that at the marine boundary ranged between 1.20 and 1.36 for the three events of August 1975. River discharge was not a factor in this amplification: low frequency stage fluctuations at B1 were not coherent with water levels at gauge E (Figure 47B) and river discharge was consistently low ($26<Q<71$ $m^3S^{-1}$) during all three events, although minor storm runoff peaks followed the first and third surges at intervals of 16 h and 21 h after high water at gauge E.

A tentative estimate of the amplification associated with

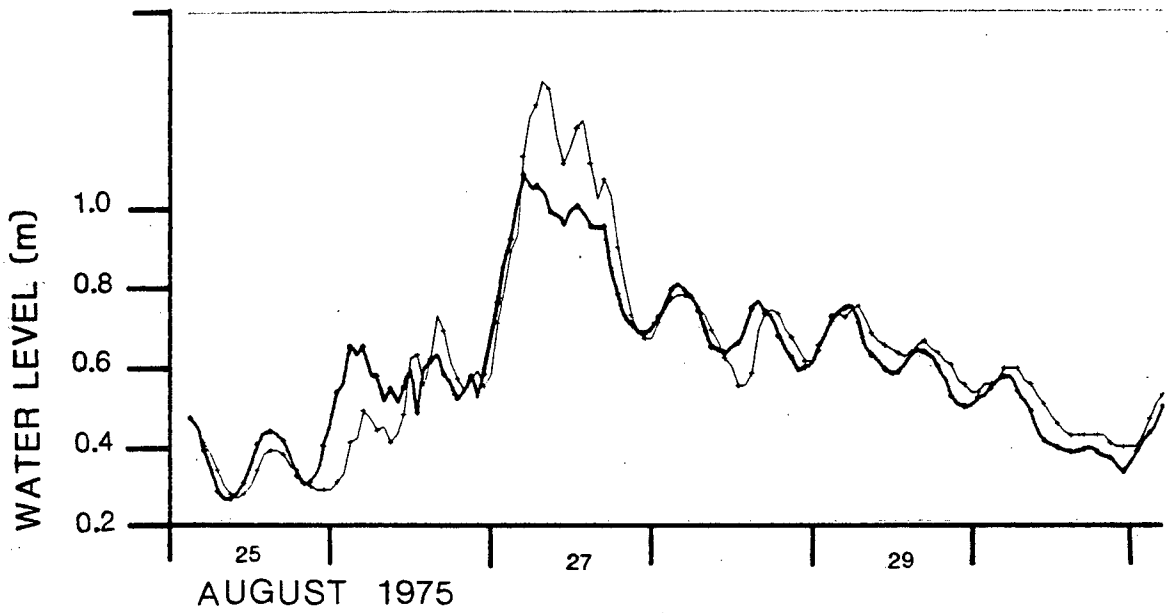


FIGURE 54

Record of storm-surge event, 27 August 1975: water levels at the marine boundary, gauge A (——), and in the upper estuary, gauge E (——).

the maximum surge can be obtained from elevations of the driftwood line at a site near Kay Point (Figure 52A; location 1 on Figure 53B) and of the highest driftwood deposit near gauge E (Figure 52C; location 3 on Figure 53B). The surveyed elevations are 1.4 m and 2.0 m respectively above local mean water level, indicating an amplitude ratio (amplification) of 1.39. There is some ambiguity associated with this result. The two lines of driftwood cannot be unequivocally related to the same event. Furthermore, the elevation of the driftwood near gauge E (site 3) is not much above the peak stage estimated for spring flood discharge through section B2 upstream, while ice-jam backwater levels may be higher. It is noteworthy, however, that little driftwood can be seen at site 3 in the 1944 photography; most of this wood must, therefore, have been moved upstream during a surge event. In any case, the elevation of a driftwood line can be somewhat difficult to define precisely (cf. Figure 52A), while maximum water level and the elevation of the associated driftwood may not be identical. It seems reasonable to suggest an elevation of 2.0±0.5 m for the maximum surge height in the upper Babbage Estuary attributable to storms in this century.

Supratidal flooding also arises during major runoff events when ice is present in the delta and lagoon. Flood level bears no consistent relation to discharge (Figure 55). The relationship depends on the amount and disposition of ice in the estuary and on the chronology of the breakup sequence (see section 3.3.3).

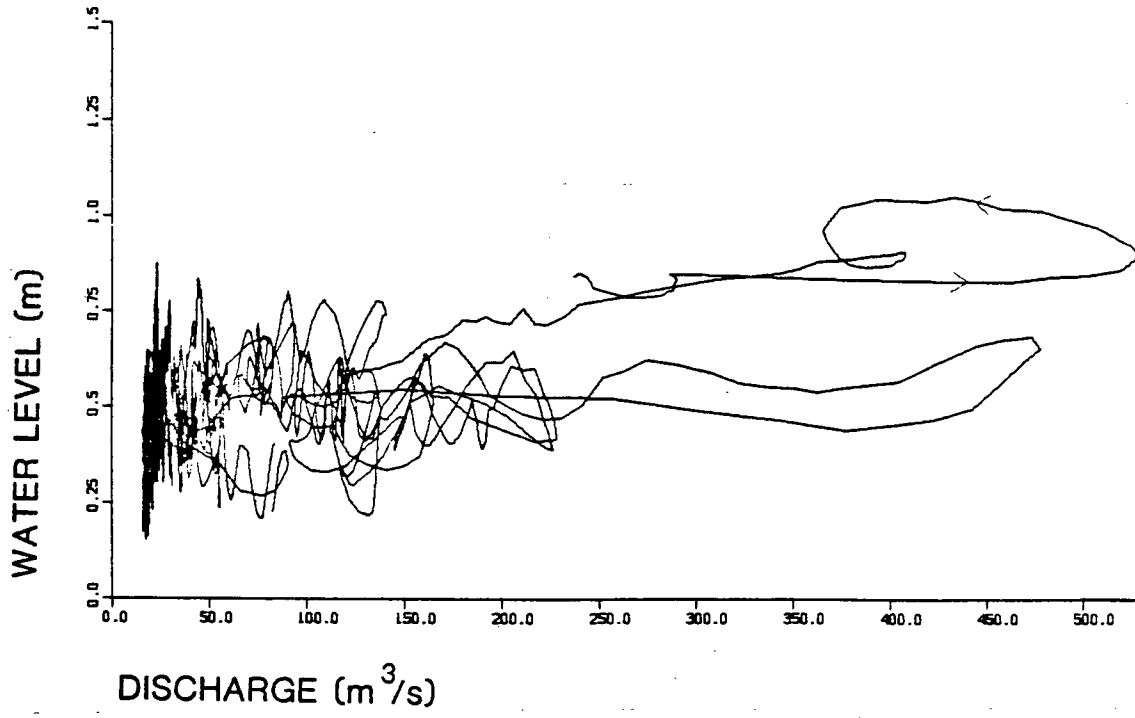


FIGURE 55

Water level at Niakolik Point (gauge B) as a function of Babbage River discharge, spring and summer 1976.

During the 1976 breakup season, the trends of ice thickness and water level were quasi-parallel during the first two weeks of June (Figure 56). Higher flooding occurred in association with the first, relatively small, discharge event of 2-3 June than with the major flood three days later. Bottomfast ice thickness at the measurement site decreased by almost 50 per cent between these events. Development of drainage channels through the ice at the bottomfast/shorefast transition, ice clearance in the entrance section, and ice-jamming in the delta, are additional factors that may have influenced the breakup flood level.

During breakup, the entire system shoreward of the marine boundary is river- and ice-dominated; flooding is essentially a channel-storage phenomenon. In 1974, the first major runoff events occurred on 8-9 June, with peak discharges of 325 $m^3s^{-1}$ and 380 $m^3s^{-1}$, respectively. Although partial drainage and ice clearance in the entrance had been observed almost two weeks earlier (section 3.3.3), large quantities of ice remained in the lagoon on 9 June (Figure 57A) and the delta was extensively flooded on the morning of 10 June (Figure 57B). The second major flood of June 1976 (Figures 55 and 56) occurred when the distributary channels and most of the lagoon were ice-free; this event did not cause supratidal flooding.

The effect of breakup flooding on the frequency distribution of water levels in the lagoon is apparent in the 1976 duration sequence (Figure 51). Storm surge flooding in

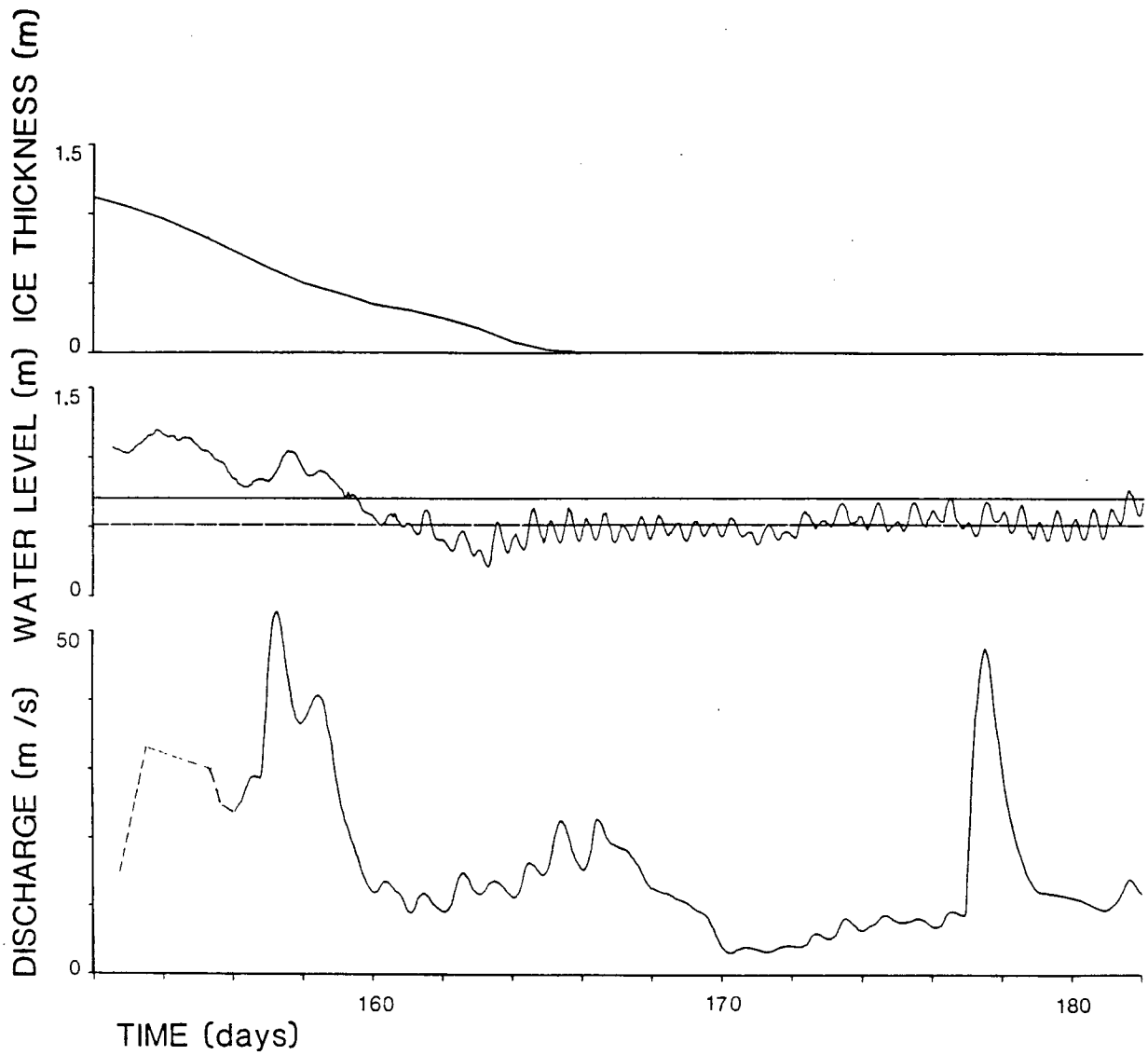


FIGURE 56

Babbage River discharge, gauge-B water level, and bottomfast ice thickness at a site in the Babbage Estuary near gauge B, 1-30 June 1976.

FIGURE 57

Supratidal flooding of Babbage Delta with bottomfast ice in the lagoon, 9-10 June 1974; upper photo shows central lagoon with distal delta in foreground, Niakolik Point in distance; lower photo shows main distributary channel at station 10, looking upstream, with flooded delta in background. At the time of the lower photograph, early on the 10th, Babbage River discharge was approximately 315 $m^3 s^{-1}$.

1975 and breakup flooding in 1976 produced similar deviations from a normal distribution in the supratidal range. A hypothetical distribution, based on an assumed breakup flood sequence identical to that of 1976 and a summer distribution identical to that of 1975, has been included in Figure 51 to indicate the general form of the overall duration sequence for a breakup-summer season in which both types of flooding occur.

Supratidal flood frequency determines the duration of potential sediment supply to the delta plain and other supratidal surfaces (ice-thrust and aeolian transport excluded). The circumstances of flood generation determine the sediment sources active at the time of flooding and therefore the potential sedimentological significance of the flood event. The frequency distribution for the combined breakup and summer seasons of 1976 (Figure 51) indicates that water levels exceeded $\zeta = 0.70$ m during about 10 per cent of the record, which included 69 per cent of the open-water season, and that the system was river-dominated during most flooding in that year. In 1975, supratidal flooding due to surge effects, when the system was wind-dominated, occupied some 5 per cent of the combined breakup and summer period, while the total proportional duration of supratidal flooding, assuming the hypothetical sequence, would be approximately 15 per cent.

The predominant role of ice in the flood regime of the Babbage Estuary is apparent from the foregoing discussion. Broadly analogous effects appear in other components of the system and constitute a recurring theme throughout the study.

It is particularly noteworthy, in the present context, that while ice inside the barrier is an essential element for the occurrence of river flooding, ice outside the barrier inhibits storm surge production during the late winter and breakup seasons, effectively decoupling the two flood processes.

### 3.3.3 ICE IN THE ESTUARY

Freezeup and breakup are major periodic thresholds that recur once per year. Due to spatial variations of temperature, salinity, and fetch, and to mesoscale climatic gradients normal to the coast, the entire freezeup or breakup sequence may span several weeks. Furthermore, because the sea functions as a heat and salt reservoir, freezeup and breakup outside the estuary generally occur somewhat later than inside.

A schematic plot showing the relative proportions of total volume in solid or liquid phase in the Babbage Estuary at the start of each month (Figure 58) emphasizes the contrast between late winter and early summer in this system. During July, August, and early September, the estuary is generally ice-free. From October to March, an increasing proportion of water in the estuary is converted to ice. During March, April, and much of May, ice accounts for more than 99 per cent of the total storage volume (Figure 59); small amounts of water at depths greater than 1.8 m remain unfrozen.

The phase distribution plotted in Figure 58B is schematic to the extent that breakup and freezeup dates may vary from year to year, storage volume and ice thickness are variable, and other factors such as the buoyancy of the ice have not been taken into account. Furthermore, ice thickness may vary, both regionally and locally, due to differences in temperature, snowfall, exposure to wind, and other variables. A mean value of 1.3 m has been reported for the thickness of ice in March

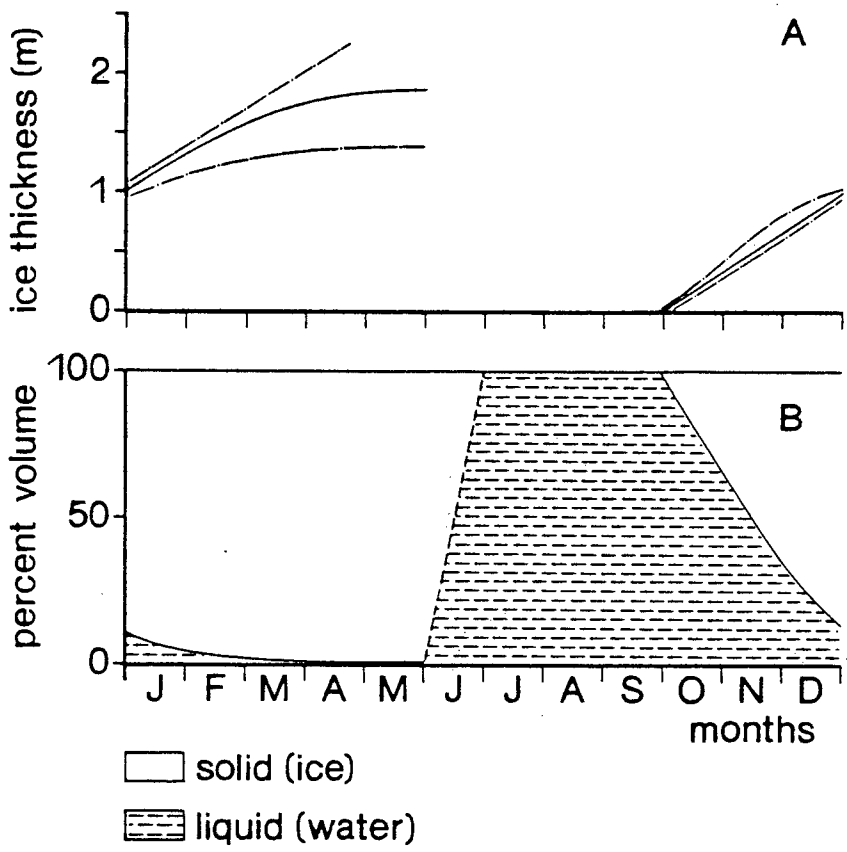


FIGURE 58

Schematic plot of monthly ice thickness (after Schell, 1974) and proportions of estuarine storage volume in solid and liquid phases.

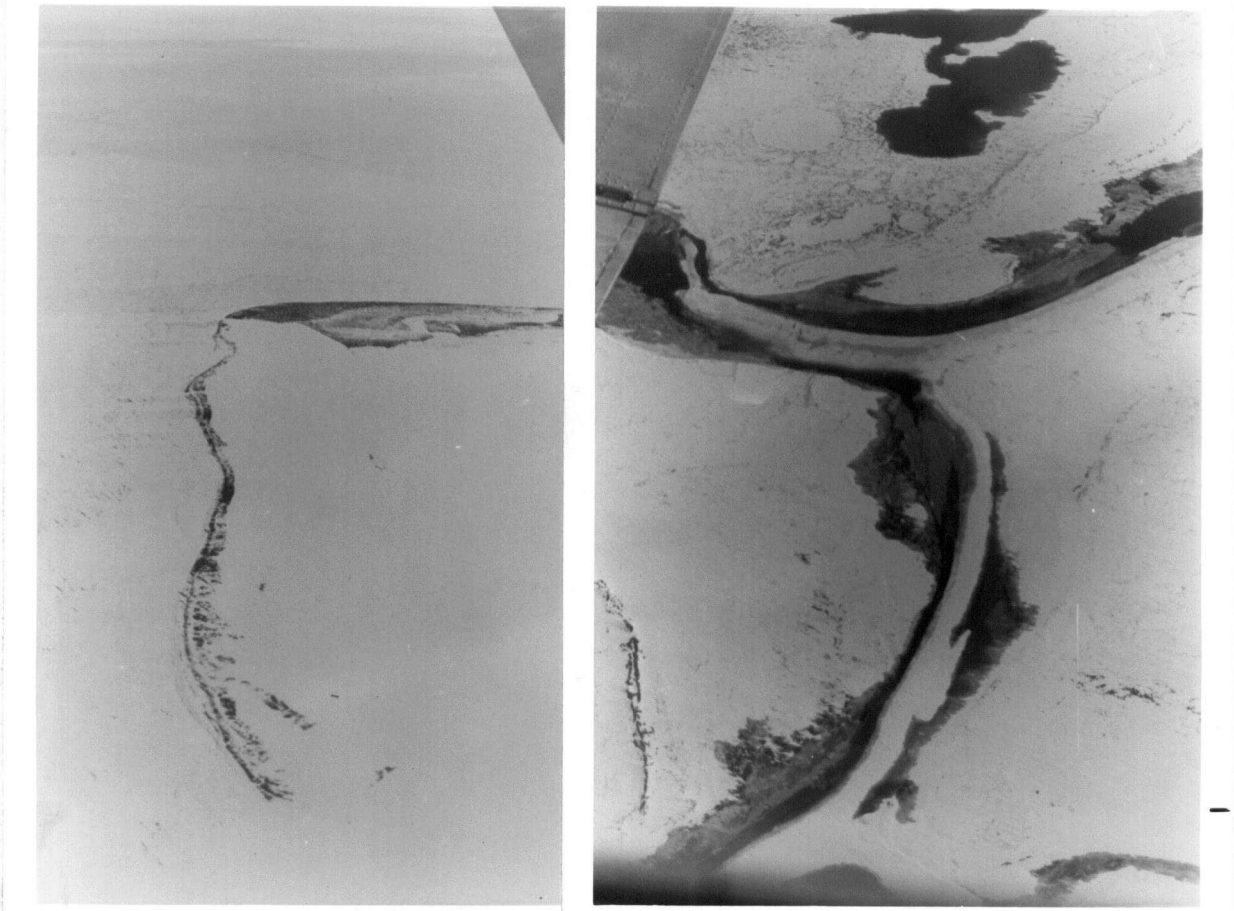

FIGURE 59

Ice in the northern Babbage Lagoon and in the proximal Babbage Delta, late May 1974; note snow-free surface of Kay Point spit (A) and pre-breakup flooding concentrated along channel margins (B).

(1972-1974) at six channel sections in the northern Mackenzie Delta (Anderson and Anderson, 1974, p.245), but all sections carried some flow beneath the ice. Limited data from the Babbage Estuary (see below) support the use of Figure 58A as a model for ice growth on the Yukon coast.

Freezeup may be viewed as a two-part process, the first involving formation of a surface ice cover, the second a progressive thickening of the ice until, in late winter, the estuary is almost entirely filled with bottomfast ice. Ice cover develops by surface freezing to form skim ice (at low Reynolds number) or by formation of frazil (at higher Reynolds number). Frazil may then coalesce at the surface to form sheet or slush ice (Michel, 1978). Slush ice may be partially remolded in transport, forming cake ice, which can later recombine to form a solid ice cover at a new location. Freezeup is often initiated in lagoons or estuaries, where lower salinity and calmer conditions promote ice formation and coalescence. Indeed, lagoons may serve as slush ice sources, the ice being flushed by wind and currents into the nearshore zone, where it promotes development of an ice cover adjacent to the coast earlier than might otherwise occur (Wiseman et al., 1973, p.146). Once formed, the ice cover in the estuary thickens with time until it becomes bottomfast. Of six boreholes drilled in the Babbage Estuary in late March 1976, five encountered bottomfast ice ranging in thickness from 0.46 to 1.37 m (H. Kerfoot, personal communication, 1976). The sixth hole, in a pool of the main distributary channel,

penetrated 1.8 m of ice over 0.9 m of water, as did a hole drilled just off the spit outside the estuary. Ice 2.6 m thick, with no underlying water, observed further offshore, may represent grounded multiyear ice. The two observations of ice over water are in agreement with the ice growth curve of Figure 58A). Assuming a mean winter sea-level roughly 0.2 m below the summer mean (cf. section 3.2.1 above) and an equilibrium ice thickness of 1.8 m, the parts of the estuary containing unfrozen water in late winter can be visualized as those areas below the 1.5 m isobath in Figure 3: viz. the two channels in the entrance section, one or both of which may maintain a free connection beneath the ice with Phillips Bay, and isolated lakes and deep sections of channels in the delta. The ice may become bottomfast down to the 0.5 m isobath during December; from this point on, tidal flushing of waters in the northern lagoon basin and in the distributary channels ceases. Ice growth has the effect, therefore, of suspending circulation in most of the estuary from December onward. Occasional winter storm surges, such as the two during the winter of 1973-1974 (R. MacKenzie, personal communication, 1974), may break up ice in Phillips Bay and flood the Babbage Delta. It is hypothesized that such events may generate strong currents under the ice in lagoon entrance channels (Reimnitz and Maurer, 1978), but no measurements have been obtained; although considerable scour might potentially occur if significant currents are generated, major winter surges represent rare anomalies in the prevailing regime of strongly inhibited circulation.

Breakup is initiated by snowmelt runoff from the Babbage River, which spreads seaward over bottomfast ice in the lagoon and out through the entrance into Phillips Bay. In 1974, the leading edge of this flow advanced through the delta at a mean rate of about 3 km per day. By May 20, the southern part of the lagoon and an area of ice outside the estuary, extending to or beyond the 2 m isobath, were flooded (Lewis and Forbes, 1974, figure 6). By the same date, winter ice in deeper parts of the delta distributary channels had begun to lift with the rising stage, while the bottomfast and bankfast ice at the channel margins remained flooded (Figure 59B).

Snowmelt runoff usually initiates breakup before in situ melting has progressed appreciably. Just as freezeup occurs earlier in the vicinity of lagoons and estuaries, so breakup begins several weeks earlier at river-mouth locations than elsewhere along the coast. The usual breakup sequence in the Babbage Estuary may be set out as follows: (1) local snow and ice melt; (2) seaward advance of meltwater over ice in delta and lagoon (pre-breakup flooding); (3) spread of meltwater as lobate front over bottomfast and shorefast ice in nearshore zone outside lagoon; (4) lifting of bottomfree ice in delta, while ice along banks and bottomfast ice on bars remains flooded; (5) drainage of floodwater through ice (initially via fractures and seal-holes) near seaward limit of bottomfast ice, vicinity of 2 m isobath; (6) removal of ice from deeper parts of entrance section; (7) development of ice jams in delta

distributary channels; (8) clearance of ice from main delta distributary; (9) clearance of ice from remaining delta channels and (primarily by in situ melting) from lagoon and delta lakes; (10) breakup in coastal nearshore zone.

A similar pattern prevails in deltaic and shallow lagoon estuaries throughout the southern Beaufort Sea region (Walker, 1972, 1973; Reimnitz and Bruder, 1972; Barnes and Reimnitz, 1972; Wiseman et al., 1973; Lewis and Forbes, 1974; Short and Wiseman, 1975). The details of the breakup at a particular site depend on the local configuration of the coast, the size and other characteristics of the drainage basin, and the unique sequence of weather and runoff occurring during a given breakup season.

Breakup chronologies for three seasons in the Babbage Estuary are given in Figure 60. Stage-1 of the breakup sequence (local thaw at the coast) may begin as soon as the temperature of the snow or ice surface rises to 0°C. Some melt, sublimation and evaporation may occur before mid-April under appropriate conditions of positive net heat flux. Although in situ melting and changes in albedo arising from snowmelt (Peake and Walker, 1971; Weller and Holmgren, 1974), from snow removal by wind, or from sedimentation on ice, are important aspects of the breakup process, no significant changes in the phase distribution of the estuary occur before stage-2, which commonly begins in early- to mid-May (Figure 60).

Numbers refer to stages of the breakup sequence defined in the text.
Entries show date of observation; if preceded by a box (□), which indicates periods in which the estuary was not observed, the actual date of occurrence may have been earlier.
Note that 8* refers to clearing of main distributary channel only.

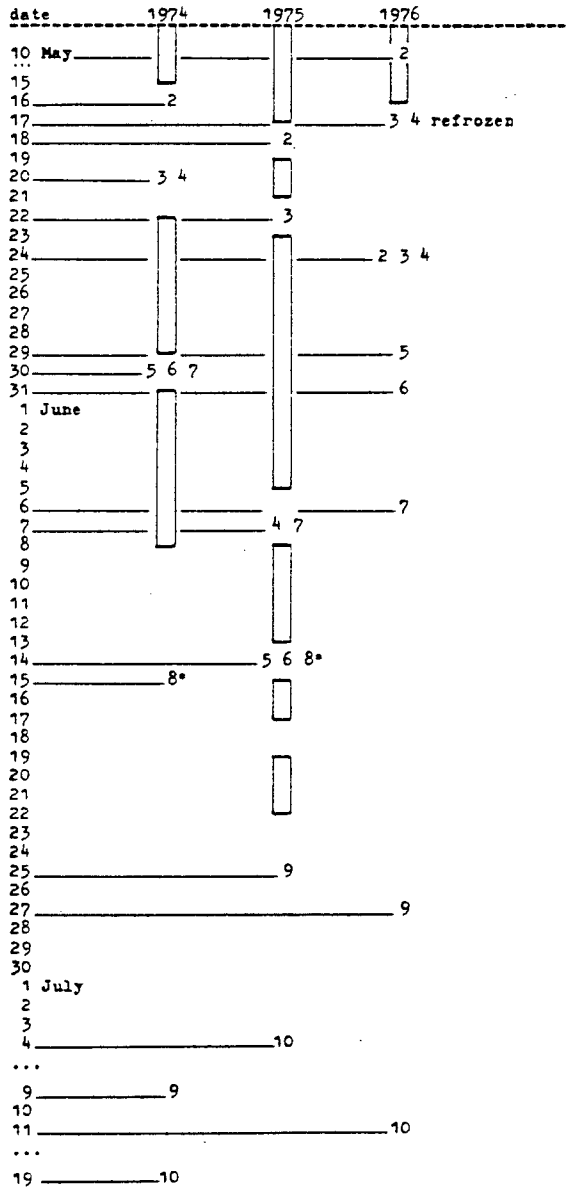


FIGURE 60

Chronology of breakup in the Babbage Estuary, 1974-1976.

FIGURE 61

A: Spring River, showing snowmelt runoff contained and deflected by the Spring River barrier; overflow of Babbage River water onto ice outside Babbage Estuary is visible in the background, 30 May 1974; B: ice floating in main distributary channel of Babbage Estuary between distal delta and Niakolik Point, 9 June 1974.

Partial or complete refreezing sometimes occurs after the first pre-breakup flooding. The Babbage River was flowing at an estimated discharge of order 1000 $ft^3/s$ (roughly 30 $m^3/s$) on 10 May 1976 (H.L. Wood, personal communication, 1976), following a period of warm weather during the first week of May; however, meltwater on ice in the lagoon was completely refrozen by May 18. Pre-breakup flow (stage-2) was reinitiated by 24 May. Breakup then proceeded without major interruption, although frazil formation and frazil-pan ice were observed in river water discharging through the lagoon early in June. During the 1974 breakup, frazil formation and slush accumulation behind winter ice at the head of the delta was a recurrent phenomenon in late May and early June.

The timing and extent of stage-3 flooding over fast ice in the nearshore zone is influenced by several factors, including: (1) the configuration of the coastal barrier, where one is present (Short and Wiseman, 1975, p.199), and the position of the river with respect to discontinuities in the barrier (cf. Figure 61A); (2) the total snowmelt runoff volume and the ratio between this volume and the storage capacity of the estuary while ice-covered; (3) the nearshore slope, which determines the seaward extent of bottomfast ice; (4) the timing of the snowmelt discharge hydrograph relative to breakup in the estuary. In the Babbage Estuary, during three seasons of record, flooding onto ice in Phillips Bay was initiated by relatively low early-snowmelt discharge. Although the annual discharge maximum occurred in every year before breakup in the

estuary entrance, drainage of floodwater through the ice had been established before the peak flow occurred and the extent of flooding over shorefast ice may have been reduced accordingly.

The fourth stage of the sequence outlined above (effectively the third stage in the delta) represents the actual beginning of breakup, as bottomfast ice rises with the rising stage in deeper parts of the river and delta channels, fractures develop along the margins of the floating ice, and previously isolated pockets of water beneath the ice are flushed out. In 1974, ice had begun to lift in the Babbage Delta by May 20, four days after the first appearance of pre-breakup flow (Figure 59B). Apart from vertical movements in response to water level changes, some of the floating ice remained essentially in place for almost three weeks, although limited horizontal movement occurred as additional fracturing and melt permitted.

Within the main distributary channel, floating ice remains in place longer in more distal reaches. Ice in the outer reach seaward of station 10 is usually the last to clear (Figure 61B), although ice may remain later in the lagoon and in the smaller distributaries.

Stage-5 of the breakup sequence is initiated when floodwater on ice outside the lagoon begins to drain. Some drainage may occur almost immediately as floodwater encounters fractures or seal holes. The floodwater loading on unsupported

shorefast ice promotes further fracturing in the vicinity of the 2 m isobath (Barnes and Reimnitz, 1972, p.1020). Reimnitz and Bruder (1972) have described the appearance of irregular drainage holes (termed strudel) with associated radial channel networks in fast ice off the north coast of Alaska. These appear to have developed along fractures, at other weak points in the ice, and as enlargements of seal holes. Some occurred in lagoons, some over depths less than 1 m, and some as much as 5 km offshore over depths up to 5 m. A shallow conical scour depression was observed beneath one such drainage feature (Reimnitz and Bruder, 1972, p.864). No drainage holes of the kind described by Reimnitz and Bruder have been found inside the Babbage Lagoon, but several appeared near the seaward limit of the baymouth shoal platform at the end of May 1974 (Figure 62A).

As water drains from the upper surface of the ice, the water level in the lagoon falls markedly and much of the lagoon ice is left relatively free of water (Figure 62B). Subsequent major increases in river discharge while ice remains in the estuary can cause extensive flooding.

The pattern of ice movement in delta distributaries is strongly dependent on the shape of the flood hydrograph in the Babbage River. In 1975, a single major flood that peaked on 15 June was characterized by a relatively prolonged rising limb and a slow recession: very little ice jamming occurred in the delta. In 1976, a major jam had developed at the main channel junction near the head of the delta by June 4. The relatively

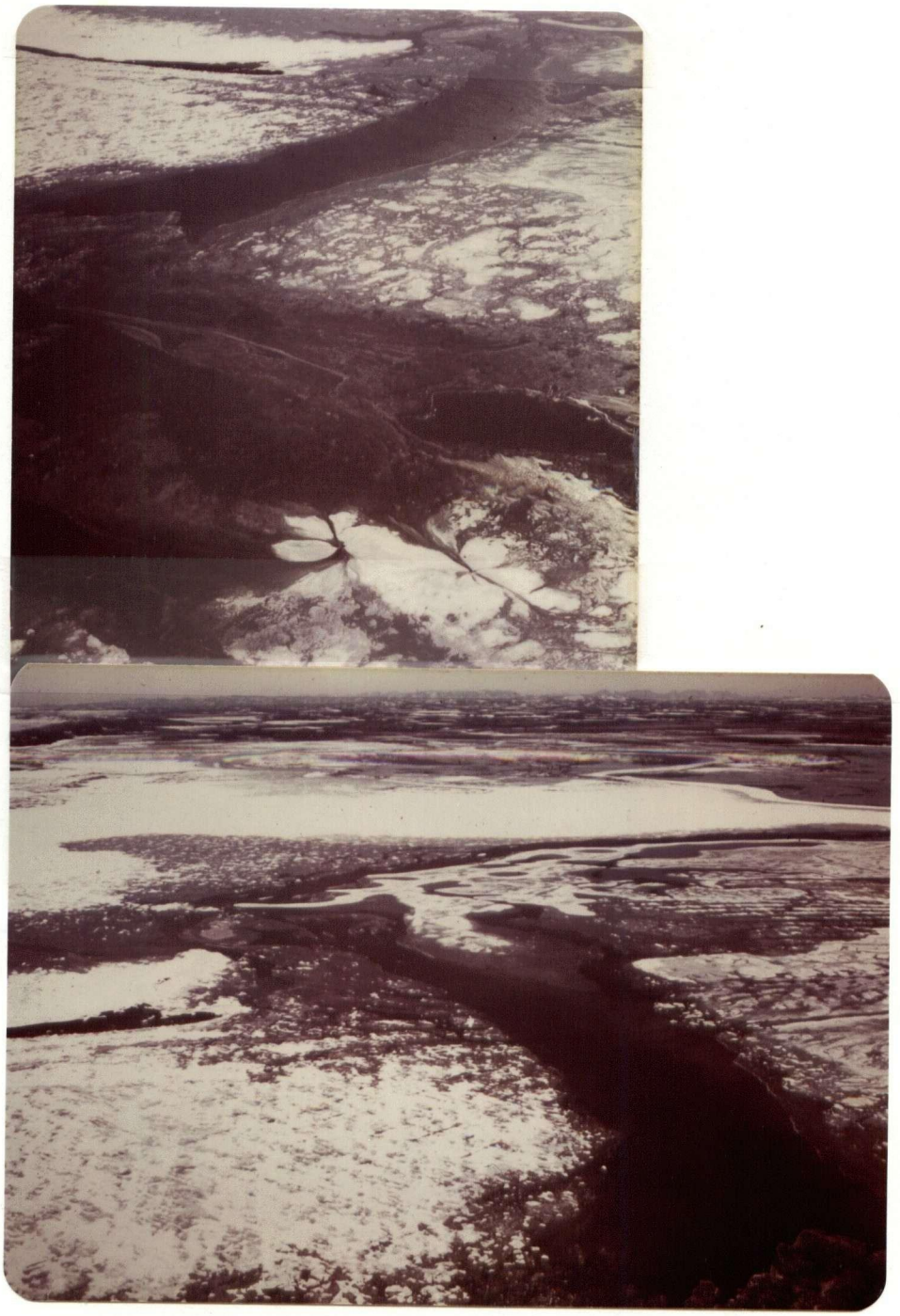

FIGURE 62

Drainage holes through ice outside main entrance section and general view of central lagoon, showing limited extent of flooding over-ice and open water in entrance channel 30 May 1974.

abrupt flood of 5-6 June moved this ice seaward to the reach between stations 10 and 12 in the delta, where the ice had jammed again on the recession late on the 6th. Although drainage had previously occurred in the entrance, the lagoon remained largely ice-filled during this flood and the water level was raised substantially in the lagoon and delta (see section 3.3.2).

While the Babbage Delta and Lagoon were essentially clear of ice by 25 June 1975 and a few days later in 1976, the estuary did not become ice-free until 9 July in 1974, a season characterized by very late and limited breakup throughout the southern Beaufort Sea. Such late clearance in the lagoon is believed to be unusual.

Breakup immediately outside the estuary is promoted by mechanical effects and heat transport associated with river discharge, as well as by dramatic changes in albedo due to sedimentation on the ice. The importance of such an albedo effect may be considerable in seasons when extensive sedimentation on the ice is followed by a period of fine weather with high positive net radiation. This was the case at the Babbage Estuary in 1976, when the early June flood left a thin veneer of sediment over a wide area of ice in the southern part of the lagoon and immediately outside the estuary in Phillips Bay. By 18 June, a large nearshore area and much of the central and southern parts of the lagoon were ice-free.

Beyond the immediate vicinity of the river outlet, ice in

Phillips Bay deteriorates slowly. Ablation of the upper surface is thought to occur primarily through radiative and convective heat transfer from the atmosphere and by conductive heat transfer from expanding pools of meltwater. Some ablation of the under-surface may also occur as an increasing volume of relatively warm water accumulates at the top of the water column beneath the ice. Phillips Bay was first ice-free by July 19 in 1974, by July 11 in 1976, and two to three weeks earlier in 1975.

The annual cycle of phase changes described above exerts a profound influence on circulation and sedimentation processes in the Babbage Estuary. Partial control of flood levels by ice and the decoupling of major fluvial and marine inputs to the estuary are but two examples of important ice effects.

### 3.3.4 PROPERTIES OF WATER IN THE ESTUARY

Interaction between waters of differing density is perhaps the most distinctive feature of estuarine hydrodynamics. Density differences $\Delta\rho/\rho \leq 0.107$ or greater may occur (see below), although values greater than 0.025 are rare and local differences within a reach are usually much smaller. Temperature and suspended solids concentration can be significant; however, density variation in estuarine waters arises primarily due to variable salinity.

River discharge into estuaries is almost invariably hypopycnal or less dense than the estuarine water (Bates, 1953), although exceptional cases of hyperpycnal (denser) discharge have been reported (Loewy, 1970; Church, 1972, p.129). Effluent buoyancy is reduced by mixing and entrainment of saline water. A broad continuum of estuarine stratification types has been recognized (eg. Stommel and Farmer, 1952; Pritchard, 1955; Cameron and Pritchard, 1963). Highly-stratified and well-mixed conditions constitute end members of this continuum. Various distinctive circulation regimes are associated with the various stratification types. In the highly-stratified 'salt-wedge' case, some entrainment of salt water into the upper freshwater layer may occur, necessitating an upstream advective transport in the lower layer to maintain continuity. If turbulence generated by tidal motions is sufficiently intense, vertical mixing may occur and the vertical density gradient between upper and lower layers will be reduced. The mass of salt advected seaward with the

upper part of the flow will then be greater than for the corresponding salt-wedge case. Under tidally-averaged quasi-steady conditions, continuity implies a 'salt balance', which is satisfied in part by advective transport of salt in the lower part of the flow (gravitational convection) and in part by turbulent diffusion. In the extreme case of vertical homogeneity, the salt balance is maintained entirely by diffusion. However, Hansen and Rattray (1965) have demonstrated that gravitational convection may occur under conditions approaching vertical homogeneity; the diffusive fraction, $\nu$, of the total headward salt flux is not uniquely related to the degree of stratification.

Water exchanges, density distribution and sediment dispersal all depend on the resultant circulation, which reflects the interaction of a diverse set of phenomena, including density gradients, tidal motions, freshwater discharge, boundary resistance and associated turbulence production, centripetal and Coriolis accelerations, wind stress, wave drift, and storage changes due to low-frequency fluctuations of water level (section 3.3.6). Salinity, temperature, and density are parameters of great physical significance, therefore, because of the role that density gradients play in the circulation regime of the estuary. An additional parameter of some dynamic importance, both for turbulence production and for suspension and deposition of sediments, is the dynamic viscosity, $\eta$.

A program of sampling and <u>in situ</u> measurements was carried

out in the Babbage Estuary to obtain information on the temporal and spatial variability of temperature, salinity, density, and viscosity. The data include daily observations in 1976 at stations 5, 6, and 7 in the estuary entrance and at station 12 in the delta (see Figure 2 for station locations; Appendix A.9 for data). Several synoptic surveys and various sequences of observations at shorter sampling intervals, to elucidate the high-frequency variability, were also obtained. The daily sequence is obviously an aliased sample with respect to major tidal frequencies, although the aliasing problem is reduced by the quasi-random sampling interval (Bâth, 1974, p.151; Wunsch, 1972).

Salinity, density, and viscosity were computed from measurements of temperature, specific electrical conductivity, and total dissolved solids concentration (total residue passing 0.45-μm membrane filters). Such computations may be biased by anomalous solute chemistry of estuarine waters. Whereas the ionic composition of ocean water is essentially constant (Dittmar, 1884), such that salinity may be determined readily from measurements of a single parameter (eg. chlorinity or electrical conductivity), major qualitative differences between river and ocean waters produce solutions of variable composition in estuaries. Therefore, values of estuarine 'salinity' computed from standard empirical relations for ocean water are, strictly, incorrect. In most cases, however, where the total dissolved solids concentration in the river water is low, the errors introduced will be minor relative to the

overall variability of salinity in the estuary.

In the present study, salinity was estimated from in situ measurements of temperature and conductivity (following Perkin and Walker, 1971; see Appendix A.8), assuming standard seawater composition, an implicit assumption in most estuarine investigations (see, however, Williams et al., 1964). Subsequent computations of density (following Knudsen, 1901) and of viscosity (following Millero, 1974) involved salinity as an input parameter; they therefore incorporate any errors in the estimation of salinity.

The proportions of major dissolved constituents in water samples from the Babbage Estuary and Phillips Bay are given in Table 12, together with standard mean seawater composition and an example of Babbage River water for comparison. Extreme overall and local variability are apparent in the data. A clear differentiation is apparent between samples that are similar to mean seawater and those that are not. The sample of river water from station B2 may be taken to represent the freshwater end of the estuarine solute continuum. The sample taken off Kay Point on 16 August 1974 (s=2ppt) indicates that the solute chemistry may approach that of standard seawater at relatively low concentrations. In contrast, results from station D in May 1975 indicate that significant departures from standard seawater composition may occur in the same salinity range during pre-breakup runoff. The station D sample (s=2ppt) shows $Ca^{++}$ enrichment characteristic of river water but contains a higher proportion of $Cl^{-}$ than mean seawater. It may

TABLE 12

Summary of dissolved constituents in water samples from the Babbage Estuary system and Phillips Bay (data derived from various sources as indicated).

| station date | concentrations in mg/L | | | | | | | | | ppt |
|---|---|---|---|---|---|---|---|---|---|---|
| | TDS | $SiO_2$ | $Ca^{++}$ | $Mg^{++}$ | $Na^{+}+K^{+}$ | $HCO_3^{-}+CO_3^{--}$ | | $Cl^{-}$ | $SO_4^{--}$ | pH | s |
| **Babbage River**[1] | | | | | | | | | | | |
| B2[3] 15/7/74 | 241.3 | 2.0 | 28.8 | 2.9 | | 78.0 | | 0.5 | 16. | 8.2 | 0 |
| **Deep Creek**[2] | | | | | | | | | | | |
| D2[4] 4/4/74 | 32372. | 2.4 | 593. | 1195. | | 346. | | 18833. | 2500. | | 27 |
| **Babbage Delta**[1/2] | | | | | | | | | | | |
| 12[5] 4/4/74 | 42822. | 2.8 | 657. | | | 335. | | 23416. | 3750. | | 35 |
| lake[6] 7/7/74 | 585.8 | 1.9 | 12.0 | 38.4 | | 74.6 | | 308. | 66. | 8.5 | 0.2 |
| **Babbage Lagoon**[1/2] | | | | | | | | | | | |
| 7?[7] 1/4/74 | 76636. | 4.2 | 1173. | 2993. | | 416. | | 43860. | 7550. | 6.8 | 67 |
| 7[7] 17/7/74 | 556.0 | 1.8 | 30.4 | 13.6 | | 76.8 | | 172. | 40. | 8.2 | 0.3 |
| **Phillips Bay**[1/2] | | | | | | | | | | | |
| Kay Pt. 1/4/74 | 27562. | 1.2 | 466. | 1277. | | 143. | | 13892. | 2600. | | |
| Kay Pt 16/8/74 | 2388. | 1.6 | 53.7 | 85.0 | | 79.0 | | 1264. | 260. | 8.7 | 2.2 |
| stnD[8] May 75 | 1336. | 4.5 | 64.5 | 89.6 | | 133. | | 1120. | 240. | 8.1 | 2.0 |
| **mean seawater**[9] | 34560. | 6.4 | 400. | 1350. | 10880. | 142. | | 19000. | 2700. | | |

**Sources:**

[1] Kendel et al., 1975

[2] Steigenberger et al., 1975

[9] Goldberg, 1963

**Stations:**

[3] section B2, this study (see Figure 1.3.1-1)

[4] downstream of confluence with uppermost Babbage River distributary

[5] near station 12, this study (see Figure 1.3.1-1)

[6] southernmost lake in delta

[7] station 7, this study (see Figure 1.3.1-1)

[8] station D of Kendel et al., 1975, off section M1

**Computational procedures:**

$Ca^{++}$ computed as 0.400(Ca-hardness as $CaCO_3$)

$Mg^{++}$ computed as 0.244[(total hardness as $CaCO_3$) - (Ca-hardness as $CaCO_3$)]

$HCO_3^{-}$ computed as 1.219(total alkalinity as $CaCO_3$) when phenolphthalein alkalinity is zero; otherwise, both $HCO_3^{-}$ and $CO_3^{--}$ are present.

be hypothesized that this sample represents early snowmelt runoff discharging into Phillips Bay in the upper layer of a salt-wedge circulation system (cf. observations off Colville River, Walker, 1973), with minor entrainment of underlying salt water into the upper layer. Alternatively, the chloride enrichment (assuming it is not due to sample contamination) may reflect entrainment of concentrated brine from winter reservoirs in the delta.

Remarkably high values of salinity are observed in the delta and lagoon in late winter (Table 12). The annual regime of monthly mean salinity and temperature is illustrated in Figure 63. As river discharge approaches zero in early to mid-winter, freshwater in the delta and lagoon is replaced by seawater and the mean salinity rises to approach the ambient value in adjacent coastal waters. This process may be inhibited or curtailed by ice growth over shoals (as demonstrated in the Colville Delta, Alaska; Arnborg et al., 1966, p.202). As ice thickness increases through the winter and the ice becomes bottomfast in depths less than 1.8 m approximately (section 3.3.3), exchange of water between the estuary and adjacent coastal waters may be inhibited or, in many parts of the estuary, cease altogether. Salinities are further increased by partial rejection of solutes on freezing (Walker, 1973, p.473). Late-winter salinities as high as 67ppt and 122ppt have been observed, respectively, in the Babbage and Spring River estuaries (Steigenberger et al., 1975, pp. 27, 439, 441). The occurrence of unfrozen salt water at 22-m depth

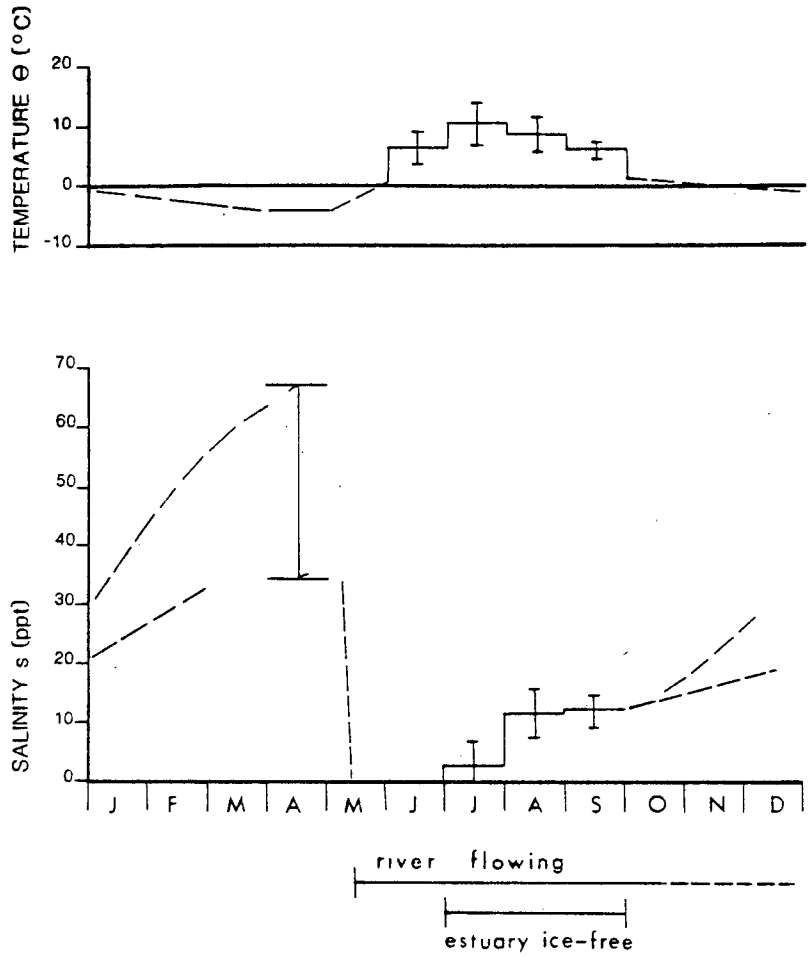


FIGURE 63

Schematic plot of monthly water temperature and salinity in the Babbage Estuary, based on 1976 observations for the summer months and 1974 data (after Steigenberger et al., 1975) for April, with other values interpolated.

in a drill-hole at the Babbage Delta front in March 1974 (R. Gilbert, personal communication, 1974; Lewis and Forbes, 1974, p.17) may be attributable in part to brine concentration in an 8-m deep scour hole of the main distributary channel adjacent to the drilling site. Salinities in excess of 60ppt have been reported from the Colville Delta (conductivity data in Arnborg et al., 1966) and from numerous lagoons on the Alaskan north coast (Schell and Hall, 1972, pp.7 and 10). These values are comparable to extremes due to excess evaporation in hypersaline lagoons at lower latitudes (eg. Behrens, 1969; Carpelan, 1969; Krumgalz et al., 1980). While much of the unfrozen water remaining in the estuary in late winter is isolated by bottomfast ice, waters that are not so restricted may be well-mixed or weakly stratified, with the salt flux maintained primarily by turbulent diffusion and a weak gravitational convection due to solute rejection at the freezing plane (cf. Matthews, in press).

When snowmelt runoff to the estuary begins, usually sometime in May, salt water is flushed rapidly from the delta and lagoon. This event, which represents an abrupt threshold in the annual regime of the estuary (Figure 63), is accompanied by a major change in the estuarine circulation. Subsequently, freshwater conditions prevail throughout the estuary until sometime in July in most years. Daily salinity data for 1976 (Figures 64 and 65) demonstrate that very low salinities were maintained in the lagoon and delta until late-July of that year, when a rather abrupt intrusion of brackish water

occurred.

The length of the lag between the end of spring flooding and the first major salinity intrusion in the lagoon suggests that mixing between river effluent and coastal waters outside the lagoon proceeds slowly. Ice remaining against the coast until early July prevents wind-induced mixing and ice-melt may provide an additional source of relatively fresh water at the surface. Although coastal waters were ice-free some time before the mid-summer salinity intrusion in both 1975 and 1976, the timing of the intrusion may be partly related to ice clearance. However, the abruptness of the intrusion implies strong local salinity gradients in Phillips Bay and therefore limited vertical mixing. In any case, the mid-summer intrusion represents a second major threshold in the annual cycle of the estuarine system. Associated changes in the circulation are discussed in section 3.3.5 below.

The abrupt transition from hypersaline to fresh conditions reflects the importance of the runoff regime as a major external parameter of the estuarine system (cf. Simmons, 1955). Runoff in Arctic basins is highly variable at a seasonal scale and largely concentrated during a short nival flood (section 3.1.1), causing severe distortion of the annual salinity cycle in shallow estuaries. In combination with winter brine concentration, the runoff sequence generates extreme seasonal-scale variance in Arctic estuarine systems, greater even than that observed in some monsoon-dominated estuaries (see, for example, Nagaraja, 1966; Dyer and

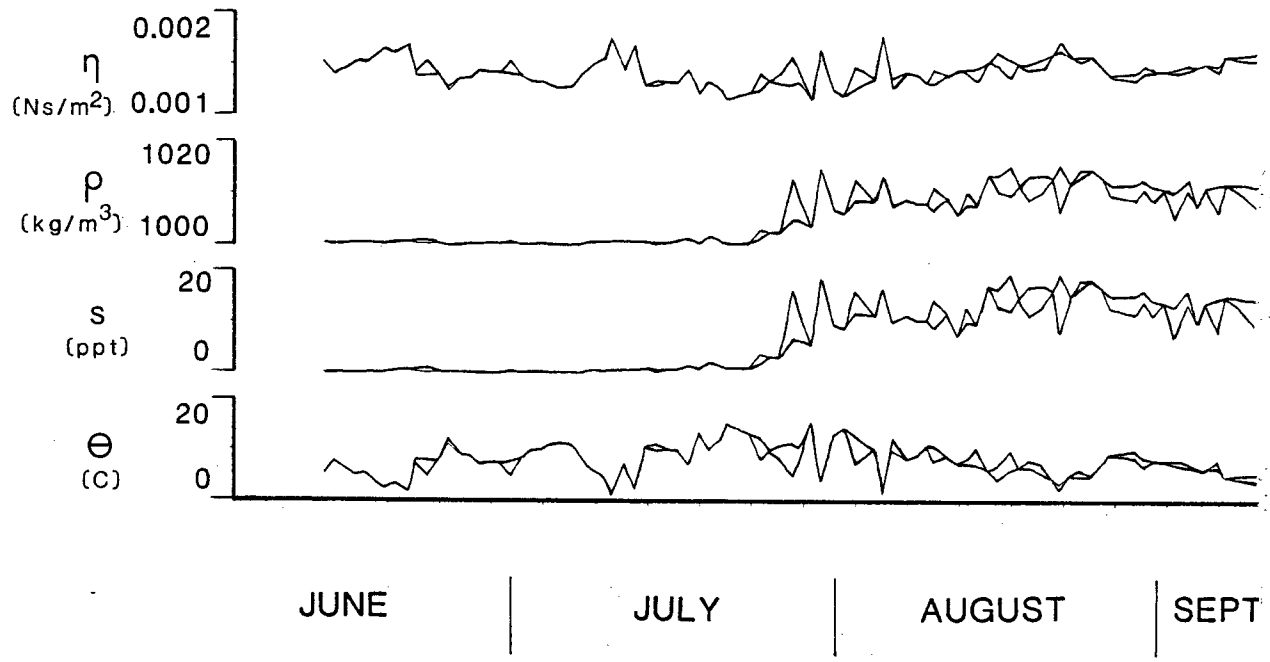


FIGURE 64

Daily sequence of water temperature, $\Theta$, salinity, s, density, $\rho$, and viscosity, $\eta$, in Babbage Estuary entrance, June-September 1976.

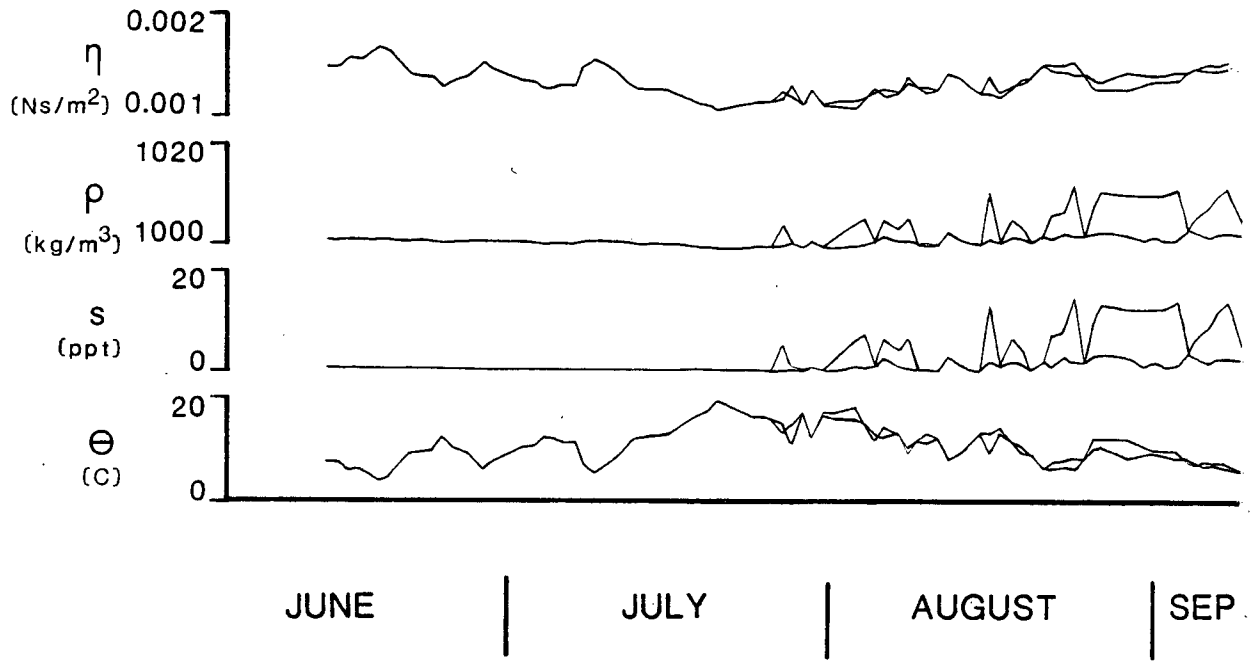


FIGURE 65

Daily sequence of water temperature, Θ, salinity, s, density, ρ, and viscosity, η, at station 12, Babbage Delta, June-September 1976.

Ramamoorthy, 1969). The magnitude of the seasonal-scale variance may distinguish Arctic estuaries from most other hypersaline systems, which typically show relatively small intra-annual variability, with the exception of high-tide pools subject to seasonal rain dilution (Jones et al., 1978, p.258) and of hypersaline lagoons exposed to hurricane surge and runoff (Behrens, 1969); in the latter case, the seasonal-scale variance may be extremely non-stationary and great between-years variability is common.

Whereas the variance of density in the Babbage Estuary is dominated by salinity fluctuations, viscosity is more sensitive to temperature effects. Daily viscosity data for 1976 exhibit a generalized minimum in mid-summer (Figures 64 and 65). Although computation of extreme winter viscosities involves extrapolation beyond the domain of empirical results (cf. Millero, 1974), the viscosity of hypersaline water (s=67ppt) at the freezing point temperature ($\Theta$ =-3.7°C) can be expected to exceed $\eta = 1.9 \times 10^{-3}$ N s m$^{-2}$. The lowest values computed from summer 1976 data are somewhat less than $\eta = 1.1 \times 10^{-3}$ N s m$^{-2}$, giving an annual range in excess of $7 \times 10^{-4}$ N s m$^{-2}$. Although the annual trend of viscosity is at a minimum in late July, relatively high values may occur briefly at that time in association with cold saline intrusions in the entrance. For example, water at $\Theta$ =0°C and s=25ppt was encountered below a depth of 1 m at station 5 on 28 July 1977 (Figure 66); this water had a computed viscosity of $1.9 \times 10^{-3}$ N s m$^{-2}$. Over the next four days, the salinity

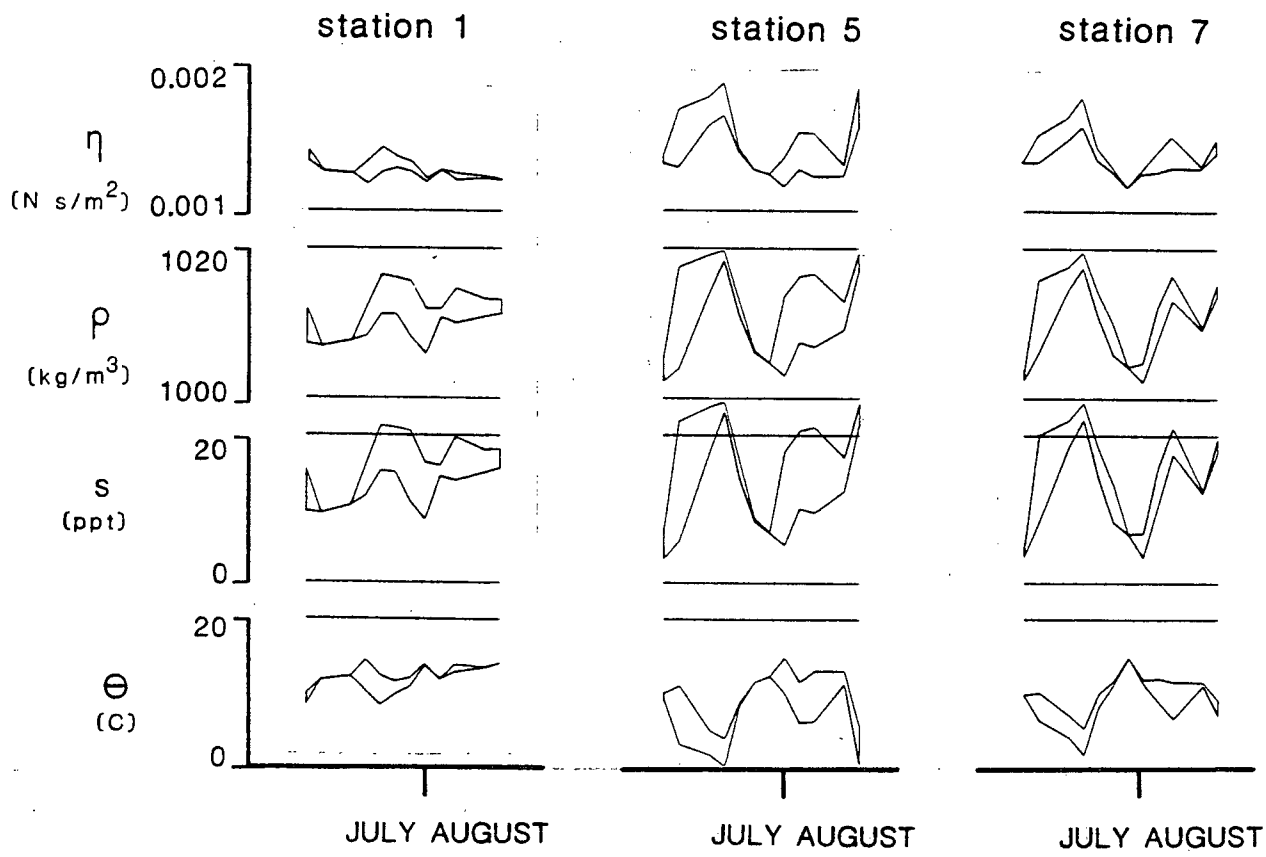


FIGURE 66

Daily temperature, salinity, density, and viscosity at stations 1, 5, and 7 in the Babbage Estuary, 24 July to 5 August 1977.

decreased rapidly, the temperature increased, and the viscosity dropped to a minimum of $1.2 \times 10^{-3}$ N s $m^{-2}$. Other major excursions of viscosity are apparent in the 1976 record for station 5 (Figure 64). Synoptic-scale variance is reduced headward into the delta (cf. station 12 data, Figure 65) and in the upper lagoon (station 1, Figure 66). The implications of high- and low-frequency viscosity fluctuations for the sedimentation regime in the estuary are considered in section 4.3.1 below.

Some appreciation of the relative contributions of various frequency bands to the total variance of density may be gained from Figure 67. This includes variance estimates derived from the series of monthly density, from successive 10-day sets of daily data, and from two sets of observations at 1-h and 3-h intervals, respectively, over periods of two to three days. The 95% confidence limits for total variance of water density, computed from the various subsets of data, are plotted against time. Limits were computed from the inequalities

$$f \hat{\sigma}_\rho^2 / \chi^2(0.025) \leq \sigma_\rho^2 \leq f \hat{\sigma}_\rho^2 / \chi^2(0.975) \quad (3.3.4\text{-}1)$$

where $\hat{\sigma}_\rho^2$ is the sample estimate of the variance, $\sigma_\rho^2$ is the population variance, and f=(n-1) is the number of degrees of freedom, on the assumption that the samples are drawn from normally distributed populations (see, for example, Snedecor and Cochran, 1967, pp.74-76). The distribution of $\hat{\sigma}_\rho^2$ is sensitive to non-normality, specifically to deviations from normal kurtosis. The variance of $\hat{\sigma}_\rho^2$ is given by

$$\mathrm{var}(\hat{\sigma}_\rho^2) = (2\sigma^4/f)\{1+[(\kappa-3)f]/[2(f+1)]\} \quad (3.3.4\text{-}2)$$

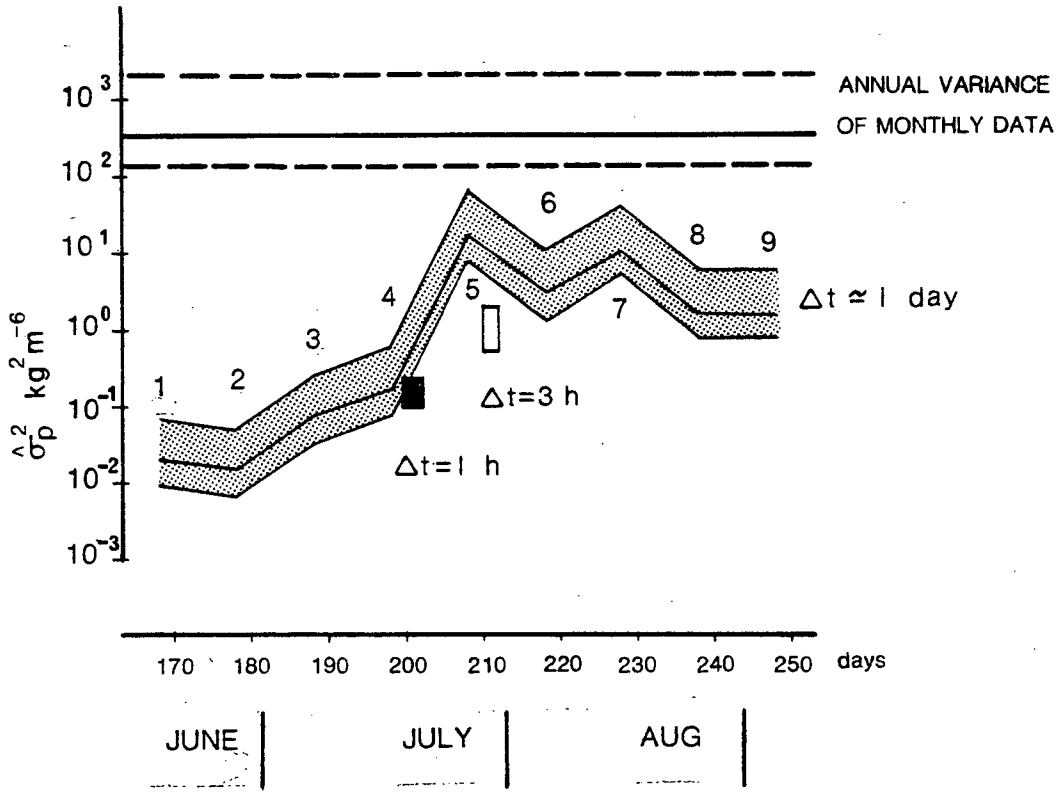


FIGURE 67

Estimates of the variance of water density for sets of data at various sampling intervals, $\Delta t$; the 95% confidence intervals for $\sigma_\rho^2$ are plotted.

where $\kappa$ is the coefficient of kurtosis, equal to 3.0 for a normal distribution, and $2\sigma^4/f$ is the variance of $\sigma^2$ for samples drawn from a normal population (Snedecor and Cochran, 1967, p.89). In the Babbage Estuary data, $\kappa<3.0$ for all but three of the samples. This suggests that the true variance of $\hat{\sigma}_\rho^2$ may be less than plotted, although the sampling variability of $\hat{\kappa}$ is high. In two cases, daily data for $174<t<183$ days and $194<t<203$ days, $\hat{\kappa} \tilde{=} 3.5$, implying that the variance of $\hat{\sigma}_\rho^2$ is greater by a factor of 1.2.

The data illustrated in Figure 67 are insufficient for the the computation of a variance density spectrum. Nevertheless, one may draw certain conclusions about the relative magnitudes of variance at seasonal, synoptic, and higher frequencies. The seasonal-scale variance ($T \simeq 1$ year) computed from the monthly data, plotted as a constant band about the estimate $\hat{\sigma}_\rho^2 = 328\ kg^2m^{-6}$, is roughly an order of magnitude greater than the highest variance observed in the daily data. The partition between synoptic and higher-frequency bands is less readily determined. While the 10-day samples of daily data are aliased and incorporate variance from both sources, the short sets of intensive observations, though largely free of alias effects and dominated by high-frequency variance, include a component of the synoptic-band signal as well.

More detailed spectral results are available for water temperature than for density or salinity. The variance density spectrum computed from hourly values of a 20-day temperature record collected at station 5 in August 1975 (Figure 38)

indicates that more than 60% of the total variance resides at subtidal frequencies, $f<0.04$ c $h^{-1}$. The relationship between the frequency distributions of temperature and density is not well established, but it is hypothesized that the two functions are highly coherent in the synoptic and tidal frequency bands. Although water temperatures in a shallow lagoon respond directly to diurnal variations of radiative heat transfer and to synoptic-scale weather, both effects that potentially reduce the coherence between temperature and density, the data generally support the notion that subtidal (synoptic- and seasonal-scale) frequencies dominate the spectra, not only of temperature and water level (cf. section 3.2.1), but of salinity and density also.

The daily temperature and salinity data for late July and early August 1977 (Figure 66) show pronounced synoptic-scale variability. During the second, third, and fourth days of the record, unusually low water levels developed in the estuary; observations at stations 5 and 7 in the entrance revealed a trend of increasing density and decreasing stratification. This was a period of easterly winds, which are frequently associated with negative surges and upwelling of deep water in Mackenzie Bay (although easterly winds are directed onshore along the Yukon coast, the associated Ekman transport is offshore). It is not known whether the cold saline water observed in the Babbage Estuary ($\theta$ =0°C, s=25ppt) was derived from Mackenzie Bay or from deep water in Herschel Basin (where a separate circulation response may have developed, with return

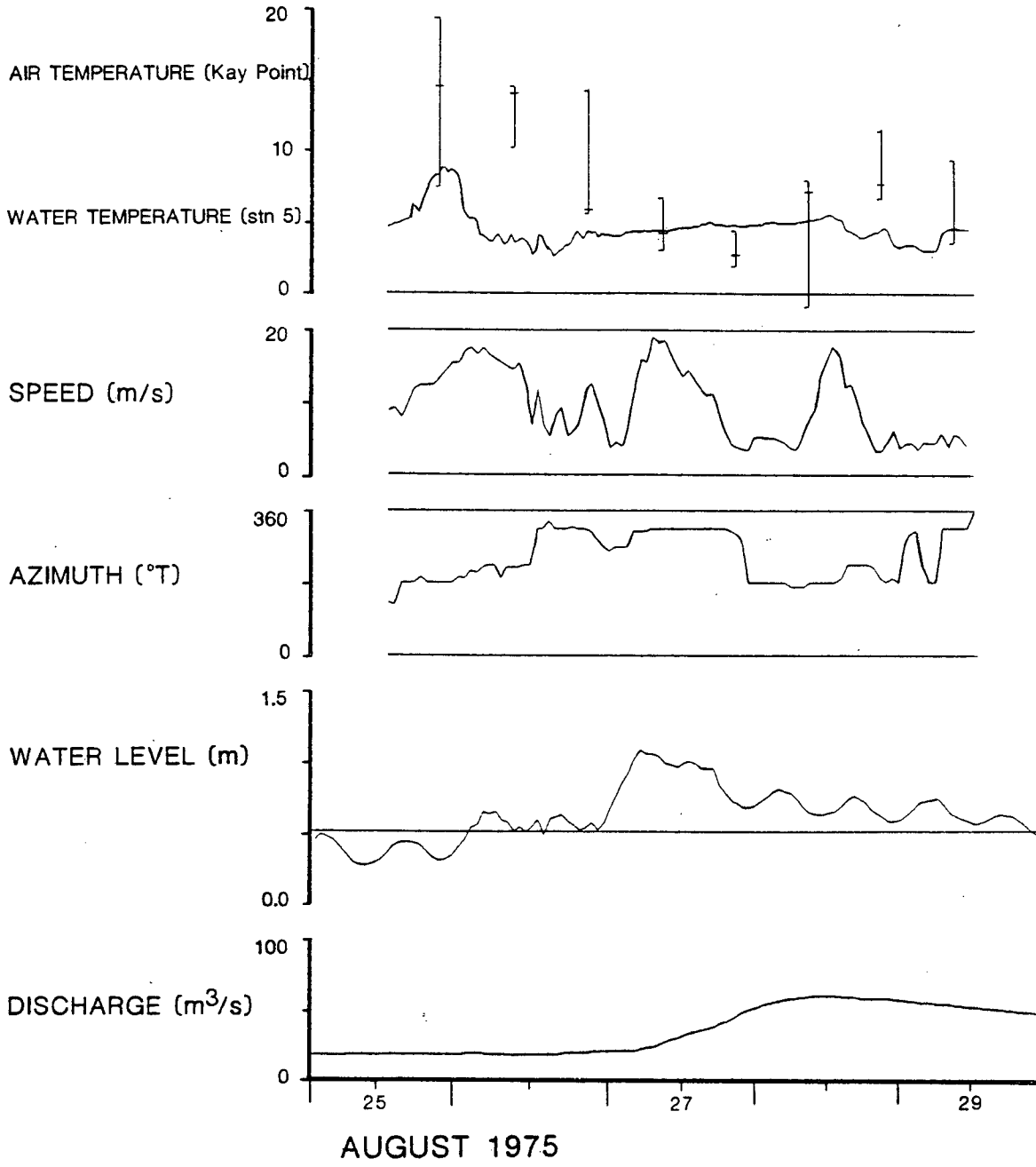


FIGURE 68

Time sequence including the storm surge event of 27 August 1975: 12h maximum, minimum, and instantaneous air temperature; half-hourly water temperature; wind speed and direction at Kay Point; water level at gauge A; and Babbage River discharge at B1.

flow and upwelling countering a westward surface transport). A return to calm conditions for several days was accompanied, in the Babbage Estuary entrance, by relaxation to $\theta$ >12°C and s<7ppt. Again, on August 1, persistent easterly winds and unusually low water levels developed, continuing to the end of the record, when extreme conditions ( $\theta$ =0.5°C and s=24ppt) were again observed.

Data obtained during positive storm surges indicate that, at least for the small-to-moderate storms of August 1975, extreme temperature and salinity conditions did not develop in the estuary. Half-hourly temperature data are available from station 5 [at (h-z)=0.9 m] for the surge of 27 August 1975 (Figure 68). A water temperature maximum of 8.7°C occurred during the evening of 25 August under a moderate, warm, southerly wind. During the following flood tide, water temperature dropped rapidly; the abrupt change in temperature can be explained plausibly by appeal either to a stratified condition with a rising thermocline, or to strong horizontal temperature gradients in a vertically homogeneous situation. Water temperature remained low through 26 August while the wind dropped and veered to northwest. The temperature record for the 26th exhibits high-frequency variance coherent but out of phase with the high-frequency fluctuations of water level. Late on the 26th the water temperature began to rise, increasing by just 1.0K over 36h, with extremely low variance about the trend ( $\hat{\sigma}_{\theta}^2$=0.01K$^2$) and no perceptible disruption by the strong northwesterly winds and associated storm surge early

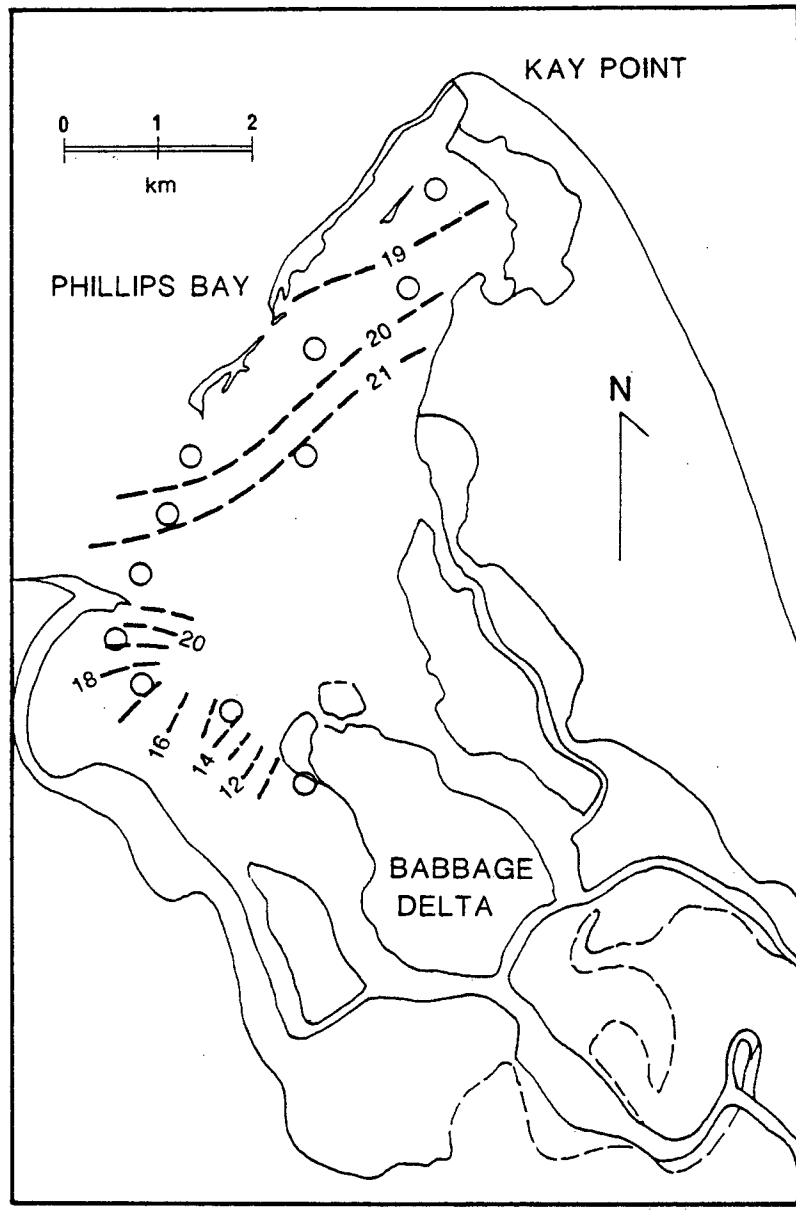


FIGURE 69

Surface salinity (ppt) in the Babbage Estuary following the storm of 27 August 1975.

on the 27th.

A synoptic survey of the estuary was carried out between 1400 and 1600h local (9-11 h after the surge peaked and 1-3 h before the major outflow began); the results showed surface salinities in the range $19<s<22$ppt (Figure 69) and surface temperatures $5< \Theta <8°C$, except in the north end of the lagoon at station 1, where warmer and less saline water occurred, and in the outer reach of the main distributary channel, where conditions may have been affected by increasing discharge in the river. Vertical differences as great as 3.3ppt were observed in the main distributary channel, but the water column in the entrance was almost homogeneous, with a maximum vertical salinity difference of 0.5ppt at station 7.

In addition to variance at periods $T \leq 1$ year, there is evidence of important year-to-year variability of salinity and density. In 1976, the first major salinity intrusion in the Babbage Estuary occurred on 27 July; in 1975, it occurred approximately two weeks earlier. Limited data for 1974 (Table 4) suggest, in contrast, that salinities may not have exceeded 10ppt in estuaries of the central Yukon coast or in surface waters of Mackenzie Bay throughout July and August of that year. Higher salinities did occur at depth (typically $s \geq 25$ppt at 10 m, $s \geq 30$ppt below 20 m; Herlinveaux et al., 1976), so that upwelling associated with offshore winds might potentially have brought more saline water to the surface at the coast. However, the summer of 1974 was characterized by a relative absence of easterly and southerly winds normally

associated with upwelling in Mackenzie Bay and no occurrences of salinity s>2.5ppt were observed in the Babbage Estuary, although a regular program of observations was not maintained. It is probable that relatively saline water moved into the Babbage Estuary by mid-September, when persistent low water levels were recorded at Kay Point spit, gauge A (Figure 35).

Salinities in 1975 (Table 4) and in 1976 (Figure 64) were more representative of the mean summer condition, under which surface waters close to the coast remain generally brackish, but salinities in excess of 20ppt are occasionally observed in the Babbage Estuary. The mean salinity at stations in the entrance was 11.4±0.4 ppt in August 1976 and 14.3±1.0 ppt for the period 24 July to 6 August 1977; mean salinity in late July and early August 1974 may have been no greater than 2 ppt. It appears, therefore, that seasons with relatively low frequencies of offshore winds and persistent heavy ice concentration near the coast may be associated with a depression of the mean mid-summer salinity of the order of 10ppt. This may have an important influence on circulation and sediment dispersal during the open-water season.

### 3.3.5 THE NON-TIDAL CIRCULATION

Variability of density and other water properties has an important bearing on the circulation of water and the dispersal of clastic sediment in an estuary, as summarized in the introduction to section 3.3.4. Although wind and ice are major factors in the circulation regime of shallow lagoons on the Beaufort Sea coast (Dygas and Burrell, 1976; Matthews, in press), the effects of tidal flows, river discharge, and geomorphology in the presence of a longitudinal density gradient are nevertheless pervasive. Major adjustments in the summer circulation related to seasonal variability of runoff and water density can be recognized. The circulation regime in the absence of wind and ice can be regarded as a reference condition from which major deviations occur (in practice the reference condition can be specified only in the most general terms).

In a narrow rectilinear estuary, assumed laterally homogeneous, the vertical density gradient and the net non-tidal circulation (mean velocity field at a time scale that is large relative to the dominant tidal periods) depend largely on the following parameters: (1) the longitudinal density gradient $(\rho_f - \rho_0)/L$, where is the density of the freshwater input and $\rho_0$ the density of the water at the entrance (the origin is taken at the entrance and L may be taken to represent the length of the salinity intrusion); (2) the longitudinal position $0 \leq x \leq L$; (3) the estuarine morphology (width b and depth h); (4) the rate of freshwater inflow, Q, and the integral mean

velocity, $u_f=Q/bh$; (5) the tidal dynamics, which may be represented in many ways, but which serve primarily as a source of turbulent energy; and (6) the wind shear, $\tau_a$, at the surface. Assuming $\tau_a=0$, a variety of distinctive circulation conditions may be recognized.

The circulation in a laterally homogeneous rectilinear estuary may be represented by four equations involving eight unknowns (see, for example, Harleman and Ippen, 1967, pp.6-7), viz. salinity, s, density, $\rho$, velocities, u and w, dispersion coefficients, $K_x$ and $K_z$, pressure, p, and Reynolds stress, $(-\rho\overline{u'w'})$. Hansen and Rattray (1965) obtained a solution based on the assumptions that the longitudinal salinity function, $\bar{s}(x)$, is linear and that the mean vertical velocity profile, $\bar{u}(z)$, is independent of x, plausible only in a central reach near x/L=0.5.

Despite the restrictive assumptions, this solution provides a basis for the most widely and readily adopted system of estuarine classification (Hansen and Rattray, 1966). Under calm conditions, the partition, $\nu$, between dispersion and gravitational convection can be represented in terms of a circulation parameter, $u_s/u_f$, and a stratification parameter, $(s_h-s_s)/[s]$, where $u_s$ is the mean longitudinal velocity at the surface, $s_s$ is the mean salinity at the surface, $s_h$ is the mean salinity at the bottom, and [s] is the section-mean salinity (Hansen and Rattray, 1966, pp.321-322). It appears that $u_s/u_f$ is correlated in a negative non-linear fashion with a Froude parameter

$$F = u_f/[gh(\Delta\rho/\rho)]^{1/2},$$

where $(\Delta\rho/\rho) = (\rho_0-\rho_f)/\rho_0$ and $\rho_0$ is the density at the entrance (Hansen and Rattray, 1966, pp.323-325). The stratification parameter, $(s_h-s_s)/[s]$, is related both to F and to $u_f/u_t$, where $u_t=(\overline{U^2})^{1/2}$ is the rms tidal speed.

Babbage Estuary data were examined in this context with a view to identifying seasonal-scale variability in the circulation regime. Mean values of $(s_h-s_s)/[s]$ and $F^{-1}$ were computed from successive 10-day samples of the daily density and salinity data for 1976 (corresponding to the 10-day intervals in Figure 67). The analysis was restricted to data from station 12, where the theoretical assumptions may be more nearly satisfied than in the entrance section. It was assumed that the quasi-random daily sampling scheme yielded reasonably unbiased estimates of tidal-average parameters for each 10-day interval. Computed values of $F^{-1}$ were not explicitly transformed to estimates of $u_s/u_f$ because substantial uncertainties concerning the relation between these two parameters remain (Hansen and Rattray, 1966, p.324; Hughes and Rattray, 1980, p.492) and because F was deemed to be more appropriately defined in terms of local density differences $(\Delta\rho/\rho) = (\rho_h-\rho_s)/\rho_h$, as is customary in the definition of interfacial Froude parameters (see, for example, Wright, 1977, p.859).

The results (Table 13) indicate a major transformation of the circulation at station 12 in late July 1976. This transformation corresponds to the first significant salinity

TABLE 13

Stratification and circulation parameters(mean ±standard error) for the Babbage Estuary at station 12 during successive ten-day intervals in the summer of 1976.

| dates | $(s_h - s_s)/[s]$ | $F^{-1}=[gh(\Delta\rho/\rho)]^{1/2}/u_f$ |
|---|---|---|
| 13 Jun - 22 Jun | 0.00 | 0.00 |
| 23 Jun - 2 Jul | 0.00 | 0.00 |
| 2 Jul - 12 Jul | 0.00 | 0.00 |
| 13 Jul - 22 Jul | 0.00 | 0.00 |
| 23 Jul - 1 Aug | 0.80±0.28 | 1.11±0.51 |
| 2 Aug - 11 Aug | 0.95±0.24 | 3.02±0.81 |
| 12 Aug - 21 Aug | 0.40±0.19 | 1.15±0.59 |
| 22 Aug - 31 Aug | 1.14±0.20 | 4.62±0.89 |
| 1 Sep - 10 Sep | 1.11±0.22 | 4.52±0.81 |

intrusion (cf. Figure 65). Prior to July 23, the data indicate consistently nonstratified or weakly stratified conditions; after that date, a shift to stratified (and highly variable) conditions is indicated. On the basis of the stratification parameter and limited velocity data, one can place this reach of the Babbage Estuary, during the intervals 2-11 August and 22 August to 10 September, in the boundary region between type 2b (partially-mixed) and type 4 (salt-wedge) regimes in the classification of Hansen and Rattray (1966, figure 2). During the intervals 23 July to 1 August and 12-21 August, partially-mixed conditions are indicated. Data from the entrance section show a similar dramatic seasonal shift, with more pronounced stratification after 23 July. Because wind-induced mixing is more effective in the lagoon, the stratification parameter, evaluated for the entrance section, has a mean value of only 0.18 for the later part of the season, much lower than the corresponding value at station 12.

During a series of hourly observations (19-21 July 1976) immediately prior to the summer salinity intrusion, mean values of the stratification and circulation parameters obtained at station 12 were $(s_h - s_s)/[s] = 5 \times 10^{-3}$ and $u_s/u_f = 1.01$, with $u_s$ taken at $z \leq 0.2h$. Measurable stratification was observed only twice. The maximum salinity at station 12 during this period was s=0.4ppt, while salinities no higher than s=2.3ppt were recorded in the entrance. At station 12, current reversals occurred at all levels during flood tide, but a seaward non-tidal mean flow was maintained at all depths, implying that

gravitational convection played no part in the small upstream salt flux occurring at this time. This accords with the behaviour predicted by the model.

Highly stratified conditions develop in the deeper parts of Babbage Delta distributaries and are occasionally observed in the lagoon after the mid-summer salinity intrusion has occurred. Pooling of high-density water in distributary channel depressions is a common feature of the late-summer circulation in the delta (Figures 70, 71, and 72). The main distributary channel consists of a series of basins with intervening shallow sills which severely inhibit development of a simple gravitational circulation regime. This may have important implications for the sediment transport system (section 4.3.1).

While the upper part of the flow, above mean sill depth, operates in late summer as a partially-mixed estuary, intermittent pronounced stratification develops at depth, particularly under ebb-flow conditions. During flood tide, higher salinity water is advected upchannel, impounding the freshwater discharge (Figure 71A). With the turn of the tide, seaward flow at the surface is re-established, the zone of maximum surface salinity gradient is moved downstream, and a major near-horizontal halocline may develop above high-density water trapped in the pools (Figure 70; Figure 72A). Considerable entrainment upward across the halocline, possibly effected by breaking internal waves, appears to take place during the ebb tide. This process may be enhanced by

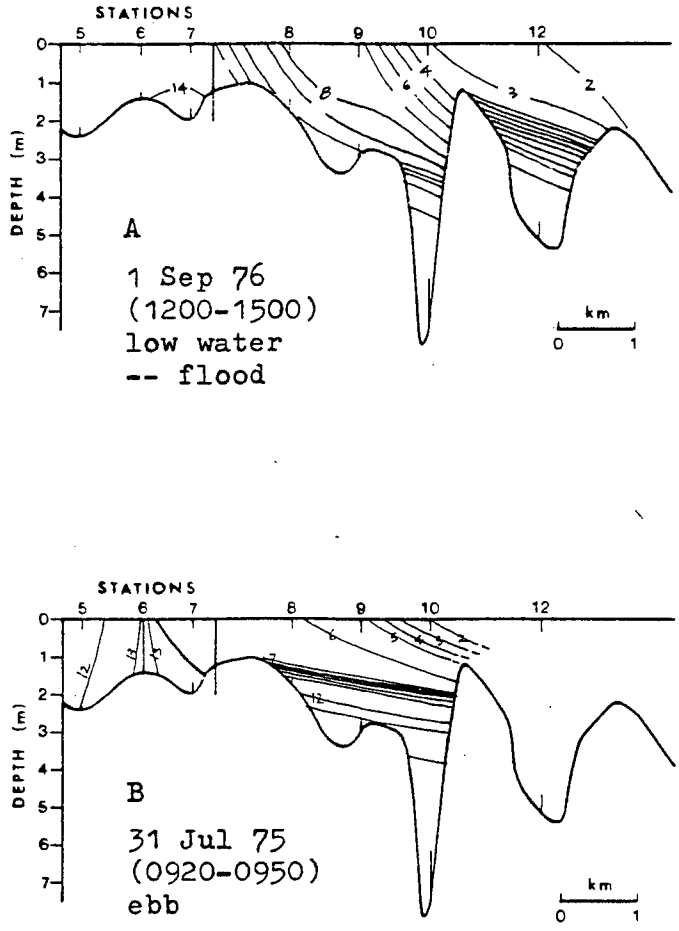


FIGURE 70

Examples of salinity stratification in main distributary channel and entrance section of Babbage Estuary, 1 September 1976 and 31 July 1975.

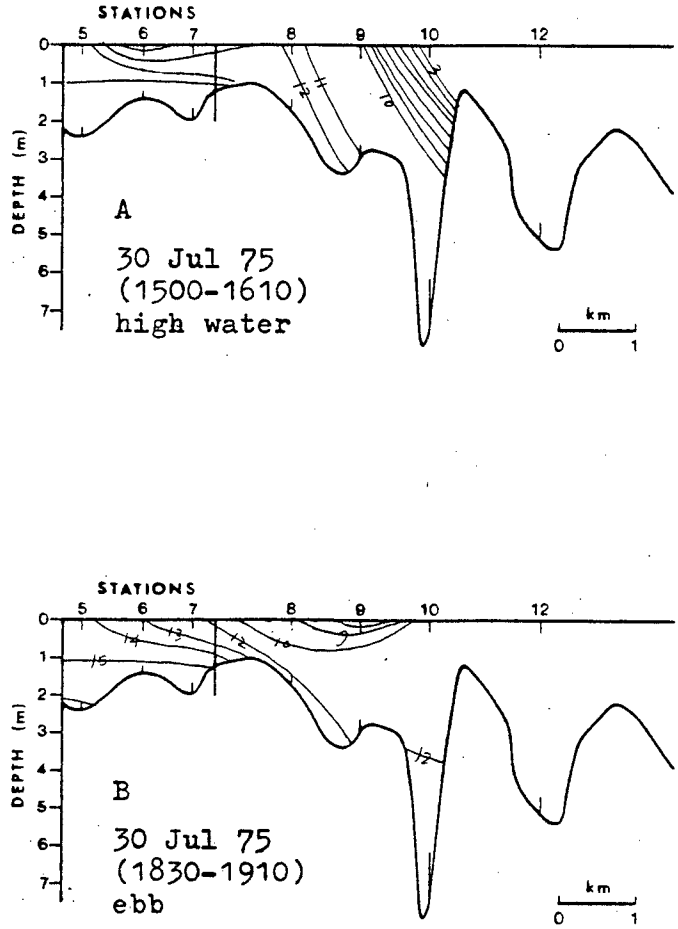


FIGURE 71

Change in pattern of salinity stratification in main distributary and entrance section of Babbage Estuary over a 3-4h period of ebb flow, 30 July 1975.

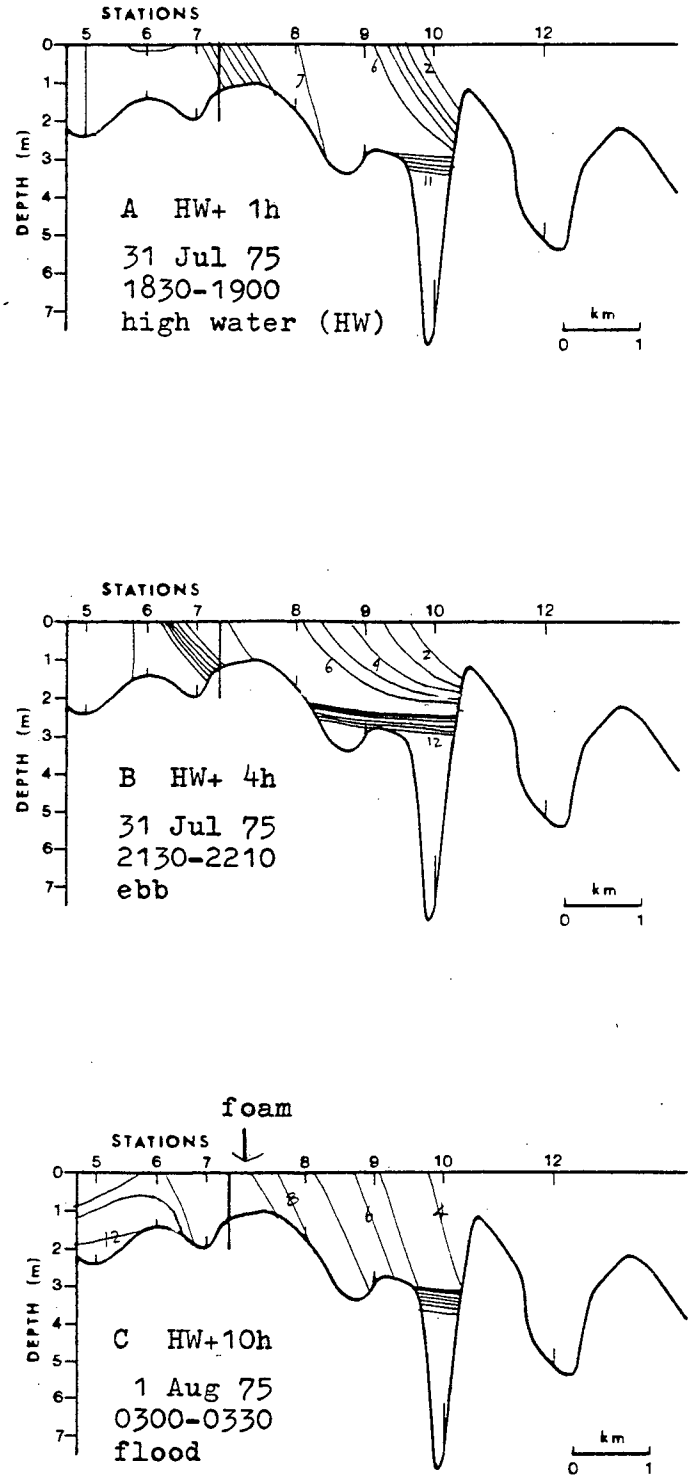


FIGURE 72

Changes in the pattern of salinity stratification over nine-hour interval, 31 July to 1 August 1975.

topographic effects, as appears to be the case in the Duwamish Estuary (Gardner and Smith, 1978).

When assumptions of lateral homogeneity and of negligible transverse velocity are relaxed, as they must be for a realistic model of any natural estuary (Fischer, 1972) and particularly in the case of shallow lagoons, the situation becomes necessarily more complex (cf. Dyer, 1973, 1974, 1977; Officer, 1976; McDowell and O'Connor, 1977). In a wide entrance section such as occurs in the Babbage Estuary, $(\partial u/\partial y)$ may be highly significant, due to characteristics of the tidal dynamics that concentrate flood flows in one part of the section and ebb flows in another (van Veen, 1950; van Straaten, 1960; Price, 1963). In addition, a characteristic ebb-flow predominance on the right side (facing seaward) and flood predominance on the left, with an associated pattern of lower mean salinity toward the right, is sometimes observed in northern hemisphere estuaries where the Coriolis acceleration makes a major contribution to the transverse dynamics (eg. Pritchard, 1956, table 3). The horizontal Coriolis parameter is $f_1 = 2\Omega \sin\phi$, where $\phi$ is latitude and $\Omega$ the angular velocity of the earth. In the latitude of the Babbage Estuary ($\phi$ =69.25°N), the Coriolis effect amounts to $f\bar{v}=(1.36\times10^{-4})\bar{v}$ m $s^{-2}$.

The transverse distribution of surface density in the Babbage Estuary entrance (stations 5-7) has been examined using 1976 daily observations and hourly data for the period 19-21 July 1976. Applying Wilcoxon's paired-sample test (see,

e.g., Snedecor and Cochran, 1967, pp.128-129), the null hypothesis that $\rho(5) = \rho(7)$ is rejected at $\alpha = 0.0001$ ($n=82$, $Z=3.71$), the mean density at station 7 (left side facing seaward) being lower. A similar conclusion is indicated for the hourly data in mid-July ($\alpha = 0.0001$, $n=48$, Student's $t=15.3$).

These results would seem, at first sight, to indicate that a preferential outflow of freshwater on the right side of the entrance (station 5) does not occur frequently. However, if the orientation of the main distributary outlet off Niakolik Point is extrapolated toward Kay Point spit, stations 5-7 may be viewed as points on a longitudinal section in an outer estuarine reach with station 5 most distal, in which case one would expect lower salinity at station 7.

Surface fronts sometimes occur near station 6 in the entrance section, separating the river plume on the Niakolik Point side from brackish marine and lagoon water to the north (Figure 70B). These are usually short-lived, the more typical condition being a relatively weak horizontal density gradient at the surface.

The bathymetry of the entrance section off Niakolik Point (Figure 73) shows a thalweg pattern that may favour flow deflection normal or parallel to the entrance section, according to the prevailing dynamic conditions. Most of the available velocity data appear to favour a model of effluent expansion seaward of Niakolik Point, with the axis of the flow

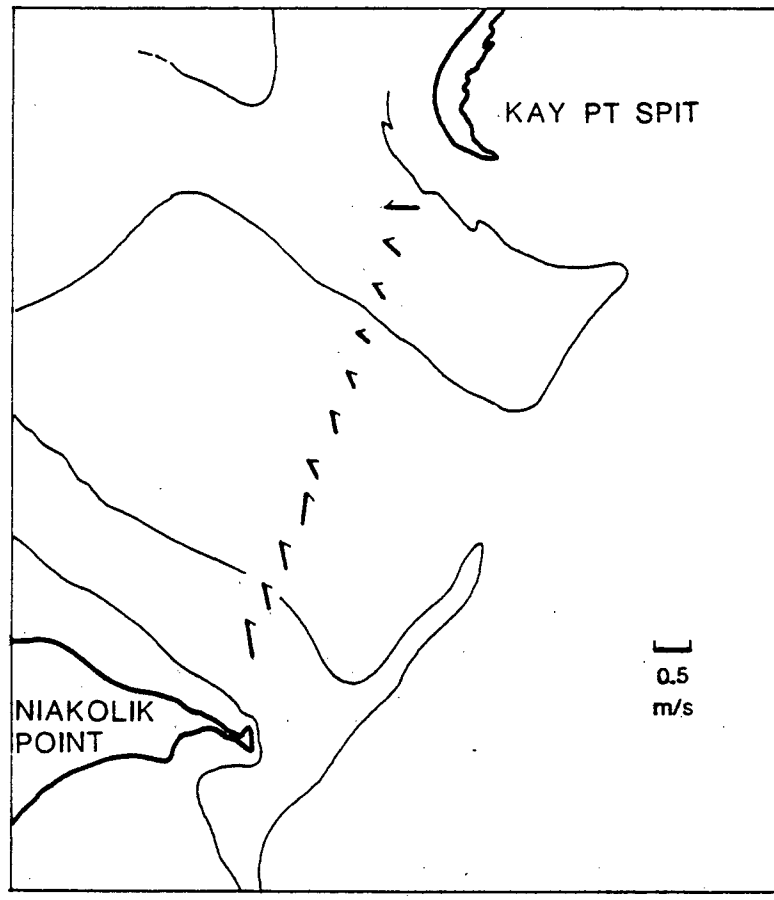


FIGURE 73

Surface velocity distribution in M1 section, Babbage Estuary, during ebb, 1423-1603h 10 August 1976; wind from 135°T at 7.7 m $s^{-1}$, Babbage River discharge Q=27 $m^3 s^{-1}$, velocity field in entrance section approximately uniform with depth. The 1-m isobath (relative to gauge datum) is also plotted.

lying initially quasi-parallel to the line of stations 5-7 and turning seaward in the vicinity of stations 5 and 6. This is the pattern suggested by an observed ebb-flow illustrated in Figure 73. In another example, surface outflow observed during a flood-tide (Figure 74) was overriding a layer of flood-directed flow in the deeper channels near stations 5 and 7 but formed a single ebb-directed boundary layer over the central shoal near station 6.

Wind plays a major role in the mixing and circulation regime of the Babbage Lagoon. Circulation in shallow lagoons is often found to be wind-dominated, a pattern confirmed for open-water conditions in certain lagoons of the north Alaska coast (Wiseman et al., 1973, pp.48-49; Dygas and Burrell, 1976; Matthews, 1979). Wind stress enters the equations of horizontal motion as terms of the form $(1/\rho)(\partial\tau_x/\partial z)$ and $(1/\rho)(\partial\tau_y/\partial z)$. If a linear shear profile is assumed, these terms can be evaluated as $(\tau_a-\tau_b)/\rho h$ (Dyer, 1977, p.26), where $\tau_a$ and $\tau_b$ are, respectively, the components of the surface and boundary shear stress. Assuming $\tau_b \leq 0$ (fully-developed response), $\rho_w$=1010 kg $m^{-3}$, $\rho_a$=1.25 kg $m^{-3}$, $C_D=1.6\times10^{-3}$ (Wiseman et al., 1973, p.29), a wind speed of 2.5 m $s^{-1}$ yields an acceleration of $1.2\times10^{-5}$ m $s^{-2}$ in 1 m of water; a wind speed of 10 m $s^{-1}$ and a depth of 1 m gives an acceleration of approximately $2\times10^{-4}$ $m.s^{-2}$. This is at least one order of magnitude greater that the anticipated values of centripetal and Coriolis terms. Locally variable response of vertical salinity distributions to wind-generated mixing processes can

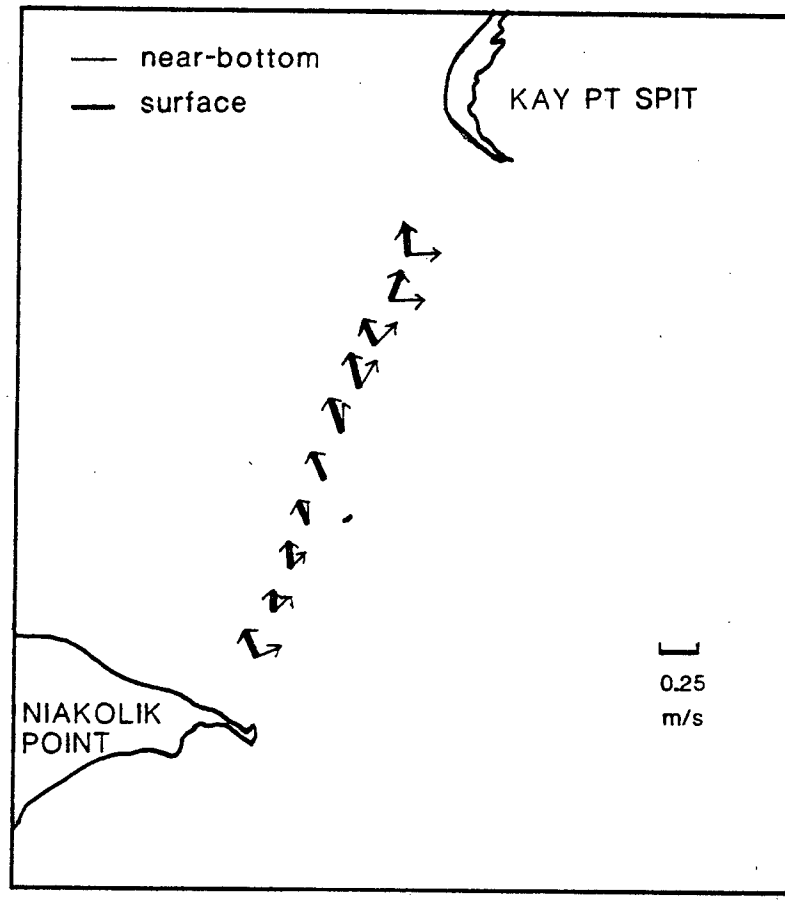


FIGURE 74

Surface and near-bottom velocities in M1 section, Babbage Estuary entrance, during flood 1200-1330h 3 August 1976, showing continued ebb flow at all depths over the central shoal, with water entering at depth via channels near stations 5 and 7 (see Figures 3 and 75 for bathymetry); wind from 315°T at 2.5 m $s^{-1}$, Babbage River discharge Q=16.5 $m^3 s^{-1}$.

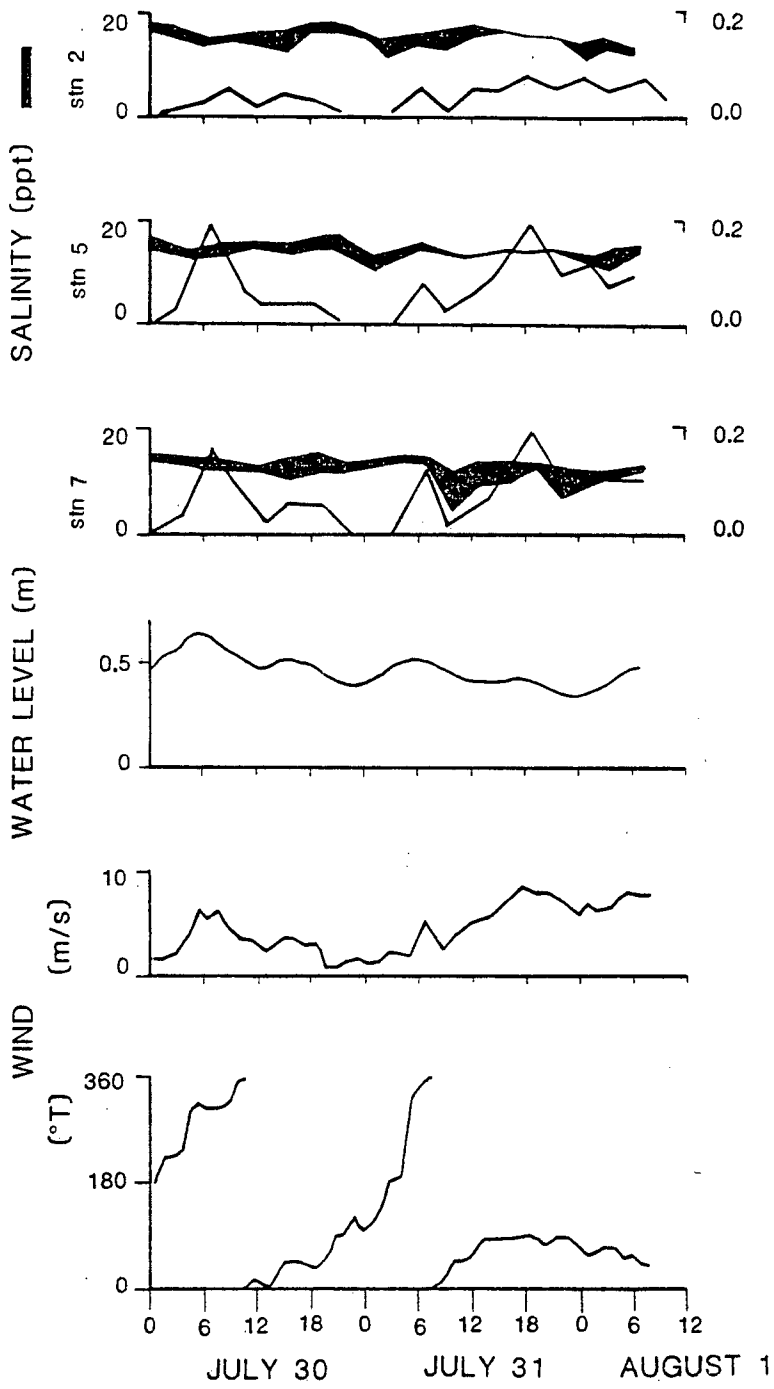


FIGURE 75

Time sequence of surface and bottom salinity at stations 2, 5, and 7 in Babbage Estuary, of gauge-A water level, and of wind speed and direction at Kay Point, showing response of vertical salinity distributions to wind-induced mixing; wave heights are superimposed on the salinity sequence.

be seen in Figure 75.

The effects of wind stress and circulation parameters on horizontal and vertical density gradients in the entrance section were investigated using simple correlation procedures and the daily density data for 1976. The maximum vertical and transverse density differences, $(\Delta\rho)_v$ and $(\Delta\rho)_t$, in each set of observations were taken as the output variables. The flow ratio R/P (Simmons, 1955), where R is the total freshwater runoff during a tidal cycle and P is the tidal prism, was selected as a simple circulation parameter; although it is inappropriate for comparative analysis of different estuaries, due to the dynamic importance of morphological factors, it provides a useful summary of synoptic-scale variability within a single system and it is proportional to the tidal mixing parameter of Hansen and Rattray (1966, p.324), the principal factor affecting vertical stratification in the absence of wind. Other variables considered were mean density, $\bar{\rho}(t)$; northwesterly and northeasterly components of hourly wind stress (see section 3.2.1) back to six hours prior to the observations; water level $\zeta(t)$; and tidal phase.

The significant portion of the correlation matrix is given in Table 14. The two output variables, $(\Delta\rho)_v$ and $(\Delta\rho)_t$, exhibited the highest correlation (r=0.64). Both transverse and vertical gradients showed weak positive correlation with the transformed circulation parameter log(R/P), $(\Delta\rho)_t$ being more highly correlated than $(\Delta\rho)_v$. On the other hand, the vertical stratification responded inversely to northwesterly

TABLE 14

Product-moment correlation coefficients for mean density, transverse stratification, and vertical stratification in the Babbage Estuary entrance (stations 5-7). Coefficients not significant at $\alpha=0.05$ have been omitted.

| | $\bar{\rho}(t)$ | $(\Delta\rho)_t$ | $(\Delta\rho)_v$ |
|---|---|---|---|
| $\bar{\rho}(t)$ | 1.00 | | |
| $(\Delta\rho)_t$ | | 1.00 | 0.64 |
| $(\Delta\rho)_v$ | | 0.64 | 1.00 |
| $\zeta(t)$ | 0.44 | | -0.26 |
| log(R/P) | | 0.42 | 0.29 |
| $\tau_{nw}(t-1+k)$ | | | -0.35 |
| $\tau_{nw}(t-2+k)$ | | | -0.36 |
| $\tau_{nw}(t-3+k)$ | | | -0.38 |
| $\tau_{nw}(t-4+k)$ | | | -0.40 |
| $\tau_{nw}(t-5+k)$ | | | -0.38 |
| $\tau_{nw}(t-6+k)$ | | | -0.36 |
| $\tau_{ne}(t-1+k)$ | -0.27 | | |

$0 \leq k \leq 1$

wind stress, the largest negative correlation being at a lag of approximately 3.5 h.

In order to assess the relative frequency of various circulation patterns in the entrance section, both for an understanding of the circulation dynamics and as input to sediment budget computations, current meters and other instrumentation were moored at stations 5 and 7 in 1975 and 1976. Unfortunately, reliable results were obtained only for the 1975 mooring of an Aanderaa RCM-4 current meter and associated temperature sensor at station 5. Due to depth and mooring limitations, the instrument was placed at a nominal elevation of 0.9 m above the bed.

Hourly values of longitudinal and transverse velocity components, low-pass and high-pass filtered sequences, and hourly water level at gauge A are given in Figure 76. The data were filtered using a 39-h nonrecursive filter developed by Groves (1955). The components are referred to a right-hand coordinate system in which x and u are positive toward 118°T (positive on flood) and y and v are positive toward 208°T (positive toward stations 6 and 7). These coordinates, determined by the overall alignment of the section, do not necessarily correspond to axial and transverse components of the mean flow (cf. figures 73 and 74). The observations cover some 20 days, beginning two days after the moderate storm surge of 10 August and including two further surges on August 17 and 27.

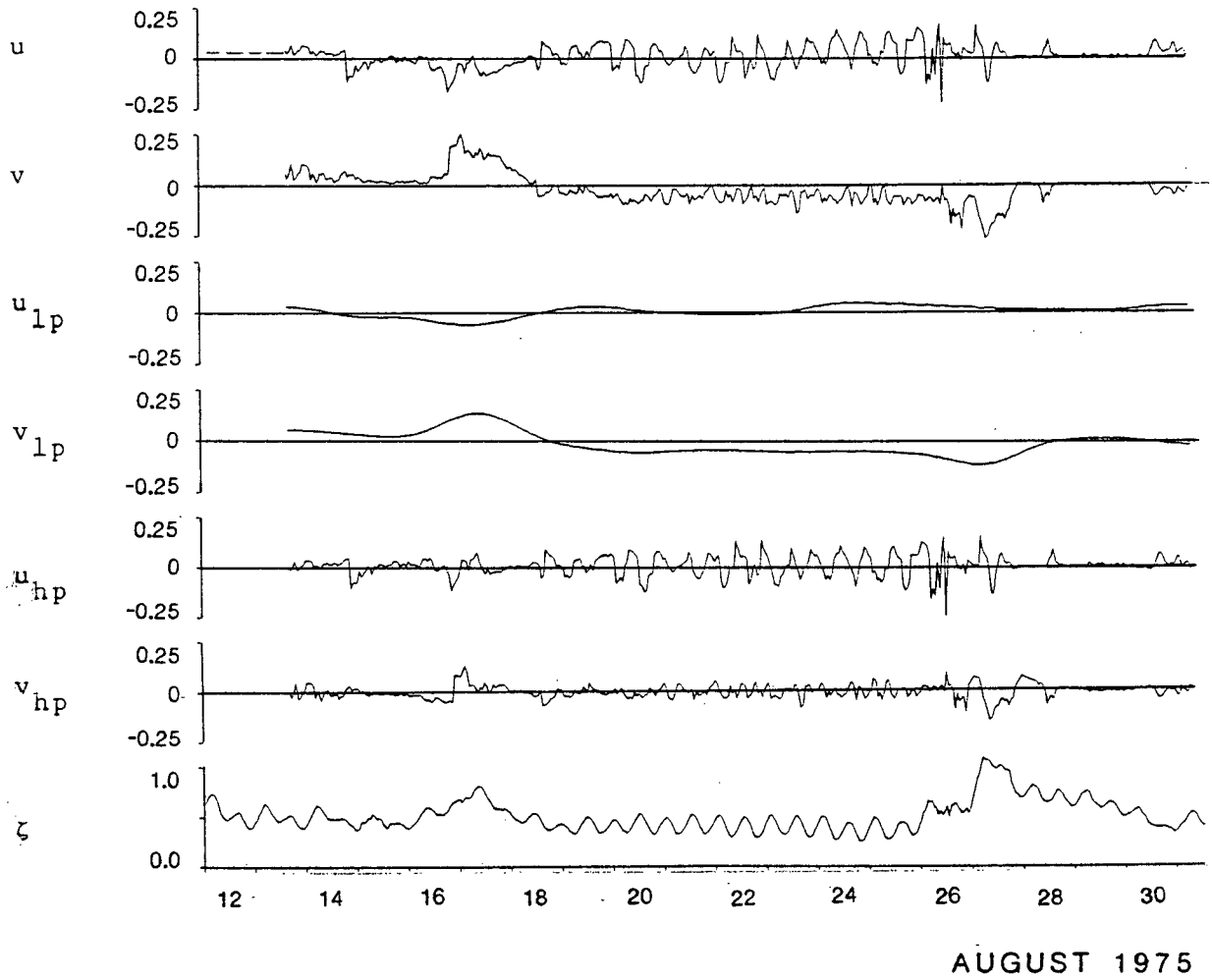


FIGURE 76

Longitudinal and transverse components of velocity at station 5, low-pass and high-pass filtered components, and water level at gauge A, Babbage Estuary, 12-31 August 1975.

Several important conclusions may be drawn from these data. First, periods of negligible flow with an extremely weak tidal component appear to have followed the two moderate surges of 10 and 27 August. Second, the data include only about seven days ($230 \leq t \leq 237$) when synoptic-scale storm effects did not dominate the velocity field. Third, during this period of quasi-equilibrium conditions, the transverse component was consistently negative and the longitudinal component contained by far the greater part of the semidiurnal tidal signal. This is consistent with a hypothesis of river discharge parallel to the section, with tide-driven deflection either seaward or into the lagoon near station 5.

Interpretation of the velocity record is complicated by the occurrence of stratification for which there is no reliable indicator in the hourly data. Low velocities persisting for several days following the two larger storm surges may represent the development of pronounced stratification in the channel at station 5, approaching an arrested salt-wedge condition during the prolonged zero flow after August 27 (although no independent corroboration of the response is available). Pronounced vertical salinity differences were observed at station 5 on the 12th and 13th of August, following the 10 August surge, differences amounting to 8.1ppt and 7.2ppt respectively. The abrupt shift from positive to negative u late on the 13th ($t=225.9$) may reflect a vertical mixing event due to wind during the afternoon and evening; a temperature increase of almost 4K accompanied this event.

The response during storms is harder to generalize, in part perhaps because local wind accelerations play a major role in the circulation dynamics at these times. Erratic high-frequency fluctuations in the section-mean velocity, [u], estimated from the water level data, are partly reproduced in the longitudinal velocity record for station 5. The longitudinal component was flood-directed during the surge inflow early on the 27th (t=238), but the transverse component of flow (directed across the section from Niakolik Point toward station 5) remained strong, increasing rapidly as soon as the surge peaked. By the end of the day, the velocity had dropped to near zero, where it remained (except for brief intervals of flood-directed flow) until the end of the record. Storm runoff from the Babbage River peaked at Q=61 $m^3s^{-1}$ close to noon on August 28 (see Figure 68). It is intriguing to note that the largest excursions of velocity during the two storm surges (August 17 and August 27) occurred in the transverse component, that they differed in sign on the two occasions, and that on the 17th the longitudinal component was ebb-directed throughout the surge, except for a brief interval coinciding with the surge maximum.

In summary, it appears that short-term fluctuations of density and other physical parameters of water in the estuary extend over a wide range of frequency, with most of the variance at synoptic and seasonal scales, the dominant period being T=1 year. Abrupt changes in the mean density occur during breakup and again in mid-summer, as the estuary switches

from hypersaline to fresh conditions and then back again to higher salinities in the range $0<s<24$ ppt. Shifts in the dominant circulation mode coincide with these changes.

Prior to the mid-summer salinity intrusion, the estuary is vertically and laterally well-mixed in the main distributary channel and in the entrance section. Gravitational convection is not an important circulation process at this time. It is inferred that highly-stratified conditions may prevail in the region of plume expansion outside the entrance section in Phillips Bay during much of June, although the distance to the shoreward limit of salinity intrusion is unknown and may be highly variable. After the mid-summer shift to higher mean salinity, the estuary is often partially-mixed, although wind is an important factor in the vertical mixing process, well-mixed conditions often occur, and the circulation regime is highly variable at this time. The presence in distributary channels of deep pools, in which denser water becomes isolated beneath abrupt near-horizontal pycnoclines, may inhibit development of a sedimentologically significant gravitational circulation system in the delta. The velocity field in the entrance section may be relatively homogeneous or it may be highly variable, with opposing mean flow in both vertical and horizontal planes being not uncommon in late summer. For this reason, although the net exchange of water between the Babbage Estuary and Phillips Bay can be computed as a residual in the water balance (see following section), complete documentation of the water budget would require an extensive array of

current-meter strings in the entrance section. Meaningful estimates of suspended sediment exchange in late summer therefore require a large logistical commitment. Fortunately, as the results of sections 4.1.2 and 4.1.3 demonstrate, a very large proportion of the annual fluvial sediment input occurs during a time of relatively simple circulation in the estuary, during the snowmelt and post-snowmelt runoff season in June, when complete water and sediment budgets are more readily obtained. On the other hand, wave-generated sediment inputs are at a maximum during that part of the season when the circulation regime is at its most complex.

### 3.3.6 WATER BUDGET AND STRUCTURE OF THE SYSTEM

The net exchange of water between the Babbage Estuary and Phillips Bay depends on both external and internal factors. External factors include the imposed water level at the marine boundary (section 3.2.1) and the rate of water supply from other sources, primarily Babbage River runoff (section 3.1.1). Internal parameters include the storage function and water surface configuration of the estuary. The latter is determined by the tidal cooscillation (section 3.3.1) during the open-water season and by ice and backwater effects during breakup flooding (see sections 3.3.2 and 3.3.3). The storage function of the system defines the volumetric capacity, V, which depends upon water level and bathymetry and reflects the system response to water inputs.

The time scale of significant bathymetric change is sufficiently great that the system geometry (Figure 3) can be considered fixed in the short run; recall, however, the major changes that may have occurred over the past 150 years (section 2.1.2). For present purposes, the storage function, $V(\zeta)$, has been defined with constant parameters (Figure 77).

Net exchanges, $Q_o(t)$, through the entrance section M1 were computed as residuals in the water balance, defined as

$$Q_r(t) = \Delta V(t) - Q_f(t-\tau) \qquad (3.3.6\text{-}1)$$

where $Q_f$ is the total gauged hourly runoff (through B1 and D1), $Q_r$ is the residual hourly flow, and $Q_o = Q_r - Q_e - Q_d \simeq Q_r$, evaporative losses ($Q_e$) and direct precipitation ($Q_d$) being

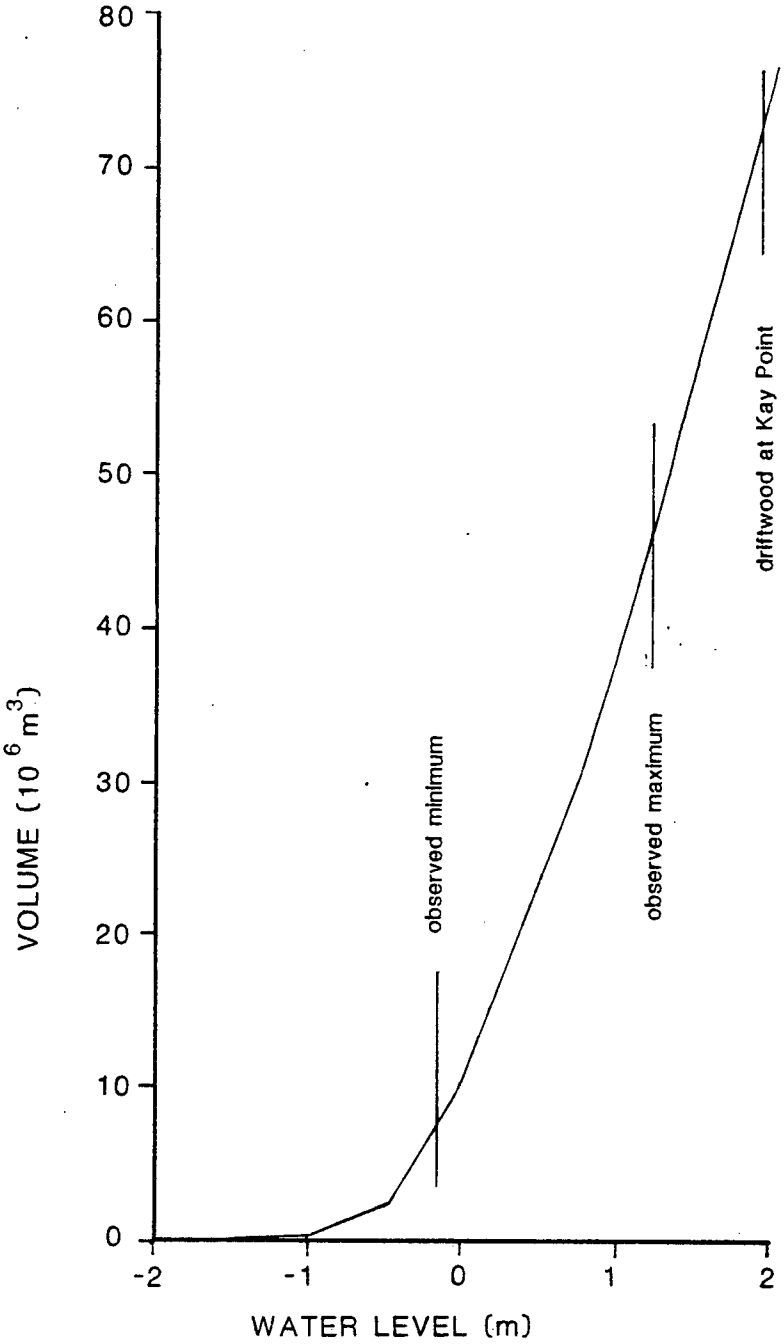


FIGURE 77

Capacity of the Babbage Estuary as a function of water level.

negligible. The hourly storage adjustment was computed as $\Delta V(t)=V(t)-V(t-1)$. The lag $\tau$, representing variable travel time between runoff gauging sections and the tidal system was assigned a constant value of 2 h for the computations. All terms were defined positive for inflow to the system, negative for outflow. It is recognized that part of the exchange flow moves through the small tidal inlet, M2 (Figure 2), and part may cross the barrier as washover flow during storms. Nevertheless, the greater part of the flow moves through the main entrance section, M1. Estimates of the exchange flow computed by equation 3.3.6-1 and corresponding values obtained from six sets of current meter data for eleven stations across the entrance section are given in Table 15.

The maximum daily precipitation observed at Kay Point was 13 mm (26 June 1976); assuming constant intensity over the 28 $km^2$ area of the estuary at mean water level, this is equivalent to a direct input of 4.2 $m^3s^{-1}$, an insignificant fraction of $Q_o$, which exhibits a daily range of order 100 $m^3s^{-1}$ (Figure 78). The maximum probable evaporative losses and ungauged runoff inputs were even smaller (see monthly totals in budget given below).

The volume of water stored in the estuary varies over an order of magnitude, the observed range being $8.0x10^6 \leq V \leq 4.6x10^7$ $m^3$ (Figure 77). A representative time sequence, V(t), for part of the summer of 1975, is illustrated in Figure 79. This sequence includes three positive storm surges in August (see Figure 35 for corresponding water level

TABLE 15

Comparison of water transfer estimates for Babbage Estuary entrance section (M1) as obtained from current meter data and by equation 3.3.6-1.

$Q_o$ is volume transfer rate derived from current meter data
$\hat{Q}_o$ is transfer rate estimated using equation 3.3.6-1

| date 1976 | $Q_o$ $m^3 s^{-1}$ | $\hat{Q}_o$ $m^3 s^{-1}$ |
|---|---|---|
| 7 June | -417.3 | -420.2 |
| 29 July | - 77.0 | -165.0 |
| 31 July | -377.0 | -350.8 |
| 1 August | -242.4 | -288.0 |
| 3 August | + 70.1 | + 67.5 |
| 10 August | -429.7 | -437.0 |

$r^2=0.963$

Assuming a least-squares relation, $\hat{Q}_o=a+bQ_o$, the null hyptheses that a=0 and b=1 cannot be rejected at $\alpha=0.1$ ($t=|\hat{b}-1|/s_b=0.89$; $t=|\hat{a}-0|/s_a=1.46$).

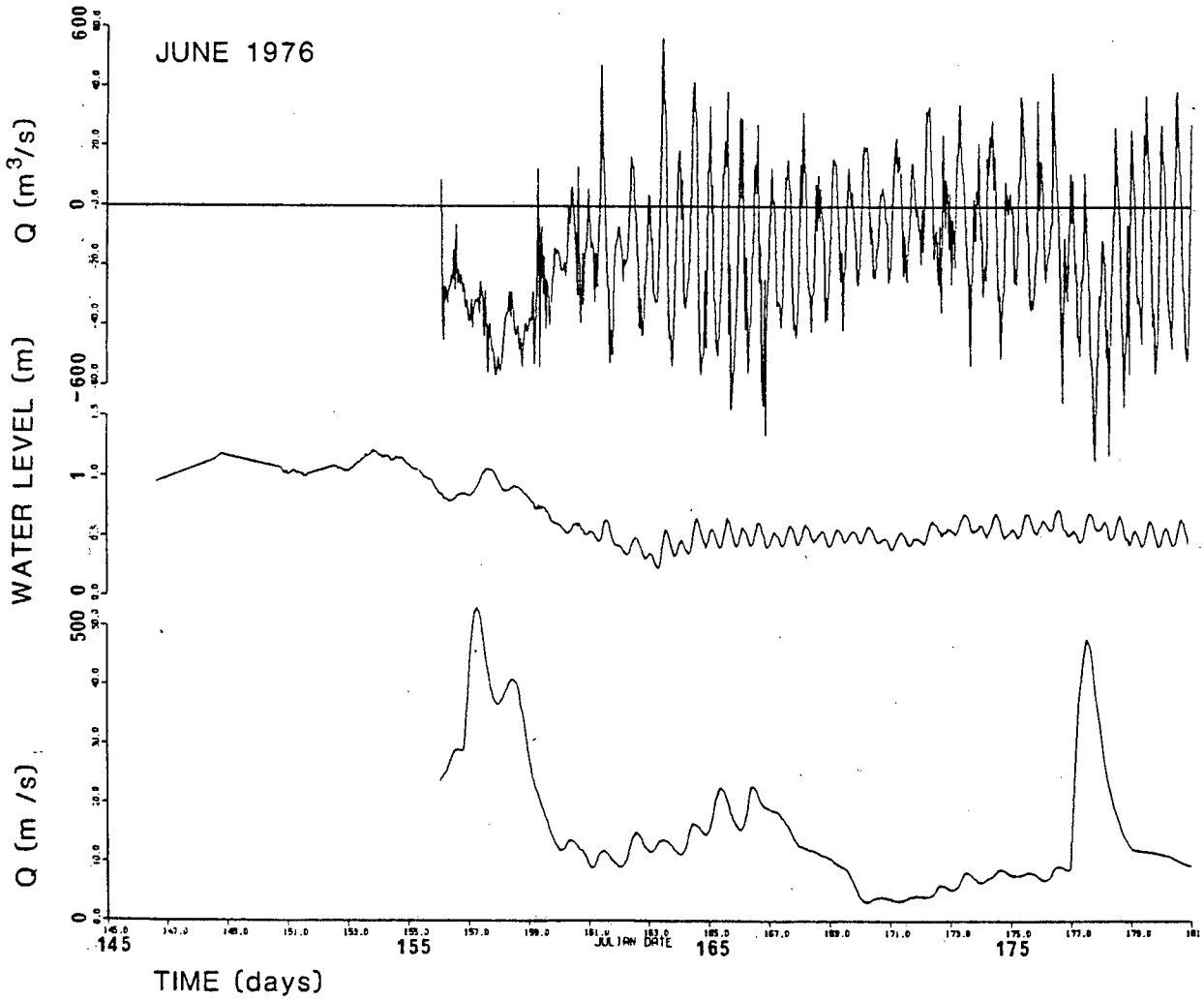


FIGURE 78

Net exchange flow through M1 section, gauge-B water level, and Babbage River discharge through B1 section, June 1976.

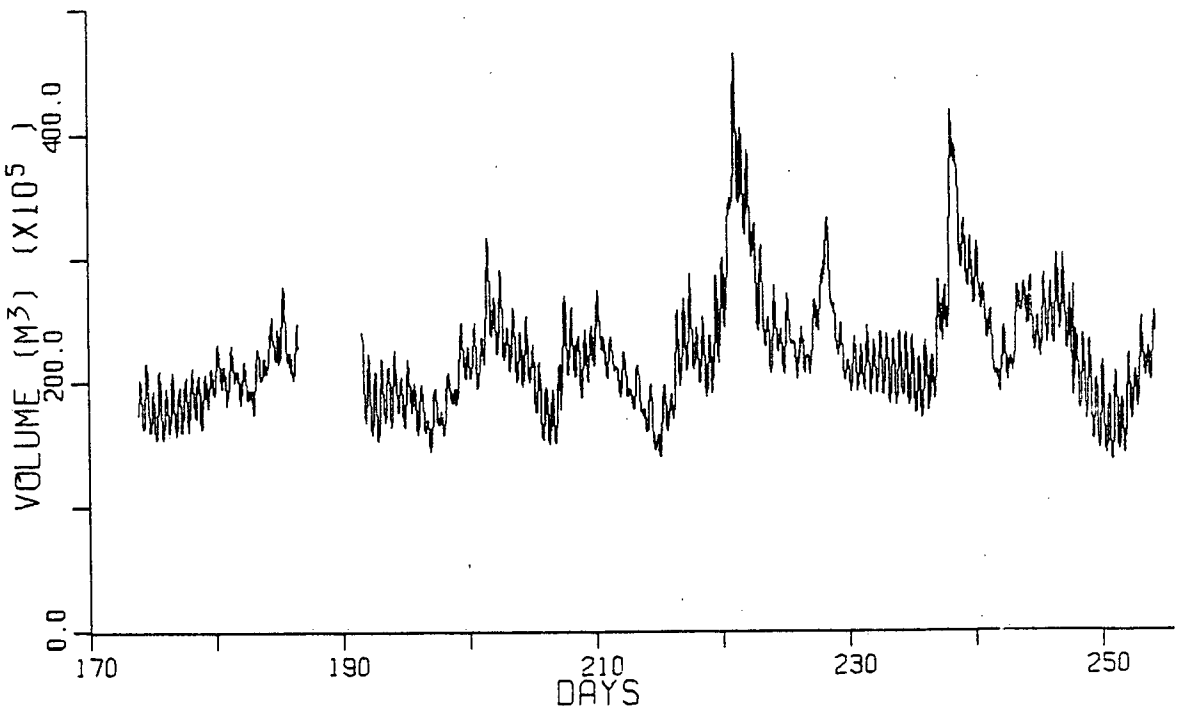


FIGURE 79

Hourly storage volume in the Babbage Estuary during summer 1975; note rapid doubling of volume in storage during early August storm surge. Time in days with origin at 0000h 1 January (see Appendix A.3 data list for conversion to date).

data). During the first of these surges, the total volume of water stored in the system increased by 91 per cent over 20 hours and more than doubled over a 31-h interval.

The August storm surges were the most prominent events of the 1975 series, but synoptic-scale variability with a range of mean daily volume approaching $10^7$ $m^3$ was evident in July also. Indeed, the frequency structure of $V(\zeta)$ (Figure 80) was almost identical to that of water level, $\zeta(t)$, which was dominated by synoptic-scale variance.

Subtidal frequencies were much less pronounced in the net exchange flow sequence, $Q_o(t)$. This was not unexpected because the magnitude of the runoff component was relatively small in late summer, such that $Q_o(t) \simeq dV/dt$ and most synoptic-scale storage adjustments were accomodated by limited modulation of the tidal-frequency exchange process.

The 1975 exchange sequence has been decomposed into a net input sequence, $Q_o^+(t)$, and a net output sequence, $Q_o^-(t)$. The output, $Q_o^-(t)$, can be regarded as a system response to two major inputs, $Q_f(t)$ and $Q_o^+(t)$. Examination of the partial coherence function for the runoff input and system output processes (Figure 81) reveals the extreme nonlinearity of runoff transfers through the estuary. This result effectively eliminates simple application of linear stochastic models such as equations 1.2.1-1 or 3.3.1-1 to represent movement of fluvial water and sediment inputs through the estuarine system, even if the system parameters could be considered constant and

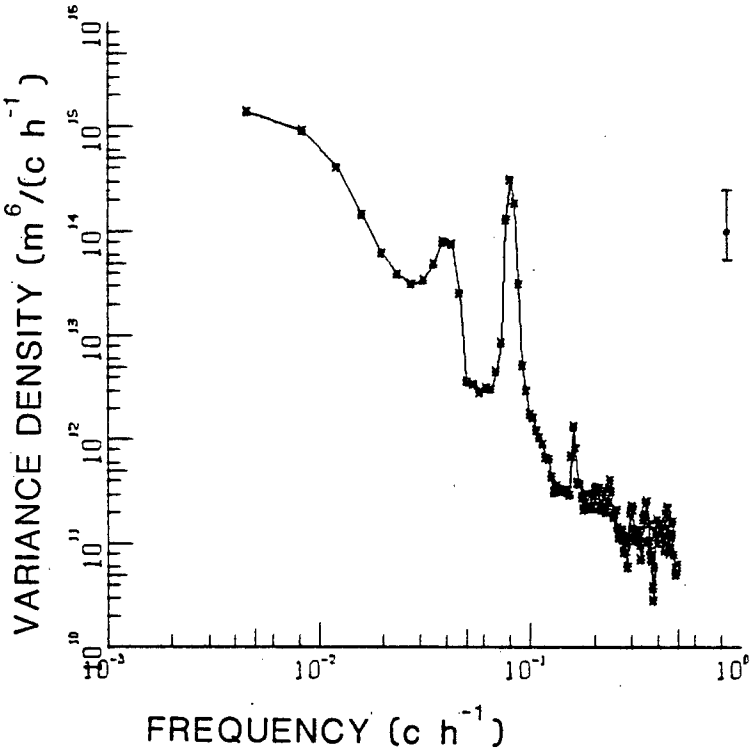


FIGURE 80

Variance density spectrum of hourly storage volume in the Babbage Estuary during summer 1975; the 90% confidence interval, assuming a chi-squared distribution with 10 degrees of freedom, is given at upper right.

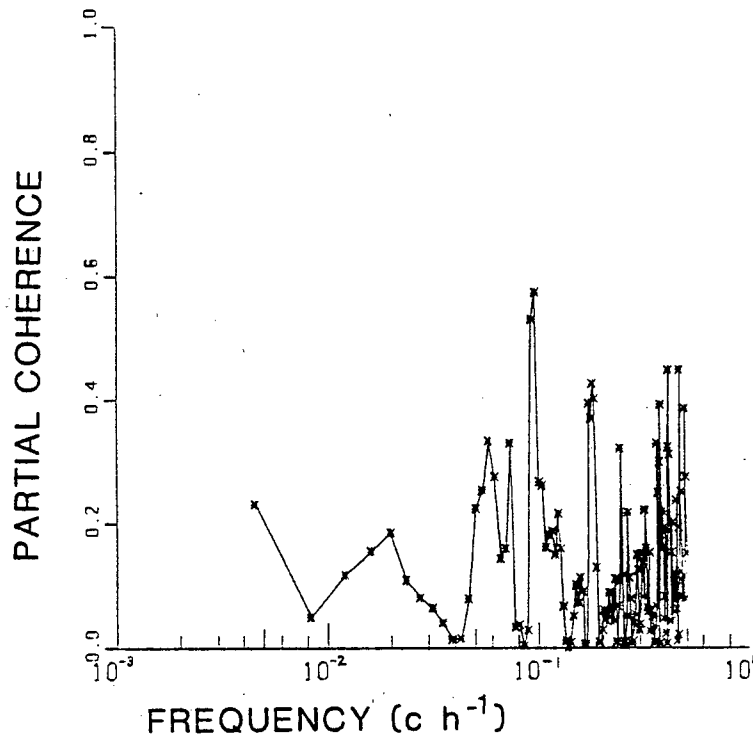


FIGURE 81

Partial coherence between Babbage River discharge, $Q_f(t)$, and M1 net output sequence, $Q_0^-(t)$, showing extreme non-linearity of runoff transfers through the estuary, particularly in the synoptic frequency band in which most of the variance of runoff resides.

if the net non-tidal circulation did not introduce additional exchanges unaccounted for in the $Q_o^+(t)$ and $Q_o^-(t)$ series.

During major runoff events, particularly during breakup when the tidal signal is weak and density stratification is negligible, much greater coherence may exist between $Q_f$ and $Q_o^-$ (which may then account for the entire exchange process). This is suggested by the time series for the flood of early June 1976 (Figure 78). A consistent outflow was maintained in the entrance section for at least three days. The estimated maximum net outflow on June 6 ($Q_o^-$=-572 $m^3s^{-1}$) was approximately equivalent to the peak discharge at B1 (Q=529 $m^{3-1}$). The output peaked some 15 hours after the input; ice effects are believed to have contributed to the very long lag time. During the 26 June flood, when a well-developed tidal signal was present in the entrance exchange flow, input from Phillips Bay was again suppressed for a time and the low tide level some 8 hours after the runoff peak was unusually high (Figure 78), indicating a significant short-term anomaly in the storage volume of the estuary attributable to the runoff input.

The monthly water budget, presented in Table 16, emphasizes the extreme seasonal variance characteristic of the Babbage Estuary system. The budget covers four months in 1976, three summer months for which time series data are available and one winter month for which the budget can be estimated on the basis of an assumed zero runoff input, an assumed constant ice surface elevation, and adoption of Shingle Point data for the precipitation input. Assuming that evaporative losses were

TABLE 16

Water budget for Babbage Estuary, January 1976 and June-August 1976.

**Volumes in cubic metres**

| date | $\Delta V$ | $Q_f$ | $Q_d$ | $Q_e$ | $Q_o$ | $Q_o^+$ | $Q_o^-$ |
|---|---|---|---|---|---|---|---|
| January | $2.7 \times 10^5$ | 0.0 | $2.7 \times 10^5$ | 0.0 | 0.0 | >0.0 | <0.0 |
| June | $-1.1 \times 10^7$ | $5.0 \times 10^8$ | $6.5 \times 10^6$ | $-1.4 \times 10^6$ | $-5.2 \times 10^8$ | $\geq 7.2 \times 10^7$ | $< -5.8 \times 10^8$ |
| July | $-1.0 \times 10^7$ | $1.3 \times 10^8$ | $2.9 \times 10^5$ | $-1.4 \times 10^6$ | $-1.4 \times 10^8$ | $\geq 2.2 \times 10^8$ | $< -3.5 \times 10^8$ |
| August | $+3.1 \times 10^6$ | $7.5 \times 10^7$ | $8.8 \times 10^5$ | $-1.4 \times 10^6$ | $-7.8 \times 10^7$ | $\geq 3.0 \times 10^8$ | $< -3.3 \times 10^8$ |

MEASURED: $\Delta V$, $Q_f$

ESTIMATED: $Q_d$, $Q_e$

RESIDUAL: $Q_o$, $Q_o^+$, $Q_o^-$

Notes:

1. Storage elements, $\Delta V$, at a time scale of order one day due to tidal exchanges are sometimes of the order of $10^7$ $m^3$. On a monthly basis, however, values of $\Delta V$ computed using daily mean volumes are equivalent to those shown above, except in August, when a value of $+4.2 \times 10^6$ $m^3$ is obtained.
2. Volume changes may occur due to steric effects or ice melt, without transfer of mass across system boundaries. At the start of June 1976 a large part of the total volume stored in the estuary remained as ice; assuming that half of the total $4 \times 10^7$ $m^3$ in storage was ice, the change in total volume due to phase changes in June would be of the order of $10^6$ $m^3$. Steric effects would be smaller (see section 3.2.1).
3. $Q_d$ for June includes an estimated $5.5 \times 10^6$ $m^3$ snowmelt runoff, computed assuming 69 mm water equivalent stored in the snowpack or as retained meltwater at the start of June and 20 per cent evaporation loss. Direct runoff from precipitation occurring during June, July, and August has been estimated on the assumption that 5 per cent of total precipitation runs off (Brown et al., 1968).

negligible, the January budget shows direct precipitation of order $10^5$ $m^3$ going entirely into storage as snow, with runoff and net exchange flow both zero (although presumably $Q_o^+ = -Q_o^- > 0$). In June, July, and August, the runoff inputs and residual outputs at the marine boundary were approximately equal in magnitude, the input term $Q_o^+$ being an order of magnitude smaller in June and an order of magnitude larger in August. During the spring and summer months, residual storage adjustments were consistently an order of magnitude smaller than the fluvial input and residual output terms, and of variable sign.

The budget summary clearly indicates that the estuarine system varies in complexity and in output behaviour on a seasonal basis, in response both to varying input conditions and to seasonally varying internal parameters. A simplified representation of the canonical structure for various seasons (Figure 82) demonstrates the dramatic changes in the number and character of internal linkages between subsystems in the estuarine cascade that recur on an annual cycle. These changes in the canonical structure of the hydrological subsystem have important implications for sediment dispersal in the estuary, a subject taken up in the following pages.

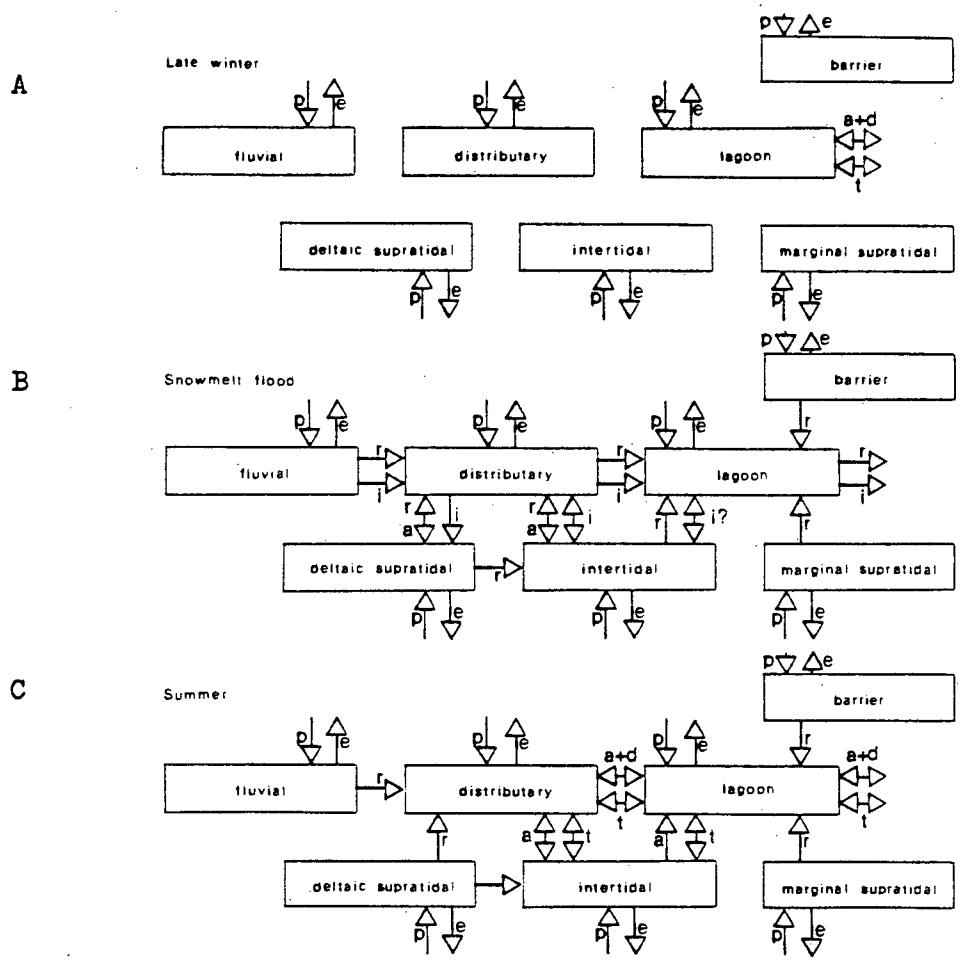


FIGURE 82

Simplified canonical structure of the hydrological subsystem during late-winter, snowmelt, and summer seasons, showing dramatic changes in the number and character of internal and external links.

p precipitation
e evaporation
r runoff
i ice-transport
t tidal transport
a non-tidal advective transport
d non-tidal dispersive transport

# 4 SEDIMENTOLOGICAL SUBSYSTEM

## 4.1 FLUVIAL SEDIMENT INPUTS TO THE ESTUARY

### 4.1.1 SEDIMENT SOURCES AND MATERIALS

The Babbage River and Deep Creek drainage basins encompass a diversity of sediment source materials and topographic conditions. Bedrock lithologies are almost exclusively sedimentary (cf. section 2.1.1). The Babbage River is incised throughout much of its middle course and major outcrops of Cretaceous or older sediments occur adjacent to the channel (Figure 83A). However, much of the sediment moving in the Babbage River is undoubtedly supplied from Tertiary and Quaternary alluvial and colluvial deposits (Figure 83B). Sediments in Deep Creek are derived primarily from unconsolidated Quaternary deposits.

Most of the drainage network consists of relatively stable single-thread channels formed in alluvial gravel (Figure 83A). Major exceptions include the lower Tulugaq (Crow) River and reaches downstream from large groundwater sources, where extensive icings and wide unstable channel zones develop. Six sites have been identified at which icings accumulate regularly to such a size that ice persists into August or later (cf. Figure 8A). On a basin-wide scale, reaches affected by icing growth represent major sediment storage sites.

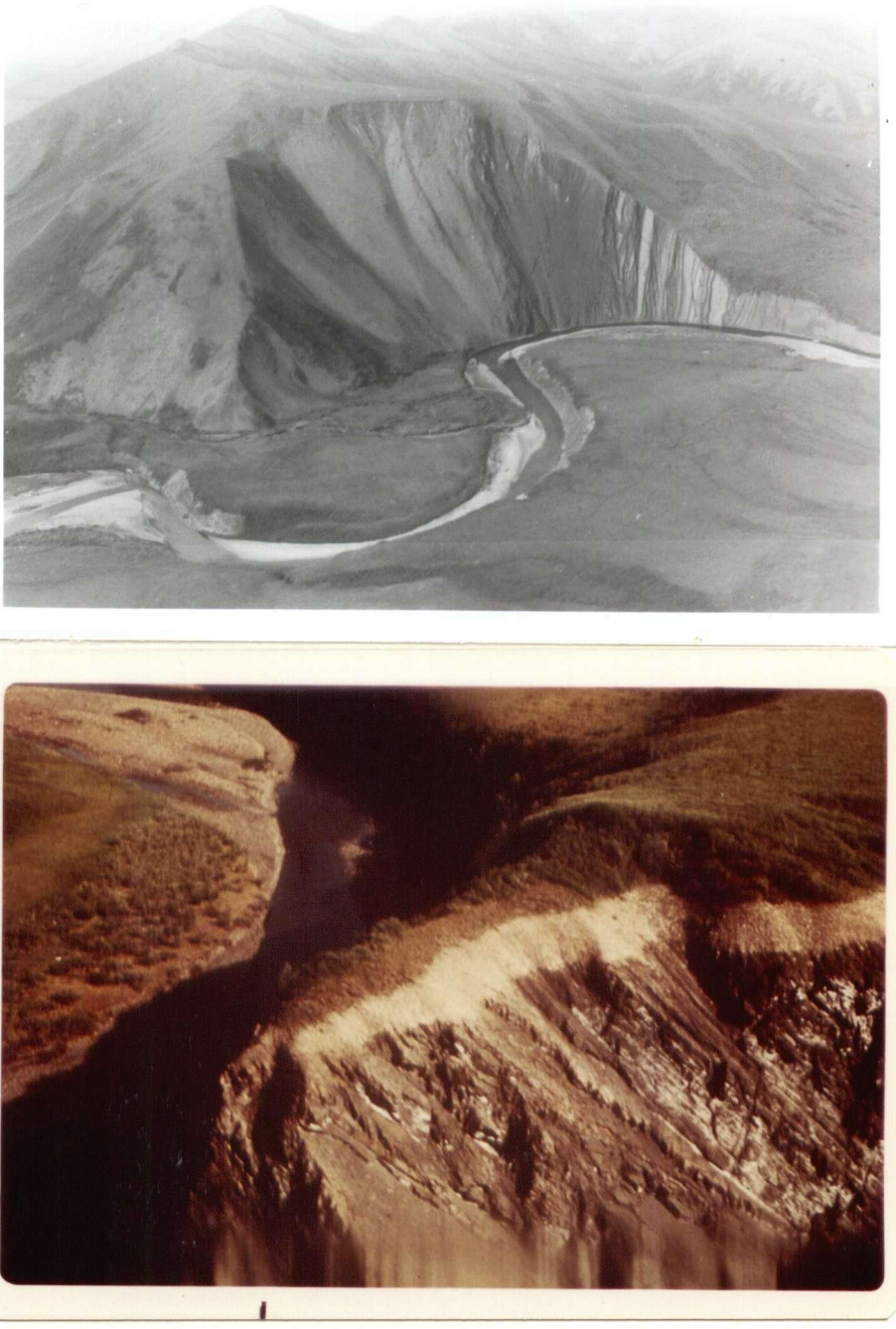

FIGURE 83

Incised middle course of Babbage River: (A) major exposure of Cretaceous or earlier sediments adjacent to the channel; (B) Tertiary gravel over older sediments in a spur above the river.

FIGURE 84

A: steep braided channels draining unvegetated ridges in Barn Mountains, eastern part of Babbage River basin, August 1976; B: block slumping due to thermo-erosional niche development, lower Babbage River, late July 1976.

There is, unfortunately, little information on which to base an assessment of weathering processes and sediment production in these basins. Permafrost, ground-ice, winter freezing, and a variety of thaw processes are major determinants of sediment production in the North Slope environment. Frost-shatter (freezing pressure) effects can be assumed to play an important role, as in other high-latitude localities (cf. Washburn, 1969). Solution processes may also be important, particularly in association with snowmelt and on carbonates, although many reactions are inhibited by low temperatures. Williams (1949) has emphasized the relatively corrosive nature of snowmelt water; however, recent evidence appears to contradict this view (T. Gallie, personal communication, 1979). Nivation processes also may represent an important component of the sediment delivery system.

In some parts of the Babbage River basin, sediments are delivered from unvegetated high-elevation surfaces via steep braided channels (Figure 84A). However, sediment delivery from sites away from channels is limited by the relatively gentle slopes and small-scale roughness characteristic of much of the catchment area (Figure 8). Solifluction transport is active locally at some sites in the mountains, where rates of movement exceeding 15 mm $a^{-1}$ are reported to be common on gentle slopes (Rampton and Dugal, 1974).

Retrogressive-thaw processes represent another means whereby valley-side materials are delivered to the channel network. Retrogressive thaw is initiated by exposure of

massive ground ice due to channel migration or other causes and can be very rapid locally. Failure proceeds back from the initial exposure, with sediment being transferred downslope from the near-vertical headwall primarily by mudflow, sheetwash, and gullying processes. A large active retrogressive-thaw feature on the Babbage River above the Trail deserves mention as a potentially important point source of sediment (see McDonald and Lewis, 1973, p.52). Retrogressive-thaw processes are often inactive during snowmelt flooding due to snow accumulation in the thaw basins.

Where channel banks are formed in fine-grained alluvium or similar deposits, block slumping may occur due to undercutting by the river. Undercutting is promoted in ice-rich bank materials by melting of interstitial ice. Thermo-erosional niching may proceed a considerable distance back from the bank face (Walker and Arnborg, 1966; McDonald and Lewis, 1973, p.49). The niching process is widespread and effective in the basins under discussion (Figure 84B) and is a major cause of lateral erosion. Whether rates of bank erosion are increased or diminished by the presence of permafrost and related processes is a debate not resolved here (cf. Scott, 1978). However, bank erosion is clearly a major source of fine sediment in the Babbage and Deep Creek basins.

The character of dissolved materials in surface waters draining to the Babbage Estuary is summarized in Table 17 (data from van Everdingen, 1974; Steigenberger et al., 1975). The data include results from four springs, which with one

TABLE 17

Summary of dissolved constituents in water samples from the Babbage River and Deep Creek drainage basins (data from various sources as indicated). Concentrations in mg/L.

| | date/ season | TDS | $SiO_2$ | $Ca^{++}$ | $Mg^{++}$ | $Na^+ + K^+$ | $HCO_3^- + CO_3^{--}$ | $Cl^-$ | $SO_4^{--}$ | pH |
|---|---|---|---|---|---|---|---|---|---|---|
| Fish Hole Creek[1] | | | | | | | | | | |
| spring | w | 184.7 | 3.9 | 35.0 | 6.9 | 1.0 | 123.2[c] | 0.4 | 14.0 | |
| icing | w | 39.3 | | 7.5 | 0.8 | 1.8 | 25.6[c] | 1.1 | 2.5 | |
| river[3] | w | 88.0 | | 17.0 | 3.3 | 0.6 | 57.3[c] | 0.2 | 9.5 | |
| Crow River[1,2] | | | | | | | | | | |
| spring | w | 269.8 | 3.9 | 59.0 | 5.0 | 2.3 | 184.2[c] | 1.2 | 14.0 | |
| river[3] | w | 40.6 | | 9.1 | 0.6 | 0.3 | 29.2[c] | 0.1 | 2.4 | |
| river[4] | 9/7/73 | 185.6 | 2.0 | 32.8[a] | 6.3[b] | | 110.2[d] | 1.9 | 12. | 8.0 |
| river[3] | 26/3/74 | 260.8 | 3.4 | 34.4[a] | 13.1[b] | | 110.0[d] | 0.5 | 15. | 7.9 |
| Trail River[2] | | | | | | | | | | |
| river[5] | 5/7/73 | 172.6 | 1.6 | 32.8[a] | 4.4[b] | | 118.2[d] | 0.7 | 10. | 8.1 |
| Babbage River[1,2] | | | | | | | | | | |
| spring[6] | w | 247.2 | 5.2 | 48.0 | 8.3 | 1.2 | 170.8[c] | 0.3 | 13.0 | 7.5 |
| river[5] | 10/7/73 | | 2.5 | 25.6[a] | 6.8[b] | | 86.5[d] | 0. | 24. | 8.1 |
| river[7] | 25/3/74 | 992.2 | 5.7 | 98.5[a] | 56.9[b] | | 348.3[d] | 3.3 | 195. | 7.1 |
| lake [8] | 17/7/73 | 55.2 | 0.5 | 2.4[a] | 3.4[b] | | 15.9[d] | 0. | 0. | 6.8 |
| lake [8] | 17/7/73 | 78.3 | 0.3 | 5.6[a] | 1.5[b] | | 15.9[d] | 0.5 | 0. | 6.9 |
| lake [8] | 25/3/74 | 330.8 | 3.2 | 48.9[a] | 24.8[b] | | 127.8[d] | 18.7 | 19. | 6.7 |
| lake [8] | 25/3/74 | 306.8 | 3.5 | 51.3[a] | 23.5[b] | | 134.1[d] | 164. | 16. | |
| Deep Creek[2] | | | | | | | | | | |
| river[5] | 11/7/73 | 197.5 | 2.0 | 16.8[a] | 4.4[b] | | 76.2[d] | 0. | 18. | 7.8 |
| river[5] | 13/7/73 | 329.1 | 2.0 | 7.6[a] | 5.1[b] | | 42.7[d] | 0.2 | 14. | 8.0 |
| lake [9] | 18/7/73 | 59.1 | 0. | 4.0[a] | 1.5[b] | | 10.1[d] | 1.9 | 0. | 7.1 |
| lake [9] | 18/7/73 | 82.9 | 0.4 | 3.2[a] | 2.9[b] | | 10.4[d] | 3.3 | 8. | 7.2 |
| spring[9] | 18/7/73 | 103.0 | 0. | 4.0[a] | 2.9[b] | | 3.7[d] | 4.7 | 0. | 7.0 |

sources of data:

[1] van Everdingen (1974)
[2] Steigenberger et al. (1975)

sample sites:

[3] at icing in vicinity of spring
[4] at CAGP crossing upstream from icing
[5] at CAGP crossing
[6] upper Babbage River
[7] isolated unfrozen pool near CAGP crossing
[8] oxbow lake at 69°01'N 138°12'W above Trail River; summer samples from surface and bottom
[9] lake and spring at 68°57'N 137°30'W: surface, bottom, spring

computational procedures:

[a] $Ca^{++}$ computed as 0.400 (Ca-hardness as $CaCO_3$)
[b] $Mg^{++}$ computed as 0.244 ((total hardness as $CaCO_3$) - (Ca-hardness as $CaCO_3$))
[c] reported as $HCO_3^-$ only
[d] $HCO_3^-$ = 1.219 (total alkalinity as $CaCO_3$) when phenolphthalein alkalinity is zero; otherwise both $HCO_3^-$ and $CO_3^{--}$ are present

w: indicates winter or early spring sampling

exception are not significantly different in ionic composition from the river and lake waters. Water from sub-permafrost aquifers is hard (total hardness as $CaCO_3$ >115 mg/L) and highly mineralized (185<$C_D$<270 mg/L). In contrast, snowmelt runoff is particularly low in dissolved solids, with concentrations during June typically less than 50 mg/L and only rarely greater than 100 mg/L (see section 4.1.2). With decline of the snowmelt freshet in late June, dissolved solids concentrations increase and may approach 300 mg/L. Concentrations are further increased in winter by exclusion of salts on freezing; Steigenberger et al. (1975) reported a concentration of total dissolved solids equal to 992 mg/L in a sample collected under ice in the Babbage River. Pockets of highly mineralized water such as this are released during breakup, at a time when most runoff is derived from snowmelt with low concentrations (see section 4.1.2).

Clastic sediments in the Babbage River include cobble and gravel fractions composed predominantly of sandstone, limestone, and chert, while the sands are predominantly quartz (Table 18). Summary size distributions for representative clastic sediments in the Babbage River system are given in Figure 85. These include samples from valley-side deposits, alluvial terrace materials, and sediments stored within the channels (data from McDonald and Lewis, 1973; Steigenberger et al., 1975). Clastic sediments available to the river exhibit a wide range of size, roughly $10^{-4}$<D<$10^{2}$ mm; in practice, in practice, the lower limit differentiating clastic sediment from

TABLE 18

Petrographic analyses of sand and gravel from Babbage River channel between Tulugaq River and section B1 (from Canada, Department of Public Works, 1971a, p.21).

| SAMPLE 5 | | SAMPLE 6 | |
|---|---|---|---|
| quartzite | 45% | quartzite | 25% |
| sandstone | 25% | sandstone | 25% |
| dark chert | 20% | dark chert | 25% |
| limestone | 10% | limestone | 25% |
| mean density | 2610 kg $m^{-3}$ | mean density | 2590 kg $m^{-3}$ |

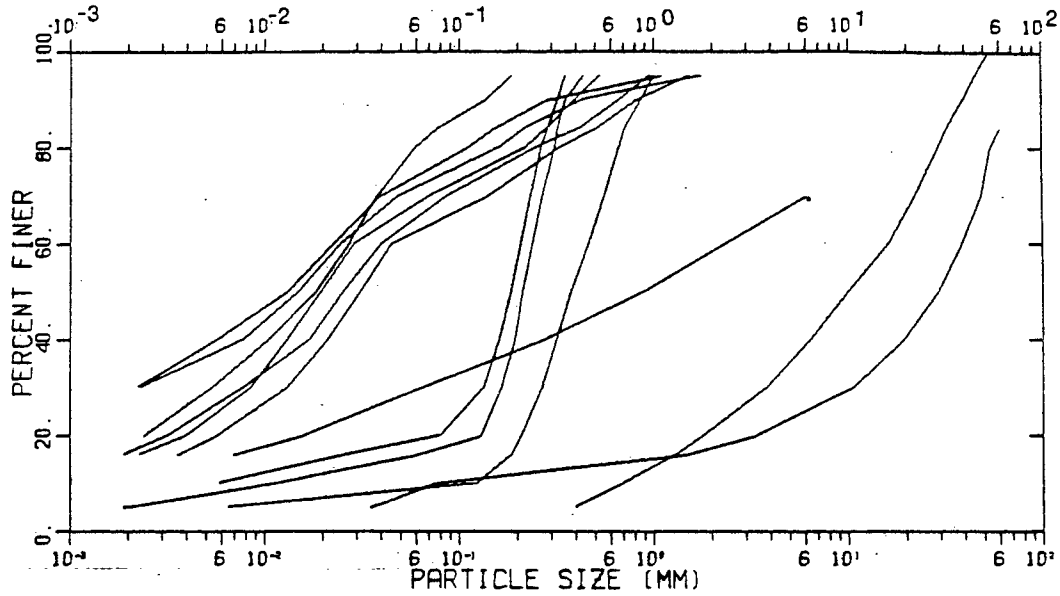


FIGURE 85

Representative particle-size distributions for source materials and for sediments stored in the channel system, Babbage River basin (data from McDonald and Lewis, 1973; Steigenberger et al., 1975).

1: valley-side; headwall and mudflow at retrogressive-thaw site upstream from Trail River confluence; 2: alluvial terrace materials (composite samples); 3: valley-side material, probably till; 4: fine sediment on bars, Babbage River; 5: gravel below armour layer in Tulugaq and Trail River channels.

solutes is somewhat arbitrary. A characteristic silt/clay ratio between 1.0 and 1.5 in the valley-side materials distinguishes them from alluvial sediments that tend, in this system, to adopt relatively consistent ratios between 1.5 and 3.0 (cf. McDonald and Lewis, 1973). Apparently, a proportion of the clay entrained from source materials bypasses alluvial storage sites in the valley.

### 4.1.2 FLUVIAL TRANSPORT PROCESSES

Organic and non-organic materials are transported in rivers as dissolved and particulate solids. The particulate sediment is classified according to its hydraulic behaviour as suspended load, which is supported by momentum transfer in anisotropic fluid turbulence, and as bedload (or bed-contact load), which is supported by constant or intermittent solid reaction forces (Bagnold, 1966). Alternatively, fine suspended materials of size fractions effectively absent from the bed in a particular reach are defined as wash load (Einstein et al., 1940), while sediments present in the bed are termed bed-material load, whether they move in suspension or along the bottom. The different definitions arise from the limitations of various measurement procedures and the assumptions of particular theoretical derivations. Parthenaides (1977) has attempted to demonstrate the applicability of general mechanical principles, particularly the concept of a bedload or exchange function (after Einstein, 1950), to the full range of clastic sediment sizes, but recognized a set of distinctive dynamic properties found only in fine cohesive materials. At the other extreme, Bagnold (1973) has argued that movement of coarse sediment as bedload involves saltation, a distinctive dynamic process unrelated to fluid turbulence and turbulent suspension (see discussion of bedload below). It appears, therefore, that three or more partially exclusive modes of transport may be distinguished according to particle size. It must be emphasized, however, that some size grades

(particularly sand) may move in different transport modes, depending upon the prevailing flow conditions (Middleton, 1976).

For the present purpose, the classification presented first above has been adopted for reporting sediment transport data. Operational definitions are as follows. Total dissolved solids (TDS) transport is taken as the product of water discharge and TDS concentration, the latter defined as total filterable residue, in mass per unit volume, passing 0.45-μm membrane filters. Total suspended sediment (TSS) transport is defined as the product of water discharge and TSS concentration, the latter defined as total non-filterable residue, in mass per unit volume, determined from depth-integrated samples collected at mid-channel with DH48 samplers (see Appendix A.4). The use of 0.45-μm filters as the criterion distinguishing dissolved from suspended solids leads to the possibility that suspended colloids or fine clays smaller than this size may be included in reported TDS concentrations and transport rates. These materials are part of the conceptual wash load and are potentially subject to deposition after flocculation in seawater. The fraction of suspended sediment remaining after combustion (2h at 550°C) is defined as incombustible suspended sediment (ISS), an estimate of clastic (inorganic) sediment in suspension. Finally, bedload has been operationally defined as sediment (D>0.2 mm) moving close to the bed and subject to interception with 76.2x76.2-mm Helley-Smith bedload samplers (Helley and Smith,

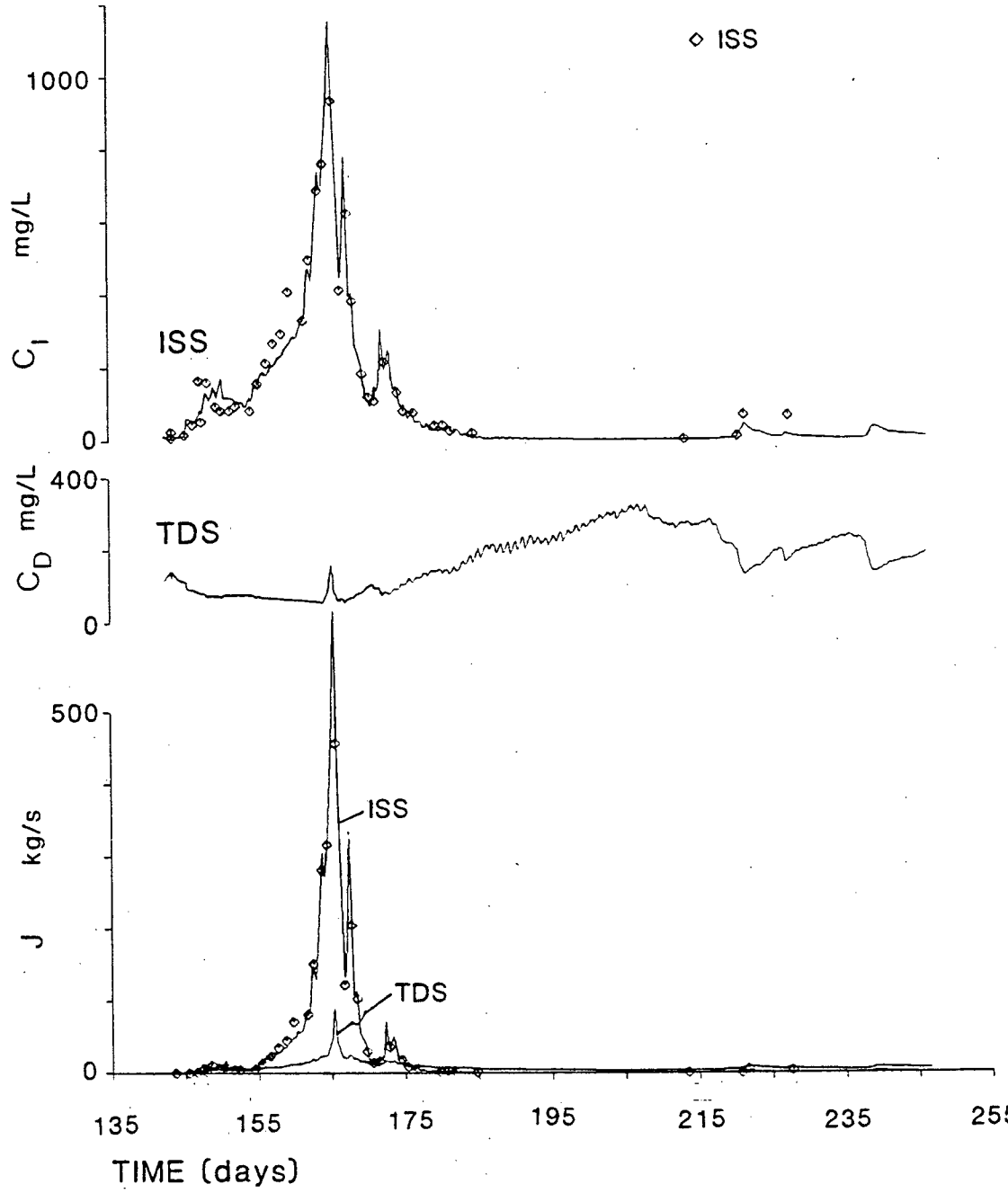


FIGURE 86

A: incombustible suspended sediment and total dissolved solids concentrations (mg/L) in Babbage River at B1, 1975; sample data and rating estimates; B: incombustible suspended sediment and total dissolved solids transport (kg/s).

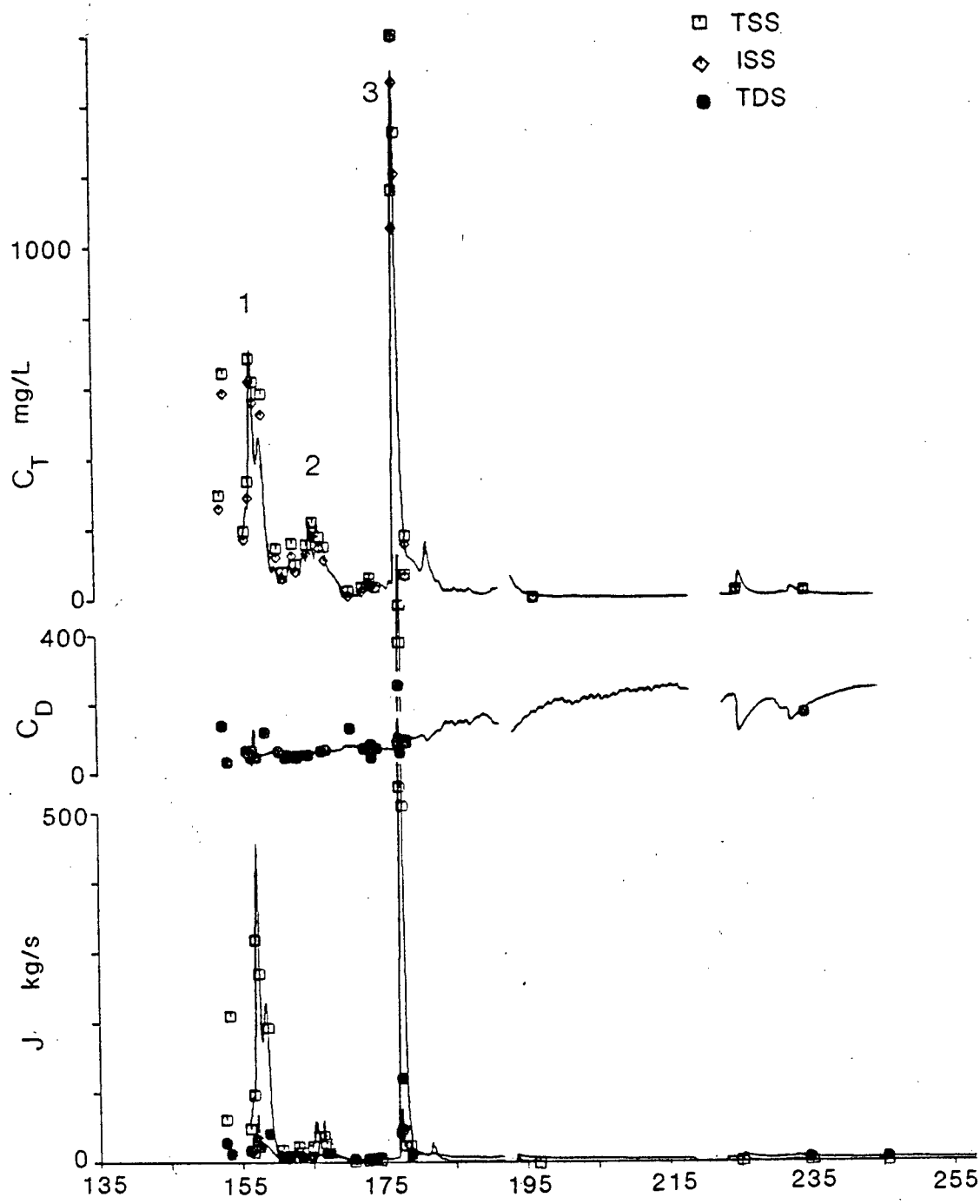


FIGURE 87

A: total suspended sediment and total dissolved solids concentrations (mg/L) in Babbage River at B1, 1976; sample data and rating estimates; B: total suspended and total dissolved solids transport (kg/s).

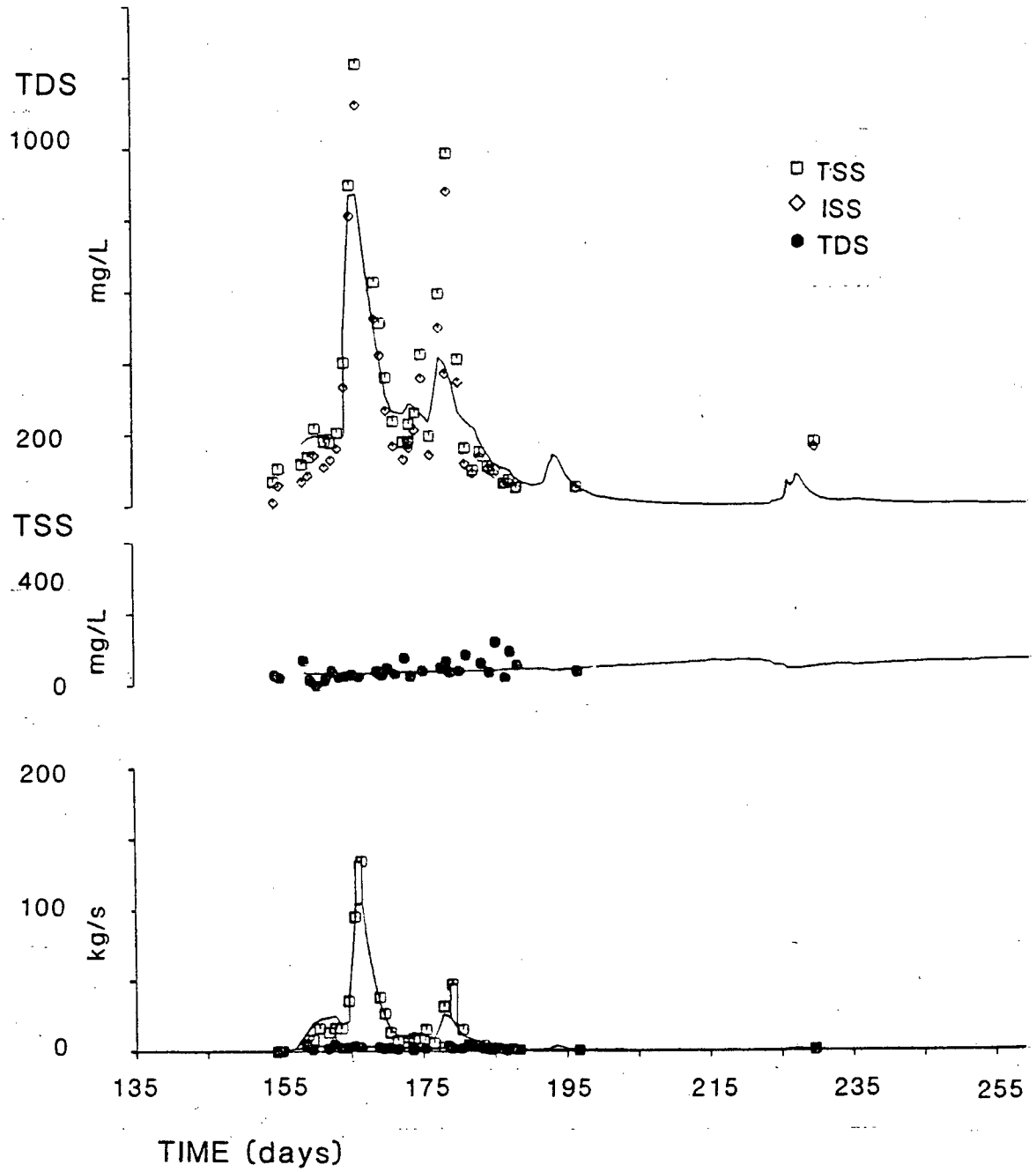


FIGURE 88

A: total suspended sediment and total dissolved solids concentrations (mg/L) in Deep Creek at D1, 1976; sample data and rating estimates; B: total suspended and total dissolved solids transport (kg/s).

1971; Emmett, 1980). This makes possible a standardized sampling procedure for bed-contact load (bedload in the sense of Bagnold, 1966), but accounts for only a part (presumably a varying part) of bed-material load (bedload in the sense of Einstein, 1950). These definitions form the basis for observational data and rating estimates presented below.

Figures 86 and 87 are time-sequence representations of solute and suspended sediment concentrations, with corresponding transport data, for the Babbage River at B1 in 1975 and 1976. Figure 88 is a similar plot for Deep Creek at D1 in 1976. The rating data represent hourly estimates, except during and prior to breakup. Note the extreme seasonal-scale variability in the data.

Whereas suspended sediment and bedload transport are steeply increasing functions of the volumetric flow, solute transport is a nearly linear function of discharge, implying relatively constant concentrations. The generalized patterns of dissolved, suspended, and bedload response to water discharge are shown in Figures 89 and 90. The dynamic basis and systematic character of these relations, and of those between concentration and discharge, are the subject of the present section. Specific rating equations adopted for the transport estimates are given in Appendix A.4; computed transport totals are presented in the following section (4.1.3).

In general, solute transport $J_D$ varies as $Q^k$ where $k \leq 1$.

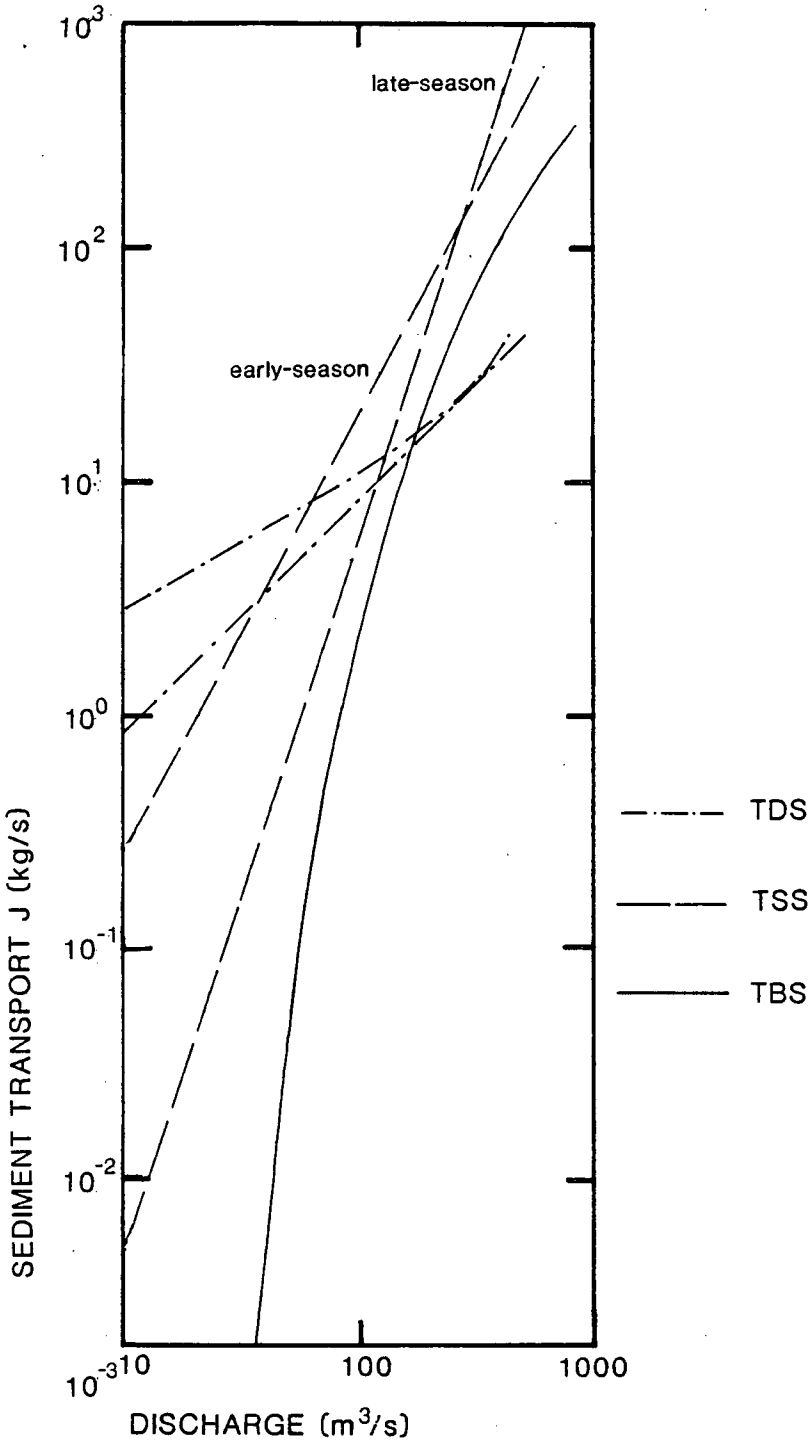


FIGURE 89

Dissolved, suspended, and bedload ratings, Babbage River at B1, 1976.

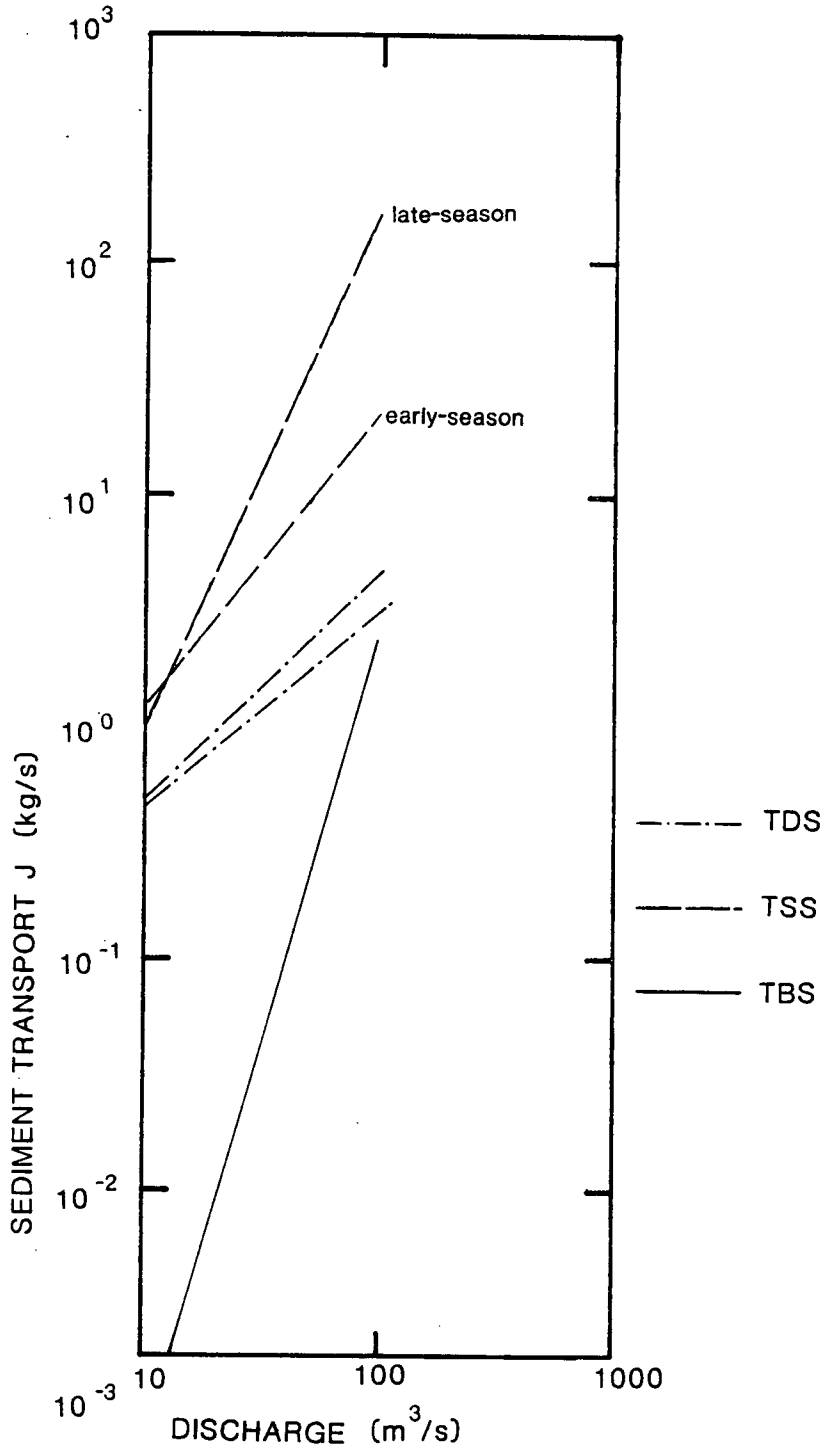


FIGURE 90

Dissolved, suspended, and bedload ratings, Deep Creek at D1, 1976.

Regression of TDS concentration on discharge, with all Babbage River data taken together, yields a relation with slope not significantly different from zero. One interpretation, therefore, is that solute concentration $C_D$ is constant, viz. $J_D=C_DQ$ and $k=1$. However, partition of the data by season indicates $k<1$ (concentration varies inversely as discharge) except, in the Babbage River, during short-lived transients in the breakup period and during floods. The former represent flushing events independent of discharge (see below); the latter tend to occur at $Q > 380$ $m^3s^{-1}$ approximately (Figure 91) and are interpreted as reflecting primarily the influence of fine suspended material ($D < 0.45$ μm), although transient solute variation may also play a role.

Total suspended load $J_T$ also varies as $Q^k$, where $1.26<k<3.09$ for the ratings plotted in Figures 89 and 90. The two alternatives in each plot differentiate early-season data, including most snowmelt transport, from late-snowmelt and summer data (see below). All 1976 data taken together yield $k=2.89$ for the Babbage River and $k=1.75$ for Deep Creek. It may be noted that the range of k reported here encompasses nearly the full set of empirical results from all environments (cf. Rannie, 1978), although Gregory and Walling (1973: pp. 215-217) have reported values as low as 0.8 in southern England and Axelsson (1967) reported values greater than three.

Whereas both dissolved and suspended loads can be represented as linear functions of $Q^k$, bedload transport $J_B$ cannot in general. In Deep Creek, the bedload transport data

do vary as $Q^k$ ($k=3.646$, $r^2=0.958$) for $Q < 31\ m^3s^{-1}$. Theoretical considerations discussed below suggest that linear extrapolation to $Q = 100\ m^3s^{-1}$ is not unwarranted. In the Babbage River, however, both the sample data and theoretical arguments suggest a highly non-linear relationship within the range of discharge encountered. Bedload transport is found to be most sensitive to discharge variation at low flow; approximation of the low-flow bedload rating by a model such as that adopted for dissolved and suspended sediment yields an exponent $k=7.74$, much higher than values obtained for the other transport modes.

Among the various types of sediment transport, therefore, we find the exponent k varies from less than 0.5 to more than 7.7: this indicates very pronounced differences in response to discharge fluctuations and corresponding differences in the variance spectra of the transport series.

Relations of the form

$$\hat{C}_D = aQ^k \ ; \quad \hat{J}_D = C_D Q = aQ^b = aQ^{k+1} \qquad (4.1.2\text{-}1)$$

provide one of the simplest solute rating models (Hem, 1959). While the information available on sources and mixing processes in the present context does not justify a more complex approach, rating parameters have been varied to account for seasonal shifts and, in the Babbage, for anomalous flood response of TDS concentration. Scatter plots of total dissolved solids concentration as a function of water discharge in the two study basins are given in Figures 91 and 92, together with rating functions. In both cases, the errors of

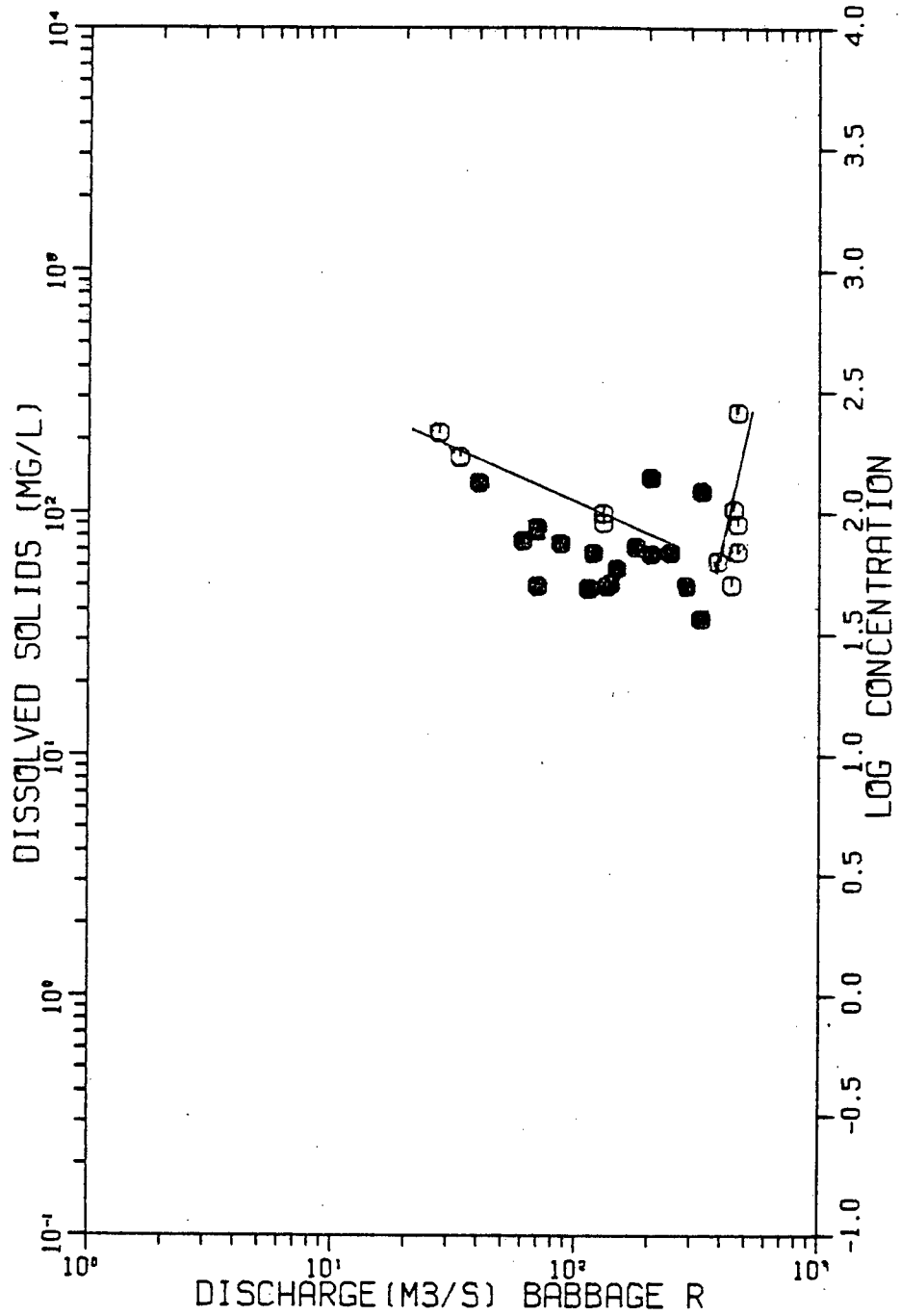


FIGURE 91

Total dissolved solids concentration as a function of discharge, Babbage River at B1, 1976; straight lines indicate high-flow and late-season low-flow ratings; shaded symbols represent early-season low-flow conditions.

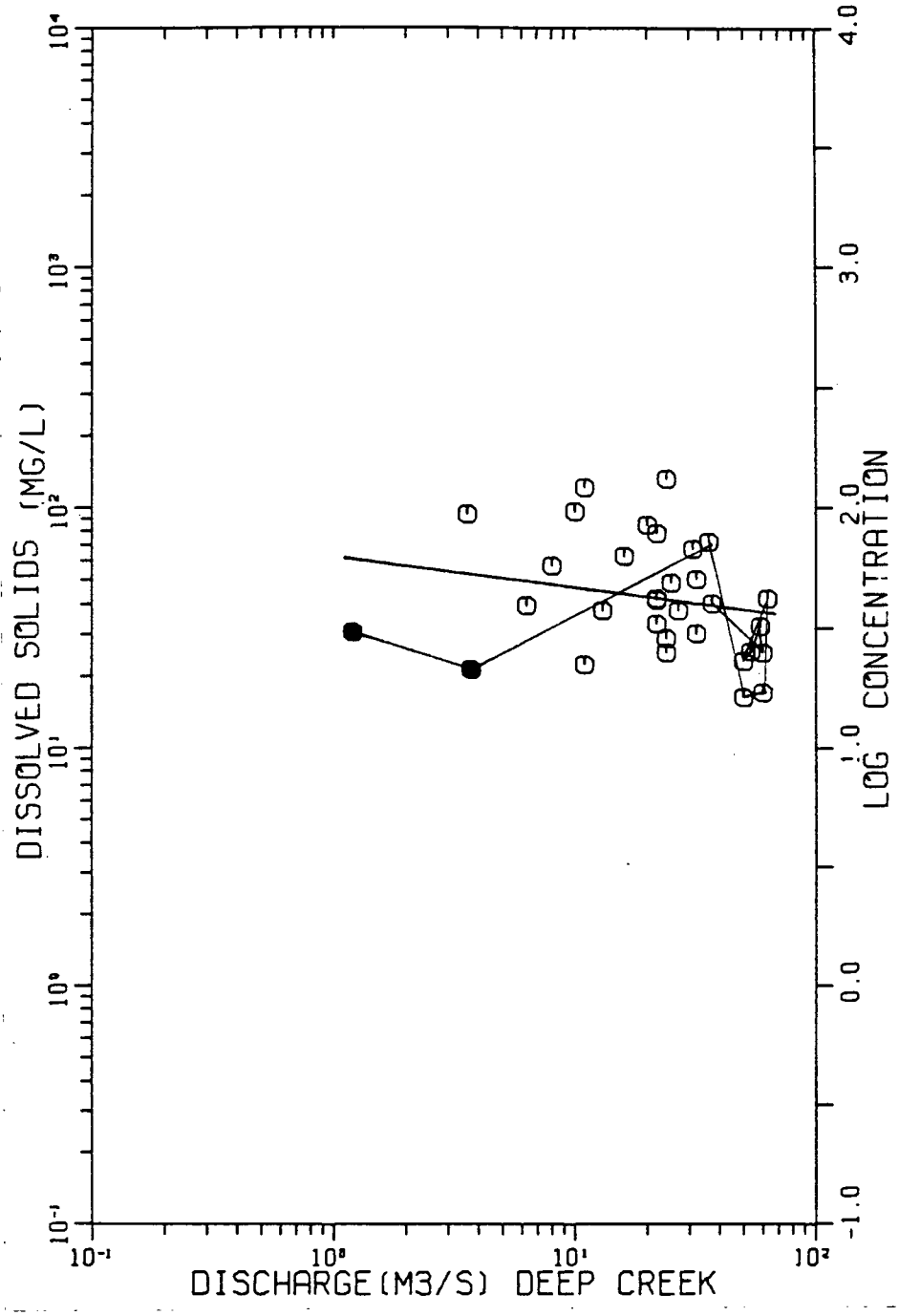


FIGURE 92

Total dissolved solids concentration as a function of dischargeDeep Creek at D1, 1976, showing phase relations for period from first flow (shaded symbols) through major snowmelt flood; heavy broken line represents general least-squares rating (slope not significantly different from zero): see discussion in text.

estimate are rather large. This undoubtedly reflects both high sampling variability (cf. Oguss and Erlebach, 1976; Kleiber and Erlebach, 1977) and the occurrence of mixing processes that the simple rating model cannot accomodate. Mixing of waters from different sources with significantly different concentrations may produce considerable variance about the simple discharge rating. Furthermore, because individual ion types may exhibit distinctive patterns of variation with discharge (Johnson et al., 1969), mixing of source waters of different composition can produce complex departures from the mean. In homogeneous basins, a relatively simple inverse relation to discharge is commonly observed, due to dilution of base flow by storm runoff (cf. Gunnerson, 1967). A broadly analogous pattern is assumed to hold in the basins considered here, although it cannot be defined unambiguously. During the snowmelt recession, solute concentrations may be expected to increase as discharge diminishes and the proportion of snowmelt decreases. At very low flows in mid-summer, groundwater sources may represent a significant part of the total discharge, despite extensive permafrost (see section 3.1.1). However, low flows in the early snowmelt period are almost entirely melt-derived, at least in reaches such as D1 well downstream from groundwater sources, and solute concentrations are correspondingly low (cf. first observations in Deep Creek, 1976, distinguished by shaded symbols in Figure 92).

Abrupt and short-lived increases in conductivity were observed occasionally in the Babbage River at relatively high

flows during the breakup period. Two such occurrences in 1975 are illustrated in Figure 93. The first of these was noted some hours after the annual flood peak on 15 June when the discharge was $Q=400\ m^3s^{-1}$; the second, four days later, during an uneventful recession when the discharge was $Q=180\ m^3s^{-1}$. Release of concentrated water from winter pools under ice provides a plausible explanation.

In the Babbage River, solute transport rates may exceed suspended sediment load at flows as high as $100\ m^3s^{-1}$ (Figure 89; cf. Figure 86), although not during the snowmelt season. In contrast, due to higher suspended sediment concentrations and lower TDS values in Deep Creek, suspended load exceeds solute load at discharges as low as $Q > 6\ m^3s^{-1}$. The greater turbidity of Deep Creek water is often apparent at its confluence with the Babbage River. During a short period in June 1976, fluvial sediment supplied from Deep Creek exceeded transport in the Babbage River. For the most part, however, the solute and sediment load in Deep Creek is very small (often negligible) compared to the quantities transported by the Babbage River.

Suspended sediment concentration and load can be estimated using ratings of the same form as those adopted for solute load. This approach has been followed widely as a pragmatic alternative to continuous sampling in many different environmental contexts (eg. Straub, 1935; Campbell and Bauder, 1940; Leopold and Maddock, 1953; Jarocki, 1957; Bobrovitskaya, 1967). In most cases, water discharge Q is found to account

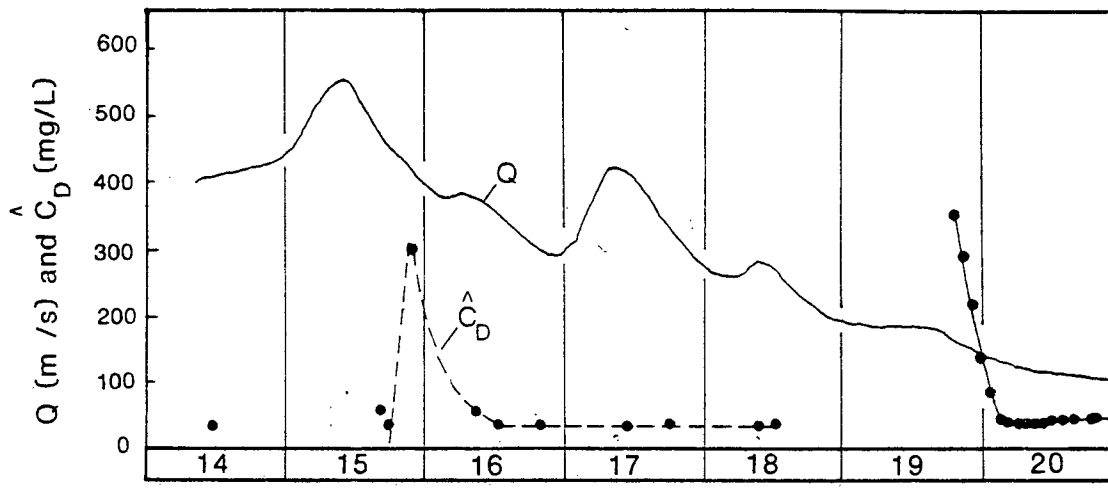


FIGURE 93

Water discharge and total dissolved solids concentration (estimated from specific conductivity corrected for $\Theta_w$), showing two transients of high TDS concentration during breakup and snowmelt flood of June 1975, Babbage River at B1.

for a large part of the variance of suspended sediment concentration, although much scatter about the rating relation may sometimes remain.

Numerous factors have been identified to explain the additional variance. In particular, one may distinguish between wash and bed-material components of the suspended load (defined with respect to a given reach): the latter is determined by the hydraulic conditions in the reach and is therefore closely correlated with discharge; the former may be only weakly related to discharge, being determined by the dynamics of erosion and sediment delivery throughout the catchment or in varying source areas. In practice, the two components of suspended load cannot easily be distinguished and factors affecting wash load must be considered to explain the variance of measured suspended load. Supply-limitation has been postulated in some cases (Campbell and Bauder, 1940) and appears to be a factor in North Slope rivers (see below). Serial correlation over a wide range of time lags, reflecting reaction and relaxation effects (Allen, 1974) at many frequencies, is another common feature of suspended sediment concentration in rivers. These effects, which, strictly speaking, invalidate the use of regression techniques for rating estimation, result from the occurrence and interaction of many factors, including shifts in the rating caused by channel adjustment during floods (Campbell and Bauder, 1940; Brown and Ritter, 1971); year-to-year and longer-term weather fluctuations (Abrahams and Kellerhals, 1973); seasonal-scale

variability of weather and related hydrological and sedimentary processes (eg. Guy, 1964; Hall, 1967); and short-term effects that may arise from a complex set of variables including precipitation patterns, antecedent soil conditions, contributing area, sediment type, and channel hydraulics.

Serial correlation in suspended sediment concentrations appears as hysteresis in the concentration-discharge relation (Figures 94 and 95). Hysteresis has been extensively documented (see, for example, Hjulström, 1935; Allen, 1974), and may reflect phase shifts at various frequencies ($10^3 < 1/f < 10^8$ s). High-frequency effects may be superimposed on low-frequency effects: for example, differences between rising and falling stage for individual short-term events (noted by Einstein et al., 1940; Johnson, 1943) may be superimposed on an annual snowmelt hydrograph. Such a pattern, similar in some respects to observations in Klarälven (Sundborg, 1956), can be seen in the 1975 Babbage River data (Figure 94A).

Separation of ratings on the basis of rising and falling stage can greatly improve the precision of rating estimates in some cases (Nilsson, 1971, 1972; W. F. Rannie in Church and Gilbert, 1975). The Babbage River data exhibit no consistent partition in terms of the sign of instantaneous dQ/dt. Regression equations computed separately for rising and falling stage are not significantly different. This result may be due in part to the occurrence of a weak diurnal melt pattern (see section 3.1.1) which determines the sign of dQ/dt, but has a rather minor effect on suspended sediment concentrations, this

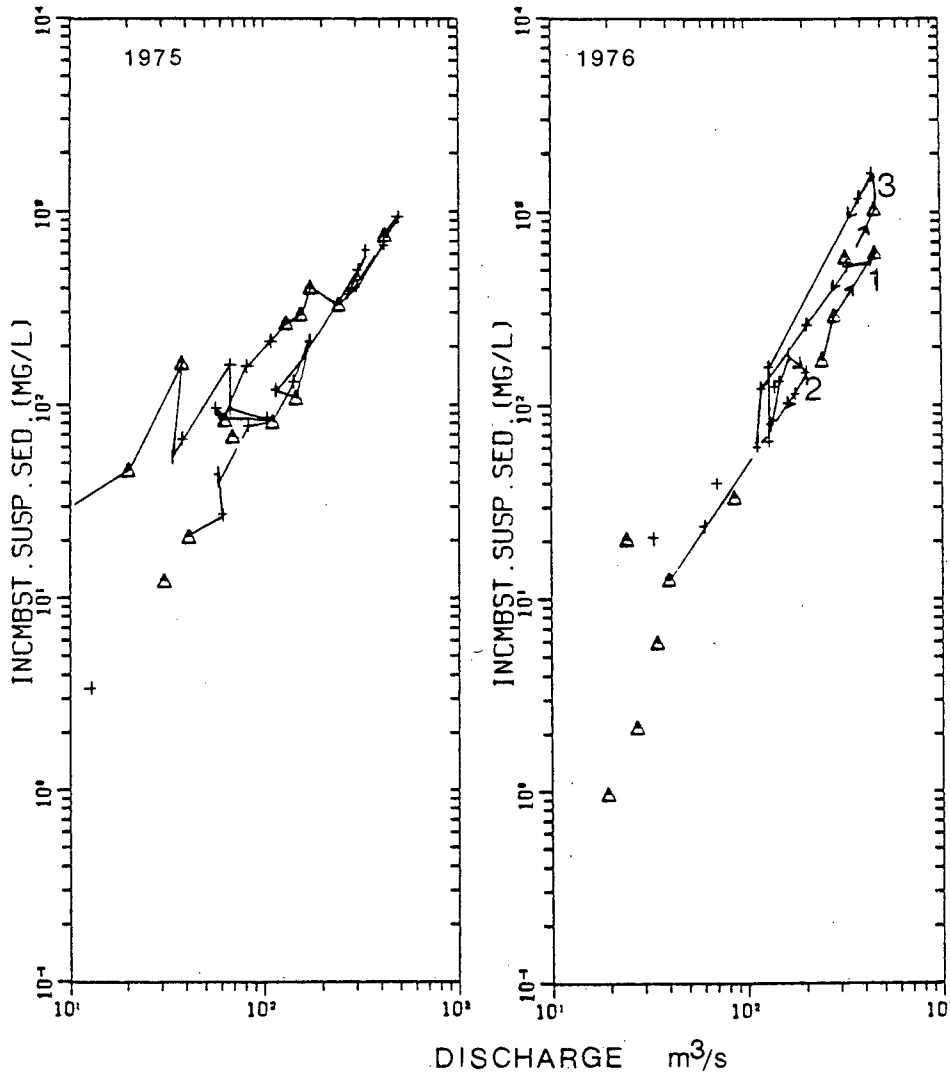


FIGURE 94

Phase relations between incombustible suspended sediment concentration (mg/L) and discharge ($m^3s^{-1}$), Babbage River at B1, 1975 and 1976. Numbered events in 1976: (1) 5-6 June; (2) 15-16 June; (3) 26 June; cf. figure 87.

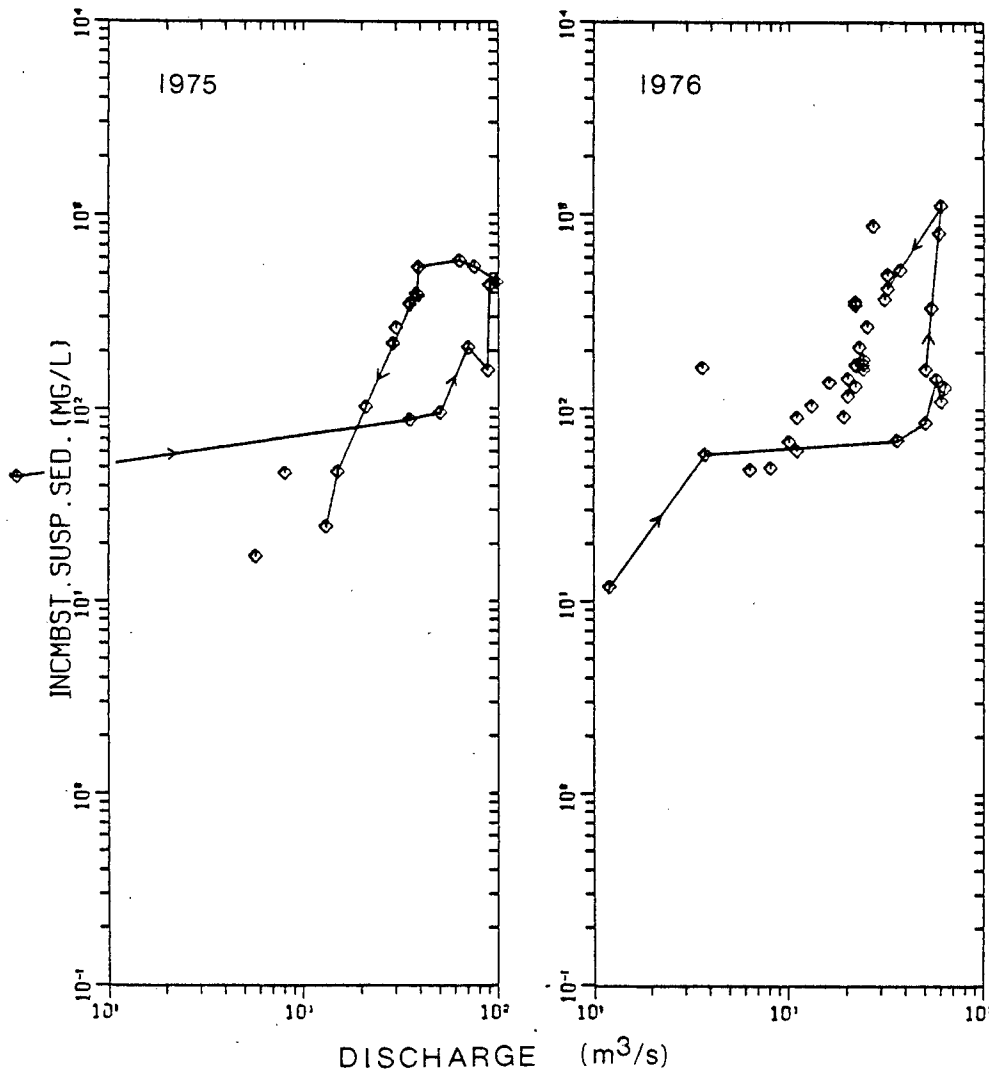


FIGURE 95

Phase relations between incombustible suspended sediment concentration (mg/L) and discharge ($m^3 s^{-1}$), Deep Creek at D1, 1975 and 1976, showing hysteresis during annual snowmelt floods.

effect being largely masked by lower-frequency events. This is not to say, however, that short-term hysteresis is lacking.

Phase lags over periods of one or more days are illustrated (Figure 94B) for three distinct flood events in the Babbage River during June 1976 (cf. Figure 87). In the two major floods of the season [(1) 6 June and (3) 26 June], suspended sediment concentration lagged discharge (although the detailed hourly pattern cannot be resolved for the flood of 6 June). During the flood of 26 June 1976, suspended sediment concentration peaked approximately 3-4 hours after discharge. In contrast, the smaller flood [(2) 15-16 June] exhibited higher suspended sediment concentrations on the rising limb, but again the detailed hourly pattern near the flood maximum cannot be resolved (indeed the sampling intervals were such that some aliasing may be present in the apparent hysteresis patterns of events 1 and 3).

Data for 8 June 1974 (Figure 96) demonstrate the degree of idealization involved in a single-input concept of sediment response. The double peak in suspended sediment concentration may represent interaction of wash load arriving from different sources (tributary basins) with different lag characteristics, different input conditions, or both. Alternatively, it may demonstrate contrasting responses of wash load and bed-material load in suspension. Counterclockwise hysteresis loops such as those of 8 June 1974 and 26 June 1976 suggest, in the case of steeply increasing functions of a simple harmonic independent variable (eg. discharge), a phase lag $\tau \leq \pi/4$ radians (Allen,

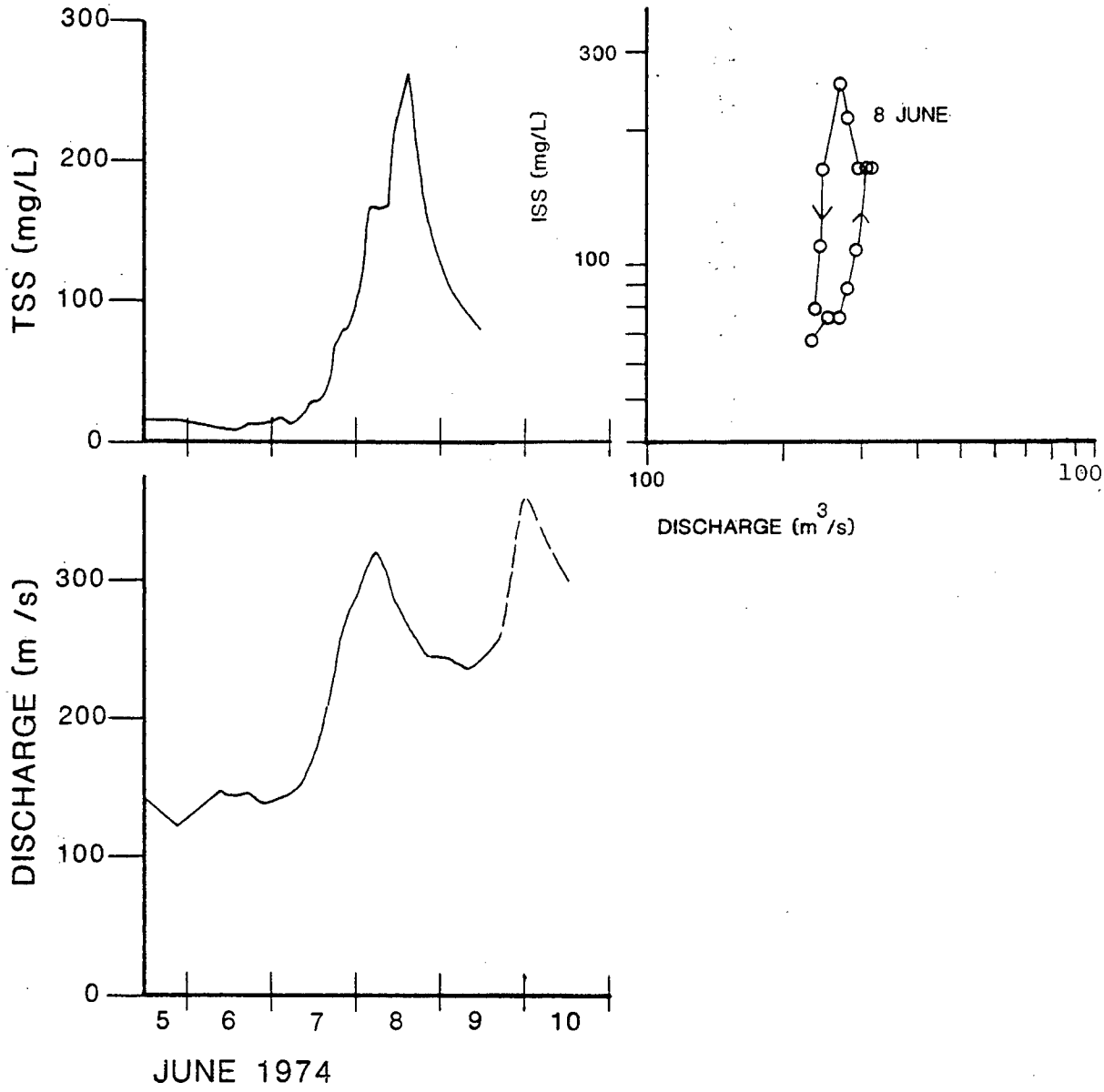


FIGURE 96

Hysteresis in suspended-sediment/discharge relation during Babbage River flood of 8 June 1974, showing peaks in TSS concentration both before and after peak stage and counter-clockwise hysteresis loop for the flood as a whole.

1974, figure 8). However, this interpretation ignores the possibility of multi-frequency components in the response variate and undoubtedly oversimplifies the sediment supply processes in the basin. The computation of a frequency response function for the water-sediment system, giving phase relations as a function of frequency [see, for example, the study by Sharma and Dickinson (1979), using daily data] requires essentially continuous sampling ($\Delta t << 1$ h) for analysis of response to individual flood events and is further complicated if the system cannot be assumed linear. Nevertheless, phase diagrams and frequency response functions may be useful tools for description of sediment delivery and for comparison of events of similar scale and frequency, or different scales and frequencies, in a single basin or in contrasting systems.

The nature of hysteresis occurring on individual floods in the Babbage River may be compared, in the phase diagrams of Figure 94, with the pattern of serial correlation on a seasonal scale. In this context, the Babbage River data will be compared with observations in Deep Creek (Figure 95) to evaluate differences in the response of two dissimilar fluvial systems to comparable input weather conditions.

In 1975, ISS concentrations during early snowmelt flooding, both in the Babbage River and in Deep Creek, were anomalously high, a pattern not clearly evident in 1976, although sampling that year began late and there is a suggestion of slightly higher-than-average concentrations in

the first days of flow in Deep Creek (Figure 95).

The Babbage River hydrographs and related transport series were very different in 1975 and 1976 (Figures 86 and 87). In 1975, there was a single major flood peak; in 1976, there were two, the first involving snowmelt almost exlusively, the second arising from rainfall with an undetermined proportion of residual snowmelt. The ISS phase diagram for 1975 indicates that suspended sediment concentration remained anomalously high for almost three weeks on the rising limb of the annual flood hydrograph, yielding a broadly clockwise loop for the annual flood as a whole. This behaviour reflects the seasonal pattern illustrated in Figure 89 (based on 1976 data), despite the appearance that suspended sediment concentrations were lower in early June 1976. They were lower at high flow during the flood of 6 June, presumably due to the high proportion of snowmelt and limited depth of thaw. The highest observed concentration on 6 June was less than half the maximum value observed on the 26th, although water discharge and, indeed, total sediment transport were higher during the earlier flood.

Higher suspended sediment concentrations at low flow during the snowmelt season are perhaps unexpected, given the widespread occurrence of bottomfast ice (see below), snow against banks, and snow-covered frozen ground. However, many channel banks have only minor snow accumulations and nivation processes may operate effectively on others (cf. Miles, 1976, 1977). Destabilization of banks by block-slumping or other processes during the previous summer may play a role similar to

that of surface weathering between storms in other regions (Hjulström, 1935). Where banks are blown relatively snow-free, entrainment may begin early in the snowmelt season. Finally, the effect of low water temperatures and associated high viscosity (cf. Harms and Fahnestock, 1965) on sediment settling velocities may be significant for the maintenance of coarser sediment in suspension.

In general, the suspended sediment ratings computed for early-season (snowmelt) data exhibit lower exponents than do those computed for late-snowmelt and summer data (Figures 89 and 90). It may be hypothesized that this pattern would hold in other Arctic rivers. The lower exponent in the early-season rating appears to represent interaction of opposing supply phenomena at high and low flows during this period of the year.

A marked contrast appears in the seasonal-scale response of Deep Creek and Babbage River, particularly in 1975 (Figures 94 and 95). Deep Creek exhibits a wide counterclockwise hysteresis loop during the first snowmelt flood in both 1975 and 1976. In both cases, a brief early period of relatively high concentrations is followed by an interval of anomalously low concentration during the rising limb of the snowmelt hydrograph. The rise and recession can be characterized by distinct quasi-parallel ratings with coefficients that differ by an order of magnitude. The reasons for this pattern can only be postulated. Relatively long relaxation effects might be expected <u>a priori</u> in Deep Creek,

due to the low hypsometric integral (Figure 11; Table 9) and elongated planform of the basin (McDonald and Lewis, 1973, p.21). Bottomfast ice, snow against banks, and a narrow sinuous channel particularly susceptible to ice-jamming may be contributing factors.

Bedload transport ratings for Babbage River and Deep Creek are illustrated in Figures 89 and 90. The rating for Deep Creek is essentially a least-squares regression through sample data, extrapolated to higher discharge. The lower segment of the bedload rating in the Babbage River is also based on sample data.

The sample data collected in section B1 (figure 97; Appendix A.4) and theoretical extensions of the rating curve derived from the Babbage River data require further discussion. Sampling extended over a wide range of discharge, $34<Q<428$ $m^3s^{-1}$. Unfortunately, measured transport rates for all flows greater than about 60 $m^3s^{-1}$ are considered unreliable, due to one or more of the following factors: high concentrations of coarse suspended organic material that may have clogged the sampler screen and reduced hydraulic efficiency on some occasions (cf. Johnson et al., 1977); poor interfacing with the armoured bed in the thalweg at flows below threshold for the armour materials; and, possibly, insufficient sample coverage at high flows. Theoretical results of Einstein (1950) and of Bagnold (1966, 1973) have been applied to the reach at B1 in order to interpret the sample data and to obtain a rating curve at higher discharges, $Q>60$ $m^3s^{-1}$.

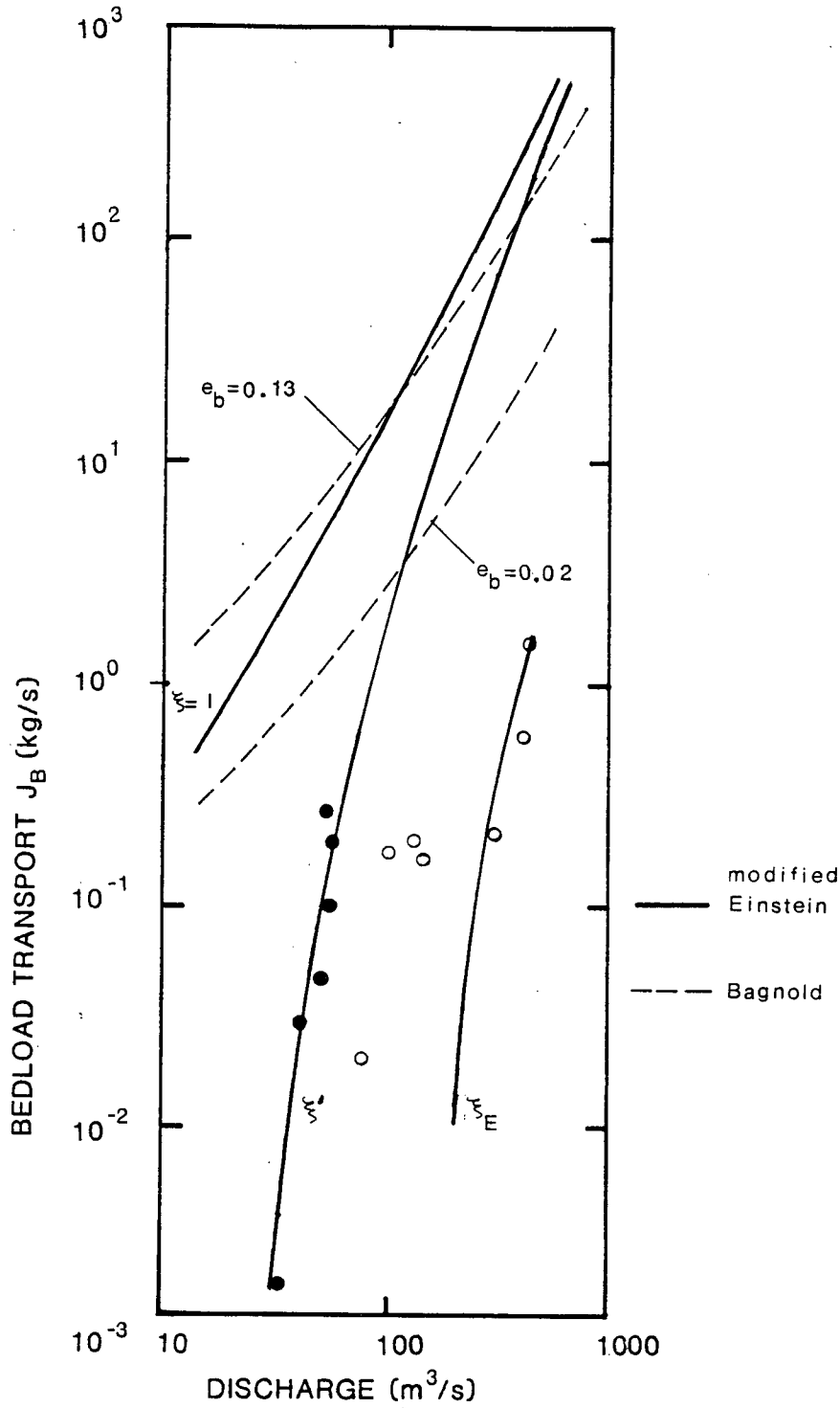


FIGURE 97

Sample data and theoretical ratings for bedload transport, Babbage River at B1, 1976; open symbols (o) denote data considered unreliable; shaded symbols (●) represent data considered realistic.

Einstein's bedload model, as modified and applied to gravel-bed rivers by M. Church (personal communication, 1977), includes the following distinctive characteristics: sediment entrainment and deposition are recognized as stochastic processes; explicit consideration is given to particle-size distributions for determination of effective resistance, hiding effects, and total transport rates; total flow resistance is partitioned (in effect following Strickler, 1923) to obtain that portion, related only to small-scale surface roughness of the bed, which is effective in the context of particle entrainment; measured hydraulic parameters (rather than the values computed in Einstein's original procedure) are employed in the calculations. The major assumptions of the model are summarized in Appendix A.4. It is implicitly assumed that sediment supply is not limited.

The dry-mass unit-width transport rate is computed, for homogeneous sediment, as:

$$j_B = \rho_s(\gamma_s - 1)^{1/2} g^{3/2} D^{3/2} \Phi_* \qquad (4.1.2\text{-}2)$$

where

$$\Phi_* = f\,[\Psi_*] \qquad (4.1.2\text{-}3)$$

as given by Einstein (1950, figure 9, equation 57). For gravel rivers (hydrodynamically rough flow):

$$\Psi_* = 0.67\xi(\gamma_s - 1)D_{35}/R_g \tan B_e = 0.67\xi(\gamma_s - 1)\rho_w D_{35}/\tau_g \qquad (4.1.2\text{-}4)$$

where $R_g$ is hydraulic radius corresponding to granular shear resistance (total flow resistance minus form resistance), $\tau_g$ is

boundary shear pertaining to granular resistance, $\tan B_e$ is the hydraulic energy slope, and $\xi$ is a hiding factor (Einstein, 1950, figure 7). Essentially, then,

$$j_B = f\,[\rho_s, D_a, D_i, \tau, \xi] \qquad (4.1.2\text{-}5)$$

where $D_a$ refers to the size distribution of sediment at the channel boundary (the armour layer in gravel rivers), defined for computational purposes by $D_{35}$ and $D_{65}$. The transport rate for individual size fractions is obtained as $j_B f_i$, where $f_i$ is the proportion of total bed-material in a given fraction represented by equivalent diameter $D_i$. Total transport through the section is then $J_B = b\,(\sum_i j_B f_i)$, where b is the width of the channel.

The modified Einstein procedure (adapted to compute only bed-contact load as defined herein) has been applied with considerable success to reaches of the Elbow River (M. Church, personal communication, 1977) and of the Chilliwack River (D. McLean, personal communication, 1977). It was found that the Einstein model was the only one of a large selection of established bedload functions (excluding the Bagnold model, which was not investigated) not to overestimate significantly the transport rate of bedload in Elbow River, relative to measured transport rates reported by Hollingshead (1971); rather, the Einstein function tended to underestimate bedload transport. To some extent, this result may reflect the extreme sensitivity of Einstein's model to grain size parameters. At high flows, moreover, when channel armouring is removed and general entrainment ('live-bed') conditions prevail, the hiding

factor $\xi$ >1.0 for all particle sizes. Church obtained improved results for Chilliwack River data using this modification. With live-bed conditions, however, the boundary roughness parameters originally specified will no longer apply and the theoretical basis of the model is undermined.

The modified Einstein model has been implemented for computation of bedload transport in the Babbage River at B1, using a program due to M. Church. Sediment size parameters were obtained from samples of sediment moving as bedload and of material in storage on the B1 bar (Figure 98). For conditions prevailing in the Babbage River at B1, computed transport rates are grossly underestimated at low flows using Einstein's hiding factor $\xi_E$ (Figure 97). This result was anticipated by Einstein (1950, p.41) and more recent work has confirmed the need for a new evaluation of the hiding factor (Yano et al., 1969). On the other hand, if the hiding factor is eliminated ($\xi$ =1), computed transport rates are much greater than observed values or extrapolated estimates, except perhaps at Q>300 $m^3s^{-1}$, when significant channel scour may occur. The Babbage River data (Figure 97, shaded symbols) indicate a modified hiding function $\xi' = 0.99+0.01\xi_E$. Einstein's function, the empirical modification adopted here, and experimental results of Yano et al. (1969) are plotted in Figure 99.

Ratings generated by equation 4.1.2-5 using $\xi$ =1 and $\xi = \xi'$ respectively are asymptotic at high flow. However, if general bed scour occurs, certain assumptions of the model

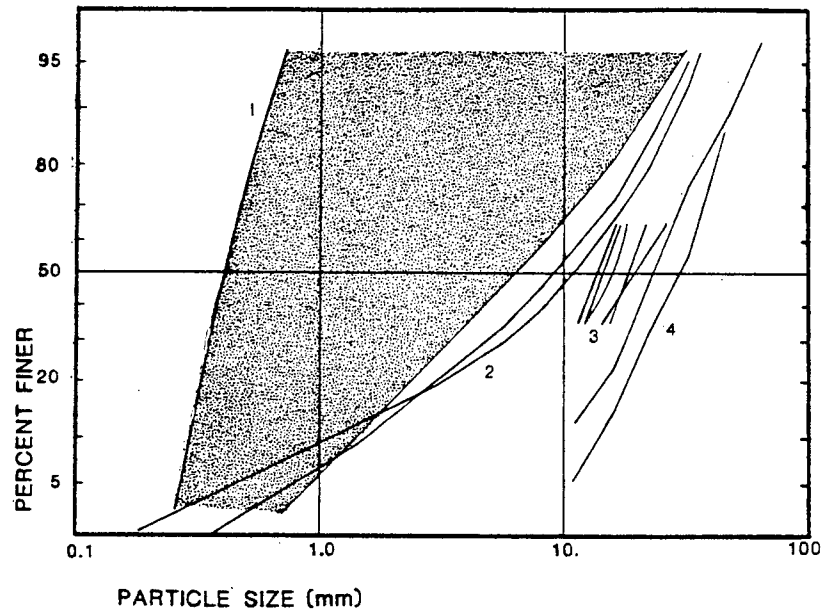


FIGURE 98

Particle-size distributions for various samples of sediment in channel deposits or moving as bedload, Babbage River at B1.
(1) sand and gravel collected in bedload samplers (sieve data, mass frequency;
(2) subsurface sediment in bar (sieve data, mass frequency);
(3) sediment on bar surface, 1976 (photo data, number frequency);
(4) sediment on bar surface, 1972 (after McDonald and Lewis, 1973; transect data, number frequency).
See Kellerhals and Bray (1971) for equivalence of number frequency results for surface samples and mass frequency results for subsurface bulk samples.

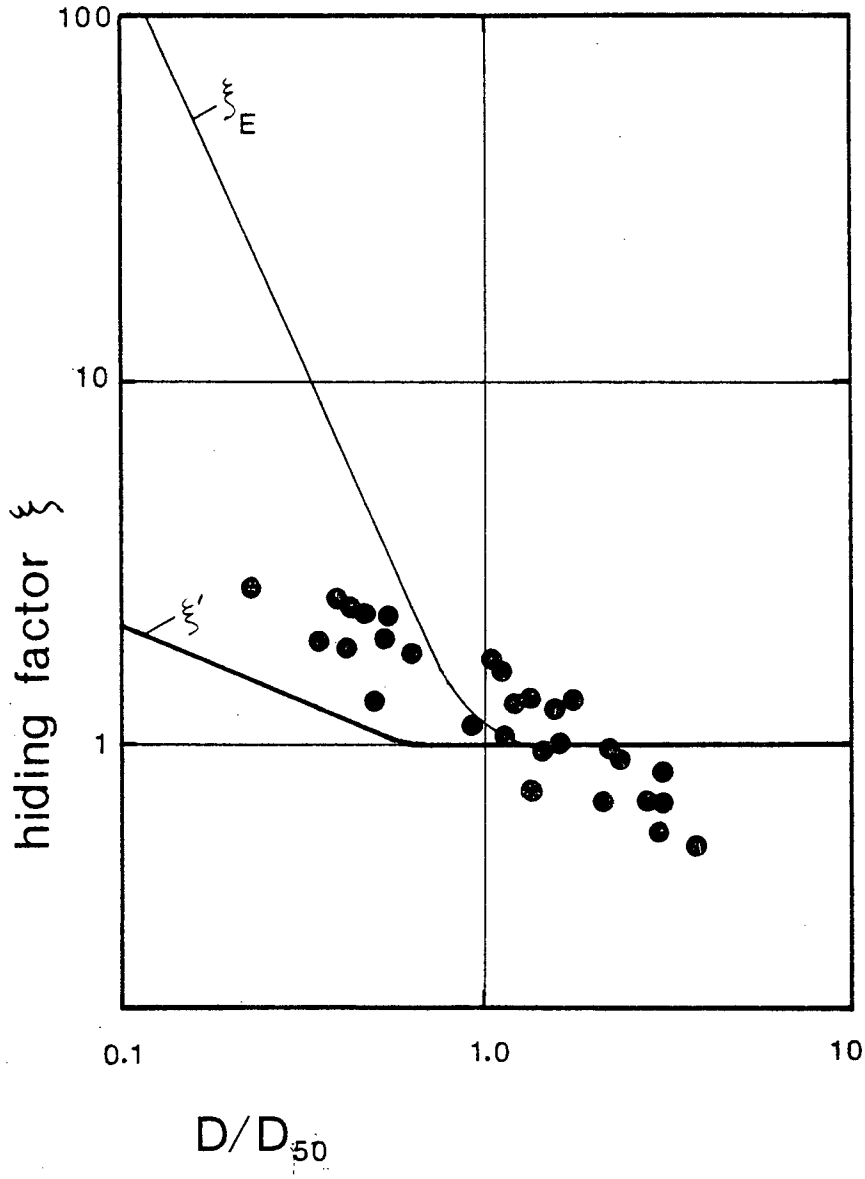


FIGURE 99

Three sets of empirical results for the hiding factor $\xi$ as a function of $D/D_{50}$ in rough turbulent flow.

(notably 3, 5, and 8; see Appendix A.4) may be seriously violated and parameters $D_a$ cannot be determined. In this case, neither version of the Einstein model may be valid and an alternative strategy must be sought. The model presented by Bagnold (1966, 1973) appears to provide the firmest physical basis for estimation of transport rates under these conditions.

Bagnold's model proceeds from the argument that sediment transport involves mechanical work, which may be taken as the product of available power and efficiency (Bagnold, 1966, p.5). The available power per unit length of stream is derived from loss of potential energy and defined by

$$P = \rho_w g Q S \qquad (4.1.2\text{-}6)$$

for the entire section; or, per unit area, by

$$p = P/b = \tau u. \qquad (4.1.2\text{-}7)$$

The fraction of total power utilized for sediment transport may be defined as $e_T p$, where $e_T$ is an efficiency factor related to total sediment transport. The bedload work rate may be defined as $i_B[\tan(f)-\tan(B)]$, where $\tan(B)$ is the slope and $\tan(f)$ is a friction coefficient for intermittent solid contact, believed to be approximately equivalent to the conventional solid friction coefficient $\tan(\phi)$. On evidence presented by Bagnold (1973, pp.480-481), $\tan(f)=0.63$ may be taken as a reasonable value, although this clearly remains a point of uncertainty.

Setting power expenditure equal to bedload work rate, we obtain:

$$i_B[\tan(f)-\tan(B)] = e_B p \qquad (4.1.2\text{-}8)$$

where $e_B<e_T<1.0$ is bedload transport efficiency and $\tan(B) \simeq 0$.

The dry-mass transport rate per unit width is then

$$j_B = \rho_s \tau u e_B / (\rho_s - \rho_w) g \tan f \qquad (4.1.2\text{-}9)$$

Major assumptions of this theory are summarized in Appendix A.4. The distribution of transport among the various size fractions of a heterogeneous sediment is not considered. Nor does the theory take explicit account of the frictional resistance characteristics of the reach, although boundary roughness is clearly implicit in the formulation of $e_B$ (cf. Bagnold, 1973, pp.492ff). Furthermore, $e_B=0$ at the transport threshold (which varies according to parameters of the sediment) and clearly increases with increasing mean velocity and shear stress to a maximum value $e_B<<1$. Of principal interest in the present context is the upper limit of $e_B$ under live-bed conditions. This concept was addressed explicitly by Bagnold (1966), wherein he deduced a theoretical maximum value of $e_B=0.13$ approximately. Substitution of $e_B=0.13$ and $\tan(f)=0.63$ in equation 4.1.2-9 yields the upper curve intersecting Einstein's model in Figure 97. In view of the uncertainties associated with the Einstein model under high-flow conditions and because the Einstein model implies $e_B>0.13$ for $Q>400 m^3 s^{-1}$ approximately, the Bagnold model has been preferred for bedload transport estimates under these conditions.

It was postulated at the outset of the study that supply limitation might be an important factor in the bedload transport regime of an Arctic river. Winter reduction of discharge to zero or near-zero is accompanied, in the rivers

described here, by freezing of water remaining in shallow low-flow channels. The ice is bottomfast except in the deepest pools and forms a temporary rapidly-degrading channel-bed (Figure 100) during initial spring discharge (McDonald and Lewis, 1973; Egginton, 1978; Forbes, 1979).

It has been hypothesized that bottomfast ice inhibits channel scour during the overflow period. However, scour of adjacent bar surfaces above the bottomfast ice level may be accelerated by the presence of the ice, which causes anomalously high stage for a given discharge. Protection from scour by bottomfast ice will also be significant only if major flows occur while the ice is in place; no major flood events were observed over bottomfast ice in the Babbage River, but high flows did occur over ice in Deep Creek. After degradation of bottomfast ice, sediment entrainment might still be inhibited if the channel perimeter remains frozen. It is difficult to define the relative impact of bottomfast ice and freezing effects on the sediment regime of the river, given the remaining general deficiencies of sediment transport theory and measurement practice. Nevertheless, these low-temperature features represent additional parameters of the sediment transport system peculiar to high-latitude streams.

The effects of bottomfast ice and a frozen channel bed are additional to those of surface armouring, which is important at all seasons. The surface lag deposit is believed to be the major factor potentially limiting bedload supply in the Babbage River case. The phenomenon is widespread, but has not yet been

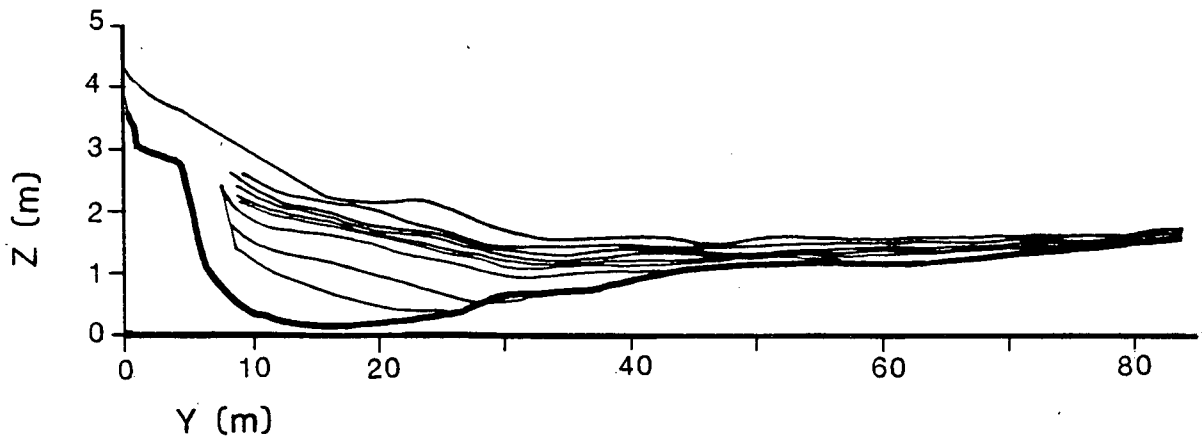


FIGURE 100

Channel bed profiles at section B1 (Babbage River) between 28 May and 8 June 1975, showing degradation of bottomfast ice; lowermost profile shows the channel ice-free at the end of this period.

satisfactorily evaluated theoretically, as the foregoing discussion of the hiding and efficiency factors demonstrates. The character of the surface armour in the Babbage River is illustrated in Figure 98, where the depletion of fine fractions in surface sediments is readily apparent.

Pragmatic recognition of the possibility of supply limitation might be accomplished by substitution of an empirical efficiency factor $e_B<0.13$ in equation 4.1.2-9. An empirical value $e_B=0.022$ for $D_{50}=8$ mm (Leopold and Emmett, 1976, figure 1) yields lower estimates of bedload transport through section B1 ($J_B \leq 40$ kg/s). The lower estimates still exceed the measured transport rates by at least a factor of ten.

Alternative ratings based on the Bagnold model (with $e_B=0.02$ and $e_B=0.13$) and on the modified Einstein model (with $\xi=\xi_E$, $\xi=\xi'$, and $\xi=1$) are presented in Figure 97. The model outlined in Figure 89 (modified Einstein model at $Q<380$ $m^3s^{-1}$, Bagnold model with $e_B=0.13$ at higher discharge) has been preferred on theoretical grounds and on evidence that some scour does occur in the B1 section during major flow events (Figure 101). The evidence for general scour (live-bed conditions) is not compelling and it must be recognized that supply limitation may be important in the bedload transport regime of rivers such as the Babbage.

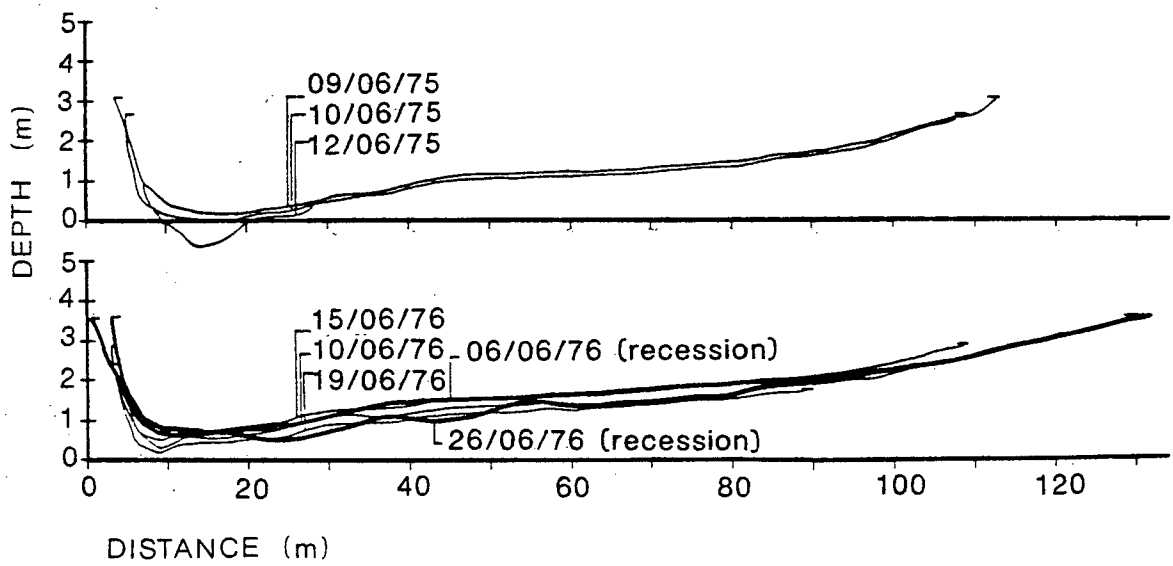


FIGURE 101

Channel bed profiles at section B1 (Babbage River); A, 1975: scour during rising limb of annual snowmelt hydrograph, showing development of scour-hole against bank in thalweg; B, 1976: profiles shortly after peak flow on 6 June and 26 June, net fill 10-15 June, and net scour 15-19 June.

### 4.1.3 TOTAL FLUVIAL SEDIMENT INPUT

The total sediment yield (including solutes) from Babbage River and Deep Creek drainage basins has been estimated using rating equations based on data and interpretations discussed above (section 4.1.2). Computed sediment transport totals are summarized in Tables 19 and 20.

The data permit a provisional estimate of annual sediment yield from two contrasting North Slope basins. Although the sample is small, there is some evidence to suggest that variance of annual sediment production may be relatively low in these basins (Cooper and Hollingshead, 1973; Scott, 1978). The total mass of sediment supplied from the Babbage River basin during the period June to August inclusive was found to be approximately $2.3 \times 10^8$ kg in 1974, $3.8 \times 10^8$ kg in 1975, and $3.0 \times 10^8$ kg in 1976 (due to gaps in the 1974 record, the total for that season may have been underestimated). These data indicate specific yields of 0.055, 0.091, and 0.072 kg $m^{-2}$ respectively. In Deep Creek, total transport computed for the same period in 1976 was $0.4 \times 10^8$ kg or 0.057 kg $m^{-2}$. Substantially less sediment was supplied from Deep Creek during June 1975 than during the same month in 1976, a pattern that contrasted with conditions in the Babbage River.

The combined yield from the Babbage River and Deep Creek provides an estimate of total fluvial sediment supply to the Babbage Estuary, amounting to $3.7 \times 10^8$ kg in June 1975 and $3.4 \times 10^8$ kg during June-August 1976.

TABLE 19

Sediment transport summary, Babbage River below Tulugaq (Crow) River, 1974-1976.

| month | days miss[1] | days comp[2] | Sediment transport in units of $10^6$ kg TDS | TSS | TBS | total | TMS |
|---|---|---|---|---|---|---|---|
| May 1974 | 26[3] | 0 | | | | | 37.08 |
| June | 14 | 0 | 30.84 | 103.96 | 48.94 | 183.74 | 70.94 |
| July | 5 | 26 | 18.89 | 8.40 | 1.70 | 28.49 | 26.38 |
| Aug | 17 | 8 | 8.80 | 8.86 | 1.90 | 19.56 | 9.78 |
| Sept | 30 | 0 | | | | | |
| May 1975 | 22[4] | 0 | 4.0 | 8.0 | 0.5 | 12.5 | 6.02 |
| June | 0 | 1 | 37.30 | 238.46 | 78.35 | 354.11 | 354.11 |
| July | 0 | 31 | 12.14 | 0.72 | 0.03 | 12.90 | 12.90 |
| Aug | 0 | 31 | 14.68 | 1.54 | 0.07 | 16.29 | 16.29 |
| Sept | 27 | 3 | | | | | 1.47 |
| May 1976 | 31[5] | 0 | | | | | |
| June | 1 | 5 | 32.17 | 167.63 | 66.42 | 266.22 | 249.13 |
| July | 1 | 28 | 17.09 | 4.13 | 0.38 | 21.60 | 18.96 |
| Aug | 5 | 26 | 12.76 | 1.20 | 0.08 | 14.04 | 13.49 |
| Sept | 11 | 19 | 10.8 | 0.3 | 0.01 | 11.1 | 7.37 |
| 1974 26 May - 15 August | | | 60.66 | 138.23 | 60.19 | 259.09 | 144.18 |
| 1975 23 May - 3 Sept | | | 67.76 | 244.67 | 78.66 | 391.12 | 391.12 |
| 1976 1 June - 19 Sept | | | 69.21 | 173.12 | 66.89 | 309.22 | 288.95 |

TDS: total dissolved solids
TSS: total suspended solids
TBS: total bed-contact solids
total: sum of TDS+TSS+TBS computed from ratings, with interpolation or limited extrapolation
TMS: total transport from ratings for intervals with observational data

1: number of days missing from record
2: number of days with continuous stage record
3: apparent first flow 16 May 1974
4: no major flow before start of observations 23 May 1975
5: flow $\sim$30 $m^3 s^{-1}$ estimated from air 10 May 1976; river observed regularly from 26 May; June totals are thought to include first major flow event

TABLE 20

Sediment transport summary, Deep Creek above Babbage distributary, 1975 and 1976.

| month | days miss[1] | days comp[2] | Sediment transport in units of $10^6$ kg TDS | TSS | TBS | total | TMS |
|---|---|---|---|---|---|---|---|
| May 1975 | 22[3] | 9 | 0. | 0. | 0. | 0. | 0. |
| June[4] | 10 | 0 | 2.78 | 25.27 | 0.80 | 28.85 | 27.27 |
| July[5] | | | | | | | |
| May 1976 | 31[6] | 0 | | | | | |
| June | 4 | 0 | 3.30 | 33.38 | 0.30 | 36.64 | 35.81 |
| July | 0 | 31 | 0.78 | 1.76 | 0.002 | 2.54 | 2.54 |
| Aug | 0 | 31 | 0.28 | 0.17 | 0.000 | 0.45 | 0.45 |
| Sept | 12 | 18 | 0.11 | 0.004 | 0.000 | 0.11 | 0.07 |

TDS: total dissolved solids
TSS: total suspended solids
TBS: total bed-contact solids
total: sum of TDS+TSS+TBS computed from ratings, with interpolation or limited extrapolation
TMS: total transport from ratings for intervals with observational data

1: number of days missing from record
2: number of days with continuous stage record
3: river observed from 23 May 1975: no flow in May
4: first flow in snow over bottomfast ice 3 June; transport estimates based on single daily discharge measurements with TDS and TSS determinations
5: no estimates for July and August due to persistent failure of stage recorder
6: irregular observations suggest that little or no flow occurred during May 1976

The high proportion of total sediment delivery occurring during the snowmelt and breakup period is illustrated in Figure 102, a plot of cumulative percent sediment transport through section B1 (Babbage River) during 1975 and 1976. As much as 18 per cent of total annual transport (and 25 per cent of the annual suspended load) may occur in a single day (as on 26 June 1976). More than 90 per cent of the annual suspended sediment yield (and more than 99 per cent of the bedload transport) may occur during June.

The relative proportions of fluvial sediment delivered by dissolved, suspended, and bed-contact transport are summarized in Table 21. Solutes (and fine suspended sediment, $D<0.45$ μm) constitute as much as 25 per cent of annual transport in the Babbage River and roughly 10 per cent of annual transport in Deep Creek. On a monthly basis, these proportions may rise to more than 95 per cent of total load in late summer. Suspended sediment transport accounts for as much as 63 per cent of total annual sediment load in the Babbage River and almost 90 per cent in Deep Creek. The proportion of bedload in Deep Creek is estimated to be roughly 2 per cent, in the Babbage River approximately 22 per cent. Alternative computations of bedload transport at high flow in the Babbage River (cf. section 4.1.2) lead to estimates ranging from 6 per cent to 23 per cent of total annual sediment transport. It is probable that the true proportion lies somewhere between. These estimates for the proportion of sediment moving as bed-contact load in the Babbage River are particularly interesting, in view of the high

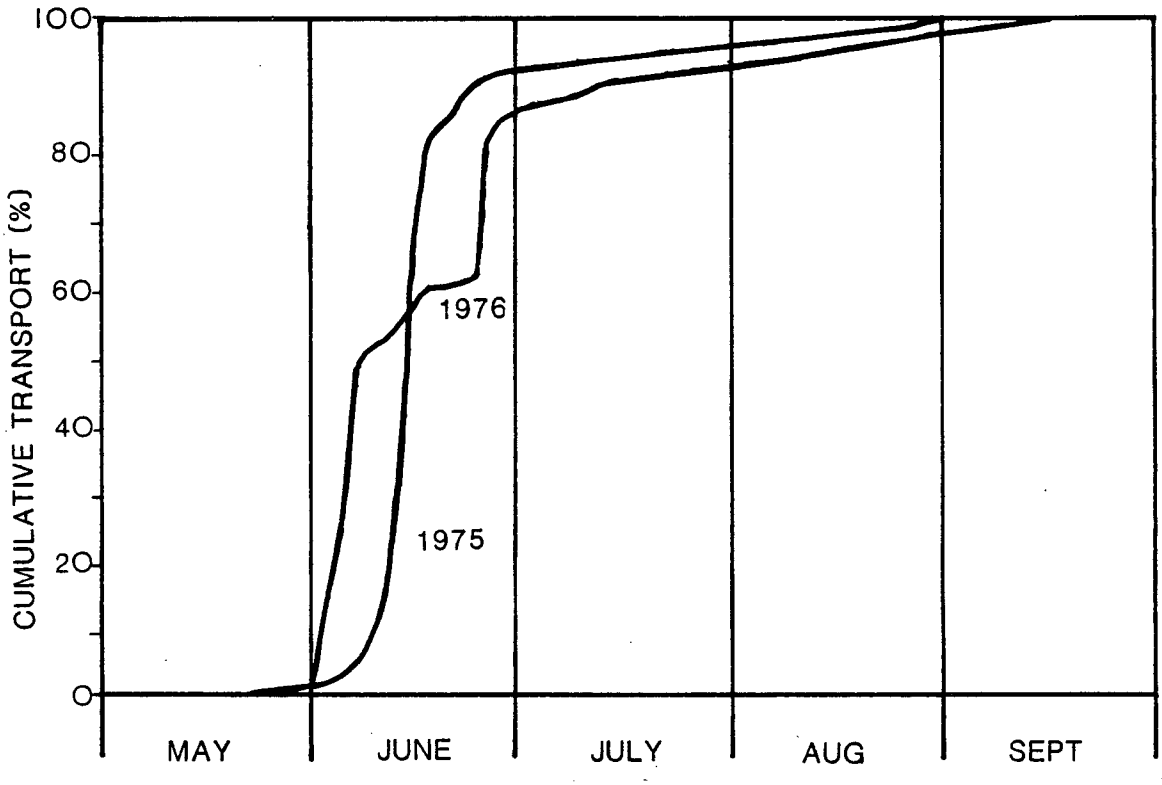


FIGURE 102

Cumulative percent of total observed sediment transport in Babbage River at B1, 1975 and 1976.

TABLE 21

Distribution of sediment transport by type, Babbage River and Deep Creek.

A: Babbage River at B1

| month/yr | percent of total transport dissolved[1] | inc-susp.[2] | total-susp.[3] | bedload[4] |
|---|---|---|---|---|
| June 1974 | 16.8 | 49.7 | 56.6 | 26.6 |
| July 1974 | 66.3 | 24.4 | 29.5 | 4.2 |
| Aug. 1974 | 45.0 | 37.4 | 45.3 | 9.7 |
| Jun-Aug74 | 25.5 | 45.5 | 52.7 | 21.8 |
| May 1975 | 32.0 | 52.0 | 64.0 | 4.0 |
| June 1975 | 10.5 | 55.5 | 67.3 | 22.1 |
| July 1975 | 94.1 | 4.6 | 5.6 | 0.2 |
| Aug. 1975 | 90.1 | 7.8 | 9.5 | 0.4 |
| Jun-Aug75 | 16.5 | 51.6 | 62.6 | 20.9 |
| June 1976 | 12.1 | 51.7 | 63.0 | 24.9 |
| July 1976 | 79.1 | 13.1 | 19.1 | 1.8 |
| Aug. 1976 | 90.9 | 7.2 | 8.5 | 0.6 |
| Sep. 1976 | 97.2 | 1.8 | 2.7 | 0.1 |
| Jun-Aug76 | 20.8 | 47.2 | 56.9 | 22.3 |

B: Deep Creek at D1

| month/yr | percent of total transport dissolved[1] | inc-susp.[2] | total-susp.[3] | bedload[4] |
|---|---|---|---|---|
| June 1975 | 9.8 | | 87.8 | 2.4 |
| June 1976 | 10.0 | 73.5 | 90.1 | 0.9 |
| July 1976 | 30.7 | 61.3 | 69.3 | 0.01 |
| Aug. 1976 | 62.2 | 35.2 | 37.8 | 0.00 |
| Sep. 1976 | 96.8 | 3.0 | 3.2 | 0.00 |
| Jun-Aug76 | 10.5 | 73.7 | 87.7 | 1.8 |

1: total residue passing 0.45-µm membrane filter
2: non-filterable residue after combustion at 550°C for 2h
3: total non-filterable residue
4: sediment supported by continuous or intermittent bed contact

width-depth ratios, pool-riffle morphology with prominent diagonal bars, and armoured gravel bed, features often taken to indicate very high proportions of bedload transport.

## 4.2 MARINE SEDIMENT SUPPLY TO THE ESTUARY

### 4.2.1 SEDIMENTARY SOURCES AND MATERIALS

McDonald and Lewis (1973) noted, from morphological evidence, the occurrence of several distinct littoral transport cells (cf. Stapor, 1971) on the Yukon coast. Each cell constitutes a partially closed system in which sediment derived from coastal erosion shows a net longshore transport toward a sediment sink, in which a large part of the total sediment supply is presumably stored, although fine sediment may be dispersed offshore (cf. Swift and Ludwick, 1976). Sediment sinks occur at Demarcation Bay (immediately west of the Yukon-Alaska boundary), in Workboat Passage (between Herschel Island and the adjacent mainland shore), at Shingle Point, and in Phillips Bay (Figure 1). The Phillips Bay sink, which may be considered to include the Spring River and Babbage estuaries, receives sediment primarily from some 15 km of coast west to Roland Bay and from a 15 km section of the Mackenzie Bay coast in Babbage Bight, extending southeast from Kay Point. Onshore transport of sediment may be another important source. Fluvial sediment is the third major input component.

The chief sources of marine sediment supply to the Babbage Estuary lie in coastal exposures of Babbage Bight and possibly in bottom deposits of Phillips Bay, including material forming the shoals north-northwest of Kay Point. Some sediment moving southeast along the western shore of Phillips Bay may also find its way into the Babbage Estuary. All of these sources expose unconsolidated Quaternary sediments, which in the coastal cliff

exposures are frozen and may contain considerable excess ice (Mackay, 1959; Mackay et al., 1972; Rampton, 1974a; cf. Figure 9). The sediments include a great variety of glacial, fluvioglacial, fluvial, lacustrine, mudflow, marine, and other facies of formations ranging in age from pre-Buckland to Holocene (Rampton, 1974b).

Southeast from Kay Point, the section of coast forming the major cliff source of sediment for the Babbage Estuary can be subdivided into two segments (Lewis and Forbes, 1974, p.21). The first segment, 1.5 km in length beginning at Kay Point, is characterized by a low steep bluff less than 10 m high (Figure 103A) in which a great variety of sediment occurs, including mud, sand, gravel, till, and peat. Large ice wedges constitute the major volume of ground ice in these deposits. Sediment delivery to the littoral transport system is dominated by ice-wedge thaw or fracture (or both), gullying along ice-wedge axes, undercutting by mechanical and thermal processes, and failure of polygonal blocks. The beach on this segment of coast is usually narrow or non-existant; however, ridge and runnel features develop at times during the open-water season.

In the second segment of coast southeast of Kay Point, the cliffs increase in height to as much as 100 m but become less steep (Figure 103B). Most exposures are in the headwalls of retrogressive-thaw features and typically reveal roughly 15 m of ice-rich mud and minor gravel, sometimes overlain by sand or till (Canada, Public Works, 1971a; Rampton, 1974a). The ice-rich sediments are highly contorted, apparently due to

FIGURE 103

A: coastal segment 1 near Kay Point, showing undercutting and failure of polygonal blocks formed by ice-wedge thaw or fracture, July 1976; B: coastal segment 2, showing major impact of retrogressive-thaw and associated mudflow transport of fine sediment across the beach, August 1977.

ice-thrusting during the Buckland Glaciation (Mackay, 1959; Mackay et al., 1972; Rampton, in press). A 60-m hole drilled at the cliff-top behind a stabilized failure zone approximately 6 km southeast of Kay Point (Lewis and Forbes, 1974, figure 11) encountered about 3 m of fine sand and silt over mud extending to the bottom of the hole; ice content decreased from 50-60 per cent by volume at the surface to 10-15 per cent at 10 m depth.

Retrogressive-thaw and associated mudflow transport dominate the sediment delivery process on this segment of coast; in some places, mudflow deposits extend across the beach so that large quantities of fine sediment can be mobilized in the surf zone during storms (Figure 103B). Gullying and slopewash may also be important (cf. results of Harper, 1978, from the Chukchi coast west of Point Barrow, Alaska).

Coastal exposures on the southern and western shores of Phillips Bay range up to 30 m in height. The cliffs west of Niakolik Point, partially protected by a broad shallow foreshore, expose up to 5 m of till or sand and gravel overlain by silt, sand, and peat; cliffs northwest of Spring River expose more than 7 m of icy pebbly clay, overlain by till, gravel, and mud (McDonald and Lewis, 1973, map 4, data due to V.N. Rampton).

Offshore sediment sources include materials on the extensive shallow bottom of Phillips Bay and in the shoal complex north-northwest of Kay Point. The latter is interpreted as an erosional remnant containing materials

similar to those present in the cliffs southeast of Kay Point. Gravel has been reported at several sites on the shoal complex and off Kay Point on the Mackenzie Bay side. Sediment over much of the bottom seaward of Kay Point spit is believed to be sand. Dune-scale bedforms with lee slopes facing onshore have been encountered locally, seaward of one or two nearshore bars up to 1 m in height parallel to the spit (Lewis and Forbes, 1974, p.25).

Hunter (1975) has reported on the petrography of three large sediment samples collected at proximal, central, and distal sites on Kay Point spit. The median size of berm sediment decreases from approximately 32 mm at the proximal site to about 3 mm at the distal end of the spit. Eight lithologies have been recognized, all of which occur in the mountains adjacent to the coastal plain. The predominant lithologies in the spit gravel are sandstone and siltstone, quartzite, and chert (Hunter, 1975, p.32).

Finally, it should be noted that the Mackenzie River represents a potential source of sediment input to the Babbage Estuary. Landsat imagery for 17 July 1975 (Figure 104A) shows suspended sediment of the Mackenzie River plume being advected westward along the Yukon coast; little if any of this sediment was dispersed into Phillips Bay. The leading edge of the plume during another such event was photographed from Kay Point on 28 July 1976 (Figure 104B). The concentration of suspended sediment (TSS) in the surface water of the plume at this time was 34 mg/L, the salinity s=3.2ppt. Events such as this were

FIGURE 104

Turbid Mackenzie River water off central Yukon coast; A: part of Landsat image 1-1089-20020-5, 17 July 1975, showing advection of suspended sediment past Kay Point; B: leading edge of Mackenzie River plume off Kay Point, 28 July 1976.

very rarely observed during field work for the present study and it is believed that the Mackenzie River does not constitute a significant sediment source for the Phillips Bay sediment sink or the Babbage Estuary system.

## 4.2.2 LITTORAL TRANSPORT PROCESSES

Sediment supplied from coastal sources southeast of Kay Point, along Kay Point spit, and west of Niakolik Point, is transported alongshore under the influence of obliquely incident waves. As in rivers, sediment entrained in the surf zone may move as bedload or in suspension. Suspended sediment concentrations are quite high on some occasions along the Yukon coast, where large quantities of fine sediment are available to the littoral transport system (Figure 103B). The distinction between wash load and bed material load (cf. section 4.1.2; Einstein et al., 1940) may be important also in the littoral environment, particularly near rivers and lagoon inlets. In Mackenzie Bay, suspended sediment of the Mackenzie River plume constitutes a wash load in the littoral transport system when it is advected westward along the Yukon coast (Figure 104). Furthermore, fine sediment entrained by surf along the coast southeast of Kay Point may be dispersed widely across the nearshore zone after refraction around Kay Point (Figure 105); west of the point, then, it may constitute a wash load with respect to local littoral transport along Kay Point spit.

Bagnold (1956, 1963, 1966) has developed an energetics model of bedload sediment transport in which the immersed weight transport rate is linearly related to the total energy expenditure due to boundary resistance (equation 4.1.2-8). Where the power is provided by surface gravity waves with energy flux per unit crest length equal to

$$P = ECn = (\rho g H^2 Cn)/8, \qquad (4.2.2\text{-}1)$$

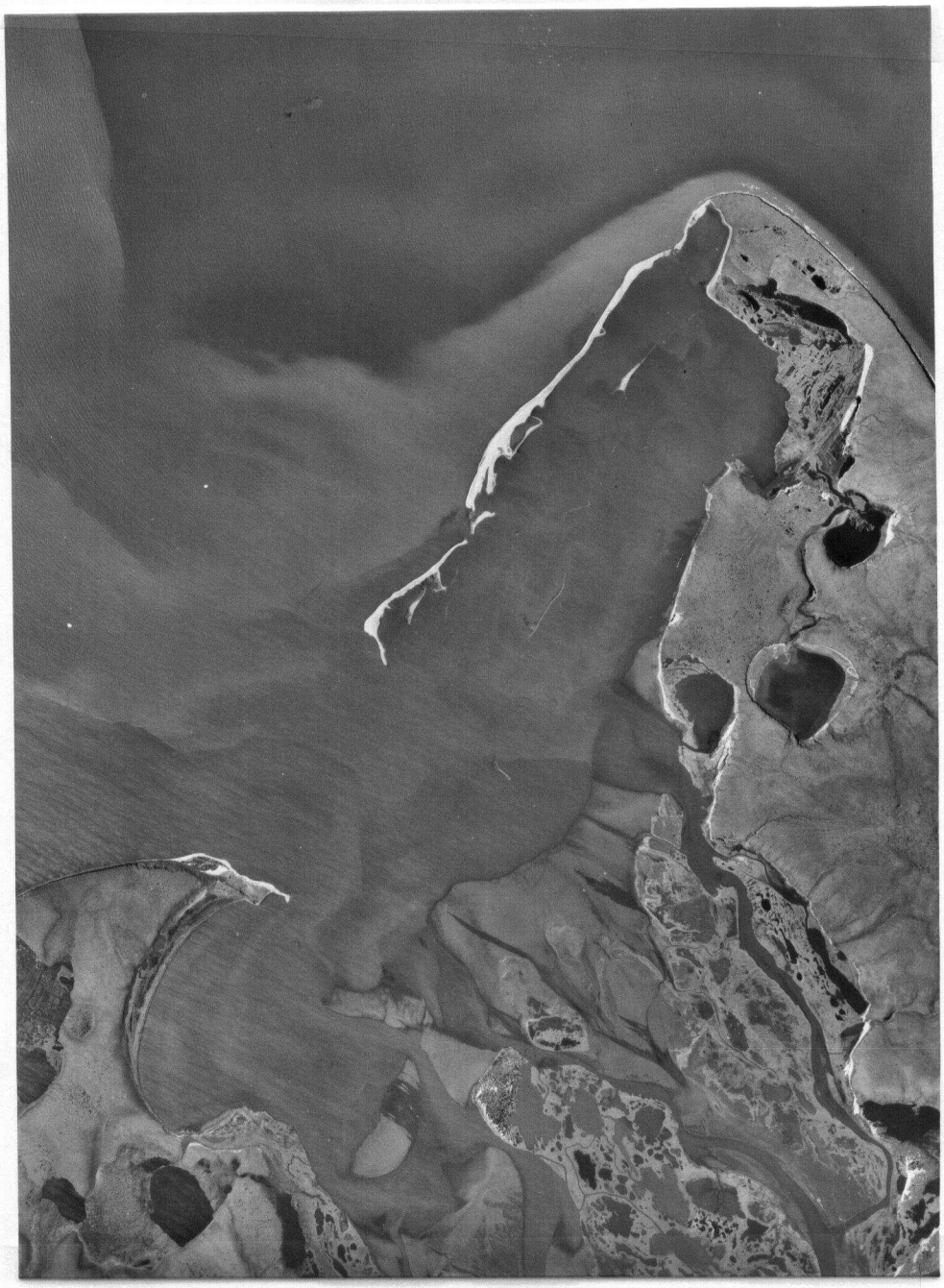

FIGURE 105

Vertical photograph of Kay Point and Babbage Estuary, showing longshore transport of suspended sediment westward past Kay Point and wide shore-normal dispersion in Phillips Bay; part of NAPL photograph A22975-56, 4 August 1972.

the rate of energy dissipation per unit area is given by

$$p = d(ECn)/dx. \qquad (4.2.2\text{-}2)$$

The total immersed weight transport per unit width may be expressed as

$$\begin{aligned} i &= i_B + i_s \\ &= p\{[e_B/(\tan\phi - \tan B)] + [e_s(1-e_B)/(W_s/\bar{U}_s - \tan B)]\} \\ &= pK \end{aligned} \qquad (4.2.2\text{-}3)$$

where $i_s$ is the unit-width immersed-weight suspended load, $e_s$ is the corresponding efficiency factor, $W_s$ is the settling speed of the sediment in still water, $\bar{U}_s$ is the mean transport speed of suspended sediment, and K is a dimensionless coefficient (Bagnold, 1963, p.517). The coefficient K is believed to reach a maximum value that is constant for a given system, a hypothesis supported by aeolian and fluvial transport data (e.g. Bagnold, 1941, pp.105-106; Bagnold, 1973; Leopold and Emmett, 1976).

In the case of sediment entrained by an oscillatory wave motion, Bagnold (1963, p.518) argued that the immersed weight of sediment supported over unit bed area would be $i/\bar{U}_s$, where $\bar{U}_s$ is the mean velocity of the oscillatory sediment motion, and further that once entrained the sediment would be transported in any direction $\theta$ by a prevailing current $u_\theta$ [empirical corroboration of this hypothesis has been reported by Komar and Inman (1970) and by Lesht et al. (1979)]. By this line of reasoning, the unit width immersed weight transport rate is given by

$$i_\theta = K\, p\, u_\theta/u_0 \qquad (4.2.2\text{-}4)$$

where $u_0$ is the horizontal orbital velocity taken at the same distance above the bed as $u_\theta$ and it is assumed that the ratio of sediment velocities is approximately equivalent to the ratio of corresponding water velocities ($U_\theta/U_0 \simeq u_\theta/u_0$).

Considering for the moment only the longshore transport, where $u_\theta = u_t$, tangential to the shore in the breaker zone, Komar and Inman (1970) have demonstrated the empirical relation

$$I_t = 0.77\ P'_t \qquad (4.2.2\text{-}5)$$

or

$$J_t = 0.77 P'_t [\rho_s/(\rho_s - \rho_w)g] \qquad (4.2.2\text{-}6)$$

where $P'_t = (ECn)_b \cos\alpha_b \sin\alpha_b$ is the shore-tangent component of incident wave power per unit length of beach ($P'_t = P_t \cos\alpha_b$; cf. section 2.3.4). This relation is also supported by results of Watts (1953), Caldwell (1956), and Knoth and Nummedal (1977). The quantity $(ECn)_b \cos\alpha_b$ represents the total incident power per unit length of beach. If it is assumed that this power is entirely dissipated in the surf zone, then equation 4.2.2-5 may be viewed as an integration of equation 4.2.2-3 across the width of transport. The coefficient incorporates an index of the proportion of total power dissipated by boundary resistance (cf. Inman and Bagnold, 1963, p.546). Equation 4.2.2-6 has been used in conjunction with the wave hindcast data described earlier (section 2.3.4) to compute approximate sediment transport rates along Kay Point spit and on the Niakolik Point shore.

In principle, the transport model (equation 4.2.2-4) should be applicable to the onshore sediment transport, in view

of the onshore mean transport velocity, $\bar{u}_n$, observed by Bagnold (1940). Unfortunately, the existing theory describing $\bar{u}_n$ (Longuet-Higgins, 1953; Longuet-Higgins in Russell and Osorio, 1958) is inapplicable when dispersed sediment is present (Bagnold, 1963, p.524) and, indeed, in the case of a very rough fixed boundary (Bijker et al., 1974). Furthermore, Inman and Bowen (1963) have demonstrated that a relatively small mean current superimposed on a wave motion over a rippled bed may reduce the symmetry of the system sufficiently to cause phase-dependent effects associated with periodic sediment suspension bursts to dominate the transport process, such that K becomes small and variable. In the wave-dominated environment, transport of sufficiently fine sediment may be fully developed within the breaker zone, but is apparently not so over rippled surfaces further seaward.

The physical system is further complicated when an onshore wind drift occurs at the surface, balanced by an offshore return flow at depth. In addition, there is now evidence to support the concept of Cornish (1898) that shore-normal sediment transport is significantly influenced by velocity asymmetry associated with harmonics of the fundamental wave motion (see Bowen, 1980b). The foregoing complications must be addressed in the application of any transport model (e.g. Kalkanis, 1964; Einstein, 1972; Madsen and Grant, 1976) and it is concluded that shore-normal sediment transport cannot at present be determined reliably other than as a residual in the littoral sediment budget. The shore-normal transport

problem remains one of the major outstanding issues in the field of sediment transport mechanics (Bowen, 1980a).

Figure 105 provides an instructive illustration of refraction effects and of the potential magnitude of the wash load in the littoral transport system at Kay Point. The deepwater wavelength can be estimated from the photograph and from this one can compute an estimate of the period $T=(2\pi\lambda_o/g)^{1/2} \simeq 4.2$ s. Assuming that the waves were fetch-limited by the coast at about 100 km, the SMB hindcast waveheight is $H \simeq 1.1$ m. The refraction coefficient for breaking waves along coastal segment 1 east of Kay Point is $K_r=0.6$ and the breaker angle is approximately 40°. Assuming realistic values for the beach slope and water density, the longshore transport rate can be estimated using equation 4.2.2-6 as $J_t \simeq 5\times10^{1}$ kg/s. Along the proximal spit shore, $K_r=0.2$ and the breaker angle is about 55°, yielding an estimate $J_t \simeq 5\times10^{0}$ kg/s. If 50 per cent of the littoral transport arriving at Kay Point was silt and clay remaining in suspension off the proximal spit, then the total transport unaccounted for off that part of the coast is roughly five times greater than the computed transport. A portion of this fine sediment may be input to the estuary; however, for present purposes it has been assumed that most washload sediment is dispersed offshore and contributions from this source to the estuary have been neglected. Inasmuch as the computed sediment inputs are overwhelmingly concentrated during northwesterly wave events, this assumption is not thought to be a significant cause of

bias.

Computed values of daily longshore transport at the distal end of Kay Point spit (positive toward the entrance section M1) are plotted in Figure 106. This shows the major importance of northwesterly waves (indicated by the vertical bars), the consistently positive sign of the transport, the extreme synoptic- and seasonal-scale variance, and the general character of year-to-year variability. Computations were also carried out for proximal spit and Niakolik shore sites, using 1976 hindcast data; the summary results of these computations as they relate to estimates of the total sediment supply, are given in the following section.

Along barrier coasts, significant quantities of sediment may be moved into lagoons by washover transport (cf. Andrews, 1970; Hayes, 1975; Schwartz, 1975; Bartberger, 1976; Leatherman, 1976), especially where the barrier is narrow and there are no dunes obstructing flow. Washover processes are important in the maintenance of barrier width during marine transgression, such as has occurred at Kay Point spit in recent time (cf. section 2.1.2).

The backshore surface of the Kay Point spit exhibits a distinct shore-normal lineation resulting from washover transport, although major washover lobes are absent. Extensive washover flows are not common; laterally restricted washover channels occasionally develop during moderate storm surges, as at Kay Point during the surge of 9-10 August 1975 (Lewis and

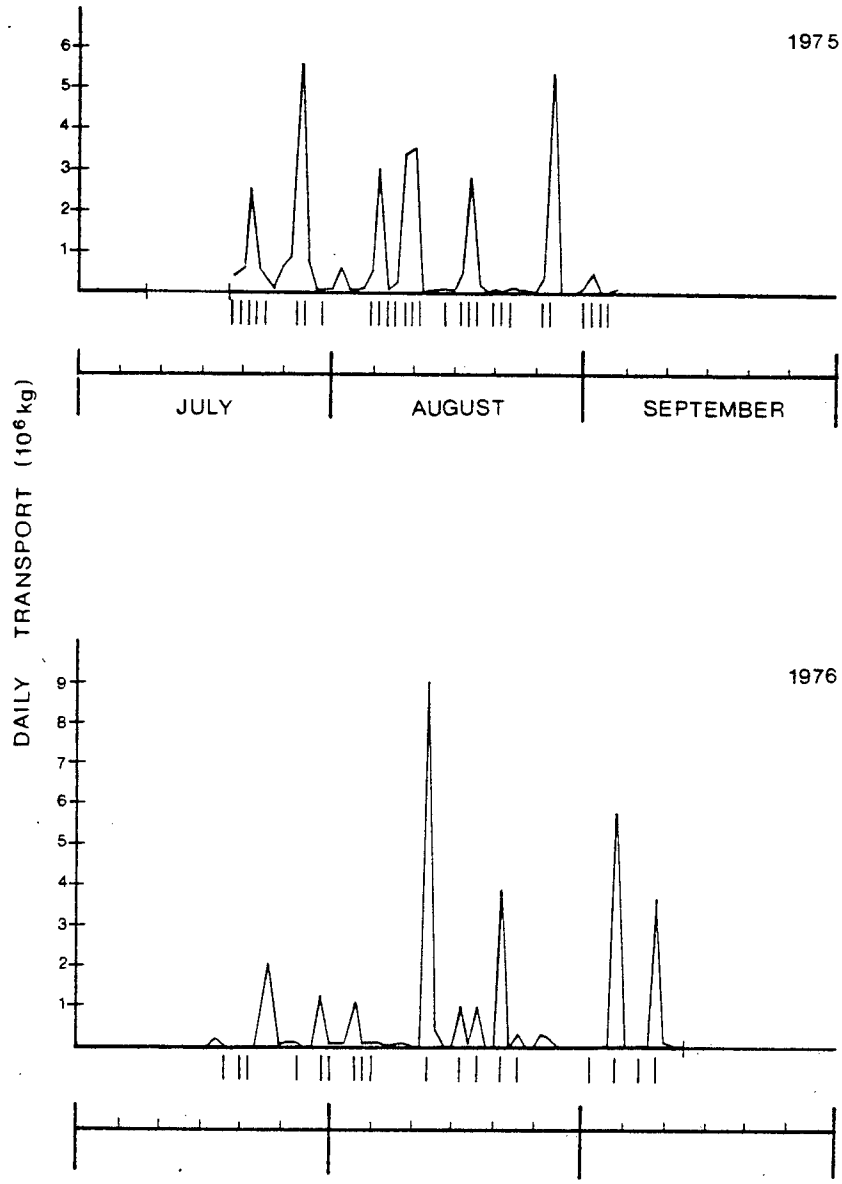


FIGURE 106

Daily longshore sediment transport at distal end of Kay Point spit, positive toward the main entrance section (M1), computed from hindcast wave data using equation 4.2.2-6; breaks in wind record during open-water conditions are indicated by lighter line in horizontal axis; note association between northwesterly wind events (indicated by vertical bars) and the major sediment transport occurrences.

Forbes, 1975, p.57). Storm channels of this kind, if scoured deeply enough, may remain after the surge has abated as temporary or quasi-permanent tidal inlets. The inlet illustrated in Figure 107 developed sometime before the exceptional storm of September 1970, which occurred less than one month after the photograph was taken. At the time it was photographed, this inlet was providing access to the lagoon for suspended sediment moving alongshore past Kay Point. The presence of the inlet may have altered the parameters of the estuarine system sufficiently to change its response to a major storm. The change may have involved, for example, higher rates of sedimentation in the north end of the lagoon than would otherwise have occurred (cf. response to small events in the absence of inlet M3, section 4.3.2 below). It is not known to what extent the development of washover channels across Kay Point spit is limited by the frozen substrate; this represents an additional potentially significant factor in the development of high-latitude barrier systems.

Because of the highly episodic nature of washover transport, an assessment of the magnitude of this input component is difficult to achieve. A rough estimate may be based on the mean 41-m transgressive migration of the barrier backshore into the lagoon during the interval 1952-1970 (measurements taken from photomosaic at 1:25000 scale). If a nominal thickness of 1 m is adopted in the computation, an annual volume of $1 \times 10^4$ $m^3$ is obtained; this corresponds to about $1.6 \times 10^7$ kg $a^{-1}$.

FIGURE 107

Proximal end of Kay Point spit, showing temporary (M3) inlet; part of NAPL photograph A21830-2, 18 August 1970.

Tidal currents are a major cause of sediment transport in many barrier inlet settings and undoubtedly generate some sediment inputs to the Babbage Estuary system through inlets M1 and M2. However, an estimate of the magnitude of the tidal transport has not been attempted, in part because the available data are quite inadequate for the purpose; in part because velocity data for station 5 suggest that threshold conditions, in the absence of waves, are rarely exceeded (cf. section 4.3.1). The entrance bathymetry (Figure 3) shows no evidence of the distinctive tide-generated features described from mesotidal and from some microtidal systems elsewhere (e.g. by Hayes, 1975; Reinson, 1977; Boothroyd, 1978; Owens and McCann, 1980) and it is judged that the error involved in neglecting tidal transport is small under most conditions.

### 4.2.3 TOTAL MARINE SEDIMENT INPUT

Longshore sediment transport totals were computed using equation 4.2.2-6 for individual hindcast wave events at the sites indicated in Figure 26; transport at all sites was defined positive toward the southwest. The results, presented as monthly totals in Table 22, indicate a total transport at the distal end of Kay Point spit (K2) amounting to approximately $3.6 \times 10^7$ kg for the period 19 July to 4 September 1975 (83 per cent of the open-water season) and about $3.4 \times 10^7$ kg for the same interval in 1976 (less than 70 per cent of the open-water season). Given the uncertainties in the computation procedure, these results are not significantly different. The annual input of clastic sediment from coastal and offshore sources is estimated to have been less than $5 \times 10^7$ kg in each year. This is somewhat greater than the long-term mean value for barrier washover transport (undoubtedly highly variable from year to year) estimated in the preceding section, very approximately, at $2 \times 10^7$ kg $a^{-1}$.

Ebb-tide currents, rip currents, and wind-drift return flow represent three mechanisms whereby sediment arriving at the Babbage Estuary entrance may be diverted offshore. In the absence of reliable procedures for the computation of shore-normal transport and of transport in combined wind-current systems, however, the results in Table 22 provide the best available estimates of the order of magnitude of marine sediment supply to the estuarine system. It is noteworthy that the estimated total sediment input across the

TABLE 22

Summary of net wave-generated longshore sediment transport for proximal and distal Kay Point spit and for site west of Niakolik Point, 1975-1976.

Note extreme seasonal structure due to ice effects.
K1: proximal end of Kay Point spit
K2: distal end of Kay Point spit [see Figure 26]
N1: foreshore west of Niakolik Point

Total longshore transport computed using equation 4.2.2-6 and hindcast wave data; transport positive toward the southwest (toward M1 section at K1 and K2; away from M1 section at N1).

| month | days miss[1] | o-w miss[2] | total transport in units of $10^6$ kg | | |
|---|---|---|---|---|---|
| | | | K1 | K2 | N1 |
| Jan 1975 | 31 | 0 | 0. | 0. | 0. |
| Feb | 28 | 0 | 0. | 0. | 0. |
| Mar | 31 | 0 | 0. | 0. | 0. |
| Apr | 30 | 0 | 0. | 0. | 0. |
| May | 31 | 0 | 0. | 0. | 0. |
| Jun | 30 | 0 | 0. | 0. | 0. |
| Jul | 18 | 10 | | >13.1 | |
| Aug | 0 | 0 | | 21.8 | |
| Sep | 26 | 0 | | 0.77 | |
| Oct | 31 | 0 | 0. | 0. | 0. |
| Nov | 30 | 0 | 0. | 0. | 0. |
| Dec | 31 | 0 | 0. | 0. | 0. |
| Jan 1976 | 31 | 0 | 0. | 0. | 0. |
| Feb | 29 | 0 | 0. | 0. | 0. |
| Mar | 31 | 0 | 0. | 0. | 0. |
| Apr | 30 | 0 | 0. | 0. | 0. |
| May | 31 | 0 | 0. | 0. | 0. |
| Jun | 30 | 0 | 0. | 0. | 0. |
| Jul | 15 | 0 | 1.78 | 4.68 | 0.23 |
| Aug | 0 | 0 | 7.30 | 18.8 | -2.93 |
| Sep | 18 | 18 | >1.48 | >10.0 | (-1.29)[3] |
| Oct | 31 | 8 | >0. | > 0. | |
| Nov | 30 | 0 | 0. | 0. | 0. |
| Dec | 31 | 0 | 0. | 0. | 0. |
| 1975 | | | | > 35.9 | |
| 1976 | | | >10.6 | > 33.5 | (-3.99)[3] |

1 number of days missing from hindcast wave record
2 number of days with open-water missing from record
3 net total for period of record

marine boundary is an order of magnitude less than the fluvial sediment yield (Tables 19 and 20). Note also that the marine inputs are highly seasonal and that fluvial and marine input processes are maximized at different times of the year.

A final point on the subject of sediment sources concerns the potential contribution from offshore sites. The transport total computed for the distal spit location was about three times greater than the total computed for the proximal spit. If this difference is significant, continuity suggests that the additional sediment at the distal site must have been derived from the estuary via inlet M2, from the spit shoreface, or from seaward of the surf zone. Supply through M2 can probably be neglected. The second source would require a mean loss of about 3.3 $m^3/m$ of shoreface along the length of the spit, assuming a dry bulk density of 1590 kg $m^{-3}$ (Terzaghi and Peck, 1967, p.28). Taking account also of uncertainties concerning the potential role of rip currents, the data provide no unequivocal evidence for net onshore transport of sediment along Kay Point spit.

## 4.3 SYSTEM RESPONSE

### 4.3.1 SEDIMENT TRANSFERS WITHIN THE ESTUARY

Sediment transportation in a subaqueous environment is fundamentally controlled by local instantaneous hydrodynamic conditions and by fixed properties of the sediment. The resulting sediment dispersal patterns depend upon the integration of this process, which includes lag and relaxation effects (Postma, 1954; Allen, 1974) over the transport path of the sediment. A distinctive set of attributes of the estuarine environment infuences the larger-scale dispersal of sediment in estuarine systems. These phenomena include: (1) tidal asymmetry; (2) temporal variability of mean depth; (3) erosional and depositional lags; (4) rotation and horizontal segregation of tidal currents; (5) net non-tidal circulation in the estuary; (6) wind-generated waves; (7) seasonally and synoptically variable rates of estuarine flushing; (8) temporal variability of density and viscosity; (9) changes in the nature of the sediment itself, due to agglomeration by flocculation, by filter-feeding organisms, or by other processes; and (10) reworking and binding of bottom sediments by benthic organisms. In Arctic estuaries and in many mid-latitude systems, ice is an additional factor. The following discussion emphasizes phenomena investigated in the Babbage Estuary and considered particularly relevant to the sedimentation process in that system.

Surface gravity waves can cause resuspension of bottom sediment in estuaries and tidal flats (Anderson, 1971, 1976;

Collins and Amos, 1973), may inhibit mud deposition and limit the vertical growth of intertidal surfaces (Postma, 1961, p.184), and may supply major quantities of sand to the estuary by longshore transport to inlets and by barrier washover (cf. section 4.2.2). There is evidence to suggest that resuspension of bottom sediments in the Babbage Lagoon may be an important feature of the system storm response, while erosion of the distal delta margin is occurring at some sites (see section 4.3.2). Inner-lagoon beach and washover facies are an important feature of lagoon-margin deposits in the Babbage Estuary (see section 4.4.5).

Stillwater settling velocities, both of muds settling according to Stokes (1851) and of sands, which may follow the relation proposed by Gibbs et al. (1971), depend upon the density and viscosity of the fluid, which can exhibit pronounced seasonal- and synoptic-scale fluctuations (section 3.3.4). The time series of Stokes settling speed

$$W_s = gD^2(\rho_s - \rho_w)/18\eta \qquad (4.3.1\text{-}1)$$

computed from daily data for station 7, Babbage Estuary (1976), shows the magnitude of the seasonal variability in $W_s$ (Figure 108). The settling speed computed for D = 1 $\mu$m ranged from a minimum of $5.0 \times 10^{-7}$ m $s^{-1}$ on 7 June to a maximum of $8.3 \times 10^{-7}$ m $s^{-1}$ on 21 July, an increase of 66 per cent. However, the true settling speed may be much greater than equation 4.3.1-1 suggests, due to turbulent effects or to particle agglomeration.

The settling velocity of a given sedimentary particle may

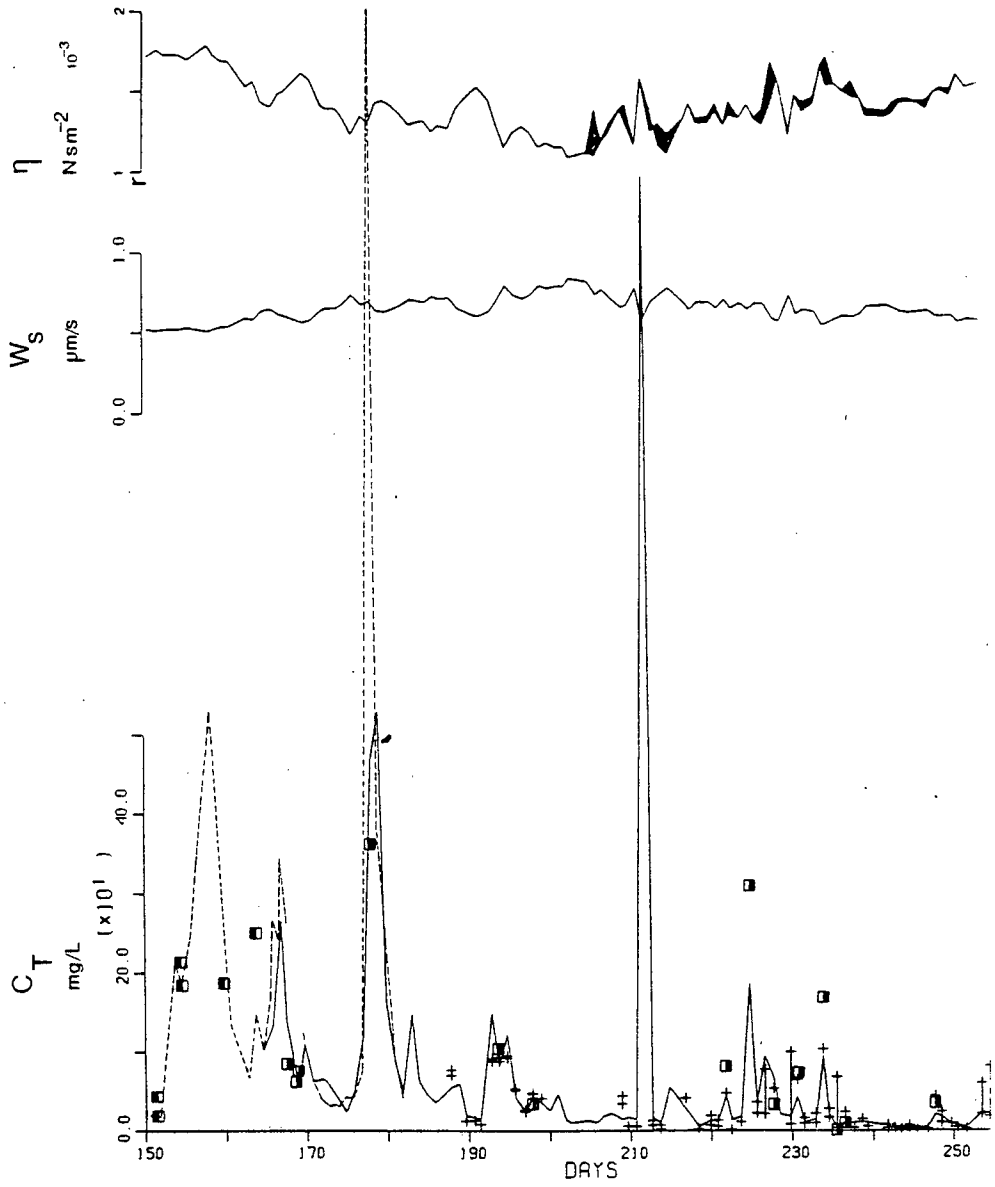


FIGURE 108

Viscosity, Stokes settling velocity for D=1 μm, and total suspended solids concentration at stations 7 and 7a, Babbage Estuary, 1976. Boxes represent sample TSS values, crosses represent estimates based on transmissometer beam attenuation, and linesrepresent estimated concentration, $C_T$, based on Secchi extinction depth.

be a function, not only of the fluid properties, but also of the agglomeration history of the particle since entering the estuary (Einstein and Krone, 1962; Schubel and Kana, 1971; Zabawa, 1978), if not before (Nelson, 1959). Agglomeration processes in an estuary may include electrochemical flocculation (Glangeaud, 1938; van Straaten and Kuenen, 1957; Schultz and Simmons, 1957), coagulation (Black et al., 1965; Chang and Anderson, 1968), production of fecal and psuedo-fecal pellets by filter-feeding organisms (Moore, 1931; Verwey, 1952), and agglomeration by diatoms (Brockmann, 1935) or by microfloral secretions (Paerl, 1973). The relative importance of the various agglomeration phenomena remains very poorly known; it may be expected to vary geographically and temporally, but there appear to be no data adequately documenting such variability. It may be important because the ratio $W_a/W_s$, where $W_a$ is the settling velocity of the agglomerate and $W_s$ the settling velocity of individual mineral particles within it, may be relatively high for pellets ($W_a/W_s >> 1$) and very much lower for inorganic agglomerates ($W_a/W_s \tilde{} 1$) (Sherman, 1953; Smayda, 1969; Zabawa, 1978).

Biogenic reworking of estuarine bottom sediments is an important process that results, not only in the production of distinctive, often abundant, sedimentary structures (e.g. van Straaten, 1952; Evans, 1965), but also in destabilization of the sediments, increasing the probability of resuspension (Rhoads, 1971; Yingst and Rhoads, 1978). On the other hand, stabilization by microfloral mucus or algal mats

may play an important seasonally-variable role, while various plant species may enhance sedimentation rates by their effects on the local hydrodynamic environment (Ginsburg and Lowenstam). Superficial reworking of muds by amphipods and isopods has been observed in the Babbage Lagoon during the present study. Sampling by Kendel et al. (1975) indicated that the abundance of amphipods may exceed 2000 $m^{-2}$ (see section 4.4.5). However, in contrast to many lower-latitude systems, there is a relative scarcity of mollusks; only two species are known from the lagoon (Kendel et al., 1975), while none has been observed in the intertidal zone. Algal mats develop in summer on ephemeral pond muds of the deltaic and marginal supratidal flats, but are not thought to play a major role in the sedimentary process. This contrasts with results in temperate regions (cf. Kellerhals and Murray, 1969; Frostick and McCave, 1979).

The nature of agglomeration in Babbage Estuary sediments was examined using scanning electron microscope imagery and settling velocity experiments. Bottom sediment from the northern lagoon basin (site 021125; see Figures 5 and 6 for reference grid) included angular and subangular silt particles (Figure 109A) and a variety of clay agglomerates of silt size, in both pellet and relatively amorphous forms (Figure 109B, 109C, 109D). In some cases, clay-size plates were attached to pellet-like particles in an angular configuration (Figure 109C). Bottom material from site 010140 (Figure 110) showed similar pellet-like composite particles in addition to open agglomerates of the sort associated with flocculation

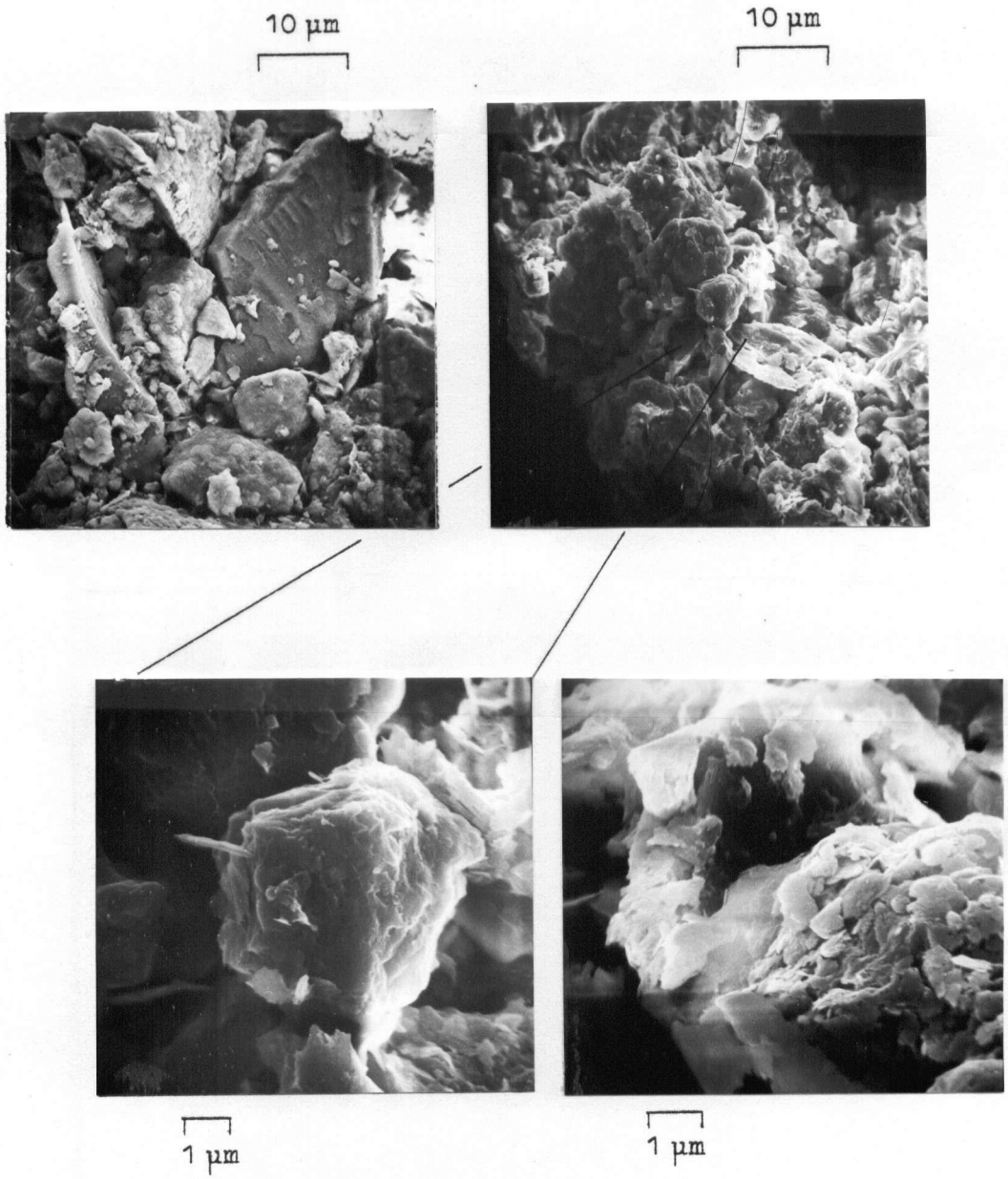


FIGURE 109

Scanning electron micrographs of sediment from the Babbage Estuary (site 021125), showing silt- and clay-size mineral particles and various composite particles of silt size.

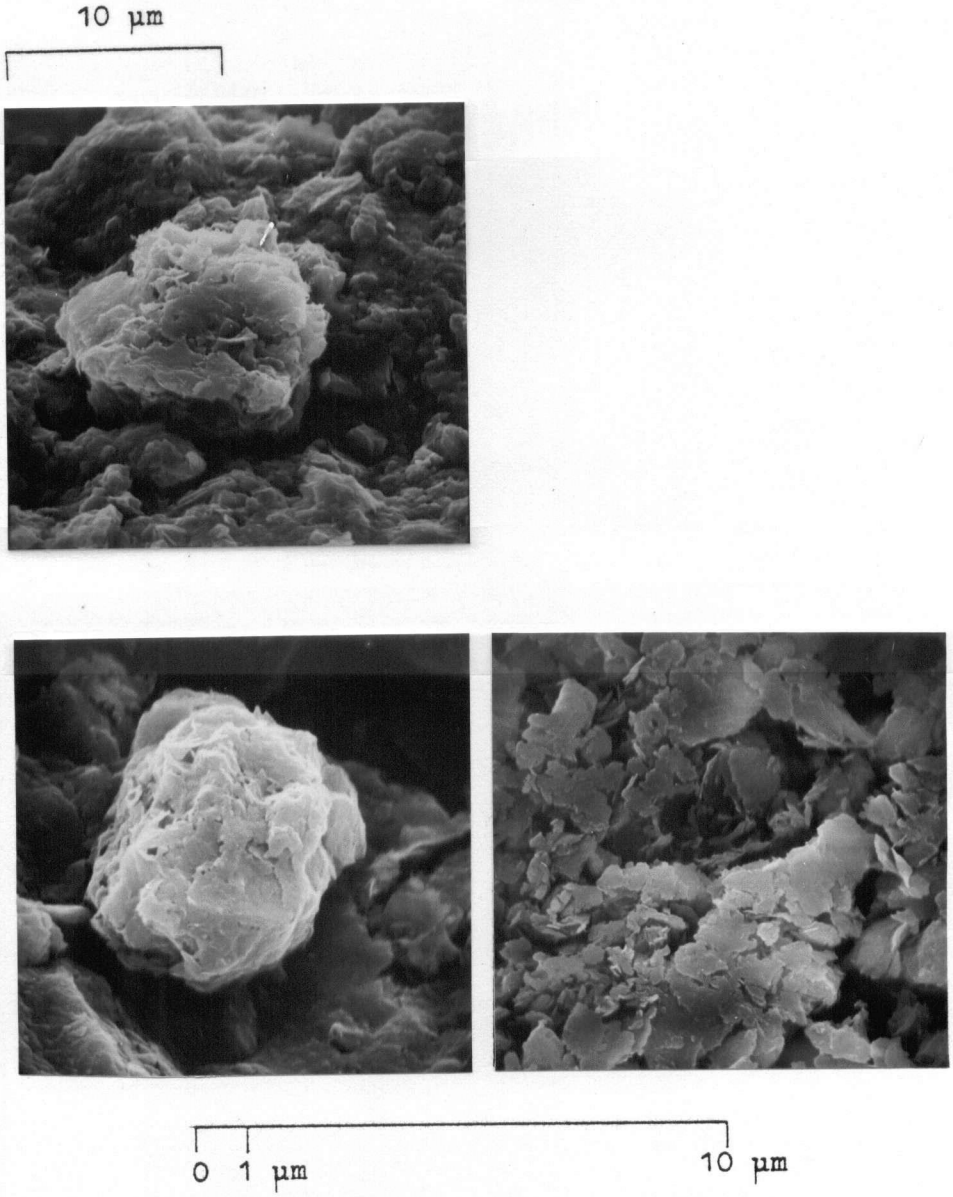


FIGURE 110

Scanning electron micrographs of sediment from the Babbage Estuary (site 010140), showing both pelletized and angular forms of agglomeration.

processes. The pellets were more common in bottom sediment; the open agglomerates in materials collected from sediment traps at the site. It may be, therefore, that biogenic pelletization occurs primarily on the bottom and is not a major factor in initial sedimentation; the settling velocity should, however, be higher in later resuspension events. Also it is not clear to what extent the open agglomerates observed in bottom sediments reflect flocculation processes in the water column, inasmuch as flocculation requires collisions between particles in suspension. The probability of collisions is relatively low at the concentrations usually prevailing in the Babbage Estuary (cf. Einstein and Krone, 1962) but increases rapidly with increasing concentration very close to the bottom.

Experiments were conducted with sediment from site 010140 to examine the effects of disaggregation and of salinity on the particle size distribution. Replicate analyses, after disaggregation with sodium metaphosphate solution, of materials collected in sediment traps at 010140 during the intervals 8-14 and 14-25 August 1976 yielded median equivalent diameters in the ranges $5.5<D_{50}<6.2$ μm and $3.0<D_{50}<3.4$ μm respectively (Figure 111). Eight subsamples of bottom sediment, treated in various ways, all including use of the disaggregating agent, yielded median values in the range $6.3\leq D_{50}\leq 12.1$ μm. In contrast, three subsamples which were maintained wet, not treated with sodium metaphosphate, and sedimented in NaCl solutions ranging in concentration from 8 to 20ppt, yielded median values $15<D_{50}<17$ μm and were much better sorted than the

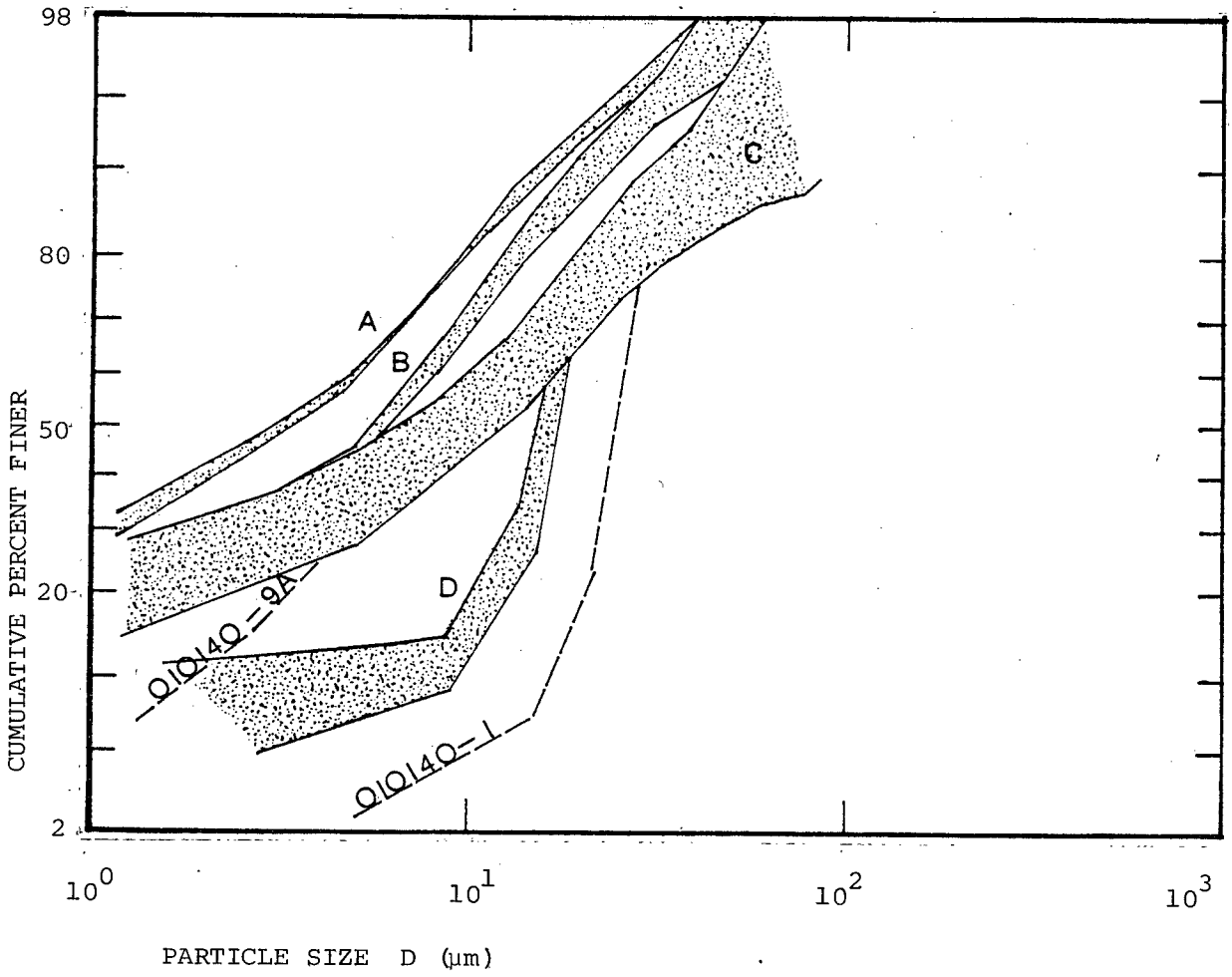


FIGURE 111

Particle-size distributions for bottom sediment and for suspended sediment collected in traps at site 010140, Babbage Lagoon, showing effects of various treatments. A and B: sediment pan samples, disaggregated; C: bottom samples, disaggregated; D: bottom samples, not disaggregated, sedimented in NaCl solution $8 \leq s \leq 20$ ppt; 010140-1: bottom sample, not disaggregated, sedimented in Babbage Estuary water; 010140-9A: same, but sedimented in distilled water.

disaggregated materials (Figure 111). Another subsample (010140-1), maintained wet, not dispersed, and sedimented in a solution of Babbage Estuary water diluted with distilled water to give a salinity of 8ppt, yielded $D_{50}$=24 μm; subsample 010140-9A, treated identically, but sedimented in distilled water, yielded a distribution within the envelope of treatments using sodium hexametaphosphate, except for a slight deficiency of fines in the range D<4 μm. The latter result suggests a deflocculation process.

The net non-tidal circulation is among the most important parameters of the sedimentary subsystem in many estuaries. In highly-stratified systems, the mean flow is commonly directed upstream within a lower layer near the bed; the landward limit of the salt wedge may be a locus of rapid shoaling (Simmons, 1966). In partially-mixed estuaries with convectional circulation, enhanced landward net flow in the lower layer is recognized as a major cause of turbidity maxima (Postma and Kalle, 1955; Nichols and Poor, 1967; Schubel, 1968; Meade, 1969). Where circulation regimes of this kind occur, maximum shoaling rates may be observed between the high- and low-tide limits of the salinity intrusion (cf. Simmons, 1955; Harleman and Ippen, 1967).

Although gravitational convection plays a part in the late-summer circulation of the Babbage Estuary (cf. section 3.3.5), it is thought to be of relatively minor importance in the sediment transport process. The extreme relief of the thalweg profile in the main distributary of the delta was

documented in Figure 70, where entrapment of dense water within the pools was illustrated. The shallow depths over the shoals between pools tend to inhibit development of an integrated convectional circulation system (see section 3.3.5). A similar situation existed in the Savannah River (eastern U.S.A.) prior to dredging of a ship channel; sedimentation became a significant problem there only after deepening of the shallower sections allowed establishment of an effective upstream residual flow in the bottom layer (Simmons, 1965).

Tidal asymmetry, or asymmetry in the time series of the horizontal current U over a tidal cycle (Postma, 1961, 1967), in concert with settling and scour lags (van Straaten and Kuenen, 1958), tends to promote net landward transport of certain size fractions of sediment on intertidal flats and in shallow flood channels. It may involve different phase shifts in flood and ebb components, inequality of flood and ebb velocity amplitudes, or both. In natural estuaries, frictional effects and the three-dimensional morphology, which often includes extensive intertidal surfaces and a network of subtidal channels, produce further modifications resulting in part from differences in mean depth and cross-sectional area at low and high tide. Tidal flows are commonly segregated horizontally into flood- and ebb-dominated channels (van Veen, 1950; van Straaten, 1960; Price, 1963). This phenomenon plays a major role in the evolution of tidal delta deposits, which are best developed in mesotidal inlets (Hayes, 1975; Hine, 1975; Boothroyd, 1978) but occur in some microtidal systems as

well (Reinson, 1977; Owens and McCann, 1980).

Echo-sounding records from the main distributary channel reveal little evidence of upstream sand transport. The data set includes five long-profiles, two of which were supplemented by side-scan sonar records, and a large number of cross-profiles, obtained at various times in late summer, in addition to extensive profiling carried out earlier in the season when a flood-dominated bottom layer would not be expected to occur. The late-summer profiles were all obtained during flooding tide. Ebb-dominated bedforms indicative of seaward sand transport were abundant in these records in both shallow and deep sections of the channel (Figure 112A). Well-developed flood-directed bedforms were observed only once (Figure 112B) in a single short reach downstream from station 10 (see Figure 2 for station locations). Although quasi-symmetrical bedforms, dunes slightly modified by flood-directed transport, and rare flood-oriented features were occasionally present in the sounding records, headward residual sand transport does not seem to be important within the deeper parts of the main distributary channel. Upstream transport does occur on intertidal channel-margin surfaces, as evidenced by the presence of flood-directed ripples and dunes on numerous occasions. Sediment can be moved upstream by these processes only limited distances, however, due to the longitudinal discontinuity of lateral bars (see Figure 5).

In many estuaries, suspended sediment accumulates (near the limit of salinity intrusion, in reaches of channel

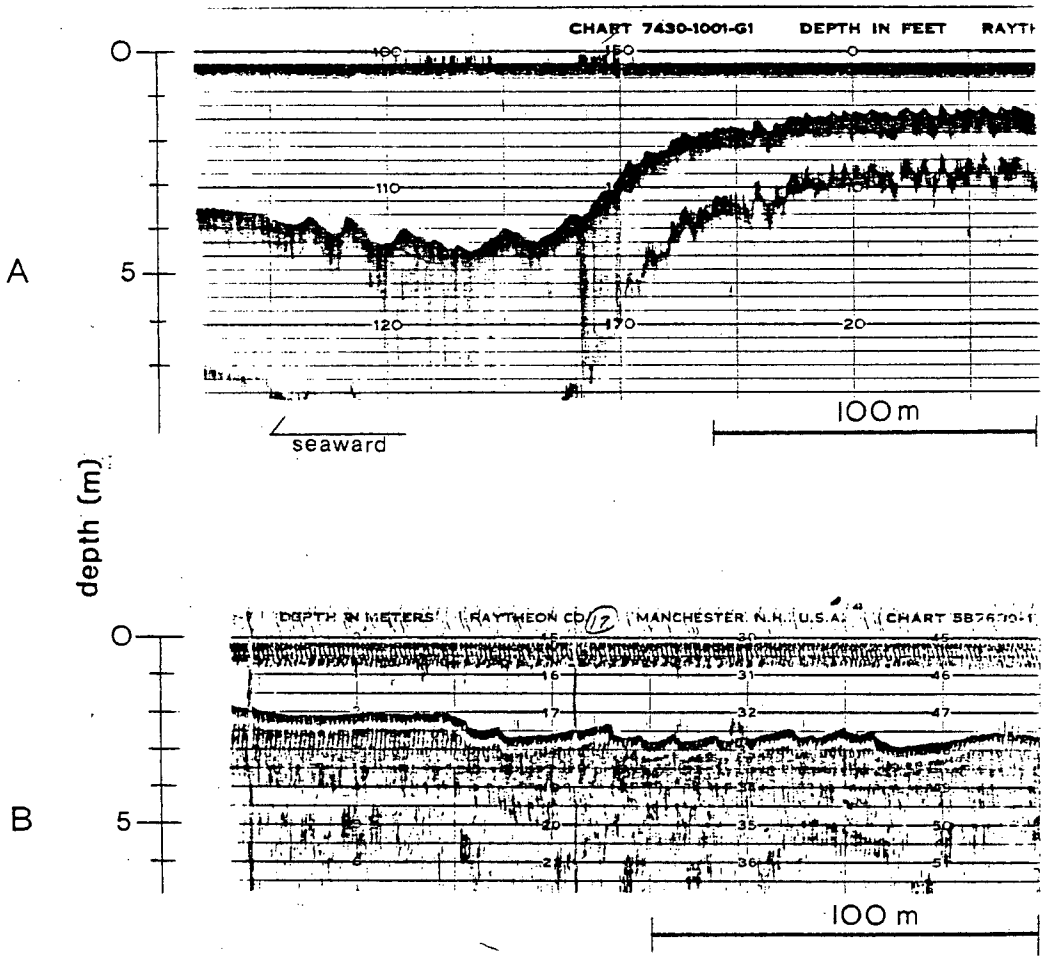


FIGURE 112

Longitudinal thalweg profiles in the main distributary channel of the Babbage Delta, showing (A) predominance of ebb-directed transport and (B) rare occurrence of flood-directed bedforms downstream from station 10.

expansion, or elsewhere) in the form of 'fluid mud', a suspension of very high concentration exceeding $10^4$ mg/L (Inglis and Allen, 1957; Allersma et al., 1966; Einstein and Krone, 1961; Kirby and Parker, 1977). The relative importance of flocculation and of hydrodynamic processes for the production of fluid mud, and the role of feedback between increasing concentration and the turbulent structure of the lower boundary layer (cf. Ippen, 1966, p.667), remain largely unexplored topics. None of the sounding records from the main distributary of the Babbage Delta showed the planar or slightly undulating reflections produced by fluid mud horizons in other estuaries (cf. Kirby and Parker, 1977, p.114). However, re-examination of 1975 cross-profiles obtained in Deep Creek has revealed reflectors in two sections, 1500 and 1750 m upstream from the first distributary bifurcation, which suggest the presence of fluid mud (Figure 113). Although the reach in question is upstream of the usual limit of salinity intrusion in the main distributary channel, runoff had been unusually low for some time prior of the date of sounding in Deep Creek and salinities as high as 15ppt were observed at station 13 eight days before. One may speculate that salt and perhaps also sediment were moved headward through the delta into Deep Creek in the lower layer of a convectional circulation regime; alternatively, the sediment may have been derived from unstable subaqueous slopes within the reach or directly from upstream.

Suspended sediment concentrations were observed in 1976 at station 12 ($h \simeq 5$ m), by sampling at irregular intervals (see

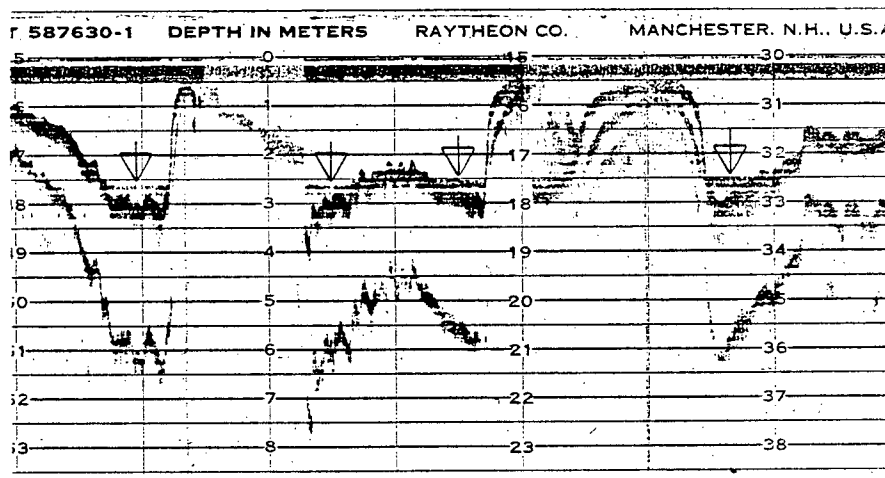


FIGURE 113

Horizontal reflectors in cross-sections of lower Deep Creek channel, suggesting presence of fluid-mud.

Appendix A.10), by daily observations of light attenuation using Secchi disks and a Hydroproducts 0.10-m pathlength beam transmissometer (see Appendix A.11 for data), and by continuous recording of light attenuation in the upper part of the flow, using an Interocean 0.10-m pathlength beam transmissometer (see Appendix A.8 for Secchi and transmissometer calibrations). The time sequence of near-surface TSS concentration, $C_T$, and other relevant variables are presented in Figure 114. The station-12 data reveal no occurrences of dense near-bottom suspensions. Between synoptic-scale transient increases in concentration, the observations indicate background values of $C_T$ of order 10 mg/L or less, with typical vertical concentration gradients less than 1 mg $L^{-1}m^{-1}$.

The time sequence of $C_T$ (Figure 114) emphasizes once again the importance of seasonal- and synoptic-scale variance in the Babbage Estuary. At this location in the system, the suspended sediment process in 1976 was dominated by delivery from the Babbage River basin, characterized by negligible variance at diurnal or shorter periods. With one exception, all major peaks in the 1976 $C_T$ series for station 12 can be related to runoff events in the Babbage River. There is some evidence of entrainment by waves during northwesterly winds on 12 August (short-lived transient preceding large event in second half of record, Figure 114) and on 21 August, when a minor surge occurred and wave and runoff effects were superimposed. Nevertheless, fluvial inputs clearly predominated at station 12 in spring and summer 1976. The difference in peak

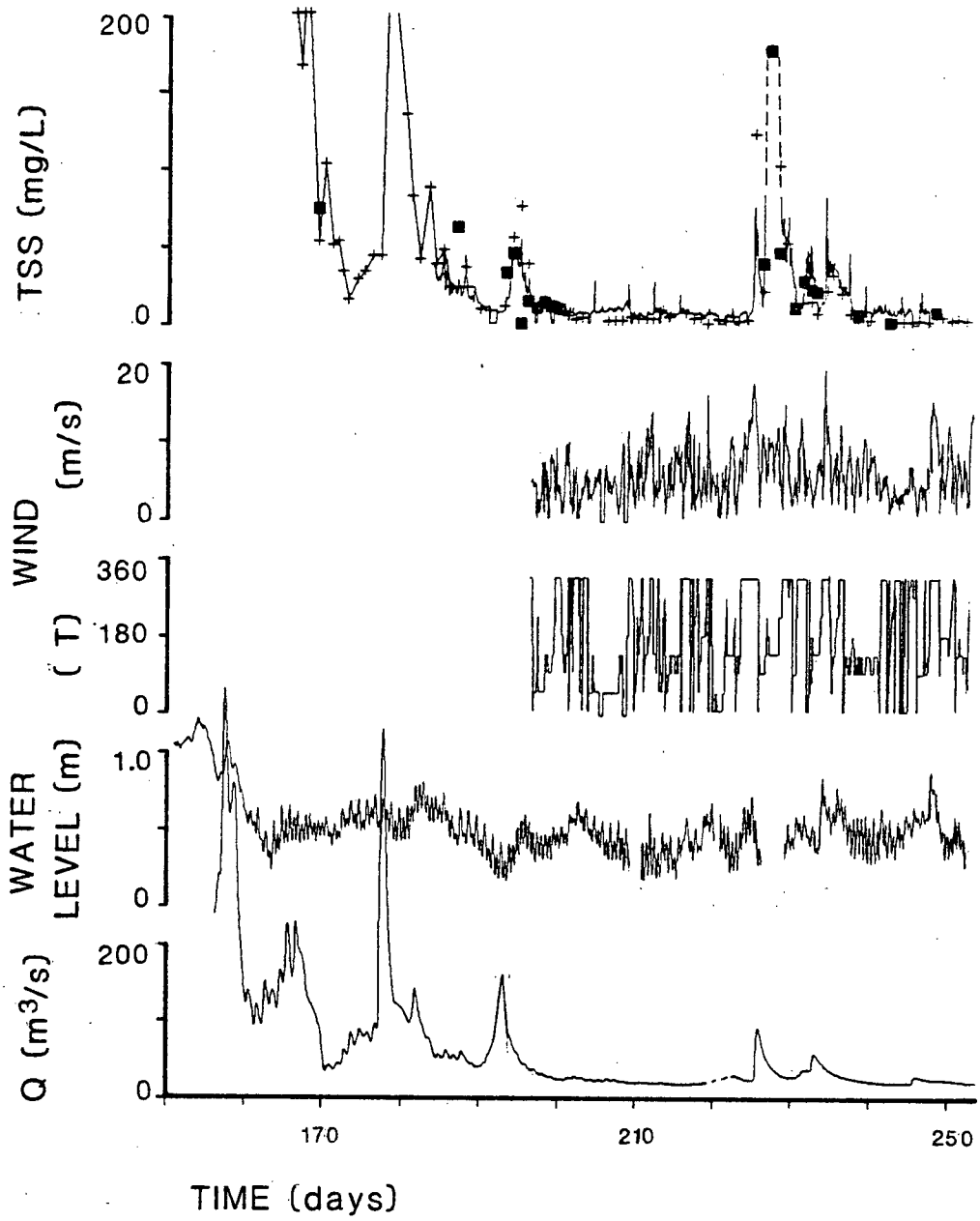


FIGURE 114

Time sequence of total suspended solids concentration at station 12, Babbage Delta, with wind speed and direction at Kay Point and Babbage River discharge, spring and summer 1976.

concentration between the small event in early July and the major transient in mid-August is attributed to readier availability of sediment in the drainage basin following the prolonged mid-summer recession (see section 4.1.2, where the increase in the exponent of the rating for late-season sediment transport was discussed). It may be inferred, from the magnitude of the early July event and from the absence of any response at station 12 to the early September runoff event that suspended sediment delivery from the river basin is indeed supply limited at some times.

At station 7 in the estuary entrance section, daily suspended sediment concentrations, $\hat{C}_T = f(H_E)$, where $H_E$ is Secchi extinction depth, show some significant departures (Figure 108) from the pattern observed in the delta at station 12 (Figure 114). In particular, very high concentrations were observed on July 30 during a nine-hour northwesterly wind event, when the entrance section lay within the surf zone. The mean value of the estimated concentration increased from 388 ±73 mg/L ($H_E$=0.077±0.009 m) about five hours after the start of this event to 1223 ±153 mg/L ($H_E$=0.035±0.003 m) two hours later, when the sample value at station 6 was $C_T$=1123 mg/L. No significant increase in concentration associated with this event was detected at station 12, where the estimated concentration was $\hat{C}_T$=3 mg/L ($H_E$=1.89 m).

In contrast, the mean estimated sediment concentration at stations in the entrance on August 11 was only 47±17 mg/L some 12 hours after the start of the 47-h northwesterly storm that

peaked on August 12; twenty-four hours later, on the afternoon of the 12th, the mean sample concentration was 349±49 mg/L, although the hindcast incident wave power was more than twice as great as on July 30. The later event of August 11-13 was associated with the only major increase in sedimentation rates observed in the lagoon.

The lower concentrations during the August event may be explicable in terms of variable position of the breaker zone with respect to the sampling stations, the breaker depth being greater (further seaward) on August 12. Differences in concentration of suspended sediment may also be attributable to differences in breaker type, plunging breakers being associated with higher mean concentrations than spilling waves (Kana, 1977). However, the breakers were of the spilling type on both occasions. A third hypothesis involves a possible depletion during July and August of finer bottom sediment in the vicinity of the entrance section. Material deposited in this area during June 1976 had a median size $D_{50}$=21 μm, whereas sediment collected at the same site in August 1975 yielded a value $D_{50}$=105 μm.

The distribution of suspended sediment concentration in the lagoon was surveyed during the storm surge of 27 August 1975 (Figure 115A), approximately 10 h after high water but before the start of any major outflow from the estuary. Concentrations of suspended sediment were somewhat elevated, the largest value being 87 mg/L at station 3. The distribution of suspended sediment concentration in the estuary on 14 August

1976, at the time of the major concentration maximum at station 12 (Figure 114), one day after the Babbage River had peaked at Q=90 $m^3s^{-1}$, is illustrated in Figure 115B. At this time, a plume of turbid water from the Babbage River filled Phillips Bay north to Kay Point, where a sharp boundary between the plume and relatively clear water of Mackenzie Bay was located approximately along the line of the submarine ridge off Kay Point. As in the August 1975 example, $C_T$ increased somewhat toward the north end of the lagoon, although values were relatively low along the eastern shore. A turbidity maximum appears to have been present also in the vicinity of stations 8 and 9 in the main distributary channel.

Tidal transport of sediment is clearly a factor in the long-term development of intertidal deposits in the Babbage Estuary, as demonstrated by the flood-oriented bedforms on distributary margin surfaces and elsewhere. However, tidal currents are not believed to generate significant variance in the suspended sediment series. Recorded velocities at station 5 in 1975 (Figure 116) exceeded an approximate minimum entrainment threshold of 0.15 m $s^{-1}$ (cf. Komar, 1976a, p.109) during only 11 per cent of the 473-h record, primarily under storm conditions and in association with an ebb-directed (negative) longitudinal component (Figure 116). Flood currents may have been more important over the broad shoal in the middle of the entrance. Unfortunately, the magnitude and residual sign of sediment transport resulting from superimposed wave motions and sub-threshold tidal currents cannot be evaluated

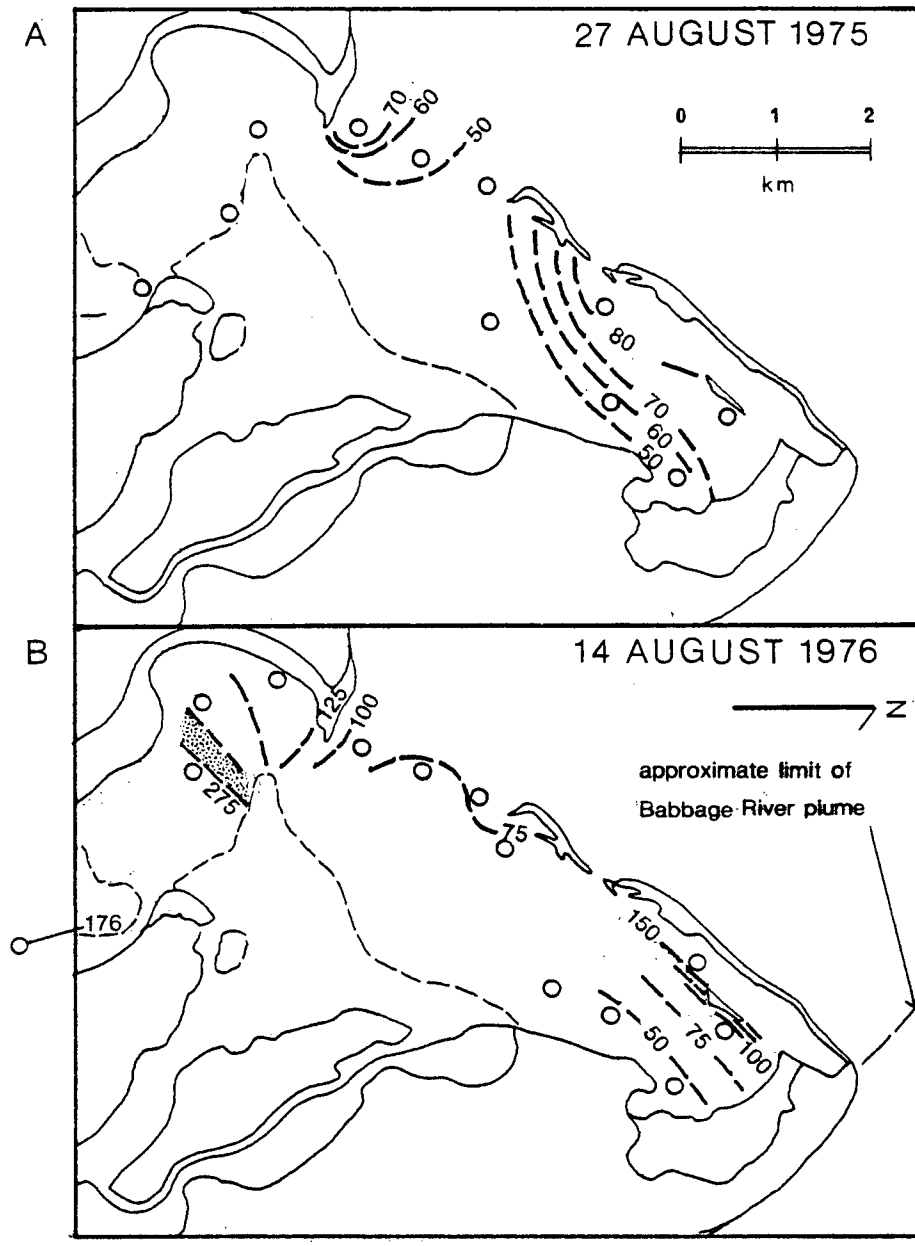


FIGURE 115

Distribution of $C_T(0)$ in the Babbage Estuary during the storm-surge of 27 August 1975 (A) and on 14 August 1976 (B), when a plume of turbid water filled Phillips Bay as far northeast as Kay Point.

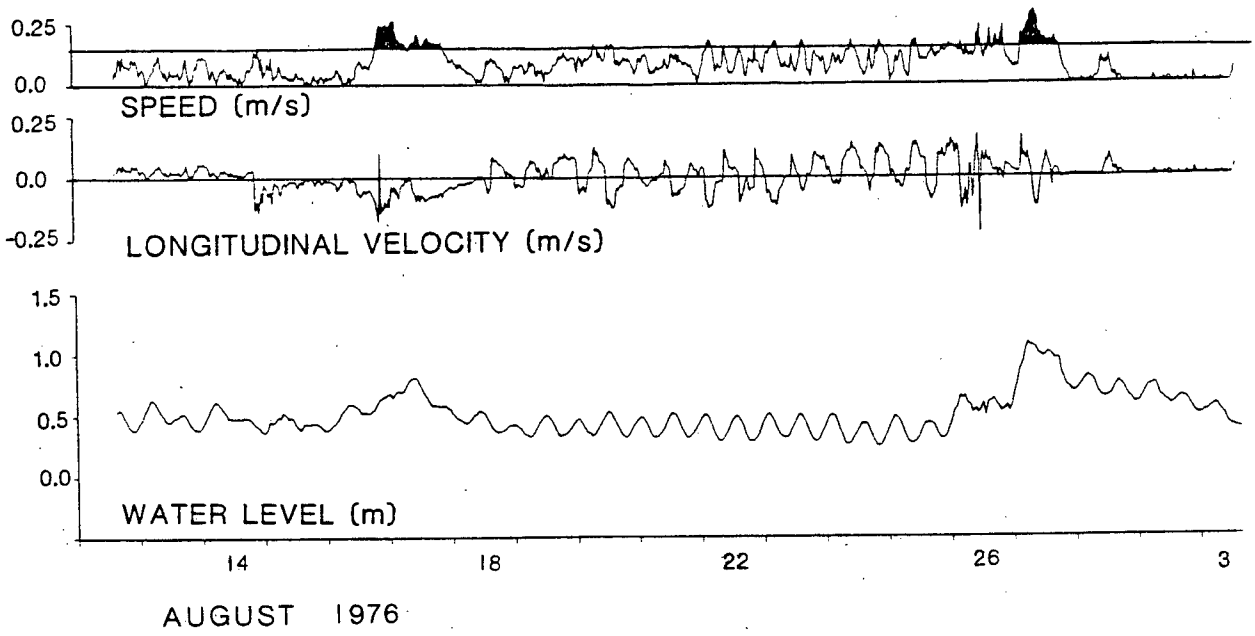


FIGURE 116

Water level and longitudinal velocity (station 5; h-z=0.9 m), second half of August 1975; uppermost record is time sequence current of speed, showing distribution of values exceeding approximate entrainment threshold of 0.15 m $s^{-1}$.

with the available data and theory.

The magnitude of the high-frequency variance present in suspended sediment concentrations may be judged from Figure 117, which shows a 48-h sequence of $C_T$ derived from hourly Secchi extinction data at stations 5, 6, 7, and 12. The variance of $H_E$ for these series may be compared with statistics for the daily series (Table 23). It is clear that, although some tidal aliasing may occur in the daily data, the greater part of the variance is associated with synoptic- and seasonal-scale effects. In fact, a part of the variance in the hourly data can be ascribed to a synoptic-scale wind event believed to have affected the first part of the record.

Because a large part of the sediment held in short-term suspensions in the Babbage Estuary is clearly derived from fluvial sources (Figures 108 and 114), the freshwater flushing rate is an important parameter affecting the trap efficiency of the system for fluvial sediment. Flushing rates may vary dramatically an estuary such as the Babbage, where runoff inputs are zero during part of the year and sufficiently great to flush salt water completely from the system at other times (see sections 3.3.4 and 3.3.5). Although the flushing parameter is difficult to specify in a meaningful way for a system as complex as the Babbage Estuary, a qualitative impression of seasonal variability can be achieved with the following simple model (cf. Officer, 1976):

$$t = fV/Q \qquad (4.3.1\text{-}2)$$

where t is the flushing time, V is the volume of the estuary, Q

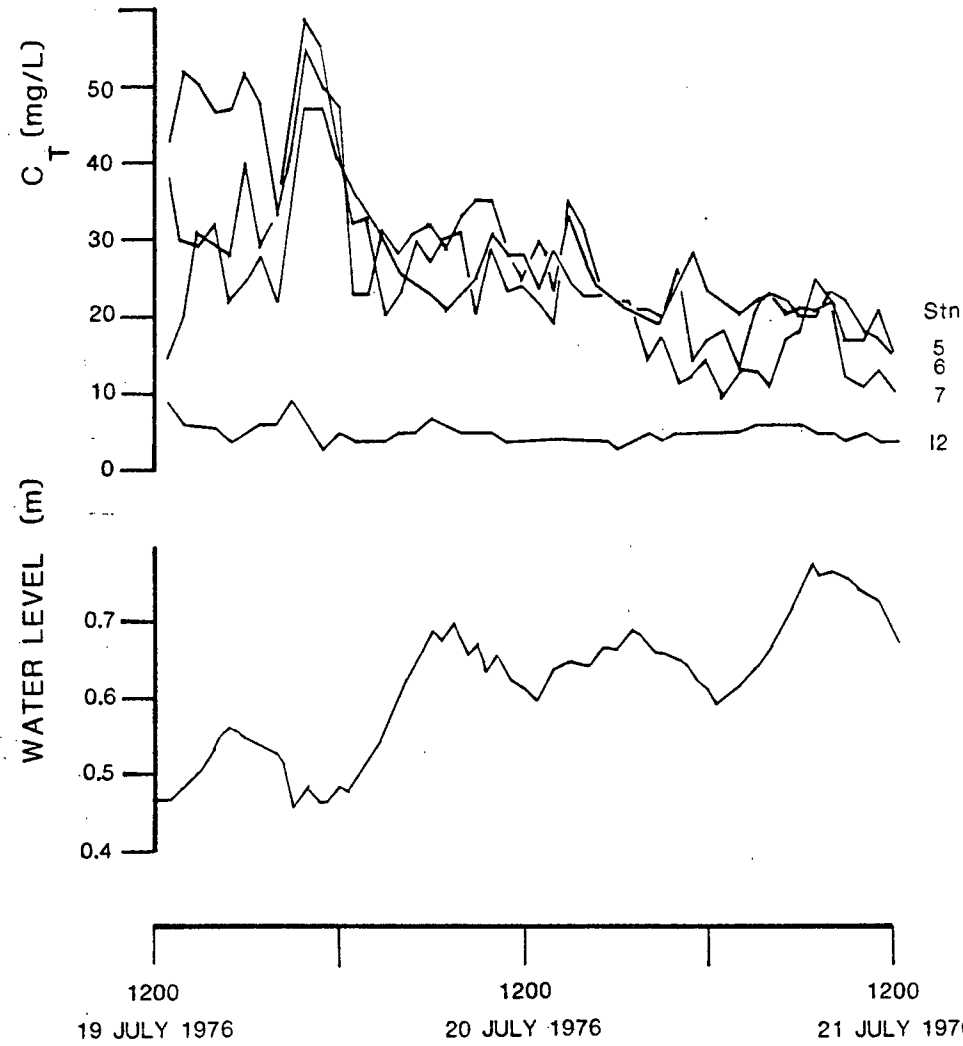


FIGURE 117

Estimated concentration of total suspended sediment, based on hourly Secchi extinction data at stations 5, 6, and 7 in the entrance section and station 12 in the delta during a 48-h period in July 1976.

TABLE 23

Statistics of Secchi extinction depth for stations in the Babbage Estuary, 1976.

HOURLY DATA: 19-21 July 1976

| | stn-5 | stn-6 | stn-7 | stn-12 |
|---|---|---|---|---|
| $\bar{H}_E$ | 0.46m | 0.44m | 0.53m | 1.40m |
| $\hat{\sigma}^2_E$ | $0.01m^2$ | $0.01m^2$ | $0.03m^2$ | $0.04m^2$ |
| n | 48 | 48 | 48 | 48 |

DAILY DATA: spring-summer 1976

| | stn-5 | stn-6 | stn-7 | stn-12 |
|---|---|---|---|---|
| $\bar{H}_E$ | 0.49m | 0.41m | 0.50m | 0.99m |
| $\hat{\sigma}^2_E$ | $0.19m^2$ | $0.09m^2$ | $0.13m^2$ | $0.53m^2$ |
| n | 94 | 94 | 93 | 88 |

the rate of total freshwater discharge to the system, $f=(s_o-\bar{s}_e)/s_o$, $s_o$ is the salinity of seawater outside the estuary, $\bar{s}_e$ is the mean salinity of the estuary, and fV is the total volume of freshwater in the system. Although this model assumes a degree of spatial homogeneity in the flushing process which simply does not occur, our ability to reproduce the settling rate in a highly variable turbulent flow is so tenuous (cf. McCave, 1970) and our knowledge of the circulation dynamics still so limited, that a more complex flushing model may not be justified for the present purpose.

A major uncertainty in the flushing rates determined from equation 4.3.1-2 relates to error in f, due to uncertainty in both $s_o$ and $\bar{s}_e$. A constant arbitrary value of $s_o$=20ppt has been adopted for the computations (cf. Table 4). Results are set out in Table 24. A major point of interest is the very short flushing time computed for the snowmelt runoff flood of 6 June 1976, when despite the high value of the freshwater fraction, the discharge rate was sufficient to reduce the estimated flushing time to t=24 hours at a time when a very high proportion of the annual fluvial sediment input was being passed through the system. Bearing in mind the large proportion of total volume that remained frozen, the true flushing time may have been considerably shorter. Typical values of the flushing time later in the season appear to fall in the range $100< t <200$ h, suggesting that the trap efficiency of the estuary is increased as fluvial sediment inputs diminish. Under certain circumstances, however, when the

TABLE 24

Flushing times for the Babbage Estuary.

Computed flushing times using equation 4.3.1-2; $\bar{s}_e$ is the mean salinity of the estuary, f the freshwater fraction, V the storage volume, Q the freshwater input rate, and t the flushing time in hours; n indicates the number of salinity observations.

| date | $\bar{s}_e$ | n | f | V | Q | t |
|---|---|---|---|---|---|---|
| | ppt | | | $m^2$ | $m^3 s^{-1}$ | h |
| 6 June 1976 | 0.0 | 5 | 1.00 | $3.73 \times 10^7$ | 436. | 24. |
| 29 July 1975 | 13.0 | 40 | 0.35 | $2.47 \times 10^7$ | 12. | 200. |
| 30 July 1975 | 12.6 | 40 | 0.37 | $2.18 \times 10^7$ | 13. | 172. |
| 24 Aug 1976 | 12.8 | 9 | 0.36 | $2.87 \times 10^7$ | 28. | 102. |
| 27 Aug 1975 | 18.4 | 10 | 0.08 | $3.73 \times 10^7$ | 38. | 22. |

freshwater fraction is reduced to very low values, as during the storm surge of 27 August 1975, short flushing times may again prevail according to the model of equation 4.3.1-2. While the validity of the equilibrium and mixing assumptions implicit in this model may be open to doubt, the contrast between rapid flushing at times of high fluvial sediment input and slow flushing when the rate of fluvial sediment input is low is thought to be valid. This behaviour, combined with low settling velocities during the snowmelt season (Figure 108) tends to reduce the probability of suspended fluvial sediment being retained in the system.

Sediment dispersal in an estuarine system is controlled, not only by hydrodynamic factors, but also by water level, which determines the surface area accessible to water borne sediments. Whereas most intertidal surfaces are submerged and potentially active on a daily basis during the open-water season, supratidal surfaces and associated lakes with closure receive sediment inputs only during breakup flooding and during rare surge events (see section 3.3.2). However, because breakup flooding is associated with snowmelt runoff carrying large concentrations of suspended material, significant annual increments of sediment are deposited in the delta during such events (see following section). Sedimentation rates on lagoon-margin supratidal flats have not been determined, but are believed to be lower. Storm surge flooding during the present study produced no measurable sedimentation on supratidal surfaces, except for localized washover transport of

sand at the north end of the lagoon.

Although ice is a major factor in the Babbage Estuary system, it effects little direct transport of sediment. Ice rafting of mud, sand , and pebbly sand, including rafting onto the supratidal delta plain, has been observed during the breakup season and minor ice thrust features can be observed occasionally (Figure 118). Ice rafting may account for very thin gravel units occasionally observed in short cores of delta plain sediments. Rare patches of gravel on intertidal distributary margin surfaces are also ice rafted.

No evidence of ice scour has been found in vertical or side-scan sounding records from the lagoon; indeed, ice scour features are rare in depths less than 10 m throughout the region (Shearer and Blasco, 1975). This does not imply that scour never occurs; it may indicate merely that recovery is rapid. While the foreshore and berm of Kay Point spit are sometimes modified by ice thrusting (cf. McDonald and Lewis, 1973, figure 33), no such occurrences have been seen on the lagoon shore of the barrier or elsewhere around the lagoon.

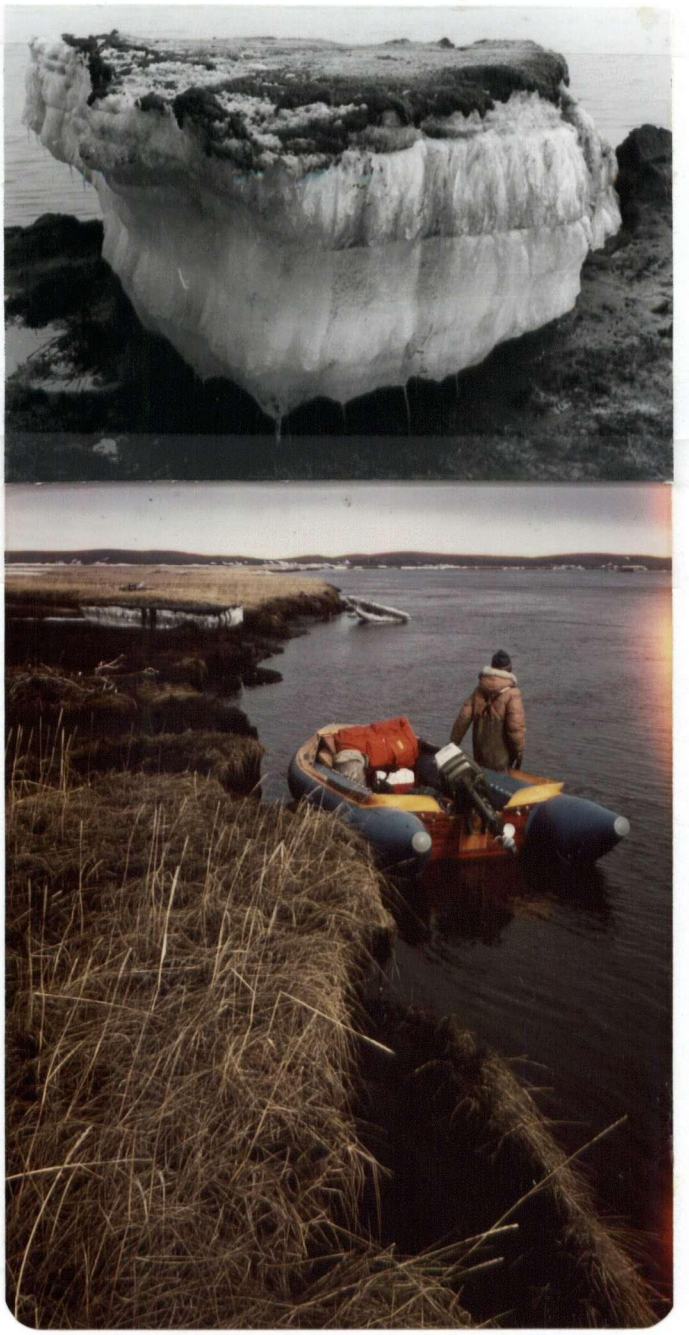

FIGURE 118

Ice rafting of sediment onto supratidal delta plain, June 1976.

### 4.3.2 SEDIMENTATION AND EROSION

Short-term (within-season) sedimentation rates in the Babbage Estuary system show marked spatial and temporal variability. This reflects topographic control and the effects of other fixed parameters, changes in the pattern of sediment supply (variable inputs) and fluctuations in the dispersal process (changing system parameters).

Direct measurements of sedimentation rates were attempted using a variety of techniques, chiefly during the 1976 open-water season. The data set is limited in scope, but provides a basis for qualitative assessment of distribution patterns and for comparison with estimated storage terms for the system as a whole.

Sedimentation on the delta plain was estimated from measurements of the thickness of fresh deposits over compacted prior-season vegetation. Observations were also made of sedimentation on ice in the lagoon. A network of sediment traps deployed in the lagoon and in selected delta lakes furnished additional data, while stakes with loosely-attached scour markers were installed on several transects in the intertidal zone (see Figure 5 for locations).

Forty-nine determinations of the thickness of freshly-deposited mud at six sites on the Babbage Delta supratidal flats were obtained in June 1976. Because the vegetated supratidal flats were not extensively flooded later in the season, these observations permit an estimate of the

total annual incrementof sediment at the measurement sites, all attributable to the snowmelt runoff flood of 5-6 June. The data are given in Table 25 and refer to sites in the elevation range $0.8 \leq \zeta \leq 1.0$ m above datum. Five of the sites constitute a longitudinal transect along the axis of the delta. The base of fresh sediment was well-defined by compressed flat-lying leaves. Similar use of buried vegetation as a reference layer has been made elsewhere (cf. Dahlskog, 1966). It is particularly favoured in the present setting provided that the data are obtained very early in the growing season and within a few days of the sedimentation event. Delay in pursuit of additional measurements explains the limited spatial coverage of the data set.

The mean thickness of fresh mud at a site varied in the range $0.17 \leq \bar{d} \leq 1.71$ mm. Differences between sites were significant at $\alpha = 0.025$. However, no clear trend with distance along the delta axis was apparent; elevation and position with respect to overbank flow distribution are probably the major factors affecting distribution of sediment on the delta plain. Assuming a dry bulk density of 1000 kg $m^{-3}$ (ten determinations yielded a mean value of 1070±110 kg $m^{-3}$), the sedimentation data in Table 25 provide an estimate of 1 kg $m^{-2}$ for the total addition of mass to sediment storage at the six sites in 1976. If this value is, very tentatively, extrapolated over the area of vegetated supratidal flats, an order of magnitude estimate of $1 \times 10^7$ kg is obtained for the annual addition of sediment to the supratidal delta plain in 1976. Estimates of the long-term

TABLE 25

Thickness of freshly deposited sediment at sites on vegetated supratidal flats, Babbage Delta, 8 June 1976

| site | thickness (mm) | | | | | | | | | mean |
|---|---|---|---|---|---|---|---|---|---|---|
| 070050 | 1. | 1. | 1. | 2. | 1. | 1. | 1. | 2. | | 1.25 |
| 080050 | 2. | 2. | 1. | 1. | 1. | 1. | 2. | 1. | | 1.38 |
| 090050 | 0.5 | 1. | 1. | 0.5 | 0.5 | 1. | 1. | 0.5 | | 0.75 |
| 100050 | 0. | 0. | 1. | 1. | 1. | 1. | 1. | 2. | 3. | 1.11 |
| 110050 | 0.5 | 0. | 0.5 | 0. | 0.5 | 0. | 0. | 0. | 0. | 0.17 |
| 100070 | 2. | 3. | 1. | 1. | 2. | 1. | 2. | | | 1.71 |

1.03±0.11 mm

ANOVA

| variance | df | SS | MS | F | |
|---|---|---|---|---|---|
| between sites | 5 | 12.01 | 2.40 | 7.07 | significant at |
| within sites | 43 | 14.69 | 0.34 | | α=0.025 |
| total | 48 | 26.70 | | | |

mean sedimentation rate, based on radiocarbon data, are presented in section 4.4.3 below.

Measurements of sediment thickness on ice in a lake with closure (site 090044) indicated an accumulation rate much higher than that obtained for the vegetated supratidal flats. Five measurements yielded a mean thickness of 10.4±3.9 mm. Observations from the air suggested that accumulation on lake ice was highly variable over the delta plain. The amount of sediment deposited on a given ice surface presumably depended in part on whether the ice was floating or remained bottomfast during the overbank flow event (cf. Figure 119). Locally thick deposits of sand were observed on the ice in a lake without closure near the distal edge of the delta (at 070043), where flow from the main distributary had been diverted north by ice jamming at station 10; the configuration of the deposit was such that the volume could not be readily determined. Elsewhere on the delta plain, higher sedimentation rates are assumed to prevail in an area bordering the main distributary channel, between intertidal transects 1 and 4 (Figure 5), where there are no lake basins and the morphology suggests a form of crevasse-controlled overbank flow (see section 4.4.3). On the other hand, the morphology of the marginal deltaic flats, between the outer distributaries and the valley walls suggests that sedimentation rates in those parts of the Babbage Delta are slower than elsewhere.

Sediment deposits on ice in the lagoon, observed during the interval 7-13 June 1976, were also highly variable in

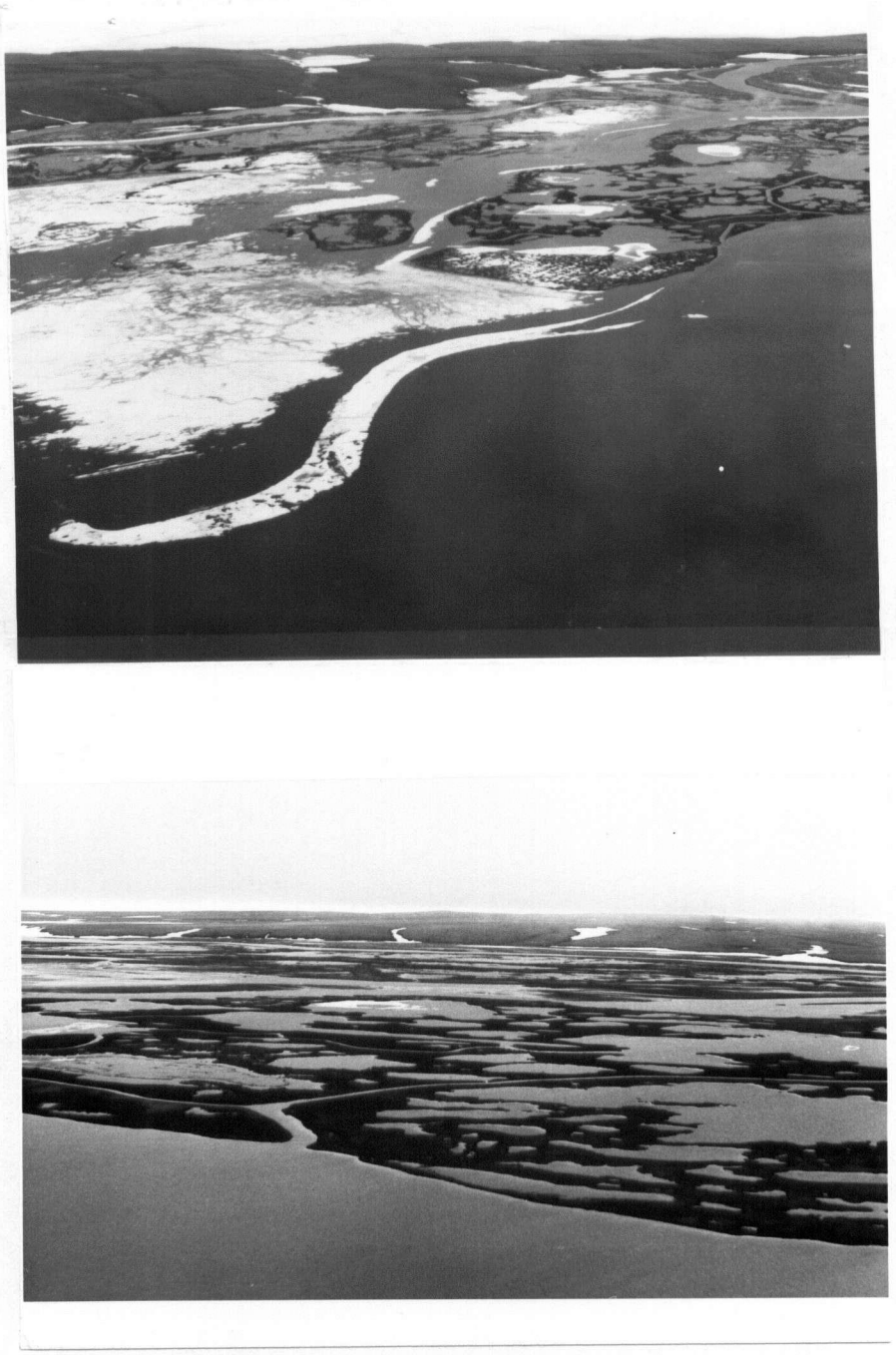

FIGURE 119

Ice in Babbage Delta lakes after spring flooding, showing basins with and without sediment on ice; (A) 15 June 1974; (B) 18 June 1976.

thickness. In some cases, the variability was due to re-entrainment of sediment from the ice surface. Measurements at a point in the lagoon near the distal end of Kay Point spit (015080) gave a mean value of 58±4 mm for parts of the deposit that had not obviously been reworked (Figure 120A). The material was organic silt with minor granules and pebbles. With a dry bulk density of 1020 kg $m^{-3}$, this deposit represented a mass of 59 kg $m^{-2}$. The original horizontal extent is unknown. It appeared that the material had been rafted from a site closer to the delta. At another site near the main distributary channel, the rippled ice surface carried 0.67±0.10 kg $m^{-2}$ of fine sand and silt; the development of thermo-erosional ripples on the upper surface implies that the ice was not in a major sedimentation zone prior to floating free, although sediment deposited on top of the ripples might plausibly have been removed by waves breaking over the floating ice.

A large mass of sediment was deposited on ice immediately seaward of the M1 entrance section. This sediment was deposited under conditions of effluent expansion and drainage through ice. The ice-surface deposit at site 000050 (Figure 120B) was an organic silt (combustible fraction 34%; dry bulk density 400 kg $m^{-2}$) which varied in thickness from 0 to 60 mm (much of the relief seen in the photograph was due to inhibited ice melt under locally thick deposits).

Information was obtained on small-scale topographic changes due to erosion and sedimentation in the intertidal

FIGURE 120

Sediment on ice, formerly bottomfast; (A) in lagoon near the distal end of the spit (015080), apparently rafted from a location closer to the delta; and (B) in Phillips Bay near section M1 (site 000050).

zone, using short lengths of light-weight brass chain attached to vertical rods by loose-fitting collars. Broadly similar devices have been successfully employed in other environments (Slaymaker and Chorley, 1964; Greenwood and Hale, 1980). Forty-one sites were monitored, distributed among eight transects, as indicated in Figure 5. Data for August and early September 1976 are given in Table 26.

The most striking feature of these results is, once again, the very high spatial and temporal variability. At a number of sites, particularly on transects 5, 7, and 8, and at the highest sites on transects 3 and 4, there were prolonged periods of stability when neither scour nor sedimentation occurred. At other locations, substantial changes were observed. The major adjustments involved net scour at sites on all transects during the interval 7-14 August (although some sites on transects 3 and 4 showed minor net gains), considerable local scour at various sites during the interval 14-22 August, and minor net gains on most transects during the interval 22 August to 11 September. The prevailing pattern of net scour at most sites during the week of 7-14 August occurred in spite of significant gross sedimentation at several sites, particularly those adjacent to the main distributary channel. This was the week in which a moderate northwesterly wind event (11-13 August), followed by storm runoff from the river basins, resulted in major accumulations in sediment traps deployed in the lagoon.

Sediment traps with an aspect (height/diameter) ratio

TABLE 26

Erosion and sedimentation on intertidal surfaces of the Babbage Delta, summer 1976.

All data in millimetres; see Figure 5 for locations.
n: number of days
z+: gross sedimentation
Δz: net change in elevation of surface

Sites are numbered consecutively moving away from the channel, except sites 3-6 and 3-7, which are located on the opposite (left-bank) bar.

| | | 7-14 August | | | 14-22 August | | | 22 Aug - 11 Sept | | |
|---|---|---|---|---|---|---|---|---|---|---|
| transect | site | n | z+ | Δz | n | z+ | Δz | n | z+ | Δz |
| 1 | 1 | 7 | +19. | -59. | 9 | +19. | -16. | | | |
| 1 | 2 | 7 | +12. | - 4. | 9 | +12. | -15. | 20 | + 5. | - 5. |
| 1 | 3 | 7 | +10. | -10. | 9 | 0. | 0. | 20 | + 3. | + 3. |
| 1 | 4 | 8 | 0. | -38. | 8 | 0. | 0. | 20 | 0. | 0. |
| 1 | 5 | 7 | + 4. | -40. | 9 | + 7. | + 7. | 20 | +15. | +15. |
| 2 | 2 | | | | 9 | +52. | ? | 20 | 0. | 0. |
| 2 | 3 | | | | 9 | + 3. | ? | 20 | + 7. | + 5. |
| 2 | 4 | | | | 9 | + 0.5 | ? | 20 | + 6. | + 4. |
| 2 | 5 | | | | 9 | + 6. | ? | 20 | +10. | + 9. |
| 3 | 7 | 8 | +22. | -31. | 8 | + 1. | -15. | | | |
| 3 | 6 | 8 | + 5. | -34. | 8 | +14. | + 5. | | | |
| 3 | 1 | 7 | +29. | -29. | 9 | 0. | -26. | 20 | +18. | +18. |
| 3 | 2 | 7 | 0. | -35. | 9 | + 3. | -10. | 20 | + 3. | -17. |
| 3 | 3 | 7 | + 5. | + 5. | 9 | + 3. | -99. | 20 | + 5. | + 5. |
| 3 | 4 | 7 | 0. | 0. | 9 | + 3. | - 3. | 20 | 0. | 0. |
| 3 | 5 | 7 | 0. | 0. | 9 | 0. | 0. | 20 | 0. | - 4. |
| 4 | 1 | 8 | + 2. | ? | 8 | + 5. | + 5. | 17 | + 4. | + 3. |
| 4 | 2 | 8 | + 3. | + 3. | 8 | 0. | - 1. | 17 | 0. | 0. |
| 4 | 3 | 8 | +15. | + 5. | 8 | + 2. | + 2. | 17 | + 6. | -14. |
| 4 | 4 | 8 | 0. | - 2. | 8 | 0. | - 3. | 17 | + 9. | - 3. |
| 4 | 5 | 8 | 0. | - 1. | 8 | 0. | 0. | 17 | + 1. | 0. |
| 5 | 1 | 8 | + 2. | -13. | 8 | + 1. | - 4. | 20 | + 9. | + 5. |
| 5 | 2 | 8 | 0. | 0. | 8 | + 5. | -12. | 20 | 0. | 0. |
| 5 | 3 | 8 | 0. | 0. | 8 | 0. | 0. | 20 | 0. | 0. |
| 5 | 4 | 8 | 0. | 0. | 8 | 0. | - 1. | 20 | 0. | 0. |
| 5 | 5 | 8 | 0. | 0. | 8 | 0. | 0. | 20 | 0. | 0. |
| 6 | 1 | 6 | + 2. | -51. | 8 | + 3. | - 5. | 19 | + 3. | + 3. |
| 6 | 2 | 6 | + 7. | -18. | 8 | + 6. | 0. | 19 | + 5. | + 2. |
| 6 | 3 | 6 | 0. | -35. | 8 | + 5. | 0. | 19 | + 5. | + 1. |
| 6 | 4 | 6 | 0. | -25. | 8 | + 4. | -19. | 19 | + 5. | 0. |
| 6 | 5 | 6 | 0. | -15. | 8 | 0. | - 6. | 19 | + 2. | 0. |
| 7 | 1 | 7 | + 2. | - 3. | 8 | 0. | - 5. | 19 | + 3. | + 3. |
| 7 | 2 | 7 | 0. | -35. | 8 | 0. | 0. | 19 | 0. | 0. |
| 7 | 3 | 7 | 0. | 0. | 8 | 0. | 0. | 19 | 0. | 0. |
| 7 | 4 | 7 | 0. | 0. | 8 | 0. | 0. | 19 | 0. | 0. |
| 7 | 5 | 7 | 0. | 0. | 8 | 0. | 0. | 19 | 0. | 0. |
| 8 | 1 | 6 | 0. | 0. | 8 | 0. | 0. | 19 | + 1. | + 1. |
| 8 | 2 | 6 | 0. | 0. | 8 | 0. | 0. | 19 | + 3. | + 3. |
| 8 | 3 | 6 | 0. | 0. | 8 | 0. | 0. | 19 | + 1. | + 1. |
| 8 | 4 | 6 | 0. | -20. | 8 | +10. | -12. | 19 | + 7. | + 7. |
| 8 | 5 | 6 | +93. | - 5. | 8 | +15. | +15. | 19 | +17. | + 1. |

H/D=0.32 and an exposure (exposure-area/basal-area) ratio $A_e/A_b$=1.83 were placed at 14 sites in the Babbage Lagoon and six sites in delta lakes during parts of the 1976 and 1977 open-water seasons (see Figures 5 and 121 for locations). Three traps were placed at each of two sites, one in the southern lagoon basin and one in the northern lagoon, where a fourth trap of a different design [H/D=0.11, $A_e/A_b$=1.00; described by Håkanson (1976)] was also deployed. The data for summer 1976 are presented in Table 27. No data were obtained for the northern end of the lagoon during the first deployment due to ice remaining in the area. Sites in delta lakes were not occupied until the second deployment in mid-July. Data are missing for later intervals at sites where traps could not be recovered. Replication at two sites, although minimal, made possible an assessment of the relative importance of within- and between-site variance in the sediment trap data. Analyses of variance for two deployments (Table 28) indicated that differences between sites were significant at $\alpha$ =0.025.

The time sequence of trap retention rates (in kg $m^{-2}day^{-1}$) is illustrated in Figure 122. Sedimentation rates in delta lakes were relatively low, with an overall mean of 0.06±0.02 kg $m^{-2}day^{-1}$, but with extremes in two lakes of 0.22 and 0.35 kg $m^{-2}day^{-1}$ during the week of 9-15 August. During the first deployment, when the second major runoff event of the season occurred on 26 June, deposition rates in the lagoon decreased seaward from the distal delta, with trap retention rates of order 1 kg $m^{-2}day^{-1}$ at the delta front (Figure 121).

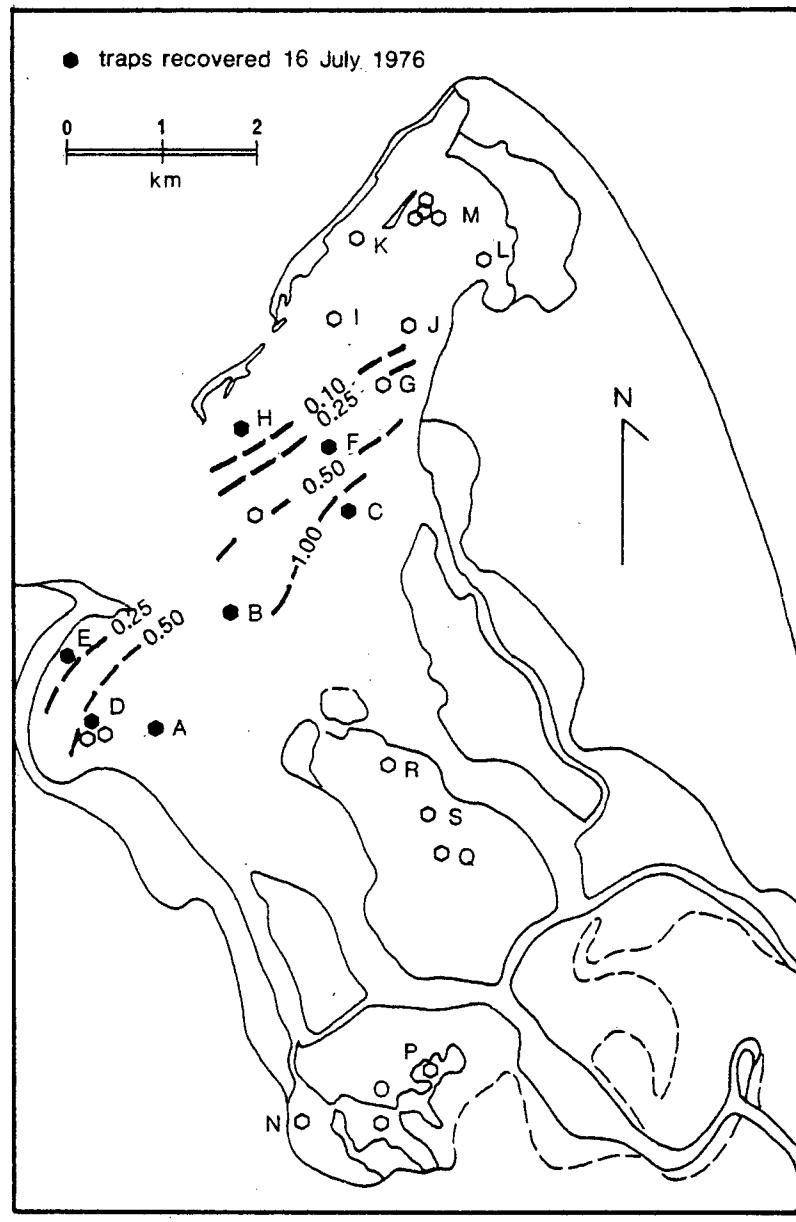


FIGURE 121

Sediment trap locations and distribution of accumulation rates (kg $m^{-2}day^{-1}$) for the interval 24 June to 16 July in 1976.

TABLE 27

Sediment accumulation rates in traps deployed in Babbage Lagoon and in lakes of the Babbage Delta, 1976.

deployment dates:

| | | | |
|---|---|---|---|
| 1: | 24 June - | 15/16 July | 22-23 days |
| 2: | 15/16 July - | 8/ 9 August | 23-25 days |
| 3: | 8/ 9 Aug - | 14/15 August | 5- 7 days |
| 4: | 14/15 Aug - | 11/12 September | 17-19 days |

| site | trap | environment | sedimentation in kg $m^{-2}day^{-1}$ | | | | |
|---|---|---|---|---|---|---|---|
| | | | deployment 1 | deployment 2 | deployment 3 | deployment 4 | deployment 5 |
| A | 1 | lagoon S | 0.739 | | | | |
| B | 6 | lagoon | 0.659 | 0.776 | | | |
| C | 11 | lagoon | 1.675 | | | | |
| D | 2 | lagoon S | 0.546 | 0.072 | 1.774 | | |
| D | 14 | lagoon S | | 0.116 | 1.114 | | |
| D | 16 | lagoon S | | 0.100 | 0.919 | | |
| E | 3 | lagoon S | 0.107 | 0.115 | 0.610 | 0.107 | 0.299 |
| F | 4 | lagoon N | 0.431 | 0.308 | | | |
| G | 22 | lagoon N | | 0.078 | 1.481 | | |
| H | 8 | lagoon N | 0.098 | 0.137 | 1.283 | | |
| I | 12 | lagoon N | 0.072 | | | | |
| J | 18 | lagoon N | | 0.050 | 0.335 | | |
| K | 19 | lagoon N | | 0.078 | 0.272 | | |
| L | 13 | lagoon N | | 0.036 | 0.197 | 0.126 | 0.054 |
| M | 15 | lagoon N | | 0.053 | 0.275 | 0.061 | |
| M | 17 | lagoon N | | 0.045 | 0.311 | 0.065 | 0.057 |
| M | 23 | lagoon N | | 0.044 | 0.262 | 0.064 | |
| M | Ua | lagoon N | | | (0.129) | (0.030) | (0.045) |
| N | 20 | delta S | | 0.009 | 0.024 | 0.023 | 0.007 |
| O | 24 | delta S | | 0.034 | 0.222 | 0.074 | |
| P | 21 | delta S | | | 0.009 | 0.002 | 0.000 |
| Q | 26 | delta | | 0.083 | 0.347 | 0.051 | 0.092 |
| R | 25 | delta | | 0.077 | 0.065 | 0.039 | 0.014 |
| S | 27 | delta | | | 0.058 | | |
| D | | | | 0.096 ±0.013 | 1.269 ±0.259 | | |
| M | | | | 0.047 ±0.003 | 0.283 ±0.015 | 0.063 ±0.001 | |

TABLE 28

Analysis of variance to determine significance of differences between sites in sediment trap data from the Babbage Estuary, 1976

Deployment 2 (15 July - 8 August):

| | | SS | MS | F |
|---|---|---|---|---|
| between sites | 1 | 0.0036 | 0.0036 | 13.6* |
| within sites | 4 | 0.0010 | 0.0003 | |
| total | 5 | 0.0046 | | |

Deployment 3 (8 August - 14 August):

| | d.f. | SS | MS | F |
|---|---|---|---|---|
| between sites | 1 | 1.459 | 1.459 | 14.5* |
| within sites | 4 | 0.403 | 0.101 | |
| total | 5 | 1.862 | | |

* both significant at $\alpha=0.025$

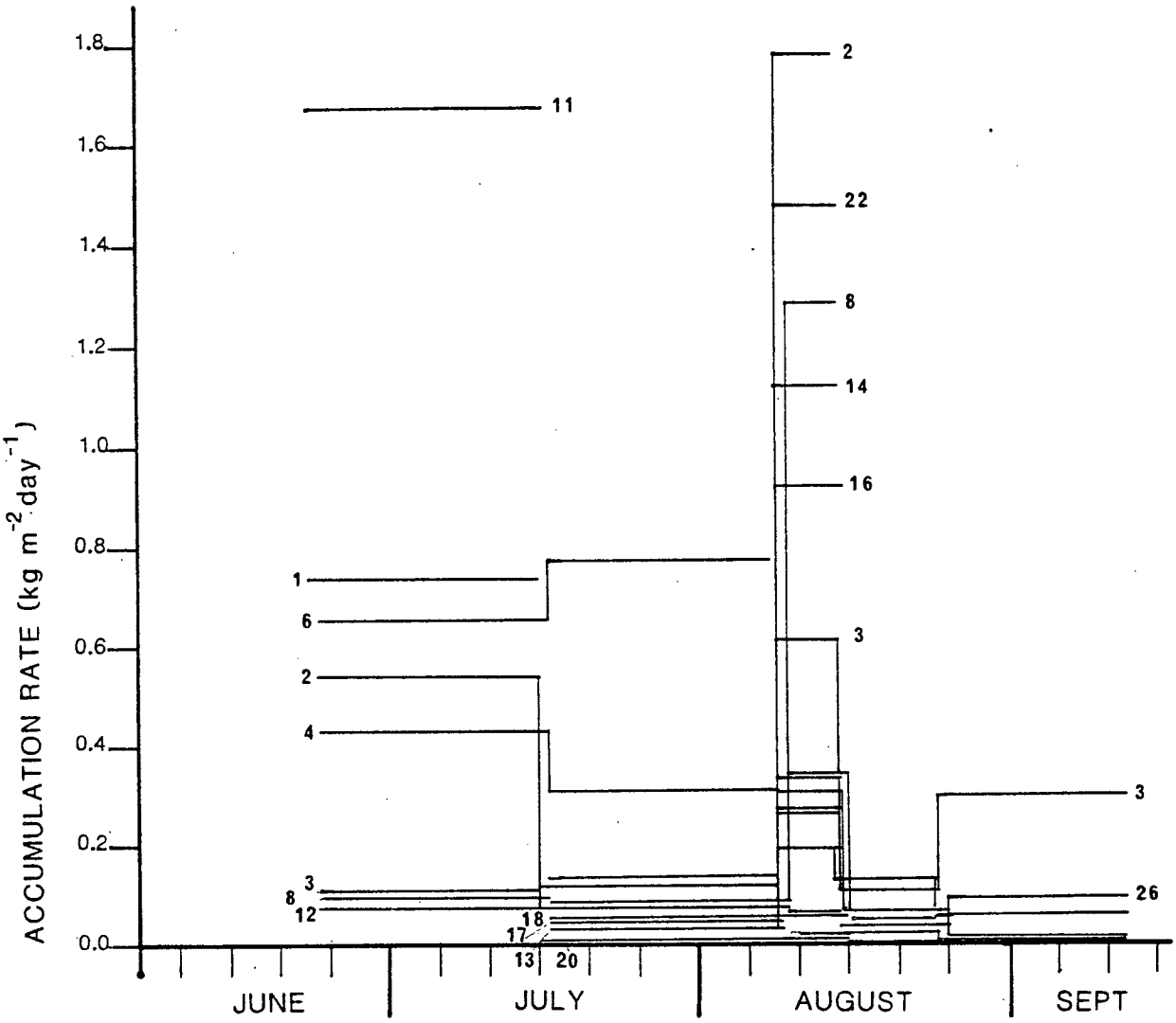


FIGURE 122

Rates of sediment accumulation (kg $m^{-2}day^{-1}$) in traps deployed at lagoon- and lake-bottom sites in the Babbage Estuary system, June-September 1976.

During the week in mid-August, when the highest trap rates in the delta lakes occurred, high accumulation rates were observed at several sites in the lagoon, the mean value for eight sites (12 traps) being 0.74±0.16 kg $m^{-2}day^{-1}$, in contrast to a mean of 0.08±0.01 kg $m^{-2}day^{-1}$ during the preceding sampling interval. Although the traps were deployed almost four times longer during the prior interval, these results clearly indicate a major sedimentation event during the week before 15 August. In this case (Figure 123), trap rates apparently increased toward the exposed section of the lagoon between the entrance and the delta. Due to trap recovery failures, the rates of sedimentation in the exposed area cannot be determined. Trap retention rates apparently exceeded 1 kg $m^{-2}day^{-1}$ over a wide area in the central lagoon.

During the week of 9-15 August, the estimated net longshore transport of littoral sediment to the estuary entrance was about $9.0x10^6$ kg, more than the total of $6.6x10^6$ kg for the entire season up to August 8 and almost 20 per cent of the estimated annual transport (cf. Table 22). A storm runoff event also occurred during the week of 9-15 August (see Figure 114), contributing some $6.1x10^5$ kg of particulate sediment (possibly as much as $1.2x10^6$ kg if late-season deviations from the summer rating are considered). Assuming complete retention of a total input amounting to $1x10^7$ kg, distributed equally over the area of the estuary at mean water level ($2.8x10^7$ $m^2$), one obtains a mean sedimentation rate of approximately 0.06 kg $m^{-2}day^{-1}$, an order of magnitude less than

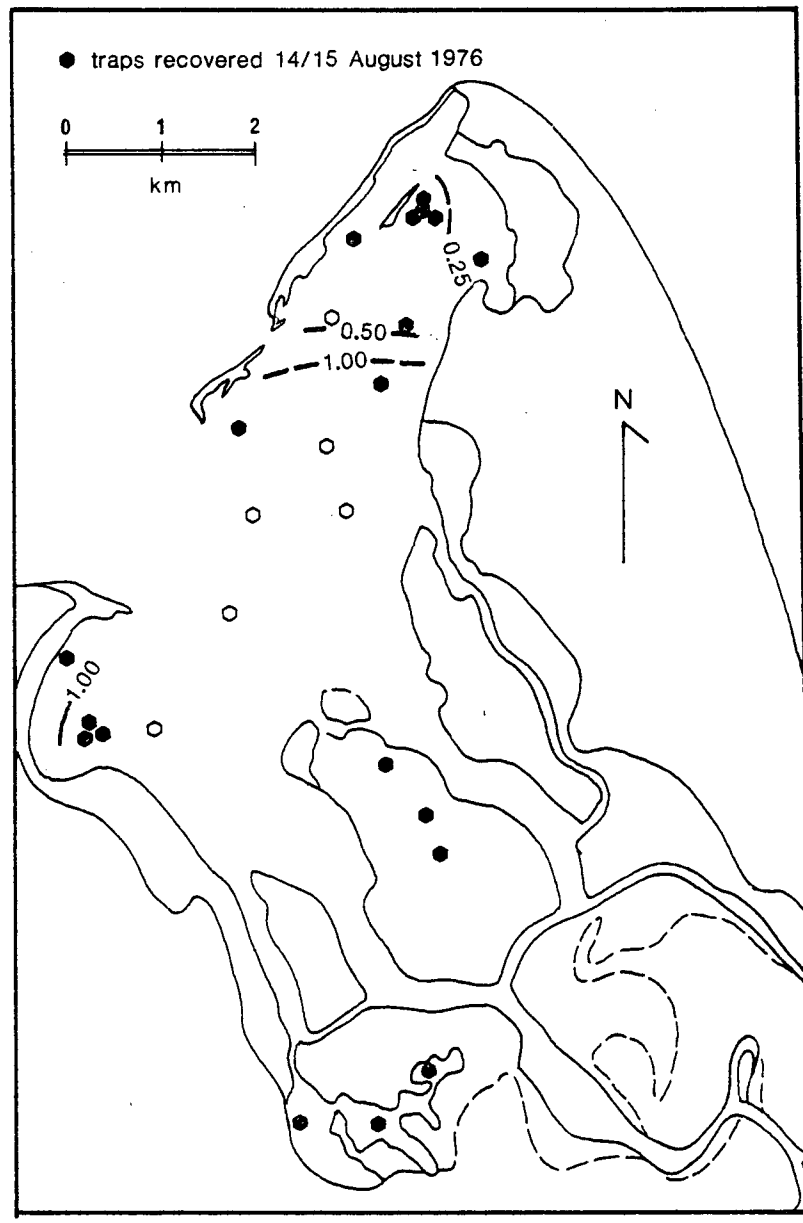


FIGURE 123

Distribution of sediment accumulation (kg $m^{-2}day^{-1}$) in traps in the Babbage Estuary, 8/9-14/15 August 1976.

the observed mean.

It is probable (in part because sampling sites appear to have been biased toward areas of lower accumulation) that much of the sediment collected in the traps during the week ending August 15 had been resuspended within the lagoon. The results would also seem, however, to favour a hypothesis of high trap efficiency for the estuary as a whole during late-season events (as suggested by evidence presented earlier in sections 3.3.5 and 4.3.1). Nevertheless, the balance between onshore and offshore transport in the surf zone on the entrance shoal, during large wave events such as the 11-13 August storm, cannot be reliably estimated (section 4.2.1) and an outflow (return flow balancing surface wind drift, rip current, or other estuarine output) may be present in part of the entrance section, even during intervals of net surge input to the estuary. Furthermore, the plume observed in Phillips Bay on 14 August attests to significant export of fluvial or resuspended lagoon-bottom sediment from the system at that time.

Due to uncertainties concerning hydrodynamic conditions in the immediate vicinity of the sediment traps, absolute sedimentation rates estimated from the trap data may show some bias. In particular, a dependence on aspect ratio is apparent at site M, where values obtained with trap Ua (H/D=0.11) were approximately half those recorded in the other three traps (H/D=0.32) during deployments 3 and 4, and somewhat lower during deployment 5 (Table 27). This is consistent with

results of Hargrave and Burns (1979), who concluded that trap efficiency is independent of aspect ratio in calm water, but increases with increase in the ratio under turbulent conditions.

Rates of bank erosion in the Babbage Delta have been investigated by comparison of bank positions in 1944 and 1970 aerial photography (see example in Figure 124). The analysis yields an estimate of $9 \times 10^4$ m$^2$ for the area of deltaic supratidal flat lost during the 26-year period. If a mean thickness of 1 m and a dry bulk density of 1100 kg m$^{-3}$ are assumed, the mass of sediment mobilized by bank erosion along distributary channels may be estimated at about $4 \times 10^6$ kg a$^{-1}$.

Additional erosion is occurring on the distal delta plain (Figure 125), but no significant differences were detectable in the aerial photographs. A further $8.5 \times 10^4$ m$^2$ of lagoon-margin supratidal flat was lost to bank erosion during the 18-year interval 1952-1970 (McDonald and Lewis, 1973, map 4). Assuming a mean thickness of 0.5 m and a bulk density of 1100 kg m$^{-3}$ for this component, a loss of $3 \times 10^6$ kg a$^{-1}$ is obtained. Whereas sediment removed from distributary banks in the delta represents one component of a channel shifting process, in which a balance may be achieved by deposition on the intertidal channel margin surface opposite, losses from the distal delta plain and from lagoon-margin flats are not compensated in this fashion.

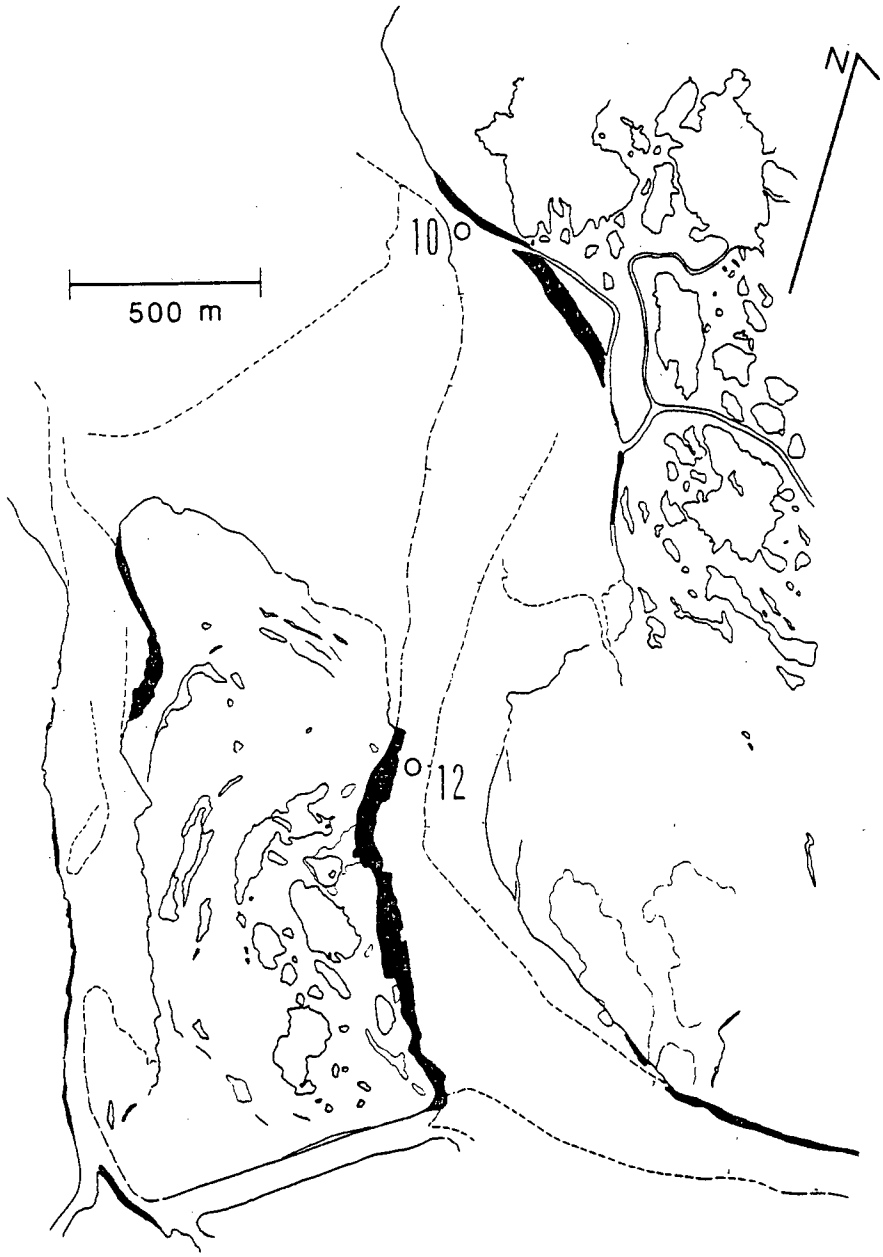


FIGURE 124

Area of supratidal flat lost to bank erosion along western and main distributary channels of the Babbage Delta, August 1944 to August 1970, determined from air photographs; extent of erosion indicated by shading; locations of stations 10 and 12 are shown for reference.

FIGURE 125

Degradation of vegetated supratidal flats, distal Babbage Delta, August 1975; horizontal bars at left margin of upper photo indicate person's height.

### 4.3.3 SEDIMENT BUDGET AND STRUCTURE OF THE SYSTEM

Most significant terms in the Babbage Estuary sediment budget have now been considered. It is the purpose of this section to present a summary of the 1976 sediment budget, insofar as it can be resolved, and to summarize the seasonal variability of sediment inputs, of the trap efficiency of the estuary, and of internal linkages in the system.

Fluvial sediment inputs, designated $J_f$, were given in Tables 19 and 20. For present purposes, $J_f$ is defined as the sum of total suspended sediment (TSS) and bedload (TBS) inputs. The magnitude of inputs, $J_o^+$, across the marine boundary was discussed in section 4.2.3. Direct inputs due to ungauged surface runoff and cliff recession are considered negligible; cliffs along the eastern shore of the estuary exhibited no significant retreat during the interval 1952-1970 (McDonald and Lewis, 1973, map 4). Erosion of the supratidal surface in the delta and bordering the lagoon (section 4.3.2) represents material released from long-term storage within the system and does not constitute a separate input. A further term, $J_e$, representing aeolian transport, may have either positive or negative residual values, but is in any case considered negligible.

Various components of the storage term, $\Delta M$, were examined in the preceding section and some evidence for seasonal variability in the trap efficiency of the estuary was adduced. The complexity of the sediment transport process in the main

entrance section is such that measurements of $J_o$ to the same precision as those of $J_f$ would require a very large logistical effort. Nevertheless, by making certain reasonable assumptions, one can obtain a qualitative picture of the estuarine sediment budget (Table 29). The tentative nature of these results deserves particular emphasis.

In mid-winter, fluvial inputs are zero and all other terms are probably negligible, although some aeolian transport of barrier sand onto ice in the lagoon may occur and limited sediment movement may take place in deeper parts of the entrance section, particularly in the event of a winter storm surge (cf. Reimnitz and Maurer, 1978).

The sediment budget for June is dominated by fluvial sediment inputs carried by snowmelt runoff with, in 1976, an additional storm runoff event in late June. Continuous outflow was maintained through the M1 entrance section until 8 June 1976 (cf. Figure 78). During this time, a rating relationship ($\log\hat{C}_T = 1.373\log\bar{Q}_o - 0.959$, $r^2=0.785$) appeared to exist between suspended sediment concentration and discharge in the M1 section. This rating yields an estimate for total suspended sediment output from the Babbage Estuary system, to 2400h 8 June 1976, of $7.1\times10^7$ kg, with upper and lower 90% tolerance limits of $1.4\times10^8$ and $3.7\times10^7$ kg respectively.

Differences between suspended sediment concentration, $C_T$, in the Babbage River at B1 and estimated concentration, based on Secchi extinction data, in the entrance (Figure 126) were

TABLE 29

Approximate sediment budget for Babbage Estuary system, 1976, January and June-August.

| | M | $J_f$ | $J_o$ | $J_o^+$ | $J_o^-$ |
|---|---|---|---|---|---|
| January | $\approx 0.$ | 0.0 | 0. | $>0.$ | $<0.$ |
| June | $<1.5 \times 10^8$ | $2.7 \times 10^8$ | $<(-1.2 \times 10^8)$ | $\approx 0.$ | $<(-1.2 \times 10^8)$ |
| July | $<1. \times 10^7$ | $6.3 \times 10^6$ | $< 4.6 \times 10^6$ | $\approx 4.6 \times 10^6$ | $< 0.$ |
| August | $<2. \times 10^7$ | $1.5 \times 10^6$ | $< 1.8 \times 10^7$ | $\approx 1.8 \times 10^7$ | $< 0.$ |
| 1976 | $<2. \times 10^8$ | $3. \times 10^8$ | $<(-1. \times 10^8)$ | $<5. \times 10^7$ | $<(-1. \times 10^8)$ |

not significant at $\alpha = 0.10$, except for two occasions during the early snowmelt runoff prior to 8 June, when $\hat{C}_T$ in the entrance fell significantly, and during the recession following the 26 June flood, when concentrations in the estuary remained significantly higher. Assuming values at M1 equal to those at B1 for the period 9-30 June, and taking the lower limit ($3.7 \times 10^7$ kg) of the estimated output for the earlier interval (1-8 June), one obtains an estimate of about $1.2 \times 10^8$ kg for the output term, $J_o^-$, for June. This results in a tentative upper limit of $1.5 \times 10^8$ kg for the mass of sediment retained in storage, or less than 41% of the total suspended sediment input from the rivers. If, on the other hand, the estimated output of $7.1 \times 10^7$ kg were adopted for the period 1-8 June, the net gain to the system would be only 24% of the fluvial suspended sediment input or 43% of the total fluvial transport, $J_f$.

Additional sediment may have been exported from the system as bedload during June 1976. Deployment of a Helley-Smith bedload sampler in section M1 yielded negligible sample weights, although accumulation of coarse suspended organics on the sampler screen is believed to have significantly reduced the hydraulic efficiency of the device.

Retention characteristics of the Babbage Estuary system during the summer months have not been well determined but the trap efficiency is assumed to be higher in summer than during the snowmelt season (see sections 4.3.1 and 4.3.2). An upper limit for $\Delta M$ in July, August, and September of 1976 may be estimated as the sum of fluvial and longshore transport totals,

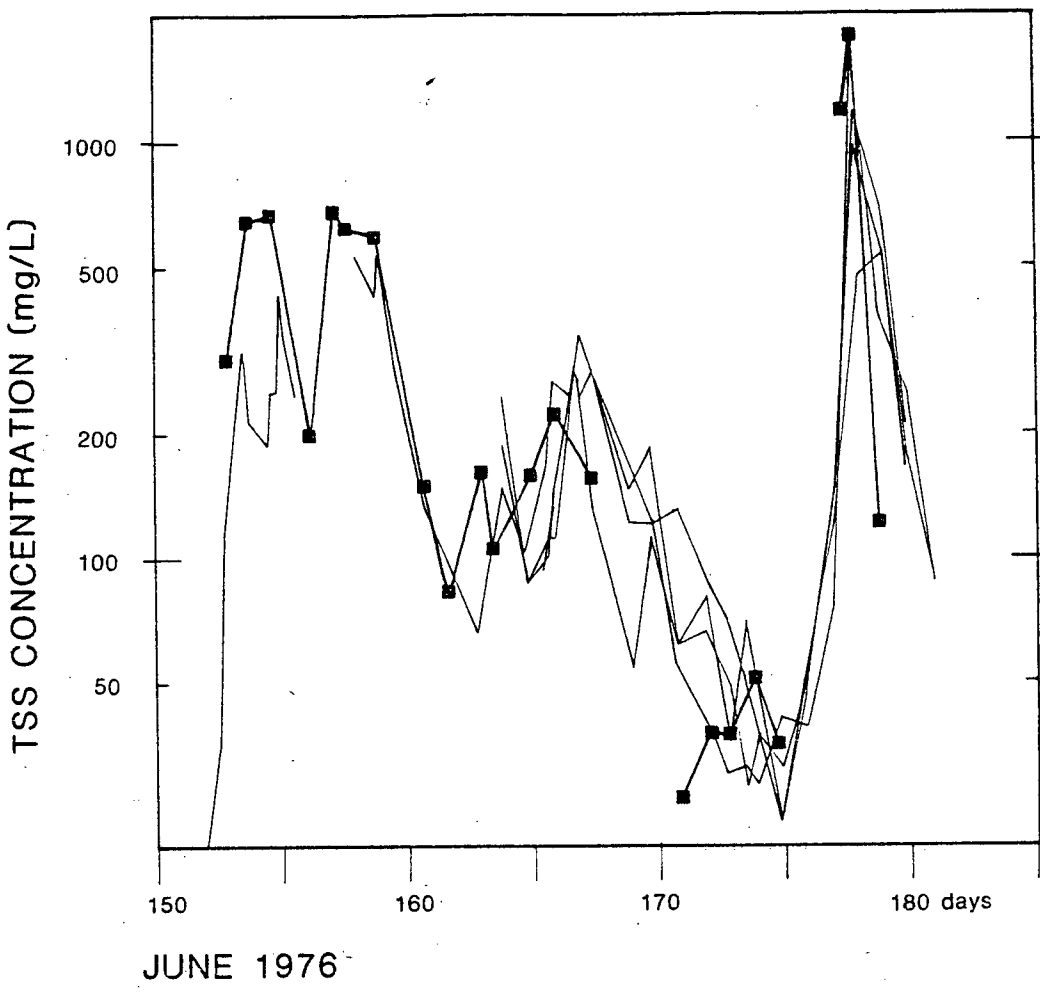


FIGURE 126

Total suspended sediment concentration at section B1, Babbage River (—■—), and estimated TSS concentration, based on Secchi extinction depth, at stations 5, 6, 7, and 7a in the estuary (——), during June 1976.

yielding results an order of magnitude smaller than the estimated upper limit for June (Table 29).

Considering the year as a whole, the foregoing assumptions and approximations lead to an estimated upper limit of $2 \times 10^8$ kg for the mass of sediment retained in the estuary in 1976. The total was probably considerably less. Taking a low bulk density of 1100 kg $m^{-3}$, it appears that the gain in sediment storage volume was somewhat less than $1.8 \times 10^5$ $m^3$, or less than 0.8 per cent of the present capacity of the estuary, $V(\bar{\zeta})$, at mean water level. Although the sedimentation rate during a single year (or during a single decade, for that matter) can hardly be considered a reliable guide to the long-term accumulation rate, an annual net gain of order $10^5$ $m^3$ might be expected to produce a more obvious expansion of intertidal surface area over a 20-year interval than is apparent in a comparison of 1952 and 1972 aerial photographs [cf. Figure 127 (1952) and Figure 105 (1972)].

The most striking feature of the sediment budget (Table 29), however imprecise the absolute values for individual terms, is again the extreme seasonal-scale variance of mass inputs and system response. The seasonal variability of the monthly budget reflects, in part, an interaction between nonlinear response to fluvial inputs (cf. section 3.3.6) and extreme seasonal-scale variance in the fluvial supply (section 3.1.1); in part, the time separation between major river inputs and longshore transport events, due to persistence of ice on coastal waters throughout the snowmelt runoff season; and, in

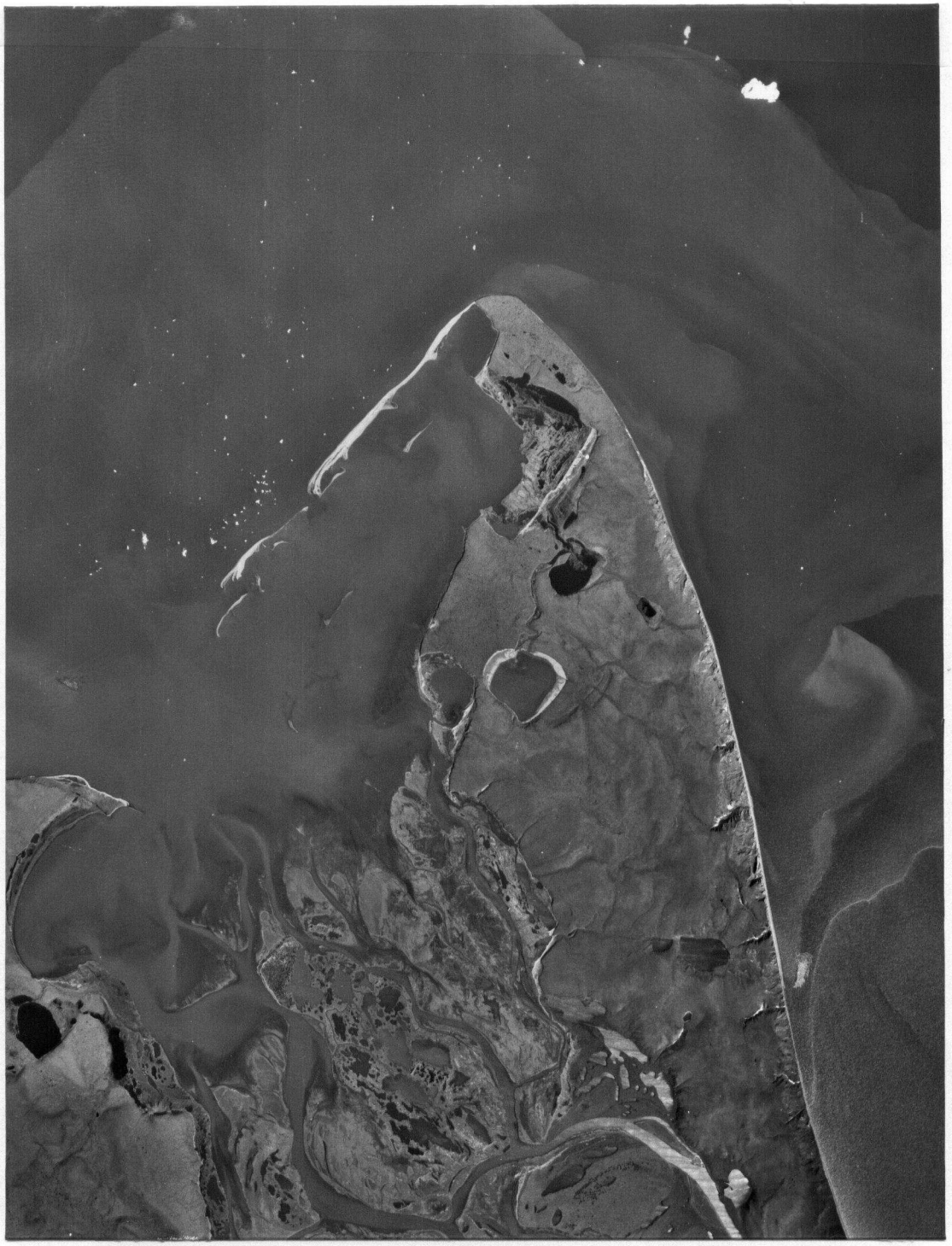

FIGURE 127

Part of NAPL photograph A13383-151, 1952, showing configuration of distributary channels seaward of the distal delta margin very different from the 1972 morphology (cf. Figure 105).

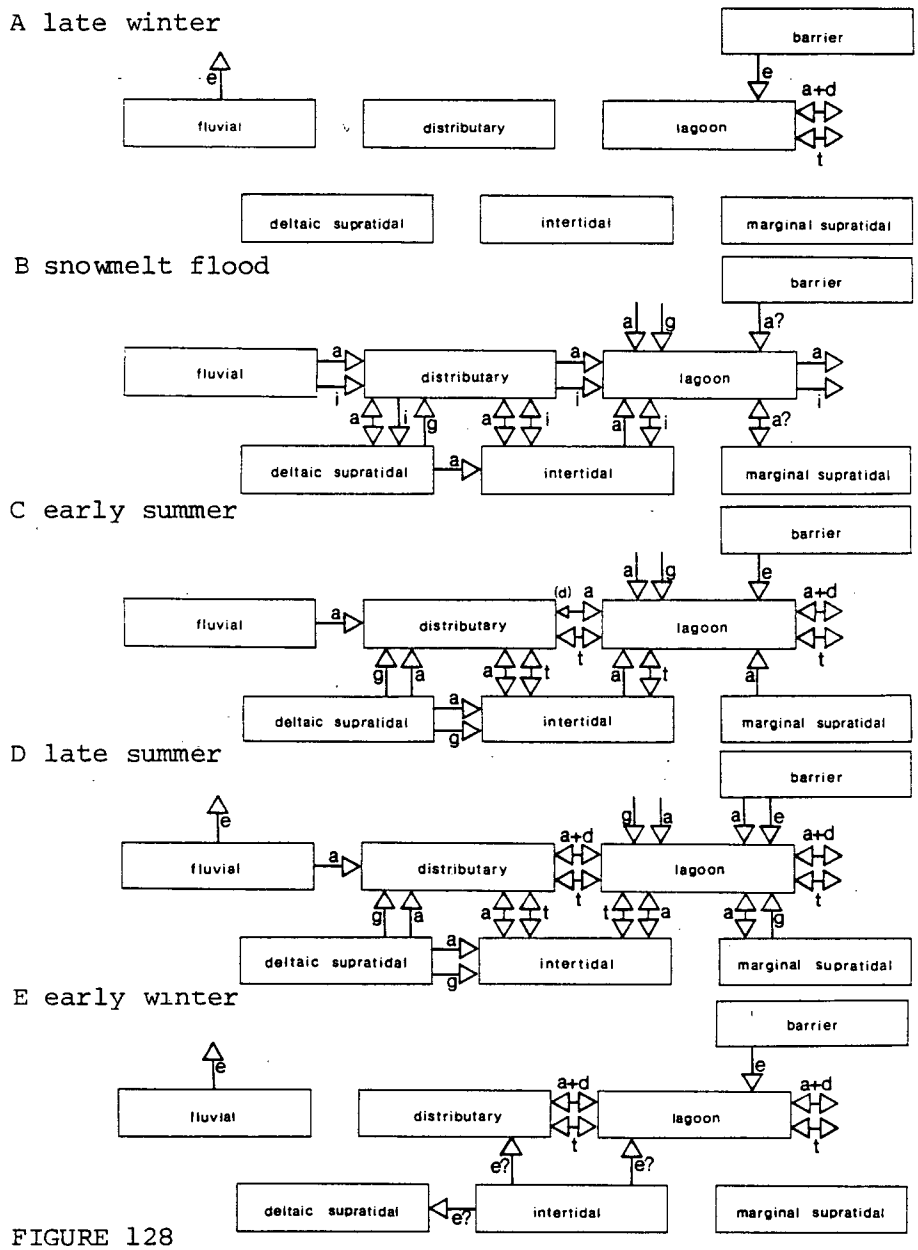


FIGURE 128

Canonical structure of the sedimentary component of the Babbage Estuary system, showing seasonal changes in the linkage network.

g gravitational transport
e aeolian transport
t tidal transport
a non-tidal advective transport
d non-tidal dispersive transport
i ice-rafting

part, significant seasonal changes in the internal structure of the estuarine system.

A heuristic representation of seasonal changes in the canonical structure of the Babbage Estuary system is provided by the simplified linkage diagrams of Figure 128. Although the numbers and types of linkages bear a strong resemblance to those of the hydrological subsystem (Figure 82), the relative magnitudes of transport via various links may be quite different. The same general pattern of seasonal change is nevertheless apparent. In particular, the cascade system is relatively inactive during the winter months, with negligible transfers occurring within or between most subsystems. Major changes occur in the relative importance and residual direction of various transport linkages, including external links through the entrance section (cf. Table 29). The number of internal links, as defined in Figure 128, ranges from one in late winter to fifteen in late summer. Under such circumstances, no fixed-parameter representation of the estuarine system can be expected to yield meaningful results.

## 4.4 THE SEDIMENT STORAGE COMPONENT

### 4.4.1 GENERAL CHARACTERISTICS

Having described the kinematic response of the estuarine system to varying sediment inputs, particularly at synoptic and seasonal scales, it is appropriate to examine the nature of the sediment retained in storage. In an environment of net deposition, which Phillips Bay and the Babbage Estuary system represent, the sediment body provides a partial record, not only of the micro- and mesoscale events emphasized thus far, but of macroscale (annual, decadal, and longer-term) variance, typically including long-term non-stationarity in the input regime and changes in system parameters (see Table 1 for definitions of scales of variance). In a depositional system, the large-scale geometry of the sediment body is associated with large time scales in the depositional process. Due to changing parameters, however, the large-scale features may not be predictable by a model based on the short-term behaviour of the system, even if non-stationarity of the inputs is taken into account.

Sediments retained in storage commonly exhibit horizontal variability reflecting inhomogeneities in the depositional environment. Sorting processes include variable response of different size fractions to hydraulic gradients in the system, as well as size-dependent lag effects within a homogeneous hydrodynamic environment (cf. Swift et al., 1972). In addition, spatial differentiation may occur if parts of a system receive sediment predominantly from different sources,

or are linked to the sediment cascade during certain seasons or events only (cf. Figure 128), when distinctive input or other conditions may prevail. Sediment sorting processes operate to produce distinctive facies types within quasi-homogeneous depositional environments (see section 1.2.2).

The major subenvironments of the Babbage Estuary system are shown in Figure 129, together with representative lithofacies types. The latter are identified by codes defined in Table 30, which presents an amended and expanded version of the classification proposed by Miall (1977, 1978). Additions to the set of lithofacies previously defined include driftwood (lithofacies W), ice (lithofacies I), and two types characteristic of tide- or wave-dominated environments (Sb and Ff). Although ice is ephemeral in the long-term stratigraphic context, it can be a major determinant of facies geometry and surface morphology in high-latitude systems. Furthermore, major ice bodies may be preserved in the record over intervals of order $10^4$-$10^5$ years, as in some of the sediments exposed along the central Yukon coast (Mackay et al., 1972; cf. Figure 9).

Deposits formed in a given depositional environment may be characterized by distinctive sets of lithofacies types. Short-term macro- or smaller-scale variance in a system input sequence may generate vertical variability in the nature of individual lithofacies or in the relative proportions of lithofacies types within a given environment. Nevertheless, assuming a constant parameter system with a stationary input

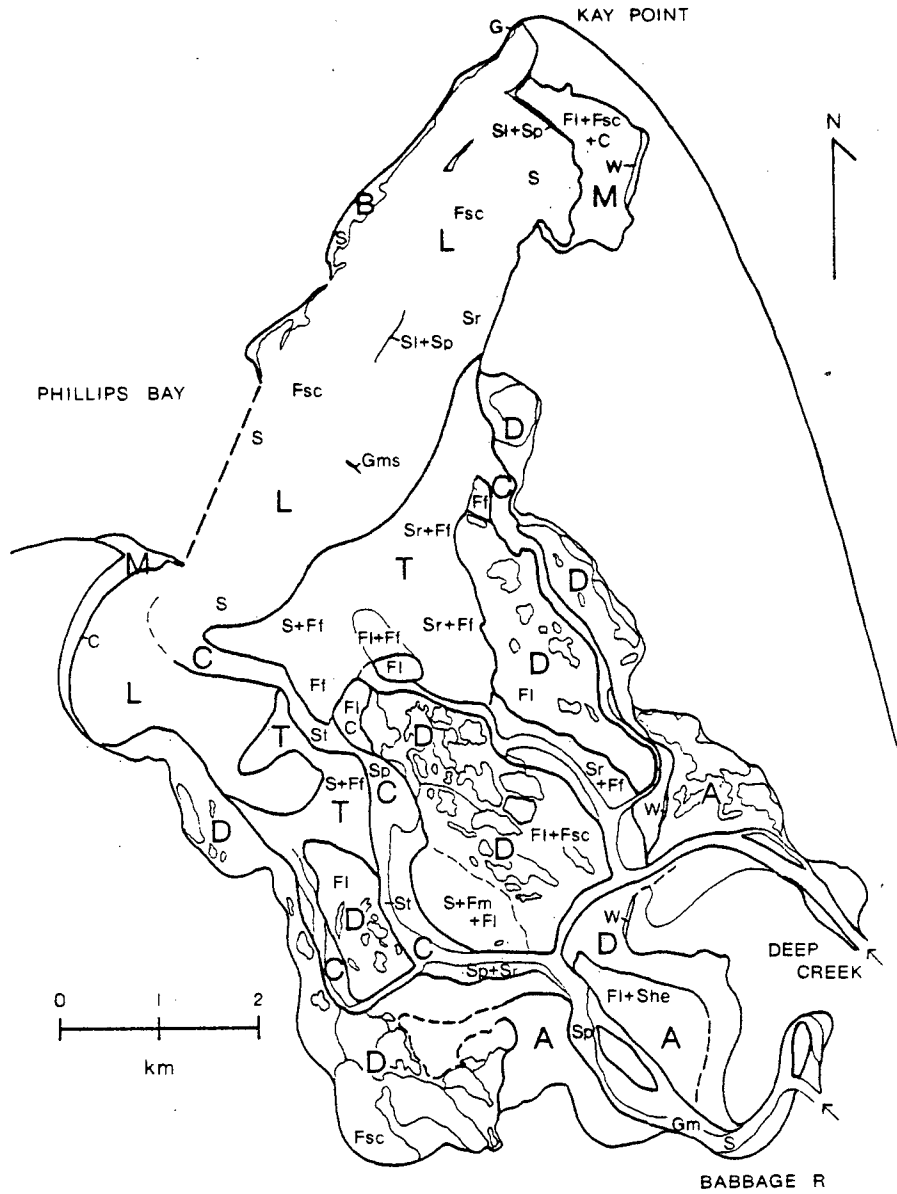


FIGURE 129

Map of Babbage Estuary system showing distribution of major depositional environments (large symbols) and representative lithofacies types (small symbols; see Table 30). Depositional environments: B barrier; M lagoon-margin supratidal; L lagoon; T intertidal; C channel; D delta plain; A alluvial terrace.

TABLE 30

Lithofacies types of lower Babbage River and Babbage Estuary.

| facies code | lithology | structure |
|---|---|---|
| G | sandy-gravel ($D_{50}$>2mm) | undifferentiated |
| Gm | gravel, sandy-gravel | massive or horizontally bedded; commonly imbricate |
| Gt | sandy-gravel | dune-scale scours with massive or trough cross-stratified fill |
| Gp | gravel, sandy-gravel | planar cross-stratified |
| Gms | muddy-gravel | matrix-supported; massive |
| S | sand, gravel-sand, silty- or muddy-sand, (0.06<$D_{50}$<2mm) | undifferentiated |
| St | sand, medium-coarse, may be pebbly | dune-scale trough cross-stratified |
| Sp | sand, medium-coarse, may be pebbly | dune- or bar-scale planar cross-stratified |
| Sb | sand, medium-coarse, may be pebbly | cross-stratified, bipolar |
| Sr | sand, fine-coarse | ripple cross-stratified |
| Sh | sand, fine-coarse, may be pebbly | horizontally laminated |
| Sl | sand, fine-coarse, may be pebbly | low-angle cross-stratified |
| Se/Sre/ She/Sle | sand | aeolian sands equivalent to S/Sr/Sh/Sl |
| Fl | sandy-silt, mud; may contain high proportion of organic material | finely laminated; rare small-scale ripple cross-stratified; roots; ice wedges |
| Fm | silt, mud | massive, dessication cracks |
| Fsc | silt, mud; may contain high proportion of organic material | massive or finely laminated |
| Ff | sand, silt, mud | fine horizontal, lenticular, or flaser lamination; small-scale ripple cross-stratified; dessication cracks; vertical drainage channels and vents |
| C | peat | massive or crudely stratified |
| W | driftwood | shore-parallel, shore-normal, or random structure |
| I | ice | massive, vertically foliated, or interstratified with other lithologies |

regime, the general character of the facies assemblage should remain constant. At longer time scales, however, major changes can develop due to horizontal shifts in the boundaries of contrasting depositional environments, as exemplified by the transgressive sequences described below (section 4.4.6). Surface sediment samples were collected within all major depositional environments or subsystems of the Babbage Estuary, at sites indicated in Figure 130. Lagoon and fluvial subsystems were further subdivided: exposed basin ('open estuary'), protected basin ('lagoon'), and marginal beach/washover subenvironments were recognized within the lagoon component; channel and alluvial terrace subenvironments were recognized in the fluvial subsystem.

Summary tables of particle size data are presented in Appendix A.12. It is important to emphasize that the size data were determined by standard techniques including disaggregation. Therefore the distributions obtained for some fine sediments, particularly those from the lagoon, may not represent the character of the sediment at the time of deposition, when the material may have been agglomerated (see Figure 111).

Proportions of sand+gravel ($D \geq 0.063$ mm), silt ($0.004 \leq D < 0.063$ mm), and clay ($D < 0.004$ mm) are presented in ternary diagrams (Figure 131). Despite considerable overlap between fields in different environments, distinctive sorting patterns are evident, indicating size-selective subsystem response characteristics.

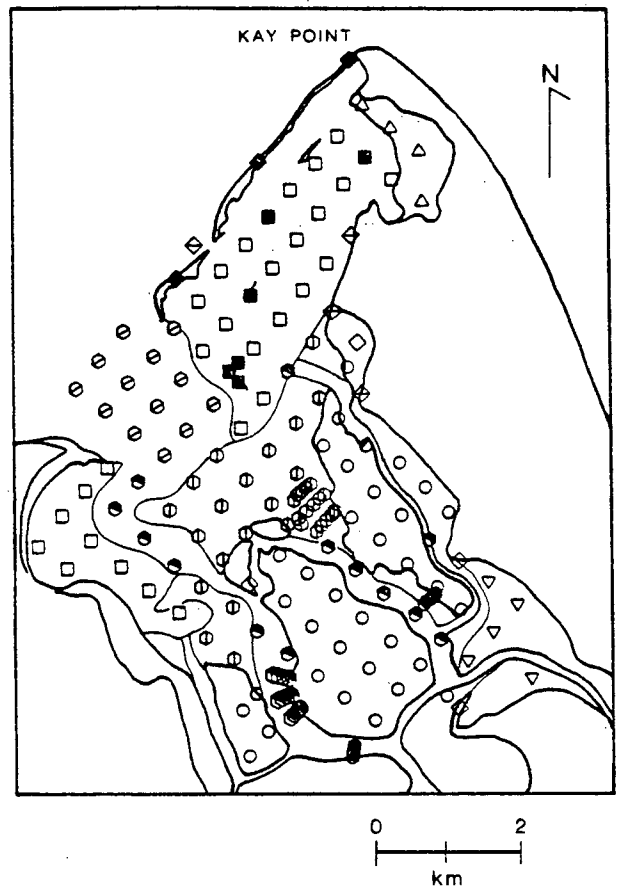


FIGURE 130

Sediment sampling locations in the Babbage Estuary, classified according to depositional environment; note subdivision of lagoon.

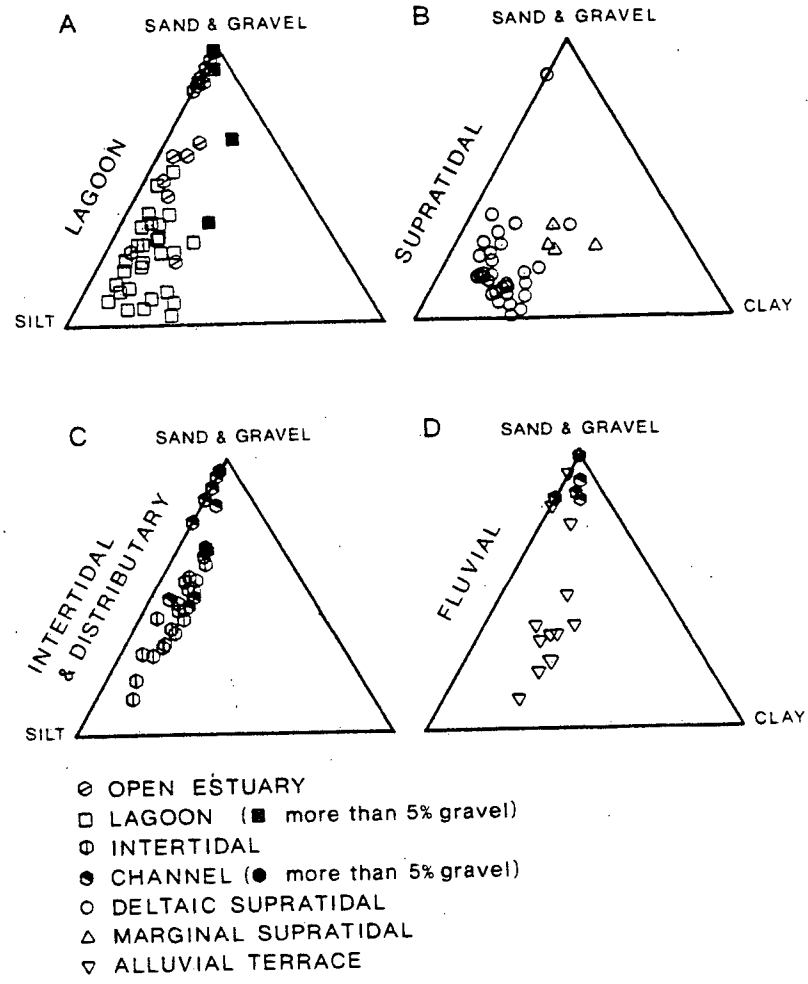


FIGURE 131

Ternary diagrams showing proportions of sand plus gravel, silt, and clay, for various components of the Babbage Estuary system.

Within the lagoon subsystem (Figure 131A), sediments of the marginal beach and open-estuary subenvironments contain higher proportions of sand, for the most part, than non-graveliferous sediments elsewhere in the lagoon. The sandy character of the bottom in the entrance section reflects the penetration of surf activity into this part of the estuary during storms. Sites on both sides of the open-estuary/intertidal boundary (030050, 030060, 040050, 040060) are also relatively coarse (the sand fraction ranges between 44 and 83 per cent), probably due primarily to wave activity on the shallow sloping bottom in this area. Finer sediments of the open-estuary subenvironment accumulate in summer in the channel trending northeast from Niakolik Point on the protected side of the entrance shoal platform (cf. Figure 3). It should be emphasized that the textural patterns presented here represent late-summer conditions; as mentioned earlier, organic-rich sandy mud ($D_{50}$=21 μm, $D_{29}$=4 μm) was deposited on the ice at site 000050 on the distal margin of the entrance shoal during snowmelt runoff in June 1976.

Apart from the open-estuary sands, non-graveliferous sediments in the lagoon are muds, sandy muds, and muddy sands, with silt/clay ratios in excess of 1.5 and highly variable sand proportions, ranging from 2 to 55 per cent. In contrast, gravels, gravelly silty sands, and gravelly muds, containing more than 5 per cent gravel (D≥2 mm), denoted by a shaded box (■) in Figures 130 and 131A, exhibit variable silt/clay ratios

as low as 0.5 and gravel fractions ranging up to 52 per cent. These materials occur locally and form shoals exposed at low water in some places. They may be relict Holocene beach or channel deposits or pre-Holocene sediments. The muddier examples may represent mixtures of lagoon mud with pre-Holocene or ice-rafted Holocene gravel. The gravel at site 010100 near the barrier may be related in some way to the former proximity of inlet M2 c.1950 (cf. Figure 127).

Sediments of the marginal supratidal flats (Figure 131B) are sandy muds with silt/clay ratios between 0.6 and 1.5; the sample from the most seaward site (010160) contained some gravel (4.9%). The silt fraction is generally lower than in sediments of the deltaic supratidal flats, which are predominantly silts of remarkably consistent textural composition. The deltaic sample plotting close to the marginal supratidal data is taken from an extreme distal site (050100) and might appropriately be classified non-deltaic. The highly anomalous sand from the delta plain, plotting near the top of Figure 131B, might be interpreted as an ice-raft deposit, although other explanations including aeolian or overbank flood transport from intertidal channel margin surfaces nearby are equally plausible.

Sediments of the intertidal facies (Figure 131C) exhibit very consistent low proportions of clay and highly variable sand/silt ratios. The wide overlap between intertidal and distributary channel fields reflects the major importance of tidal processes on intertidal bars in the deltaic channel

network. Except for very rare ice-rafted deposits, gravel is entirely absent from intertidal and delta distributary sites. In contrast, fluvial channel samples contain very low proportions of silt and clay (Figure 131D) and large gravel fractions. Almost all gravel transported through section B1 is deposited in the river above the delta.

Figure 132 is a ternary plot showing relative proportions of gravel, sand, and mud (D<0.063 mm) for representative samples from the river and valley and for all other samples containing material larger than 2 mm. Data for barrier samples are take from Hunter (1975). Gravels in the river and barrier contain negligible proportions of mud. Gravel is present in trace quantities in a few samples from most other environments. Only in the pre-Holocene source materials and in the lagoon are significant fractions of both gravel and mud present.

Due to the large proportions of clay in some samples, statistical moments for the estuarine sediments could not be computed without some dubious assumptions about lower size limits. Likewise, because, for many samples with extreme fine tails, the fifth percentile is less than 0.5 μm, graphic measures requiring this statistic could not be employed. Various extrapolation procedures have been suggested for fine sediments (e.g. by Folk, 1966; Jaquet and Vernet, 1976), but arbitrary extrapolation cannot reveal distinctive features in the tails of individual sample distributions. It seems more appropriate, therefore, to interpret only known parts of the distributions; if information is required on the very fine

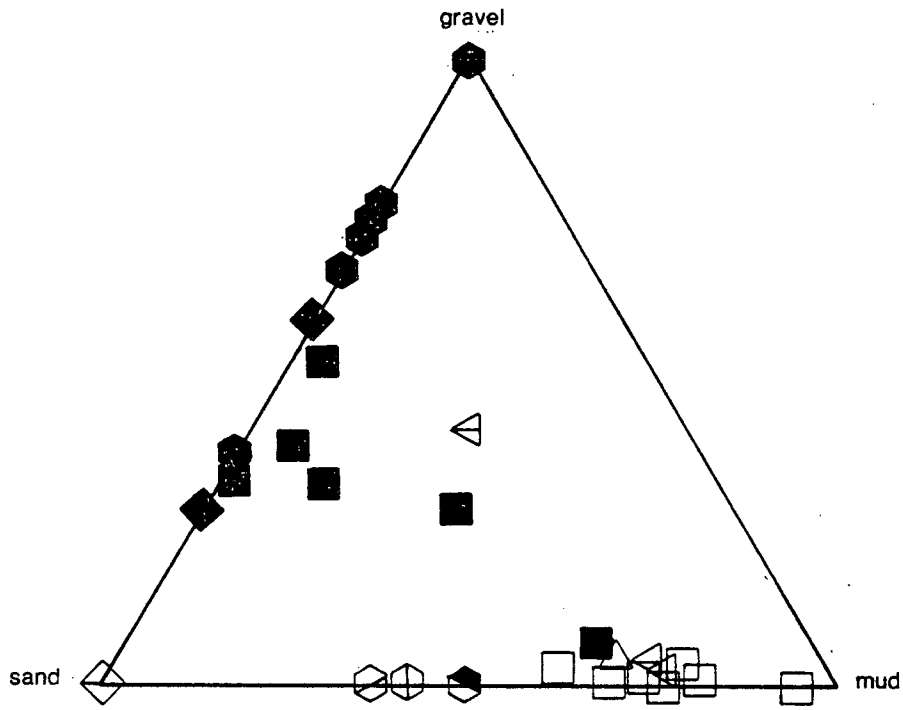


FIGURE 132

Ternary diagram showing proportions of gravel, sand, and mud in sediments of the Babbage River and Estuary; symbols as in Figure 131, except ◁: source materials in valley.

fraction of a sample, an analysis procedure should be adopted that can discriminate very small particle sizes [for example, the lower limit can be extended to about 0.01 μm using centrifugal sedimentation at order $10^3$rpm (Irani and Callis, 1963)]. Furthermore, it appears that the Folk-Ward graphic measures of skewness and kurtosis (Folk and Ward, 1957) are highly erratic (Swan et al., 1978), although the graphic mean and graphic standard deviation are highly correlated with the corresponding grouped or ungrouped weight-frequency parameters (Davis and Erlich, 1970; Jones, 1970; Swan et al., 1978).

For present purposes, therefore, the graphic mean, $\tilde{D}$, where $\log\tilde{D}=[\log(D'_{16}D_{50}D_{84})]/3$ (after Folk and Ward, 1957), and the graphic standard deviation, $\tilde{s}=(\log_2 D_{84}-\log_2 D_{16})/2$ (after Inman, 1952), have been computed (Appendix A.12); skewness and kurtosis, however, have not been examined other than qualitatively. The sediments of the Babbage Estuary are predominantly negative skewed (phi skewness positive).

The relation between $\tilde{s}$ and $\tilde{D}$ is presented in Figure 133. This indicates a partial separation between storage components of the various estuarine subsystems. The delta plain sediments are much better sorted ($\tilde{s} \leq 2.7$ phi) than materials from the marginal supratidal ($\tilde{s} \geq 4.4$ phi), with the single exception of the distal delta sample (050100) noted earlier as being similar to marginal supratidal sediments. Values of $\tilde{s} > 2.7$ phi are rare; however, some of the graveliferous materials from the lagoon and four other anomalous lagoon samples containing less than 4 per cent gravel are poorly sorted ($\tilde{s} > 2.9$ phi). Sample

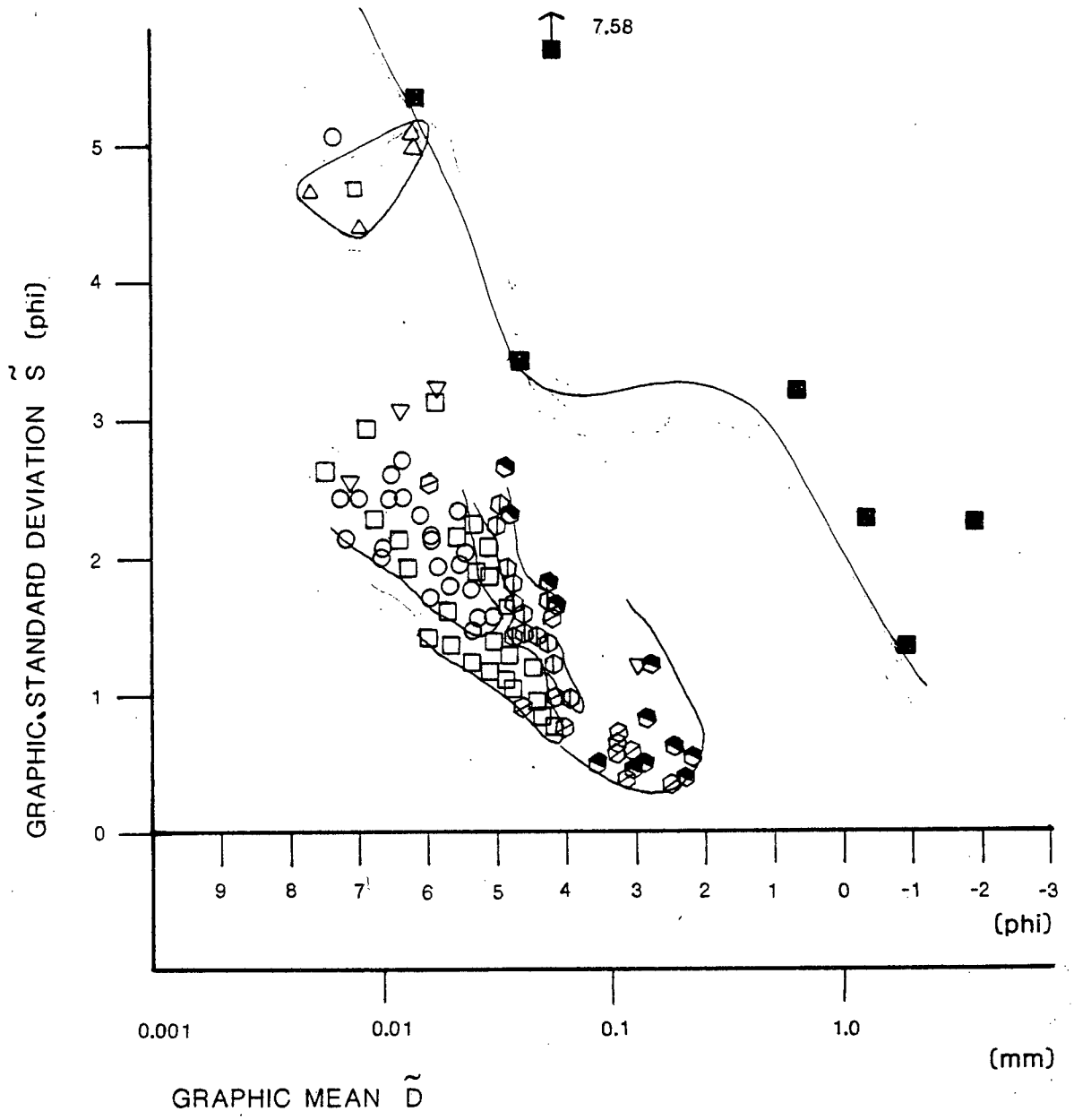


FIGURE 133

Relation between graphic standard deviation $\tilde{s}$ and graphic mean $\tilde{D}$ for surface sediments of the Babbage Delta and Estuary; see Figure 131 for legend.

030010 is very poorly sorted ($\tilde{s}$ =4.66 phi) but contains no gravel; proximity to shore and to the site of a shoal visible in 1952 photography (Figure 127) are the only obvious site anomalies.

Open-estuary, lagoon, intertidal, distributary, and delta plain sediments cannot be differentiated on the basis of $\tilde{s}$, although the lower boundary of the lagoon envelope falls below that for the delta plain and some open-estuary samples are better sorted than samples from other parts of the lagoon. Open-estuary and distributary sediments can be largely differentiated from other materials on the basis of mean size $\tilde{D}$. The intertidal data tend to fall above and to the right of the delta plain and lagoon envelopes. There is, in general, a striking correspondence between the lagoon (protected-basin) and deltaic supratidal fields, both in Figure 133 and in the ternary diagrams of Figure 131.

Qualitative information on subsurface sediments is available from seismic refraction profiling in the lagoon and in adjacent parts of Phillips Bay (Carson et al., 1975) and from boreholes at lagoon, delta, and alluvial terrace sites (Figure 134). Because the textural interpretation of the seismic data depends in part on whether the material is ice-bonded, and because both ice-bonded and non-bonded sediments were encountered beneath the lagoon during drilling, only the borehole data will be presented here. There appear to be some conflicts between the two sets of results, but these may reflect significant local horizontal variability rather

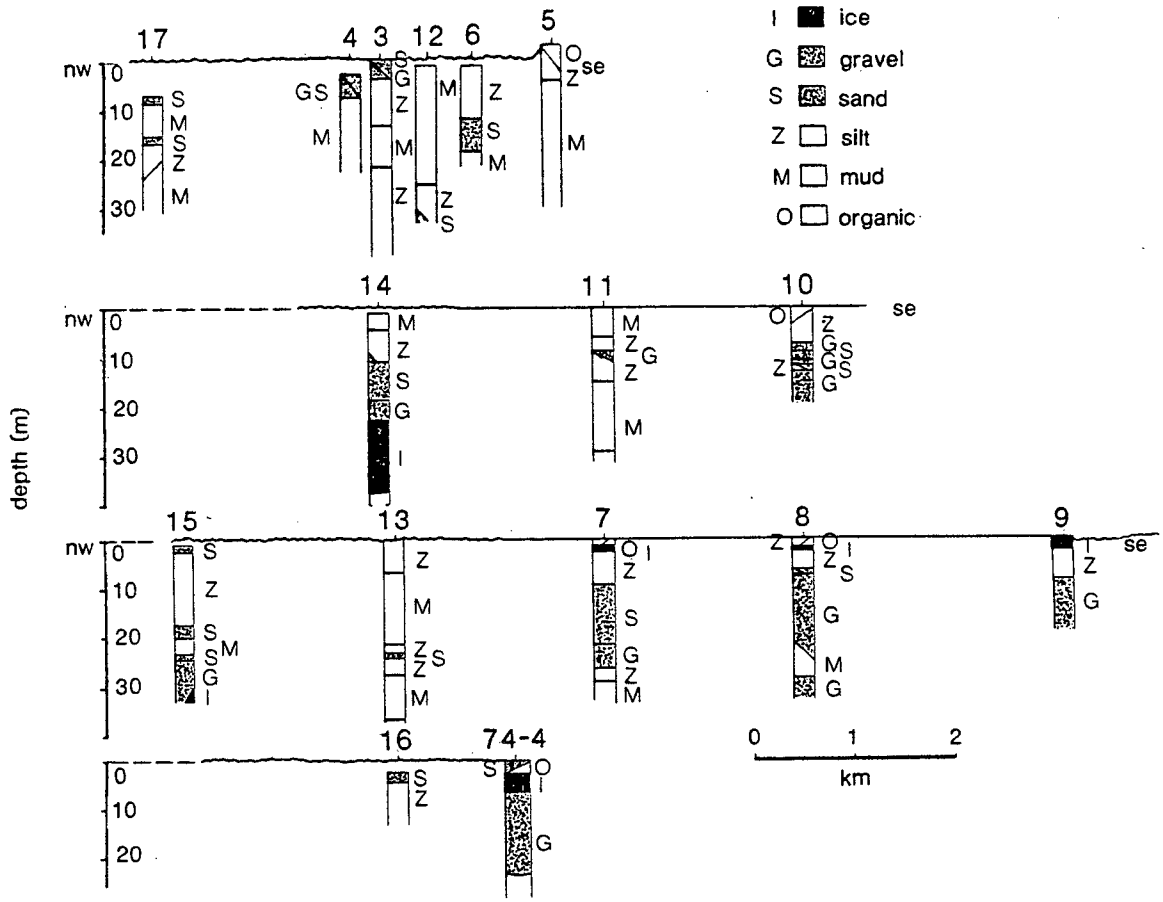


FIGURE 134

Borehole data, Babbage Estuary and Delta.

than errors of interpretation.

Barrier sands and gravels up to 11 m thick (borehole 3 and a nearby borehole reported by Lewis and Forbes, 1974, p.25) are underlain by silts and muds similar to those found beneath the lagoon (boreholes 6, 12, 13, 14, and 15, Figure 134). In the delta plain (boreholes 7, 8, and 10), silts and organic silts 6-21 m thick are underlain by sand and gravel, except in borehole 11. Segregated ice up to 2.1 m thick is common at very shallow depths in the delta plain. Extensive gravels occurring at depth beneath the Babbage Delta have been interpreted as fluvioglacial valley fill (Lewis and Forbes, 1974; Carson et al., 1975); however, other interpretations are plausible (see section 4.4.6). Sand and gravel at depths no greater than 14 m may represent fluvial channel deposits of late-Wisconsinan and Holocene age.

4.4.2 FLUVIAL FACIES

The lower Babbage River may be considered part of the estuarine sediment cascade to the extent that the gravel fraction passing section B1 is deposited at present upstream from the delta. The river may therefore be regarded as the first sink for fluvial sediment entering the estuarine system. The lower Babbage River (Figures 135 and 136) is a sinuous gravel-bed stream similar to the poorly-documented class-5 meandering channel facies assemblage of Jackson (1978). Furthermore, the Babbage and two narrow distributaries flowing to Deep Creek form an anastomosing channel system in the sense of Smith and Smith (1980). The morphology and distribution of channel deposits in the lower valley have been strongly influenced by sediment discharge from the braided tributary Tulugaq (Crow) River and by deposition and channel avulsion on the Tulugaq fan (Figure 135). Some fluvial sediments are believed to have been preserved at the base of a Holocene transgressive sequence beneath the Babbage Delta (see section 4.4.6).

The Babbage River channel between the Tulugaq River and the limit of storm-surge backwater has a sinuosity of 1.89, a variable width/depth ratio ($24<b/h^*<226$), and a mean slope of $7.4 \times 10^{-4}$ at low flow. The channel is locally divided and is dominated by alternating lateral (or point) bars, diagonal bars, and a prominent pool-riffle sequence (Figures 136 and 137). While the riffles may function primarily as hydraulic resistance elements, the lateral bars constitute the

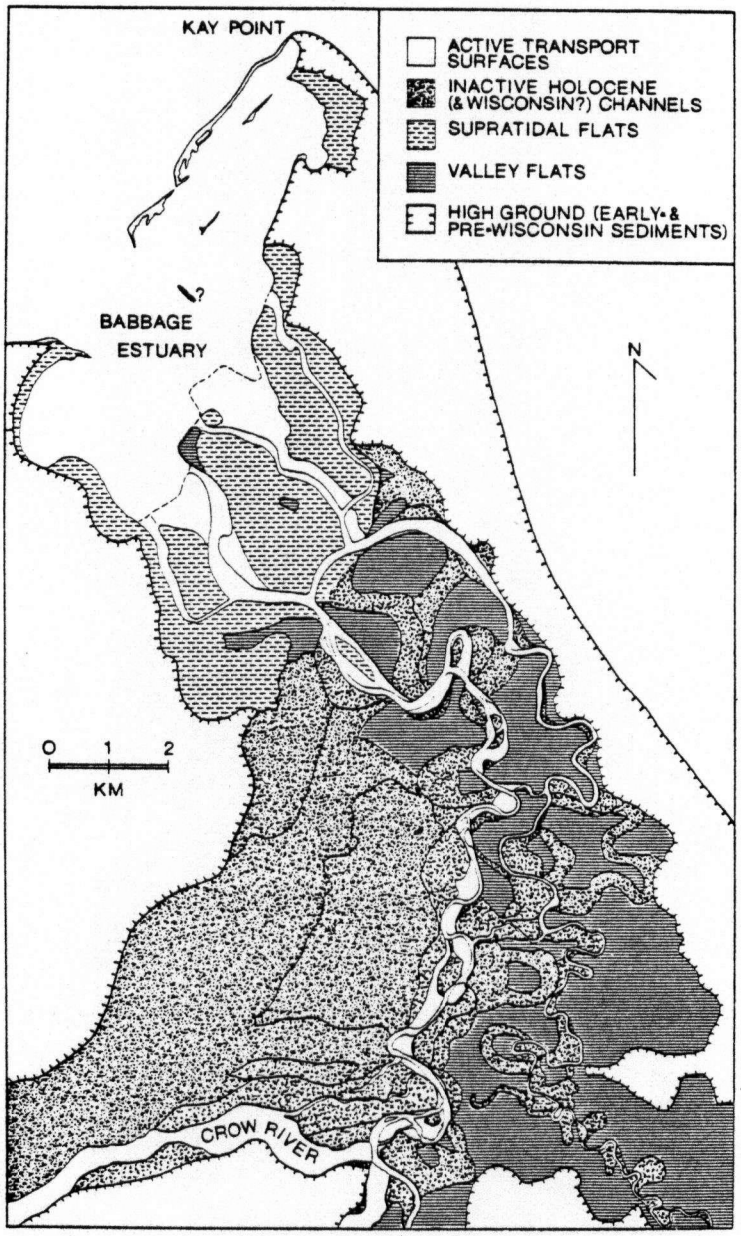


FIGURE 135

Distribution of Holocene channel deposits in the lower valley, as interpreted from surface morphology and limited exposures, showing major impact of Tulugaq river fan on sedimentation in this part of the valley.

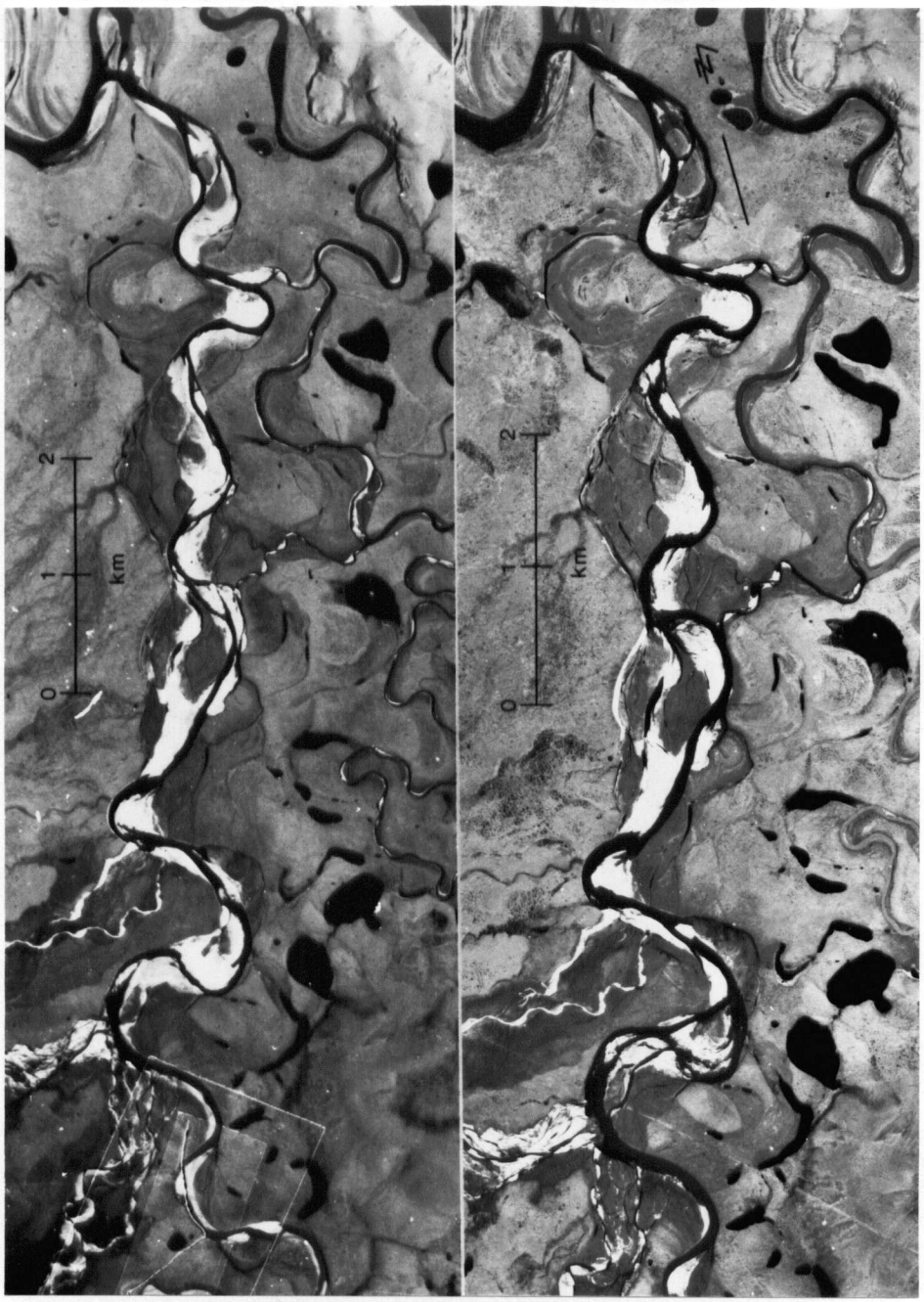


FIGURE 136

Lower Babbage River between Trail River and furthest-seaward gravel riffle, in 1954 (left) and 1976 (right); parts of NAPL photographs A14406-48 and A24502-170.

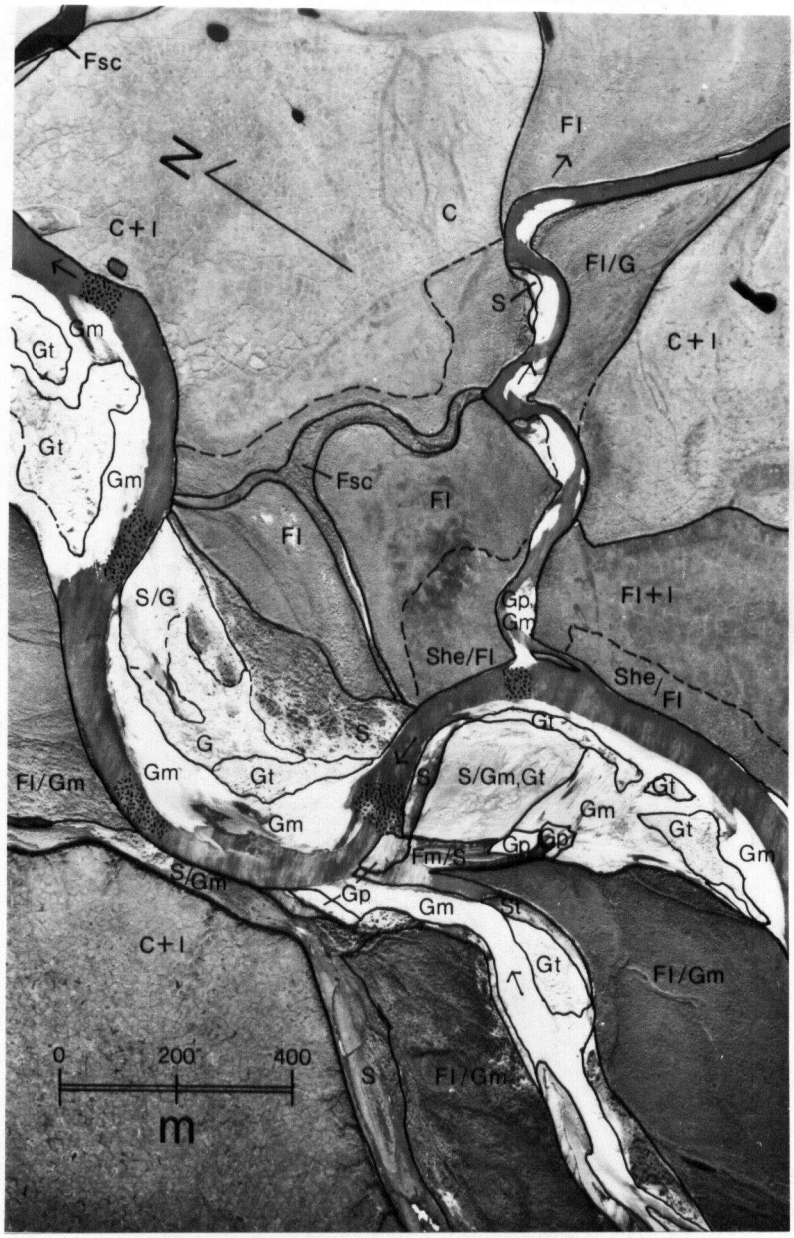


FIGURE 137

Distribution of lithofacies types at the surface, Babbage River and distributary channel immediately downstream from section B1; part of NAPL photograph A21826-87, August 1970.

major gravel and sand storage sites in the fluvial subsystem (cf. Church and Jones, in press).

Bar deposits (Figure 137) are predominantly sandy gravel ($6<D_{50}<12$ mm) of lithofacies Gm, massive or with crude horizontal bedding, formed by progradation of thin gravel sheets across the bar surface. Planar cross-stratified gravel (lithofacies Gp) is formed in diagonal, transverse, and chute bars. Extensive dune-scale scours may generate trough-fill deposits of lithofacies Gt on upper bar surfaces, while similar features are seen locally in the channel. Imbricate lag gravel ($12<D_{50}<20$ mm) is characteristic of most bar and channel surfaces, except where sand or mud have been deposited over gravel. Channel-fill sands of lithofacies St, Sr, and Sh may be preserved locally in some quantity, while minor deposits of lithofacies Sr, Sh, Sre, She, Fm, and C, observed on bars at low flow, are believed to have relatively low preservation potential. All of the foregoing features are attributable to events at synoptic or longer time scales, primarily to the annual snowmelt flood and to rare storm runoff events of comparable magnitude.

The vertical sequence exhibits abrupt upward transitions from gravel to overbank and terrace deposits of facies Fl and She ($0.01<D_{50}<0.3$ mm). In some cases, a more gradual transition through sand occurs where bar topography grades smoothly upward to the valley flat level. An important aspect of the sediment distribution in the lower valley is the limited horizontal extent of channel gravel (Figure 135). Extensive

overbank fines, aeolian sand, lacustrine deposits, and peat occur in the intervening areas. These materials with associated ground ice may acquire thicknesses greater than 8 m, the maximum observed value.

### 4.4.3 DELTA PLAIN FACIES

Depositional environments of the delta plain (Figure 138) include vegetated supratidal flats, ephemeral ponds, lakes with and without closure, tidal channels, and flood splays. The supratidal delta plain ranges in elevation between 0.7 and 1.6 m above mean water level (Figure 139). The upvalley boundary is delineated by driftwood accumulations (Figure 53), by the limit of halophytic flora, and by morphological criteria, in particular the absence of unmodified low-centre polygons on the delta-plain.

Vegetation on the delta plain is dominated by very short salt-tolerant grasses and sedges (mainly Carex Ramenskii and Puccinellia phryganodes). A tall grass, Elymus arenarius, dominates some marginally higher levee surfaces and other relatively well-drained sites that appear pale in Figure 138A. No upright woody plants grow on the delta plain. Stands of Hippuris are found in shallow ephemeral ponds (Figure 138B), often with Ranunculus Pallasii and R. Gmelini (J. Teversham, personal communication, 1975).

The high concentration of lakes on Arctic deltas has been remarked upon by other workers (Mackay, 1963a; Ugolini, 1975). The proportion of the total area of Babbage Delta supratidal flats occupied by lakes larger than 100 $m^2$ is 0.23; this compares with a value of 0.09 for an area of comparable size in the lower valley. The lake-area distribution in the central delta plain (bounded by the outer distributary channels)

FIGURE 138

Air and ground views of Babbage Delta, showing distributary, lacustrine, and supratidal components of the sediment system.

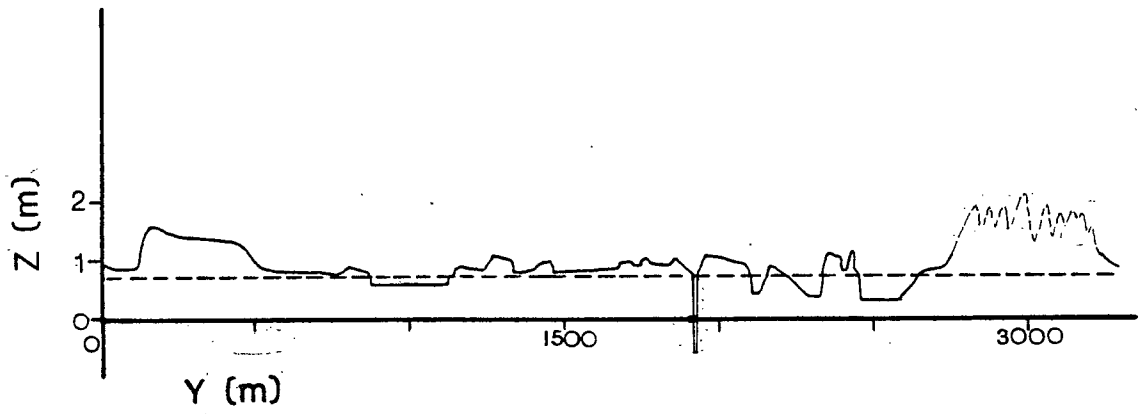


FIGURE 139

Topographic profile of central Babbage Delta along grid line yyy=040 (see Figure 5); proximal delta at left, distal margin with anomalous elevated surface at right.

differs substantially from that in the delta-margin areas (between the the outer distributaries and the valley sides, excluding the area of very large lakes in the southern corner of the delta). The distributions are presented in Figure 140. While lakes smaller than 100 $m^2$ represent between 40 and 60 per cent of the total population in the central delta, they consitute just under 90 per cent of the total in the marginal areas.

Dionne (1972) proposed a mechanism for the formation of shallow angular depressions on intertidal flats by removal of material when bottomfast ice is floated off the bottom. Ugolini (1975) proposed a mechanism for the initiation of thermokarst lakes on an Arctic delta plain by differential thaw beneath ice-rafted sediments. Whatever the initiating mechanism (spatially variable snow depth and ponding of floodwaters may be important factors), thermokarst processes are believed to play a major role in the development of Babbage Delta lakes.

These basins, which form distinctive depositional subenvironments on the delta plain, represent a form of long-term adjustment in the system. Lake depths are highly variable and may be as great as 5 m (Figure 141). Within individual lakes, the variance spectrum of the sedimentation process depends in large part on whether a tidal channel connection exists; if so, synoptic-scale events may be important during the summer months (see Table 27); if not, the basin is essentially decoupled from the sediment cascade,

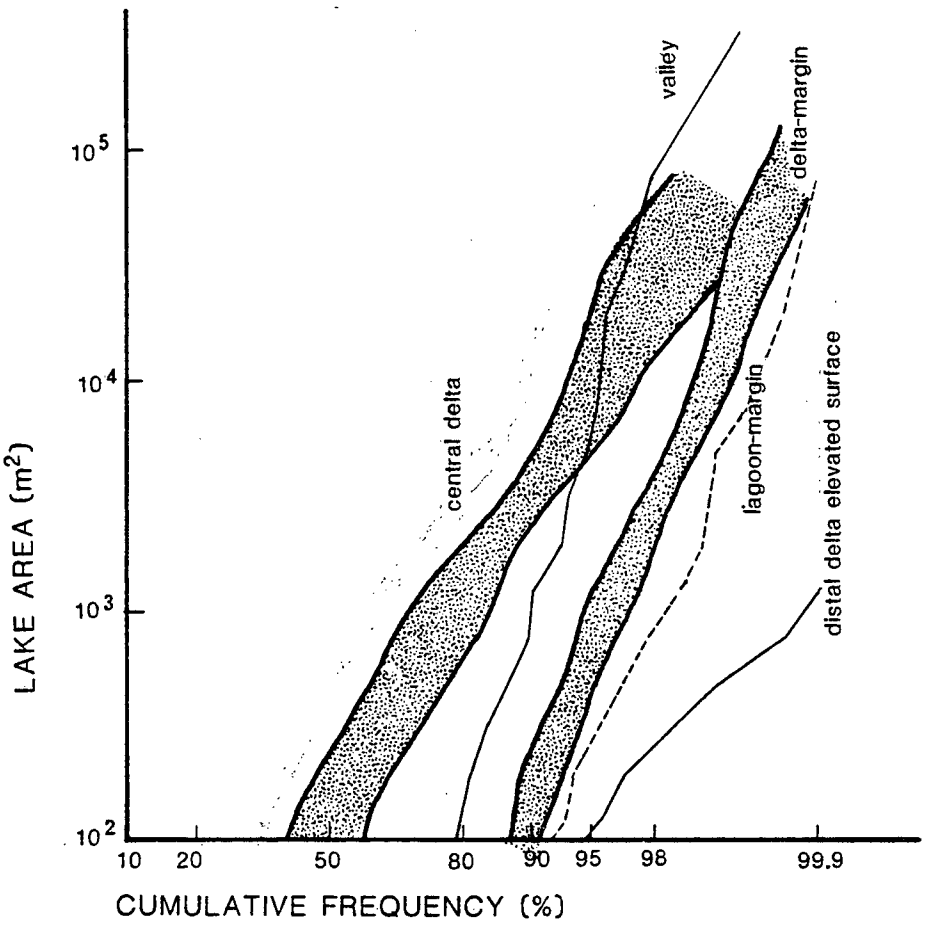


FIGURE 140

Frequency distributions of surface area for various subsets of the pond and lake population on the Babbage Delta; also plotted are distributions for an area of lagoon-margin supratidal flats, for anomalous surface with rugged microrelief on distal delta, and for a representative area in the lower valley.

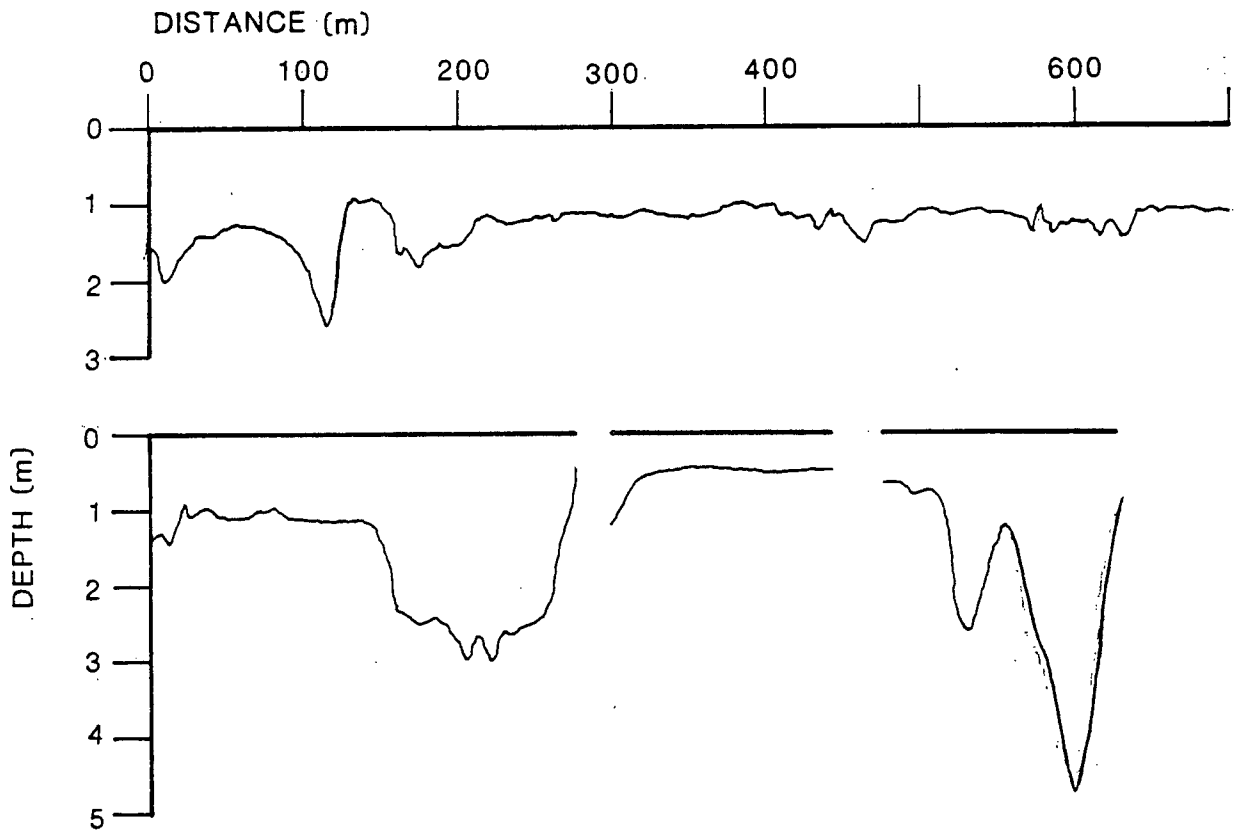


FIGURE 141

Long profile of tidal channel and cross-profiles of three lakes in the central Babbage Delta.

except during snowmelt/breakup flood events, and no significant synoptic-scale variance may occur (measurable sedimentation due to storm-surge flooding has not been observed on the delta plain). In both cases, however, the snowmelt flood may produce the largest inputs of inorganic sediment. Lake sediments vary from black ooze to sandy silt, depending upon location, tidal and floodwater access, and probably depth. Sand is believed to be largely restricted to sites of flow expansion in through-flow basins and accumulates primarily during spring flooding. Shallow basins (Figure 138B) accumulate stratified muds of lithofacies Fl, with algal mats and dessication cracks. Deeper basins may contain massive or finely laminated silts or muds of facies Fsc.

Levees of the Babbage Delta are low and poorly developed (Figure 142). It is not clear to what extent this may be due to the absence of trees and shrubs and to the low hydraulic resistance generated by Elymus during overbank flow. Low levees are characteristic of the distal Mackenzie Delta, north of the tree line (Mackay, 1963a) and of the Blow and Running River deltas. A distinctive area without lakes bordering the main distributary channel (Figures 143 and 144) can be considered a poorly developed crevasse-splay (cf. Welder, 1959); the term 'flood-splay' has been adopted in the present context. There is no well-defined levee and the interdistributary surface (the supratidal delta plain) is high relative to mean water level (Figure 139). The surface is largely unvegetated and receives sediment during annual

FIGURE 142

Levees in the Babbage Delta; A: prominent levee beside minor distributary channel, northern distal margin of delta plain; B: bank with negligible levee development, more typical of the distal delta, right bank of main distributary channel between stations 10 and 12.

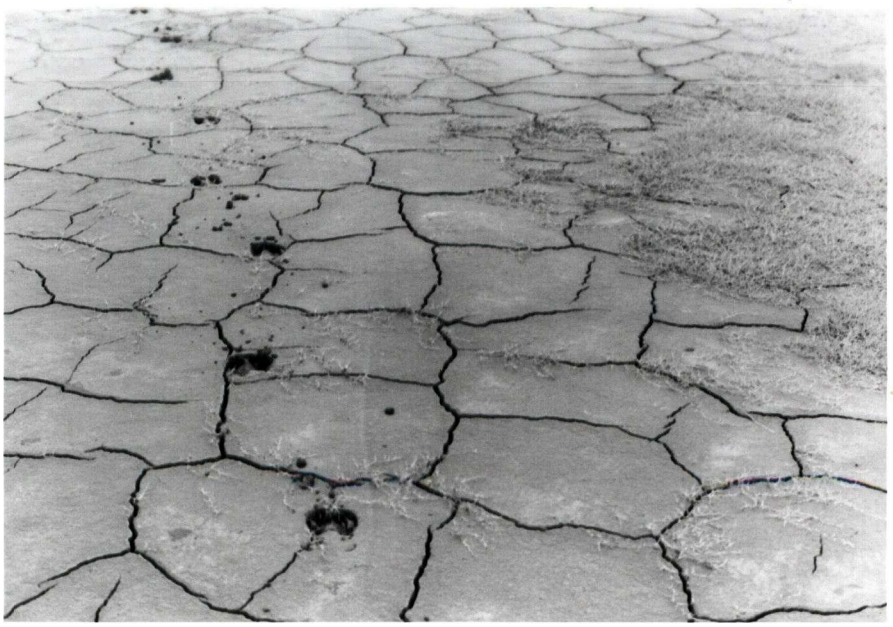

FIGURE 143

Proximal delta plain; (A) looking upvalley, showing vegetated supratidal surface with lakes at left and flood-splay unit at bottom right; note abandonned Babbage River channel in middle distance; (B) sparsely vegetated supratidal flood-splay surface.

FIGURE 144

Flood-splay sedimentation surface adjacent to main distributary channel, central Babbage Delta; part of NAPL photograph A21826-81, August 1970.

snowmelt/breakup flooding. Proximal flood-splay deposits are sandy silt ($20<D_{50}<52$ μm) of lithofacies Fl or Fm, with dessication cracks and various imprints (Figure 143B) sand of lithofacies Sr, Sh, and Se occurs also (note wind-drift lineation in Figure 144 centre).

Deposits of the deltaic supratidal flats are predominantly stratified organic silts ($8.3<D_{50}<36$ μm) of lithofacies Fl (Figure 145). Combustible fractions (12 h at 550°C) range from 5 to 16 per cent. Roots, peat layers, and thin sand units are common; minor gravel is very rare. These deposits are primarily attributable to snowmelt/breakup flood events. Driftwood scattered over the delta plain may be incorporated into sediment of lithofacies Fl (Figure 145A), and locally forms accumulations that may be classified as lithofacies W, associated with synoptic-scale storm surge events. Ice-scour grooves and blocky deposits associated with ice-thrusting occur locally; these probably have low preservation potential, being most common along erosional banks. Organic silts of the delta plain are ice-rich near the surface at many sites. Shallow cores about 2 m in length obtained for the present study confirmed earlier reconnaissance results, indicating an excess ice content typically "greater than 10 per cent [by volume] and occurring in pure ice lenses as thick as 25 cm" (McDonald and Lewis, 1973, p.86). Ice wedges are present in some parts of the delta plain.

An anomalous rugged surface with local relief exceeding 2 m (known in the field as 'Chaos Island') occurs near the

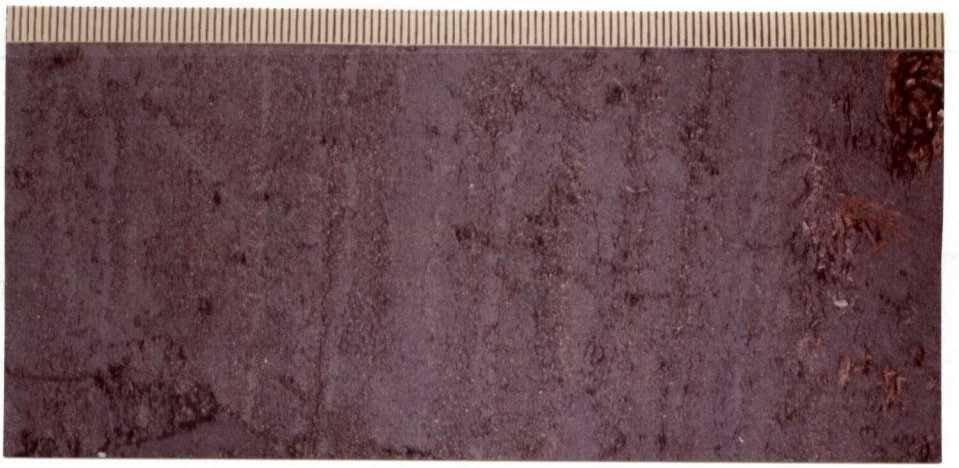

FIGURE 145

A: spruce logs (driftwood) in supratidal sediments of the Babbage Delta; B: stratified organic silts of the supratidal delta plain, part of section 405 in the central delta (see Figure 6 for location); upper part of section to left; millimetre scale.

distal margin of the Babbage Delta (Figure 146; McDonald and Lewis, 1973, figures 55 and 56). A smaller area of similar morphology is found in the central delta plain. The mean elevation of 'Chaos Island' is higher than that of the adjacent supratidal flats. This may be due in part to a massive ice body underlying part or all of the rough surface area (see stratigraphy in borehole 74-4, Figure 134). A heavy driftwood accumulation surrounds the elevated surface. Numerous ponds occupy closed depressions surrounded by high irregular ridges. The size distribution of these basins is plotted in Figure 140, indicating that more than 94 per cent are smaller than 100 $m^2$. The chaotic morphology of this anomalous surface may have developed by a combination of thermokarst and heaving processes. Rising sea level and thermal degradation of an ice-wedge polygon net may have been important factors. Ice-wedge thaw is occurring at present on the lower supratidal surface along the seaward edge of 'Chaos Island'. Similar morphological development, but with more subdued relief, can be found on delta- and lagoon-margin supratidal surfaces (see Figure 147 and section 4.4.5 below).

Estimates of long-term mean sedimentation rates in the Babbage Delta are provided by radiocarbon dates from three sites (see Figure 6 for locations), two on the deltaic supratidal flats (sites 405 and 408) and one on a high intertidal surface in a shallow flood basin on the distal delta plain (site 406). Samples were taken from peat horizons in stratified organic silts at sites 405 and 408 and from peat

FIGURE 146

Anomalous raised surface of rugged microrelief at distal margin of central delta plain, June 1976.

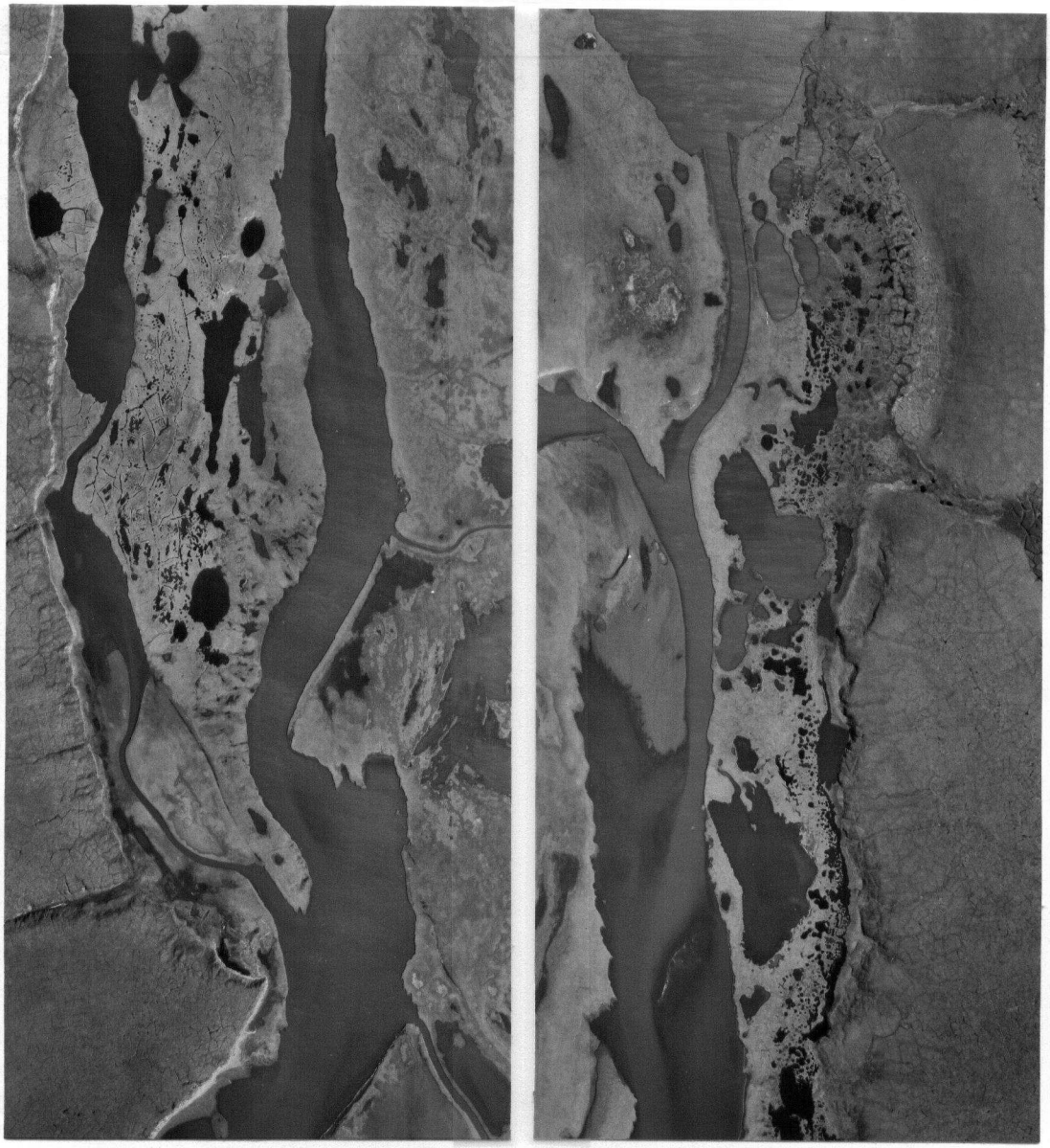


FIGURE 147

Marginal supratidal flats of Babbage Delta, showing complex morphology arising in part, at least, from degradation of ice-wedge polygons; similar features occur on anomalous elevated surfaces in the delta and on lagoon-margin supratidal flats, but are absent from most of the central delta. Parts of NAPL photos A21826-220 (left) and A21826-70 (right), August 1970.

underlying interlaminated sand and mud at site 406. Material from site 408, 420-520 mm below the surface, was dated 1380±80 years B.P. (GSC-2330). The sample from a depth of 870 mm at site 405 gave a date of 2110±90 years B.P. (GSC-2691). A date of 2250±130 years B.P. (S-1482) was obtained on peat underlying 0.91 m stratified mud and sand at site 406. The radiocabon dates suggest net accumulation rates greater than or equal to 0.34±0.05 mm $a^{-1}$ (408), 0.41±0.02 mm $a^{-1}$ (405), and 0.41±0.02 mm $a^{-1}$ (406). These remarkably consistent results are not incompatible with the mean thickness, 1.03 mm freshly deposited, of the 1976 sediment increment in the central delta plain (Table 25). Nevertheless, the long-term estimates are considered minimum values because another sample (S-1481), collected 250 mm above GSC-2691 in the same exposure (site 405), yielded a date some 1000 years younger (see Appendix A.13), confirming suspicions that some or all of the dated material may have been reworked from other Holocene peat exposures in the area.

### 4.4.4 DISTRIBUTARY AND INTERTIDAL FACIES

Four major tidal distributary channels carry runoff across the Babbage Delta. Maximum depths range from 0.9 to 8 m, widths from 26 to 519 m, and width/depth ratios from 19 to 465. Channel sinuosities are generally less than 1.2, considerably less than in the river.

Thalweg sediments of the main distributary channel are predominantly sands of facies St and Sb (cf. Figures 112 and 148A). Bar-scale cross-stratification of lithofacies Sp is present in some 7 kHz sounding records (Figure 148B, after McDonald and Lewis, 1973, figure 59). These deposits record events predominantly at synoptic or longer time scales.

Sediments of the intertidal distributary bars (channel-margin environment) contain higher proportions of silt (Figure 131) and exhibit flood-oriented bedforms generating dune-scale planar cross-stratification of lithofacies Sp and ripple-scale cross-stratification of lithofacies Sr (Figure 149A). Horizontally laminated silty sands of lithofacies Sh or Ff may predominate. Diurnal-scale (tidal) processes evidently play a role in the development of these deposits; however, synoptic-scale events are also important. Ice-rafted gravel (Figure 149B) is a rare feature associated with seasonal-scale processes.

Channel-margin surfaces merge in places with intertidal flats remote from the channels (Figure 150); although the distinction between the two is largely arbitrary,

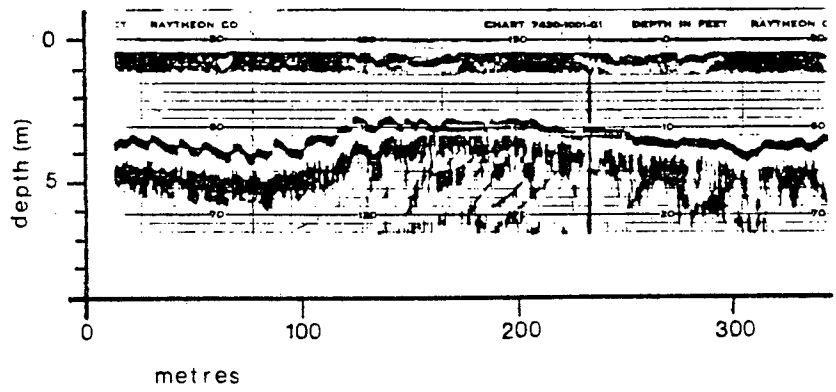


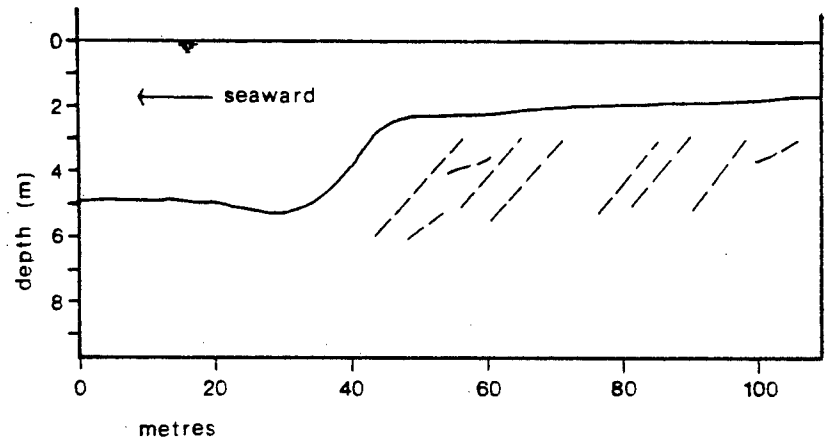


FIGURE 148

A: 7-kHz record from main distributary channel, proximal delta; B: interpretation of 7-kHz record from main distribuary, distal delta near station 10. These records show both dune-scale cross-stratification of lithofacies St and bar-scale cross-bedding of lithofacies Sp.

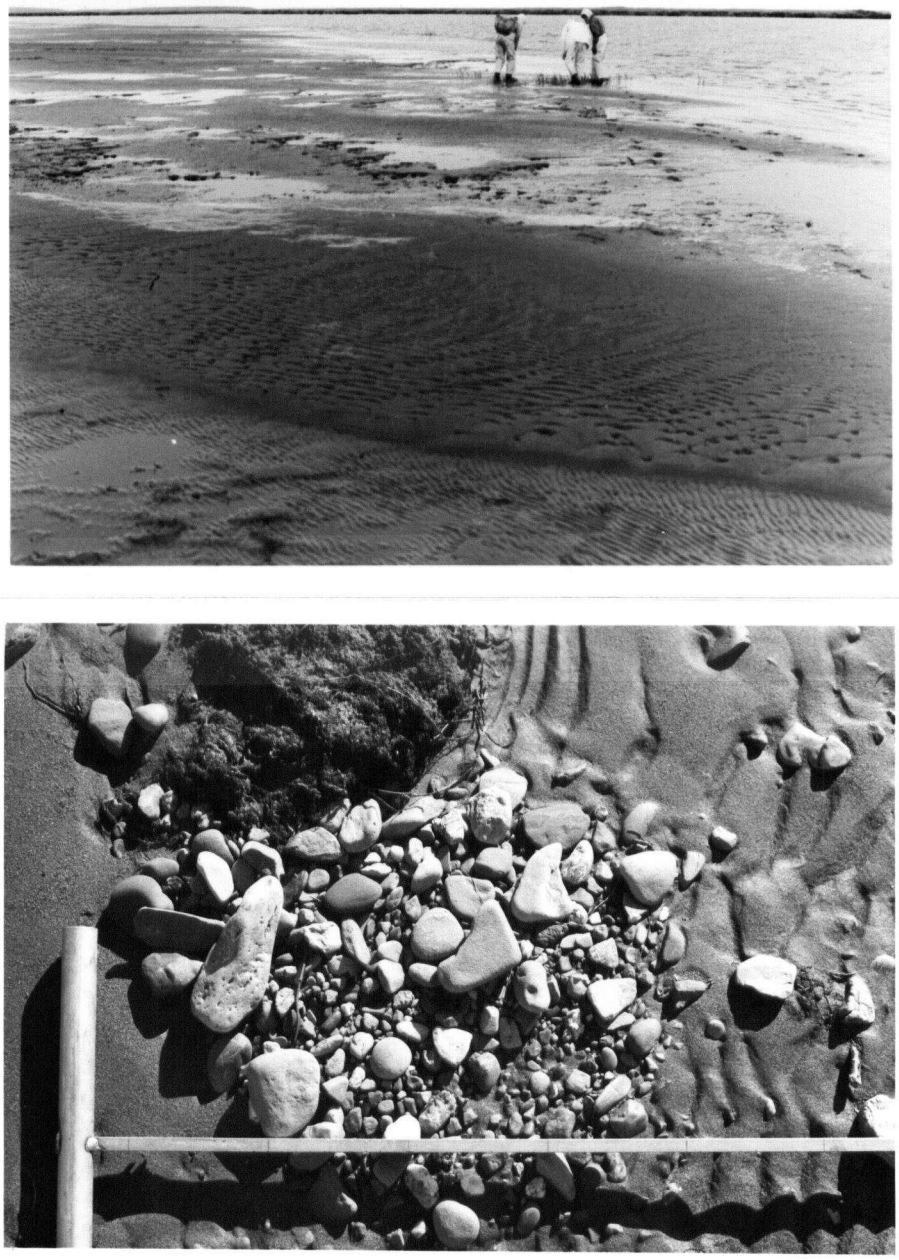

FIGURE 149

A: flood-directed dune- and ripple-scale bedforms on distributary-margin surface near transect 4, proximal Babbage Delta; B: ice-rafted gravel on distributary-margin intertidal surface, central delta (probe is 10x10 mm in section and graduated at 100-mm intervals).

flood-oriented deposits of lithofacies Sp have been observed only adjacent to major channels. Sediments of the upper intertidal appear to be accumulating over an eroded supratidal surface and to be infilling former lake basins of the supratidal flats (Figures 150 and 151A; cf. Figure 125). Dendritic tidal channel networks are well developed in some areas (Figure 151A). Patches of colonizing vegetation, primarily Puccinellia phryganodes, occur on low hummocks and levees bordering the small channels; stands of the same species bordering the tidal basins appear to be vestiges of supratidal surface, over which tidal sediments are prograding from the basin side, while erosion of the distal edge (often a low scarp) continues (see Figure 151A).

Sediments of the intertidal subsystem are sands and silts ($34<D_{50}<92$ μm) of lithofacies Sr and Ff (Figure 152). Individual units range from order 0.1 mm to order 10 mm in thickness, reflecting synoptic-scale variance in the system (cf. Table 26) but probably also including storm events of multiyear rank and seasonal snowmelt-runoff inputs that vary from year to year. Dessication cracks and scour enlargement of cracks are common post-depositional features, which may be associated with diurnal time scales. Drainage vents are sometimes observed on low intertidal surfaces exposed during synoptic-scale spring-tide or negative surge events (Figure 151B). Vents such as these are associated with vertical drainage channels in the sediment (cf. Migniot, 1968, figure 12C).

FIGURE 150

Channel-margin and lagoon-margin intertidal surfaces in the Babbage Delta, August 1974.

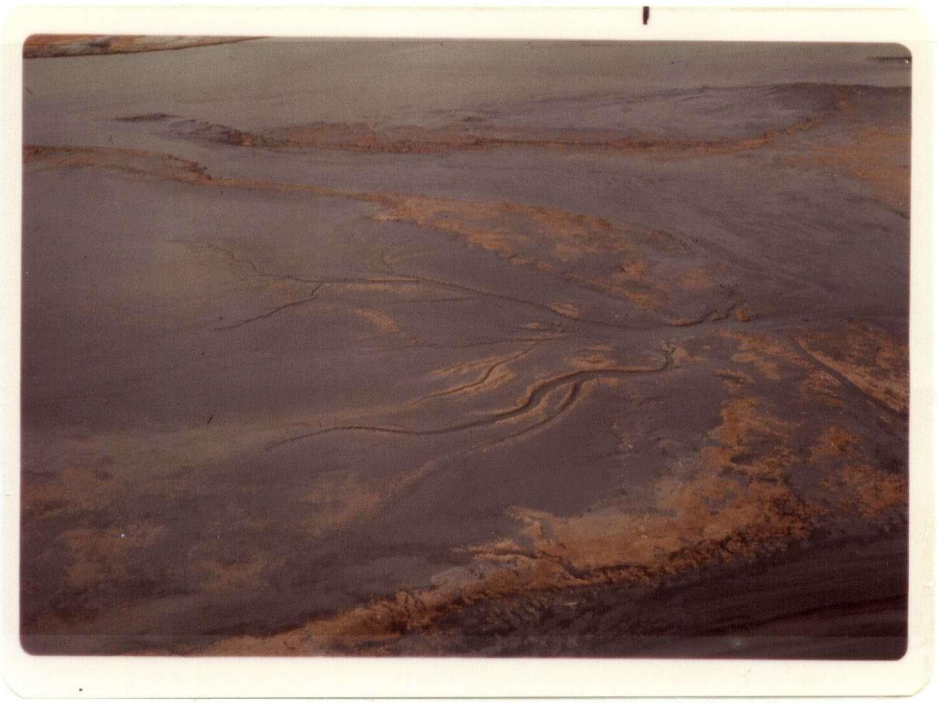

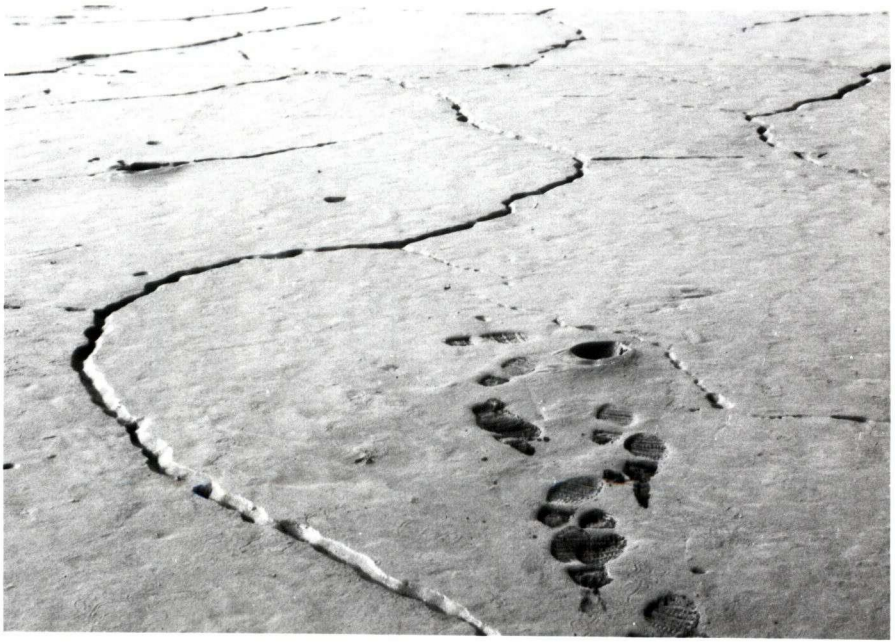

FIGURE 151

A: intertidal flats near transect 8, distal Babbage Delta, showing tidal channel network, with patches of colonizing Puccinellia on levees, and erosion of supratidal surface, September 1976; B: dessication cracks, associated small-scale scour, and drainage vents on low intertidal surface.

FIGURE 152

Core sections from high intertidal surface in shallow basin, distal delta plain (site 406, Figure 6). Left: 130-285 mm below surface; right: 380-470 mm below surface; millimetre scale at right. Note interlaminated mud and sand, scour structure at upper left, and minor small-scale cross-lamination.

Major changes in the surface configuration have occurred during recent decades near the main distributary outlet in the southern lagoon. In 1952 (Figure 127), the channel bifurcated seaward of the distal delta margin. By 1970, a single channel had developed, as seen in 1972 photography (Figure 105). The evolution of the channel in this area seems to be consistent with a model of temporary channel bifurcation in a non-stratified outlet (Bates, 1953; Welder, 1959; Mikhailov, 1966), followed by abandonment of one branch, in this case the branch more exposed to waves propagating into the lagoon through the main entrance section. At present, low intertidal and subtidal levees extend seaward to a point about two-thirds of the distance from station 10 (distal delta) to Niakolik Point. A distributary mouth bar is present at the distal limit of the levee (see Figure 3). Applicability of a non-stratified flow model would support the concept that most significant changes in the channel outlet occur during spring runoff, when the estuary is entirely fresh and non-stratified (section 3.3.4).

### 4.4.5 LAGOON, BARRIER, AND MARGINAL FACIES

The Babbage Lagoon can be subdivided into a northern basin transected by a long narrow shoal parallel to the barrier, a southern basin south of Niakolik Point, and a central region (the 'open-estuary') that receives discharge from the main distributary channel and is exposed to waves moving into the entrance (see Figure 3 for bathymetry). The entrance area contains a broad central shoal, which differs from the morphology commonly associated with tidal inlets in mesotidal and some microtidal estuaries (Hayes, 1975; Reinson, 1977). Existing models for microtidal inlets in medium wave energy environments (Hayes, 1979, figure 4) involve extensive flood-tidal deltas and relatively minor ebb-tidal deposits (cf. also Reinson, 1980, figure 3.18; Armon, 1980). The entrance shoal morphology in the Babbage Estuary bears little resemblance to the model. Furthermore, no major bedforms have been observed in the entrance section, except on the distal margin of the central shoal and around the end of Kay Point spit, where bars were present in 1976 (Figure 153), apparently associated with synoptic-scale wave-transport of sediment onto the shoal and into the estuary.

Sediments of the open-estuary are predominantly silty sands (see section 4.4.1), presumably stratified, possibly with extensive ripple cross-stratification (lithofacies Sr). A wide variety of stratification types may be present in association with the bar morphology illustrated (cf. Davidson-Arnott and Greenwood, 1976). The mean combustible fraction, estimated

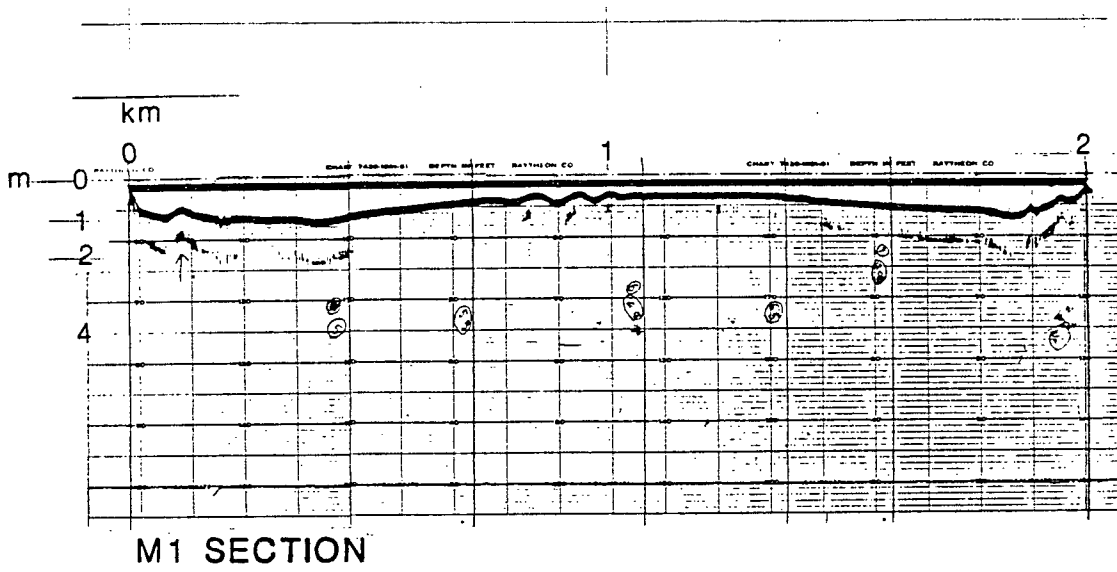


FIGURE 153

Profile of M1 (main entrance) section, Babbage Estuary marine boundary, 12 August 1976.

from four open-estuary samples, is 6.1±0.9 per cent.

Sediments of the protected lagoon basins include a wide variety of silt, mud, silty sand, and muddy gravel (Figure 131) of lithofacies Fsc, S, Sp, and Gms. The silts and muds are massive or finely laminated; structures are disrupted by benthic organisms and, it is surmised, by adfreezing to bottomfast ice. The composition of the benthic invertebrate fauna at a site in the southern lagoon basin is given in Table 31. The mean combustible fraction of lagoon samples (excluding open-estuary sites) is 6.8±0.6 per cent (n=13) and ranges from 3.5 per cent in gravel-rich material at site 020150 to a maximum of 11.8 per cent in the pebbly mud at site 030090.

No evidence of ice-scouring was found in extensive side-scan sonar surveys within the lagoon, but ice-scour features were observed on shoal gravels (Figure 154). Scattered driftwood logs occur in the lagoon; in the small embayment at the north end of the lagoon near Kay Point, numerous logs litter the shallow subtidal surface and form a significant component of the deposit accumulating there. Movement of grounding driftwood by ice or wind may generate linear grooves similar to ice-scour features, but the preservation potential of these in the shallow lagoon environment is apparently low.

The barrier morphology also differs significantly from the microtidal model of Hayes (1979) and from other microtidal barriers of the Texas coast (Scott et al., 1969), the west

TABLE 31

Benthic invertebrates in Ekman dredge samples from the Babbage Estuary near station 7a, 24 July 1975 (data from Kendel et al., 1975, pp. 85-88).

depth h=1.4 m — area sampled: 0.234 $m^2$
temperature $\Theta_w(h)$=9.1°C
salinity $s_h$=7.5ppt

| order | number species | number individuals | individual abundance |
|---|---|---|---|
| Polychaeta | 2 | 201 | 859 $m^{-2}$ |
| Amphipoda | 3 | 526 | 2248 $m^{-2}$ |
| Isopoda | 1 | 15 | 64 $m^{-2}$ |
| Mysidacea | 2 | 6 | 26 $m^{-2}$ |
| total | 8 | 748 | 3196 $m^{-2}$ |

FIGURE 154

Gravel forming low intertidal shoal (site 032080) in Babbage Lagoon, showing linear grooves attributed to ice scour.

Alaska coast (Hayes, 1979), and the Gulf of St Lawrence coast (Owens, 1975, 1977; McCann, 1979; Armon, 1979). The Babbage Estuary barrier (Figure 155A), and others on the Yukon coast, lack aeolian dunes and the major washover fans observed elsewhere; however, some Yukon coast barriers such as Shingle Point spit (Figure 155B) possess complex backbarrier morphology, reflecting a postulated history of vertical aggradation, seaward progradation, more extensive washover transport, and major ice-thrust events.

Kay Point spit is characterized by narrow width (30-300 m), a low driftwood-strewn berm, and laterally extensive washover deposits forming a long gently-sloping backshore surface on the lagoon side of the berm (Figures 155A and 156). Washover transport during infrequent storm events forms cross-stratified sands of lithofacies Sp at the backbarrier shore (Figure 157), where subsequent modification by waves within the lagoon may form bipolar cross-stratified sands (lithofacies Sb) and low-angle stratification (Sl). Wide subtidal backbarrier platform deposits have developed at some sites as a result of long-term inlet migration, local progradation, and distal extension of the spit (cf. Figures 105 and 127). Figure 156B shows the backbarrier platform at the distal end of the spit as it was in 1974.

On the seaward side of the barrier, small bar features associated with synoptic-scale wave events may generate local cross-sets of lithofacies Sp, directed toward shore, in association with widespread deposits of lithofacies Sl.

FIGURE 155

A: Kay Point barrier, with Phillips Bay at right and Babbage Lagoon at left, showing wide backshore surface largely snow-free, May 1976; B: Shingle Point spit, showing extensive and complex backbarrier deposits, August 1975.

FIGURE 156

A: distal Kay Point spit, 27 August 1975, following a severe storm and moderate surge, showing limited extent of washover deposits, aeolian sand accumulation near large logs on berm, and ice incorporated in foreshore sediments; B: distal end of spit, 2 August 1974, showing subtidal backbarrier platform and post-1972 extension of the spit.

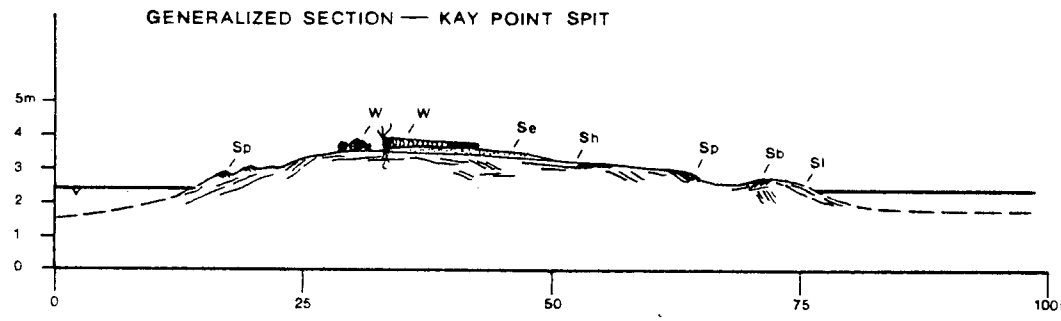


FIGURE 157

Schematic section through Kay Point spit, showing distribution of upper barrier lithofacies (in part after McDonald and Lewis, 1973).

Horizontally-laminated sands and pebbly sands (lithofacies Sh), formed by minor washover transport that may not extend to the backbarrier shore (Figure 156A), occur on the backshore surface, back of the berm (Figure 157). Minor aeolian sand deposits (lithofacies Se) occur, especially as drifts in the lee of large logs (Figure 156A).

Ice-thrust ridges with heights approaching 2 m have been observed on Kay Point spit (McDonald and Lewis, 1973, pp.59-60) but occur only infrequently (none was observed in 1974-1976; minor thrusting in gravel at Kay Point occurred in 1977) and are generally destroyed within a single open-water season. Deposition of ice cakes on the foreshore and subsequent burial can result in formation of small kettle holes (cf. Thompson, 1953; Nichols, 1961); chaotic microtopography can develop due to melt of buried snow and ice layers originating in various other ways (Short and Wiseman, 1974). Ice- and thaw-generated features are believed to have low preservation potential.

Three distinctive 'end-member' models have been proposed for barrier deposits (Reinson, 1979): these are the regressive (or prograding) model (Bernard and Leblanc, 1965), the transgressive model (Hoyt, 1967; Kraft, 1971); and the barrier-inlet model (Kumar and Sanders, 1974; Barwis and Makurath, 1978). Kay Point spit is a transgressive barrier which has undergone rapid onshore migration during the past 150 years (cf. Figure 12). Minor local progradation has also occurred, however, and migration of inlet M2 during the interval 1952-1972 (cf. Figures 105 and 127) introduces the

possibility of a thin inlet-migration sequence. Distal extension of the spit (Figure 156B) may generate a large-scale cross-stratified (spit-platform) deposit at the base of the transgressive barrier sequence (cf. Kumar and Sanders, 1974). In the present case, however, because of the shallow nature of the inlet channels (Figure 153) and the rapid migration of the barrier, little barrier sediment may have been preserved during historical time. The transgressive sequence is considered further in the following section.

Lagoon-margin supratidal flats (Figure 158A) bear a strong morphological resemblance to the delta-margin supratidal flats illustrated in Figure 147. However, the sandy muds of the lagoon-margin flats (lithofacies Fl) are much more poorly sorted than all but one sample from the delta (see section 4.4.1). These deposits are formed by synoptic-scale storm-surge flooding at seasonal- or annual-scale (multiyear) intervals.

The lagoon-margin supratidal subsytem includes vegetated flats with halophytic Carex-Puccinellia and Elymus communities very similar to those of the delta plain, ephemeral ponds with algal and Hippuris communities, and lakes with and without closure. A major driftwood deposit occurs at the eastern end of the Kay Point flats, while beach and storm-generated washover sands and pebbly sands (lithofacies S, Sl, Sp) interfinger with deposits of the supratidal flats along the lagoon shore (Figure 158).

FIGURE 158

A: lagoon-margin supratidal flats at north end of Babbage Lagoon, showing numerous lakes and ponds, local rugged microrelief, and marginal beach and washover facies, August 1975; B: Carex-Puccinellia and Elymus communities and the landward limit of marginal washover sand.

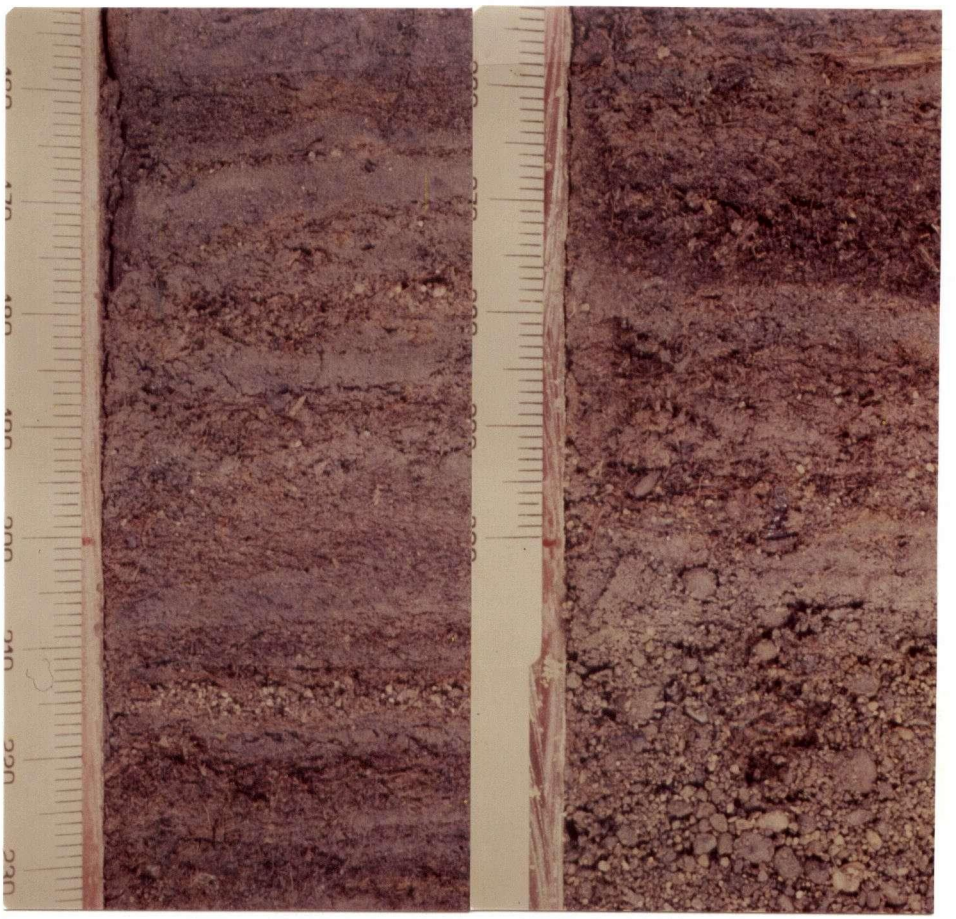

FIGURE 159

Parts of core taken in ephemeral pond near edge of supratidal flats, showing: (at left) near-surface interlaminated algal mud, peat, and sand; (at right) pebbly sand washover unit at a depth of 400 mm.

A core taken in an ephemeral pond about 10 m landward of the most advanced washover sediment at the surface, showed a 400-mm sequence of interlaminated algal mud, peat, sand, and pebbly sand (Figure 159) with a gravel-sand overwash unit at the base. Attempts to date the lower washover unit were frustrated by the presence of fine detrital coal.

### 4.4.6 THE TRANSGRESSIVE SEQUENCE

The behaviour of the estuarine system at very low frequencies (e.g. T>100 years) is dominated by parametric changes associated with coastal erosion and sea level adjustments, in addition to non-stationarity of energy and mass inputs due to climatic fluctuations. The remarkable recession of Kay Point since 1826, suggested by data of Franklin (1828), was documented in section 2.1.2. In addition, there is some evidence to support the concept of a late-Holocene, possibly continuing, submergence of the central Yukon coast (Forbes, 1980). The contemporary stratigraphic context of the Babbage Estuary system is, therefore, transgressive in the sense both of a landward translation of the barrier complex and of a rising relative sea level. This appears to have been the case throughout Holocene time.

While the nature of the sedimentary body within a given subsystem of the estuary is determined largely by short-term conditions, it is the response of the system to long-term trends that establishes the preservation potential and stratigraphic relationship of the various storage components. In a transgressive context, a sequence (progressing seaward) of surficial facies assemblages provides a predictive model for the vertical sequence to be expected if all facies are preserved. Kraft (1971, pp.2140-2145) has presented a surficial transgressive sequence, for sedimentary environments on the coast of Delaware (U.S.A.), which is broadly analogous to the vertical sequence found beneath the Delaware coastal

barrier. An adapted version of Kraft's surficial sequence for a mid-latitude mesotidal system, with a tentative assignment of lithofacies codes, is presented in Table 32A.

The surficial transgressive sequence at the north end of the Babbage Lagoon is presented in Table 32B. Major contrasts between the Delaware and Babbage sequences include the nature of the transgressive limit, of lagoon-margin surfaces, and of the benthic community in the central lagoon; backbarrier margin and aeolian dune components are missing from the Babbage sequence. Similarities between the two cases include the presence of an inner lagoon beach and washover unit and the general pattern of lagoon-margin, lagoon, and barrier environments.

In the Babbage Estuary system, much of the Holocene barrier and lagoon record, at least for the recent part of the transgression, may have been eliminated due to the very rapid rate of barrier migration in historical time and the shallow depths of inlet channels. Figure 160 shows a section normal to the barrier axis, across the Babbage Lagoon, Kay Point spit, and the shoreface in Phillips Bay. The pattern clearly conforms to the transgressive barrier model of Kraft (1971). If the large lagoon depicted in Figure 12 was deeper than the present lagoon, specifically if depths exceeded 6 m seaward of the present barrier, then the entire sand unit observed beneath the shoreface may represent barrier facies of Kay Point spit; otherwise, an undetected unconformity exists within the large sand unit seaward of the barrier and little or none of the

TABLE 32

A

Delaware surficial transgressive sequence
(adapted from Kraft, 1971)

1. HIGH GROUND; Pleistocene surface.
2. TRANSGRESSIVE LIMIT; marsh fringe with sand, silt, and clay; stumps, roots, and marsh flora (Fl, C)
3. LAGOON MARGIN; Spartina alterniflora and S. patens marshes (Fl, C).
4. INNER LAGOON BEACH AND WASHOVER; sand (Sl, Sp).
5. SHALLOW LAGOON; sand and mud (S, Fsc).
6. CENTRAL LAGOON; clay-silt with Elphidium-Crassostrea community, abundant molluscan fauna (Fsc).
7. BACKBARRIER PLATFORM; sand (Sb, Sp).
8. BACKBARRIER MARGIN; Spartina marsh and Pinus community (Fl, C, S).
9. AEOLIAN DUNES; sand (Se).
10. BARRIER BERM-WASHOVER; sand (Sl, Sh, Sp).
11. BARRIER BEACHFACE; sand (Sl, Sp).
12. SHOREFACE; sand (S).

B

Babbage Lagoon surficial transgressive sequence

1. HIGH GROUND; Holocene peat and colluvium over pre-Holocene sediments.
2. TRANSGRESSIVE LIMIT; driftwood (W).
3. SUPRATIDAL FLAT; silt and clay with Elymus, Carex-Puccinellia, Hippuris, and algal communities (Fl, Fsc, C).
4. INNER LAGOON BEACH AND WASHOVER; pebbly sand (Sl, Sp).
5. SHALLOW LAGOON; sand and mud (S, Fsc).
6. LAGOON SHOAL; muddy gravel (G, Gms).
7. CENTRAL LAGOON; mud with Amphipoda-Polychaeta-Isopoda community (Fsc).
8. BACKBARRIER WASHOVER AND BEACH; gravel-sand, sand (Sp, Sl, Sb).
9. BARRIER BERM; gravel-sand and sand (Sh, Sl, Se, W).
10. BARRIER BEACHFACE; gravel-sand and sand (Sl, Sp).
11. SHOREFACE; sand (S,Sp, Sr).

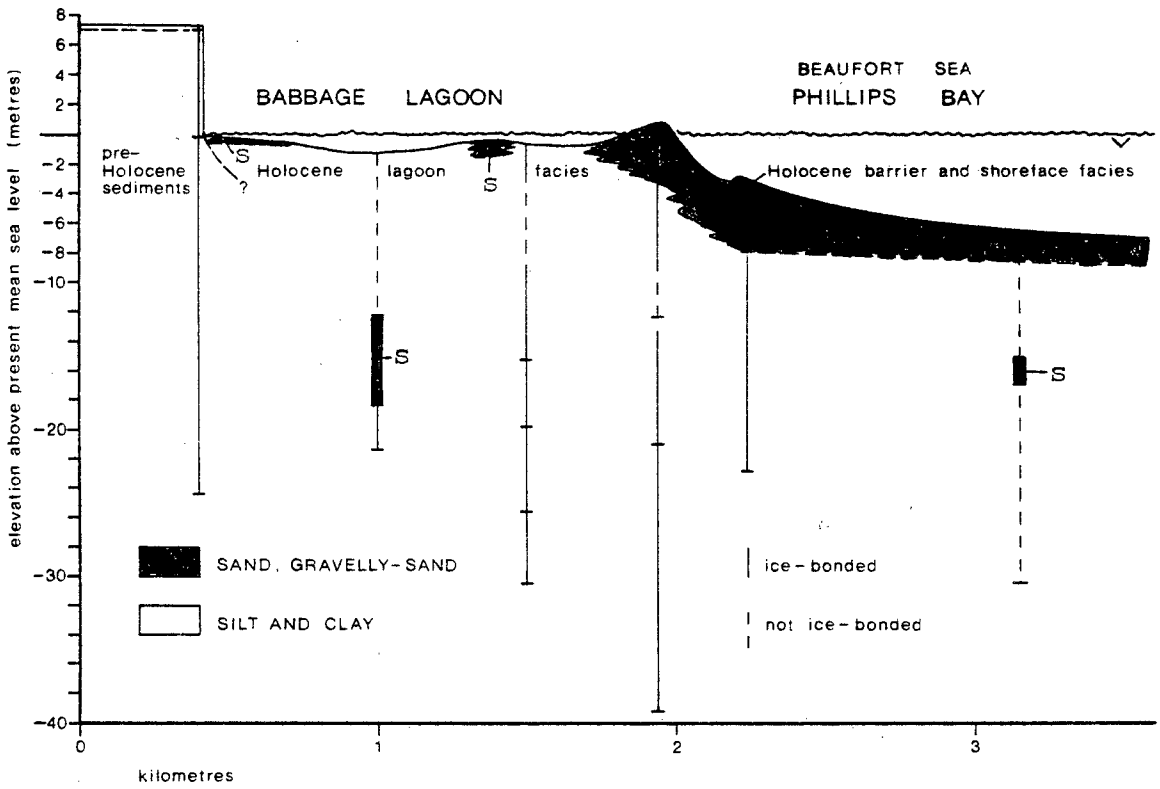


FIGURE 160

Section through Babbage Lagoon, Kay Point spit, and Phillips Bay, showing the distribution of sand and gravelly-sand lithofacies and the transgressive character of the barrier sequence (see Figure 6 for borehole locations).

former barrier deposit may be preserved. Similarly, the depth of the former lagoon would determine whether or not lagoon facies are present beneath Phillips Bay.

It is instructive to compare the late Holocene deposits of the Babbage Estuary system with barrier sequences elsewhere on the Yukon coast. At King Point, where spit progradation between 1954 and 1972 closed the inlet to isolate the lagoon (Figure 161), much of the barrier backshore preserves small-scale beach ridge topography, interpreted as the surficial expression of large-scale inlet-fill cross-stratification (see Figure 162A). At the right-hand side of the photograph, the original morphology has been obscured by washover deposits infilling the swales; note the limit of recent washover just visible in the extreme top right corner (cf. Figure 10B).

The Spring River barrier complex lies directly opposite the Babbage Estuary on the western shore of Phillips Bay (see Figure 12). Whereas Kay Point spit conforms to the transgressive model of Kraft (1971), the Spring River barrier appears superficially to resemble the prograding model of Bernard and Leblanc (1965). Although some erosion occurred on the proximal spit shore between 1952 and 1970, there was substantial accretion at the distal end (Figure 163) and the multiple ridges attest to long-term barrier progradation.

Swift (1975) proposed an informal model for shoreface profile adjustment on a transgressive barrier coast, based on

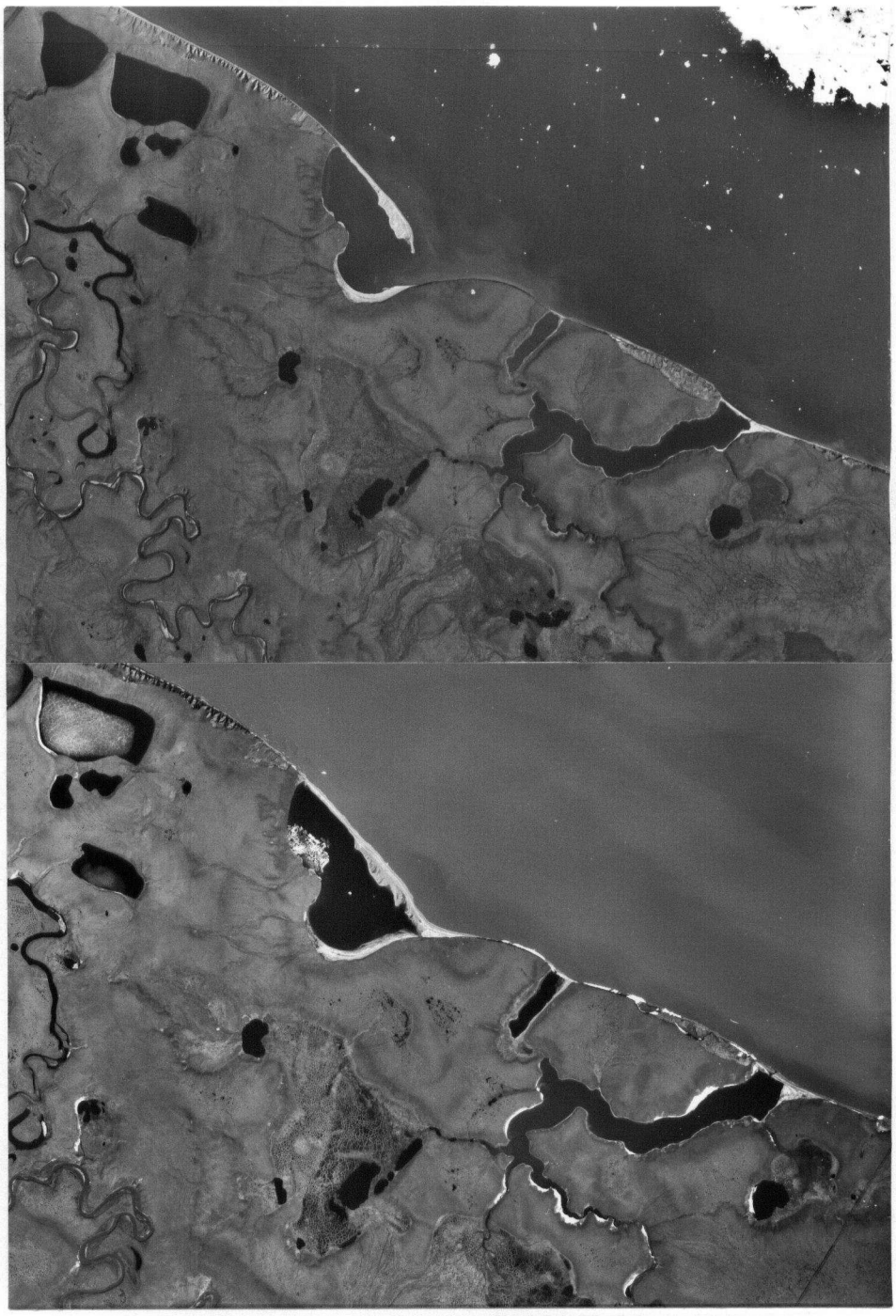

FIGURE 161

Changes in the King Point barrier, 1954-1972, showing development of an inlet-fill sequence by distal extension of the spit; parts of NAPL photographs A14363-54 (1954) and A22879-105 (1972).

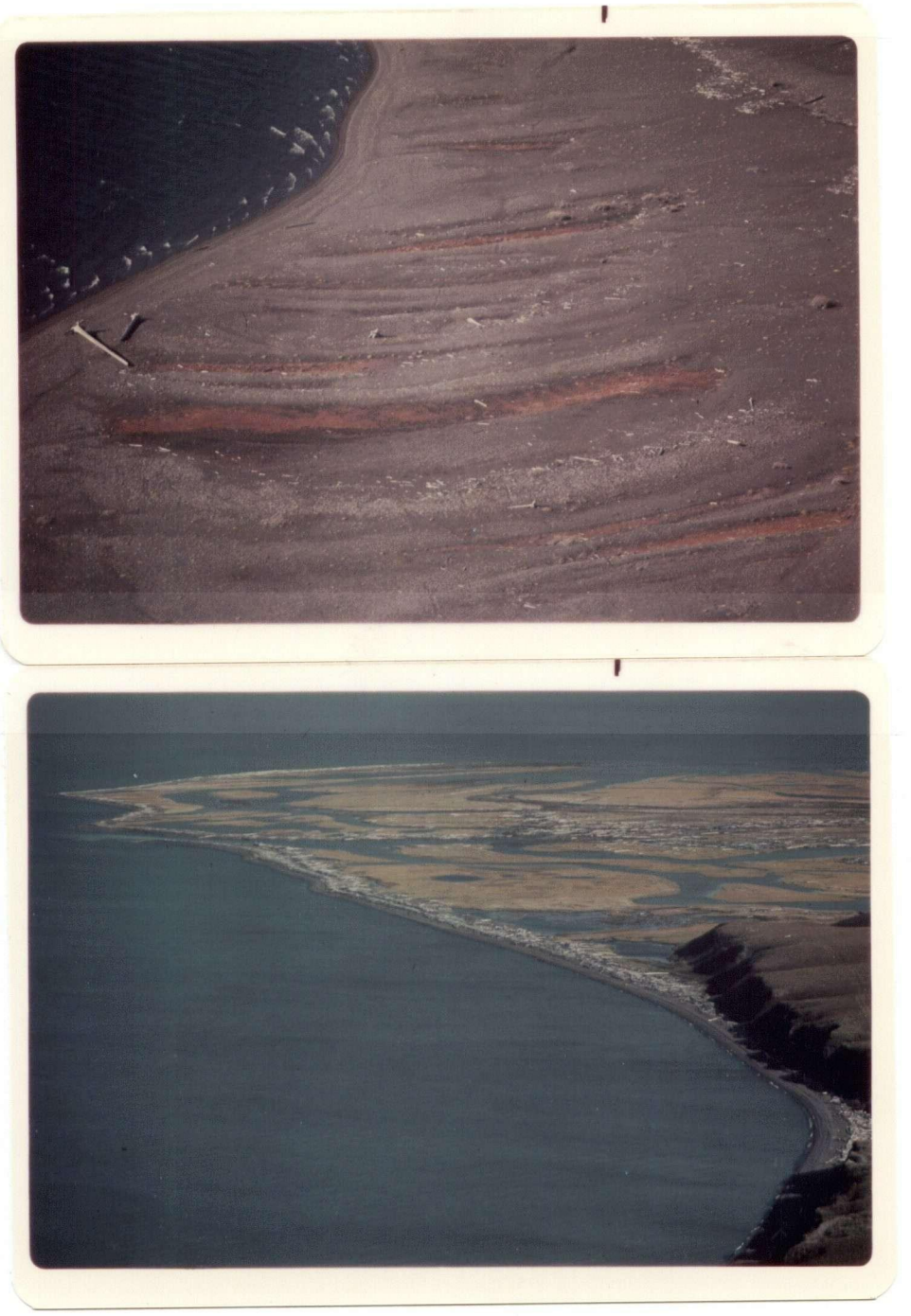

FIGURE 162

A: low-level oblique photograph of surface morphology on the King Point barrier backshore, August 1975; B: Running River delta near Shingle Point, showing beach and washover facies at the seaward margin of deltaic supratidal flats.

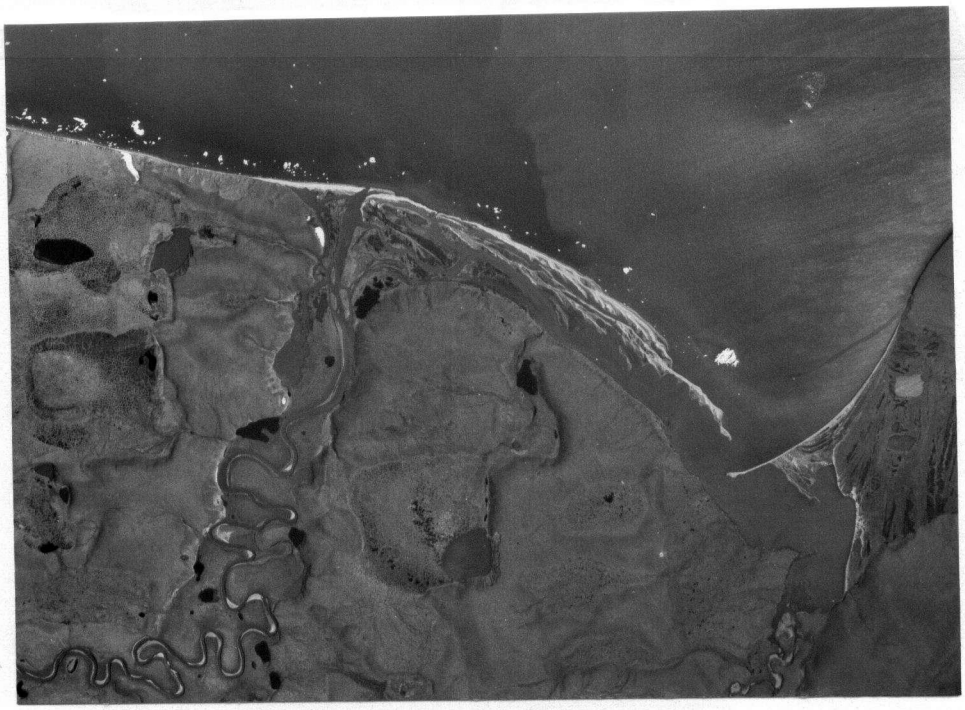

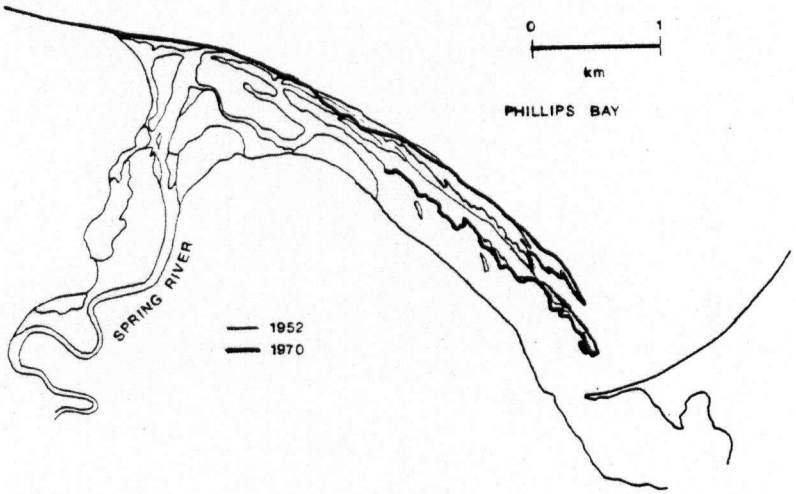


FIGURE 163

Spring River barrier in 1952 (part of NAPL photograph A13383-155) and changes occurring between 1952 and 1970.

continuity principles. He demonstrated the theoretical plausibility both of shoreface retreat, where longshore sediment exports equal or exceed imports (cf. Bruun, 1962), and of shoreface advance, where imports exceed exports (cf. Curray et al., 1969). The results from the Yukon coast confirm that contrasting progradational and erosional regimes may occur in close proximity where differing barrier orientation or other factors alter the local sediment budget. Owens and McCann (1980) have noted a similar juxtaposition on the east coast of the Magdalen Islands, Gulf of St Lawrence.

The surficial transgressive sequence for the Babbage Delta, set out in Table 33), includes all the major environments of the deltaic estuarine system, with the exception of the laterally discontinuous fluvial channel component and anomalous elevated surfaces with extreme microrelief (Figure 146). A three-dimensional schematic representation of the fluvial and deltaic sequence (components 1-6 in Table 33) is shown in Figure 164. This illustrates the hypothesized geometry of channel gravels produced under the contemporary Babbage River regime and a conceptual model for the vertical transition to deltaic and estuarine facies.

In practice, it is unclear to what extent late-Wisconsinan and Holocene sediments analogous to the sinuous gravel river assemblage observed at present in the lower valley have been preserved beneath transgressive deposits of the Babbage Delta. Assuming that the terrace in Herschel Basin at -15±1 m developed as a delta in the late-Wisconsinan/early-Holocene

TABLE 33

Babbage Delta surficial transgressive sequence

1. ALLUVIAL TERRACE; sand, silt, and peat (Fl, She, C).
2. TRANSGRESSIVE LIMIT; driftwood (W).
3. DELTAIC SUPRATIDAL FLAT; silt and clay with Elymus, Carex-Puccinellia, Hippuris, and algal communities (Fl, Fsc).
4. FLOOD-SPLAY; sand and sandy silt (Fl, Fm, Sr, Sh, Se).
5. DISTRIBUTARY CHANNEL; sand (St, Sb, Sr, Sh, Sp).
6. DISTRIBUTARY MARGIN; sand and silt (Sp, Sr, Sh, Ff).
7. INTERTIDAL FLAT; sand and silt with local patches of Arctophila and Puccinellia (Sr, Ff).
8. SHALLOW LAGOON; sand and mud (Sr, Fsc).
9. LAGOON SHOAL; muddy gravel (G, Gms).
10. CENTRAL LAGOON; mud with Amphipoda-Polychaeta-Isopoda community (Fsc).
11. BACKBARRIER PLATFORM; pebbly muddy sand (Sl, Sr, Fm)
12. BACKBARRIER WASHOVER AND BEACH; gravel-sand and sand (Sp, Sl).
13. BARRIER BERM; gravel-sand and sand (Sh, Sl, Se, W).
14. BARRIER BEACHFACE; gravel-sand and sand (Sl, Sp).
15. SHOREFACE; sand (S, Sr, Sp).

Note that units 8-10 and 12-15 correspond to units 5-11 of the Babbage Lagoon sequence (Table 32B).

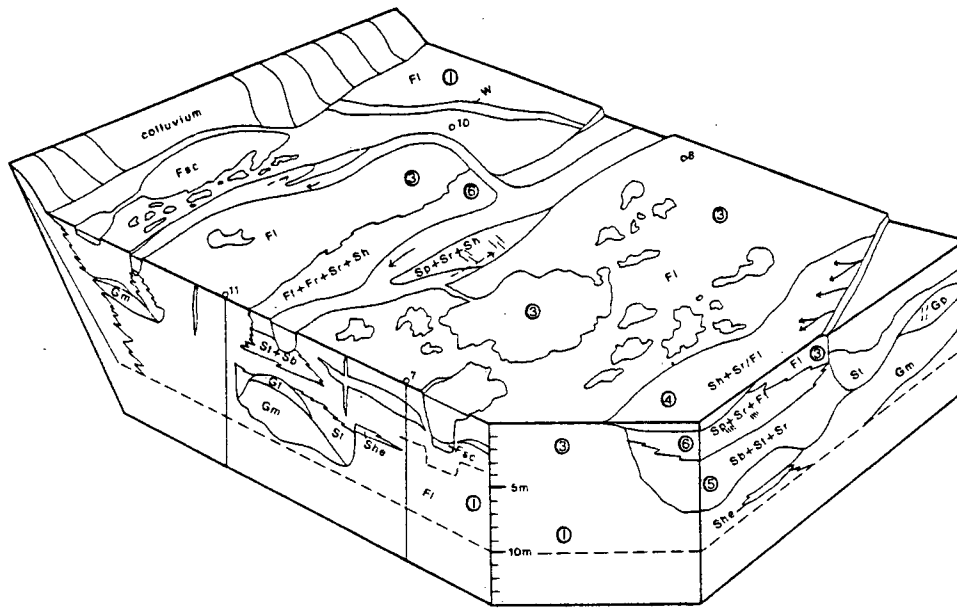


FIGURE 164

Schematic diagram showing hypothetical distribution of lithofacies forming transgressive sequence beneath the Babbage Delta. See Table 30 for explanation of lithofacies codes. Note lateral discontinuity of channel, overbank, and lacustrine facies. Small numbers refer to boreholes (Figures 6 and 134). Circled numbers refer to units of the transgressive sequence (Table 33).

Lake Herschel (Figure 12), extrapolation of realistic valley-axis slopes would put the river well below lake level at the site of the former delta, even assuming a higher channel elevation than present in the vicinity of the modern estuary (see Figure 13). It is therefore postulated that a gravel- to sand-bed transition, due to a change in gradient, may have been present in the Babbage River downstream from the present estuary during late Wisconsinan time. Consideration of the valley geometry suggests 10 m as a maximum plausible depth for late Wisconsinan Babbage River gravels beneath the modern delta. It appears that the gravels occurring extensively at depths greater than 10 m beneath the Babbage Delta may be early Wisconsinan outwash gravels of the Buckland Glaciation (see section 2.1.2) or even pre-Buckland sediments [cf. gravels exposed in coastal cliffs nearby (Rampton, 1974a)]. Given the hypothesized rise in sea level of order 1 m over the past 1000 years, transgression of estuarine and deltaic sediments over Babbage River alluvium can be assumed to have occurred, but the Holocene transgressive sequence may be quite thin.

Whereas extensive intertidal surfaces are present at the seaward margin of the Babbage Delta, intertidal facies are poorly developed in the Spring and Running River deltas, which otherwise strongly resemble the Babbage. In the Running River system (Figure 162B), an inner-lagoon beach and washover complex, with heavy driftwood accumulation, is present at the seaward margin of the deltaic supratidal flats. In the Babbage Delta, this juxtaposition is found only at the far-lateral

distal margins. These observations suggest that, as in the case of the barrier sequences described above, local variability in the sediment budgets of deltaic systems may lead to contrasting patterns of sediment storage and therefore to different vertical sequences in the sedimentary record. Because changes in the sediment budget may result from adjustments of system inputs or parameters over time, analogous differences may exist in the form of the transgressive sequence within deposits associated with a single system. For example, the deltaic transgressive sequence produced in the Babbage Estuary system 6000-4000 years B.P. may have been somewhat different from the sequence being produced at the present time. Such differences represent the long-term end of the spectrum of variance introduced in section 1.1.1.

# 5 CONCLUSIONS

The nature of the estuarine system during deposition of much of the sediment now in storage is not entirely open to resolution by short-term investigations such as the present study, or even by continued monitoring over many decades. This is true, in part, because of long-term statistical dependence in the input series (cf. Mandelbrot and Wallis, 1969), whereby a monitoring program of any practical duration may never see the full range of sedimentologically significant input conditions or system thresholds. Furthermore, a system subject to such rapid marine transgression as seems to be occurring near Kay Point may change significantly over a time interval that is short relative to the time required for accumulation of a significant thickness of sediment. Whatever inaccuracies may exist in Franklin's map of the 1826 shoreline in the Babbage Estuary, there can be little doubt that the lagoon has been reduced in size during historical time, such that the system parameters of the 1970s may have borne little resemblance to the parameters of the 1770s and even less to those 1000 years earlier. Clearly, any attempt to understand the full range of variance in such a system must employ both direct and indirect measures.

Sediments in storage provide one form of indirect record,

more complete in some settings than in others. Whereas the entire body of barrier sediment in the present spit at Kay Point can be related with some confidence to environmental conditions of the recent past, the nearby progradational Spring River barrier may record a longer interval of accumulation; older sediments present in the deposit may have accumulated under conditions quite different from those prevailing at the present time. Recognition of major local differences in the morphology and anticipated facies relationships of barrier features on the central Yukon coast, including examples of transgressive, prograding, and inlet-fill sequences, all occurring within a 40-km segment of coast, is an important finding of this study.

Just as major differences in the estuarine transgressive sequence can occur within a relatively small region, so too the dynamic characteristics of Yukon coast estuaries may be highly variable, due to variable geometries, large differences in catchment size relative to lagoon area, and differences in the volume of the tidal prism relative to inlet width (see Table 2). The role of fluvial inputs in the estuarine circulation process, emphasized many years ago by Simmons (1955), has been shown to be especially marked in the Babbage Estuary, where the large amplitude of the Arctic nival runoff regime contributes to development, on an annual cycle, of a wide spectrum of salinity, stratification, and circulation conditions. This spectrum ranges from fresh to hypersaline, from highly-stratified to well-mixed, and from a cascading

reservoir system through a dispersion-dominated system to a regime in which gravitational convection plays an important role, but is freqently disrupted by wind-induced mixing events.

In the Babbage Estuary system, the variance of salinity, temperature, and runoff inputs is apparently maximized at T=1 year. Rapid flushing of the delta and lagoon by early snowmelt runoff, followed closely by breakup, produces a very rapid transition between the two extremes of the annual salinity cycle (Figure 63) and constitutes a major periodic threshold in the circulation regime. A second seasonal threshold occurs in late July, in most years, when brackish water intrudes from Phillips Bay (Figure 64). Other systems on the central Yukon coast, such as the Stokes Point lagoon complex (Figure 10A), which receives very little freshwater discharge, are not flushed completely during the snowmelt runoff and retain hypersaline water near the bottom until mid-summer or later (see, for example, Kendel et al., 1975; cf. Wiseman, 1979). Nevertheless, these systems too exhibit a striking seasonal-scale variance that is largely predictable, although the timing of the transitions is somewhat variable, the annual cycle being modulated by synoptic-scale events or persistent anomalies in the large-scale circulation of the atmosphere. Dramatic seasonal changes in the canonical structure of the Babbage Estuary system (Figures 82 and 128) reflect seasonal changes in the circulation regime and the presence of various thresholds that determine the occurrence and nature of internal links.

The role of ice, a seasonal-scale variable, in littoral, estuarine, and fluvial environments of the northern Yukon, is more clearly discernible as a result of this study. Although ice has attracted considerable attention as a dominant feature of the high-latitude coastal environment (e.g. Owens and McCann, 1960; Nichols, 1961; Schalk and Hume, 1966; Reimnitz and Bruder, 1972; Taylor, 1977), it can be important at lower latitudes as well (cf. Dionne, 1969; Dionne and Laverdiere, 1972; Owens, 1976). Furthermore, Leffingwell (1919), in the first comprehensive account of geomorphological processes on the Beaufort Sea coast, concluded that wind and waves are more important than ice as agents of sediment transport and morphological change in the coastal zone. Results of the present study support Leffingwell's conclusion to the extent that ice-thrust and ice-rafting processes have been found to be relatively unimportant in the coastal zone of Mackenzie Bay, sediment transport is overwhelmingly dominated by fluvial and storm-wave dynamics, waves are rarely fetch-limited by ice during the open-water season, and ice-generated structures (apart from thaw basins in deltaic and lagoon-margin supratidal deposits) are not common in the estuarine sedimentary record.

Nevertheless, the indirect effects of ice are pervasive and include the following: (1) storage of precipitation as snow and of groundwater in icings causes cessation of river flow in winter, profoundly affecting conditions in the estuaries; (2) ice formation in shallow estuaries may produce hypersaline conditions (with values as high as 122 ppt) in remaining

unfrozen water; in the absence of freshwater runoff, a reverse gravitational circulation may develop; and water in deep basins may become isolated by bottomfast ice; (3) the sedimentologically important spring flood events on supratidal flats of the Babbage Delta are controlled by ice jamming in the delta, bottomfast ice in the lagoon, or both; (4) scour of bottom sediments by freshwater runoff draining through ice [strudel-scour of Reimnitz and Bruder (1972)] may form shallow depressions beneath lagoon and nearshore waters; in the Babbage Estuary, the ice-surface expression of these features was observed immediately outside the entrance section but never within the lagoon; (5) storm-surge development is inhibited and high-frequency storm-wave generation precluded by ice cover on coastal waters during some 8-9 months of the year [cf. 3-4 months in the Gulf of St Lawrence (Owens, 1976)]; (6) thaw of ground ice in coastal exposures contributes substantially to very rapid rates of coastal recession; (7) the morphology of deltaic and lagoon-margin supratidal surfaces in the Babbage Estuary system is dominated by pond and lake basins believed to be largely of thermokarst origin.

Synoptic-scale wind effects have been widely recognized as a dominant feature of the circulation, exchange process, density structure, and sedimentology of shallow lagoons (e.g. Posner, 1959; Behrens, 1969; Kjerfve, 1975; Dygas and Burrell, 1976; Smith, 1978), while wind and storm runoff effects have also been described, with increasing frequency in recent years, from fjords and other types of estuaries as well

(e.g. Petterson, 1920; Farmer, 1972; Schubel, 1974; Elliott, 1976; Weisberg, 1976; Nichols, 1977; Grano and Pritchard, 1978).

In the Babbage Estuary, synoptic-scale wind processes dominate the spectrum of post-breakup water levels to an extreme degree (see section 3.2.1) and account for the largest anomalies of suspended sediment concentration observed in the lagoon. During northwesterly storms, the total volume of water stored in the system may more than double over 24-36 hours (Figure 79), while suspended sediment concentration may increase by more than two orders of magnitude in the same length of time (Figure 108). Late summer salinity and temperature in the lagoon appear to be dominated by synoptic-scale processes (section 3.3.4); reaction and relaxation times are short. In the Babbage Delta, major synoptic-scale anomalies are related to storm runoff (Figure 114), peak suspended sediment concentrations may lag the runoff peak 15 km upstream by some 24 hours, and relaxation times are long, in part probably because of the long time scale of late summer recessions in the river (section 3.1.1). A relatively minor storm in August 1976, which accounted for about 18 per cent ($9 \times 10^6$ kg) of the estimated total annual longshore sediment transport to the lagoon entrance ($5 \times 10^7$ kg) and was followed by storm runoff contributing some $1 \times 10^6$ kg of fluvial sediment, produced a major increase in sedimentation rates within the lagoon and an extensive plume of turbid water filling Phillips Bay.

In 1976, four storms accounted for 67 per cent of the estimated longshore sediment transport during the field season at the distal end of Kay Point spit. This result accords with observations of Wiseman et al. (1973) on the Beaufort and Chukchi coasts of Alaska, where storm transport was found to be even more important. In the fluvial transport system (sections 4.1.2 and 4.1.3), approximately 25 per cent ($4.4 \times 10^7$ kg) of the annual suspended sediment transport through section B1 ($1.7 \times 10^8$ kg) occurred on 26 June 1976 and more than 90 per cent of the observed annual suspended sediment discharge was delivered in June; more than 99 per cent of total annual bedload transport may occur during the same month.

The estuarine system, in its present configuration, responds to the major annual input of fluvial sediment during the snowmelt and immediate post-snowmelt season by moving a large proportion directly through the system into Phillips Bay. It is estimated that at least 59 per cent of suspended sediment discharged to the estuary during June 1976 was exported to depositional sites seaward of the barrier and entrance section. The low retention is ascribed to the short flushing time, non-convectional circulation, low settling velocities, and partially inoperative agglomeration processes characteristic of the system at this time of year. The sediment trap efficiency of the estuary appears to be much greater later in the summer, when most marine sediment inputs occur.

Although the propagation of tidal and synoptic-scale water

level perturbations within the estuary may be treated as a quasi-linear stochastic process, transfers of runoff and fluvial sediment inputs through the system are highly non-linear. Furthermore, the parameters of the system change dramatically on a seasonal time-scale. The short-term behaviour of the Babbage Estuary system is dominated by extreme synoptic- and seasonal-scale variance. Tidal processes play a relatively minor role in the operation of the system; the large-scale estuarine morphology exhibits none of the distinctive tidal delta phenomena characteristic even of many microtidal systems. Water level, storage volume, salinity, and suspended sediment sequences in the lagoon during the open-water season are dominated by synoptic-scale wind effects. On an annual basis, however, the synoptic-scale variance of salinity, density, and sediment transport processes is greatly exceeded by seasonal-scale effects.

At longer intervals, opening or closing of inlets through the barrier and other changes in the configuration of the estuary may alter the parameters of the system response to input variance over a broad range of frequencies. The mean and variance of the input terms may also change significantly at decadal and longer time scales. In the long run, system parameters and sedimentary deposits in the estuarine system are profoundly affected by transgression due to rising sea level and coastal erosion.

Distinctive features of the transgressive sequence in the Babbage Estuary system include the absence or limited

development of aeolian, backbarrier-margin, tidal-delta, and intertidal marsh facies, a largely afaunal intertidal component, and deltaic deposits with poorly developed levees and numerous lake basins occupying a very large proportion of the total area. Lagoon-margin supratidal surfaces are morphologically similar to parts of the delta plain. Whereas the small-scale characteristics of lithofacies sets within individual subsystems of the estuary reflect a quasi-consistent system response to input variance at annual and shorter time scales, the large-scale features of the sediment body result from long-term non-stationarity in the input regime and changes in the configuration or other parameters of the system.

REFERENCES

Aagaard, K., and Coachman, L.K., 1977, Recent studies on Arctic currents; in M.J. Dunbar, ed., Polar oceans; Proceedings, Polar Oceans Conference, May 1974; Arctic Institute of North America, Calgary; pp. 87-98.

Abrahams, A.D., and Kellerhals, R., 1973, Correlations between water discharge and concentration of suspended solids for four large Prairie rivers; in Fluvial processes and sedimentation; Proceedings, Hydrology Symposium no. 9, Edmonton, May 1973; pp. 96-113.

Ackley, S.F., and Hibler, W.D. III, 1977, Measurements of Arctic Ocean ice deformation and fracture patterns from satellite imagery; in M.J. Dunbar, ed., Polar oceans; Proceedings, Polar Oceans Conference, May 1974; Arctic Institute of North America, Calgary; pp. 227-238.

Alexander, V., Burrell, D.C., Chang, J., Cooney, R.T., Coulon, C., Crane, J.J., Dygas, J.A., Hall, C.E., Kinney, P.J., Kogl, D., Mowatt, T.C., Naidu, A.S., Osterkamp, T.E., Schell, D.M., Seifert, R.D., and Tucker, R.W., 1974, Environmental studies of an estuarine system; University of Alaska, Institute of Marine Science, I.M.S. Report R-74-1; 543 p.

Allen, J.R.L., 1973, Phase differences between bed configuration and flow in natural environments, and their geological relevance; Sedimentology, v. 20, pp. 323-329.

Allen, J.R.L., 1974, Reaction, relaxation and lag in natural sedimentary systems: general principles, examples and lessons; Earth-Science Reviews, v. 10, pp. 263-342.

Allersma, E., Hoekstra, A.J., and Bijker, E.W., 1966, Transport patterns in the Chao Phya estuary; Proceedings, 10th Conference on Coastal Engineering, Tokyo; v. 1, pp. 632-650.

Amorocho, J., and Brandstetter, A., 1971, Determination of non-linear functional response functions in rainfall-runoff processes; Water Resources Research, v. 7, pp. 1087-1101.

Amundsen, R., 1908, The north west passage; A. Constable, London; 2 volumes.

Anderson, F.E., 1971, Resuspension of estuarine sediments by low amplitude waves [abstract]; in D.S. Gorsline, ed., Abstract volume, 2nd National Coastal and Shallow Water Research Conference; University of Southern California, Los Angeles; p. 10.

Anderson, F.E., 1976, Rapid settling rates observed in sediments resuspended by boat waves over a tidal flat; Netherlands Journal of Sea Research, v.10, pp. 44-58.

Anderson, J.C., and Anderson, R.J., 1974, Progress report on winter distribution of flow in the Mackenzie Delta, N.W.T.; Canada, Environmental-Social Committee, Northern Pipelines, Task Force on Northern Oil Development, Report 74-12; pp. 225-258.

Andrews, P.B., 1970, Facies and genesis of a hurricane washover fan, St Joseph Island, central Texas coast; University of Texas, Austin; Bureau of Economic Geology, Report of Investigation no. 67; 147 p.

Armon, J.W., 1979, Landward sediment transfers in a transgressive barrier island system, Canada; in S.P. Leatherman, ed., Barrier islands from the Gulf of St Lawrence to the Gulf of Mexico; Proceedings of a coastal research symposium, Boston, March 1978; Academic Press, New York; pp. 65-80.

Armon, J.W., 1980, Changeability in small flood tidal deltas and its effects, Malpeque barrier system, Prince Edward Island; in S.B. McCann, ed., The coastline of Canada; Geological Survey of Canada, Paper 80-10; pp. 41-50.

Arnborg, L., Walker, H.J., and Peippo, J., 1966, Water discharge in the Colville River, Alaska, 1962; Geografiska Annaler, v. 48A, pp. 195-210.

Axelsson, V., 1967, The Laitaure delta: a study of deltaic morphology and processes; Geografiska Annaler, v. 49A, 127 p.

Bagnold, R.A., 1940, Beach formation by waves; some model experiments in a wave tank; Journal of the Institute of Civil Engineering, v. 15, pp. 27-52.

Bagnold, R.A., 1941, Physics of blown sand and desert dunes; William Morrow, New York; reprinted 1954 by Methuen, London; 265 p.

Bagnold, R.A., 1956, Flow of cohesionless grains in fluids; Philosophical Transactions, Royal Society (London), v. 249A, pp. 235-297.

Bagnold, R.A., 1963, Mechanics of marine sedimentation; in M.N. Hill, ed., The sea: ideas and observations on progress in the study of the seas; J. Wiley and Sons, New York; v. 3, p. 507.

Bagnold, R.A., 1966, An approach to the sediment transport problem from general physics; U.S. Geological Survey, Professional Paper 422-I; 37 p.

Bagnold, R.A., 1973, The nature of saltation and of 'bed-load' transport in water; Proceedings, Royal Society (London), v. 322A, pp. 473-504.

Barber, F.G., 1968, On the water of Tuktoyaktuk Harbour; Canada, Marine Sciences Branch, Manuscript Report Series no. 9; 32 p.

Barnes, P.W., and Reimnitz, E., 1972, River overflow onto sea ice off the north coast of Alaska spring 1972 [abstract]; Transactions , American Geophysical Union, v. 53, p. 1020.

Bartberger, C.E., 1976, Sediment sources and sedimentation rates, Chincoteague Bay, Maryland and Virginia; Journal of Sedimentary Petrology, v. 46, pp. 326-336.

Barwis, J.H., and Makurath, J.H., 1978, Recognition of ancient tidal inlet sequences: an example from the Upper Silurian Keyser Limestone in Virginia; Sedimentology, v. 25, pp. 61-82.

Bates, C.C., 1953, Rational theory of delta formation; American Association of Petroleum Geologists Bulletin, v. 37, pp. 2119-2161.

Båth, M., 1974, Spectral analysis in geophysics; Elsevier Scientific Publishing Company, Amsterdam; 563 p.

Beal, M.A., 1968, The seasonal variation in sea level at Barrow, Alaska; in J.E. Sater, coordinator, Arctic drifting stations; Arctic Institute of North America; pp. 327-341.

Behrens, E.W., 1969, Hurricane effects on a hypersaline bay; in A.A. Castanares and F.B. Phleger, eds, Lagunas costeras, un simposio; Proceedings, International Symposium on Coastal Lagoons, Mexico, D.F., November 1967; pp. 301-311.

Bendat J.S., and Piersol, A.G., 1971, Random data: analysis and measurement procedures; Wiley-Interscience, New York; 407 p.

Benson, C.S., 1969, The seasonal snow cover of Arctic Alaska; Arctic Institute of North America, Research Paper no. 51; 86 p.

Bernard, H.A., and Leblanc, R.J., 1965, Resume of the Quaternary geology of the northwestern Gulf of Mexico Province; in H.E. Wright, Jr, and D.G. Frey, eds, The Quaternary of the United States; Princeton University Press, Princeton; pp. 137-185.

Bijker, E.W., Kalkwijk, J.P.Th., and Pieters, T., 1974, Mass transport in gravity waves on a sloping bottom; Proceedings, 14th Conference on Coastal Engineering, Copenhagen; American Society of Civil Engineers, New York; pp. 447-465.

Black, A.P., Birkner, F.B., and Morgan, J.J., 1965, Destabilization of dilute clay suspensions with labelled polymers; Journal of the American Water Works Association, v. 57, pp. 1547-1560.

Blatt, H., Middleton, G., and Murray, R., 1972, Origin of sedimentary rocks; Prentice-Hall, Englewood Cliffs, N.J.; 634 p.

Bobrivitskaya, N.N., 1967, Discharge of suspended sediments as a function of hydrological characteristics; Soviet Hydrology, no. 4, pp. 173-183.

Boothroyd, J.C., 1978, Mesotidal inlets and estuaries; in R.A. Davis, ed., Coastal sedimentary environments; Springer-Verlag, New York; chapter 6, pp. 287-360.

Bornhold, B.D., 1975, Suspended matter in the southern Beaufort Sea; Canada, Department of Environment, Beaufort Sea Project, Technical Report 25b; 23 p.

Bostock, H.S., 1948, Physiography of the Canadian Cordillera, with special reference to the area north of the fifty-fifth parallel; Geological Survey of Canada, Memoir 247; 106 p.

Bowden, K.F., 1953, Note on wind drift in a channel in the presence of tidal currents; Proceedings, Royal Society (London), v. 219A, pp. 426-446.

Bowen, A.J., 1980a, Simple models of nearshore sedimentation; beach profiles and longshore bars; in S.B. McCann, ed., The coastline of Canada; Geological Survey of Canada, Paper 80-10; pp. 1-11.

Bowen, A.J., 1980b, Nearshore velocity measurements and beach equilibrium; in Proceedings, Canadian Coastal Conference 1980; Burlington, April 1980; pp. 21-30.

Brockmann, C., 1935, [Diatoms and mud in Jade-Gebeit (in German)]; Abh. Senckenberg. Naturf. Ges., 430, 64 p.; cited by van Straaten (1961).

Brown, J., Dingman, S., and Lewellan, R., 1968, Hydrology of a drainage basin on the Alaskan coastal plain; U.S.A., Cold Regions Research and Engineering Laboratory, Research Report 240; 18 p.

Brown, W.M., and Ritter, J.R., 1971, Sediment transport and turbidity in the Eel River basin, California; U.S. Geological Survey, Water Supply Paper 1986.

Bruun, P., 1962, Sea level rise as a cause of shore erosion; Journal of the Waterways and Harbors Division, Proceedings, American Socitey of Civil Engineers, v. 88, pp. 117-13-.

Bryson, R.A., 1966, Air masses, streamlines and the boreal forest; Geogaphical Bulletin, v. 8, pp. 228-269.

Bryson, R.A., 1974, A perspective on climatic change; Science, v. 184, pp. 753-760.

Burns, B.M., 1973, The climatology of the Mackenzie Valley - Beaufort Sea; Canada, Department of Environment, Atmospheric Environment Service, Climatological Studies 24, 2 volumes.

Caldwell, J.M., 1956, Wave action and sand movement near Anaheim Bay, California; U.S.A., Beach Erosion Board, Technical Memorandum no. 68; 21 p.

Cameron, W.M., 1953, Hydrography and oceanography of the southeast Beaufort Sea and Amundsen Gulf; part 2: hydrographic and oceanographic observartions in the Beaufort Sea 1952; University of British Columbia, Institute of Oceanography.

Cameron, W.M., and Pritchard, D.W., 1963, Estuaries; in M.N. Hill, ed., The sea: ideas and observations on progress in the study of the seas; J. Wiley and Sons, New York; v. 2, pp. 306-324.

Campbell, F.B., and Bauder, H.A., 1940, A rating curve method for determining silt discharge of streams; Transactions, American Geophysical Union, v. 21, pp. 603-607.

Canada, Department of Public Works, 1971a, Herschel Island: feasibility of a marine terminal; Engineering Programs Branch, Ottawa; 141 p. and 19 plates.

Canada, Department of Public Works, 1971b, Beaufort Sea storm, September 13-16, 1970: investigation of effects in the Mackenzie Delta region; Engineering Programs Branch, Ottawa; 22 p.

Canadian Hydrographic Service, 1971, Herschel Island to Kay Point; scale 1:60,000; Chart 7603.

Canadian Hydrographic Service, 1972, Mackenzie Bay; scale 1:150,000; Chart 7602.

Carlson, R.F., and Kane, D.L., 1975, Hydrology of Alaska's Arctic; in G. Weller and S.A. Bowling, eds, Climate of the Arctic; Proceedings, 24th Alaska Science Conference, Fairbanks, August 1973; University of Alaska, Geophysical Institute, Fairbanks; pp. 367-373.

Carlson, R.F., Norton, W., and Birtch, R., 1972, Modelling snowmelt runoff in an Arctic coastal basin; in The role of snow and ice in hydrology; Proceedings of the Banff Symposia; Symposium on Measurement and Forecasting; Banff, September 1972; v. 2, pp. 1004-1016.

Carpelan, L.H., 1969, Physical characteristics of southern California coastal lagoons; in A.A. Castanares and F.B. Phleger, eds, Lagunas costeras, un simposio; Proceedings, International Symposium on Coastal Lagoons, Mexico, D.F., November 1967; pp. 319-334.

Carson, J.M., Hunter, J.A., and Lewis, C.P., 1975, Marine seismic refraction profiling, Kay Point, Yukon Territory; in Report of Activities, Part B; Geological Survey of Canada, Paper 75-1B; pp. 9-12.

Chang, C.W., and Anderson, J.V., 1968, Flocculation of clays and soils by organic compounds; Soil Science Society of America, Proceedings, v. 32, pp. 23-27.

Childers, J.M., Sloan, C.E., Meckel, J.P., and Nauman, J.W., 1977, Hydrologic reconnaissance of the eastern North Slope, Alaska, 1975; U.S. Geological Survey, Anchorage; Open-file Report 77-492; 65 p.

Chorley, R.J., and Kennedy, B., 1971, Physical geography: a systems approach; Prentice-Hall International, London; 370 p.

Church, M., 1972, Baffin Island sandurs: a study of Arctic fluvial processes; Geological Survey of Canada, Bulletin 216; 208 p.

Church, M., 1974, Hydrology and permafrost with reference to northern North America; in Permafrost hydrology; Proceedings of a workshop seminar, Calgary, February 1974; Canada, Department of Environment, Canadian National Committee, International Hydrological Decade; pp. 7-20.

Church, M., and Gilbert, R., 1975, Proglacial fluvial and lacustrine environments; in A.V. Jopling and B.C. McDonald, eds, Glaciofluvial and glaciolacustrine sedimentation; Society of Economic Paleontologists and Mineralogists, Special Publication no. 23, pp. 22-100.

Church, M., and Jones, D., in press, in R.D. Hey, ed., Engineering problems in the management of gravel-bed rivers; J. Wiley and Sons, Chichester.

Coachman, L.K., 1963, Water masses of the Arctic; in Proceedings, Arctic Basin Symposium, Hershey, Pa., October 1962; Arctic Institute of North America; pp. 143-172.

Coachman, L.K., and Barnes, C.A., 1962, Surface water in the Eurasian Basin of the Arctic Ocean; Arctic, v. 15, pp. 251-277.

Cogley, J.G., and McCann, S.B., 1975, Surface runoff characteristicw of an arctic nival catchment: Mecham River, Cornwallis Island; in Proceedings, Canadian Hydrology Symposium; pp. 282-288.

Coleman, J.M., Gagliano, S.M., and Smith, W.G., 1970, Sedimentation in a Malaysian high tide tropical delta; in J.P. Morgan, ed., Deltaic sedimentation, modern and ancient; Society of Economic Paleontologists and Mineralogists, Tulsa, Oklahoma; Special Publication no. 15; pp. 185-197.

Collins, M.B., and Amos, C.L., 1973, The effect of waves on an intertidal sand flat of the Wash; in J. Hails and A. Carr, eds, Nearshore sediment dynamics and sedimentation, an interdisciplinary review; J. Wiley and Sons, London; pp. 304-306.

Cooper, P.F., Jr, 1974, Landfast ice in the southeastern part of the Beaufort Sea; in J.C. Reed and J.E. Sater, eds, The coast and shelf of the Beaufort Sea; Arctic Institute of North America, Arlington, Va.; pp. 235-242.

Cooper, R.H., and Hollingshead, A.B., 1973, River bank erosion in regions of permafrost; in Fluvial processes and sedimentation; Proceedings, Hydrology Symposium no. 9; Edmonton, May 1973; pp. 272-283.

Cornish, V., 1898, On sea beaches and sand banks; Geographical Journal, v. 2, pp. 628-674.

Curray, J.R., Emmel, F.J., and Crampton, P.J.S., 1969, Holocene history of a strand plain, lagoonal coast, Nayarit, Mexico; in A.A. Castanares and F.B. Phleger, eds, Lagunas costeras, un simposio; Proceedings, International Symposium on Coastal Lagoons, Mexico, D.F., November 1967; pp. 63-100.

Dahlskog, S., 1966, Sedimentation and vegetation in a Lapland mountain delta; Geografiska Annaler, v. 48A, pp. 86-101.

Davidson-Arnott, R.G.D., and Greenwood, B., 1976, Facies relationships on a barred coast, Kouchibouguac Bay, New Brunswick, Canada; in R.A. Davis, Jr, and R.L. Ethington, eds, Beach and nearshore sedimentation; Society of Economic Paleontologists and Mineralogists, Special Publication no. 24, pp. 149-168.

Davies, J.L., 1964, A morphogenic approach to world shorelines; Zeitschrift fur Geomorphologie, v. 8, pp. 127-142.

Davis, M.W., and Erlich, R., 1970, Relationships between measures of sediment-size-frequency distributions and the nature of sediments; Geological Society of America Bulletin, v. 81, pp. 3537-3548.

Defant, A., 1953, [Ebb and flow of the tides of the sea, atmosphere, and earth (in German)]; Springer-Verlag, Berlin; translated and published in English, 1958: Ebb and flow: the tides of earth, air, and water; University of Michigan Press, Ann Arbor; 121 p.

Defant, A., 1961, Physical oceanography; Pergamon Press, Oxford; v. 1.

Dey, B., 1980, Orbital sensing of Mackenzie Bay ice dynamics; Arctic, v. 33, pp. 280-291.

Dionne, J-C., 1969, Tidal flat erosion by ice at La Pocatiere, St Lawrence Estuary; Journal of Sedimentary Petrology, v. 39, pp. 1174-1181.

Dionne, J-C., and Laverdiere, C., 1972, Ice-formed beach features from Lake St Jean, Quebec; Canadian Journal of Earth Sciences, v. 9, pp. 979-990.

Dittmar, W., 1884, Report on the scientific results of the exploring voyage of H.M.S. Challenger; Physics and chemistry; H.M. Stationery Office, London; v. 1.

Doodson, A.T., 1924, Meteorological perturbations of sea-level and tides; Monthly Notices, Royal Astronomical Society, Geophysical Supplement 1; pp. 124-127.

Dyer, K.R., 1973, Estuaries: a physical introduction; J. Wiley and Sons, New York; 140 p.

Dyer, K.R., 1974, The salt balance in stratified estuaries; Estuarine and Coastal Marine Science, v. 2, pp. 273-281.

Dyer, K.R., 1977, Lateral circulation effects in estuaries; in Estuaries, geophysics, and the environment; National Academy of Sciences, Washington, D.C.; pp. 22-29.

Dyer, K.R., and Ramamoorthy, K., 1969, Salinity and water circulation in the Vellar Estuary; Limnology and Oceanography, v. 14, pp.4-15.

Dygas, J.A., and Burrell, D.C., 1976, Wing and current patterns in an arctic coast lagoon; Ocean Engineering, v. 3, pp. 317-327.

Egginton, P.A., 1978, The effect of bottomfast ice on the stage-discharge relation; in Current Research, Part A; Geological Survey of Canada, Paper 78-1A; pp. 493-495.

Einstein, H.A., 1950, Th bedload function for sediment transportation in open channel flows; U.S.D.A. Technical Bulletin 1026; 70 p.

Einstein, H.A., 1972, Sediment transport by wave action; Proceedings, 13th Conference on Coastal Engineering, Vancouver, July 1972; American Society of Civil Engineers, New York; v. 2, pp. 933-952.

Einstein, H.A., Anderson, A.G., and Johnson, J.W., 1940, A distinction between bed-load and suspended load in natural streams; Transactions, American Geophysical Union, v. 21, pp. 628-633.

Einstein, H.A., and Krone, R.B., 1961, Estuarial sediment transport patterns; Journal of the Hydraulics Division, Proceedings, American Society of Civil Engineers, v. 87, p. 51.

Einstein, H.A., and Krone, R.B., 1962, Experiments to determine modes of cohesive sediment transport in salt water; Journal of Geophysical Research, v. 67, pp. 1451-1461.

Elliott, A.J., 1976, A study of the effect of meteorological forcing on the circulation in the Potomac estuary; Chesapeake Bay Institute, The Johns Hopkins University, Baltimore, Special Report 56.

Emmett, W.W., 1980, A field calibration of the sediment-trapping characteristics of the Helley-Smith bedload sampler; U.S. Geological Survey, Professional Paper 1139; 44 p.

Evans, G., 1965, Intertidal flat sediments and their environments of deposition in the Wash; Quarterly Journal, Geological Society of London, v. 121, pp. 209-241.

Faas, R.W., 1966, Paleoecology of an arctic estuary; Arctic, v. 19, pp. 343-348.

Farmer, D.M., 1972, The influence of wind on the surface waters of Alberni Inlet; Ph.D. dissertation, University of British Columbia, Vancouver.

Fischer, H.B., 1972, Mass transport mechanisms in partially stratified estuaries; Journal of Fluid Mechanics, v. 53, pp. 671-687.

Fjelstad, J.E., 1929, Contributions to the dynamics of free progressive tidal waves; Norwegian North Polar Expedition with the Maud, 1918-1925; Scientific Results, v. 4, 80 p.

Folk, R.L., 1966, A review of grain-size parameters; Sedimentology, v. 6,, pp. 73-93.

Folk, R.L., and Ward, W.C., 1957, Brazos River bar -- a study in the significance of grain size parameters; Journal of Sedimentary Petrology, v. 27, pp. 3-26.

Forbes, D.L., 1979, Bottomfast ice in northern rivers: hydraulic effects and hydrometric implications; Proceedings, Canadian Hydrology Symposium: 79, Cold Climate Hydrology; Vancouver, May 1979; pp. 175-184.

Forbes, D.L., 1980, Late-Quaternary sea levels in the southern Beaufort Sea; in Current Research, Part B; Geological Survey of Canada, Paper 80-1B; pp. 75-87.

Ford, W.L., and Hattersley-Smith, G., 1965, On the oceanography of the Nansen Sound fiord system; Arctic, v. 18, pp. 158-171.

Foreman, M.G.G., 1977, Manual for tidal heights analysis and prediction; Canada, Department of Fisheries and the Environment, Institute of Marine Sciences, Patricia Bay, B.C.; Pacific Marine Science Report 77-10; 97 p.

Francis, J.R.D., 1973, Experiments on the motion of solitary grains along the bed of a water stream; Proceedings of the Royal Society (London), v. 332A, pp. 443-471.

Franklin, J., 1828, Narrative of a second expedition to the shores of the Polar Sea in the years 1825, 1826, and 1827; John Murray, London; reprinted 1969 by Greenwood, New York; 320 p. with appendices.

Frey, R.w., and Basan, P.B., 1978, Coastal salt marshes; in R.A. Davis, Jr, ed., Coastal sedimentary environments; Springer-Verlag, New York; pp. 101-169.

Frostick, L., and McCave, I.N., 1979, Seasonal shifts of sediment within an estuary mediated by algal growth; Estuarine and Coastal Marine Science, v. 9, pp. 569-576.

Fyles, J.G., 1966, Quaternary stratigraphy, Mackenzie Delta and Arctic coastal plain; in Report of Activities, May-October 1965; Geological Survey of Canada, Paper 66-1; pp. 30-31.

Galloway, W.E., 1976, Sediments and stratigraphic framework of the Copper River fan-delta, Alaska; Journal of Sedimentary Petrology, v. 46, pp. 726-737.

Gardner, G.B., and Smith, J.D., 1978, Turbulent mixing in a salt wedge estuary; in J.C.J. Nihoul, ed., Hydrodynamics of estuaries and fjords; Proceedings, 9th International Liege Colloquium on Ocean Hydrodynamics; Elsevier Scientific Publishing Company, Amsterdam; pp. 79-108.

Garfinkel, H.L., and Brubaker, L.B., 1980, Modern climate -- tree growth relationships and climatic reconstruction in sub-arctic Alaska; Nature, v. 286, pp. 872-874.

Garland, G.D., and Lennox, D.H., 1962, Heat flow in western Canada; Royal Astronomical Society, Geophysical Journal, v. 6, pp. 245-262.

Gibbs, R.J., Matthews, M.D., and Link, D.A., 1971, Relationship between sphere size and settling velocity; Journal of Sedimentary Petrology, v. 41, pp. 7-18.

Gill, D., 1972, The point bar environment in the Mackenzie River Delta; Canadian Journal of Earth Sciences, v. 9, pp. 1382-1393.

Ginsberg, R.N., and Lowenstam, H.A., 1958, The influence of marine bottom communities on the depositional environment of sediments; Journal of Geology, v. 66, pp. 310-318.

Glangeaud, L., 1938, [Transport and sedimentation in the Gironde Estuary (in French)]; Bulletin de la Société Géologique de France, 5e ser., 8, pp. 599-631.

Godin, G., 1972, The analysis of tides; University of Toronto Press, Toronto; 264 p.

Gold, L.W., and Lachenbruch, A.H., 1973, Thermal conditions in permafrost -- a review of North American literature; in Permafrost, North American contribution, 2nd International Conference, Yakutsk, July 1973; National Academy of Sciences, Washington; pp. 3-25.

Goldberg, E.D., 1963, The oceans as a chemical system; in M.N. Hill, ed., The sea: ideas and observations on progress in the study of the seas; J. Wiley and Sons, New York; v. 2, pp. 3-25.

Gordon, C.M., 1974, Sediment transport in tides; Eos, v. 56; p. 1139.

Grano, V., and Pritchard, D.W., 1978, Wind-driven, nontidal circulation of the upper Chesapeake Bay; Eos, v.50, p. 1102.

Greenwood, B., and Hale, P.B., 1980, Depth of activity, sediment flux, and morphological change in a barred nearshore environment; in S.B. McCann, ed., The coastline of Canada; Geological Survey of Canada, Paper 80-10; pp. 89-109.

Gregory, K.J., and Walling, D.E., 1973, Drainage basin form and process: a geomorphological approach; Edward Arnold, London; 485 p.

Gressly, A., 1838, [Geological observations in the Solothurnian Jura (in French)]; Neue Denkschrift fur Allgemeine Schweizerische Gesellschaft ges. Naturwissenschaft., v. 2, pp. 1-112; cited by Krumbein and Sloss (1963, p. 607).

Griggs, R.F., 1937, Timberlines as indicators of climatic trends; Science, v. 85, pp. 251-255.

Groen, P., and Groves, G.W., 1962, Surges; in M.N. Hill, ed., The sea: ideas and observations on progress in the study of the seas; J. Wiley and Sons, New York; v. 1, pp. 611-646.

Groves, G.W., 1955, Numerical filters for discrimination against tidal periodicities; Transactions, American Geophysical Union, v. 36, pp. 1073-1084.

Groves. G.W., and Hannan, E.J., 1968, Time series regression of sea level on weather; Reviews of Geophysics, v. 6, pp. 129-174.

Gunnerson, C.G., 1967, Streamflow and quality of the Columbia River basin; Journal of the Sanitary Engineering Division, American Society of Civil Engineers, v. 39, pp. 1-16.

Guy, H.P., 1964, An analysis of some storm-period variables affecting stream sediment transport; U.S. Geological Survey, Professional Paper 462-E.

Hakanson, L., 1976, A bottom sediment trap for recent sedimentary deposits; Limnology and Oceanography, v. 21, pp. 170-175.

Hall, D.G., 1967, The pattern of sediment movement in the River Tyne; International Association of Scientific Hydrology, Publication 75; General Assembly of Bern, Symposium on River Morphology; pp. 117-140.

Hansen, D.V., and Rattray, M., Jr, 1965, Gravitational circulation in straits and estuaries; Journal of Marine Research, v. 23, pp. 104-122.

Hansen, D.V., and Rattray, M., Jr, 1966, New dimensions in estuary classification; Limnology and Oceanography, v.11, pp. 319-326.

Harden, D., Barnes, P., and Reimnitz, E., 1977, Distribution and character of naleds in northeastern Alaska; Arctic, v. 30, pp. 28-40.

Hare, F.K., 1969, The atmospheric circulation and Arctic meteorology; Arctic, v. 22, pp. 185-194.

Hargrave, B.T., and Burns, N.M., 1979, Assessment of sediment trap collection efficiency; Limnology and Oceanography, v. 24, pp. 1124-1136.

Harleman, D.R.F., and Ippen, A.T., 1967, Two-dimensional aspects of salinity intrusion in estuaries: analysis of salinity and velocity distributions; U.S.A., Corps of Engineers, Committee on Tidal Hydraulics, Technical Bulletin 13.

Harms, J.C., and Fahnestock, R.K., 1965, Stratification, bed forms, and flow phenomena (with an example from the Rio Grande); in G.V. Middleton, ed., Primary sedimentary structures and their hydrodynamic interpretation; Society of Economic Paleontologists and Mineralogists, Special Publication 12; pp. 84-115.

Harper, J.R., 1978, Coastal erosion rates along the Chukchi Sea coast near Barrow, Alaska; Arctic, v. 31, pp. 428-433.

Hayes, M.O., 1975, Morphology of sand accumulations in estuaries; in L.E. Cronin, ed., Estuarine research; v. 2, Geology and engineering; Academic Press, New York; pp. 3-22.

Hayes, M.O., 1979, Barrier island morphology as a function of tidal and wave regime; in S.P. Leatherman, ed., Barrier islands from the Gulf of St Lawrence to the Gulf of Mexico; Academic Press, New York; pp. 1-27.

Healey, D.A., 1971, Oceanographic observations in the Beaufort Sea, July 15- Sepetmber 4, 1970; Canada, Marine Sciences Branch, Pacific Region, Victoria; 36 p.

Helley, E.J., and Smith, W., 1971, Development and calibration of a pressure-difference bedload sampler; U.S. Geological Survey, Open-file Report; 18 p.

Hem, J.D., 1959, Study and interpretation of the chemical characteristics of natural water; U.S. Geological Survey, Water Supply Paper 1473; 269 p. (revised edition published in 1970).

Henry, R.F., 1975, Storm surges; Canada, Department of Environment, Beaufort Sea Project, Technical Report 19; 41 p.

Henry, R.F., and Foreman, M.G.G., 1977, Numerical model studies of semi-diurnal tides in the southern Beaufort Sea; Canada, Department of Fisheries and the Environment, Institute of Ocean Sciences, Patricia Bay, B.C.; Pacific Marine Science Report 77-11; 71 p.

Henry, R.F., and Heaps, N.S., 1976, Storm surges in the southern Beaufort Sea; Journal of the Fisheries Research Board of Canada, v. 33, pp. 2362-2376.

Herlinveaux, R.H., and de Lange Boom, B.R., 1975, Physical oceanography of the southeastern Beaufort Sea; Canada, Department of Environment, Beaufort Sea Project, Technical Report 18; 97 p.

Herlinveaux, R.H., de Lange Boom, B.R., and Wilton, G.R., 1976, Salinity, temperature, turbidity and meteorological observations in the Beaufort Sea: summer 1974, spring and summer 1975; Canada, Department of Environment, Institute of Ocean Sciences, Patricia Bay; Pacific Marine Science Report 76-26; 224 p.

Hine, A.C., 1975, Bedform distribution and migration patterns on tidal deltas in the Chatham Harbor Estuary, Cape Cod, Massachusetts; in L.E. Cronin, ed., Proceedings, 2nd International Estuarine Research Conference; Academic Press, New York; v. 2, pp. 235-254.

Hjulström, F., 1935, Studies of the morphological activity of rivers as illustrated by the River Fyris; Bulletin of the Geological Institute of Uppsala, v. 25, pp. 221-527.

Hollingshead, A.B., 1971, Sediment transportation measurements in a gravel river; Journal of the Hydraulics Division, American Society of Civil Engineers, v. 97, pp. 1817-1834.

Holmgren, B., Benson, C., and Weller, G., 1975, A study of the breakup of the arctic slope of Alaska by ground, aircraft, and satellite observations; in G. Weller and S.A. Bowling, eds, Climate of the Arctic; Proceedings, 24th Alaska Science Conference, Fairbanks, August 1973; University of Alaska, Geophysical Institute, Fairbanks; pp. 358-366.

Howard, A.D., 1965, Geomorphological systems -- equilibrium and dynamics; American Journal of Science, v. 263, pp. 302-312.

Hoyt, J.H., 1967, Barrier island formation; Geological Society of America Bulletin, v. 78, pp. 1125-1136.

Hufford, G.L., 1975, Some characteristics of the Beaufort Sea shelf current; Journal of Geophysical Research, v. 80, pp. 3465-3468.

Huggett, W.S., Woodward, M.J., Stephenson, F., Hermiston, F.V., and Douglas, A., 1975, Near bottom currents and offshore tides; Canada, Department of Environment, Beaufort Sea Project, Technical Report 16; 38 p.

Hughes, F.W., and Rattray, M., Jr, 1980, Salt flux and mixing in the Columbia River Estuary; Estuarine and Coastal Marine Science, v. 10, pp. 479-493,

Hughes, O.L., 1972, Surficial geology of northern Yukon Territory and northwestern District of Mackenzie, Northwest Territories; Geological Survey of Canada, Paper 69-36; 11 p.

Hume, J.D., 1971, Sedimentology of Elson Lagoon, Arctic Alaska [abstract]; in D.S. Gorsline, ed., Abstract volume, 2nd National Coastal and Shallow Water Research Conference; University of Southern California, Los Angeles; p. 114.

Hume, J.D., and Schalk, M., 1967, Shoreline processes near Barrow, Alaska: a comparison of the normal and the catastrophic; Arctic, v. 20, pp. 86-103.

Hunter, D.R., 1975, Three Arctic spits; unpublished B.Sc. dissertation, University of Waterloo, Waterloo, Ontario; 44 p. and appendix.

Hunter, J.A., Neave, K.G., MacAulay, H.A., and Hobson, G.D., 1978, Interpretation of sub-seabottom permafrost in the Beaufort Sea by seismic methods; Part 1: seismic refraction methods; in Proceedings, 3rd International Conference on Permafrost, Edmonton, July 1978; National Research Council of Canada, Ottawa; pp. 514-520.

Ince, S., 1962, Winter regime of a tidal inlet in the Arctic and the use of air bubblers for the protection of wharf structures; Proceedings, 8th International Conference on Coastal Engineering, Mexico; pp. 521-532.

Inglis, C.C., and Allen, F.H., 1957, The regime of the Thames Estuary as affected by currents, salinities, and river flow; Proceedings, Institute of Civil Engineers, v. 7, pp. 827-878; discussion, v. 8, pp. 437-439.

Inman, D.L., 1952, Measures for describing the size distribution of sediments; Journal of Sedimentary Petrology, v. 22, pp. 125-145.

Inman, D.L., and Bagnold, R.A., 1963, Littoral processes; in M.N. Hill, ed., The sea: ideas and observations on progress in the study of the seas; J. Wiley and Sons, New York; v. 3, pp. 529-553.

Inman, D.L., and Bowen, A.J., 1963, Flume experiments on sand transport by waves and currents; Proceedings, 8th Conference on Coastal Engineering, American Society of Civil Engineers; pp. 137-150.

Ippen, A.T., 1966, Sedimentation in estuaries; in A.T. Ippen, ed., Estuary and coastline hydrodynamics; McGraw-Hill, New York; chapter 15, pp. 648-672.

Ippen, A.T., and Harleman, D.R.F., 1961, One-dimensional analysis of salinity intrusion in estuaries; U.S.A., Corps of Engineers, Committee on Tidal Hydraulics, Technical Bulletin 5; 52 p. and 4 tables.

Irani, R.R., and Callis, C.F., 1963, Particle size: measurement, interpretation, and application; J. Wiley and Sons, New York.

Iversen, H.W., 1953, Waves and breakers in shoaling water; Proceedings, 3rd Conference on Coastal Engineering, Cambridge, Massachusetts.

Jackson, R.G. II, 1978, Preliminary evaluation of lithofacies models for meandering alluvial streams; in A.D. Miall, ed., Fluvial sedimentology; Canadian Society of Petroleum Geologists, Memoir 5; pp. 543-576.

Jaguet, J-M., and Vernet, J-P., 1976, Moment and graphic size parameters in sediments of Lake Geneva (Switzerland); Journal of Sedimentary Petrology, v. 46, pp. 305-312.

Jarocki, W., 1957, [Empirical methods for the calculation of material in suspension (in French)]; International Association of Scientific Hydrology, Toronto General Assembly, v. 1, pp. 387-398.

Johnson, C.W., Engleman, R.L., Smith, J.P., and Hanson, C.L., 1977, Helley-Smith bedload samplers; American Society of Civil Engineers, Journal of the Hydraulics Division, v. 103, pp. 1217-1221.

Johnson, J.W., 1943, Distribution graphs of suspended matter concentrations; Transactions, American Society of Civil Engineers, v. 69, pp. 941-956.

Johnson, N.M., Likens, G.E., Bormann, F.H., Fisher, D.W., and Pierce, R.S., 1969, A working model for the variation in stream water chemistry at the Hubbard Brook Experimental Forest, New Hampshire; Water Resources Research, v. 5, pp. 1353-1363.

Jones, D.A., Price, A.R.G., and Hughs, R.N., 1978, Ecology of the high saline lagoons Dawhat as Sayh, Arabian Gulf, Saudi Arabia; Estuarine and Coastal Marine Science, v. 6, pp. 253-262.

Judge, A.S., 1973, The prediction of permafrost thickness; Canadian Geotechnical Journal, v. 10, pp. 1-11.

Kalkanis, G., 1964, Transportation of bed material due to wave action; U.S.A., Coastal Engineering Research Center, Technical Memorandum no. 2; 38 p.

Kana, T.W., 1977, Suspended sediment transport at Price Inlet, South Carolina; in Coastal sediments '77; Proceedings, 5th Symposium of Waterway, Port, Coastal and Ocean Division, American Society of Civil Engineers, New York; pp. 366-382.

Kanasewich, E.R., 1975, Time sequence analysis in geophysics; University of Alberta Press, Edmonton; 2nd revised edition; 364 p.

Kellerhals, R., and Bray, D.L., 1971, Sampling procedures for coarse fluvial sediments; Journal of the Hydraulics Division, American Society of Civil Engineers, v. 97, pp. 1165-1180.

Kellerhals, P., and Murray, J.W., 1969, Tidal flats at Boundary Bay, Fraser River Delta, B.C.; Bulletin of Canadian Petroleum Geology, v. 17, pp. 67-91.

Kendel, R.E., Johnston, R.A.C., Lobsiger, U., and Kozak, M.D., 1975, Fishes of the Yukon coast; Canada, Department of Environment, Beaufort Sea Project, Technical Report 6; 114 p.

Keulegan, G.H., 1938, Laws of turbulent flow in open channels; Journal of Research, National Bureau of Standards (U.S.A.), v. 21, pp. 707-741.

Kinney, J.J., Schell, D.M., Alexander, V., Burrell, D.C., Cooney, R., and Naidu, A.S., 1972, Baseline data study of the Alaskan Arctic aquatic environment; University of Alaska, Institute of Marine Science, Fairbanks, Report R72-3; 257 p.

Kirby, R.R., and Parker, W.R., 1977, The physical characteristics and environmental significance of fine-sediment suspensions in estuaries; in Estuaries, geophysics and the environment; National Academy of Sciences, Washington, D.C.; pp. 110-120.

Kjerfve, B., 1975, Tide and fair-weather wind effects in a bar-built Louisiana estuary; in L.E. Cronin, ed., Proceedings, 2nd International Estuarine Research Conference; Academic Press, New York; v. 2, pp. 47-62.

Kjerfve, B., Greer, J.E., and Crout, R.L., 1978, Low-frequency response of estuarine sea level to non-local forcing; in M.L. Wiley, ed., Estuarine interactions; Proceedings, 4th International Estuarine Research Conference; Academic Press, New York; pp. 497-513.

Kleiber, P., and Erlebach, W.E., 1977, Limitations of single water samples in representing mean water quality; III, Effect of variability in concentration measurements on estimates of nutrient loadings in the Squamish River, B.C.; Canada, Department of Environment, Water Quality Branch, Vancouver, ; Technical Bulletin no. 103; 9 p.

Knight, J., 1971, Distributional trends in the recent marine sediments of Tasiujaq Cove of Ekalugad Fiord, Baffin Island, N.W.T.; Maritime Sediments, v. 7, pp. 1-18.

Knight, R.J., and Church, M., 1970, Tasiujaq Cove, Ekalugad Fiord, Baffin Island; Canadian Oceanographic Data Centre, 1970 Data Record Series, no. 1, pp. 31-45, 57-62.

Knoth, J.S., and Nummedal, D., 1977, Longshore sediment transport using fluorescent tracer; in Coastal sediments '77; Proceedings, 5th Symposium of Waterway, Port, Coastal and Ocean Division of American Society of Civil Engineers, Charleston, S.C., November 1977; American Society of Civil Engineers, New York; pp. 383-398.

Knudsen, M., ed., 1901, Hydrographical tables; G.E.C. Gad, Copenhagen.

Komar, P.D., 1976a, The transport of cohesionless sediments on continental shelves; in D.J. Stanley and D.J.P. Swift, eds, Marine sediment tranport and environmental management; American Geological Institute and J. Wiley and Sons, New York; pp. 107-125.

Komar, P.D., 1976b, Beach processes and sedimentation; Prentice-Hall Inc., Englewood Cliffs, N.J.; 429 p.

Komar, P.D., and Inman, D.L., 1970, Longshore sand transport on beaches; Journal of Geophysical Research, v. 75, pp. 5914-5927.

Kovacs, A., and Mellor, M., 1971, Investigation of ice islands in Babbage Bight; Creare Inc., Hanover, N.H.; Technical Note TN-118; 17 p. and 7 figures.

Kovacs, A., and Mellor, M., 1974, Sea ice morphology and ice as a geologic agent in the southern Beaufort Sea; in J.C. Reed and J.E. Sater, eds, The coast and shelf of the Beaufort Sea; Arctic Institute of North America, Arlington, Va.; pp. 113-161.

Kraft, J.C., 1971, Sedimentary facies patterns and geologic history of a Holocene marine transgression; Geological Society of America Bulletin, v. 82, pp. 2131-2158.

Krumbein, W.C., 1963, A geological process-response model for analysis of beach phenomena; U.S.A., Beach Erosion Board, Bulletin 17; pp. 1-15.

Krumbein, W.C., and Sloss, L.L., 1963, Stratigraphy and sedimentation; 2nd edition; W.H. Freeman and Company, San Francisco and London; 660 p.

Krumgalz, B.S., Hornung, H., and Oren, O.H., 1980, The study of a natural hypersaline lagoon in a desert area (the Bardawil Lagoon in northern Sinai); Estuarine and Coastal Marine Science, v. 10, pp. 403-415.

Kumar, N., and Sanders, J.E., 1974, Inlet sequence: a vertical succession of sedimentary structures and textures created by the lateral migration of tidal inlets; Sedimentology, v. 21, pp. 491-532.

Lachenbruch, A.H., and Brewer, M.C., 1961, Geothermal evidence for recent climatic change near Barrow, Alaska [abstract]; Geological Society of America, Special Paper 68; p. 117.

Lachenbruch, A.H., and Marshall, B.V., 1969, Heat flow in the Arctic; Arctic, v. 22, pp. 300-311.

Lake, R.A., and Walker, E.R., 1973, Notes on the oceanography of d'Iberville Fiord; Arctic, v. 26, pp. 222-229.

Langbein, W.B., and Leopold, L.B., 1964, Quasi-equilibrium states in channel morphology; American Journal of Science, v. 262, pp. 782-794.

Leatherman, S.P., 1976, Barrier island dynamics: overwash processes and eolian transport; Proceedings, 15th International Conference on Coastal Engineering, Honolulu; pp. 1958-1974.

Leffingwell, E. de K., 1919, The Canning River region, northern Alaska; U.S. Geological Survey, Professional Paper 109; 251 p.

Leopold, L.B., and Emmett, W.W., 1976, Bedload measurements, East Fork River, Wyoming; Proceedings, National Academy of Science (U.S.A.), v. 73, pp. 1000-1004.

Leopold, L.B., and Maddock, T.M., Jr, 1953, The hydraulic geometry of stream channels and some physiographic implications; U.S. Geological Survey, Professional Paper 252; 56 p.

Lesht, B.M., Clarke, T.L., Young, R.A., and Swift, D.J.P., 1979, Point measurement of sediment flux in a combined wave-current flow: observations compared with calculated transport [abstract]; Eos, v. 60, p. 285.

Lewellen, R.I., 1973, The occurrence and characteristics of near-shore permafrost; in Permafrost, North American contribution; 2nd International Conference, Yakutsk, July 1973; National Academy of Sciences, Washington, D.C.; pp. 131-136.

Lewis, C.P., 1975, Sediments and sedimentary processes, Yukon Beaufort Sea coast; in Report of Activities, Part B; Geological Survey of Canada, Paper 75-1B; pp. 165-170.

Lewis, C.P., 1977, Deltaic processes and delta morphology, Mackenzie Delta, N.W.T. [abstract]; in Geological Association of Canada, Program with Abstracts, v. 2, p. 32.

Lewis, C.P., and Forbes, D.L., 1974, Sediments and sedimentary processes, Yukon Beaufort Sea coast; Canada, Environmental-Social Committee, Northern Pipelines, Task Force on Northern Oil Development, Report no. 74-29; 40 p.

Lewis, C.P., and Forbes, D.L., 1975, Coastal sedimentary processes and sediments, southern Canadian Beaufort Sea; Canada, Beaufort Sea Project, Technical Report 24; 68 p.

Likes, E.H., 1966, Surface water discharge of Ogotoruk Creek; in N.J. Wilimovsky and J.N. Wolfe, eds, Environment of the Cape Thompson region, Alaska; U.S. Atomic Energy Commission; pp. 125-131.

Lisitzin, E., 1957, On the reducing influence of sea ice on the piling-up of water due to wind stress; Societas Scientiarum Fennica, Physics-Mathematics; pp. 20-27.

Loewy, E., 1970, Model tests and studies for Port Rashid, Dubai; in Proceedings, 12th Coastal Engineering Conference, Washington, D.C., September 1970; American Society of Civil Engineers, New York; pp. 1137-1149.

Longuet-Higgins, M.S., 1952, On the statistical distribution of the height of sea waves; Journal of Marine Research, v. 11, pp. 245-266.

Longuet-Higgins, M.S. 1953, Mass transport in water waves; Philosophical Transactions, Royal Society (London), v. 245A, pp. 535-581.

McCann, S.B., 1979, Barrier islands in the southern Gulf of St Lawrence, Canada; in S.P. Leatherman, ed., Barrier islands from the Gulf of St Lawrence to the Gulf of Mexico; Proceedings of a coastal research symposium, Boston, Massachusetts, 1978; Academic Press, New York; pp. 29-63.

McCave, I.N., 1970, Deposition of fine-grained suspended sediment from tidal currents; Journal of Geophysical Research, v. 75, pp. 4151-4159.

McCloy, J.M., 1970, Hydrometeorological relationships and their effects on the levees of a small Arctic delta; Geografiska Annaler, v. 52A, pp. 223-241.

McCloy, J.M., 1971, Accretionary channel features in a small Arctic delta [abstract]; in D.S. Gorsline, ed., Abstract volume, 2nd National Coastal and Shallow Water Research Conference, University of Southern California, Los Angeles; p. 139.

McDonald, B.C., and Lewis, C.P., 1973, Geomorphic and sedimentologic processes of rivers and coast, Yukon Coastal Plain; Canada, Environmental-Social Committee, Northern Pipelines, Task Force on Northern Oil Development, Report 73-39; 245 p.

McDowell, D.M., and O'Connor, B.A., 1977, Hydraulic behaviour of estuaries; Macmillan, London; 292 p.

MacKay, D.K., 1966, Characteristics of river discharge and runoff in Canada; Geographical Bulletin, v. 8, pp. 219-227.

Mackay, J.R., 1959, Glacier ice-thrust features of the Yukon coast; Geographical Bulletin, no. 13, pp. 5-21.

Mackay J.R., 1960, Notes on small boat harbours of the Yukon coast; Geographical Bulletin, no. 15, pp. 19-30.

Mackay, J.R., 1963a, The Mackenzie Delta area, N.W.T.; Canada, Department of Mines and Technical Surveys, Geographical Branch, Memoir 8; 202 p.

Mackay, J.R., 1963b, Notes on the shoreline recession along the coast of the Yukon Territory; Arctic, v. 16, pp. 195-197.

Mackay, J.R., 1972, Offshore permafrost and ground ice, southern Beaufort Sea, Canada; Canadian Journal of Earth Sciences, v. 9, pp. 1550-1561.

Mackay, J.R., 1975a, Relict ice wedges, Pelly Island, N.W.T. (107 C/12); in Report of Activities, Part A; Geological Survey of Canada, Paper 75-1A; pp. 469-470.

Mackay, J.R., 1975b, The stability of permafrost and recent climatic change in the Mackenzie Valley, N.W.T.; in Report of Activities, Part B; Geological Survey of Canada, Paper 75-1B; pp. 173-176.

Mackay, J.R., 1976, Ice wedges as indicators of recent climatic change, western Arctic coast; in Report of Activities, Part A; Geological Survey of Canada, Paper 76-1A; pp. 233-234.

Mackay, J.R., 1978, Freshwater shelled invertebrate indicators of paleoclimate in northwestern Canada during late glacial times: discussion; Canadian Journal of Earth Sciences, v. 15, pp. 461-462.

Mackay, J.R., and MacKay, D.K., 1974, Snow cover and ground temperatures, Garry Island, N.W.T.; Arctic, v. 27, pp. 287-296.

Mackay, J.R., and Stager, J.K., 1966, The structure of some pingos in the Mackenzie Delta area, N.W.T.; Geographical Bulletin, v. 8, pp. 360-368.

Mackay, J.R., Rampton, V.N., and Fyles, J.G., 1972, Relic Pleistocene permafrost, western Arctic, Canada; Science, v. 176, pp. 1321-1323.

McLeod, W.R., and Hodder, D.T., 1978, An examination of long term ice forecast and periodicities of the Beaufort Sea; in D.B. Muggeridge, ed., Proceedings, 4th International Conference on Port and Ocean Engineering under Arctic Conditions; Memorial University, St John's, Newfoundland, 1977; v. 2, pp. 1035-1050.

MacNeill, M.R., and Garrett, J.F., 1975, Open water surface currents; Canada, Beaufort Sea Project, Technical Report no. 17; 113 p.

Madsen, O.S., and Grant, W.D., 1976, Quantitative description of sediment transport by waves; in Proceedings, 15th Conference on Coastal Engineering, Honolulu, July 1976; American Society of Civil Engineers, New York; v. 2, pp. 1093-1112.

Mandelbrot, B.B., and Wallis, J.R., 1969, Some long-run properties of geophysical records; Water Resources Research, v. 5, pp. 321-340.

Mann, H.B., and Whitney, D.R., 1947, On a test of whether one of two random variables is stochastically larger than the other; Annals of Mathematical Statistics, v. 18, pp. 52-54.

Markham, W.E., 1975, Ice climatology of the Beaufort Sea; Canada, Beaufort Sea Project, Technical Report no. 26; 87 p.

Marko, J.R., 1975, Satellite observations of the Beaufort Sea ice cover; Canada, Beaufort Sea Project, Technical Report no. 34; 114 p.

Mather, J.R., and Thornthwaite, C.W., 1956, Microclimatic investigations at Point Barrow, Alaska, 1956; Drexel Institute of Technology, Centerton, N.J., Laboratory of Climatology; Publications in Climatology, v. 9, 51 p.

Matthews, J.B., 1970, Tides at Point Barrow; The Northern Engineer, v. 2, pp. 12-13.

Matthews, J.B., 1979, Circulation in a seasonally ice-covered Arctic lagoon estuary [abstract]; in Abstracts, Interdisciplinary Symposia, International Union of Geodesy and Geophysics, 17th General Assembly, Canberra, December 1979; p. 124.

Matthews, J.B., in press, Observations of underice circulation in a shallow lagoon in the Alaskan Beaufort Sea; Ocean Management.

Meade, R.H., 1969, Landward transport of bottom sediments in estuaries of the Atlantic Coastal Plain; Journal of Sedimentary Petrology, v. 39, pp. 222-234.

Miall, A.D., 1977, A review of the braided-river depositional environment; Earth Science Reviews, v. 13, pp. 1-62.

Miall, A.D., 1978, Lithofacies types and vertical profile models in braided river deposits: a summary; in A.D. Miall, ed., Fluvial sedimentology; Canadian Society of Petroleum Geologists, Memoir 5; pp. 597-604.

Michel, B., 1978, Ice mechanics; Les Presses de l'Universite Laval, Quebec; 499 p.

Middleton, G.V., 1976, Hydraulic interpretation of sand size distributions; Journal of Geology, v. 84, pp. 405-426.

Migniot, C., 1968, [Investigation of physical properties and hydraulic behaviour of different very fine sediments (in French)]; La Houille Blanche, v. 23, pp. 591-620.

Mikhailov, V.N., 1966, Hydrology and formation of river mouth bars; in Scientific problems of the humid tropical zone deltas and their implications; Proceedings, Dacca Symposium; UNESCO, Paris; pp. 59-64.

Miles, M., 1976, An investigation of riverbank and coastal erosion, Banks Island, District of Franklin; in Report of Activities, Part A; Geological Survey of Canada, Paper 76-1A; pp. 195-200.

Miles, M., 1977, Coastal and riverbank stability on Banks Island, N.W.T., Canada; in Proceedings, 3rd National Hydrotechnical Conference, Quebec, May 1977; pp. 972-991.

Millero, F.J., 1974, Seawater as a multicomponent electrolyte solution; in E.D. Goldberg, ed., The sea: ideas and observations on progress in the study of the seas; J. Wiley and Sons, New York; v. 5, pp. 3-80.

Mitchell, J.M., Jr, 1961, Changes of mean temperature since 1870; Annals of the New York Academy of Sciences, v. 95, pp. 235-250.

Moore, H.B., 1931, The specific identification of faecal pellets; Journal of the Marine Biological Association of the United Kingdom, v. 17 (n.s.), p. 325.

More, R.J., 1967, Hydrological models and geography; in R.J. Chorley and P. Haggett, eds, Models in geography; Methuen, London; pp. 145-185.

Morison, S.R., and Taylor, R.B., 1978, Physical characteristics and seasonal changes in an Arctic estuarine environment; in Current Research, Part B; Geological Survey of Canada, Paper 78-1B; pp. 101-106.

Munk, W.H., 1962, Long ocean waves; in M.N. Hill, ed., The sea: ideas and observations on progress in the study of the seas; J. Wiley and Sons, New York; v. 1, pp. 647-663.

Nagaraja, V.N., 1966, Hydrometeorological and tidal problems of the deltaic areas in India; in Scientific problems of the humid tropical zone deltas and their implications; Proceedings, Dacca Symposium, February-March 1964; UNESCO, Paris; pp. 115-120.

Nelson, B.W., 1959, Transportation of colloidal sediment in the freshwater marine transition zone [abstract]; in M. Sears, ed., 1st International Oceanographic Congress preprints; American Association for the Advancement of Science, Washington, D.C.; pp. 640-641.

Nelson, B.W., 1970, Hydrography, sediment dispersal, and recent historical development of the Po River Delta, Italy; in J.P. Morgan, ed., Deltaic sedimentation, modern and ancient; Society of Economic Paleontologists and Mineralogists, Tulsa, Oklahoma; Special Publication no. 15; pp. 152-184.

Nichols, R.L., 1961, Characteristics of beaches formed in polar climates; American Journal of Science, v. 259, pp. 694-708.

Nichols, M.M., 1977, Response and recovery of an estuary following a river flood; Journal of Sedimentary Petrology, v. 47, pp. 1171-1186.

Nichols, M.M., and Poor, G., 1967, Sediment transport in a coastal plain estuary; Journal of the Waterways and Harbors Division; Proceedings, American Society of Civil Engineers, v. 93, pp. 83-95.

Nilsson, B., 1971, [Sediment transport in Swedish rivers, an International Hydrological Decade project; part 1, methods (in Swedish)]; Uppsala Universitet, Naturgeografiska Institutionen, UNGI Rapport 4; 83 p. and appendix.

Nilsson, B., 1972, [Sediment transport in Swedish rivers, an International Hydrological Decade project; part 2, catchment areas, stations and results in 1967-69 (in Swedish)]; Uppsala Universitet, Naturgeografiska Institutionen, UNGI Rapport 16; 250 p.

Norris, D.K., 1973, Tectonic styles of northern Yukon Territory and northwestern District of Mackenzie, Canada; in M.C. Ritcher, ed., Arctic geology; American Association of Petroleum Geologists, Memoir 19; pp. 23-40.

Norris, D.K., Price, R.A., and Mountjoy, E.W., 1963, Geology, northern Yukon Territory and northwestern District of Mackenzie; Geological Survey of Canada, Map 10-1963.

Officer, C.B., 1976, Physical oceanography of estuaries (and associated coastal waters); J. Wiley and Sons, New York; 465 p.

Officer, C.B., and Geophysics Study Committee, 1977, Overview and recommendations; in Estuaries, geophysics, and the environment; National Academy of Sciences, Washington, D.C.; pp. 1-10.

Oguss, E., and Erlebach, W.E., 1976, Limitations of single water samples in representing mean water quality; I, Thompson River at Shaw Spring, British Columbia; Canada, Department of Environment, Water Quality Branch, Vancouver; Technical Bulletin no. 95; 7 p. and Appendix.

O'Neill, J.J., 1924, Geology of the Arctic coast of Canada, west of the Kent Peninsula; in Report of Canadian Arctic expedition 1913-1918; v. 2, Geology and geography; pp. 10A-18A.

Owens, E.H., 1975, Barrier beaches and sediment transport in the southern Gulf of St Lawrence, Canada; in Proceedings, 14th Coastal Engineering Conference, Copenhagen, June 1974; American Society of Civil Engineers, New York; v. 2, pp. 1177-1193.

Owens, E.H., 1976, The effects of ice on the littoral zone, Richibucto Head, eastern New Brunswick; Revue de Geographie de Montreal, v. 30, pp. 95-104.

Owens, E.H., 1976, Temporal variations in beach and nearshore dynamics; Journal of Sedimentary Petrology, v. 47, pp. 168-190.

Owens, E.H., and McCann, S.B., 1970, The role of ice in the Arctic beach environment with special reference to Cape Ricketts, southwest Devon Island, N.W.T., Canada; American Journal of Science, v. 268, pp. 397-414.

Owens, E.H., and McCann, S.B., 1980, The coastal geomorphology of the Magdalen Islands, Quebec; in S.B. McCann, ed., The coastline of Canada; Geological Survey of Canada, Paper 80-10; pp. 51-72.

Paerl, H.W., 1973, Detritus in Lake Tahoe: structural modification by attached microflora; Science, v. 180, pp. 496-498.

Paquette, R.G., and Bourke, R.H., 1974, Observations on the coastal current of Arctic Alaska; Journal of Marine Research, v. 32, pp. 195-207.

Parthenaides, E., 1977, Unified view of wash load and bed-material load; Journal of the Hydraulics Division, American Society of Civil Engineers, v. 103, pp. 1037-1057.

Pattullo, J., Munk, W., Revelle, R., and Strong, E., 1955, The seasonal oscillations in sea level; Journal of Marine Research, v. 14, pp. 88-156.

Peake, J.S., and Walker, H.J., 1971, Albedo changes in an Arctic delta [abstract]; in D.S. Gorsline, ed., Abstract Volume, 2nd National Coastal and Shallow Water Research Conference, University of Southern California, Los Angeles; p. 176.

Pearson, A.M., and Nagy, J., 1976, The summer climate at Sam Lake, Yukon Territory; Arctic, v. 29, pp. 159-164.

Pelletier, B.R., 1980, Geology, Beaufort-Mackenzie Basin, District of Mackenzie and Yukon Territory; Geological Survey of Canada, Map 1509A.

Perkin, R.G., and Walker, E.R., 1971, Salinity calculations from in situ measurements; Canada, Department of Environment, Pacific Marine Science Report no. 71-1.

Petterson, H., 1920, Internal movements in coastal waters and meteorological phenomena; Geografiska Annaler, v. 1, pp. 32.

Pissart, A., 1967, [The nature of the runoff regime on Prince Patrick Island, Canadian Arctic) (in French)]; Biuletyn Periglacjalny, v. 16, pp. 217-224.

Posner, G.S., 1959, Preliminary oceanographic studies of the positive bar-built estuaries of North Carolina, U.S.A. [abstract]; in M. Sears, ed., 1st International Oceanographic Congress preprints; American Association for the Advancement of Science, Washington, D.C.; pp. 704-705.

Postma, H., 1954, Hydrology of the Dutch Wadden Sea; Archives Neerlandaises de Zoologie, v. 10, pp. 405-511.

Postma, H., 1961, Transport and accumulation of suspended matter in the Dutch Wadden Sea; Netherlands Journal of Sea Research, v. 1, pp. 148-190.

Postma, H., 1967, Sediment transport and sedimentation in the estuarine environment; in G. Lauff, ed., Estuaries; American Association for the Advancement of Science, Publication 83; pp. 158-179.

Postma, H., and Kalle, K., 1955, [The origin of the turbidity zone in the lower reaches of rivers (in German)]; Deutsche Hydrographische Zeitschrift, v. 8, pp. 137-144.

Prest, V.K., 1969, Retreat of Wisconsin and Recent ice in North America; Geological Survey of Canada, Map 1257A.

Price, W.A., 1963, Patterns of flow and channeling in tidal inlets; Journal of Sedimentary Petrology, v. 33, pp. 279-290.

Pritchard, D.W., 1955, Estuarine circulation patterns; American Society of Civil Engineers, Proceedings, v. 8, pp. 717/1-717/11.

Pritchard, D.W., 1956, The dynamic structure of a coastal plain estuary; Journal of Marine Research, v. 15, pp. 33-42.

Proudman, J., 1955, The propagation of tide and surge in an estuary; Proceedings, Royal Society (London), v. 231A, pp. 8-24.

Rampton, V.N., 1974a, Terrain evaluation with respect to pipeline construction, Mackenzie Transportation Corridor, northern part, latitude 68°N to coast; Canada, Environmental-Social Committee, Northern Pipelines, Task Force on Northern Oil Development, Report no. 73-47; 44 p.

Rampton, V.N., 1974b, Surficial geology, Herschel Island map-sheet; in Geological Survey of Canada, Open-file no. 191.

Rampton, V.N., in press, Quaternary geology of the Yukon Coastal Plain; Geological Survey of Canada, Bulletin 317.

Rampton, V.N., and Dugal, J.B., 1974, Quaternary stratigraphy and geomorphic processes on the Arctic coastal plain and adjacent areas, Demarcation Point, Yukon Territory, to Malloch Hill, District of Mackenzie; in Report of Activities, Part A; Geological Survey of Canada, Paper 74-1A; p. 283.

Rannie, W.F., 1978, An approach to the prediction of suspended sediment rating curves; in R. Davidson-Arnott and W. Nickling, eds, Research in fluvial geomorphology; Proceedings, 5th Guelph Symposium on Geomorphology, 1977; Geo Abstracts, Norwich (in association with University of Guelph); pp. 149-167.

Reed, R.J., and Kunkel, B.A., 1960, The Arctic circulation in summer; Journal of Meteorology, v. 17, pp. 489-506.

Reimnitz, E., and Bruder, K.F., 1972, River discharge into an ice-covered ocean; Geological Society of America Bulletin, v. 83, pp. 861-866.

Reimnitz, E., and Maurer, D.K., 1978, Storm surges in the Alaskan Beaufort Sea; U.S. Geological Survey, Open-file Report 78-593; 26 p.

Reimnitz, E., and Maurer, D.K., 1979, Effects of storm surges on the Beaufort Sea coast, northern Alaska; Arctic, v. 32, pp. 329-344.

Reineck, H.E., and Singh, I.B., 1973, Depositional sedimentary environments, with reference to terrigenous clastics; Springer-Verlag, New York; 439 p.

Reinson, G.E., 1977, Tidal-current control of submarine morphology at the mouth of the Miramichi Estuary, New Brunswick; Canadian Journal of Earth Sciences, v. 14, pp. 2524-2532.

Reinson, G.E., 1979, Facies models 6: barrier island systems; in R.G. Walker, ed., Facies models; Geoscience Canada, Reprint series no. 1; pp. 57-74.

Reinson, G.E., 1980, Variations in tidal-inlet morphology and stability, northeast New Brunswick; in S.B.McCann, ed., The coastline of Canada; Geological Survey of Canada, Paper 80-10; pp. 23-39.

Rhoads, D.C., 1971, Near-bottom turbidity related to biogenic reworking of bottom muds [abstract]; in D.S. Gorsline, ed., Abstract Volume, 2nd National Coastal and Shallow Water Research Conference, University of Southern California, Los Angeles; p. 189.

Ritchie, J.C., 1972, Pollen analysis of late-Quaternary sediments from the Arctic treeline of the Mackenzie River Delta region, Northwest Territories; in D.E. Kerfoot, ed., Mackenzie Delta Monograph; Brock University, St Catherines, Ontario; pp. 29-50.

Ritchie, J.C., and Hare, F.K., 1971, Late-Quaternary vegetation and climate near the Arctic tree line of northwestern North America; Quaternary Research, v. 1, pp. 331-342.

Rogers, J.C., 1978, A meteorological basis for long-range forecasting of summer and early autumn sea ice conditions in the Beaufort Sea; in D.B. Muggeridge, ed., Proceedings, 4th International Conference on Port and Ocean Engineering under Arctic Conditions; Memorial University, St John's, Newfoundland, 1977; v. 2, pp. 952-962.

Russell, R.C.H., and Osorio, J.D.C., 1958, An experimental investigation of drift profiles in a closed channel, with appendix by M.S. Longuet-Higgins; in Proceedings, 6th Conference on Coastal Engineering, Council on Wave Research, University of California; pp. 171-183.

Schalk, M., and Hume, J.D., 1966, Sea ice movement of beach material in the vicinity of Point Barrow, Alaska [abstract]; Journal of Geophysical Research, v. 66, pp. 2558-2559.

Schell, D.M., 1974, Seasonal variation in nutrient chemistry and conservative constituents in coastal Alaskan Beaufort Sea waters; in V. Alexander et al., Environmental studies of an Arctic estuarine system; University of Alaska, Institute of Marine Science, Report R-74-1; 543 p.

Schell, D.M., and Hall, G., 1972, Water chemistry and nutrient regeneration process studies; in P.J. Kinney, D.M. Schell, and V. Alexander, Baseline data study of the Alaskan Arctic aquatic environment; University of Alaska, Institute of Marine Science, Report R-72-3; pp. 3-28.

Schubel, J.R., 1968, Turbidity maximum of the northern Chesapeake Bay; Science, v. 161, pp. 1013-1015.

Schubel, J.R., 1974, Effects of tropical storm Agnes on the suspended solids of the northern Chesapeake Bay; in R.J. Gibbs, ed., Suspended solids in water; Plenum Press, New York.

Schubel, J.R., and Kana, T.W., 1972, Agglomeration of fine-grained suspended sediment in northern Chesapeake Bay; Powder Technology, v. 6, pp. 9-16.

Schultz, E.A., and Simmons, H.B., 1957, Freshwater-saltwater density currents, a major cause of siltation in estuaries; U.S.A., Corps of Engineers, Committee on Tidal Hydraulics, Technical Bulletin no. 2; 28 p.

Schumm, S.A., and Lichty, R.W., 1965, Time, space, and causality in geomorphology; American Journal of Science, v. 263, pp. 110-119.

Schwartz, P.K., 1975, Nature and genesis of some storm washover deposits; U.S.A., Corps of Engineers, Coastal Engineering Research Center, Technical Memorandum 61; 69 p.

Scott, K.M., 1978, Effects of permafrost on stream channel behaviour in Arctic Alaska; U.S. Geological Survey, Professional Paper 1068; 19 p.

Scott, A.J., Hoover, R.A., and McGowen, J.H., 1969, Effects of hurricane Beulah on Texas coastal lagoons and barriers; in A.A. Castanares and F.B. Phleger, eds, Lagunas costeras, un simposio; Proceedings, International Symposium on Coastal Lagoons, Mexico, D.F., November 1967; pp. 221-236.

Scruton, P.C., 1960, Delta building and the deltaic sequence; in F.P. Shepard, F.B. Phleger, and Tj. van Andel, eds, Recent sediments, northwest Gulf of Mexico; American Association of Petroleum Geologists, Tulsa, Oklahoma; pp. 82-102.

Sharma, T.C., and Dickinson, W.T., 1979, Unit step and frequency response functions applied to the watershed fluvial system; Journal of Hydrology, v. 40, pp. 323-335.

Shearer, J.M, 1972, Geologic structure of the Mackenzie Canyon area of the Beaufort Sea; in Report of Activities, Part A; Geological Survey of Canada, Paper 72-1A; pp. 179-180.

Shearer, J.M., and Blasco, S., 1975, Further observations of the scouring phenomenon in the Beaufort Sea; in Report of Activities, Part A; Geological Survey of Canada, Paper 75-1A; pp. 483-493.

Sherman, I., 1953, Flocculent structure of sediment suspended in Lake Mead; Transactions, American Geophysical Union, v. 34, pp. 394-406.

Short, A.D., 1979, Barrier island development along the Alaska-Yukon coastal plains; Geological Society of America Bulletin, part II, v. 90, pp. 77-103.

Short, A.D., and Wiseman, W.J., Jr, 1974, Freeze-up processes on Arctic beaches; Arctic, v. 27, pp. 215-224.

Short, A.D., and Wiseman, W.J., Jr, 1975, Coastal breakup in the Alaskan Arctic; Geological Society of America Bulletin, v. 86, pp. 199-202.

Shpaikher, A.O., Federova, Z.P., and Yankina, Z.S., 1968, [Variations of thermal conditions in the Chukchi Sea during the last decade (in Russian)]; Problemy Arktiki i Antarktiki, v. 29, pp. 19-28.

Simmons, H.B., 1955, Some effects of upland discharge on estuarine hydraulics; Proceedings, American Society of Civil Engineers, v. 81, pp. 1-20.

Simmons, H.B., 1965, Channel depth as a factor in estuarine sedimentation; in Proceedings, Federal Interagency Sedimentation Conference, 1963; U.S. Department of Agriculture, Miscellaneous Publication 970; pp. 722-730.

Simmons, H.B., 1966, Field experience in estuaries; in A.T. Ippen, ed., Estuary and coastline hydrodynamics; Mc%graw-Hill, New York; chapter 16, pp. 673-690.

Slaymaker, H.O., and Chorley, R.J., 1964, The vigil network system; Journal of Hydrology, v. 2, pp. 19-24.

Smayda, T., 1969, Some measurements of the sinking rate of fecal pellets; Limnology and Oceanography, v. 14, p. 621.

Smith, N.P., 1977, Meteorological and tidal exchanges between Corpus Christi Bay, Texas, and the northwestern Gulf of Mexico; Estuarine and Coastal Marine Science, v. 5, pp. 511-520.

Smith, N.P., 1978, Long-period, estuarine-shelf exchanges in response to meteorological forcing; in J.C.J. Nihoul, ed., Hydrodynamics of estuaries and fjords; Proceedings, 9th International Liege Colloquium on Ocean Hydrodynamics; Elsevier Scientific Publishing Company, Amsterdam; pp. 147-159.

Smith, N.P., 1979, Meteorological forcing of coastal waters by the inverse barometer effect; Estuaries and Coastal Marine Science, v. 8, pp. 149-156.

Smith, D.G., and Smith, N.D., 1980, Sedimentation in anastomozed river systems: examples from alluvial valleys near Banff, Alberta; Journal of Sedimentary Petrology, v. 50, pp. 157-164.

Snedecor, G.W., and Cochran, W.G., 1967, Statistical methods; 6th edition; Iowa State University Press, Ames, Iowa; 593 p.

Stapor, F.W., 1971, Sediment budgets on a compartmented low-to-moderate energy coast in northwest Florida; Marine Geology, v. 10, pp. M1-M7.

Steigenberger, L.W., Robertson, R.A., Johansen, K., and Elson, M.S., 1975, Biological/engineering evaluation of the proposed pipeline crossing sites in northern Yukon Territory; Canada, Department of Environment, Fisheries and Marine Service, Pacific Region, Report PAC/T-75-11; 456 p.

Stenborg, T., 1970, Delay of runoff from a glacier basin; Geografiska Annaler, v. 52A, pp. 1-30.

Stokes, G.G., 1851, On the effect of the internal friction of fluids on the motion of pendulums; Philosophical Transactions, Cambridge, v. 9, pp. 8-106.

Stommel, H., and Farmer, H.G., 1952, Abrupt change in width in two-layer open-channel flow; Journal of Marine Research, v. 11, pp. 205-214.

Strahler, A.,S., 1950, Equilibrium theory of erosional slopes approached by frequency distribution analysis; American Journal of Science, v. 248, pp. 673-696, 800-814.

Strahler, A.N., 1952, Hypsometric (area-altitude) analysis of erosional topography; Geological Society of America Bulletin, v. 63, pp. 1117-1142.

Straub, L.G., 1935, Missouri River; 73rd U.S. Congress, Session 2, House Document 238, Appendix 6; pp. 1032-1235.

Strickler, A., 1923, [Contribution to the study of the velocity formula and the resistance coefficient for streams, canals, and closed pipes (in German)]; Mitteilungen des Amtes fur Wasserwirtschaft, Bern; no. 16; 77 p.

Stringer, W.J., 1974, Morphology of the Beaufort Sea shorefast ice; in J.C. Reed and J.E. Sater, eds, The coast and shelf of the Beaufort Sea; Arctic Institute of North America, Arlington, Va.; pp. 165-172.

Sundborg, Å., 1956, The river Klaralven: a study of fluvial processes; Geografiska Annaler, v. 38.

Sverdrup, H.V., 1926, Dynamics of tides on the North Siberian shelf, results from the Maud expedition; Geofiziske Publikasjoner, v. 4, no. 5, pp. 1-75.

Swan, D., Clague, J.J., and Luternauer, J.L., 1978, Grain-size statistics I: evaluation of the Folk and Ward measures; Journal of Sedimentary Petrology, v. 48, pp. 863-878.

Swift, D.J.P., 1975, Barrier-island genesis: evidence from the central Atlantic shelf, eastern U.S.A.; Sedimentary Geology, v. 14, pp. 1-43.

Swift, D.J.P., and Ludwick, J.C., 1976, Substrate response to hydraulic process: grain-size frequency distributions and bed forms; in D.J. Stanley and D.J.P. Swift, eds, Marine sediment transport and environmental management; American Geological Institute; J. Wiley and Sons, New York; chapter 10, pp. 159-196.

Swift, D.J.P., Ludwick, J.C., and Boehmer, W.R., 1972, Shelf sediment transport: a probability model; in D.J.P. Swift, D.B. Duane, and O.H. Pilkey, eds, Shelf sediment transport: process and pattern; Dowden, Hutchinson and Ross, Stroudsburg, Pennsylvania; pp. 195-223.

Taylor, R.B., 1977, The occurrence of grounded ice ridges and shore ice piling along the northern coast of Somerset Island, N.W.T.; Arctic, v. 31, pp. 133-149.

Terzaghi, K., and Peck, R.B., 1967, Soil mechanics in engineering practice; 2nd edition; J. Wiley and Sons, New York; 729 p.

Thompson, H.R., 1953, Geology and geomorphology in the southeastern Nordaustland (Northeast Land), Spitsbergen; Proceedings, Geologists' Association, v. 64, pp. 293-312.

Treshnikov, A.F., 1977, Water masses of the Arctic Basin; in M.J. Dunbar, ed., Polar oceans; Proceedings, Polar Oceans Conference, Montreal, May 1974; Arctic Institute of North America, Calgary; pp. 17-31.

Treshnikov, A.F., and Baranov, G.I., 1977, The structure of the circulation and budget dynamics of the waters of the North Polar region; in M.J. Dunbar, ed., Polar oceans; Proceedings, Polar Oceans Conference, Montreal, May 1974; Arctic Institute of North America, Calgary; pp. 33-44.

Treshnikov, A.F., Borisenkov, E.P., Nikiforov, E.G., Mustafin, N.V., Chaplygin, E.I., and Shpaikher, A.O., 1968, [Full-scale experiment on the problem of ocean-atmosphere interaction (in Russian)]; Problemy Arktiki i Antarktiki, v. 28, pp. 5-20.

Tucker, R.W., and Burrell, D.C., 1977, The sedimentary environment of a lagoon on the Beaufort Sea coast of Alaska; Marine Science Communications, v. 3, pp. 93-116.

Ugolini, F.C., 1975, Ice-rafted sediments as a cause of some thermokarst lakes in the Noatak River Delta, Alaska; Science, v. 188, pp. 51-53.

U.S.A., Coastal Engineering Research Center, 1973, Shore protection manual; U.S.A., Corps of Engineers, Fort Belvoir, Va.,; 3 volumes.

van Dorn, W.G., 1953, Wind stress on an artificial pond; Journal of Marine Research, v. 12, pp. 249-276.

van Everdingen, R.O., 1974, Groundwater in permafrost regions of Canada; in Permafrost hydrology; Proceedings of workshop seminar, Calgary, February 1974; Canada, Department of Environment, Canadian National Committee, International Hydrological Decade; pp. 83-93.

van Straaten, L.M.J.U., 1952, Biogene textures and the formation of shell beds in the Dutch Wadden Sea; Proceedings, Koninklijke Nederlandse Akademie van Wetenschappen, v. B55, pp. 500-516.

van Straaten, L.M.J.U., 1960, Transport and composition of sediments; in Das Ems-Estuarium, Nordsee; Verhandelingen Koninklijk Nederlande Geologisch Mijnbouwkundig Genootschap, Geologische Serie 19; pp. 279-292.

van Straaten, L.M.J.U., and Kuenen, Ph.H., 1957, Accumulation of fine-grained sediments in the Dutch Wadden Sea; Geologie en Mijnbouw, v. 19, pp. 329-354.

van Straaten, L.M.J.U., and Kuenen, Ph.H., 1958, Tidal action as a cause for clay accumulation; Journal of Sedimentary Petrology, v. 28, pp. 406-413.

van Veen, J., 1950, [Ebb- and flood-channel systems in Dutch tidal waters (in Dutch)]; in Waddensymposium, tijdschrift nederlandse Aardrijkskunde Genootschap, pp. 43-65.

Verwey, J., 1952, On the ecology of distribution of cockle and mussel in the Dutch Wadden Sea, their role in sedimentation and the source of the food supply; Archives Neerlandaises de Zoologie, v. 10, pp. 171-239.

Volker, A., 1966, Surface hydrology of deltaic area; in Scientific problems of the humid tropical zone deltas and their implications; Proceedings, Dacca Symposium, February-March 1964; UNESCO, Paris; pp. 143-150.

Walcott, R.I., 1975, Recent and late Quaternary changes in water level; Eos, v. 56, pp. 62-72.

Walker, H.J., 1969, Some aspects of erosion and sedimentation in an Arctic delta during breakup; in Hydrologie des deltas; Association Internationale d'Hydrologie Scientifique, Actes du Colloque de Bucarest; pp. 209-219.

Walker, H.J., 1971, Salinity changes occurring during breakup in an Arctic delta [abstract]; in D.S. Gorsline, ed., Abstract Volume, 2nd National Coastal and Shallow Water Research Conference, University of Southern California, Los Angeles; p. 247.

Walker, H.J., 1972, Salinity changes in the Colville River Delta, Alaska, during breakup; in The Role of snow and ice in hydrology; Proceedings of the Banff Symposia; Banff, September 1972; v. 1, pp. 514-527.

Walker, H.J., 1973, Spring discharge of an Arctic river determined from salinity measurements beneath sea ice; Water Resources Research, v. 9, pp. 474-480.

Walker, H.J., 1974, The Colville River and the Beaufort Sea: some interactions; in J.C. Reed and J.E. Sater, eds, The coast and shelf of the Beaufort Sea; Arctic Institute of North America, Arlington, Va.; pp. 513-540.

Walker, H.J., and Arnborg, L., 1965, Permafrost and ice-wedge effects on riverbank erosion; in Permafrost, Proceedings, 1st International Conference, Purdue University, West Lafayette, Indiana, 1963; pp. 164-171.

Walker, R.G., 1979, Facies and facies models 1: general introduction; in R.G. Walker, ed., Facies models; Geoscience Canada, reprint series no. 1; pp. 1-7.

Walsh, J.E., and Johnson, C.M., 1979, An analysis of Arctic sea ice fluctuations, 1953-1977; Journal of Physical Oceanography, v. 9, pp. 580-591.

Wang, D-P., 1979, Subtidal sea level variations in the Chesapeake Bay and relations to atmospheric forcing; Journal of Physical Oceanography, v. 9, pp. 413-421.

Washburn, A.L., 1969, Weathering, frost action and patterned ground in the Mesters Vig district, northeast Greenland; Meddelelser om Gronland, v. 176, no, 4, 296 p.

Watts, G.M., 1953, A study of sand movement at South Lake Worth Inlet, Florida; U.S.A., Beach Erosion Board, Technical Memorandum no. 42; 24 p.

Weigel, R.L., 1954, Gravity wave tables of functions; Council on Wave Research, Engineering Foundation, University of California, Berkeley; cited by Komar (1976b, p. 74).

Wein, R.W., Hettinger, L.R., Janz, A.V., and Cody, W.J., 1974, Vascular plant range extensions in northern Yukon Territory and northwestern Mackenzie District, Canada; Canadian Field Naturalist, v. 88, pp. 57-66.

Weisberg, R.H., 1976, The nontidal flow in the Providence River of Narragansett Bay; a stochastic approach to estuarine circulation; Journal of Physical Oceanography, v. 6, pp. 721-734.

Welder, F.A., 1959, Processes of deltaic sedimentation in the lower Mississippi River; Lousiana State University , Baton Rouge; Coastal Studies Institute, Technical Report no. 12; 90 p.

Weller, G., and Holmgren, B., 1974, The microclimates of the Arctic tundra; Journal of Applied Meteorology, v. 13, pp. 854-862.

Welsh, S.L., and Rigby, J.K., 1971, Botanical and physiographic reconnaissance of northern Yukon; Brigham Young University, Science Bulletin, Biological Series, v. 14; 64 p.

Wendler, G., 1978, Snow blowing and snow fall on the North Slope, Alaska; University of Alaska, Fairbanks; Geophysical Institute, Report U.A.G. R-259; 22 p.; prepared for Arctic Pipeline Study Group.

Whitten, E.H.T., 1964, Process-response models in geology; Geological Society of America Bulletin, v. 75, pp. 455-464.

Williams, J.E., 1949, Chemical weathering at low temperatures; Geographical Review, v. 39, pp. 129-135.

Williams, H.B., Farrugia, V., Ekker, A., and Haden, E.L., 1964, Chlorinity determination in estuarine waters by physical measurement; Journal of Marine Research, v. 22, pp. 190-196.

Wilson, H.P., 1974, Winds and currents in the Beaufort Sea; in J.C. Reed and J.E. Sater, eds, The coast and shelf of the Beaufort Sea; Arctic Institue of North America, Arlington, Va.; pp. 13-23.

Wiseman, W.J., Jr, 1979, Hypersaline bottom water: Peard Bay, Alaska; Estuaries, v. 2, pp. 189-193.

Wiseman, W.J., Jr, and Short, A.D., 1976, Mesoscale thermal variations along the Arctic North Slope; in D.W. Hood and D.C. Burrel, eds, Assessment of the Arctic marine environment: selected topics; University of Alaska, Fairbanks; Institute of Marine Science, Occasional Publication no. 4; pp. 229-240.

Wiseman, W.J., Jr, Coleman, J.M., Gregory, A., Hsu, S.A., Short, A.D., Suhayda, J.N., Walters, C.D., Jr, and Wright, L.D., 1973, Alaskan Arctic coastal processes and morphology; Louisiana State University, Baton Rouge; Coastal Studies Institute, Technical Report no. 149; 171 p..

Wright, L.D., 1970, Circulation, effluent diffusion and sediment transport, mouth of South Pass, Mississippi River Delta; Louisiana State University, Baton Rouge; Coastal Studies Institute, Technical Report no. 84; 56 p.

Wright, L.D., 1977, Sediment transport and deposition at river mouths: a synthesis; Geological Society of America Bulletin, v. 88, pp. 857-868.

Wunsch, C., 1972, Bermuda sea level in relation to tides, weather, and baroclinic fluctuations; Reviews of Geophysics and Space Physics, v. 10, pp. 1-49.

Yano, K., Tsuchiya, Y., and Michiye, M., 1969, Studies on the sand transport in streams with tracers; Bulletin of the Disaster Prevention Research Institute, Kyoto University, v. 18, part 3, no. 141; 16 p.

Yingst, J.Y., and Rhoads, D.C., 1978, Seafloor stability in central Long Island Sound: part 2, biological interactions and their potential importance for seafloor erodibility; in M.L. Wiley, ed., Estuarine interactions; Proceedings, 4th International Estuarine Research Conference, Mount Pocono, Pennsylvania, October, 1977; Academic Press, New York; p. 245.

Yorath, C.J., 1973, Geology of Beaufort-Mackenzie Basin and eastern part of northern Interior Plains; in M.C. Ritcher, ed., Arctic Geology; American Association of Petroleum Geologists, Memoir 19; pp. 41-47.

Zabawa, C.F., 1978, Microstructure of agglomerated suspended sediments in northern Chesapeake Bay estuary; Science, v. 202, pp. 49-51.

APPENDIX A.1

LIST OF NOTATION

| | |
|---|---|
| $x \pm e$ | sample mean and standard error |
| $[x]$ | section-mean value |
| $\langle x \rangle$ | reach-mean value |
| $\hat{x}$ | estimated value or sample statistic |
| $\bar{x}$ | mean value |
| $\simeq$ | approximately equal |
| $\sim$ | of order of magnitude |
| | |
| $A$ | area, cross-sectional area |
| $A_D$ | drainage-basin area |
| $A_I$ | icing area |
| $A_L$ | lagoon or lake area |
| $A_b$ | basal area |
| $A_e$ | exposure area |
| $a$ | amplitude |
| $B$ | slope (angle) |
| $B_e$ | energy-slope (angle) |
| $b$ | width |
| $C$ | phase speed |
| $C$ | concentration (mass per unit volume) |
| $C_D$ | drag coefficient |

$C_D$ concentration of total dissolved solids

$C_I$ concentration of incombustible suspended solids

$C_S$ concentration of suspended sediment

$C_T$ concentration of total suspended solids

$D$ particle size

$D_n$ n-percentile size ($0 \leq n \leq 100\%$)

$D_a$ representative particle size in armour layer

$\tilde{D}$ graphic mean size ($\log\tilde{D} = \log(D_{84} D_{50} D_{16})/3$

$d$ sediment thickness

$E$ energy

$e$ error term

$e_B$ efficiency factor, bedload transport

$e_S$ efficiency factor, suspended load transport

$e_T$ efficiency factor, total transport

$f$ frequency

$f$ friction angle

$f_i$ relative frequency, class i

$f_l$ horizontal Coriolis parameter

$g$ gravitational acceleration

$H$ Fourier transform of $h(\tau)$

$H$ wave height

$H_E$ Secchi extinction depth

$H_b$ breaking wave height

$H_n$ n-percentile wave height ($0 \leq n \leq 100\%$)

$H_0$ deepwater wave height

$H_{rms}$ r.m.s. wave height

$h$ weighting function

| | |
|---|---|
| $h$ | depth |
| $h^*$ | mean depth $h^*=A/b$ |
| $I_t$ | total longshore transport rate (immersed weight) |
| $i_B$ | unit-width bedload transport rate (immersed weight) |
| $i_S$ | unit-width suspended load transport rate (immersed weight) |
| $J$ | mass transport rate (dry mass), total transport |
| $J_B$ | bedload transport rate (dry mass) |
| $J_D$ | solute transport rate (dry mass) |
| $J_e$ | aeolian sediment input to estuarine system |
| $J_f$ | fluvial sediment input to estuarine system |
| $J_0$ | sediment exchange across marine boundary of estuarine system |
| $J_T$ | total suspension transport rate (dry mass) |
| $j$ | unit-width transport rate (dry mass) |
| $j_B$ | unit-width bedload transport rate (dry mass) |
| $j_d$ | deposition rate (dry mass) |
| $K_x$ | refraction coefficient |
| $k$ | phase angle per unit distance (wave number) |
| $k$ | exponent |
| $L$ | basin or estuary length |
| $L_I$ | inlet length |
| $L_B$ | barrier length |
| $M$ | mass of sediment in storage |
| $m$ | mass |
| $N$ | record length |
| $N$ | coefficient of eddy viscosity |
| $n$ | sample size |

| | |
|---|---|
| $n$ | group speed coefficient |
| $P$ | power |
| $P_n$ | shore-normal component of wave power per unit crest length |
| $P_t$ | shore-tangent component of wave power per unit crest length |
| $P'_t$ | shore-tangent component of wave power per unit beach length |
| $p$ | power per unit boundary area |
| $p$ | pressure |
| $p$ | probability |
| $Q$ | discharge (volume transport rate) |
| $Q_d$ | direct precipitation input to estuarine system |
| $Q_e$ | evapotranspiration output from estuarine system |
| $Q_f$ | fluvial input to estuarine system |
| $Q_0$ | volume transfer across marine boundary |
| $Q_r$ | residual volume transfer |
| $Q_s$ | specific runoff |
| $Ra$ | Rayleigh parameter |
| $Re$ | Reynolds parameter |
| $R$ | hydraulic radius |
| $R_s$ | spring-tide range |
| $r$ | radius of curvature |
| $r_C$ | circularity ratio |
| $r_H$ | hypsometric integral |
| $S$ | deviation of s about s at tidal frequency |
| $s$ | salinity |
| $\bar{s}$ | tidal mean salinity |

| | |
|---|---|
| $s'$ | high-frequency deviation of s |
| $\bar{s}_e$ | mean salinity of estuary |
| $s_h$ | bottom salinity |
| $s_o$ | salinity at estuary entrance |
| $s_s$ | surface salinity |
| $\tilde{s}$ | graphic standard deviation $\tilde{s}=(\log_2 D_{84}-\log_2 D_{16})/2$ |
| T | period T=1/f |
| $T_a$ | dimensionless wind-stress parameter |
| t | time, duration |
| t* | recession constant |
| U | deviation of u about $\bar{u}$ at tidal frequency |
| $\bar{U}$ | mean speed of (oscillatory) sediment motion |
| $U_\theta$ | speed of sediment in direction $\theta$ |
| u | speed, longitudinal component of velocity |
| $\bar{u}$ | tidal mean value of u |
| $u'$ | high-frequency deviation of u |
| $u_f$ | integral mean velocity u =Q/bh |
| $u_s$ | longitudinal velocity at surface |
| $u_\theta$ | speed in direction $\theta$ |
| $u_0$ | horizontal orbital velocity |
| $u_m$ | maximum orbital velocity |
| $u_n$ | shore-normal current |
| $u_t$ | shore-tangent (longshore) current |
| V | volumetric capacity of system |
| V | deviation of v about $\bar{v}$ at tidal frequency |
| v | transverse component of velocity |
| $\bar{v}$ | tidal mean value of v |
| $v'$ | high-frequency deviation of v |

| | |
|---|---|
| $W$ | settling velocity |
| $W_s$ | still-water settling velocity |
| $W_a$ | still-water settling velocity of agglomerated particle |
| $W$ | deviation of w about $\bar{w}$ at tidal frequency |
| $w$ | vertical component of velocity |
| $\bar{w}$ | tidal mean value of w |
| $w'$ | high-frequency deviation of w about $\bar{w}$ |
| $X$ | Fourier transform of x(t) |
| $X$ | Characteristic grain size of sediment mixture |
| $x$ | system input |
| $x$ | longitudinal distance |
| $Y$ | Fourier transform of y(t) |
| $y$ | system output |
| $y$ | transverse distance |
| $Z$ | standardized normal deviate |
| $z$ | vertical distance |
| $\alpha$ | probability of type-I error |
| $\alpha$ | phase shift |
| $\alpha_b$ | angle between breaking wave crest and shore |
| $\gamma^2$ | coherence |
| $\gamma_s$ | specific gravity of sediment |
| $\Delta$ | dissipation parameter |
| $\varepsilon$ | noise function |
| $Z$ | Fourier transform of $\zeta(t)$ |
| $\zeta$ | water level |
| $\zeta_n$ | n-percentile water level ($0 \leq n \leq 100\%$) |
| $\eta$ | dynamic viscosity |
| $\Theta$ | temperature |

| | |
|---|---|
| $\kappa$ | coefficient of kurtosis |
| $\lambda$ | Poisson parameter |
| $\lambda$ | wavelength |
| $\lambda_0$ | deepwater wave length |
| $\mu$ | damping coefficient |
| $\nu$ | diffusive fraction of headward salt flux in estuary |
| $\xi$ | hiding factor |
| $\xi_E$ | hiding factor according to Einstein (1950) |
| $\xi'$ | modified hiding factor |
| $\rho$ | density, water density |
| $\rho_a$ | air density |
| $\rho_f$ | freshwater density |
| $\rho_h$ | water density at bottom (z=h) |
| $\rho_0$ | water density at estuary entrance (x=0) |
| $\rho_s$ | water density at surface (z=0); sediment density |
| $\rho_w$ | water density |
| $\sigma^2$ | variance |
| $\tau$ | lag time |
| $\tau$ | shear stress |
| $\tau_a$ | wind stress |
| $\tau_g$ | shear due to granular resistance only |
| $\tau_{ne}$ | northeasterly component of wind stress |
| $\tau_{nw}$ | northwesterly component of wind stress |
| $\Phi$ | phase |
| $\Phi_*$ | dimensionless transport coefficient |
| $\phi$ | streamfunction |
| $\phi$ | latitude |
| $\phi$ | solid friction angle |

$\chi^2$ parameter of chi-square distribution

$\Psi_*$ dimensionless shear coefficient

$\Omega$ angular velocity of the earth

$\omega$ phase angle per unit time (radial frequency)

APPENDIX A.2

FIELD INVESTIGATIONS AND PROCEDURES

Runoff inputs to the Babbage Estuary through sections B1 (Babbage River) and D1 (Deep Creek) were determined during parts of 1974-1976 using stage records and stage-discharge relations established for each section (see Appendix A.3 below). Stilling wells with Stevens type-A35 and type-F recorders were maintained at each section during the summer months. Prior to ice clearance, when stilling wells could not be installed and the stage-discharge relation was unstable due to ice effects, estimates of flow through the Babbage River section were obtained from discharge measurements taken approximately once daily and from frequent direct observations of stage for interpolation of discharge. In Deep Creek, daily discharge measurements were undertaken and the results adopted as representative for the day. Discharge measurements were carried out with Price-Gurley type-622AA meters suspended from the bow of a boat held stationary in the current against a tag wire. Current meters were calibrated by the Hydraulics Division, Canada Centre for Inland Waters, before and at the end of the study; the calibrations showed relatively minor changes. Initial (1974) calibrations were adopted for 1974 and 1975 measurements; subsequent (1977) calibrations were employed for 1976 measurements.

Net exchanges between the estuary and coastal waters of Phillips Bay were determined using water-level records with corroboration from velocity measurements in section M1. Water-level recorders were established at various sites within the estuary (see Figure 2 for locations). Stevens type-F recorders on stilling wells were used at gauge sites C and D in the delta; Foxborough pressure-diaphragm gauges were installed at sites B and E; and an Ottboro pressure-diaphragm gauge was employed at site A (C.H.S. station 6515), located on the lagoon side of Kay Point spit near the small inlet M2.

During parts of 1974, 1975, and 1976, a meteorological station was operated near Kay Point at a tundra site (Figure 2) approximately 6 m above sea level. Observations included hourly mean wind velocity at z=10 m; atmospheric pressure; air temperature and relative humidity; 12-h maximum and minimum air temperature; 12-h precipitation totals; and 12-h visibility and cloud conditions.

Estimates of fluvial sediment inputs were based on sample

data for suspended sediment concentration, obtained using DH48 depth-integrating samplers, and bedload transport data obtained with Helley-Smith bedload samplers. Ratings were established for dissolved and particulate solids transport using the sample data and for bedload transport using modified-Einstein and Bagnold models, partially calibrated by the Helley-Smith results (see section 4.1.2 and Appendix A.4).

Water samples for determination of filterable and non-filterable solids were collected using van Dorn samplers under various sampling regimes at stations indicated in Figure 2. Non-filterable solids concentrations were determined using 0.45-µm membrane filters. The sample data supplemented in situ measurements of water temperature, conductivity, and light attenuation, obtained with YSI SCT-33 temperature-conductivity meters, Interocean and Hydroproducts 0.10m-pathlength beam transmissometers, and standard 0.30-m Secchi disks on rods graduated at 5-mm intervals.

Sedimentation in the lagoon and in selected delta lakes was monitored with traps deployed during parts of the 1976 and 1977 open-water seasons (Figure 5). Sedimentation due to snowmelt flooding was estimated from measurements of accumulation on bottomfast ice and over prior-season vegetation. Erosion and sedimentation on intertidal surfaces were monitored using stakes with light-chain scour indicators at 41 sites on eight transects (Figure 5). Long-term sedimentation rates were estimated from radiocarbon dates on organic materials at selected sites in the delta and lower valley.

Bathymetric surveys were carried out with a Raytheon DE719 200-kHz narrow-beam (3°) sounding system, mounted on 16-foot boats. Additional surveys were conducted with a Raytheon RTT1000 200- and 7-kHz system, supplemented by side-scan sonar, mounted on a 19-foot boat. Horizontal control was provided by transection, using theodolites and two-way radio communication, and by trilateration using a ComDev Marine trisponder system with a nominal precision of ±1 m. Bathymetry of river and delta channels was obtained in cross-sections at 250-m intervals, supplemented by numerous longitudinal profiles; bathymetric surveys were also carried out in selected lakes in the Babbage Delta. Topographic profiles and elevation control were obtained with Zeiss Ni-2 levels and bubble-equipped survey rods.

Surface sediment samples were collected for particle size, bulk density, combustible fraction, and other analyses, at sites indicated in Figure 130 and at additional channel and terrace sites in the lower valley. Samples (m>0.5 kg) were collected from subaqueous surfaces with an Ekman box sampler;

samples from subaerial surfaces were obtained with simple cylindrical samplers or spades. Subsurface samples were obtained using modified-CRREL corers in frozen deposits and a simple piston corer, custom-built at UBC, in non-frozen materials. Larger samples ($m \leq 50$ kg) were collected as required for statistically valid analyses of graveliferous deposits. Particle size analyses were conducted by standard dry sieve and hydrometer procedures (see Appendix A.12).

APPENDIX A.3

DAILY DISCHARGE DATA, BABBAGE RIVER AND DEEP CREEK

Runoff inputs to the Babbage Estuary through sections B1 (Babbage River) and D1 (Deep Creek) were determined during parts of 1974-1976 using stage records and stage-discharge relations established for each section according to procedures outlined in Appendix A.2. The rating curve for ice-free conditions in the Babbage River section was based on 16 determinations in 1975 and 18 in 1976. A minor systematic difference between years may be present in the data, reflecting the adoption of different meter calibrations, changes in the reference elevation, or channel adjustmennts during the flood of 5-6 June 1976. The highest measured flow through section b1 was $Q=435\ m^3s^{-1}$; higher discharges were estimated by extrapolation of the stage-discharge relation. The Deep Creek rating was based on 25 discharge measurements under ice-free conditions in 1976.

The ratings adopted for summer-season data presented in this report were as follows (elevations in metres above arbitrary local datum):

Babbage River at B1

$$\log(Q)=3.467\log(z)+0.733,\quad r^2=0.961,\quad s=0.076$$

Deep Creek at D1

$Q>23.3\ m^3s^{-1}$: $\log(Q)=2.713\log(z)+0.209,\ r^2=0.974,\ s=0.026$

$Q<23.3\ m^3s^{-1}$: $\log(Q)=6.534\log(z)-1.422,\ r^2=0.985,\ s=0.024$

Mean, maximum, and minimum daily discharge are given below. For days for which continuous stage records are not available, observed maximum and minimum instantaneous discharge only are given; when continuous stage records are available, the data have been sampled at hourly intervals, yielding 24 hourly discharge values and the daily mean Q given below.

Babbage River below Crow River 1974

| | date | $\bar{Q}$ ($m^3 s^{-1}$) | max. | min. |
|---|---|---|---|---|
| 146. | 27 May 1974 | | >163.4 | <163.4 |
| 147. | 28 May 1974 | | >200.7 | <174.1 |
| 148. | 29 May 1974 | | >230.2 | <229.0 |
| 149. | 30 May 1974 | | >253.4 | <237.4 |
| 150. | 31 May 1974 | | >232.1 | <223.5 |
| 151. | 1 June 1974 | | >229.0 | <226.9 |
| 152. | 2 June 1974 | | >236.0 | <215.4 |
| 153. | 3 June 1974 | | >192.4 | <178.5 |
| 154. | 4 June 1974 | | >197.5 | <197.5 |
| 155. | 5 June 1974 | | >124.0 | <124.0 |
| 156. | 6 June 1974 | | >148.1 | <135.3 |
| 157. | 7 June 1974 | | >282.4 | <144.1 |
| 158. | 8 June 1974 | | >320.7 | <245.3 |
| 159. | 9 June 1974 | | >275.4 | <235.3 |
| 160. | 10 June 1974 | | >311.6 | <311.6 |
| 165. | 15 June 1974 | | >151.6 | <151.6 |
| 167. | 17 June 1974 | | >109.8 | < 62.9 |
| 168. | 18 June 1974 | | > 57.1 | < 27.5 |
| 169. | 19 June 1974 | | > 59.9 | < 34.4 |
| 170. | 20 June 1974 | | > 42.1 | < 30.2 |
| 171. | 21 June 1974 | | > 36.3 | < 15.4 |
| 181. | 1 July 1974 | | >108.2 | <108.2 |
| 182. | 2 July 1974 | | >146.9 | <146.9 |
| 184. | 4 July 1974 | 42.0 | 53.1 | 51.9 |
| 185. | 5 July 1974 | 46.7 | 50.3 | 45.2 |
| 186. | 6 July 1974 | 44.2 | 45.5 | 43.1 |
| 187. | 7 July 1974 | 55.1 | 66.6 | 45.3 |
| 188. | 8 July 1974 | 69.6 | 83.6 | 64.5 |
| 189. | 9 July 1974 | 82.2 | 86.7 | 74.6 |
| 190. | 10 July 1974 | 67.6 | 72.3 | 65.1 |
| 191. | 11 July 1974 | 63.1 | 68.7 | 58.6 |
| 192. | 12 July 1974 | 70.2 | 77.4 | 66.4 |
| 193. | 13 July 1974 | 64.1 | 69.3 | 59.2 |
| 194. | 14 July 1974 | 57.2 | 62.4 | 52.5 |
| 195. | 15 July 1974 | 50.2 | 55.0 | 47.2 |
| 196. | 16 July 1974 | 45.2 | 49.9 | 41.8 |
| 197. | 17 July 1974 | 41.8 | 47.2 | 38.8 |
| 198. | 18 July 1974 | 40.9 | 44.1 | 38.0 |
| 199. | 19 July 1974 | 39.2 | 42.6 | 36.5 |
| 200. | 20 July 1974 | 40.5 | 45.9 | 37.4 |
| 201. | 21 July 1974 | 50.5 | 80.5 | 44.4 |
| 202. | 22 July 1974 | 103.4 | 110.4 | 92.8 |

A.3 continued

| | | | | | |
|---|---|---|---|---|---|
| 203. | 23 | July | 1974 | | |
| 204. | 24 | July | 1974 | | |
| 205. | 25 | July | 1974 | | |
| 206. | 26 | July | 1974 | | |
| 207. | 27 | July | 1974 | | |
| 208. | 28 | July | 1974 | | |
| 209. | 29 | July | 1974 | | |
| 210. | 30 | July | 1974 | 38.6 | 41.3 | 36.6 |
| 211. | 31 | July | 1974 | 35.0 | 38.9 | 32.6 |
| 212. | 1 | Augt | 1974 | 31.8 | 33.9 | 29.7 |
| 213. | 2 | Augt | 1974 | 31.0 | 33.2 | 29.7 |
| 214. | 3 | Augt | 1974 | 36.1 | 37.8 | 34.5 |
| 215. | 4 | Augt | 1974 | 33.0 | 35.5 | 30.6 |
| 216. | 5 | Augt | 1974 | | | |
| 217. | 6 | Augt | 1974 | | | |
| 218. | 7 | Augt | 1974 | | | |
| 219. | 8 | Augt | 1974 | | | |
| 220. | 9 | Augt | 1974 | | | |
| 221. | 10 | Augt | 1974 | | | |
| 222. | 11 | Augt | 1974 | | | |
| 223. | 12 | Augt | 1974 | | | |
| 224. | 13 | Augt | 1974 | 39.0 | 47.0 | 34.8 |
| 225. | 14 | Augt | 1974 | 131.4 | 226.1 | 47.8 |

## A.3 continued

Babbage River (section B1) below Crow River

| | date | $\bar{Q}$ ($m^3 s^{-1}$) | max. | min. |
|---|---|---|---|---|
| 142. | 23 May 1975 | | > 3.4 | < 3.4 |
| 143. | 24 May 1975 | | > 2.6 | < 1.0 |
| 144. | 25 May 1975 | | > 3.4 | < 3.4 |
| 145. | 26 May 1975 | | > 26.0 | < 4.3 |
| 146. | 27 May 1975 | | > 23.5 | < 20.1 |
| 147. | 28 May 1975 | | > 41.0 | < 34.3 |
| 148. | 29 May 1975 | | > 72.8 | < 55.2 |
| 149. | 30 May 1975 | | > 84.4 | < 61.1 |
| 150. | 31 May 1975 | | >102.8 | < 61.1 |
| 151. | 1 June 1975 | | > 63.6 | < 61.9 |
| 152. | 2 June 1975 | | > 56.9 | < 53.5 |
| 153. | 3 June 1975 | | > 54.0 | < 44.8 |
| 154. | 4 June 1975 | | > 78.9 | < 53.2 |
| 155. | 5 June 1975 | | >111.5 | < 77.2 |
| 156. | 6 June 1975 | | >118.1 | <107.3 |
| 157. | 7 June 1975 | | >136.9 | <126.1 |
| 158. | 8 June 1975 | | >154.2 | <135.1 |
| 159. | 9 June 1975 | | >186.2 | <166.5 |
| 160. | 10 June 1975 | | >205.1 | <183.9 |
| 161. | 11 June 1975 | | >252.2 | <241.2 |
| 162. | 12 June 1975 | | >309.6 | <293.7 |
| 163. | 13 June 1975 | | >413.8 | <343.2 |
| 164. | 14 June 1975 | | >409.9 | <394.4 |
| 165. | 15 June 1975 | | >554.4 | <489.4 |
| 166. | 16 June 1975 | | >379.2 | <296.9 |
| 167. | 17 June 1975 | | >429.9 | <281.4 |
| 168. | 18 June 1975 | | >281.4 | <210.0 |
| 169. | 19 June 1975 | | >188.5 | <144.4 |
| 170. | 20 June 1975 | | >138.7 | <108.0 |
| 171. | 21 June 1975 | | >146.3 | <133.2 |
| 172. | 22 June 1975 | | >233.1 | <152.2 |
| 173. | 23 June 1975 | | >205.1 | <158.2 |
| 174. | 24 June 1975 | | >146.3 | <109.6 |
| 175. | 25 June 1975 | | >112.7 | < 89.0 |
| 176. | 26 June 1975 | | > 97.4 | < 74.8 |
| 177. | 27 June 1975 | | > 77.2 | < 65.5 |
| 178. | 28 June 1975 | | > 71.2 | < 62.3 |
| 179. | 29 June 1975 | | > 65.1 | < 56.1 |
| 180. | 30 June 1975 | 56.4 | 62.3 | 52.2 |
| 181. | 1 July 1975 | 58.6 | 65.5 | 53.2 |
| 182. | 2 July 1975 | 52.7 | 58.1 | 47.0 |
| 183. | 3 July 1975 | 41.9 | 49.4 | 38.1 |
| 184. | 4 July 1975 | 36.3 | 40.5 | 31.7 |
| 185. | 5 July 1975 | 30.8 | 37.0 | 25.2 |
| 186. | 6 July 1975 | 25.4 | 31.7 | 22.8 |
| 187. | 7 July 1975 | 24.5 | 29.7 | 22.1 |
| 188. | 8 July 1975 | 25.8 | 29.7 | 22.1 |
| 189. | 9 July 1975 | 25.6 | 30.7 | 21.3 |
| 190. | 10 July 1975 | 24.2 | 29.7 | 20.6 |
| 191. | 11 July 1975 | 21.8 | 26.1 | 18.6 |
| 192. | 12 July 1975 | 20.1 | 25.2 | 17.3 |
| 193. | 13 July 1975 | 20.3 | 22.8 | 18.6 |
| 194. | 14 July 1975 | 20.7 | 22.8 | 19.2 |
| 195. | 15 July 1975 | 20.2 | 23.6 | 17.9 |

A.3 continued

| | date | $\bar{Q}$ ($m^3 s^{-1}$) | max. | min. |
|---|---|---|---|---|
| 196. | 16 July 1975 | 18.4 | 20.6 | 16.1 |
| 197. | 17 July 1975 | 17.8 | 21.3 | 15.5 |
| 198. | 18 July 1975 | 15.6 | 17.3 | 13.9 |
| 199. | 19 July 1975 | 14.6 | 16.1 | 13.4 |
| 200. | 20 July 1975 | 13.6 | 14.4 | 12.4 |
| 201. | 21 July 1975 | 12.3 | 12.9 | 11.5 |
| 202. | 22 July 1975 | 11.4 | 11.9 | 11.1 |
| 203. | 23 July 1975 | 10.9 | 11.5 | 10.6 |
| 204. | 24 July 1975 | 11.1 | 11.9 | 10.2 |
| 205. | 25 July 1975 | 10.3 | 10.6 | 9.8 |
| 206. | 26 July 1975 | 9.6 | 10.2 | 9.1 |
| 207. | 27 July 1975 | 9.7 | 10.2 | 9.1 |
| 208. | 28 July 1975 | 10.3 | 11.5 | 9.1 |
| 209. | 29 July 1975 | 12.0 | 12.4 | 11.5 |
| 210. | 30 July 1975 | 12.7 | 13.4 | 11.9 |
| 211. | 31 July 1975 | 13.8 | 14.4 | 13.4 |
| 212. | 1 Augt 1975 | 14.2 | 15.0 | 13.4 |
| 213. | 2 Augt 1975 | 13.2 | 13.4 | 12.9 |
| 214. | 3 Augt 1975 | 13.7 | 14.4 | 12.9 |
| 215. | 4 Augt 1975 | 13.7 | 14.4 | 12.9 |
| 216. | 5 Augt 1975 | 12.8 | 13.4 | 11.9 |
| 217. | 6 Augt 1975 | 13.5 | 14.4 | 11.9 |
| 218. | 7 Augt 1975 | 19.0 | 22.1 | 15.0 |
| 219. | 8 Augt 1975 | 22.7 | 22.8 | 22.1 |
| 220. | 9 Augt 1975 | 27.2 | 38.1 | 22.8 |
| 221. | 10 Augt 1975 | 58.3 | 70.1 | 40.5 |
| 222. | 11 Augt 1975 | 57.0 | 65.5 | 50.3 |
| 223. | 12 Augt 1975 | 48.2 | 50.3 | 47.0 |
| 224. | 13 Augt 1975 | 40.4 | 47.0 | 34.8 |
| 225. | 14 Augt 1975 | 30.6 | 34.8 | 27.9 |
| 226. | 15 Augt 1975 | 27.5 | 29.7 | 26.1 |
| 227. | 16 Augt 1975 | 37.8 | 41.8 | 30.7 |
| 228. | 17 Augt 1975 | 31.5 | 35.9 | 28.8 |
| 229. | 18 Augt 1975 | 27.3 | 29.7 | 26.1 |
| 230. | 19 Augt 1975 | 25.9 | 26.9 | 25.2 |
| 231. | 20 Augt 1975 | 24.5 | 25.2 | 23.6 |
| 232. | 21 Augt 1975 | 22.7 | 23.6 | 21.3 |
| 233. | 22 Augt 1975 | 20.7 | 22.1 | 19.2 |
| 234. | 23 Augt 1975 | 19.3 | 19.9 | 18.6 |
| 235. | 24 Augt 1975 | 18.6 | 19.2 | 17.9 |
| 236. | 25 Augt 1975 | 18.7 | 19.2 | 17.9 |
| 237. | 26 Augt 1975 | 19.8 | 21.3 | 18.6 |
| 238. | 27 Augt 1975 | 33.4 | 52.2 | 22.1 |
| 239. | 28 Augt 1975 | 59.1 | 61.2 | 53.2 |
| 240. | 29 Augt 1975 | 53.2 | 58.1 | 48.4 |
| 241. | 30 Augt 1975 | 44.9 | 48.4 | 43.0 |
| 242. | 31 Augt 1975 | 40.5 | 43.0 | 39.3 |
| 243. | 1 Sept 1975 | 38.1 | 39.3 | 37.0 |
| 244. | 2 Sept 1975 | 37.0 | 38.1 | 35.9 |
| 245. | 3 Sept 1975 | 33.2 | 34.8 | 31.7 |

A.3 continued

Babbage River (section B1) below Crow River

| | date | $\bar{Q}$ ($m^3 s^{-1}$) | max. | min. |
|---|---|---|---|---|
| 150. | 30 May 1976 | | > 63. | < 63. |
| 151. | 31 May 1976 | | > 88. | < 88. |
| 152. | 1 June 1976 | | >151. | <151. |
| 153. | 2 June 1976 | | >326. | <326. |
| 154. | 3 June 1976 | | >311. | <311. |
| 155. | 4 June 1976 | | >282. | <282. |
| 156. | 5 June 1976 | 289.0 | 434.0 | 237.0 |
| 157. | 6 June 1976 | 445.0 | 529.0 | 365.0 |
| 158. | 7 June 1976 | 367.7 | 407.0 | 271.0 |
| 159. | 8 June 1976 | 179.6 | 261.0 | 120.0 |
| 160. | 9 June 1976 | 121.5 | 137.0 | 93.0 |
| 161. | 10 June 1976 | 103.9 | 119.0 | 90.0 |
| 162. | 11 June 1976 | 123.8 | 150.0 | 91.0 |
| 163. | 12 June 1976 | 126.5 | 138.0 | 113.0 |
| 164. | 13 June 1976 | 145.3 | 165.0 | 112.0 |
| 165. | 14 June 1976 | 190.8 | 226.0 | 154.0 |
| 166. | 15 June 1976 | 196.0 | 228.0 | 153.0 |
| 167. | 16 June 1976 | 161.7 | 187.0 | 126.0 |
| 168. | 17 June 1976 | 115.6 | 126.0 | 105.0 |
| 169. | 18 June 1976 | 80.0 | 104.0 | 40.0 |
| 170. | 19 June 1976 | 37.3 | 41.0 | 32.0 |
| 171. | 20 June 1976 | 38.3 | 43.0 | 33.0 |
| 172. | 21 June 1976 | 50.4 | 60.8 | 40.7 |
| 173. | 22 June 1976 | 69.3 | 83.4 | 52.8 |
| 174. | 23 June 1976 | 78.6 | 87.6 | 65.1 |
| 175. | 24 June 1976 | 78.3 | 82.8 | 70.6 |
| 176. | 25 June 1976 | 86.8 | 149.3 | 69.3 |
| 177. | 26 June 1976 | 381.7 | 477.0 | 202.0 |
| 178. | 27 June 1976 | 180.9 | 274.0 | 122.0 |
| 179. | 28 June 1976 | 116.9 | 121.0 | 112.0 |
| 180. | 29 June 1976 | 102.6 | 112.0 | 94.0 |
| 181. | 30 June 1976 | 119.7 | 141.0 | 96.0 |
| 182. | 1 July 1976 | 94.0 | 114.4 | 77.5 |
| 183. | 2 July 1976 | 70.3 | 76.7 | 56.3 |
| 184. | 3 July 1976 | 51.8 | 55.0 | 49.3 |
| 185. | 4 July 1976 | 53.9 | 59.6 | 48.6 |
| 186. | 5 July 1976 | 50.3 | 53.3 | 47.8 |
| 187. | 6 July 1976 | 52.5 | 57.7 | 46.5 |
| 188. | 7 July 1976 | 44.7 | 50.6 | 41.9 |
| 189. | 8 July 1976 | 38.6 | 41.8 | 36.7 |
| 190. | 9 July 1976 | 44.6 | 54.1 | 38.9 |
| 191. | 10 July 1976 | 63.0 | 141. | 53.1 |
| 192. | 11 July 1976 | | 140. | |
| 193. | 12 July 1976 | | | 68.3 |
| 194. | 13 July 1976 | 58.2 | 68.3 | 49.0 |
| 195. | 14 July 1976 | 42.6 | 48.0 | 38.7 |
| 196. | 15 July 1976 | 35.4 | 38.3 | 34.1 |

A.3 continued

| | date | $\bar{Q}$ ($m^3 s^{-1}$) | max. | min. |
|---|---|---|---|---|
| 197. | 16 July 1976 | 30.7 | 33.7 | 29.1 |
| 198. | 17 July 1976 | 27.0 | 29.8 | 25.7 |
| 199. | 18 July 1976 | 24.6 | 27.0 | 23.2 |
| 200. | 19 July 1976 | 23.2 | 25.2 | 22.2 |
| 201. | 20 July 1976 | 25.2 | 27.6 | 24.0 |
| 202. | 21 July 1976 | 25.9 | 27.6 | 24.7 |
| 203. | 22 July 1976 | 23.0 | 25.4 | 21.6 |
| 204. | 23 July 1976 | 22.0 | 23.6 | 20.5 |
| 205. | 24 July 1976 | 21.6 | 23.2 | 20.1 |
| 206. | 25 July 1976 | 22.5 | 23.8 | 21.1 |
| 207. | 26 July 1976 | 21.3 | 22.8 | 20.1 |
| 208. | 27 July 1976 | 19.8 | 20.9 | 18.4 |
| 209. | 28 July 1976 | 18.3 | 18.9 | 17.4 |
| 210. | 29 July 1976 | 18.6 | 19.1 | 17.6 |
| 211. | 30 July 1976 | 18.2 | 19.2 | 17.2 |
| 212. | 31 July 1976 | 17.8 | 18.6 | 17.1 |
| 213. | 1 Augt 1976 | 17.7 | 18.9 | 16.6 |
| 214. | 2 Augt 1976 | 16.8 | 17.4 | 16.1 |
| 215. | 3 Augt 1976 | 16.4 | 16.9 | 15.6 |
| 216. | 4 Augt 1976 | 16.3 | 16.6 | 15.8 |
| 217. | 5 Augt 1976 | 17.8 | 18.1 | 16.9 |
| 218. | 6 Augt 1976 | | | |
| 219. | 7 Augt 1976 | | | |
| 220. | 8 Augt 1976 | | | |
| 221. | 9 Augt 1976 | | | |
| 222. | 10 Augt 1976 | | | |
| 223. | 11 Augt 1976 | 24.7 | 27.7 | 22.3 |
| 224. | 12 Augt 1976 | 21.9 | 23.0 | 21.6 |
| 225. | 13 Augt 1976 | 69.1 | 90.3 | 23.8 |
| 226. | 14 Augt 1976 | 53.1 | 68.4 | 42.7 |
| 227. | 15 Augt 1976 | 36.3 | 42.0 | 31.8 |
| 228. | 16 Augt 1976 | 28.4 | 31.4 | 26.5 |
| 229. | 17 Augt 1976 | 25.6 | 26.4 | 24.9 |
| 230. | 18 Augt 1976 | 26.6 | 29.9 | 25.0 |
| 231. | 19 Augt 1976 | 34.1 | 35.2 | 30.4 |
| 232. | 20 Augt 1976 | 44.1 | 55.2 | 34.0 |
| 233. | 21 Augt 1976 | 45.9 | 53.0 | 40.3 |
| 234. | 22 Augt 1976 | 35.2 | 39.2 | 31.8 |
| 235. | 23 Augt 1976 | 29.6 | 31.6 | 27.7 |
| 236. | 24 Augt 1976 | 26.2 | 27.6 | 25.0 |
| 237. | 25 Augt 1976 | 23.9 | 24.9 | 22.9 |
| 238. | 26 Augt 1976 | 22.1 | 22.8 | 21.4 |
| 239. | 27 Augt 1976 | 20.7 | 21.4 | 20.0 |
| 240. | 28 Augt 1976 | 19.5 | 20.0 | 19.0 |
| 241. | 29 Augt 1976 | 18.6 | 19.0 | 18.1 |
| 242. | 30 Augt 1976 | 18.0 | 18.2 | 17.8 |
| 243. | 31 Augt 1976 | 17.8 | 18.0 | 17.6 |
| 244. | 1 Sept 1976 | 17.7 | 17.8 | 17.6 |
| 245. | 2 Sept 1976 | 23.5 | 27.6 | 17.7 |
| 246. | 3 Sept 1976 | 24.8 | 26.6 | 23.8 |
| 247. | 4 Sept 1976 | 22.8 | 23.7 | 22.1 |
| 248. | 5 Sept 1976 | 21.7 | 22.0 | 21.6 |
| 249. | 6 Sept 1976 | 21.5 | 21.7 | 21.1 |
| 250. | 7 Sept 1976 | 20.5 | 21.1 | 19.8 |
| 251. | 8 Sept 1976 | 19.2 | 19.8 | 18.6 |
| 252. | 9 Sept 1976 | 18.1 | 18.5 | 17.8 |
| 253. | 10 Sept 1976 | 17.8 | 18.0 | 17.6 |
| 254. | 11 Sept 1976 | 17.6 | 17.7 | 17.6 |
| 255. | 12 Sept 1976 | 17.4 | 17.6 | 17.1 |
| 256. | 13 Sept 1976 | 16.7 | 17.1 | 16.4 |
| 257. | 14 Sept 1976 | 16.0 | 16.3 | 15.7 |
| 258. | 15 Sept 1976 | 15.6 | 15.8 | 15.3 |
| 259. | 16 Sept 1976 | 16.2 | 17.0 | 15.8 |
| 260. | 17 Sept 1976 | 17.7 | 18.2 | 17.1 |

A.3 continued

Deep Creek above Babbage River distributary
(section D1) 1975

| date | Q ($m^3 s^{-1}$) |
|---|---|
| 28 MAY 1975 | 0. |
| 29 MAY | 0. |
| 30 MAY | 0. |
| 31 MAY | 0. |
| 1 JUNE | 0. |
| 2 JUNE | 0. |
| 3 JUNE | 0.02 |
| 4 JUNE | 0.1 |
| 5 JUNE | 0.1 |
| 6 JUNE | 0.1 |
| 7 JUNE | 0.1 |
| 8 JUNE | 0.1 |
| 9 JUNE | 0.1 |
| 10 JUNE | 0.3 |
| 11 JUNE | 10. |
| 12 JUNE | 35. |
| 13 JUNE | 50. |
| 14 JUNE | 70. |
| 15 JUNE | 87. |
| 16 JUNE | 90. |
| 17 JUNE | 98. |
| 18 JUNE | 75. |
| 19 JUNE | 63. |
| 20 JUNE | 39. |
| 21 JUNE | 38. |
| 22 JUNE | 39. |
| 23 JUNE | 37. |
| 24 JUNE | 35. |
| 25 JUNE | 29. |
| 26 JUNE | 30. |
| 27 JUNE | 21. |
| 28 JUNE | 17. |
| 29 JUNE | 15. |
| 30 JUNE | 14. |
| 1 JULY | 13. |
| 2 JULY | 11. |
| 3 JULY | 10. |
| 4 JULY | 8. |
| 7 JULY | 6. |
| 26 JULY | 3. |

A.3 continued

Deep Creek above Babbage River distributary (section D1) 1976

| date | $\bar{Q}$ ($m^3 s^{-1}$) | max. | min. |
|---|---|---|---|
| 154. 3 June 1976 | | > 1.2 | < 1.2 |
| 155. 4 June 1976 | | > 3.7 | < 3.7 |
| 158. 7 June 1976 | | >36.4 | <36.4 |
| 159. 8 June 1976 | | >49.9 | <49.9 |
| 160. 9 June 1976 | | >57.1 | <57.1 |
| 161. 10 June 1976 | | >60.0 | <60.0 |
| 162. 11 June 1976 | | >63.0 | <63.0 |
| 163. 12 June 1976 | | >49.9 | <49.9 |
| 164. 13 June 1976 | | >54.3 | <54.3 |
| 165. 14 June 1976 | | >59.3 | <59.3 |
| 166. 15 June 1976 | | >59.6 | <59.6 |
| 168. 17 June 1976 | | >36.7 | <36.7 |
| 169. 18 June 1976 | | >31.5 | <31.5 |
| 170. 19 June 1976 | | >25.3 | <25.3 |
| 171. 20 June 1976 | | >22.3 | <22.3 |
| 172. 21 June 1976 | | >21.7 | <21.7 |
| 173. 22 June 1976 | | >23.9 | <23.9 |
| 174. 23 June 1976 | | >23.2 | <23.2 |
| 175. 24 June 1976 | | >21.9 | <21.9 |
| 176. 25 June 1976 | | >20.0 | <20.0 |
| 177. 26 June 1976 | | >32.4 | <32.4 |
| 178. 27 June 1976 | | >31.1 | <31.1 |
| 179. 28 June 1976 | | >27.4 | <27.4 |
| 180. 29 June 1976 | | >22.1 | <22.1 |
| 181. 30 June 1976 | | >20.4 | <20.4 |
| 182. 1 July 1976 | | >19.1 | <18.2 |
| 183. 2 July 1976 | 16.1 | 17.7 | 14.5 |
| 184. 3 July 1976 | 13.4 | 14.4 | 11.9 |
| 185. 4 July 1976 | 11.3 | 11.7 | 10.7 |
| 186. 5 July 1976 | 10.4 | 10.6 | 10.2 |
| 187. 6 July 1976 | 9.9 | 10.2 | 9.1 |
| 188. 7 July 1976 | 8.1 | 9.0 | 7.5 |
| 189. 8 July 1976 | 7.0 | 7.4 | 6.7 |
| 190. 9 July 1976 | 6.5 | 6.7 | 6.4 |
| 191. 10 July 1976 | 6.7 | 6.9 | 6.6 |
| 192. 11 July 1976 | 8.8 | 11.4 | 6.9 |
| 193. 12 July 1976 | 12.7 | 13.4 | 11.4 |
| 194. 13 July 1976 | 11.6 | 12.9 | 10.0 |
| 195. 14 July 1976 | 8.6 | 9.9 | 7.5 |
| 196. 15 July 1976 | 6.6 | 7.4 | 5.9 |
| 197. 16 July 1976 | 5.2 | 5.8 | 4.8 |
| 198. 17 July 1976 | 4.5 | 9.9 | 3.8 |
| 199. 18 July 1976 | 3.5 | 3.8 | 3.2 |
| 200. 19 July 1976 | 3.1 | 3.3 | 3.0 |
| 201. 20 July 1976 | 2.8 | 3.0 | 2.6 |
| 202. 21 July 1976 | 2.4 | 2.6 | 2.3 |
| 203. 22 July 1976 | 2.2 | 2.3 | 2.1 |
| 204. 23 July 1976 | 2.0 | 2.1 | 1.9 |
| 205. 24 July 1976 | 1.8 | 1.9 | 1.6 |
| 206. 25 July 1976 | 1.5 | 1.6 | 1.4 |
| 207. 26 July 1976 | 1.4 | 1.4 | 1.3 |
| 208. 27 July 1976 | 1.2 | 1.3 | 1.1 |
| 209. 28 July 1976 | 1.1 | 1.1 | 1.0 |
| 210. 29 July 1976 | 1.0 | 1.0 | 0.9 |
| 211. 30 July 1976 | 0.8 | 0.9 | 0.8 |
| 212. 31 July 1976 | 0.7 | 0.8 | 0.7 |

A.3 continued

| date | $\bar{Q}$ ($m^3 s^{-1}$) | max. | min. |
|---|---|---|---|
| 213. 1 Augt 1976 | 0.6 | 0.7 | 0.6 |
| 214. 2 Augt 1976 | 0.5 | 0.6 | 0.5 |
| 215. 3 Augt 1976 | 0.4 | 0.5 | 0.4 |
| 216. 4 Augt 1976 | 0.5 | 0.5 | 0.4 |
| 217. 5 Augt 1976 | 0.5 | 0.5 | 0.5 |
| 218. 6 Augt 1976 | 0.4 | 0.5 | 0.4 |
| 219. 7 Augt 1976 | 0.4 | 0.4 | 0.4 |
| 220. 8 Augt 1976 | 0.4 | 0.4 | 0.4 |
| 221. 9 Augt 1976 | 0.5 | 0.5 | 0.4 |
| 222. 10 Augt 1976 | 0.6 | 0.7 | 0.4 |
| 223. 11 Augt 1976 | 1.0 | 1.7 | 0.7 |
| 224. 12 Augt 1976 | 1.9 | 2.2 | 1.7 |
| 225. 13 Augt 1976 | 4.3 | 7.5 | 2.2 |
| 226. 14 Augt 1976 | 6.7 | 8.6 | 5.9 |
| 227. 15 Augt 1976 | 8.2 | 8.8 | 6.9 |
| 228. 16 Augt 1976 | 5.5 | 6.7 | 4.5 |
| 229. 17 Augt 1976 | 3.7 | 4.4 | 3.2 |
| 230. 18 Augt 1976 | 2.7 | 3.1 | 2.3 |
| 231. 19 Augt 1976 | 2.1 | 2.3 | 2.0 |
| 232. 20 Augt 1976 | 1.9 | 2.0 | 1.8 |
| 233. 21 Augt 1976 | 1.8 | 1.9 | 1.7 |
| 234. 22 Augt 1976 | 1.9 | 2.2 | 1.8 |
| 235. 23 Augt 1976 | 2.2 | 2.3 | 2.1 |
| 236. 24 Augt 1976 | 1.9 | 2.1 | 1.8 |
| 237. 25 Augt 1976 | 1.7 | 1.8 | 1.6 |
| 238. 26 Augt 1976 | 1.4 | 1.6 | 1.4 |
| 239. 27 Augt 1976 | 1.3 | 1.3 | 1.2 |
| 240. 28 Augt 1976 | 1.1 | 1.2 | 1.1 |
| 241. 29 Augt 1976 | 1.0 | 1.1 | 1.0 |
| 242. 30 Augt 1976 | 0.9 | 1.0 | 0.9 |
| 243. 31 Augt 1976 | 0.8 | 0.9 | 0.8 |
| 244. 1 Sept 1976 | 0.8 | 0.8 | 0.7 |
| 245. 2 Sept 1976 | 0.7 | 0.7 | 0.7 |
| 246. 3 Sept 1976 | 0.7 | 0.7 | 0.7 |
| 247. 4 Sept 1976 | 0.7 | 0.7 | 0.7 |
| 248. 5 Sept 1976 | 0.8 | 0.9 | 0.8 |
| 249. 6 Sept 1976 | 0.8 | 0.9 | 0.8 |
| 250. 7 Sept 1976 | 0.7 | 0.8 | 0.7 |
| 251. 8 Sept 1976 | 0.7 | 0.7 | 0.7 |
| 252. 9 Sept 1976 | 0.6 | 0.7 | 0.6 |
| 253. 10 Sept 1976 | 0.6 | 0.6 | 0.6 |
| 254. 11 Sept 1976 | 0.5 | 0.6 | 0.5 |
| 255. 12 Sept 1976 | 0.5 | 0.5 | 0.4 |
| 256. 13 Sept 1976 | 0.4 | 0.4 | 0.4 |
| 257. 14 Sept 1976 | 0.5 | 0.5 | 0.4 |
| 258. 15 Sept 1976 | 0.5 | 0.5 | 0.5 |
| 259. 16 Sept 1976 | 0.5 | 0.6 | 0.5 |
| 260. 17 Sept 1976 | 0.6 | 0.6 | 0.6 |

APPENDIX A.4

SEDIMENT TRANSPORT MEASUREMENTS AND RATINGS, BABBAGE RIVER AND DEEP CREEK

Water samples were collected for determination of suspended and dissolved solids concentrations using US-DH48 depth-integrating samplers. On the basis of five sets of samples collected to determine the transverse variability of suspended sediment transport, it was concluded that the transport rate estimated from a depth-integrated sample at a single vertical near mid-channel was not significantly different at $\alpha = 0.05$ from the transport rate determined from data at three verticals. The reported transport data are therefore based on concentrations at a single station.

Dissolved and suspended fractions were defined on the basis of filtration through 0.45 μm membrane filters, as described in section 4.1.2 of the text. Total non-filterable residue per unit volume (mg/L) was taken to be the total suspended solids (TSS) concentration, $C_T$; the non-filterable residue after ashing for 2 h at 550°C was defined as the incombustible suspended solids (ISS) fraction, giving an ISS concentration $C_I$; the combustible fraction (CSS) was obtained as the difference TSS-ISS. Total filterable residue, which may contain very fine suspended particulates, was taken to represent the total dissolved solids (TDS) fraction, yielding a concentration $C_D$. The sample data are given in accompanying lists below.

Separate ratings were adopted for transport of suspended and dissolved solids under distinctive regimes, defined by seasonal shifts or absolute discharge criteria (see section 4.1.2). The rating equations employed for the total transport estimates are set out below.

Suspended sediment ratings, Babbage River, 1974:

| | |
|---|---|
| before 25 June: | $\log(C_I) = 1.624 \log(Q) - 1.665$ |
| | $\log(C_T) = 1.468 \log(Q) - 1.036$ |
| after 25 June: | $\log(C_I) = 1.807 \log(Q) - 1.665$ |
| | $\log(C_T) = \log(Q) - 1.581$ |

Suspended sediment ratings, Babbage River, 1975:

| | |
|---|---|
| before 11 June: | $\log(C_I)=0.737\log(Q)+0.757$ |
| | $\log(C_T)=0.737\log(Q)+0.841$ |
| 11-25 June: | $\log(C_I)=1.527\log(Q)-1.127$ |
| | $\log(C_T)=1.527\log(Q)-1.043$ |
| after 25 June: | $\log(C_I)=1.807\log(Q)-1.665$ |
| | $\log(C_T)=1.807\log(Q)-1.581$ |

Suspended sediment ratings, Babbage River, 1976:

| | |
|---|---|
| before 4 June | $\log(C_I)=1.624\log(Q)-1.473$ |
| and 8-25 June: | $\log(C_T)=1.468\log(Q)-1.036$ |
| 4-7 June (major | $\log(C_I)=1.624\log(Q)-1.572$ |
| snowmelt flood: | $\log(C_T)=1.624\log(Q)-1.489$ |
| after 25 June: | $\log(C_I)=1.807\log(Q)-1.665$ |
| | $\log(C_T)=1.807\log(Q)-1.581$ |

Solute ratings, Babbage River, 1974:

| | |
|---|---|
| $Q<382$ m$^3$s$^{-1}$: | $\log(C_D)=-0.443\log(Q)+2.934$ |
| $Q>382$ m$^3$s$^{-1}$: | $\log(C_D)=4.578\log(Q)-10.05$ |

Solute ratings, Babbage River, 1975:

| | |
|---|---|
| $Q<443$ m$^3$s$^{-1}$ | |
| before 13 June: | $\log(C_D)=-0.149\log(Q)+2.156$ |
| after 13 June: | $\log(C_D)=-0.443\log(Q)+2.934$ |
| $Q>443$ m$^3$s$^{-1}$: | $\log(C_D)=4.578\log(Q)-10.05$ |

Solute ratings, Babbage River, 1976:

| | |
|---|---|
| before 6 June $Q<369\ m^3s^{-1}$: | $\log(C_D)=-2.779\log(Q)+8.529$ |
| before 6 June $Q>369\ m^3s^{-1}$, 6-21 June $Q>443\ m^3s^{-1}$: | $\log(C_D)=4.578\log(Q)-10.05$ |
| 21-26 June $Q<383\ m^3s^{-1}$: | $\log(C_D)=-0.149\log(Q)+2.156$ |
| after 21 June $Q>383\ m^3s^{-1}$: | $\log(C_D)=4.578\log(Q)-10.05$ |
| after 26 June $Q<383\ m^3s^{-1}$: | $\log(C_D)=-0.443\log(Q)+2.934$ |

Suspended sediment ratings, Deep Creek, 1976:

| | |
|---|---|
| before 13 June: | $\log(C_I)=0.542\log(Q)+1.202$ |
| | $\log(C_T)=0.264\log(Q)+1.833$ |
| from 13 June: | $\log(C_I)=1.165\log(Q)+0.789$ |
| | $\log(C_T)=1.210\log(Q)+0.793$ |

Solute ratings, Deep Creek, 1976:

$$\log(C_D)=-0.141\log(Q)+1.798$$

The foregoing relations were established on the basis of sample data given in the following data listing, interpretations of seasonal adjustments being supplemented with in situ turbidity and conductivity data. Due to the evident instability of the ratings with respect both to absolute discharge rate and date, and in view of the hysteresis effects described in section 4.1.2, meaningful error terms for the transport estimates are difficult to establish. Suspended sediment transport, in particular, is highly episodic, with a very large proportion of the total transport occurring during brief extreme events that are not readily modelled using regression techniques. Furthermore, as was pointed out in the text, serial correlation in the sediment concentration series violates an important assumption of regression theory.

The data lists below and on the following two pages give suspended and dissolved solids concentrations in mg/L, with corresponding values of the discharge Q in $m^3s^{-1}$, and the date and time in units of days (with origin at 0000h 1 January; see data list, Appendix A.3, for conversion to date).

1975 BABBAGE RIVER

| date | Q | ISS |
|---|---|---|
| | $m^3s^{-1}$ | mg/L |
| 143.69 | 1.5 | 9.03 |
| 143.69 | 1.5 | 26.60 |
| 145.54 | 4.8 | 18.60 |
| 146.65 | 20.1 | 46.54 |
| 147.54 | 38. | 166.0 |
| 147.79 | 34. | 54.61 |
| 148.56 | 67. | 161.1 |
| 149.77 | 67. | 95.20 |
| 150.49 | 103. | 84.81 |
| 151.67 | 63. | 83.73 |
| 152.46 | 56. | 96.35 |
| 154.52 | 60. | 84.69 |
| 155.50 | 81. | 157.9 |
| 156.67 | 108. | 214.6 |
| 157.70 | 131. | 267.3 |
| 158.85 | 154. | 294.5 |
| 159.79 | 173. | 408.6 |
| 161.77 | 244. | 330.3 |
| 162.58 | 304. | 496.6 |
| 163.81 | 410. | 685.8 |
| 164.46 | 415. | 760.7 |
| 165.66 | 489. | 932.9 |
| 166.85 | 297. | 412.4 |
| 167.76 | 330. | 622.0 |
| 168.51 | 270. | 382.1 |
| 169.81 | 165. | 183.5 |
| 170.66 | 115. | 119.6 |
| 171.52 | 146. | 110.0 |
| 172.82 | 171 | 216.8 |
| 174.60 | 142. | 132.3 |
| 175.42 | 111. | 82.43 |
| 176.81 | 83. | 78.23 |
| 179.69 | 58. | 41.18 |
| 180.79 | 58. | 44.81 |
| 181.76 | 62. | 27.09 |
| 184.77 | 41. | 21.19 |
| 213.58 | 13. | 3.43 |
| 220.83 | 31. | 12.46 |
| 221.75 | 69. | 69.11 |
| 227.71 | 38. | 67.91 |

A.4 continued

1976 BABBAGE RIVER concentrations in mg/L

| date | Q | TSS | ISS | CSS | TDS |
|---|---|---|---|---|---|
| 152.82 | 203.6 | 298.18 | 259.94 | 38.24 | 139.3 |
| 153.53 | 326.1 | 643.26 | 586.70 | 56.56 | 36.6 |
| 154.62 | | 668.34 | 609.89 | 58.45 | 56.1 |
| 156.16 | 245.5 | 196.22 | 172.75 | 23.47 | 68.3 |
| 157.08 | 464. | 685.44 | 620.42 | 65.02 | 69.4 |
| 157.61 | 435.9 | 619.93 | 559.63 | 60.30 | 50.8 |
| 158.82 | 329.8 | 586.23 | 525.25 | 60.98 | 122.9 |
| 160.66 | 119.0 | 147.44 | 122.54 | 24.90 | 68.0 |
| 161.59 | 113.9 | 80.21 | 62.45 | 17.75 | 49.1 |
| 162.87 | 140.2 | 162.21 | 125.18 | 37.03 | 51.4 |
| 163.43 | 135.1 | 102.33 | 79.09 | 23.24 | 50.1 |
| 164.87 | 147.3 | 157.85 | 132.36 | 25.49 | 58.8 |
| 165.83 | 166.9 | 222.91 | 182.41 | 40.50 | |
| 166.69 | 203.3 | 179.96 | 147.28 | 32.68 | 67.6 |
| 167.42 | 177.7 | 151.65 | 114.40 | 37.25 | 72.6 |
| 170.82 | 40.2 | 25.59 | 12.67 | 12.92 | 133.5 |
| 156.80 | 286.7 | 338.50 | 290.18 | 48.32 | 50.4 |
| 172.68 | 60.8 | 36.74 | 23.89 | 12.85 | 76.8 |
| 173.82 | 70.1 | 61.67 | 44.63 | 17.04 | 49.9 |
| 173.82 | 70.1 | 46.02 | 40.40 | 5.62 | 87.5 |
| 173.82 | 70.1 | 46.66 | 43.61 | 3.05 | 84.3 |
| 174.65 | 87.5 | 35.04 | 33.89 | 1.15 | 75.4 |
| 177.41 | 463.0 | 1157.65 | 1050.39 | 107.26 | 89.9 |
| 177.56 | 464.2 | 1598.77 | 1463.53 | 135.24 | 258.7 |
| 177.62 | 449.0 | 1770.17 | 1592.49 | | 103.8 |
| 177.77 | 385.0 | 1322.73 | 1204.44 | 118.29 | 63.2 |
| 178.85 | 131.0 | 71.25 | 66.29 | 4.96 | 91.5 |
| 178.85 | 131.0 | 182.81 | 157.06 | 25.75 | 99.6 |
| 196.68 | 35.1 | 5.93 | 6.00 | | |
| 225.08 | 24.6 | 22.87 | 20.77 | 2.10 | |
| 234.75 | 33.5 | 19.48 | 20.73 | | 169.5 |
| 245.73 | 27.4 | 2.82 | 2.19 | 0.63 | 214.1 |
| 262.30 | 19.5 | 0.32 | 0.98 | | |

A.4 continued

1975 DEEP CREEK concentrations in mg/L

| date | Q | ISS |
|---|---|---|
| 159.71 | .07 | 77.93 |
| 160.71 | .34 | 44.58 |
| 162.75 | 35. | 87.65 |
| 163.65 | 50. | 95.68 |
| 164.52 | 70. | 209.5 |
| 165.72 | 88. | 158.4 |
| 166.88 | 90. | 436.8 |
| 167.71 | 98. | 451.6 |
| 168.54 | 75. | 543.5 |
| 169.58 | 63. | 582.4 |
| 170.79 | 39. | 537.8 |
| 171.58 | 38. | 395.3 |
| 172.84 | 39. | 384.4 |
| 174.67 | 35. | 347.3 |
| 175.44 | 29. | 218.5 |
| 176.54 | 30. | 262.0 |
| 177.58 | 21. | 102.3 |
| 179.64 | 15. | 47.35 |
| 181.58 | 13. | 24.55 |
| 184.69 | 8.0 | 46.63 |
| 187.72 | 5.7 | 17.19 |

1976 DEEP CREEK

| date | Q | TSS | ISS | CSS | TDS |
|---|---|---|---|---|---|
| 154.77 | 1.2 | 69.78 | 12.01 | 57.77 | 30.4 |
| 155.52 | 3.7 | 105.20 | 58.92 | 46.28 | 21.5 |
| 158.80 | 36. | 117.99 | 70.24 | 47.75 | 72.4 |
| 159.66 | 50. | 137.19 | 86.05 | 51.14 | 16.5 |
| 160.63 | 57. | 217.83 | 144.96 | 72.87 | |
| 161.92 | 60. | 182.18 | 110.69 | 71.49 | 17.1 |
| 162.85 | 63. | 177.15 | 129.63 | 47.52 | 42.1 |
| 163.67 | 50. | 206.45 | 162.66 | 43.79 | 23.1 |
| 164.70 | 54. | 402.41 | 334.13 | 68.28 | 25.3 |
| 165.64 | 59. | 896.76 | 810.57 | 86.19 | 32.2 |
| 166.48 | 60. | 1236.14 | 1120.07 | 116.07 | 25.0 |
| 168.98 | 37. | 626.17 | 522.34 | 103.83 | 40.5 |
| 169.67 | 32. | 509.88 | 422.43 | 87.45 | 30.1 |
| 170.53 | 25. | 360.68 | 267.97 | 92.71 | 49.2 |
| 171.46 | 22. | 238.56 | 168.92 | 69.64 | 33.3 |
| 172.86 | 22. | 179.01 | 131.08 | 47.93 | 78.7 |
| 173.72 | 24. | 230.26 | 171.42 | 58.84 | 132.1 |
| 173.72 | 24. | 181.05 | 182.77 | | 28.8 |
| 173.72 | 24. | 178.30 | 162.46 | 15.84 | 25.1 |
| 174.48 | 23. | 261.27 | 211.14 | 50.13 | |
| 175.44 | 22. | 424.76 | 357.65 | 67.11 | 42.4 |
| 176.49 | 20. | 196.43 | 144.69 | 51.74 | |
| 177.89 | 32. | 592.82 | 496.81 | 96.01 | 50.7 |
| 178.67 | 31. | | 369.8 | | 67.8 |
| 179.06 | 27. | 984.27 | 876.21 | 109.06 | 37.7 |
| 180.48 | 22. | 409.06 | 346.98 | 62.08 | 41.5 |
| 181.43 | 20. | 161.74 | 117.47 | 44.27 | 85.5 |
| 182.47 | 19. | 100.38 | 92.71 | 7.67 | |
| 183.55 | 16. | 151.60 | 138.53 | 13.07 | 63.3 |
| 184.60 | 13. | 111.75 | 104.13 | 7.62 | 37.5 |
| 185.55 | 11. | 101.92 | 91.61 | 10.31 | 122.3 |
| 186.76 | 11. | 64.64 | 61.38 | 3.26 | 22.4 |
| 187.50 | 10. | 73.71 | 68.03 | 5.68 | 96.5 |
| 188.54 | 8.0 | 52.07 | 50.35 | 1.72 | 57.6 |
| 196.76 | 6.3 | 53.41 | 49.07 | 4.34 | 39.2 |
| 229.67 | 3.6 | 177.93 | 164.96 | 12.97 | 94.4 |
| 262.3 | 0.9 | 3.22 | 4.19 | | |

Bedload transport rates were computed using modified-Einstein and Bagnold models, as described in section 4.1.2. The derivation of the modified Einstein transport model assumes the following (Einstein, 1950, pp. 8-9 and 30-33): (1) entrainment and deposition are in equilibrium, with a constant mass (number) of particles in motion at any instant, this mass being represented by an 'exchange probability', p; (2) the probability of particle entrainment is a function of particle characteristics and local hydraulic conditions only; (3) entrainment is determined solely in terms of instantaneous dynamic lift greater than immersed weight; (4) the probability of deposition is equal at all points where the local lift force is less than critical; (5) the average travel distance is constant for a given particle size and is assumed to equal 100D; (6) saltation may be neglected (explicit antithesis of Bagnold's theory); (7) the dynamic lift force is normally distributed; (8) the vertical velocity profile is adequately represented by the logarithmic models of Keulegan (1938), even over very rough boundaries; (9) unlimited sediment supply. Particular sources of error may be anticipated in assumptions 3, 5, 6, 8, and 9.

Major assumptions of the Bagnold model include the following (Bagnold, 1966, 1973): (1) motion by shearing of successive layers of granular solids immersed in fluid of lesser density; (2) motion maintained by tractive force in direction of transport; (3) steady open-channel flow with all forces in statistical equilibrium; (4) unlimited sediment supply; (5) flow may be laminar or turbulent (cf. Francis, 1973, for experimental justification); (6) bedload is defined as fraction of total sediment transport wholly supported by solid-contact normal stress.

Bedload transport data were obtained using Helley-Smith samplers with inlet section area of 76.2x76.2 $mm^2$ and 0.21-mm mesh screens (Helley and Smith, 1971; Emmett, 1980). The samplers were deployed at three to five sites across the section for intervals ranging from 3.3 to 16 minutes; the longer deployment times were chosen to take account of the intermittent behaviour of bedload transport. Bed conditions ranged from coarse cobble-gravel armouring, with which the samplers interfaced poorly, to rippled sand moving over gravel; dune-scale bedforms in sand were not observed. Problems were encountered with coarse suspended organic material clogging the screens at high discharge rates; under these conditions, the hydraulic efficiency of the samplers was reduced rapidly and longer deployment times were undoubtedly disadvantageous. This is believed to have been a major cause of the anomalously low transport rates observed at $Q>60\ m^3s^{-1}$. Insufficient sample size may have been a factor in some cases also (cf. standard procedure proposed by Emmett, 1980). The results of the bedload sampling program in the Babbage River and Deep Creek are summarized below.

A.4 continued

Observed rates of bedload transport, Babbage River at B1

| date 1976 | Q ($m^3s^{-1}$) | $J_B$ (kg/s) |
|---|---|---|
| 5 June | 313 | 0.210 |
| 10 June | 106 | 0.170 |
| 11 June | 146 | 0.161 |
| 24 June | 80 | 0.020 |
| 26 June | 428 | 1.56 |
| 26 June | 402 | 0.577 |
| 30 June | 133 | 0.194 |
| 3 July | 52 | 0.045 |
| 4 July | 58 | 0.143 |
| 5 July | 53 | 0.277 |
| 6 July | 57 | 0.100 |
| 7 July | 42 | 0.029 |
| 15 July | 34 | 0.002 |

Observed rates of bedload transport, Deep Creek at D1

| date 1976 | Q ($m^3s^{-1}$) | $J_B$ (kg/s) |
|---|---|---|
| 19 June | 25 | 0.022 |
| 24 June | 22 | 0.013 |
| 27 June | 31 | 0.435 |
| 2 July | 17 | 0.003 |
| 3 July | 14 | 0.001 |
| 4 July | 10 | 0.001 |
| 6 July | 10 | 0.001 |
| 7 July | 8 | 0.000 |

# APPENDIX A.5

## DAILY SEDIMENT TRANSPORT, BABBAGE RIVER AT B1

Babbage River (section B1)

DAILY TRANSPORT TOTALS (TONNES)

| | 1975 | | | | 1976 | | | |
|---|---|---|---|---|---|---|---|---|
| date | TDS | ISS | TSS | TBS | TDS | ISS | TSS | TBS |
| 1 JUNE | 392. | 602. | 730. | 5. | 102. | . | 219. | 76. |
| 2 JUNE | 305. | 435. | 527. | 6. | 42. | . | 755. | 270. |
| 3 JUNE | 507. | 668. | 810. | 4. | 48. | . | 430. | 234. |
| 4 JUNE | 416. | 654. | 789. | 18. | 57. | . | 332. | 180. |
| 5 JUNE | 582. | 1330. | 1609. | 50. | 1352. | 7026. | 8519. | 4851. |
| 6 JUNE | 619. | 1629. | 1975. | 200. | 3215. | 21437. | 25992. | 13846. |
| 7 JUNE | 916. | 2885. | 3493. | 528. | 1890. | 13215. | 15849. | 9551. |
| 8 JUNE | 924. | 3213. | 3897. | 714. | 1024. | 2679. | 3201. | 1275. |
| 9 JUNE | 1012. | 4047. | 4907. | 1096. | 736. | 877. | 1129. | 343. |
| 10 JUNE | 1063. | 4666. | 5657. | 1445. | 644. | 581. | 766. | 202. |
| 11 JUNE | 1337. | 7005. | 8494. | 2764. | 747. | 948. | 1212. | 376. |
| 12 JUNE | 2068. | 16595. | 20122. | 7423. | 762. | 963. | 1234. | 384. |
| 13 JUNE | 1634. | 20062. | 24327. | 9491. | 857. | 1412. | 1765. | 598. |
| 14 JUNE | 3092. | 25060. | 30400. | 9500. | 1081. | 2908. | 3480. | 1374. |
| 15 JUNE | 4145. | 42265. | 51242. | 17253. | 1106. | 3100. | 3698. | 1475. |
| 16 JUNE | 2629. | 23600. | 28610. | 11157. | 939. | 1882. | 2311. | 834. |
| 17 JUNE | 1936. | 18260. | 22140. | 8321. | 706. | 759. | 986. | 288. |
| 18 JUNE | 1314. | 6440. | 7810. | 2624. | 514. | 321. | 436. | 91. |
| 19 JUNE | 1548. | 3730. | 4520. | 1276. | 269. | 39. | 59. | 1. |
| 20 JUNE | 1032. | 1130. | 1370. | 313. | 276. | 42. | 64. | 1. |
| 21 JUNE | 1337. | 1990. | 2410. | 603. | 347. | 89. | 131. | 9. |
| 22 JUNE | 1374. | 3985. | 4835. | 1437. | 455. | 205. | 287. | 45. |
| 23 JUNE | 1223. | 2345. | 3445. | 970. | 508. | 278. | 383. | 70. |
| 24 JUNE | 1045. | 1460. | 1780. | 437. | 506. | 271. | 375. | 67. |
| 25 JUNE | 1052. | 810. | 980. | 192. | 552. | 419. | 556. | 114. |
| 26 JUNE | 849. | 480. | 580. | 93. | 3235. | 36081. | 43746. | 10234. |
| 27 JUNE | 844. | 320. | 390. | 52. | 1333. | 4742. | 5749. | 1340. |
| 28 JUNE | 708. | 200. | 240. | 25. | 1053. | 1192. | 1445. | 299. |
| 29 JUNE | 662. | 140. | 180. | 12. | 979. | 832. | 1010. | 188. |
| 30 JUNE | 711. | 157. | 191. | 14. | 1064. | 1316. | 1596. | 329. |
| 1 JULY | 716. | 173. | 210. | 18. | 931. | 665. | 807. | 141. |
| 2 JULY | 675. | 128. | 155. | 8. | 792. | 291. | 353. | 45. |
| 3 JULY | 594. | 67. | 82. | 1. | 669. | 121. | 146. | 7. |
| 4 JULY | 548. | 45. | 54. | 0. | 684. | 137. | 166. | 10. |
| 5 JULY | 500. | 28. | 35. | 0. | 658. | 111. | 135. | 6. |
| 6 JULY | 449. | 16. | 20. | 0. | 673. | 127. | 154. | 9. |
| 7 JULY | 441. | 14. | 18. | 0. | 616. | 80. | 97. | 2. |
| 8 JULY | 453. | 17. | 21. | 0. | 568. | 53. | 64. | 1. |
| 9 JULY | 451. | 17. | 20. | 0. | 615. | 81. | 99. | 3. |
| 10 JULY | 437. | 14. | 17. | 0. | 700. | . | 420. | 34. |

A.5 continued

| | 1975 | | | | 1976 | | | |
|---|---|---|---|---|---|---|---|---|
| date | TDS | ISS | TSS | TBS | TDS | ISS | TSS | TBS |
| 11 JULY | 412. | 10. | 13. | 0. | 683. | . | 742. | 61. |
| 12 JULY | 394. | 8. | 10. | 0. | 382. | 170. | 206. | 29. |
| 13 JULY | 397. | 8. | 10. | 0. | 713. | 171. | 208. | 18. |
| 14 JULY | 401. | 9. | 11. | 0. | 599. | 70. | 85. | 2. |
| 15 JULY | 395. | 8. | 10. | 0. | 541. | 41. | 50. | 0. |
| 16 JULY | 375. | 6. | 8. | 0. | 500. | 27. | 33. | 0. |
| 17 JULY | 369. | 6. | 7. | 0. | 465. | 19. | 23. | 0. |
| 18 JULY | 343. | 4. | 5. | 0. | 441. | 14. | 17. | 0. |
| 19 JULY | 330. | 3. | 4. | 0. | 423. | 12. | 15. | 0. |
| 20 JULY | 317. | 2. | 3. | 0. | 448. | 15. | 19. | 0. |
| 21 JULY | 301. | 2. | 2. | 0. | 455. | 17. | 20. | 0. |
| 22 JULY | 288. | 2. | 2. | 0. | 426. | 12. | 15. | 0. |
| 23 JULY | 280. | 1. | 2. | 0. | 415. | 10. | 13. | 0. |
| 24 JULY | 284. | 1. | 2. | 0. | 411. | 10. | 12. | 0. |
| 25 JULY | 272. | 0. | 1. | 0. | 420. | 11. | 13. | 0. |
| 26 JULY | 261. | 0. | 0. | 0. | 408. | 9. | 11. | 0. |
| 27 JULY | 263. | 0. | 1. | 0. | 391. | 8. | 9. | 0. |
| 28 JULY | 272. | 1. | 1. | 0. | 374. | 6. | 7. | 0. |
| 29 JULY | 295. | 2. | 2. | 0. | 378. | 6. | 7. | 0. |
| 30 JULY | 306. | 2. | 2. | 0. | 373. | 6. | 7. | 0. |
| 31 JULY | 320. | 2. | 3. | 0. | 369. | 5. | 7. | 0. |
| 1 AUGT | 325. | 3. | 3. | 0. | 368. | 5. | 7. | 0. |
| 2 AUGT | 312. | 2. | 2. | 0. | 357. | 5. | 5. | 0. |
| 3 AUGT | 318. | 2. | 3. | 0. | 353. | 4. | 5. | 0. |
| 4 AUGT | 319. | 2. | 3. | 0. | 351. | 4. | 5. | 0. |
| 5 AUGT | 306. | 2. | 2. | 0. | 369. | 6. | 7. | 0. |
| 6 AUGT | 316. | 2. | 3. | 0. | . | . | . | . |
| 7 AUGT | 382. | 7. | 9. | 0. | . | . | . | . |
| 8 AUGT | 422. | 12. | 13. | 0. | . | . | . | . |
| 9 AUGT | 466. | 20. | 25. | 0. | . | . | . | . |
| 10 AUGT | 712. | 179. | 217. | 20. | . | . | . | . |
| 11 AUGT | 705. | 161. | 195. | 15. | 345. | 11. | 13. | 0. |
| 12 AUGT | 643. | 98. | 120. | 3. | 414. | 10. | 12. | 0. |
| 13 AUGT | 582. | 61. | 74. | 1. | 772. | 340. | 412. | 60. |
| 14 AUGT | 499. | 27. | 33. | 0. | 676. | 136. | 165. | 12. |
| 15 AUGT | 469. | 20. | 24. | 0. | 548. | 45. | 54. | 0. |
| 16 AUGT | 560. | 50. | 61. | 0. | 478. | 22. | 27. | 0. |
| 17 AUGT | 506. | 29. | 36. | 0. | 451. | 16. | 20. | 0. |
| 18 AUGT | 468. | 19. | 24. | 0. | 461. | 18. | 22. | 0. |
| 19 AUGT | 454. | 16. | 21. | 0. | 530. | 37. | 45. | 0. |
| 20 AUGT | 440. | 14. | 17. | 0. | 608. | 85. | 103. | 4. |
| 21 AUGT | 422. | 11. | 13. | 0. | 625. | 87. | 106. | 3. |
| 22 AUGT | 401. | 9. | 11. | 0. | 539. | 41. | 50. | 0. |
| 23 AUGT | 386. | 7. | 9. | 0. | 489. | 25. | 30. | 0. |
| 24 AUGT | 378. | 6. | 8. | 0. | 457. | 17. | 21. | 0. |
| 25 AUGT | 379. | 7. | 8. | 0. | 435. | 13. | 16. | 0. |
| 26 AUGT | 391. | 8. | 10. | 0. | 416. | 10. | 13. | 0. |
| 27 AUGT | 519. | 42. | 51. | 1. | 401. | 8. | 10. | 0. |
| 28 AUGT | 720. | 175. | 213. | 18. | 388. | 7. | 9. | 0. |
| 29 AUGT | 679. | 131. | 159. | 8. | 378. | 6. | 8. | 0. |
| 30 AUGT | 618. | 81. | 99. | 2. | 371. | 6. | 7. | 0. |
| 31 AUGT | 583. | 60. | 74. | 0. | 369. | 6. | 6. | 0. |
| 1 SEPT | 563. | 51. | 61. | 0. | 367. | 5. | 6. | 0. |
| 2 SEPT | 553. | 46. | 56. | 0. | 429. | 13. | 16. | 0. |
| 3 SEPT | 521. | 35. | 42. | 0. | 444. | 15. | 18. | 0. |
| 4 SEPT | | | | | 423. | 11. | 14. | 0. |
| 5 SEPT | | | | | 412. | 10. | 12. | 0. |
| 6 SEPT | | | | | 409. | 9. | 12. | 0. |
| 7 SEPT | | | | | 399. | 8. | 10. | 0. |
| 8 SEPT | | | | | 385. | 7. | 8. | 0. |
| 9 SEPT | | | | | 373. | 6. | 7. | 0. |
| 10 SEPT | | | | | 369. | 6. | 6. | 0. |
| 11 SEPT | | | | | 367. | 5. | 6. | 0. |
| 12 SEPT | | | | | 364. | 5. | 6. | 0. |
| 13 SEPT | | | | | 356. | 5. | 6. | 0. |
| 14 SEPT | | | | | 348. | 4. | 5. | 0. |
| 15 SEPT | | | | | 342. | 3. | 5. | 0. |
| 16 SEPT | | | | | 350. | 4. | 5. | 0. |

APPENDIX A.6

OBSERVED WIND AND HINDCAST WAVE CONDITIONS

Wave data were synthesized using Kay Point wind records and the SMB hindcast procedure, as described in section 2.3.4 of the text. The mean wind speed and direction, storm duration, and hindcast maximum significant wave conditions are tabulated below for each storm event. Breaker height, $H_b$, and the unit shorelength component of tangential wave power, $P'$, were computed according to procedures given in section 4.2.2.

Distal end Kay Point spit, 1975 hindcast wave conditions

| date starting | $\bar{u}$ wind m/s | $\theta_T$ | t h | T s | $H_b$ m | $\alpha_b$ ° | $P'_t$ W/m |
|---|---|---|---|---|---|---|---|
| 19/07 | 15.9 | 315 | 15 | 3.0 | 0.70 | 5 | 64. |
| 20/07 | 18.9 | 315 | 12 | 3.4 | 0.88 | 5 | 112. |
| 21/07 | 26.3 | 315 | 9 | 4.0 | 1.33 | 10 | 612. |
| 21/07 | 15.3 | 315 | 24 | 3.0 | 0.70 | 5 | 64. |
| 23/07 | 16.0 | 315 | 13 | 3.0 | 0.70 | 5 | 64. |
| 24/07 | 20.3 | 90 | 4 | 4.2 | 0.33 | 35 | 58. |
| 25/07 | 15.7 | 90 | 24 | 4.4 | 0.35 | 35 | 69. |
| 26/07 | 13.3 | 112 | 8 | 3.6 | 0.14 | 50 | 7. |
| 26/07 | 15.1 | 45 | 7 | 3.8 | 0.62 | 47 | 288. |
| 27/07 | 31.0 | 315 | 5 | 4.3 | 1.58 | 11 | 1024. |
| 27/07 | 24.1 | 315 | 7 | 3.8 | 1.18 | 8 | 369. |
| 27/07 | 29.3 | 315 | 4 | 4.2 | 1.45 | 10 | 771. |
| 28/07 | 18.2 | 315 | 20 | 3.3 | 0.83 | 5 | 98. |
| 30/07 | 10.3 | 315 | 3 | 2.3 | 0.39 | 5 | 15. |
| 31/07 | 12.4 | 90 | 10 | 3.6 | 0.24 | 40 | 28. |
| 1/08 | 12.3 | 45 | 8 | 3.4 | 0.49 | 47 | 165. |
| 2/08 | 10.9 | 90 | 11 | 3.3 | 0.20 | 45 | 18. |
| 2/08 | 10.8 | 90 | 5 | 2.7 | 0.14 | 55 | 7. |
| 4/08 | 15.1 | 135 | 9 | 4.3 | 0.20 | 50 | 22. |
| 4/08 | 19.7 | 135 | 6 | 4.5 | 0.22 | 50 | 28. |
| 5/08 | 13.5 | 315 | 5 | 2.8 | 0.60 | 5 | 43. |
| 5/08 | 23.7 | 315 | 3 | 3.8 | 1.16 | 8 | 352. |
| 6/08 | 21.4 | 315 | 9 | 3.6 | 1.37 | 8 | 503. |
| 6/08 | 17.7 | 315 | 15 | 3.3 | 0.97 | 5 | 141. |
| 7/08 | 14.1 | 315 | 8 | 2.8 | 0.63 | 5 | 49. |
| 8/08 | 18.8 | 315 | 5 | 3.4 | 0.88 | 5 | 113. |
| 8/08 | 12.5 | 135 | 4 | 2.9 | 0.09 | 50 | 3. |
| 9/08 | 25.3 | 315 | 8 | 3.9 | 1.26 | 9 | 487. |
| 9/08 | 31.6 | 315 | 3 | 4.4 | 1.61 | 11 | 1090. |
| 10/08 | 25.0 | 315 | 16 | 3.9 | 1.26 | 9 | 487. |
| 11/08 | 13.0 | 315 | 3 | 2.7 | 0.56 | 5 | 37. |
| 11/08 | 11.5 | 135 | 2 | 2.3 | 0.06 | 50 | 1. |
| 12/08 | 13.8 | 135 | 8 | 3.7 | 0.15 | 50 | 9. |
| 14/08 | 14.5 | 315 | 2 | 3.0 | 0.67 | 5 | 58. |
| 15/08 | 11.0 | 135 | 2 | 2.2 | 0.06 | 50 | 1. |
| 16/08 | 20.9 | 315 | 7 | 3.5 | 0.99 | 6 | 179. |
| 17/08 | 24.2 | 315 | 12 | 3.8 | 1.19 | 9 | 422. |
| 17/08 | 16.5 | 315 | 12 | 3.1 | 0.74 | 5 | 73. |
| 18/08 | 11.6 | 315 | 7 | 2.5 | 0.78 | 5 | 74. |
| 20/08 | 13.4 | 315 | 6 | 2.8 | 0.57 | 5 | 39. |
| 21/08 | 10.7 | 315 | 3 | 2.4 | 0.42 | 5 | 18. |
| 22/08 | 11.7 | 315 | 3 | 2.5 | 0.78 | 5 | 74. |
| 24/08 | 10.5 | 90 | 2 | 2.2 | 0.09 | 55 | 0. |
| 25/08 | 13.5 | 90 | 2 | 2.6 | 0.12 | 55 | 2. |
| 26/08 | 16.7 | 315 | 11 | 3.2 | 0.76 | 5 | 80. |
| 27/08 | 28.0 | 315 | 3 | 4.2 | 1.46 | 10 | 780. |
| 27/08 | 36.0 | 315 | 3 | 4.7 | 1.86 | 12 | 1692. |
| 27/08 | 24.8 | 315 | 9 | 3.9 | 1.27 | 9 | 494. |
| 30/08 | 10.5 | 90 | 6 | 2.0 | 0.07 | 55 | 1. |
| 30/08 | 13.5 | 135 | 2 | 2.5 | 0.07 | 50 | 1. |
| 31/08 | 12.1 | 315 | 12 | 2.6 | 0.50 | 5 | 27. |
| 31/08 | 10.9 | 315 | 7 | 2.4 | 0.43 | 5 | 19. |
| 1/09 | 15.1 | 315 | 20 | 3.0 | 0.69 | 5 | 61. |
| 2/09 | 12.3 | 315 | 3 | 2.7 | 0.49 | 5 | 27. |
| 3/09 | 11.3 | 135 | 4 | 2.2 | 0.06 | 50 | 1. |
| 3/09 | 13.0 | 315 | 2 | 2.7 | 0.53 | 5 | 32. |
| 4/09 | 14.0 | 315 | 3 | 2.8 | 0.59 | 5 | 42. |
| 4/09 | 12.8 | 315 | 6 | 2.7 | 0.53 | 5 | 32. |

A.6 continued

Distal end Kay Point spit, 1976 hindcast wave conditions

| date start | $\bar{u}$ wind m/s | $\theta_T$ | t h | T s | $H_b$ m | $\theta^b$ | $P'_t$ W/m |
|---|---|---|---|---|---|---|---|
| 16/07 | 13.0 | 45 | 3 | 2.8 | 0.35 | 47 | 67. |
| 17/07 | 14.5 | 90 | 12 | 4.1 | 0.29 | 30 | 39. |
| 18/07 | 16.8 | 315 | 2 | 2.6 | 0.54 | 5 | 33. |
| 19/07 | 15.6 | 112 | 10 | 4.3 | 0.20 | 50 | 17. |
| 20/07 | 11.1 | 315 | 7 | 2.5 | 0.47 | 5 | 24. |
| 21/07 | 10.9 | 315 | 8 | 2.5 | 0.47 | 5 | 24. |
| 23/07 | 10.9 | 45 | 20 | 3.3 | 0.45 | 47 | 133. |
| 24/07 | 11.7 | 45 | 14 | 3.3 | 0.47 | 47 | 143. |
| 25/07 | 10.6 | 45 | 4 | 2.6 | 0.35 | 47 | 70. |
| 26/07 | 15.2 | 112 | 21 | 4.2 | 0.19 | 50 | 15. |
| 27/07 | 11.3 | 315 | 11 | 2.5 | 0.47 | 5 | 24. |
| 28/07 | 13.4 | 90 | 6 | 3.4 | 0.21 | 40 | 19. |
| 28/07 | 12.5 | 135 | 4 | 2.9 | 0.09 | 50 | 3. |
| 29/07 | 19.3 | 112 | 10 | 4.8 | 0.25 | 50 | 32. |
| 30/07 | 21.8 | 315 | 9 | 3.7 | 1.08 | 8 | 299. |
| 31/07 | 14.7 | 315 | 3 | 2.9 | 0.68 | 5 | 59. |
| 31/07 | 11.8 | 68 | 7 | 3.2 | 0.22 | 38 | 22. |
| 1/08 | 12.6 | 68 | 5 | 3.2 | 0.22 | 38 | 22. |
| 1/08 | 11.5 | 90 | 6 | 3.4 | 0.21 | 40 | 20. |
| 2/08 | 15.2 | 112 | 19 | 4.2 | 0.19 | 50 | 16. |
| 3/08 | 14.4 | 135 | 3 | 3.1 | 0.10 | 50 | 3. |
| 3/08 | 19.5 | 315 | 19 | 3.4 | 0.93 | 5 | 130. |
| 4/08 | 18.8 | 315 | 3 | 3.3 | 0.89 | 5 | 116. |
| 5/08 | 15.6 | 315 | 4 | 3.0 | 0.72 | 5 | 68. |
| 6/08 | 18.7 | 337 | 9 | 4.2 | 0.27 | 33 | 37. |
| 7/08 | 11.3 | 22 | 3 | 2.6 | 0.26 | 28 | 27. |
| 8/08 | 11.2 | 0 | 3 | 2.6 | 0.34 | 35 | 59. |
| 8/08 | 12.6 | 68 | 3 | 2.7 | 0.18 | 38 | 13. |
| 9/08 | 17.3 | 112 | 16 | 4.1 | 0.18 | 50 | 14. |
| 10/08 | 13.9 | 112 | 9 | 3.8 | 0.15 | 50 | 9. |
| 12/08 | 20.1 | 315 | 5 | 3.5 | 0.97 | 6 | 173. |
| 12/08 | 16.8 | 315 | 10 | 3.2 | 0.79 | 5 | 87. |
| 12/08 | 23.9 | 315 | 11 | 3.8 | 1.17 | 8 | 369. |
| 12/08 | 30.5 | 315 | 13 | 4.3 | 1.53 | 11 | 961. |
| 12/08 | 20.1 | 315 | 8 | 3.5 | 0.97 | 6 | 173. |
| 13/08 | 18.3 | 90 | 13 | 4.8 | 0.40 | 30 | 92. |
| 14/08 | 18.5 | 135 | 9 | 4.3 | 0.19 | 50 | 17. |
| 16/08 | 19.6 | 315 | 17 | 3.4 | 0.93 | 5 | 130. |
| 18/08 | 19.4 | 315 | 17 | 3.4 | 0.93 | 5 | 130. |
| 20/08 | 13.7 | 135 | 12 | 3.4 | 0.13 | 50 | 6. |
| 21/08 | 26.6 | 315 | 14 | 4.0 | 1.31 | 10 | 605. |
| 22/08 | 12.3 | 68 | 6 | 3.2 | 0.23 | 38 | 24. |
| 23/08 | 18.6 | 315 | 7 | 3.3 | 0.89 | 5 | 116. |
| 24/08 | 17.3 | 135 | 6 | 4.1 | 0.18 | 50 | 14. |
| 25/08 | 14.7 | 112 | 9 | 4.0 | 0.17 | 50 | 13. |
| 26/08 | 19.6 | 90 | 8 | 4.9 | 0.43 | 30 | 105. |
| 27/08 | 15.1 | 90 | 11 | 4.2 | 0.32 | 35 | 56. |
| 1/09 | 13.4 | 292 | 3 | 2.4 | 0.38 | -16 | -43. |
| 1/09 | 12.1 | 315 | 4 | 2.6 | 0.54 | 5 | 33. |
| 3/09 | 13.2 | 90 | 3 | 2.8 | 0.15 | 55 | 8. |
| 4/09 | 17.2 | 315 | 5 | 3.5 | 0.97 | 6 | 173. |
| 4/09 | 25.9 | 315 | 20 | 4.0 | 1.31 | 10 | 605. |
| 5/09 | 15.3 | 90 | 3 | 3.2 | 0.18 | 40 | 14. |
| 7/09 | 13.3 | 315 | 4 | 2.7 | 0.60 | 5 | 44. |
| 7/09 | 15.1 | 135 | 7 | 3.8 | 0.15 | 50 | 8. |
| 8/09 | 14.0 | 112 | 8 | 3.8 | 0.15 | 50 | 9. |
| 9/09 | 16.8 | 315 | 10 | 3.2 | 0.79 | 5 | 87. |
| 9/09 | 25.0 | 315 | 15 | 3.9 | 1.25 | 9 | 478. |
| 10/09 | 18.5 | 135 | 30 | 4.2 | 0.20 | 50 | 18. |
| 12/09 | 13.9 | 135 | 6 | 3.5 | 0.13 | 50 | 7. |
| 12/09 | 16.1 | 135 | 12 | 3.9 | 0.16 | 50 | 11. |

APPENDIX A.7

LONGSHORE SEDIMENT TRANSPORT

Computed values of the longshore sediment transport for individual storm events in 1976, obtained using equation 4.2.2-6 and the hindcast wave data, are set out below. Estimates are presented for two locations on Kay Point spit and one location west of Niakolik Point. Although the data are subject to considerable uncertainty, they provide order of magnitude estimates of longshore sediment supply to the Babbage Estuary and a striking illustration of local alongshore variability in the sediment budget.

| 1976 event no. | starting date | TONNES proximal spit K1 | distal spit K2 | Niakolik foreshore N1 |
|---|---|---|---|---|
| 1 | 16 July | 28. | 92. | 29. |
| 3 | 17 | 436. | 212. | 76. |
| 4 | 18 | 2. | 30. | -67. |
| 5 | 19 | 66. | 79. | 14. |
| 6 | 20 | 6. | 76. | -51. |
| 7 | 21 | 8. | 86. | -58. |
| 8 | 23 | 394. | 1221. | 291. |
| 9 | 24 | 294. | 900. | 222. |
| 10 | 25 | 38. | 127. | 32. |
| 11 | 26 | 123. | 144. | 25. |
| 12 | 27 | 11. | 119. | -79. |
| 13 | 28 | 93. | 52. | 14. |
| 14 | 28 | 4. | 6. | 1. |
| 15 | 29 | 136. | 148. | 28. |
| 16 | 30 | 58. | 1230. | -228. |
| 17 | 31 | 6. | 81. | -53. |
| 18 | 31 | 76. | 71. | 31. |
| 19 | 1 August | 54. | 50. | 22. |
| 20 | 1 | 95. | 54. | 14. |
| 21 | 2 | 122. | 137. | 25. |
| 22 | 3 | 4. | 4. | 1. |
| 23 | 3 | 86. | 1130. | -473. |
| 24 | 4 | 12. | 159. | -75. |
| 25 | 5 | 9. | 124. | -91. |
| 26 | 6 | 898. | 149. | 0. |
| 27 | 7 | 46. | 37. | 0. |
| 28 | 8 | 80. | 80. | 0. |
| 29 | 8 | 19. | 17. | 11. |
| 30 | 9 | 89. | 98. | 18. |
| 31 | 10 | 34. | 39. | 7. |
| 32 | 12 | 2785. | 9010. | -1412. |
| 33 | 13 | 1100. | 548. | 170. |
| 34 | 14 | 62. | 71. | 13. |
| 35 | 16 | 77. | 1010. | -423. |
| 36 | 18 | 77. | 1010. | -423. |
| 37 | 20 | 30. | 35. | 6. |
| 38 | 21 | 152. | 3890. | -386. |
| 39 | 22 | 72. | 67. | 30. |
| 40 | 23 | 28. | 373. | -174. |
| 41 | 24 | 33. | 37. | 7. |
| 42 | 25 | 45. | 52. | 9. |
| 43 | 26 | 770. | 386. | 112. |
| 44. | 27 | 524. | 281. | 78. |
| 45. | 1 September | -40. | -58. | 0. |
| 46. | 1 | 5. | 61. | -41. |
| 47. | 3 | 21. | 12. | 3. |
| 48. | 4 | 743. | 5830. | -655. |
| 49. | 5 | 35. | 19. | 5. |
| 50. | 7 | 6. | 81. | -55. |
| 51 | 7 | 24. | 25. | 2. |
| 52 | 8 | 30. | 35. | 2. |
| 53 | 9 | 380. | 3690. | -613. |
| 54 | 10 | 211. | 238. | 45. |
| 56 | 12 | 16. | 19. | 3. |
| 57 | 12 | 51. | 61. | 11. |

APPENDIX A.8

DETERMINATION OF WATER PROPERTIES AND SEDIMENT CONCENTRATIONS

In situ measurements of temperature and conductivity were obtained using YSI model 33 SCT meters with YSI 3300 series conductivity and temperature probes. Two or more meters with associated probes were maintained in the field for cross-checking. Although readings were usually within the 6% worst-case error specified by the manufacturer, deviations exceeding 15% were occasionally encountered, the major presumed causes being water at the probe jack, or inside the meter, and oil or organic fouling of probes. Particular care was taken during the 1976 field season to avoid these problems. Empirical correlation between the logarithm of the TDS concentration determined from sample data and the logarithm of the in situ conductivity, adjusted to 25°C (following Perkin and Walker, 1971), yielded a coefficient of determination $r^2=0.951$ (n=59).

Salinity was computed from the in situ temperature and conductivity data using results of Perkin and Walker (1971). Errors in the salinity data are believed to be less than ± 1 ppt in most cases.

Density, $\rho(s,\Theta)$, was determined from the temperature and salinity results using the standard hydrographical tables of Knudsen (1901). Differences between the density determined by this procedure and density computed from sample TDS concentrations did not exceed 10 kg $m^{-3}$ (n=59). Viscosity, $\eta(s,\Theta)$, was computed using equations developed by Millero (1974) from experimental data. The equation used was

$$\eta(s,\Theta) = \eta(0,\Theta)[1+A(Cl)^{1/2}+B(Cl)]$$

where Cl, the volume chlorinity, is the product of chlorinity and specific gravity; the cholorinity was computed as (s-0.03)/1.805 (Knudsen, 1901, p.iii); and the constants A and B, determined experimentally only at 5°C and 25°C, were obtained for other temperatures by linear interpolation or extrapolation.

Water samples were collected using 1-L van Dorn samplers and were stored in new 1-L polyethylene bottles. After determination of sample volume, samples were passed through pre-weighed Sartorius 13106 47-mm diameter cellulose nitrate membrane filters having a nominal pore diameter of 0.45 µm. Filters were dried at 105°C, cooled in a dessicator, and re-weighed to the nearest 0.01 mg to obtain total suspended

solids (TSS) concentration. The incombustible fraction (ISS) was determined by ashing for 2 h at 550°C. Total dissolved solids (TDS) concentration was determined by evaporation of an aliquot of the sample after filtration through the 0.45-μm membrane filter. The TDS results are considered good to within 1 mg/L. The major source of error in the suspended sediment data is due to undetermined residual salt remaining on the filter before drying. A correction for the remaining salt was applied to the concentration data for samples from stations in the estuary. The correction was based on the water salinity and the estimated volume of voids in the filter and retained sediment; was negligible prior to the mid-summer salinity intrusion; and exceeded 3 mg/L in only six cases, the most extreme being 7.2 mg/L. Residual salt on five filters treated with samples of salinity $18.2<s<19.5$ ppt, determined by rinsing with distilled water, amounted to 1.97±1.04 mg. It is concluded that the TSS and ISS concentration data are probably good to within 5 mg/L; this is more than adequate to resolve the major sources of variance of suspended sediment concentration in the Babbage Estuary system.

In situ observations of light attenuation for estimation of TSS concentrations, $C_T$, were obtained using 0.30-m Secchi disks and two 0.10-m pathlength beam transmissometers. The Secchi disks, painted gloss white above and matte black below, were mounted on aluminum snow-survey rods graduated at 5-mm intervals. Calibrations of percent transmissivity ($T_L$) and Secchi extinction depth ($H_E$) were obtained in terms of $C_T$. Sample concentrations ranged from 0.94 mg/L to 1123 mg/L (see Appendix sections A.4 and A.10). Least-squares relations for estimation of $C_T$ took the form

$$\hat{C}_T=ae^{-T_L} \quad \text{and} \quad \hat{C}_T=cH_E^{-d}$$

where a, b, c, and d are constants which may vary geographically or seasonally because light transmission is affected not only by total particulate concentration, but also by other factors including particle size and shape. The Secchi disk calibration extended over the full range of sample concentrations. However, estimates based on Secchi data suffer from three major disadvantages: turbidity is integrated over a depth interval that varies inversely with concentration; the calibration is altered if extinction depth approaches total water depth; and surface waves may introduce additional variance. Nevertheless, the Secchi disk proved to be a robust, relatively precise, and simple (therefore reliable) instrument. Beam extinction in the 0.10-m transmissometers occurred at mean concentrations of 94 and 75 mg/L; in addition, the calibrations were erratic at T >60%, approximately, relative to a standard of 100% in distilled water. Calibrations adopted for estimation of $C_T$ are given below (the coefficients assume $H_E$ in metres and $C_T$ in mg/L).

Hydroproducts 0.10-m pathlength beam transmissometer:
$\ln(\hat{C}_T) = -0.052 T_L + 4.541$, $r^2 = 0.724$, $s = 0.695$, $n = 48$

Interocean 0.10-m pathlength beam transmissometer:
$\ln(\hat{C}_T) = -0.042 T_L + 4.323$, $r^2 = 0.830$, $s = 0.372$, $n = 15$

Secchi disk 0.30-m diameter:
$\ln(\hat{C}_T) = -1.442 \ln(H_E) + 2.189$, $r^2 = 0.868$, $s = 0.572$, $n = 84$

APPENDIX A.9

DAILY TEMPERATURE, SALINITY, DENSITY, AND VISCOSITY, BABBAGE ESTUARY, 1976 (IN SITU DATA)

Data for stations 5-7 are referenced to date in days with origin at 0000h 1 January 1976 (see data list, Appendix A.3 for conversion to date).

Babbage Estuary station 5 1976

Daily temperature, salinity, density, and viscosity near-surface (z=0) and near-bottom (z=h)

| date | time | θ(0) | s(0) | ρ(0) | η(0) | θ(h) | s(h) | ρ(h) | η(h) |
|---|---|---|---|---|---|---|---|---|---|
| | | | | $kg/m^3$ | $N\ s/m^2$ | | | $kg/m^3$ | $N\ s/m^2$ |
| days | hr/min | °C | ppt | | | °C | ppt | | |
| 163.774 | 1835 | 5.1 | 0.2 | 1000.3 | 0.001515 | 5.1 | 0.2 | 1000.3 | 0.001515 |
| 164.726 | 1725 | 7.9 | 0.3 | 1000.2 | 0.001391 | 7.9 | 0.3 | 1000.2 | 0.001391 |
| 165.840 | 2010 | 6.4 | 0.1 | 1000.2 | 0.001455 | 6.4 | 0.1 | 1000.2 | 0.001455 |
| 166.802 | 1915 | 5.0 | 0.2 | 1000.3 | 0.001520 | 5.0 | 0.2 | 1000.3 | 0.001520 |
| 167.861 | 2040 | 5.5 | 0.2 | 1000.3 | 0.001496 | 5.5 | 0.2 | 1000.3 | 0.001496 |
| 168.953 | 2252 | 3.5 | 0.2 | 1000.3 | 0.001594 | 3.5 | 0.2 | 1000.3 | 0.001594 |
| 169.717 | 1712 | 2.5 | 0.3 | 1000.3 | 0.001647 | 2.5 | 0.3 | 1000.3 | 0.001647 |
| 170.667 | 1600 | 3.6 | 0.6 | 1000.6 | 0.001590 | 3.6 | 0.6 | 1000.6 | 0.001590 |
| 171.999 | 2359 | 2.0 | 0.6 | 1000.6 | 0.001675 | 2.0 | 0.6 | 1000.6 | 0.001675 |
| 172.650 | 1536 | 8.3 | 0.3 | 1000.2 | 0.001374 | 7.4 | 0.9 | 1000.6 | 0.001413 |
| 173.873 | 2057 | 8.1 | 0.1 | 1000.1 | 0.001382 | 5.0 | 1.0 | 1000.8 | 0.001522 |
| 174.833 | 2000 | 7.9 | 0.3 | 1000.2 | 0.001391 | 7.9 | 0.3 | 1000.2 | 0.001391 |
| 175.800 | 1912 | 12.4 | 0.2 | 999.7 | 0.001222 | 11.2 | 0.2 | 999.8 | 0.001264 |
| 176.947 | 2243 | 9.0 | 0.2 | 1000.1 | 0.001346 | 9.0 | 0.2 | 1000.1 | 0.001346 |
| 177.878 | 2105 | 9.0 | 0.2 | 1000.1 | 0.001346 | 9.0 | 0.2 | 1000.1 | 0.001346 |
| 178.838 | 2007 | 7.0 | 0.2 | 1000.2 | 0.001429 | 7.0 | 0.2 | 1000.2 | 0.001429 |
| 179.809 | 1925 | 7.5 | 0.1 | 1000.1 | 0.001407 | 7.5 | 0.1 | 1000.1 | 0.001407 |
| 180.862 | 2041 | 7.5 | 0.1 | 1000.1 | 0.001407 | 7.5 | 0.1 | 1000.1 | 0.001407 |
| 181.792 | 1901 | 7.8 | 0.2 | 1000.2 | 0.001395 | 5.0 | 0.6 | 1000.6 | 0.001521 |
| 182.970 | 2317 | 8.6 | 0.1 | 1000.0 | 0.001362 | 8.6 | 0.1 | 1000.0 | 0.001362 |
| 183.782 | 1846 | 10.1 | 0.1 | 999.9 | 0.001303 | 9.7 | 0.2 | 1000.0 | 0.001319 |
| 184.837 | 2005 | 10.1 | 0.2 | 1000.0 | 0.001304 | 10.1 | 0.2 | 1000.0 | 0.001304 |
| 185.774 | 1835 | 11.3 | 0.1 | 999.8 | 0.001260 | 11.3 | 0.1 | 999.8 | 0.001260 |
| 186.631 | 1508 | 11.5 | 0.2 | 999.9 | 0.001253 | 11.5 | 0.2 | 999.9 | 0.001253 |
| 187.764 | 1820 | 11.0 | 0.1 | 999.8 | 0.001270 | 11.0 | 0.1 | 999.8 | 0.001270 |
| 188.750 | 1800 | 8.0 | 0.1 | 1000.1 | 0.001386 | 8.0 | 0.1 | 1000.1 | 0.001386 |
| 189.598 | 1421 | 6.2 | 0.7 | 1000.6 | 0.001465 | 6.2 | 0.7 | 1000.6 | 0.001465 |
| 190.701 | 1650 | 4.8 | 0.2 | 1000.3 | 0.001529 | 4.9 | 0.5 | 1000.5 | 0.001525 |
| 191.441 | 1035 | 1.0 | 0.7 | 1000.6 | 0.001733 | 1.0 | 0.7 | 1000.6 | 0.001733 |
| 192.747 | 1755 | 7.3 | 0.7 | 1000.6 | 0.001417 | 7.3 | 0.7 | 1000.6 | 0.001417 |
| 193.642 | 1525 | 2.5 | 0.7 | 1000.6 | 0.001648 | 2.5 | 0.7 | 1000.6 | 0.001648 |
| 194.726 | 1725 | 10.8 | 0.9 | 1000.4 | 0.001280 | 10.8 | 0.9 | 1000.4 | 0.001280 |
| 195.726 | 1725 | 11.0 | 0.1 | 999.8 | 0.001270 | 10.0 | 0.5 | 1000.2 | 0.001308 |
| 196.858 | 2035 | 10.0 | 0.7 | 1000.4 | 0.001309 | 10.0 | 0.7 | 1000.4 | 0.001309 |
| 197.783 | 1848 | 10.1 | 0.7 | 1000.4 | 0.001305 | 10.1 | 0.7 | 1000.4 | 0.001305 |
| 198.861 | 2040 | 7.0 | 1.5 | 1001.2 | 0.001432 | 7.0 | 1.5 | 1001.2 | 0.001432 |
| 199.885 | 2115 | 13.5 | 0.6 | 999.9 | 0.001187 | 13.0 | 1.0 | 1000.2 | 0.001204 |
| 200.875 | 2100 | 10.0 | 2.2 | 1001.5 | 0.001312 | 10.0 | 2.2 | 1001.5 | 0.001312 |
| 201.875 | 2100 | 12.2 | 1.4 | 1000.6 | 0.001232 | 12.2 | 1.4 | 1000.6 | 0.001232 |
| 202.542 | 1300 | 15.1 | 0.9 | 999.9 | 0.001138 | 15.1 | 0.9 | 999.9 | 0.001138 |
| 204.798 | 1909 | 13.0 | 1.2 | 1000.4 | 0.001204 | 13.0 | 1.2 | 1000.4 | 0.001204 |
| 205.819 | 1940 | 12.4 | 1.9 | 1001.0 | 0.001226 | 8.0 | 3.7 | 1002.8 | 0.001395 |
| 206.622 | 1455 | 9.9 | 3.1 | 1002.2 | 0.001318 | 9.9 | 3.1 | 1002.2 | 0.001318 |
| 207.583 | 1400 | 10.7 | 2.9 | 1002.0 | 0.001288 | 8.5 | 3.2 | 1002.4 | 0.001373 |
| 208.858 | 2035 | 11.3 | 6.7 | 1004.8 | 0.001275 | 5.0 | 16.0 | 1012.7 | 0.001558 |
| 209.566 | 1335 | 10.5 | 6.3 | 1004.6 | 0.001303 | 8.2 | 11.0 | 1008.5 | 0.001403 |
| 210.635 | 1515 | 15.6 | 5.2 | 1003.1 | 0.001132 | 15.6 | 5.2 | 1003.1 | 0.001132 |

A.9 continued

station 5

| | | | | | | | | | |
|---|---|---|---|---|---|---|---|---|---|
| 211.545 | 1305 | 3.8 | 18.5 | 1014.7 | 0.001624 | 3.8 | 18.5 | 1014.7 | 0.001624 |
| 212.795 | 1905 | 13.0 | 9.2 | 1006.5 | 0.001222 | 13.0 | 9.2 | 1006.5 | 0.001222 |
| 213.792 | 1900 | 14.3 | 8.4 | 1005.7 | 0.001178 | 14.3 | 8.4 | 1005.7 | 0.001178 |
| 214.833 | 2000 | 12.5 | 11.8 | 1008.6 | 0.001244 | 7.1 | 15.9 | 1012.4 | 0.001462 |
| 216.801 | 1914 | 10.1 | 11.1 | 1008.4 | 0.001329 | 10.1 | 11.1 | 1008.4 | 0.001329 |
| 217.526 | 1238 | 1.2 | 16.5 | 1013.2 | 0.001762 | 1.2 | 16.5 | 1013.2 | 0.001762 |
| 218.438 | 1030 | 12.0 | 9.7 | 1007.1 | 0.001257 | 9.9 | 10.0 | 1007.6 | 0.001334 |
| 219.868 | 2050 | 8.0 | 11.2 | 1008.7 | 0.001412 | 8.0 | 11.2 | 1008.7 | 0.001412 |
| 220.858 | 2035 | 8.8 | 10.0 | 1007.7 | 0.001377 | 8.8 | 10.0 | 1007.7 | 0.001377 |
| 221.769 | 1827 | 10.8 | 10.4 | 1007.8 | 0.001301 | 10.8 | 10.4 | 1007.8 | 0.001301 |
| 222.465 | 1110 | 11.0 | 8.8 | 1006.5 | 0.001290 | 7.9 | 14.2 | 1011.0 | 0.001423 |
| 223.684 | 1625 | 9.0 | 11.5 | 1008.8 | 0.001372 | 9.0 | 11.5 | 1008.8 | 0.001372 |
| 224.708 | 1700 | 7.5 | 7.0 | 1005.4 | 0.001423 | 7.5 | 7.0 | 1005.4 | 0.001423 |
| 225.597 | 1420 | 8.2 | 10.0 | 1007.7 | 0.001401 | 7.5 | 12.8 | 1010.0 | 0.001437 |
| 226.542 | 1300 | 10.5 | 9.8 | 1007.3 | 0.001311 | 7.2 | 9.2 | 1007.2 | 0.001441 |
| 227.660 | 1550 | 6.1 | 17.0 | 1013.4 | 0.001509 | 6.1 | 17.0 | 1013.4 | 0.001509 |
| 228.486 | 1140 | 6.9 | 13.2 | 1010.3 | 0.001464 | 4.2 | 16.3 | 1013.0 | 0.001598 |
| 229.790 | 1858 | 9.8 | 12.2 | 1009.3 | 0.001343 | 6.0 | 19.3 | 1015.2 | 0.001519 |
| 230.533 | 1247 | 6.5 | 14.4 | 1011.3 | 0.001485 | 6.5 | 14.4 | 1011.3 | 0.001485 |
| 231.504 | 1206 | 7.9 | 11.0 | 1008.5 | 0.001416 | 6.7 | 16.8 | 1013.2 | 0.001481 |
| 232.876 | 2102 | 7.1 | 13.1 | 1010.2 | 0.001455 | 5.5 | 17.0 | 1013.4 | 0.001537 |
| 233.792 | 1900 | 4.5 | 16.0 | 1012.7 | 0.001583 | 4.5 | 16.0 | 1012.7 | 0.001583 |
| 234.497 | 1155 | 3.4 | 7.6 | 1006.1 | 0.001618 | 2.3 | 19.2 | 1015.4 | 0.001706 |
| 235.529 | 1242 | 5.1 | 14.7 | 1011.7 | 0.001550 | 5.1 | 14.7 | 1011.7 | 0.001550 |
| 236.510 | 1215 | 6.0 | 16.8 | 1013.2 | 0.001513 | 5.0 | 18.0 | 1014.2 | 0.001563 |
| 237.618 | 1450 | 5.0 | 18.2 | 1014.4 | 0.001564 | 5.0 | 18.2 | 1014.4 | 0.001564 |
| 238.604 | 1430 | 7.3 | 16.5 | 1012.9 | 0.001454 | 7.3 | 16.5 | 1012.9 | 0.001454 |
| 239.278 | 0640 | 9.3 | 12.6 | 1009.6 | 0.001363 | 9.0 | 15.0 | 1011.5 | 0.001380 |
| 241.769 | 1827 | 10.0 | 11.3 | 1008.6 | 0.001333 | 8.6 | 15.1 | 1011.7 | 0.001397 |
| 242.649 | 1535 | 8.2 | 14.0 | 1010.8 | 0.001410 | 6.9 | 16.0 | 1012.5 | 0.001471 |
| 243.466 | 1111 | 8.1 | 11.0 | 1008.5 | 0.001408 | 7.9 | 14.1 | 1011.0 | 0.001423 |
| 244.500 | 1200 | 8.0 | 13.8 | 1010.7 | 0.001418 | 8.0 | 13.8 | 1010.7 | 0.001418 |
| 245.472 | 1120 | 8.1 | 6.8 | 1005.2 | 0.001398 | 7.4 | 12.8 | 1010.0 | 0.001441 |
| 246.848 | 2021 | 7.6 | 13.5 | 1010.5 | 0.001434 | 6.8 | 16.1 | 1012.6 | 0.001475 |
| 247.725 | 1724 | 6.7 | 9.6 | 1007.5 | 0.001464 | 6.7 | 9.6 | 1007.5 | 0.001464 |
| 248.456 | 1056 | 6.2 | 13.7 | 1010.8 | 0.001496 | 6.2 | 13.7 | 1010.8 | 0.001496 |
| 249.719 | 1715 | 7.6 | 8.0 | 1006.2 | 0.001422 | 6.8 | 14.7 | 1011.5 | 0.001472 |
| 250.448 | 1045 | 4.8 | 14.9 | 1011.8 | 0.001565 | 4.8 | 14.9 | 1011.8 | 0.001565 |
| 251.578 | 1353 | 5.2 | 13.2 | 1010.5 | 0.001542 | 4.5 | 14.8 | 1011.8 | 0.001580 |
| 253.437 | 1029 | 5.2 | 9.0 | 1007.2 | 0.001532 | 4.1 | 14.1 | 1011.2 | 0.001598 |
| 254.458 | 1100 | 4.7 | 14.2 | 1011.3 | 0.001568 | 3.2 | 18.6 | 1014.8 | 0.001656 |
| 255.511 | 1216 | 4.1 | 16.8 | 1013.4 | 0.001605 | 2.7 | 20.5 | 1016.4 | 0.001687 |

A.9 continued

Babbage Estuary station 6 1976

Daily temperature, salinity, density, and viscosity near-surface (z=0) and near-bottom (z=h)

| date | time | θ(0) | s(0) | ρ(0) | η(0) | θ(h) | s(h) | ρ(h) | η(h) |
|---|---|---|---|---|---|---|---|---|---|
| | | | | $kg/m^3$ | $N\ s/m^2$ | | | $kg/m^3$ | $N\ s/m^2$ |
| days | hr/min | C | ppt | | | C | ppt | | |
| 163.792 | 1900 | 4.0 | 0.1 | 1000.2 | 0.001568 | 4.0 | 0.1 | 1000.2 | 0.001568 |
| 164.701 | 1650 | 7.0 | 0.2 | 1000.2 | 0.001429 | 7.0 | 0.2 | 1000.2 | 0.001429 |
| 165.844 | 2015 | 6.9 | 0.1 | 1000.1 | 0.001433 | 6.9 | 0.1 | 1000.1 | 0.001433 |
| 166.806 | 1920 | 5.0 | 0.2 | 1000.3 | 0.001520 | 5.0 | 0.2 | 1000.3 | 0.001520 |
| 167.865 | 2045 | 4.2 | 0.1 | 1000.2 | 0.001558 | 4.2 | 0.1 | 1000.2 | 0.001558 |
| 168.925 | 2212 | 3.5 | 0.1 | 1000.2 | 0.001594 | 3.5 | 0.1 | 1000.2 | 0.001594 |
| 169.721 | 1718 | 3.1 | 0.7 | 1000.6 | 0.001616 | 3.1 | 0.7 | 1000.6 | 0.001616 |
| 170.674 | 1610 | 4.5 | 0.1 | 1000.2 | 0.001544 | 4.5 | 0.1 | 1000.2 | 0.001544 |
| 171.997 | 2356 | 7.0 | 0.9 | 1000.7 | 0.001430 | 7.0 | 0.9 | 1000.7 | 0.001430 |
| 172.646 | 1530 | 7.9 | 0.1 | 1000.1 | 0.001390 | 7.9 | 0.1 | 1000.1 | 0.001390 |
| 173.912 | 2154 | 8.0 | 0.1 | 1000.1 | 0.001386 | 8.0 | 0.1 | 1000.1 | 0.001386 |
| 174.840 | 2009 | 7.9 | 0.3 | 1000.2 | 0.001391 | 7.9 | 0.3 | 1000.2 | 0.001391 |
| 175.799 | 1910 | 12.0 | 0.1 | 999.7 | 0.001235 | 12.0 | 0.1 | 999.7 | 0.001235 |
| 176.944 | 2239 | 9.1 | 0.1 | 1000.0 | 0.001342 | 9.1 | 0.1 | 1000.0 | 0.001342 |
| 177.875 | 2100 | 9.2 | 0.2 | 1000.1 | 0.001338 | 9.2 | 0.2 | 1000.1 | 0.001338 |
| 178.835 | 2003 | 7.6 | 0.2 | 1000.2 | 0.001403 | 7.6 | 0.2 | 1000.2 | 0.001403 |
| 179.811 | 1928 | 6.1 | 0.1 | 1000.2 | 0.001468 | 6.1 | 0.1 | 1000.2 | 0.001468 |
| 180.860 | 2038 | 6.5 | 0.1 | 1000.2 | 0.001450 | 6.5 | 0.1 | 1000.2 | 0.001450 |
| 181.790 | 1858 | 8.9 | 0.1 | 1000.0 | 0.001350 | 8.9 | 0.1 | 1000.0 | 0.001350 |
| 182.968 | 2314 | 9.3 | 0.1 | 1000.0 | 0.001334 | 9.3 | 0.1 | 1000.0 | 0.001334 |
| 183.787 | 1853 | 10.0 | 0.1 | 999.9 | 0.001307 | 10.0 | 0.1 | 999.9 | 0.001307 |
| 184.835 | 2003 | 10.1 | 0.1 | 999.9 | 0.001303 | 10.1 | 0.1 | 999.9 | 0.001303 |
| 185.771 | 1830 | 11.2 | 0.2 | 999.9 | 0.001264 | 11.2 | 0.2 | 999.9 | 0.001264 |
| 186.628 | 1505 | 11.3 | 0.3 | 999.9 | 0.001260 | 11.3 | 0.3 | 999.9 | 0.001260 |
| 187.767 | 1825 | 11.3 | 0.1 | 999.8 | 0.001260 | 11.3 | 0.1 | 999.8 | 0.001260 |
| 188.752 | 1803 | 7.8 | 0.2 | 1000.2 | 0.001395 | 7.8 | 0.2 | 1000.2 | 0.001395 |
| 189.593 | 1414 | 6.8 | 0.3 | 1000.3 | 0.001438 | 6.8 | 0.3 | 1000.3 | 0.001438 |
| 190.712 | 1705 | 5.0 | 0.3 | 1000.3 | 0.001520 | 5.0 | 0.3 | 1000.3 | 0.001520 |
| 191.447 | 1043 | 3.0 | 0.8 | 1000.7 | 0.001622 | 3.0 | 0.8 | 1000.7 | 0.001622 |
| 192.753 | 1805 | 8.1 | 0.6 | 1000.4 | 0.001383 | 8.1 | 0.6 | 1000.4 | 0.001383 |
| 193.647 | 1532 | 4.0 | 0.8 | 1000.7 | 0.001570 | 4.0 | 0.8 | 1000.7 | 0.001570 |
| 194.729 | 1730 | 5.0 | 1.0 | 1000.9 | 0.001522 | 5.0 | 1.0 | 1000.9 | 0.001522 |
| 195.721 | 1718 | 12.5 | 0.1 | 999.7 | 0.001218 | 12.5 | 0.1 | 999.7 | 0.001218 |
| 196.854 | 2030 | 11.2 | 0.3 | 1000.0 | 0.001264 | 11.2 | 0.3 | 1000.0 | 0.001264 |
| 197.781 | 1845 | 13.0 | 0.5 | 999.9 | 0.001203 | 13.0 | 0.5 | 999.9 | 0.001203 |
| 198.858 | 2035 | 7.7 | 1.3 | 1001.0 | 0.001402 | 7.7 | 1.3 | 1001.0 | 0.001402 |
| 199.882 | 2110 | 14.0 | 0.5 | 999.8 | 0.001171 | 14.0 | 0.5 | 999.8 | 0.001171 |
| 200.875 | 2100 | 9.7 | 2.1 | 1001.4 | 0.001324 | 9.7 | 2.1 | 1001.4 | 0.001324 |
| 201.875 | 2100 | 13.0 | 1.0 | 1000.2 | 0.001204 | 13.0 | 1.0 | 1000.2 | 0.001204 |
| 202.542 | 1300 | 16.4 | 0.3 | 999.2 | 0.001098 | 16.4 | 0.3 | 999.2 | 0.001098 |
| 204.796 | 1906 | 15.6 | 0.3 | 999.4 | 0.001121 | 15.6 | 0.3 | 999.4 | 0.001121 |
| 205.826 | 1950 | 16.0 | 1.1 | 999.9 | 0.001112 | 16.0 | 1.1 | 999.9 | 0.001112 |
| 206.624 | 1459 | 11.8 | 2.6 | 1001.6 | 0.001248 | 11.8 | 2.6 | 1001.6 | 0.001248 |
| 207.590 | 1410 | 11.3 | 2.9 | 1001.9 | 0.001266 | 11.3 | 2.9 | 1001.9 | 0.001266 |
| 208.854 | 2030 | 7.9 | 13.5 | 1010.5 | 0.001422 | 7.9 | 13.5 | 1010.5 | 0.001422 |
| 209.573 | 1345 | 9.8 | 6.1 | 1004.5 | 0.001329 | 9.8 | 6.1 | 1004.5 | 0.001329 |
| 210.660 | 1550 | 15.5 | 5.8 | 1003.5 | 0.001136 | 15.5 | 5.8 | 1003.5 | 0.001136 |
| 211.542 | 1300 | 4.0 | 18.0 | 1014.3 | 0.001613 | 4.0 | 18.0 | 1014.3 | 0.001613 |

A.9 continued

station 6

| | | | | | | | | | |
|---|---|---|---|---|---|---|---|---|---|
| 212.767 | 1825 | 14.0 | 8.9 | 1006.1 | 0.001189 | 14.0 | 8.9 | 1006.1 | 0.001189 |
| 213.764 | 1820 | 14.8 | 8.3 | 1005.6 | 0.001163 | 14.8 | 8.3 | 1005.6 | 0.001163 |
| 214.835 | 2002 | 10.3 | 13.8 | 1010.4 | 0.001327 | 10.3 | 13.8 | 1010.4 | 0.001327 |
| 216.799 | 1910 | 12.6 | 12.6 | 1009.2 | 0.001243 | 12.6 | 12.6 | 1009.2 | 0.001243 |
| 217.529 | 1242 | 10.6 | 13.4 | 1010.1 | 0.001315 | 10.6 | 13.4 | 1010.1 | 0.001315 |
| 218.440 | 1034 | 11.0 | 10.5 | 1007.8 | 0.001294 | 11.0 | 10.5 | 1007.8 | 0.001294 |
| 219.865 | 2045 | 10.5 | 10.0 | 1007.5 | 0.001311 | 10.5 | 10.0 | 1007.5 | 0.001311 |
| 220.851 | 2025 | 9.0 | 6.1 | 1004.6 | 0.001360 | 9.5 | 9.1 | 1006.9 | 0.001347 |
| 221.765 | 1821 | 12.0 | 4.9 | 1003.4 | 0.001246 | 12.0 | 4.9 | 1003.4 | 0.001246 |
| 222.472 | 1120 | 10.1 | 9.1 | 1006.8 | 0.001324 | 8.9 | 11.7 | 1009.0 | 0.001377 |
| 223.681 | 1620 | 9.5 | 11.0 | 1008.4 | 0.001351 | 9.5 | 11.0 | 1008.4 | 0.001351 |
| 224.703 | 1653 | 7.5 | 5.0 | 1003.9 | 0.001419 | 7.5 | 5.0 | 1003.9 | 0.001419 |
| 225.618 | 1450 | 8.0 | 9.0 | 1007.0 | 0.001407 | 8.0 | 9.0 | 1007.0 | 0.001407 |
| 226.549 | 1310 | 10.2 | 6.2 | 1004.6 | 0.001314 | 8.0 | 12.7 | 1009.9 | 0.001416 |
| 227.667 | 1600 | 7.0 | 16.6 | 1013.0 | 0.001468 | 2.9 | 20.3 | 1016.2 | 0.001676 |
| 228.497 | 1155 | 5.0 | 18.0 | 1014.2 | 0.001563 | 5.0 | 18.0 | 1014.2 | 0.001563 |
| 229.785 | 1850 | 9.0 | 13.8 | 1010.6 | 0.001377 | 6.5 | 17.7 | 1013.9 | 0.001492 |
| 230.544 | 1303 | 6.4 | 16.2 | 1012.7 | 0.001493 | 6.4 | 16.2 | 1012.7 | 0.001493 |
| 231.513 | 1219 | 9.3 | 6.8 | 1005.1 | 0.001350 | 8.1 | 14.6 | 1011.3 | 0.001416 |
| 232.872 | 2055 | 9.5 | 5.3 | 1003.9 | 0.001339 | 7.5 | 13.7 | 1010.7 | 0.001439 |
| 233.799 | 1910 | 3.8 | 18.2 | 1014.5 | 0.001623 | 3.8 | 18.2 | 1014.5 | 0.001623 |
| 234.510 | 1215 | 4.1 | 12.6 | 1010.1 | 0.001594 | 3.0 | 17.5 | 1014.0 | 0.001664 |
| 235.533 | 1248 | 5.0 | 16.0 | 1012.7 | 0.001558 | 5.0 | 16.0 | 1012.7 | 0.001558 |
| 236.521 | 1230 | 6.0 | 15.2 | 1012.0 | 0.001509 | 6.0 | 16.7 | 1013.1 | 0.001513 |
| 237.622 | 1455 | 5.5 | 17.4 | 1013.7 | 0.001538 | 5.5 | 17.4 | 1013.7 | 0.001538 |
| 238.608 | 1435 | 7.2 | 17.0 | 1013.3 | 0.001460 | 7.2 | 17.0 | 1013.3 | 0.001460 |
| 239.290 | 0657 | 9.6 | 13.7 | 1010.4 | 0.001354 | 9.6 | 13.7 | 1010.4 | 0.001354 |
| 241.777 | 1839 | 10.2 | 9.2 | 1006.9 | 0.001321 | 8.8 | 15.9 | 1012.3 | 0.001390 |
| 242.656 | 1545 | 8.5 | 14.0 | 1010.8 | 0.001398 | 7.8 | 15.4 | 1012.0 | 0.001430 |
| 243.470 | 1117 | 8.4 | 11.1 | 1008.6 | 0.001395 | 8.2 | 14.4 | 1011.2 | 0.001411 |
| 244.505 | 1207 | 7.9 | 13.2 | 1010.2 | 0.001421 | 7.9 | 13.2 | 1010.2 | 0.001421 |
| 245.479 | 1130 | 7.9 | 9.6 | 1007.4 | 0.001413 | 7.5 | 14.4 | 1011.3 | 0.001441 |
| 246.849 | 2023 | 8.2 | 11.5 | 1008.9 | 0.001405 | 7.3 | 15.6 | 1012.2 | 0.001452 |
| 247.729 | 1730 | 6.8 | 12.0 | 1009.4 | 0.001466 | 6.8 | 12.0 | 1009.4 | 0.001466 |
| 248.462 | 1105 | 5.5 | 11.4 | 1009.0 | 0.001523 | 5.6 | 14.6 | 1011.5 | 0.001526 |
| 249.724 | 1722 | 6.8 | 13.2 | 1010.3 | 0.001468 | 6.4 | 15.3 | 1012.0 | 0.001491 |
| 250.453 | 1052 | 4.2 | 16.6 | 1013.2 | 0.001599 | 4.2 | 16.6 | 1013.2 | 0.001599 |
| 251.585 | 1403 | 5.3 | 13.8 | 1010.9 | 0.001538 | 4.8 | 15.8 | 1012.5 | 0.001567 |
| 253.444 | 1040 | 4.7 | 9.1 | 1007.3 | 0.001556 | 4.7 | 9.1 | 1007.3 | 0.001556 |
| 254.465 | 1110 | 5.0 | 12.1 | 1009.6 | 0.001549 | 4.0 | 18.2 | 1014.5 | 0.001613 |
| 255.520 | 1229 | 4.0 | 12.4 | 1009.9 | 0.001599 | 4.0 | 16.5 | 1013.1 | 0.001609 |

A.9 continued

Babbage Estuary station 7 1976

Daily temperature, salinity, density, and viscosity near-surface (z=0) and near-bottom (z=h)

| date | time | θ(0) | s(0) | ρ(0) | η(0) | θ(h) | s(h) | ρ(h) | η(h) |
|---|---|---|---|---|---|---|---|---|---|
| days | | C | ppt | $kg/m^3$ | $N\ s/m^2$ | C | ppt | $kg/m^3$ | $N\ s/m^2$ |
| 163.785 | 1850 | 4.2 | 0.1 | 1000.2 | 0.001558 | 4.2 | 0.1 | 1000.2 | 0.001558 |
| 164.705 | 1655 | 7.0 | 0.2 | 1000.2 | 0.001429 | 7.0 | 0.2 | 1000.2 | 0.001429 |
| 165.847 | 2020 | 7.8 | 0.1 | 1000.1 | 0.001394 | 7.8 | 0.1 | 1000.1 | 0.001394 |
| 166.813 | 1930 | 5.9 | 0.2 | 1000.2 | 0.001478 | 5.9 | 0.2 | 1000.2 | 0.001478 |
| 167.865 | 2045 | 5.4 | 0.1 | 1000.2 | 0.001500 | 5.4 | 0.1 | 1000.2 | 0.001500 |
| 168.934 | 2225 | 4.0 | 0.1 | 1000.2 | 0.001568 | 4.0 | 0.1 | 1000.2 | 0.001568 |
| 169.724 | 1722 | 3.2 | 0.2 | 1000.3 | 0.001610 | 3.2 | 0.2 | 1000.3 | 0.001610 |
| 170.677 | 1615 | 4.1 | 0.1 | 1000.2 | 0.001563 | 4.1 | 0.1 | 1000.2 | 0.001563 |
| 171.994 | 2351 | 7.3 | 0.2 | 1000.2 | 0.001416 | 7.6 | 0.6 | 1000.5 | 0.001404 |
| 172.635 | 1515 | 8.0 | 0.2 | 1000.1 | 0.001386 | 8.0 | 0.2 | 1000.1 | 0.001386 |
| 173.861 | 2040 | 8.0 | 0.1 | 1000.1 | 0.001386 | 8.0 | 0.1 | 1000.1 | 0.001386 |
| 174.835 | 2003 | 9.7 | 0.3 | 1000.1 | 0.001319 | 9.7 | 0.3 | 1000.1 | 0.001319 |
| 175.795 | 1905 | 12.3 | 0.4 | 999.9 | 0.001226 | 12.3 | 0.4 | 999.9 | 0.001226 |
| 176.958 | 2300 | 9.1 | 0.1 | 1000.0 | 0.001342 | 9.1 | 0.1 | 1000.0 | 0.001342 |
| 177.872 | 2055 | 10.5 | 0.2 | 1000.0 | 0.001289 | 10.5 | 0.2 | 1000.0 | 0.001289 |
| 178.832 | 1958 | 7.2 | 0.2 | 1000.2 | 0.001420 | 7.2 | 0.2 | 1000.2 | 0.001420 |
| 179.813 | 1931 | 6.8 | 0.1 | 1000.1 | 0.001437 | 6.8 | 0.1 | 1000.1 | 0.001437 |
| 180.858 | 2035 | 7.8 | 0.1 | 1000.1 | 0.001394 | 7.8 | 0.1 | 1000.1 | 0.001394 |
| 181.787 | 1854 | 8.9 | 0.1 | 1000.0 | 0.001350 | 8.9 | 0.1 | 1000.0 | 0.001350 |
| 182.966 | 2311 | 10.8 | 0.1 | 999.9 | 0.001278 | 10.8 | 0.1 | 999.9 | 0.001278 |
| 183.790 | 1857 | 10.3 | 0.1 | 999.9 | 0.001296 | 10.3 | 0.1 | 999.9 | 0.001296 |
| 184.833 | 2000 | 10.0 | 0.1 | 999.9 | 0.001307 | 10.0 | 0.1 | 999.9 | 0.001307 |
| 185.771 | 1830 | 12.0 | 0.1 | 999.7 | 0.001235 | 12.0 | 0.1 | 999.7 | 0.001235 |
| 186.625 | 1500 | 10.9 | 0.2 | 999.9 | 0.001274 | 10.9 | 0.2 | 999.9 | 0.001274 |
| 187.776 | 1837 | 11.4 | 0.1 | 999.8 | 0.001256 | 11.4 | 0.1 | 999.8 | 0.001256 |
| 188.754 | 1806 | 8.1 | 0.2 | 1000.1 | 0.001382 | 8.1 | 0.2 | 1000.1 | 0.001382 |
| 189.589 | 1408 | 7.0 | 0.2 | 1000.2 | 0.001429 | 7.0 | 0.2 | 1000.2 | 0.001429 |
| 190.715 | 1710 | 5.7 | 0.1 | 1000.2 | 0.001486 | 5.7 | 0.1 | 1000.2 | 0.001486 |
| 191.449 | 1047 | 5.1 | 0.2 | 1000.3 | 0.001515 | 5.1 | 0.2 | 1000.3 | 0.001515 |
| 192.764 | 1820 | 7.0 | 0.1 | 1000.1 | 0.001428 | 7.0 | 0.1 | 1000.1 | 0.001428 |
| 193.651 | 1538 | 10.7 | 0.3 | 1000.0 | 0.001282 | 10.7 | 0.3 | 1000.0 | 0.001282 |
| 194.729 | 1730 | 15.0 | 0.2 | 999.4 | 0.001139 | 15.0 | 0.2 | 999.4 | 0.001139 |
| 195.717 | 1712 | 12.2 | 0.1 | 999.7 | 0.001228 | 12.2 | 0.1 | 999.7 | 0.001228 |
| 196.851 | 2025 | 11.0 | 0.1 | 999.8 | 0.001270 | 11.0 | 0.1 | 999.8 | 0.001270 |
| 197.774 | 1835 | 12.2 | 0.1 | 999.7 | 0.001228 | 12.2 | 0.1 | 999.7 | 0.001228 |
| 198.854 | 2030 | 15.0 | 0.3 | 999.5 | 0.001139 | 15.0 | 0.3 | 999.5 | 0.001139 |
| 199.878 | 2105 | 14.0 | 0.2 | 999.5 | 0.001170 | 14.0 | 0.2 | 999.5 | 0.001170 |
| 200.875 | 2100 | 15.0 | 1.5 | 1000.3 | 0.001142 | 15.0 | 1.5 | 1000.3 | 0.001142 |
| 201.875 | 2100 | 14.9 | 0.5 | 999.6 | 0.001143 | 14.9 | 0.5 | 999.6 | 0.001143 |
| 202.542 | 1300 | 17.1 | 0.2 | 999.1 | 0.001078 | 17.1 | 0.2 | 999.1 | 0.001078 |
| 204.792 | 1900 | 16.0 | 0.3 | 999.3 | 0.001110 | 16.0 | 0.3 | 999.3 | 0.001110 |
| 205.830 | 1955 | 16.7 | 0.2 | 999.1 | 0.001089 | 8.5 | 3.7 | 1002.8 | 0.001374 |
| 206.628 | 1504 | 14.3 | 1.2 | 1000.2 | 0.001163 | 13.8 | 1.9 | 1000.8 | 0.001180 |
| 207.592 | 1413 | 12.1 | 2.3 | 1001.3 | 0.001237 | 10.8 | 2.8 | 1001.9 | 0.001284 |
| 208.851 | 2025 | 9.0 | 11.9 | 1009.1 | 0.001373 | 9.0 | 11.9 | 1009.1 | 0.001373 |
| 209.576 | 1350 | 10.9 | 6.0 | 1004.3 | 0.001288 | 8.2 | 12.0 | 1009.3 | 0.001406 |
| 210.663 | 1555 | 14.8 | 5.7 | 1003.6 | 0.001157 | 14.8 | 5.7 | 1003.6 | 0.001157 |
| 211.538 | 1255 | 4.8 | 17.0 | 1013.5 | 0.001570 | 4.8 | 17.0 | 1013.5 | 0.001570 |
| 212.740 | 1745 | 9.2 | 7.7 | 1005.9 | 0.001356 | 12.6 | 8.8 | 1006.3 | 0.001234 |

A.9 continued

station 7

| | | | | | | | | | |
|---|---|---|---|---|---|---|---|---|---|
| 213.719 | 1715 | 15.0 | 7.8 | 1005.1 | 0.001156 | 11.0 | 9.6 | 1007.1 | 0.001292 |
| 214.831 | 1957 | 16.9 | 6.7 | 1004.0 | 0.001098 | 13.2 | 10.4 | 1007.4 | 0.001218 |
| 216.792 | 1900 | 10.5 | 12.3 | 1009.3 | 0.001316 | 10.5 | 12.3 | 1009.3 | 0.001316 |
| 217.531 | 1245 | 8.2 | 13.5 | 1010.4 | 0.001409 | 8.2 | 13.5 | 1010.4 | 0.001409 |
| 218.444 | 1040 | 11.1 | 9.8 | 1008.0 | 0.001289 | 10.5 | 11.2 | 1008.4 | 0.001314 |
| 219.854 | 2030 | 11.0 | 8.0 | 1005.9 | 0.001289 | 10.1 | 10.9 | 1008.2 | 0.001328 |
| 220.847 | 2020 | 8.9 | 5.8 | 1004.4 | 0.001363 | 8.0 | 11.0 | 1008.5 | 0.001412 |
| 221.760 | 1814 | 11.2 | 5.1 | 1003.6 | 0.001275 | 11.2 | 5.1 | 1003.6 | 0.001275 |
| 222.478 | 1128 | 9.8 | 11.0 | 1008.3 | 0.001340 | 8.0 | 15.7 | 1012.2 | 0.001423 |
| 223.677 | 1615 | 10.3 | 9.8 | 1007.4 | 0.001318 | 10.3 | 9.8 | 1007.4 | 0.001318 |
| 224.698 | 1645 | 7.9 | 5.6 | 1004.3 | 0.001403 | 7.9 | 5.6 | 1004.3 | 0.001403 |
| 225.625 | 1500 | 10.0 | 4.2 | 1003.0 | 0.001317 | 10.0 | 4.2 | 1003.0 | 0.001317 |
| 226.563 | 1330 | 11.4 | 10.3 | 1006.7 | 0.001279 | 9.0 | 12.9 | 1009.9 | 0.001375 |
| 227.677 | 1615 | 8.0 | 12.7 | 1009.9 | 0.001416 | 3.0 | 19.5 | 1015.6 | 0.001669 |
| 228.500 | 1200 | 5.0 | 20.0 | 1015.8 | 0.001568 | 5.0 | 20.0 | 1015.8 | 0.001568 |
| 229.781 | 1845 | 13.0 | 6.0 | 1004.1 | 0.001215 | 13.0 | 15.5 | 1011.4 | 0.001235 |
| 230.551 | 1314 | 7.0 | 15.5 | 1012.1 | 0.001465 | 7.0 | 15.5 | 1012.1 | 0.001465 |
| 231.518 | 1226 | 9.0 | 7.2 | 1005.5 | 0.001362 | 8.0 | 15.0 | 1011.6 | 0.001421 |
| 232.867 | 2048 | 7.8 | 6.0 | 1003.2 | 0.001408 | 7.2 | 13.8 | 1010.8 | 0.001452 |
| 233.802 | 1915 | 3.5 | 21.0 | 1016.7 | 0.001646 | 3.5 | 21.0 | 1016.7 | 0.001646 |
| 234.517 | 1224 | 5.1 | 4.3 | 1003.4 | 0.001525 | 2.4 | 20.1 | 1016.1 | 0.001703 |
| 235.537 | 1254 | 5.5 | 16.0 | 1012.6 | 0.001534 | 5.5 | 16.0 | 1012.6 | 0.001534 |
| 236.531 | 1245 | 6.5 | 17.0 | 1013.3 | 0.001491 | 6.5 | 17.0 | 1013.3 | 0.001491 |
| 237.630 | 1507 | 6.9 | 10.2 | 1008.0 | 0.001457 | 5.2 | 18.7 | 1014.8 | 0.001555 |
| 238.619 | 1452 | 7.5 | 16.5 | 1012.9 | 0.001446 | 7.5 | 16.5 | 1012.9 | 0.001446 |
| 239.290 | 0658 | 10.0 | 11.3 | 1008.6 | 0.001333 | 9.0 | 14.2 | 1010.9 | 0.001378 |
| 241.785 | 1850 | 10.1 | 10.6 | 1008.0 | 0.001328 | 9.4 | 14.8 | 1011.3 | 0.001364 |
| 242.660 | 1550 | 9.4 | 10.3 | 1007.9 | 0.001354 | 8.1 | 15.4 | 1011.9 | 0.001418 |
| 243.476 | 1125 | 8.0 | 13.5 | 1010.5 | 0.001418 | 7.6 | 15.5 | 1012.1 | 0.001439 |
| 244.508 | 1212 | 7.8 | 13.2 | 1010.3 | 0.001425 | 7.4 | 14.4 | 1011.2 | 0.001445 |
| 245.483 | 1136 | 7.8 | 13.7 | 1010.7 | 0.001426 | 7.8 | 13.7 | 1010.7 | 0.001426 |
| 246.838 | 2007 | 8.7 | 10.5 | 1008.1 | 0.001382 | 7.7 | 15.1 | 1011.8 | 0.001434 |
| 247.735 | 1738 | 6.4 | 13.7 | 1010.8 | 0.001487 | 6.4 | 13.7 | 1010.8 | 0.001487 |
| 248.469 | 1115 | 6.0 | 11.2 | 1008.8 | 0.001500 | 5.9 | 14.2 | 1011.2 | 0.001511 |
| 249.728 | 1728 | 6.9 | 12.8 | 1010.0 | 0.001463 | 6.3 | 16.2 | 1012.7 | 0.001498 |
| 250.458 | 1059 | 4.3 | 16.8 | 1013.4 | 0.001595 | 4.3 | 16.8 | 1013.4 | 0.001595 |
| 251.590 | 1409 | 5.7 | 12.0 | 1009.5 | 0.001515 | 4.8 | 15.1 | 1012.0 | 0.001566 |
| 253.452 | 1051 | 4.8 | 7.6 | 1006.1 | 0.001547 | 4.2 | 13.3 | 1010.6 | 0.001591 |
| 254.474 | 1122 | 4.9 | 13.8 | 1011.0 | 0.001558 | 3.9 | 18.2 | 1014.5 | 0.001618 |
| 255.527 | 1239 | 5.1 | 9.4 | 1007.5 | 0.001537 | 3.4 | 18.7 | 1014.9 | 0.001645 |

A.9 continued

Babbage Estuary station 12 1976

Daily temperature, salinity, density, and viscosity near-surface (z=0) and near-bottom (z=h)

| time/date 1976 | θ(0) | s(0) | ρ(0) | η(0) | θ(h) | s(h) | ρ(h) | η(h) |
|---|---|---|---|---|---|---|---|---|
| 1515h 13 June | 7.0 | 0.2 | 1000.2 | 0.001429 | 7.0 | 0.2 | 1000.2 | 0.001429 |
| 1945h 14 June | 6.9 | 0.1 | 1000.1 | 0.001433 | 6.9 | 0.1 | 1000.1 | 0.001433 |
| 1910h 15 June | 5.1 | 0.1 | 1000.2 | 0.001515 | 5.1 | 0.1 | 1000.2 | 0.001515 |
| 2030h 16 June | 5.5 | 0.1 | 1000.1 | 0.001496 | 5.5 | 0.1 | 1000.1 | 0.001496 |
| 2110h 17 June | 4.1 | 0.1 | 1000.2 | 0.001563 | 4.1 | 0.1 | 1000.2 | 0.001563 |
| 1745h 18 June | 3.1 | 0.1 | 1000.2 | 0.001615 | 3.1 | 0.1 | 1000.2 | 0.001615 |
| 1645h 19 June | 4.0 | 0.1 | 1000.2 | 0.001568 | 4.0 | 0.1 | 1000.2 | 0.001568 |
| 2330h 20 June | 7.0 | 0.1 | 1000.1 | 0.001428 | 7.0 | 0.1 | 1000.1 | 0.001428 |
| 1655h 21 June | 8.5 | 0.2 | 1000.1 | 0.001366 | 8.5 | 0.2 | 1000.1 | 0.001366 |
| 2030h 22 June | 9.0 | 0.1 | 1000.0 | 0.001346 | 9.0 | 0.1 | 1000.0 | 0.001346 |
| 1930h 23 June | 9.1 | 0.1 | 1000.0 | 0.001342 | 9.1 | 0.1 | 1000.0 | 0.001342 |
| 1945h 24 June | 12.0 | 0.1 | 999.7 | 0.001235 | 12.0 | 0.1 | 999.7 | 0.001235 |
| 2220h 25 June | 9.8 | 0.1 | 999.9 | 0.001315 | 9.8 | 0.1 | 999.9 | 0.001315 |
| 2030h 26 June | 9.1 | 0.1 | 1000.0 | 0.001342 | 9.1 | 0.1 | 1000.0 | 0.001342 |
| 1710h 27 June | 8.1 | 0.1 | 1000.1 | 0.001382 | 8.1 | 0.1 | 1000.1 | 0.001382 |
| 2230h 28 June | 5.5 | 0.1 | 1000.2 | 0.001496 | 5.5 | 0.1 | 1000.2 | 0.001496 |
| 2015h 29 June | 7.2 | 0.1 | 1000.1 | 0.001420 | 7.2 | 0.1 | 1000.1 | 0.001420 |
| 1930h 30 June | 8.2 | 0.1 | 1000.1 | 0.001378 | 8.2 | 0.1 | 1000.1 | 0.001378 |
| 2235h 1 July | 9.2 | 0.1 | 1000.0 | 0.001338 | 9.2 | 0.1 | 1000.0 | 0.001338 |
| 1915h 2 July | 10.0 | 0.1 | 999.9 | 0.001307 | 10.0 | 0.1 | 999.9 | 0.001307 |
| 1925h 3 July | 10.1 | 0.1 | 999.9 | 0.001303 | 10.1 | 0.1 | 999.9 | 0.001303 |
| 1810h 4 July | 12.0 | 0.1 | 999.7 | 0.001235 | 12.0 | 0.1 | 999.7 | 0.001235 |
| 1410h 5 July | 11.8 | 0.1 | 999.7 | 0.001242 | 11.8 | 0.1 | 999.7 | 0.001242 |
| 1405h 6 July | 10.9 | 0.1 | 999.8 | 0.001274 | 10.9 | 0.1 | 999.8 | 0.001274 |
| 1915h 7 July | 11.0 | 0.1 | 999.8 | 0.001270 | 11.0 | 0.1 | 999.8 | 0.001270 |
| 1330h 8 July | 6.7 | 0.2 | 1000.2 | 0.001442 | 6.7 | 0.2 | 1000.2 | 0.001442 |
| 1746h 9 July | 5.0 | 0.1 | 1000.2 | 0.001519 | 5.0 | 0.1 | 1000.2 | 0.001519 |
| 1715h 11 July | 7.8 | 0.1 | 1000.1 | 0.001394 | 7.8 | 0.1 | 1000.1 | 0.001394 |
| 1710h 12 July | 10.2 | 0.1 | 999.9 | 0.001300 | 10.2 | 0.1 | 999.9 | 0.001300 |
| 1535h 13 July | 11.9 | 0.1 | 999.7 | 0.001239 | 11.9 | 0.1 | 999.7 | 0.001239 |
| 1410h 14 July | 12.0 | 0.1 | 999.7 | 0.001235 | 12.0 | 0.1 | 999.7 | 0.001235 |
| 1740h 16 July | 12.5 | 0.1 | 999.7 | 0.001218 | 12.5 | 0.1 | 999.7 | 0.001218 |
| 1240h 19 July | 16.4 | 0.3 | 999.2 | 0.001098 | 16.4 | 0.3 | 999.2 | 0.001098 |
| 1310h 20 July | 17.0 | 0.2 | 999.1 | 0.001081 | 17.0 | 0.2 | 999.1 | 0.001081 |
| 1300h 21 July | 19.2 | 0.2 | 998.7 | 0.001023 | 19.2 | 0.2 | 998.7 | 0.001023 |
| 2025h 24 July | 16.1 | 0.2 | 999.2 | 0.001107 | 16.1 | 0.2 | 999.2 | 0.001107 |
| 1610h 25 July | 16.3 | 0.1 | 999.1 | 0.001100 | 16.3 | 0.1 | 999.1 | 0.001100 |
| 1520h 26 July | 15.6 | 0.1 | 999.2 | 0.001121 | 15.6 | 0.1 | 999.2 | 0.001121 |
| 1825h 27 July | 14.9 | 0.1 | 999.3 | 0.001142 | 13.0 | 5.1 | 1003.4 | 0.001213 |
| 1410h 28 July | 10.8 | 0.1 | 999.9 | 0.001278 | 14.6 | 0.9 | 1000.0 | 0.001153 |
| 1640h 29 July | 17.1 | 0.1 | 999.0 | 0.001078 | 17.1 | 0.4 | 999.2 | 0.001079 |
| 1215h 30 July | 12.0 | 0.8 | 1000.2 | 0.001237 | 12.0 | 0.8 | 1000.2 | 0.001237 |
| 1640h 31 July | 17.2 | 0.1 | 999.0 | 0.001075 | 16.5 | 0.2 | 999.2 | 0.001095 |
| 1210h 1 Aug | 17.0 | 0.1 | 999.0 | 0.001081 | 16.0 | 2.0 | 1000.5 | 0.001114 |
| 1712h 3 Aug | 18.1 | 0.9 | 999.4 | 0.001053 | 15.8 | 6.1 | 1003.7 | 0.001128 |

A.9 continued

station 12

| time/date 1976 | θ(0) | s(0) | ρ(0) | η(0) | θ(h) | s(h) | ρ(h) | η(h) |
|---|---|---|---|---|---|---|---|---|
| 1535h 4 Aug | 14.6 | 0.5 | 999.7 | 0.001152 | 14.9 | 7.3 | 1004.8 | 0.001158 |
| 1346h 5 Aug | 11.5 | 1.0 | 1000.4 | 0.001255 | 12.7 | 1.3 | 1000.5 | 0.001215 |
| 1110h 6 Aug | 14.1 | 2.7 | 1001.4 | 0.001172 | 12.1 | 6.5 | 1004.6 | 0.001246 |
| 2010h 7 Aug | 13.0 | 0.9 | 1000.2 | 0.001204 | 13.0 | 4.1 | 1002.6 | 0.001211 |
| 1935h 8 Aug | 10.0 | 0.6 | 1000.3 | 0.001309 | 9.0 | 6.5 | 1004.9 | 0.001361 |
| 1535h 9 Aug | 11.5 | 0.3 | 999.9 | 0.001253 | 11.5 | 0.3 | 999.9 | 0.001253 |
| 1215h 10 Aug | 12.9 | 0.1 | 999.6 | 0.001205 | 11.2 | 0.5 | 1000.1 | 0.001264 |
| 1532h 11 Aug | 12.1 | 0.1 | 999.7 | 0.001232 | 12.1 | 0.1 | 999.7 | 0.001232 |
| 1425h 12 Aug | 7.9 | 3.0 | 1002.3 | 0.001397 | 7.9 | 3.0 | 1002.3 | 0.001397 |
| 1625h 13 Aug | 9.0 | 1.2 | 1000.8 | 0.001349 | 9.0 | 1.2 | 1000.8 | 0.001349 |
| 1350h 14 Aug | 10.9 | 0.3 | 1000.0 | 0.001275 | 10.9 | 0.3 | 1000.0 | 0.001275 |
| 1645h 15 Aug | 13.0 | 0.1 | 999.6 | 0.001202 | 13.0 | 0.1 | 999.6 | 0.001202 |
| 1415h 16 Aug | 13.0 | 1.9 | 1000.9 | 0.001206 | 9.0 | 13.0 | 1010.0 | 0.001376 |
| 1450h 17 Aug | 14.0 | 0.8 | 1000.0 | 0.001171 | 13.0 | 1.1 | 1000.3 | 0.001204 |
| 1819h 18 Aug | 11.5 | 2.0 | 1001.2 | 0.001257 | 11.4 | 6.5 | 1004.7 | 0.001271 |
| 1945h 19 Aug | 9.2 | 1.1 | 1000.7 | 0.001340 | 10.1 | 3.8 | 1002.7 | 0.001312 |
| 1245h 20 Aug | 9.0 | 0.1 | 1000.0 | 0.001346 | 9.0 | 0.1 | 1000.0 | 0.001346 |
| 1935h 21 Aug | 6.0 | 2.0 | 1001.6 | 0.001478 | 6.0 | 2.0 | 1001.6 | 0.001478 |
| 1313h 22 Aug | 7.3 | 0.8 | 1000.6 | 0.001417 | 6.2 | 7.1 | 1005.6 | 0.001481 |
| 1820h 23 Aug | 7.5 | 2.7 | 1002.1 | 0.001413 | 6.4 | 7.9 | 1006.2 | 0.001474 |
| 1745h 24 Aug | 8.2 | 1.8 | 1001.3 | 0.001382 | 6.0 | 14.6 | 1011.5 | 0.001508 |
| 1630h 25 Aug | 8.0 | 1.8 | 1001.3 | 0.001390 | 8.0 | 1.8 | 1001.3 | 0.001390 |
| 1510h 26 Aug | 12.0 | 3.2 | 1002.0 | 0.001243 | 10.1 | 10.2 | 1007.7 | 0.001327 |
| 0714h 27 Aug | 11.9 | 3.3 | 1002.1 | 0.001246 | 10.4 | 13.2 | 1010.0 | 0.001322 |
| 1910h 29 Aug | 11.9 | 2.8 | 1001.7 | 0.001245 | 8.1 | 12.2 | 1009.5 | 0.001410 |
| 1144h 31 Aug | 10.5 | 1.0 | 1000.5 | 0.001291 | 8.9 | 12.2 | 1009.4 | 0.001378 |
| 1330h 1 Sept | 9.5 | 1.9 | 1001.3 | 0.001331 | 9.1 | 12.2 | 1009.4 | 0.001370 |
| 1214h 2 Sept | 9.5 | 0.7 | 1000.4 | 0.001328 | 8.7 | 12.4 | 1009.6 | 0.001386 |
| 1815h 3 Sept | 9.5 | 1.1 | 1000.7 | 0.001329 | 7.9 | 13.8 | 1010.7 | 0.001422 |
| 1816h 4 Sept | 7.3 | 3.6 | 1002.8 | 0.001424 | 7.8 | 3.8 | 1002.9 | 0.001403 |
| 1140h 5 Sept | 6.6 | 2.7 | 1002.1 | 0.001452 | 6.9 | 6.4 | 1005.0 | 0.001448 |
| 1743h 6 Sept | 7.3 | 1.4 | 1001.1 | 0.001419 | 6.2 | 8.8 | 1006.9 | 0.001485 |
| 1125h 7 Sept | 7.0 | 2.5 | 1001.9 | 0.001434 | 6.7 | 11.6 | 1009.1 | 0.001469 |
| 1437h 8 Sept | 6.8 | 2.7 | 1002.1 | 0.001444 | 6.0 | 13.7 | 1010.8 | 0.001506 |
| 1116h 10 Sept | 5.2 | 2.1 | 1001.7 | 0.001515 | 5.1 | 2.2 | 1001.8 | 0.001520 |
| 1157h 11 Sept | 5.4 | 4.7 | 1003.8 | 0.001512 | 5.2 | 9.0 | 1007.2 | 0.001532 |
| 1335h 12 Sept | 5.8 | 3.4 | 1002.7 | 0.001490 | 5.9 | 9.3 | 1007.4 | 0.001500 |

APPENDIX A.10

SUSPENDED AND DISSOLVED SOLIDS CONCENTRATIONS, BABBAGE ESTUARY, 1976 (SAMPLE DATA)

| DATE | STN | DEPTH | TSS(MG/L) | ISS(MG/L) | TDS(G/L) |
|---|---|---|---|---|---|
| 16 JUNE | 5 | 0. | 219.96 | 212.17 | 0.10 |
| 17 JUNE | 5 | 0. | 150.29 | 141.19 | 0.11 |
| 17 JUNE | 5 | 0. | 150.10 | 141.79 | 0.09 |
| 26 JUNE | 5 | 0. | 767.65 | 706.59 | 0.05 |
| 12 JULY | 5 | 0. | 88.22 | 77.31 | 0.40 |
| 16 JULY | 5 | 0. | 31.57 | 29.75 | 0.58 |
| 9 AUGT | 5 | 0. | 34.24 | 32.89 | 12.70 |
| 12 AUGT | 5 | 0. | 290.90 | 266.91 | 8.18 |
| 15 AUGT | 5 | 0. | 27.22 | 23.60 | 20.78 |
| 21 AUGT | 5 | 0. | 72.22 | 64.46 | 19.31 |
| 22 AUGT | 5 | 0. | | 11.27 | 6.19 |
| 22 AUGT | 5 | 1. | 12.38 | 7.15 | 19.24 |
| 22 AUGT | 5 | 2. | 21.41 | 21.03 | 22.51 |
| 23 AUGT | 5 | 0. | 6.14 | 2.80 | 19.84 |
| 24 AUGT | 5 | 0. | 1.36 | | 18.75 |
| 25 AUGT | 5 | 0. | 6.11 | 4.17 | |
| 25 AUGT | 5 | 1.1 | | 10.45 | 12.23 |
| 29 AUGT | 5 | 0. | 3.53 | 3.13 | 14.26 |
| 4 SEPT | 5 | 0. | 101.71 | 89.85 | 15.37 |
| 16 JUNE | 6 | 0. | | 188.22 | 0.07 |
| 17 JUNE | 6 | 0. | 183.96 | 171.60 | 0.09 |
| 26 JUNE | 6 | 0. | 587.37 | 116.94 | 0.11 |
| 12 JULY | 6 | 0. | 138.83 | 128.00 | 0.66 |
| 16 JULY | 6 | 0. | 49.80 | 44.45 | 0.26 |
| 30 JULY | 6 | 0. | 1122.95 | | 18.31 |
| 10 AUGT | 6 | 0. | 4.41 | | |
| 10 AUGT | 6 | 0.8 | 5.98 | | 12.09 |
| 12 AUGT | 6 | 0. | 446.17 | 404.90 | 4.59 |
| 13 AUGT | 6 | 0. | 163.48 | 152.16 | 9.72 |
| 14 AUGT | 6 | 0. | 50.21 | 40.67 | 6.78 |
| 14 AUGT | 6 | 0.8 | 430.74 | | 11.23 |
| 15 AUGT | 6 | 0. | 47.61 | 43.18 | 12.52 |
| 15 AUGT | 6 | 0.7 | 48.22 | 45.74 | 22.39 |
| 21 AUGT | 6 | 0. | 87.11 | 73.75 | 16.73 |
| 29 AUGT | 6 | 0. | | 1.63 | 11.52 |
| 4 SEPT | 6 | 0. | 63.48 | 56.59 | 19.41 |
| 16 JUNE | 7 | 0. | 85.39 | 76.80 | 0.13 |
| 17 JUNE | 7 | 0. | 62.23 | 59.34 | 0.14 |
| 17 JUNE | 7 | 0. | 75.61 | 72.82 | 0.11 |
| 26 JUNE | 7 | 0. | 362.68 | 334.54 | 0.15 |
| 12 JULY | 7 | 0. | 103.88 | 97.61 | 0.33 |
| 16 JULY | 7 | 0. | 34.39 | 34.36 | 0.21 |
| 9 AUGT | 7 | 0. | 81.22 | 71.13 | 4.24 |
| 12 AUGT | 7 | 0. | 309.69 | 288.06 | |
| 15 AUGT | 7 | 0. | 32.52 | 30.60 | 16.58 |
| 15 AUGT | 7 | 1.0 | 153.42 | 128.69 | 12.46 |
| 18 AUGT | 7 | 0. | 72.69 | 66.19 | 20.35 |
| 21 AUGT | 7 | 0. | 168.86 | 154.35 | 23.29 |
| 23 AUGT | 7 | 0. | 0.98 | 0.00 | 16.19 |
| 24 AUGT | 7 | 0. | 9.55 | 8.75 | 15.71 |
| 30 AUGT | 7 | 0. | | 0.95 | 13.38 |
| 4 SEPT | 7 | 0. | 35.21 | 28.63 | |
| 31 MAY | 7a | 0. | 19.46 | 9.39 | 0.13 |
| 31 MAY | 7a | 0. | 40.02 | 8.68 | 0.05 |
| 3 JUNE | 7a | 0. | 184.84 | 144.20 | 0.09 |
| 3 JUNE | 7a | 1. | 213.16 | 161.98 | 0.06 |
| 8 JUNE | 7a | 0. | 187.94 | 147.62 | 0.13 |
| 12 JUNE | 7a | 0. | 250.56 | 210.32 | 0.06 |

A.10 continued

| DATE | STN | DEPTH | TSS(MG/L) | ISS(MG/L) | TDS(G/L) |
|---|---|---|---|---|---|
| 17 JUNE | 12 | 0. | 73.24 | 67.51 | |
| 5 JULY | 12 | 0. | | 80.48 | |
| 11 JULY | 12 | 0. | 32.39 | | 0.16 |
| 12 JULY | 12 | 0. | 44.86 | 39.79 | |
| 13 JULY | 12 | 0. | | 33.09 | |
| 14 JULY | 12 | 0. | 14.30 | 14.30 | 0.10 |
| 15 JULY | 12 | 0. | 9.90 | 9.50 | 0.13 |
| 16 JULY | 12 | 0. | 13.36 | 10.14 | |
| 17 JULY | 12 | 0. | 11.14 | 7.18 | 0.10 |
| 18 JULY | 12 | 0. | 9.62 | 7.40 | 0.11 |
| 13 AUGT | 12 | 0. | 38.81 | 35.86 | 0.51 |
| 14 AUGT | 12 | 0. | 176.62 | 153.00 | |
| 15 AUGT | 12 | 0. | 46.10 | 42.75 | 0.11 |
| 17 AUGT | 12 | 0. | 10.59 | | 0.18 |
| 18 AUGT | 12 | 0. | 27.91 | 26.99 | 0.18 |
| 18 AUGT | 12 | 5.1 | 21.09 | 18.80 | |
| 19 AUGT | 12 | 0. | 22.26 | 20.93 | 0.19 |
| 20 AUGT | 12 | 0. | 21.13 | 18.56 | |
| 21 AUGT | 12 | 0. | 33.00 | 31.85 | 0.68 |
| 25 AUGT | 12 | 0. | 6.08 | | |
| 29 AUGT | 12 | 0. | 1.57 | 0.40 | 0.69 |
| 4 SEPT | 12 | 0. | 8.75 | 8.75 | 2.11 |
| 20 AUGT | 13 | 0. | 29.92 | 26.28 | 0.22 |

APPENDIX A.11

SUSPENDED SOLIDS CONCENTRATIONS IN BABBAGE ESTUARY, 1976

The following listings include daily Secchi extinction depth, $H_E$, surface and near-bottom transmissivity, $T_L(0)$ and $T_L(h)$ (Hydroproducts meter), and estimated total suspended solids concentration, $C_T=f(H_E)$, for stations 5, 6, 7, 7a, and 12 in the Babbage Estuary during the 1976 open-water season. Dates are given in units of days, with the origin at 0000h 1 January 1976 (see Appendix A.3 for conversion to date). Units are: $C_T$ (mg/L); $H_E$ (m); $T_L$ (%).

STATION 5

| date | $\hat{C}_T$ | $H_E$ | $T_L(0)$ | $T_L(h)$ |
|---|---|---|---|---|
| 158.88 | 697. | 0.050 | . | . |
| 163.77 | 246. | 0.100 | . | . |
| 164.73 | 87. | 0.200 | . | . |
| 165.56 | 111. | 0.170 | . | . |
| 165.84 | 111. | 0.170 | . | . |
| 166.54 | 289. | 0.090 | . | . |
| 166.80 | 344. | 0.080 | . | . |
| 167.46 | 289. | 0.090 | . | . |
| 168.95 | 122. | 0.160 | . | . |
| 169.72 | 122. | 0.160 | . | . |
| 170.67 | 134. | 0.150 | . | . |
| 172.00 | 87. | 0.200 | . | . |
| 172.65 | 71. | 0.230 | . | . |
| 173.46 | 52. | 0.280 | . | . |
| 173.87 | 38. | 0.350 | . | . |
| 174.83 | 31. | 0.400 | . | . |
| 175.80 | 50. | 0.290 | . | . |
| 176.95 | 149. | 0.140 | . | . |
| 177.88 | 1192. | 0.035 | . | . |
| 178.84 | 697. | 0.050 | . | . |
| 179.81 | 213. | 0.110 | . | . |
| 180.86 | 289. | 0.090 | . | . |
| 181.79 | 149. | 0.140 | . | . |
| 182.97 | 187. | 0.120 | . | . |
| 183.78 | 75. | 0.220 | . | . |
| 184.84 | 41. | 0.330 | . | . |
| 185.77 | 41. | 0.330 | . | . |
| 186.63 | 47. | 0.300 | . | . |
| 187.76 | 59. | 0.260 | 7. | 7. |
| 188.75 | 421. | 0.070 | . | . |
| 189.60 | 52. | 0.280 | 8. | 6. |
| 190.70 | 71. | 0.230 | 3. | 1. |
| 191.44 | 87. | 0.200 | 12. | 12. |
| 192.75 | 289. | 0.090 | 0. | 0. |
| 193.64 | 59. | 0.260 | 14. | 13. |
| 194.73 | 66. | 0.240 | 15. | 15. |
| 195.73 | 75. | 0.220 | 7. | 7. |
| 196.86 | 55. | 0.270 | 6. | 4. |
| 197.78 | 38. | 0.350 | 20. | 20. |
| 198.86 | 59. | 0.260 | 12. | 12. |
| 199.89 | 26. | 0.450 | . | . |
| 200.88 | 33. | 0.380 | . | . |
| 201.88 | 20. | 0.530 | . | . |
| 202.54 | 16. | 0.620 | . | . |
| 204.80 | 31. | 0.400 | . | . |
| 205.82 | 26. | 0.450 | . | . |
| 206.62 | 30. | 0.410 | . | . |
| 207.58 | 22. | 0.500 | . | . |
| 208.86 | 18. | 0.580 | 25. | 10. |
| 209.57 | 18. | 0.580 | 46. | 46. |
| 210.64 | 19. | 0.560 | 48. | 48. |
| 211.46 | 289. | 0.090 | 0. | 0. |
| 211.55 | 975. | 0.040 | 0. | 0. |
| 212.41 | 17. | 0.600 | 38. | 37. |

A.11 continued

station 5

| date | $\hat{C}_T$ | $H_E$ | $T_L(0)$ | $T_L(h)$ |
|---|---|---|---|---|
| 212.80 | 16. | 0.610 | 39. | 33. |
| 213.41 | 13. | 0.700 | 54. | 54. |
| 213.79 | 9. | 0.880 | 55. | 51. |
| 214.83 | 30. | 0.410 | . | . |
| 215.62 | . | . | 42. | 36. |
| 216.80 | 23. | 0.490 | 25. | 25. |
| 217.53 | 31. | 0.400 | . | . |
| 218.44 | . | . | 58. | 62. |
| 219.87 | 14. | 0.680 | 46. | 46. |
| 220.86 | 10. | 0.850 | 45. | 44. |
| 221.77 | 8. | 0.980 | 32. | 32. |
| 222.47 | 8. | 0.970 | 69. | 67. |
| 223.68 | 47. | 0.300 | 7. | 2. |
| 224.71 | 213. | 0.110 | . | . |
| 225.60 | 75. | 0.220 | 7. | 0. |
| 226.54 | 75. | 0.220 | 8. | 8. |
| 227.66 | 35. | 0.370 | 24. | 15. |
| 228.49 | 62. | 0.250 | 7. | 2. |
| 229.79 | 10. | 0.850 | 44. | 38. |
| 230.53 | 22. | 0.500 | 19. | 19. |
| 231.50 | 12. | 0.730 | 41. | 20. |
| 232.88 | 7. | 1.110 | 52. | 52. |
| 233.79 | 45. | 0.310 | 9. | 1. |
| 234.50 | 17. | 0.590 | 30. | 21. |
| 235.53 | 7. | 1.100 | 45. | 26. |
| 236.51 | 6. | 1.150 | 51. | 51. |
| 237.62 | 4. | 1.680 | 67. | 70. |
| 238.60 | 4. | 1.550 | 52. | 52. |
| 239.28 | 13. | 0.720 | 59. | 62. |
| 241.77 | 5. | 1.350 | 57. | 49. |
| 242.65 | 3. | 1.870 | 59. | 60. |
| 243.47 | 3. | 2.000 | 68. | 66. |
| 244.50 | 8. | 1.000 | 49. | 33. |
| 245.47 | 4. | 1.610 | 57. | 58. |
| 246.85 | . | . | 63. | 63. |
| 247.73 | 47. | 0.300 | 10. | 10. |
| 248.46 | 16. | 0.620 | 37. | 30. |
| 249.72 | 16. | 0.630 | 39. | 51. |
| 250.45 | 9. | 0.930 | 53. | 49. |
| 251.58 | 3. | 1.770 | 65. | 64. |
| 253.44 | 21. | 0.520 | 28. | 10. |
| 254.46 | 19. | 0.560 | 31. | 12. |
| 255.51 | 29. | 0.420 | 18. | 6. |

A.11 continued

station 6

STATION 6

| date | $\hat{C}_T$ | H E | T (O) L | T (h) L |
|---|---|---|---|---|
| 158.83 | 697. | 0.050 | . | . |
| 163.79 | 187. | 0.120 | . | . |
| 164.70 | 87. | 0.200 | . | . |
| 165.53 | 102. | 0.180 | . | . |
| 165.84 | 149. | 0.140 | . | . |
| 166.55 | 289. | 0.090 | . | . |
| 166.81 | 246. | 0.100 | . | . |
| 167.47 | 289. | 0.090 | . | . |
| 168.93 | 149. | 0.140 | . | . |
| 169.72 | 187. | 0.120 | . | . |
| 170.67 | 62. | 0.250 | . | . |
| 171.99 | 81. | 0.210 | . | . |
| 172.65 | 36. | 0.360 | . | . |
| 173.46 | 71. | 0.230 | . | . |
| 173.91 | 47. | 0.300 | . | . |
| 174.84 | 23. | 0.490 | . | . |
| 175.80 | 47. | 0.300 | . | . |
| 176.94 | 149. | 0.140 | . | . |
| 177.88 | 975. | 0.040 | . | . |
| 178.84 | 530. | 0.060 | . | . |
| 179.81 | 187. | 0.120 | . | . |
| 180.86 | 94. | 0.190 | . | . |
| 181.79 | 55. | 0.270 | . | . |
| 182.97 | 187. | 0.120 | . | . |
| 183.79 | 102. | 0.180 | . | . |
| 184.84 | 38. | 0.350 | . | . |
| 185.77 | 39. | 0.340 | . | . |
| 186.63 | 55. | 0.270 | . | . |
| 187.77 | 45. | 0.310 | 13. | 13. |
| 188.75 | 134. | 0.150 | . | . |
| 189.59 | 29. | 0.420 | 27. | 27. |
| 190.71 | 23. | 0.480 | 24. | 24. |
| 191.45 | 102. | 0.180 | 5. | 5. |
| 192.75 | 246. | 0.100 | 0. | 0. |
| 193.65 | 94. | 0.190 | 5. | 4. |
| 194.73 | 75. | 0.220 | 10. | 9. |
| 195.72 | 38. | 0.350 | 16. | 16. |
| 196.85 | 33. | 0.380 | 13. | 13. |
| 197.78 | 59. | 0.260 | 12. | 12. |
| 198.86 | 55. | 0.270 | 12. | 12. |
| 199.88 | 33. | 0.380 | . | . |
| 200.88 | 41. | 0.330 | . | . |
| 201.88 | 21. | 0.520 | . | . |
| 202.54 | 15. | 0.640 | . | . |
| 204.80 | 31. | 0.400 | . | . |
| 205.83 | 23. | 0.480 | . | . |
| 206.62 | 36. | 0.360 | . | . |
| 207.59 | 20. | 0.540 | . | . |
| 208.85 | 26. | 0.450 | 16. | 16. |
| 209.57 | 17. | 0.600 | 45. | 45. |
| 210.66 | 26. | 0.450 | 43. | 43. |
| 211.46 | 530. | 0.060 | 0. | 0. |
| 211.54 | 1502. | 0.030 | 0. | 0. |
| 212.41 | 23. | 0.480 | 27. | 27. |

A.11 continued

station 6

| date | $\hat{C}_T$ | $H_E$ | $T_L(0)$ | $T_L(h)$ |
|---|---|---|---|---|
| 212.77 | 19. | 0.550 | 34. | 34. |
| 213.41 | 12. | 0.730 | 48. | 48. |
| 213.76 | 11. | 0.790 | 57. | 57. |
| 214.84 | 30. | 0.410 | . | . |
| 215.61 | . | . | 45. | 39. |
| 216.80 | 75. | 0.220 | 5. | 1. |
| 217.53 | 59. | 0.260 | . | . |
| 218.44 | . | . | 59. | 59. |
| 219.87 | 24. | 0.470 | 26. | 26. |
| 220.85 | 12. | 0.750 | 51. | 19. |
| 221.77 | 62. | 0.250 | 13. | 13. |
| 222.47 | 9. | 0.89 | 71. | 71. |
| 223.68 | 75. | 0.220 | 5. | 2. |
| 224.70 | 246. | 0.100 | . | . |
| 225.62 | 166. | 0.130 | 6. | 6. |
| 226.55 | 62. | 0.250 | 10. | 0. |
| 227.67 | 75. | 0.220 | 7. | 1. |
| 228.50 | 379. | 0.075 | 0. | 0. |
| 229.79 | 10. | 0.86 | 47. | 47. |
| 230.54 | 45. | 0.310 | 10. | 10. |
| 231.51 | 13. | 0.710 | 40. | 30. |
| 232.87 | 14. | 0.670 | 39. | 39. |
| 233.80 | 94. | 0.190 | 2. | 2. |
| 234.51 | 14. | 0.670 | 30. | 27. |
| 235.53 | 7. | 1.050 | 44. | 44. |
| 236.52 | 8. | 1.000 | 48. | 48. |
| 237.62 | 6. | 1.150 | 64. | 64. |
| 238.61 | 8. | 0.95 | 44. | 44. |
| 239.29 | 13. | 0.700 | 53. | 53. |
| 241.78 | 9. | 0.90 | 58. | 45. |
| 242.66 | 8. | 0.95 | 58. | 55. |
| 243.47 | 10. | 0.85 | 66. | 66. |
| 244.51 | 8. | 0.95 | 55. | 46. |
| 245.48 | 7. | 1.09 | 57. | 61. |
| 246.85 | . | . | 62. | 62. |
| 247.73 | 62. | 0.250 | 6. | 6. |
| 248.46 | 14. | 0.690 | 42. | 25. |
| 249.72 | 13. | 0.70 | 44. | 48. |
| 250.45 | 8. | 0.950 | 52. | 51. |
| 251.59 | 9. | 0.93 | 61. | 61. |
| 253.44 | 23. | 0.490 | 25. | 24. |
| 254.47 | 18. | 0.580 | 32. | 16. |
| 255.52 | 19. | 0.550 | 30. | 7. |

A.11 continued

station 7

STATION 7

| date | $\hat{C}_T$ | $H_E$ | $T_L$ (0) | $T_L$ (h) |
|---|---|---|---|---|
| 158.81 | 530. | 0.060 | . | . |
| 163.79 | 166. | 0.130 | . | . |
| 165.48 | 94. | 0.190 | . | . |
| 165.85 | 134. | 0.150 | . | . |
| 166.55 | 289. | 0.090 | . | . |
| 166.81 | 266. | 0.095 | . | . |
| 167.47 | 134. | 0.150 | . | . |
| 168.94 | 55. | 0.270 | . | . |
| 169.72 | 111. | 0.170 | . | . |
| 170.68 | 62. | 0.250 | . | . |
| 171.99 | 66. | 0.240 | . | . |
| 172.64 | 59. | 0.260 | . | . |
| 173.46 | 28. | 0.430 | . | . |
| 173.86 | 38. | 0.350 | . | . |
| 174.83 | 23. | 0.480 | . | . |
| 175.79 | 50. | 0.290 | . | . |
| 176.96 | 122. | 0.160 | . | . |
| 177.88 | 470. | 0.065 | . | . |
| 178.83 | 530. | 0.060 | . | . |
| 179.81 | 166. | 0.130 | . | . |
| 180.90 | 87. | 0.200 | . | . |
| 181.79 | 47. | 0.300 | . | . |
| 182.96 | 149. | 0.140 | . | . |
| 183.79 | 62. | 0.250 | . | . |
| 184.83 | 45. | 0.310 | . | . |
| 185.81 | 35. | 0.370 | . | . |
| 186.63 | 43. | 0.320 | . | . |
| 187.78 | 55. | 0.270 | 8. | 6. |
| 188.75 | 59. | 0.260 | . | . |
| 189.58 | 19. | 0.550 | 36. | 36. |
| 190.71 | 16. | 0.630 | 35. | 35. |
| 191.46 | 14. | 0.680 | 42. | 42. |
| 192.76 | 149. | 0.140 | 4. | 3. |
| 193.65 | 81. | 0.210 | 4. | 3. |
| 194.73 | 122. | 0.160 | 3. | 3. |
| 195.71 | 41. | 0.330 | 13. | 12. |
| 196.85 | 23. | 0.480 | 25. | 24. |
| 197.78 | 45. | 0.310 | 14. | 13. |
| 198.85 | 35. | 0.370 | 16. | 16. |
| 199.88 | 25. | 0.460 | . | . |
| 200.88 | 47. | 0.300 | . | . |
| 201.88 | 14. | 0.680 | . | . |
| 202.54 | 10. | 0.850 | . | . |
| 204.79 | 13. | 0.700 | . | . |
| 205.83 | 10. | 0.850 | . | . |
| 206.63 | 19. | 0.560 | . | . |
| 207.59 | 22. | 0.500 | . | . |
| 208.85 | 14. | 0.670 | 19. | 15. |
| 209.58 | 17. | 0.600 | 48. | 48. |
| 210.67 | 14. | 0.660 | 51. | 48. |
| 211.47 | 344. | 0.080 | 0. | 0. |
| 211.54 | 1192. | 0.035 | 0. | 0. |
| 212.41 | 14. | 0.690 | 41. | 41. |
| 212.74 | 17. | 0.590 | 46. | 35. |

A.11 continued

station 7

| date | $\hat{C}_T$ | $H_E$ | $\bar{T}_L(0)$ | $\bar{T}_L(h)$ |
|---|---|---|---|---|
| 213.42 | 12. | 0.730 | 46. | 44. |
| 213.72 | 9. | 0.890 | 61. | 45. |
| 214.83 | 55. | 0.270 | . | . |
| 215.61 | . | . | 47. | 32. |
| 216.68 | 19. | 0.560 | 26. | 18. |
| 216.79 | 27. | 0.440 | 16. | 16. |
| 217.53 | 18. | 0.570 | . | . |
| 218.45 | . | . | 61. | 61. |
| 219.85 | 13. | 0.700 | 44. | 28. |
| 220.85 | 11. | 0.780 | 51. | 35. |
| 221.76 | 45. | 0.310 | 14. | 14. |
| 222.48 | 13. | 0.700 | 70. | 70. |
| 223.68 | 18. | 0.580 | 37. | 0. |
| 224.70 | 187. | 0.120 | . | . |
| 225.63 | 35. | 0.370 | 26. | 18. |
| 226.56 | 94. | 0.190 | 27. | 6. |
| 227.68 | 66. | 0.240 | 12. | 0. |
| 228.50 | 344. | 0.080 | 0. | 0. |
| 229.78 | 18. | 0.580 | 42. | 2. |
| 230.55 | 43. | 0.320 | 9. | 9. |
| 231.53 | 10. | 0.820 | 41. | 31. |
| 232.87 | 15. | 0.650 | 39. | 26. |
| 233.80 | 94. | 0.190 | 2. | 2. |
| 234.51 | 20. | 0.540 | 30. | 22. |
| 235.54 | 4. | 1.450 | 56. | 8. |
| 236.54 | 11. | 0.800 | 41. | 25. |
| 237.63 | 10. | 0.830 | 53. | 60. |
| 238.62 | 12. | 0.750 | 32. | 32. |
| 239.29 | 10. | 0.840 | 51. | 48. |
| 241.79 | 6. | 1.190 | 58. | 42. |
| 242.66 | 4. | 1.55 | 58. | 49. |
| 243.48 | 4. | 1.45 | 66. | 63. |
| 244.51 | 5. | 1.400 | 57. | 45. |
| 245.49 | 4. | 1.450 | 61. | 59. |
| 246.83 | . | . | 63. | 63. |
| 247.74 | 21. | 0.520 | 15. | 15. |
| 248.47 | 17. | 0.600 | 38. | 25. |
| 249.73 | . | . | 41. | 57. |
| 250.46 | 6. | 1.250 | 54. | 52. |
| 251.59 | 4. | 1.46 | 61. | 61. |
| 253.45 | 23. | 0.490 | 27. | 10. |
| 254.47 | 21. | 0.520 | 30. | 5. |
| 255.53 | 19. | 0.550 | 29. | 1. |

A.11 continued

station 7a

STATION 7a

| date | $\hat{C}_T$ | H E | T (O) L | T (h) L |
|---|---|---|---|---|
| 150.58 | 20. | 0.530 | . | . |
| 151.46 | 21. | 0.510 | . | . |
| 151.80 | 17. | 0.600 | . | . |
| 152.50 | 35. | 0.370 | . | . |
| 153.54 | 314. | 0.085 | . | . |
| 153.73 | 213. | 0.110 | . | . |
| 154.50 | 187. | 0.120 | . | . |
| 155.58 | 246. | 0.100 | . | . |
| 158.04 | 530. | 0.060 | . | . |
| 158.75 | 421. | 0.070 | . | . |
| 158.89 | 530. | 0.060 | . | . |
| 159.50 | 289. | 0.090 | . | . |
| 159.77 | 246. | 0.100 | . | . |
| 160.63 | 134. | 0.150 | . | . |
| 162.76 | 66. | 0.240 | . | . |
| 163.74 | 149. | 0.140 | . | . |
| 164.61 | 102. | 0.180 | . | . |
| 165.48 | 166. | 0.130 | . | . |
| 165.85 | 266. | 0.095 | . | . |
| 166.54 | 246. | 0.100 | . | . |
| 166.81 | 344. | 0.080 | . | . |
| 167.47 | 266. | 0.095 | . | . |
| 169.73 | 122. | 0.160 | . | . |
| 170.69 | 55. | 0.270 | . | . |
| 171.99 | 38. | 0.350 | . | . |
| 172.63 | 30. | 0.410 | . | . |
| 173.45 | 31. | 0.400 | . | . |
| 173.86 | 28. | 0.430 | . | . |
| 174.83 | 41. | 0.330 | . | . |
| 175.81 | 39. | 0.340 | . | . |
| 176.92 | 75. | 0.220 | . | . |
| 177.86 | 1502. | 0.030 | . | . |
| 178.44 | 379. | 0.075 | . | . |
| 179.92 | 246. | 0.100 | . | . |
| 180.85 | 87. | 0.200 | . | . |
| 181.83 | 39. | 0.340 | . | . |
| 182.96 | 122. | 0.160 | . | . |
| 183.79 | 47. | 0.300 | . | . |
| 184.83 | 47. | 0.300 | . | . |
| 185.77 | 41. | 0.330 | . | . |
| 186.66 | 31. | 0.400 | . | . |
| 187.61 | 59. | 0.260 | . | . |
| 187.80 | 45. | 0.310 | 13. | 13. |
| 188.76 | 102. | 0.180 | . | . |
| 189.58 | 17. | 0.600 | 38. | 38. |
| 190.72 | 15. | 0.65 | 46. | 46. |
| 191.50 | 18. | 0.570 | 39. | 39. |
| 192.77 | 94. | 0.190 | 6. | 6. |
| 193.66 | 36. | 0.360 | 17. | 17. |
| 194.72 | 94. | 0.190 | 9. | 8. |
| 195.71 | 59. | 0.260 | 9. | 9. |
| 196.84 | 15. | 0.65 | 28. | 28. |
| 197.77 | 17. | 0.600 | 39. | 39. |
| 198.85 | 26. | 0.450 | 34. | 33. |
| 199.85 | 20. | 0.540 | . | . |

A.11 continued

station 12

STATION 12

| date | $\hat{C}_T$ | $H_E$ | $T_L$ (O) | $T_L$ (h) |
|---|---|---|---|---|
| 165.83 | 289. | 0.090 | . | . |
| 166.54 | 166. | 0.130 | . | . |
| 166.79 | 246. | 0.100 | . | . |
| 167.50 | 289. | 0.090 | . | . |
| 168.88 | 52. | 0.280 | . | . |
| 169.75 | 102. | 0.180 | . | . |
| 170.71 | 50. | 0.290 | . | . |
| 171.42 | 52. | 0.280 | . | . |
| 172.00 | 33. | 0.380 | . | . |
| 172.71 | 15. | 0.650 | . | . |
| 173.88 | 28. | 0.430 | . | . |
| 174.83 | 33. | 0.380 | . | . |
| 175.83 | 43. | 0.320 | . | . |
| 176.92 | 43. | 0.320 | . | . |
| 177.46 | 1502. | 0.030 | . | . |
| 177.88 | 1975. | 0.025 | . | . |
| 178.71 | 289. | 0.090 | . | . |
| 179.96 | 134. | 0.150 | . | . |
| 180.83 | 81. | 0.210 | . | . |
| 181.83 | 41. | 0.330 | . | . |
| 182.96 | 87. | 0.200 | . | . |
| 183.79 | 38. | 0.350 | . | . |
| 184.79 | 47. | 0.300 | . | . |
| 185.75 | 23. | 0.480 | . | . |
| 186.58 | 23. | 0.480 | . | . |
| 187.58 | 36. | 0.360 | . | . |
| 187.79 | 23. | 0.490 | 29. | 29. |
| 189.54 | 9. | 0.910 | 59. | 59. |
| 190.75 | 8. | 1.000 | 49. | 49. |
| 192.63 | 11. | 0.800 | 43. | 43. |
| 193.71 | 55. | 0.270 | 11. | 10. |
| 194.67 | 75. | 0.220 | 14. | 12. |
| 195.58 | 38. | 0.350 | 27. | 28. |
| 196.71 | 11. | 0.770 | 36. | 35. |
| 197.75 | 15. | 0.640 | 50. | 43. |
| 198.79 | 13. | 0.700 | . | . |
| 199.75 | 10. | 0.850 | . | . |
| 200.75 | 5. | 1.350 | . | . |
| 201.75 | 3. | 1.700 | . | . |
| 202.54 | 4. | 1.660 | . | . |
| 205.83 | 2. | 2.200 | . | . |
| 206.67 | 2. | 2.200 | . | . |
| 207.63 | 2. | 2.200 | . | . |
| 208.75 | 4. | 1.500 | 51. | 45. |
| 209.58 | 3. | 1.700 | 73. | 69. |
| 210.71 | 3. | 1.710 | 78. | 73. |
| 211.50 | 3. | 1.890 | 59. | 55. |
| 212.42 | 8. | 0.980 | 57. | 50. |
| 212.71 | 9. | 0.890 | 66. | 57. |
| 213.50 | 4. | 1.530 | 82. | 48. |
| 213.67 | 5. | 1.380 | 78. | 64. |
| 215.71 | 7. | 1.120 | 68. | 54. |
| 216.67 | 3. | 1.880 | 55. | 45. |
| 217.58 | 4. | 1.620 | . | . |

A.11 continued

station 12

| date | $\hat{C}_T$ | $H_E$ | $T_L(0)$ | $T_L(h)$ |
|---|---|---|---|---|
| 218.46 | . | . | 77. | 65. |
| 219.83 | 3. | 2.000 | 74. | 58. |
| 220.83 | 2. | 2.500 | 74. | 54. |
| 221.67 | 5. | 1.350 | 67. | 63. |
| 222.50 | 2. | 2.200 | 82. | 79. |
| 223.67 | 3. | 1.950 | 65. | 65. |
| 224.58 | 122. | 0.160 | . | . |
| 225.67 | 21. | 0.510 | 31. | 30. |
| 227.71 | 102. | 0.180 | 6. | 6. |
| 228.58 | 52. | 0.280 | 18. | 34. |
| 229.63 | 14. | 0.660 | 47. | 40. |
| 230.75 | 14. | 0 680 | 26. | 36. |
| 231.83 | 15. | 0.650 | 25. | 25. |
| 232.54 | 7. | 1.030 | 62. | 64. |
| 233.83 | 22. | 0.500 | 22. | 22. |
| 234.54 | 32. | 0.390 | 24. | 31. |
| 235.58 | 20. | 0.530 | . | . |
| 236.75 | 7. | 1.080 | 57. | 48. |
| 237.71 | 4. | 1.450 | 67. | 58. |
| 238.63 | 9. | 0.900 | 27. | 44. |
| 239.29 | 3. | 1.860 | 76. | 58. |
| 241.79 | 2. | 2.200 | 62. | 53. |
| 242.67 | 2. | 2.200 | 62. | 54. |
| 243.50 | 2. | 2.200 | 71. | 61. |
| 244.58 | 2. | 2.200 | 64. | 54. |
| 245.50 | 3. | 1.900 | 67. | 56. |
| 246.75 | 2. | 2.300 | 71. | 63. |
| 247.75 | 6. | 1.250 | 42. | 40. |
| 248.50 | 5. | 1.350 | 59. | 51. |
| 249.75 | 3. | 1.950 | 61. | 49. |
| 250.46 | 4. | 1.550 | 63. | 49. |
| 251.63 | 3. | 2.000 | 45. | 38. |
| 253.46 | 5. | 1.400 | 51. | 48. |
| 254.50 | 6. | 1.200 | 51. | 35. |
| 255.58 | 5. | 1.400 | 48. | 28. |

APPENDIX A.12

PARTICLE-SIZE DATA: SURFACE SEDIMENTS

Particle-size data are given below for surface samples collected at grid-intersections (Figure 6). Samples were split, treated with hydrogen peroxide, dried at 60°C, weighed and wet-sieved to separate coarse and fine fractions at D=0.063mm. Coarse fractions were dry-sieved for 20 minutes at half-phi intervals. Fine fractions were disaggregated with 100 mL/L 5% sodium metaphosphate solution at pH=10 and stirred for 3 minutes in a mechanical mixer; suspensions were brought to a total volume of 1L, mixed, and allowed to settle at constant temperature, particle size being determined as equivalent diameter using hydrometers and assuming equation 4.3.1-1 (Stokes, 1851). See section 4.4.1 for discussion and explanation of statistics.

| site | clay | silt | sand | gravel | D50 (um) | D (0) | s (0) | depositional environment |
|---|---|---|---|---|---|---|---|---|
| | proportions | | | | | | | |
| 000050 | 0.00 | 0.15 | 0.85 | 0.00 | 107.0 | 3.28 | 0.63 | E |
| 000060 | 0.00 | 0.12 | 0.88 | 0.00 | 104.0 | 3.28 | 0.57 | E |
| 000070 | 0.00 | 0.09 | 0.01 | 0.00 | 128.0 | 3.05 | 0.58 | E |
| 000100 | 0.00 | 0.01 | 0.99 | 0.00 | 187.0 | 2.48 | 0.35 | B |
| 010050 | 0.06 | 0.34 | 0.60 | 0.00 | 69.3 | 4.00 | 0.75 | E |
| 010060 | 0.00 | 0.04 | 0.96 | 0.00 | 117.0 | 3.11 | 0.38 | E |
| 010070 | 0.14 | 0.23 | 0.63 | 0.00 | 79.0 | 4.16 | 1.28 | E |
| 010080 | 0.10 | 0.30 | 0.60 | 0.00 | 79.0 | 4.15 | 1.56 | E |
| 010090 | 0.16 | 0.62 | 0.20 | 0.02 | 30.5 | 5.55 | 2.16 | L |
| 010100 | 0.08 | 0.72 | 0.19 | 0.01 | 43.8 | 4.78 | 1.05 | L |
| 010110 | 0.10 | 0.82 | 0.08 | 0.00 | 38.3 | 5.07 | 1.17 | L |
| 010120 | 0.27 | 0.37 | 0.29 | 0.07 | 35.5 | 6.13 | 5.30 | L |
| 010130 | 0.22 | 0.73 | 0.05 | 0.00 | 16.0 | 6.73 | 2.27 | L |
| 010140 | 0.34 | 0.64 | 0.02 | 0.00 | 9.0 | 7.41 | 2.64 | L |
| 010150 | 0.21 | 0.53 | 0.26 | 0.00 | 26.0 | 5.88 | 3.13 | L |
| 010160 | 0.28 | 0.40 | 0.27 | 0.05 | 18.8 | 6.16 | 5.08 | M |
| 020010 | 0.14 | 0.82 | 0.04 | 0.00 | 20.2 | 5.96 | 1.42 | L |
| 020020 | 0.13 | 0.80 | 0.07 | 0.00 | 25.2 | 5.63 | 1.37 | L |
| 020030 | 0.11 | 0.77 | 0.12 | 0.00 | 29.0 | 5.32 | 1.23 | L |
| 020040 | 0.10 | 0.61 | 0.29 | 0.00 | 25.2 | 5.10 | 2.07 | L |
| 020050 | 0.21 | 0.56 | 0.23 | 0.00 | 24.2 | 5.97 | 2.54 | E |
| 020060 | 0.09 | 0.64 | 0.27 | 0.00 | 48.8 | 4.55 | 0.92 | E |
| 020070 | 0.02 | 0.12 | 0.86 | 0.00 | 107.0 | 3.28 | 0.62 | E |
| 020080 | 0.16 | 0.63 | 0.21 | 0.00 | 36.0 | 5.53 | 2.06 | L |
| 020090 | 0.07 | 0.53 | 0.40 | 0.00 | 56.2 | 4.40 | 0.94 | L |
| 020100 | 0.02 | 0.06 | 0.54 | 0.38 | 1160.0 | -0.39 | 2.27 | L |
| 020110 | 0.16 | 0.45 | 0.36 | 0.03 | 45.8 | 4.62 | 3.39 | L |
| 020120 | 0.14 | 0.76 | 0.10 | 0.00 | 26.6 | 5.69 | 1.61 | L |
| 020130 | 0.21 | 0.70 | 0.09 | 0.00 | 19.0 | 6.40 | 2.14 | L |
| 020140 | 0.26 | 0.62 | 0.12 | 0.00 | 16.1 | 6.85 | 2.93 | L |
| 020150 | 0.20 | 0.14 | 0.38 | 0.28 | 500.0 | 4.14 | 7.58 | L |
| 020160 | 0.30 | 0.45 | 0.25 | 0.00 | 17.1 | 6.17 | 4.97 | M |
| 030010 | 0.28 | 0.46 | 0.28 | 0.00 | 29.8 | 7.05 | 4.66 | L |
| 030020 | 0.05 | 0.45 | 0.50 | 0.00 | 62.0 | 4.15 | 0.75 | L |
| 030030 | 0.09 | 0.22 | 0.69 | 0.00 | 94.0 | 4.06 | 1.62 | C |
| 030040 | 0.00 | 0.11 | 0.89 | 0.00 | 132.0 | 3.03 | 0.63 | C |
| 030050 | 0.13 | 0.43 | 0.44 | 0.00 | 56.5 | 4.46 | 1.18 | E |
| 030060 | 0.00 | 0.17 | 0.83 | 0.00 | 113.0 | 3.28 | 0.70 | E |
| 030070 | 0.07 | 0.41 | 0.52 | 0.00 | 64.6 | 4.15 | 0.97 | E |
| 030080 | 0.00 | 0.15 | 0.53 | 0.32 | 685.0 | 0.63 | 3.21 | L |

A.12 continued

| site | clay | silt | sand | gravel | D50 (um) | D (0) | s (0) | depositional environment |
|---|---|---|---|---|---|---|---|---|
| | proportions | | | | | | | |
| 030086 | 0.00 | 0.02 | 0.66 | 0.32 | 5500.0 | -1.91 | 2.25 | L |
| 030090 | 0.09 | 0.69 | 0.21 | 0.01 | 37.8 | 4.84 | 1.08 | L |
| 030100 | 0.15 | 0.54 | 0.31 | 0.00 | 42.1 | 5.28 | 1.88 | L |
| 030110 | 0.17 | 0.77 | 0. 5 | 0.00 | 21.4 | 6.21 | 1.91 | L |
| 030120 | 0.18 | 0.58 | 0.24 | 0.00 | 35.0 | 5.14 | 1.87 | L |
| 030130 | 0.00 | 0.02 | 0.98 | 0.00 | 212.0 | 2.25 | 0.38 | B |
| 030150 | 0.08 | 0.58 | 0.34 | 0.00 | 41.5 | 4.54 | 1.46 | L |
| 030160 | 0.32 | 0.43 | 0.25 | 0.00 | 14.3 | 6.91 | 4.36 | M |
| 032080 | 0.00 | 0.04 | 0.44 | 0.52 | 2060.0 | -0.92 | 1.35 | L |
| 040020 | 0.06 | 0.38 | 0.56 | 0.00 | 70.2 | 4.14 | 1.29 | L |
| 040030 | 0.11 | 0.25 | 0.64 | 0.00 | 96.0 | 4.21 | 1.82 | C |
| 040040 | 0.08 | 0.37 | 0.55 | 0.00 | 72.0 | 4.20 | 1.24 | T |
| 040050 | 0.08 | 0.34 | 0.58 | 0.00 | 74.0 | 3.96 | 0.96 | T |
| 040060 | 0.13 | 0.37 | 0.50 | 0.00 | 62.5 | 4.73 | 1.82 | T |
| 040070 | 0.09 | 0.54 | 0.37 | 0.00 | 54.1 | 4.35 | 0.84 | L |
| 040080 | 0.16 | 0.54 | 0.30 | 0.00 | 52.0 | 5.32 | 2.24 | L |
| 040090 | | | 0.55 | 0.00 | | | | C |
| 040100 | 0.07 | 0.65 | 0.28 | 0.00 | 38.2 | 4.80 | 1.30 | T |
| 040110 | 0.00 | 0.04 | 0.96 | 0.00 | 184.0 | 2.45 | 0.59 | B |
| 040150 | 0.44 | 0.32 | 0.24 | 0.00 | 6.7 | 7.66 | 4.64 | M |
| 050020 | 0.12 | 0.52 | 0.36 | 0.00 | 48.2 | 4.85 | 1.64 | L |
| 050030 | 0.00 | 0.07 | 0.93 | 0.00 | 148.0 | 2.83 | 0.51 | C |
| 050040 | 0.14 | 0.48 | 0.38 | 0.00 | 41.0 | 5.01 | 2.23 | T |
| 050050 | 0.14 | 0.44 | 0.42 | 0.00 | 50.0 | 4.92 | 2.39 | T |
| 050060 | 0.10 | 0.42 | 0.48 | 0.00 | 59.0 | 4.51 | 1.47 | T |
| 050070 | 0.10 | 0.38 | 0.52 | 0.00 | 64.3 | 4.40 | 1.35 | T |
| 050080 | 0.13 | 0.36 | 0.51 | 0.00 | 62.7 | 4.61 | 1.59 | T |
| 050090 | 0.11 | 0.34 | 0.55 | 0.00 | 67.0 | 4.48 | 1.44 | T |
| 050100 | 0.34 | 0.35 | 0.31 | 0.00 | 22.6 | 7.33 | 5.03 | D |
| 050110 | 0.10 | 0.80 | 0.10 | 0.00 | 51.2 | 4.53 | 0.59 | K |
| 060020 | 0.11 | 0.61 | 0.28 | 0.00 | 42.3 | 4.81 | 1.33 | L |
| 060030 | 0.14 | 0.40 | 0.46 | 0.00 | 58.0 | 4.86 | 1.94 | T |
| 060040 | 0.13 | 0.42 | 0.45 | 0.00 | 57.8 | 4.75 | 1.82 | T |
| 060050 | 0.14 | 0.52 | 0.34 | 0.00 | 47.7 | 5.03 | 1.64 | T |
| 060060 | 0.12 | 0.56 | 0.32 | 0.00 | 48.4 | 4.81 | 1.48 | T |
| 060070 | 0.11 | 0.59 | 0.30 | 0.00 | 45.2 | 4.78 | 1.43 | T |
| 060080 | 0.12 | 0.72 | 0.16 | 0.00 | 36.5 | 5.29 | 1.53 | D |
| 060090 | 0.22 | 0.69 | 0.09 | 0.00 | 21.4 | 6.37 | 2.42 | D |
| 060100 | 0.00 | 0.00 | 0.99 | 0.01 | 225.0 | 2.12 | 0.55 | B |
| 070020 | 0.07 | 0.51 | 0.42 | 0.00 | 56.5 | 4.33 | 0.93 | T |
| 070030 | 0.12 | 0.48 | 0.40 | 0.00 | 50.9 | 4.75 | 1.67 | T |
| 070050 | 0.15 | 0.64 | 0.21 | 0.00 | 31.2 | 5.50 | 1.96 | D |
| 070060 | 0.10 | 0.70 | 0.20 | 0.00 | 34.2 | 5.03 | 1.39 | T |
| 070070 | 0.12 | 0.73 | 0.15 | 0.00 | 33.1 | 5.34 | 1.52 | T |
| 070080 | 0.12 | 0.68 | 0.20 | 0.00 | 35.2 | 5.33 | 1.76 | D |
| 070090 | 0.18 | 0.69 | 0.13 | 0.00 | 27.1 | 5.92 | 2.17 | D |
| 080020 | 0.12 | 0.24 | 0.64 | 0.00 | 92.0 | 4.24 | 1.70 | T |
| 080030 | 0.00 | 0.21 | 0.79 | 0.00 | 88.0 | 3.56 | 0.49 | C |
| 080040 | 0.18 | 0.68 | 0.14 | 0.00 | 25.0 | 5.94 | 2.14 | D |
| 080050 | 0.29 | 0.67 | 0.04 | 0.00 | 10.0 | 7.14 | 2.14 | D |

A.12 continued

| site | clay | silt | sand | gravel | D50 (um) | D (0) | s (0) | depositional environment |
|---|---|---|---|---|---|---|---|---|
| | proportions | | | | | | | |
| 080060 | 0.08 | 0.42 | 0.50 | 0.00 | 63.0 | 4.24 | 1.38 | C |
| 080070 | 0.12 | 0.73 | 0.15 | 0.00 | 33.5 | 5.31 | 1.49 | D |
| 080080 | 0.25 | 0.67 | 0.08 | 0.00 | 11.7 | 6.99 | 2.43 | D |
| 080090 | 0.29 | 0.56 | 0.15 | 0.00 | 15.3 | | | D |
| 090010 | 0.13 | 0.71 | 0.16 | 0.00 | 23.6 | 5.66 | 1.79 | D |
| 090020 | 0.20 | 0.70 | 0.10 | 0.00 | 26.0 | 6.38 | 2.70 | D |
| 090030 | 0.00 | 0.06 | 0.94 | 0.00 | 124.0 | 3.05 | 0.44 | C |
| 090040 | 0.24 | 0.71 | 0.05 | 0.00 | 12.9 | 6.62 | 2.00 | D |
| 090050 | 0.13 | 0.72 | 0.15 | 0.00 | 14.5 | 5.94 | 1.71 | D |
| 090060 | 0.11 | 0.22 | 0.67 | 0.00 | 93.0 | 4.14 | 1.66 | C |
| 090070 | 0.16 | 0.64 | 0.20 | 0.00 | 21.2 | 5.55 | 2.34 | D |
| 090080 | 0.30 | 0.69 | 0.01 | 0.00 | 9.9 | | | D |
| 090090 | 0.31 | 0.61 | 0.08 | 0.00 | 10.6 | | | D |
| 100000 | 0.15 | 0.59 | 0.26 | 0.00 | 35.5 | 5.44 | 2.05 | D |
| 100010 | 0.17 | 0.48 | 0.34 | 0.00 | 34.0 | | | D |
| 100030 | 0. 6 | 0.56 | 0.38 | 0.00 | 51.8 | 4.46 | 1.21 | D |
| 100040 | 0.30 | 0.58 | 0.12 | 0.00 | 8.6 | | | D |
| 100060 | 0.16 | 0.35 | 0.49 | 0.00 | 60.0 | 4.86 | 2.67 | C |
| 100070 | 0.22 | 0.66 | 0.12 | 0.00 | 14.4 | 6.57 | 2.42 | D |
| 100080 | 0.14 | 0.39 | 0.47 | 0.00 | 58.0 | 4.82 | 2.33 | C |
| 100090 | 0.30 | 0.53 | 0.17 | 0.00 | 14.4 | | | D |
| 110030 | 0.10 | 0.63 | 0.27 | 0.00 | 39.2 | 5.03 | 1.57 | D |
| 110040 | 0.30 | 0.57 | 0.13 | 0.00 | 10.0 | | | D |
| 110050 | 0.22 | 0.67 | 0.11 | 0.00 | 13.0 | 6.61 | 2.08 | D |
| 110060 | 0.00 | 0.13 | 0.87 | 0.00 | 162.0 | 2.82 | 0.84 | C |
| 110070 | 0.00 | 0.17 | 0.83 | 0.00 | 107.0 | 3.13 | 0.93 | D |
| 120020 | | | 0.72 | 0.00 | 143. | | | C |
| 120030 | 0.15 | 0.68 | 0.17 | 0.00 | 20.0 | 5.83 | 1.95 | D |
| 120040 | 0.20 | 0.71 | 0.09 | 0.00 | 23.3 | 6.11 | 2.31 | D |
| 120050 | 0.25 | 0.62 | 0.13 | 0.00 | 17.7 | 6.51 | 2.62 | D |
| 120060 | 0.05 | 0.13 | 0.82 | 0.00 | 198.0 | 2.76 | 1.24 | C |
| 120070 | 0.24 | 0.66 | 0.10 | 0.00 | 11.2 | 6.76 | 2.26 | D |
| 120080 | 0.30 | 0.36 | 0.34 | 0.00 | 26.4 | | | A |
| 130050 | 0.32 | 0.65 | 0.03 | 0.00 | 8.3 | 7.27 | 2.42 | D |
| 130060 | 0.00 | 0.20 | 0.80 | 0.00 | 145.0 | 2.91 | 1.24 | A |
| 130070 | 0.23 | 0.44 | 0.33 | 0.00 | 38.5 | 5.81 | 3.24 | A |
| 130080 | 0.22 | 0.68 | 0.10 | 0.00 | 11.8 | 7.08 | 2.55 | A |
| 140070 | 0.27 | 0.51 | 0.22 | 0.00 | 20.0 | 6.34 | 3.09 | A |

depositional environments:
B: beach
E: open estuary (exposed basin)
L: lagoon (protected basin)
T: intertidal
M: lagoon-margin supratidal
D: deltaic-supratidal
C: distributary channel
A: alluvial terrace
K: lacustrine

## A.13 RADIOCARBON DATES: LATE HOLOCENE OF CENTRAL YUKON COAST

Radiocarbon dates relevant to sea-level history and sedimentation in late Holocene time on the central Yukon coast are given below. Sites in the Babbage Estuary are identified in Figure 6. The laboratories are: GSC- Geological Survey of Canada, Ottawa; S- National Research Council and University of Saskatchewan, Saskatoon.

| Lab. no. | site | elevation | description | date | reference |
|---|---|---|---|---|---|
| S- 1533 | Herschel Island | -0.7m | charcoal in basal midden below house floor | 990± 95 | B. Walker-Yorga, pers. comm., 1979 |
| S- 1532 | Herschel Island | -0.7m | charcoal in basal midden | 1570± 60 | B. Walker-Yorga, pers. comm., 1979 |
| S- 1534 | Herschel Island | -0.7m | charred fat in basal midden | 1510± 90 | B. Walker-Yorga, pers. comm., 1979 |
| S- 1481 | Babbage site 405 | 0 m | silty peat 0.62m below surface of deltaic silt | 3075±180 | Forbes, 1980 |
| GSC-2691 | Babbage site 405 | 0 m | silty peat 0.87m below surface of deltaic silt | 2110± 90 | Forbes, 1980 |
| GSC-2330 | Babbage site 408 | +0.8m | sandy peat 0.42m below surface in distal delta | 1380± 80 | Forbes, 1980 |
| GSC-2323 | Babbage site 408 | -1.3m | peat from base of 2.6m ice-rich peat silt and sand over massive ice | 2100± 80 | Forbes, 1980 |
| S- 1482 | Babbage site 406 | -0.5m | peat underlying 0.91m stratified silt and sand | 2260±130 | Forbes, 1980 |